



UNIVERSITAT DE
BARCELONA

Nous antagonistes del receptor NMDA pel tractament de la malaltia d'Alzheimer

Caracterització farmacològica *in vivo*

Júlia Companys Alemany



Aquesta tesi doctoral està subjecta a la llicència Reconeixement- NoComercial – SenseObraDerivada 4.0. Espanya de Creative Commons.

Esta tesis doctoral está sujeta a la licencia Reconocimiento - NoComercial – SinObraDerivada 4.0. España de Creative Commons.

This doctoral thesis is licensed under the Creative Commons Attribution-NonCommercial-NoDerivs 4.0. Spain License.



UNIVERSITAT DE
BARCELONA

Facultat de Farmàcia i Ciències de l'Alimentació
Departament de Farmacologia, Toxicologia i Química Terapèutica

Nous antagonistes del receptor NMDA pel tractament de la malaltia d'Alzheimer

Caracterització farmacològica *in vivo*

Júlia Companys Alemany

2022



UNIVERSITAT DE
BARCELONA

Facultat de Farmàcia i Ciències de l'Alimentació
Departament de Farmacologia, Toxicologia i Química Terapèutica

Programa de doctorat en Biotecnologia

Nous antagonistes del receptor NMDA pel tractament de la malaltia d'Alzheimer

Caracterització farmacològica *in vivo*

*Memòria presentada per **Júlia Companys Alemany** per optar al títol de doctor per
la Universitat de Barcelona*

Director

Director

Estudiant de
doctorat

Dra. Mercè Pallàs

Dr. Christian Griñán

Júlia Companys Alemany

Júlia Companys Alemany

2022

Aquesta tesi doctoral s'ha dut a terme al departament de Farmacologia, Toxicologia i Química Terapèutica de la Facultat de Farmàcia i Ciències de l'Alimentació de la Universitat de Barcelona i ha estat finançada per:



Institut de Neurociències
UNIVERSITAT DE BARCELONA

Institut de Neurociències
Universitat de Barcelona



**EXCELENCIA
MARÍA
DE MAEZTU**



**Generalitat
de Catalunya**

Generalitat de Catalunya



Ministerio de Ciencia, Innovación y
Universidades (Agencia Estatal de
Investigación)



Unión Europea

Fondo Europeo
de Desarrollo Regional
"Una manera de hacer Europa"

Fondo Europeo de Desarrollo Regional



Bosch i Gimpera
UNIVERSITAT DE BARCELONA

Fundació Bosch i Gimpera

Als meus pares, Magí i Margarita
A la meva germana, Judit

Agraïments

Un cop arribat a aquest punt, m'agradaria agrair a totes aquelles persones en algun moment o altre d'aquesta etapa, m'han ajudat, recolzat, animat o aportat qualsevol cosa que m'hagi servit per arribar a presentar aquesta tesi doctoral.

En primer lloc, m'agradaria dirigir-me als meus directors Mercè i Christian. Mercè, gràcies per obrir-me les portes d'aquest grup, una de les coses que recordo amb més afecte és la rapidesa amb què vas donar-me l'oportunitat de venir a fer la que va ser la primera estada al laboratori, en aquell moment com a estudiant de grau. Gràcies per haver confiat en mi i per tota la paciència, comprensió, i ajuda que m'has ofert al llarg d'aquesta etapa, m'he sentit molt cuidada i acompanyada tant en l'aspecte personal com en el professional. Christian, gràcies a tu per inspirar-me en els meus inicis com a investigadora i per motivar-me a realitzar la tesi. Per ensenyar-me i deixar-me acompanyar-te en molts dels projectes del grup, que m'han servit per formar-me en diferents àmbits de la ciència. És cert, que no estaria presentant aquesta tesi si no fos per tot el que he après amb tu.

Agrair també al Dr. Santi Vázquez per deixar-me participar en aquest projecte que ha derivat en la present tesi doctoral. Ha estat molt gratificant participar-hi. A més, agrair al Dr. Chillón i al Joan Roig la seva ajuda en la part de l'estudi de neurogènesi.

M'agradaria agrair a la meva companya Foteini, que ha estat el meu suport incondicional durant aquesta etapa. Una vez me dijiste que no esperabas encontrar una amiga como yo aquí, la verdad es que yo tampoco me lo esperaba. La ciencia nos unió, y aunque ahora nos ha separado, sé que siempre tendré a mi amiga griega para lo que necesite. Gracias por todo, sin ti todo habría sido diferente.

No em puc oblidar de la que va ser una de les meves primeres alumnes que s'ha acabat convertint en companya de doctorat. Aina, la veritat és que t'has convertit en una amiga molt especial i que has marcat la meva última etapa d'aquesta

aventura. Mil gràcies per tota la paciència que tens amb mi, per la companyia que m'has fet, per l'ajuda i el suport que m'has donat, no podria haver tingut millor companyia. Saps que la Poma i jo sempre et farem un lloc a casa nostra.

Gràcies també a totes les companyes que he tingut al grup. Gràcies Dolors per ajudar-me i acompanyar-me durant els meus inicis. Gracias a Vero y Vanessa por vuestra ayuda siempre que la necesité. També agrair a la Júlia J. la seva predisposició a ajudar sempre. A les alumnes que he tingut Amalia i Anna, per sempre amb esforç intentar ajudar i participar en el que fes falta, tinc un molt bon record vostre.

Una menció especial a tots els companys del departament pel seu suport tant a nivell personal com professional durant aquests anys, gràcies Emma, Miren, Oriol, Nuri, Raul, Leti, David, Mona, Javi, Triana, Kat, Marina, Núria, Pol, Ana i Roger ha estat un plaer compartir aquesta etapa amb tots vosaltres, heu fet aquesta experiència molt més divertida!

Agrair l'ajuda també al personal del departament, gràcies Mar, Silvia i Quim per la vostra ajuda, així com a tots els professors del departament per haver-me fet sentir part d'aquesta gran família. També agrair al personal de l'estabulari per sempre oferir una solució a tots els problemes amb els quals ens hem trobat. En especial a la Marta, la Tere i la Malika.

Per altra banda, voldria recordar a la meva família a Barcelona, Polo, Magí i Anna em van acollir al vostre pis just abans de començar aquesta etapa, i la vostra companyia va fer aquesta etapa fos única al vostre costat.

Gràcies Sònia, perquè encara que aquests anys hem estat lluny l'una de l'altra sempre ser-hi d'alguna manera. A la Francina, per sempre amb la cosa més mínima treure'm un somriure. A l'Agnès, pels mil i un viatges Santa Coloma-Barcelona que ens vam fer un tip de fer, amb les seves respectives eternes converses.

A la meva germana Judit i al Bernat, per acollir-me durant el confinament, on vam estar treballant plegats al menjador, colze amb colze. Per les tardes de futbol, de pàdel, de passejades, de jocs de la *play* i un llarg etcètera. Gràcies per sempre ser-hi. En especial a la Judit, per ser la meva ma dreta i per les forces que m'has donat en aquesta última etapa d'escriptura de la tesi.

Ivan, no tinc paraules per agrair-te tot el que has fet i fas per mi. Encara que no ha estat un camí fàcil, tot i la distància que ens separava, sempre m'has encoratjat a tirar endavant, a no rendir-me, i a afrontar totes les adversitats. El teu suport ha estat fonamental per a que hagi pogut arribar a presentar aquesta tesi. Gràcies per cuidar-me i per sempre creure en mi, a vegades fins i tot més del que hi crec jo mateixa.

Als meus avis, per acompanyar-me en tots els passos de la vida.

Finalment, però per a mi més important, gràcies als meus pares. Per sempre confiar en mi. Per no posar-me mai barreres i donar-me ales. Per compartir amb mi totes les victòries i per ajudar-me a combatre totes les adversitats, perquè a casa sempre es repeteix la frase “si una porta es tanca, és perquè se n’ha d’obrir una altra”. Gràcies per ser al meu costat sempre, no podria tenir una família millor. Us estimo molt.

Declaració d'Originalitat

Declaro que la present tesi doctoral és original i inclou el contingut de dos articles que han estat publicats prèviament en revistes internacionals després de l'avaluació per part d'experts. Dos articles més s'han entregat a dues revistes internacionals i estan en procés de revisió per la seva publicació.

Júlia Companys

Maig 2022

Resum

Actualment, el tractament de la MA és una necessitat mèdica no coberta, ja que només existeixen tres grups de fàrmacs aprovats que no són suficientment eficaços pel control de la malaltia. La naturalesa complexa de la fisiopatologia de la MA i la manca de biomarcadors són els principals obstacles per al desenvolupament de nous fàrmacs pel tractament de la MA. Tenint en compte l'alta taxa de fracàs, l'optimització dels fàrmacs ja en el mercat representa una eina interessant ja que es reduirien els costos en comparació amb l'assaig de nous compostos dirigits a noves dianes.

La memantina, un antagonista dels receptors NMDA, ha demostrat beneficis clínics en relació tant en aspectes cognitius i no cognitius, com en vies moleculars implicades en el procés neurodegeneratiu. Malgrat tot, la seva efectivitat és limitada. Per aquest motiu, aquesta tesi doctoral s'ha centrat en caracteritzar farmacològicament en models *in vivo* dos nous compostos anàlegs a la memantina (l'RL-208 i l'UB-ALT-EV) que s'han desenvolupat amb l'objectiu de millorar l'eficàcia terapèutica de la memantina. Durant la tesi doctoral, es van dur a terme estudis cognitius i de comportament en el nematode *C.elegans*, en un model de ratolí amb senescència accelerada (SAMP8) i en un model de ratolí transgènic de la MA, el 5XFAD, després del tractament amb els nous antagonistes. A més, es va avaluar molecularment vies associades a la MA per poder avaluar l'efecte modulador dels antagonistes dels receptors NMDA sobre elles.

Els resultats obtinguts en els models animals de ratolí demostren com el tractament crònic per via oral a una dosi baixa amb els nous compostos és capaç de millorar les alteracions de la memòria, així com regular les alteracions de la conducta social i el comportament de tipus ansiós. Per altra banda, el compost UB-ALT-EV va demostrar efectes positius sobre els dèficits locomotors i del comportament els

cucs *C.elegans* causats per l'acumulació del pèptid β -amiloide. Així mateix, els antagonistes del receptor NMDA avaluats van reduir els marcadors neuropatològics típics de la MA com la formació i l'acumulació del pèptid A β i la fosforilació de la proteïna tau. De la mateixa manera es va demostrar l'efectivitat dels nous compostos en la modulació de vies de senyalització molecular implicades en la neurodegeneració, com la desregulació dels nivells de calci intracel·lular, l'estrès oxidatiu, el flux autofàgic i la neuroinflamació.

De manera global, els estudis duts a terme en aquesta tesi permeten demostrar l'efecte neuroprotector dels dos antagonistes del receptor NMDA a més de suggerir que l'optimització de fàrmacs aprovats suposa una estratègia de desenvolupament de nous fàrmacs que permetria l'abordatge de la MA de manera més eficaç. Particularment, donada la capacitat dels nous compostos de regular no només aspectes cognitius i no cognitius sinó també vies moleculars implicades en el procés neurodegeneratiu, aquestes noves teràpies podrien acabar sent considerades com teràpies modificadores de la malaltia i no només tractaments simptomatològics.

Estructura de la tesi

La present tesi doctoral es presenta en els següents capítols:

Capítol 1- Introducció: Presenta els antecedents i resumeix la informació existent sobre la temàtica en la qual s'emmarca aquesta tesi, en aquest cas, els receptors NMDA i la malaltia d'Alzheimer, amb especial consideració a la seva estreta relació.

Capítol 2- Objectius: Conté l'objectiu general i els aspectes centrals que es van abordar durant el desenvolupament d'aquesta tesi i al començament de cada treball científic.

Capítol 3- Mètodes i Resultats: Es divideix en quatre estudis on es demostren els efectes beneficiosos, després del tractament amb els nous antagonistes del receptor NMDA, sobre la cognició, el comportament i sobre vies moleculars alterades durant la malaltia d'Alzheimer en el nematode *C.elegans*, i en dos models de ratolí de la malaltia d'Alzheimer.

Capítol 4- Discussió: Ofereix una interpretació en profunditat dels resultats obtinguts al llarg de la tesi doctoral, procurant establir relacions entre les conclusions i les evidències descrites a la bibliografia.

Capítol 5- Conclusions: Conté un conjunt de conclusions finals basades en les troballes recollides en els quatre treballs d'investigació.

L'**Annex:** Conté resultats preliminars obtinguts durant la realització de la tesi, els quals no s'han tingut en compte per al contingut principal de la tesi.

A continuació es mostren els quatre articles científics que conformen el contingut de la present tesi doctoral: dos d'ells publicats, i els altres dues enviats a dos revistes per la seva publicació:

Article 1

Comanys-Alemanys J., Turcu A. L., Bellver-Sanchis A., Loza M. I., Brea J. M., Canudas A. M., Leiva R., Vázquez S., Pallàs M., Griñán-Ferré C. (2020). A Novel NMDA Receptor Antagonist Protects against Cognitive Decline Presented by Senescent Mice. *Pharmaceutics*, 12(3), 284. doi: <https://doi.org/10.3390/pharmaceutics12030284>.

Article 2

Turcu A. L.*, **Comanys-Alemanys J.***, Phillips M. B., Patel D. S., Griñán-Ferré C., Loza M. I., Brea J. M., Pérez B., Soto D., Sureda F. X., Kurnikova M. G., Johnson J.W., Pallàs M., Vázquez S. (2022). Design, synthesis, and *in vitro* and *in vivo* characterization of new memantine analogs for Alzheimer's disease. *European Journal of Medicinal Chemistry*, 8;236:114354 doi: <https://doi.org/10.1016/j.ejmech.2022.114354>. *han contribuït per igual

Article 3

Comanys-Alemanys J., Turcu A. L., Schneider M., Müller C. E., Vázquez S., Griñán-Ferré C., Pallàs M. NMDA receptor antagonists reduce amyloid- β deposition by modulating calpain-1 signaling and autophagy, rescuing cognitive impairment in 5XFAD mice. [enviat a la revista *Cellular and Molecular Life Sciences*]

Article 4

Comanys-Alemanys J., Turcu A. L., Vázquez S., Pallàs M., Griñán-Ferré C. Glial cell activation and oxidative stress prevention in Alzheimer's disease mice model by an optimized NMDA receptor antagonist. [enviat a la revista *Scientific Reports*]

A més, s'han publicat cinc articles científics addicionals durant el període de la tesi doctoral com a resultat de la participació de l'autor en altres estudis realitzats per membres del mateix grup de recerca. El contingut d'aquestes publicacions no s'ha inclòs en el document principal ja que l'autor va contribuir com a col·laborador en lloc de dirigir la investigació:

Cosín-Tomás M, Álvarez-López MJ, **Comanys-Alemanys J**, Kaliman P, González-Castillo C, Ortuño-Sahagún D, Pallàs M, Griñán-Ferré, C. (2018). Temporal integrative analysis of mRNA and microRNAs expression profiles and epigenetic alterations in female SAMP8, a model of age-related. *Frontiers in Genetics*. 11(9):596. doi: 10.3389/fgene.2018.00596.

Griñán-Ferré C, Codony S, Pujol E, Yang J, Leiva R, Escolano C, Puigoriol-Illamola D, **Companys-Alemaný J**, Corpas R, Sanfeliu C, Pérez B, Loza MI, Brea J, Morisseau C, Hammock BD, Vázquez S, Pallàs M, Galdeano C. (2020). Pharmacological Inhibition of Soluble Epoxide Hydrolase as a New Therapy for Alzheimer's Disease. *Neurotherapeutics*. 17(4):1825-1835. doi: 10.1007/s13311-020-00854-1.

Griñán-Ferré C, **Companys-Alemaný J**, Jarné-Ferrer J, Codony S, González-Castillo C, Ortuño-Sahagún D, Vilageliu L, Grinberg D, Vázquez S, Pallàs M. (2021). Inhibition of Soluble Epoxide Hydrolase Ameliorates Phenotype and Cognitive Abilities in a Murine Model of Niemann Pick Type C Disease. *International Journal of Molecular Sciences*. 26;22(7):3409. doi: 10.3389/fgene.2018.00596.

Puigoriol-Illamola, D., **Companys-Alemaný J**, McGuire, K., Homer, N., Leiva, R., Vázquez, S., Mole, D. J., Griñán-Ferré, C., & Pallàs, M. (2021). Inhibition of 11 β -HSD1 Ameliorates Cognition and Molecular Detrimental Changes after Chronic Mild Stress in SAMP8 Mice. *Pharmaceuticals*. 13;14(10):1040. doi: 10.3390/ph14101040.

Bellver-Sanchis A, Choudhary BS, **Companys-Alemaný J**, Sukanya S, A Ávila-López P, Martínez Rodríguez AL, Brea Floriani JM, Malik R, Pérez B, Pallàs M, Griñán-Ferré C. (2022). Structure based virtual screening, in vitro and in vivo analysis revealed novel potent methyltransferase G9a inhibitors as prospective anti-Alzheimer's agents. *ChemMedChem*. doi: 10.1002/cmdc.202200002. doi: 10.1002/cmdc.202200002

Índex

Agraïments	ix
Declaració d'Originalitat	xiii
Resum	xv
Estructura de la tesi	xvii
Llista de figures	xxv
Llista d'abreviatures	xxvii
1 Introducció	1
1.1 Glutamat al Sistema Nerviós Central.....	3
1.2 Els receptors NMDA.....	4
1.2.1 Subunitats i subtipus de receptors NMDA	4
1.2.2 Expressió i localització dels receptors NMDA al SNC	5
1.2.3 Funció dels receptors NMDA	7
1.2.4 Fosforilació dels receptors NMDA.....	8
1.2.5 Localització sinàptica i extrasinàptica dels receptors NMDA.....	10
1.3 Envel·liment i deteriorament cognitiu.....	12
1.4 La malaltia d'Alzheimer	14
1.4.1 Etiologia i factors de risc	15
1.5 Neuropatologia de la malaltia d'Alzheimer	16
1.6 Mecanismes bioquímics i cel·lulars de la malaltia d'Alzheimer	21
1.6.1 Excitotoxicitat.....	21
1.6.1.1 Desregulació dels nivells de Ca^{2+} intracel·lular.....	22
1.6.1.2 Estrès oxidatiu i disfunció mitocondrial	23
1.6.1.3 Mort neuronal i pèrdua sinàptica	24
1.6.1.4 Alteracions en el procés autofàgic	25
1.6.2 Neuroinflamació	26

1.7	Tractaments actuals per la malaltia d'Alzheimer.....	30
1.7.1	Inhibidors d'acetilcolinesterases.....	30
1.7.2	Antagonistes dels receptors NMDA	31
1.7.3	Anticossos monoclonals	34
1.7.4	Recerca de nous tractaments.....	35
1.7.4.1	RL-208	36
1.7.4.2	UB-ALT-EV	37
1.8	Models animals per l'estudi de la malaltia d'Alzheimer	37
1.8.1	El model <i>Caenorhabditis elegans</i>	38
1.8.2	Models de ratolí	39
1.8.2.1	Ratolins 5XFAD	40
1.8.2.2	Ratolins SAMP8	41
2	Objectius	43
3	Mètodes i Resultats	47
3.1	Article 1. A novel NMDA receptor antagonist protects against cognitive decline presented by senescent mice.....	49
3.2	Article 2. Design, synthesis, and <i>in vitro</i> and <i>in vivo</i> characterization of new memantine analogs for Alzheimer's disease	73
3.3	Article 3. NMDA receptor antagonists reduce amyloid- β deposition by modulating calpain-1 signaling and autophagy, rescuing cognitive impairment in 5XFAD mice	105
3.4	Article 4. Glial cell activation and oxidative stress prevention in Alzheimer's disease mice model by an optimized NMDA receptor antagonist	143
4	Discussió	177
4.1	Efecte de nous compostos antagonistes del receptor NMDA sobre la funció cognitiva.....	180
4.2	Efecte dels nous antagonistes del receptor NMDA sobre la neuropatologia de la malaltia d'Alzheimer.....	183
4.2.1	Producció i acumulació del pèptid A β	183
4.2.2	Hiperfosforilació de la proteïna tau	184
4.3	Efecte del tractament amb nous antagonistes del receptor NMDA sobre vies moleculars implicades en el procés neurodegeneratiu.....	186

4.3.1 Efectes sobre l'expressió dels receptors NMDA	186
4.3.2 Efectes produïts sobre la desregulació dels nivells de Ca ²⁺ intracel·lular	188
4.3.3 Efectes sobre la pèrdua sinàptica i neuronal	189
4.3.4 Efectes del tractament amb UB-ALT-EV sobre l'autofàgia.....	191
4.3.5 Efectes sobre l'estrès oxidatiu	193
4.4 Efectes produïts sobre la neuroinflamació mitjançant el tractament amb UB-ALT-EV.....	194
4.5 Consideracions finals	197
5 Conclusions	199
Referències	203
Annex	247
Annex 1. Resultats preliminars sobre l'efecte de l'UB-ALT-EV sobre la neurogènesi en femelles SAMP8 de 10 mesos d'edat	249

Llista de figures

Figura 1. Esquema de l'estructura dels receptors NMDA.....	5
Figura 2. Els mecanismes d'LTP i LTD regulen la plasticitat sinàptica.	8
Figura 3. Efectes oposats de l'activació dels receptors NMDA sinàptics i extrasinàptics.....	12
Figura 4. Canvis macroscòpics i microscòpics característics de la MA. Figura adaptada de (Drew, 2018).....	16
Figura 5. Vies de processament de la proteïna APP. Figura adaptada de (Patterson et al., 2008).	18
Figura 6. Funció estabilitzadora dels microtúbuls de tau. Desestabilització dels microtúbuls a causa de la hiperfosforilació i agregació insoluble de tau.	19
Figura 7. Funció de les cèl·lules inflamatòries en condicions fisiològiques i durant la MA.	30
Figura 8. Estructura química dels inhibidors de l'acetilcolinesterasa. Donepezil (A), Rivastigmina (B) i Galantamina (C)	31
Figura 9. Estructura química de la memantina	32
Figura 10. Mecanisme d'acció de la memantina. Procés d'entrada de Ca^{2+} a través dels receptors NMDA en condicions fisiològiques (A); Procés d'entrada de Ca^{2+} a través dels receptors NMDA durant la MA, on el Mg^{2+} deixa de bloquejar el canal degut a l'acció dels oligòmers d' $A\beta$ (B); Mecanisme d'acció dependent de voltatge de la memantina, ocupant el lloc del Mg^{2+} , regulant la	

senyalització de Ca ²⁺ (C). Figura adaptada de (Danysz & Parsons, 2012)	33
Figura 11. RL-208; (3,4,8,9-Tetrametiltetracido[4.4.0.0 ^{3,9} .0 ^{4,8}]dec-1-il) metilamina hidrocloreur.....	37
Figura 12. UB-ALT-EV; 9-Fluoro-5,6,8,9,10,11-hexahidro-7H-5,9:7,11-dimetanobenzo[9]annulè-7-amina hidrocloreur	37
Figura 13. Representació esquemàtica de les vies moleculars del SNC modificades per l'acció dels nous antagonistes del receptor NMDA optimitzats respecte la memantina, i dels efectes a nivell cognitiu i del comportament.	198

Llista d'abreviatures

- A β** : β -amiloide
- ADAM10**: De l'anglès *A disintegrin and metalloproteinase 10*
- AINE**: Medicament antiinflamatori no esteroïdal
- AMPA**: α -amino-3-hidroxi-5-metil-4-isoxazolpropioníc
- ANOVA**: anàlisi de variància
- APOE**: Apolipoproteïna E
- APP**: De l'anglès *Amyloid precursor protein*
- ARG1**: Arginasa 1
- ARNm**: ARN missatger
- ATP**: Adenosina trifosfat
- BACE1**: De l'anglès *beta-site amyloid precursor protein cleaving enzyme 1*
- BAD**: De l'anglès *Bcl-2 associated agonist of cell death*
- Bax**: De l'anglès *Bcl-2 associated X*
- Bcl-2**: De l'anglès *B cell lymphoma 2*
- BDNF**: De l'anglès *Brain derived neurotrophic factor*
- BrdU**: Bromodeoxiuridina
- BSA**: Albúmina de sèrum boví
- CaM**: Calmodulina
- CaMKII**: De l'anglès *Calcium/calmodulin-dependent protein kinase II*
- CaN**: Calcineurina
- CAT**: Catalasa
- CCL1**: De l'anglès *Chemokine (C-C motif) ligand 1*
- CCL2**: De l'anglès *Chemokine (C-C motif) ligand 2*
- CCL3**: De l'anglès *Chemokine (C-C motif) ligand 3*
- Cdk5**: de l'anglès *Cyclin dependent kinase 5*
- Caenorhabditis elegans***: *C. elegans*
- CKII**: Caseína quinasa II

CREB: De l'anglès *cAMP response element-binding*
CXCL1: De l'anglès *chemokine (C-X-C motif) ligand 1*
D-APV: àcid D(-)-2-amino-5-fosfonopentanoic
DCX: Doblecortina
EMA: De l'anglès *European medicine agency*
ERK: De l'anglès *Extracellular signal-regulated kinase*
ERO: Espècies reactives d'oxigen
FDA: De l'anglès *Food and drug administration*
GFAP: De l'anglès *Glial fibrillar acidic protein*
GPx: Glutatió peroxidasa
GPX1: Glutatió peroxidasa 1
GSK3 β : De l'anglès *Glycogen synthase kinasa 3 β*
GLP1: De l'anglès *Glucagon-like peptide-1*
GR: Glutatió reductasa
iGluR: Receptor ionotròpic de glutamat
Hmox1: De l'anglès *Heme oxygenase 1*
ID: Índex de discriminació
Ifn- γ : Interferó γ
IL-1 β : Interleucina-1 β
IL-6: Interleucina-6
IL-18: Interleucina-18
iNOS: De l'anglès *inducible nitric oxide synthase*
LAMP1: De l'anglès *lysosomal-associated membrane protein 1*
LC3B: De l'anglès *microtubule-associated proteins 1A/1B light chain 3*
LTP: De l'anglès *long term potentiation*
LTD: De l'anglès *long term depression*
MA: Malaltia d'Alzheimer
MAPK: De l'anglès *mitogen-activated protein kinase*
MWM: De l'anglès *Morris water maze*
Ngf: De l'anglès *nerve growth factor*
NFAT: De l'anglès *nuclear factor of activated T-cells*
NF- κ B: De l'anglès *nuclear factor kappa-light-chain-enhancer of activated B cells*
NMDA: N-metil-D-aspartat
NO: Òxid nítric
NORT: De l'anglès *Novel object recognition test*
OF: De l'anglès *Open field*
OLT: De l'anglès *Object location test*
p62: proteïna d'unió a ubiquitina p62

- PFA:** Paraformaldehid
- PKA:** De l'anglès *protein kinase A*
- PKB:** De l'anglès *protein kinase B*
- PKC:** De l'anglès *protein kinase C*
- PLD:** De l'anglès *Phospholipase D*
- PSEN:** Presenilina
- PSD95:** De l'anglès *post synaptic density protein 95*
- SAMP:** De l'anglès *Senescence accelerated mouse-prone*
- SAMR:** De l'anglès *Senescence accelerated mouse resistant*
- sAPP:** Proteïna precursora amiloide soluble
- SEM:** Error estàndard de la mitjana
- SNAP25:** Proteïna associada als sinaptosomes, 25kDa
- SNC:** Sistema nerviós central
- SOD:** Superòxid dismutasa
- SOD1:** Superòxid dismutasa 1
- TC:** temps d'exploració de l'objecte conegut
- TCT:** De l'anglès *Three chamber test*
- TN:** Temps d'exploració de l'objecte nou
- TNF:** De l'anglès *tumor necrosis factor*
- TREM2:** De l'anglès *triggering receptor expressed on myeloid cells 2*
- TrkB:** De l'anglès *Tropomyosin receptor kinase B*
- ULK1:** De l'anglès *Unc-51 like autophagy activating kinase*
- Vgf:** De l'anglès *Nerve growth factor inducible*
- YM1:** Proteïna de tipus quitinasa 3

Capítol 1

Introducció

1.1 Glutamat al Sistema Nerviós Central

Des de la dècada dels anys setanta es coneix el glutamat com el principal neurotransmissor excitador del sistema nerviós central (SNC) dels mamífers. El glutamat és alliberat a nivell presinàptic a través de vesícules mitjançant un mecanisme dependent de calci (Ca^{2+}) i posteriorment actua a nivell postsinàptic unint-se a receptors ionotròpics i metabotròpics específics (Reiner & Levitz, 2018). Els receptors ionotròpics de glutamat (iGluRs) es troben tant a cèl·lules neuronals com no neuronals, sent essencials per la senyalització de glutamat en diferents processos associats a funcions fisiològiques, com ara l'aprenentatge i la memòria (Reiner & Levitz, 2018).

Els iGluRs són associacions de proteïnes integrals de membrana formades per 4 subunitats grans (amb més de 900 residus) que conformen un canal iònic central (Traynelis et al., 2010). Les subunitats dels receptors de glutamat són estructures modulares que contenen 4 dominis semi-autònoms: el domini extracel·lular amino-terminal, el domini extracel·lular d'unió al lligand, el domini transmembrana, i el domini intracel·lular carboxi-terminal (Traynelis et al., 2010). S'han identificat múltiples tipus d'iGluRs; entre ells es troben els receptors N-metil-D-aspartat (NMDA), els receptors α -amino-3-hidroxi-5-metil-4-isoxazolpropioníc (AMPA) i els receptors kainat. Aquestes famílies es caracteritzen per ser canals permeables a cations, essent variable la permeabilitat als ions de sodi (Na^+) i Ca^{2+} segons la família i la composició de subunitats de cada receptor. Cadascun dels receptors està format per homo- o hetero-tetràmers de subunitats específiques, generant un gran nombre de subtipus de receptors, amb diferents propietats fisiològiques (Meldrum, 2000).

La família dels receptors NMDA és essencial durant els processos de memòria i aprenentatge donada la seva funció reguladora de la transmissió i la plasticitat sinàptica (Hansen et al., 2018). Hi ha un gran nombre de malalties causades per mutacions en els gens que codifiquen pels receptors NMDA i la majoria d'elles estan relacionades amb trastorns del desenvolupament neurològic (Endele et al., 2010; C. Hu, Chen, Myers, Yuan, & Traynelis, 2016; Stroebel & Paoletti, 2021; XiangWei, Jiang, & Yuan, 2018). Per aquest motiu, els receptors NMDA es consideren dianes farmacològiques amb un alt potencial terapèutic (Yan Zhang, Li, Feng, & Wu, 2016).

1.2 Els receptors NMDA

Els receptors NMDA presenten una sèrie de característiques que els fan únics entre els iGluRs. Són els únics receptors sinàptics que necessiten la unió de dos agonistes, el glutamat i la glicina (o D-serina) per a la seva activació (Benveniste & Mayer, 1991; Kleckner & Dingledine, 1988). Aquesta activació però, està condicionada per l'alliberació presinàptica de glutamat (Berger, Dieudonné, & Ascher, 1998). Són permeables principalment a l'entrada de Ca^{2+} , però a més permeten l'entrada de Na^+ i potassi (K^+). A més, es caracteritzen per tenir un filtre de selectivitat del canal iònic, on un conjunt de residus d'asparagina doten al receptor d'una gran sensibilitat als canvis locals de potencial de membrana, a través del bloqueig del canal mitjançant el ió magnesi (Mg^{2+}) (Stroebel & Paoletti, 2021).

1.2.1 Subunitats i subtipus de receptors NMDA

Les subunitats dels receptors NMDA estan codificades per 7 gens diferents. Un únic gen anomenat *GRIN1*, quatre gens *GRIN2* i dos gens *GRIN3* que codifiquen per les subunitats GluN1, GluN2A-D i GluN3A-B (Traynelis et al., 2010). Aquestes unitats presenten un assemblatge hetero-tetramèric de subunitats que conjuntament formen el canal iònic central del receptor NMDA. Cada subtipus de receptor es caracteritza per tenir unes propietats funcionals úniques i específiques que venen determinades per les combinacions de subunitats que formen l'heteròmer. De fet, la combinació de diferents subunitats determina l'afinitat al glutamat, la sensibilitat al Mg^{2+} i la cinètica del canal de cada subtipus de receptor NMDA (S. G. Cull-Candy & Leszkiewicz, 2004).

Totes les subunitats dels receptors NMDA comparteixen una tipologia d'inserció a la membrana, sempre formada per quatre dominis: un domini extracel·lular amino-terminal encarregat de la regulació alostèrica i de l'assemblatge de la subunitat, que contribueix al control de l'obertura del canal; un domini d'unió a lligand format per dos segments discontinus (S1 i S2), que s'uneix als agonistes i antagonistes per controlar l'obertura del canal iònic; un domini transmembrana que conté tres segments transmembrana (M1, M3 i M4) i un "bucle de porus" re-entrants (M2) que forma part del porus del canal i que conté un residu d'asparagina, encarregat de determinar la permeabilitat del Ca^{2+} del canal i controlar el bloqueig per Mg^{2+} . Finalment trobem un domini intracel·lular carboxi-terminal que interactua amb les proteïnes citosòliques (J. Liu, Chang, Song, Li, & Wu, 2019). Els dominis d'unió a lligand de les subunitats GluN2

contenen el lloc d'unió a glutamat, mentre que els mateixos dominis per GluN1 contenen el lloc d'unió del co-activador glicina (Hackos & Hanson, 2017). En la majoria dels casos, els receptors NMDA estan formats per dues subunitats d'unió a glicina GluN1 i per dues subunitats d'unió a glutamat GluN2 (C.-H. Lee et al., 2014) (**Figura 1**). Encara que, també poden incloure subunitats d'unió a glicina GluN3. Aquesta última subunitat s'ha demostrat que pot actuar com una subunitat reguladora en algunes regions durant el desenvolupament (Chatterton et al., 2002).

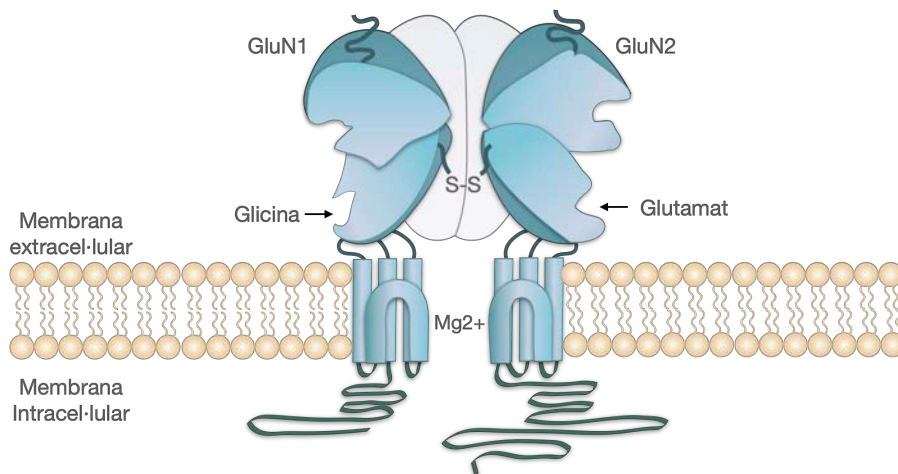


Figura 1. Esquema de l'estructura dels receptors NMDA.

1.2.2 Expressió i localització dels receptors NMDA al SNC

Dins el SNC, els receptors NMDA s'expressen a les neurones, als astròcits i als oligodendròcits (Káradóttir, Cavelier, Bergersen, & Attwell, 2005; Lalo, Pankratov, Kirchhoff, North, & Verkhratsky, 2006). A les neurones, es troben a les zones presinàptiques i postsinàptiques, mentre que a les interneurons GABAèrgiques corticals els receptors NMDA es troben distribuïts al llarg dels eixos dendrítics (Goldberg, Yuste, & Tamas, 2003). Respecte als diferents subtipus de receptors NMDA, aquests es distribueixen per tot el cervell i, existeix la possibilitat que durant el desenvolupament cerebral la combinació de subunitats dins dels receptors variïn. Durant la vida adulta, l'exposició a determinades experiències o alteracions fisiològiques o patològiques de la funció sinàptica poden produir variacions en la composició dels receptors (Mothet, Le Bail, & Billard, 2015).

Respecte a la composició i expressió per subunitats dels receptors NMDA:

- La subunitat GluN1 s'expressa des de fases embrionàries fins a la vida adulta per tot el cervell, destacant la seva expressió en àrees com l'hipocamp i l'escorça cerebral (Paoletti, Bellone, & Zhou, 2013).
- La subunitat GluN2A s'expressa de manera general a l'hipocamp i a l'escorça cerebral durant la vida adulta. Concretament, s'expressa a les zones sinàptiques de les neurones madures, sent l'extrem C-terminal el responsable d'aquesta localització, però també s'ha trobat aquesta subunitat a zones extra-sinàptiques (S. Cull-Candy, Brickley, & Farrant, 2001; Thomas, Miller, & Westbrook, 2006).
- La subunitat GluN2B es troba a la majoria de regions cerebrals durant el desenvolupament neuronal, i la seva expressió va decreixent a mesura que s'arriba a la maduresa, encara que es mantenen nivells considerables a l'escorça i hipocamp cerebrals durant la vida adulta. Es localitza tant en zones sinàptiques com extra-sinàptiques durant el desenvolupament i a mesura que les neurones maduren es troba de manera predominant a zones extra-sinàptiques (S. Cull-Candy et al., 2001).
- La subunitat GluN2C s'expressa principalment a les cèl·lules granulars del cerebel. A més, també actua en altres zones cerebrals, per exemple en processos dels oligodendròcits, que són responsables de la mielinització (Káradóttir et al. 2005; Micu et al. 2006; Salter i Fern 2005).
- La subunitat GluN2D s'expressa a l'etapa embrionària, i va decreixent de manera contundent durant l'edat adulta, on s'expressa de manera molt baixa al diencèfal i mesencèfal (Paoletti, Bellone i Zhou 2013).
- La subunitat GluN3A es troba expressada a l'etapa post-natal i va decaient de manera progressiva mentre que l'expressió de la subunitat GluN3B actua contràriament, augmentant la seva expressió durant el desenvolupament, i durant l'edat adulta s'expressa en altes concentracions a les neurones motores (Henson, Roberts, Pérez-Otaño, & Philpot, 2010).

1.2.3 Funció dels receptors NMDA

Funció sinàptica

El glutamat alliberat des dels terminals presinàptics després de l'arribada d'un potencial d'acció s'elimina de forma ràpida de l'espai intersinàptic per l'acció de transportadors de glutamat i dels astròcits propers (Rothstein et al., 1994). De tal manera que, només es troba disponible per la unió als receptors durant un període breu durant la transmissió sinàptica de baixa freqüència. Atès que els receptors NMDA tenen una afinitat relativament alta pel glutamat, els pics de mil·lisegons del neurotransmissor són capaços d'activar-los parcialment. No obstant això, aquest fenomen per si sol no dona lloc a l'entrada de Ca^{2+} a causa d'una segona propietat d'aquests receptors, la dependència de voltatge. Quan els potencials de membrana es troben en repòs, els ions de Mg^{2+} entren al canal NMDA, on s'hi uneixen de manera que impedeixen l'entrada de ions (Nowak, Bregestovski, Ascher, Herbet, & Prochiantz, 1984). Es necessita una despolarització de suficient amplitud i duració per a desplaçar i expulsar els ions de Mg^{2+} del canal, permetent així el flux de ions com el Ca^{2+} . Aquest doble requisit d'entrada, juntament amb la cinètica d'activació i desactivació lenta, permeten als receptors NMDA integrar i descodificar l'activitat sinàptica entrant (Blanke & VanDongen, 2009).

Potenciació i depressió a llarg termini

La forta despolarització requerida per eliminar el bloqueig produït pel Mg^{2+} als canals NMDA es pot produir per diferents mecanismes involucrats en processos de memòria i aprenentatge. Els senyals sinàptics d'alta freqüència permeten que els potencials postsinàptics excitadors generats indueixin l'anomenada potenciació a llarg termini (LTP, de l'anglès *long term potentiation*). Els ions de Ca^{2+} que entren a través dels receptors NMDA són capaços d'actuar localment sobre grans complexes de transducció de senyals com ara enzims dependents de Ca^{2+} , segons missatgers, proteïnes quinases i fosfatases, pèptids com el GLP1 (de l'anglès *Glucagon-Like Peptide-1*) i molècules d'adhesió (Husi, Ward, Choudhary, Blackstock, & Grant, 2000). De manera que, l'activació d'un conjunt de cascades de senyalització acaba donant lloc a l'enfortiment de les sinapsis, augmentant la localització de receptors AMPA a la superfície cel·lular (Deisseroth, Mermelstein, Xia, & Tsien, 2003). En canvi, la depressió a llarg termini (LTD, de l'anglès *long term depression*) es genera a partir de l'estimulació prolongada a baixa freqüència de les sinapsis excitadores. Aquest procés redueix l'activitat sinàptica mitjançant la desfosforilació dels receptors AMPA i

promovent la seva endocitosi i la pèrdua d'espines (Blanke & VanDongen, 2009). Aquest procés de formació i eliminació d'espines dendrítiques s'ha proposat com la base molecular de la formació de la memòria (Nabavi et al., 2014) (**Figura 2**).

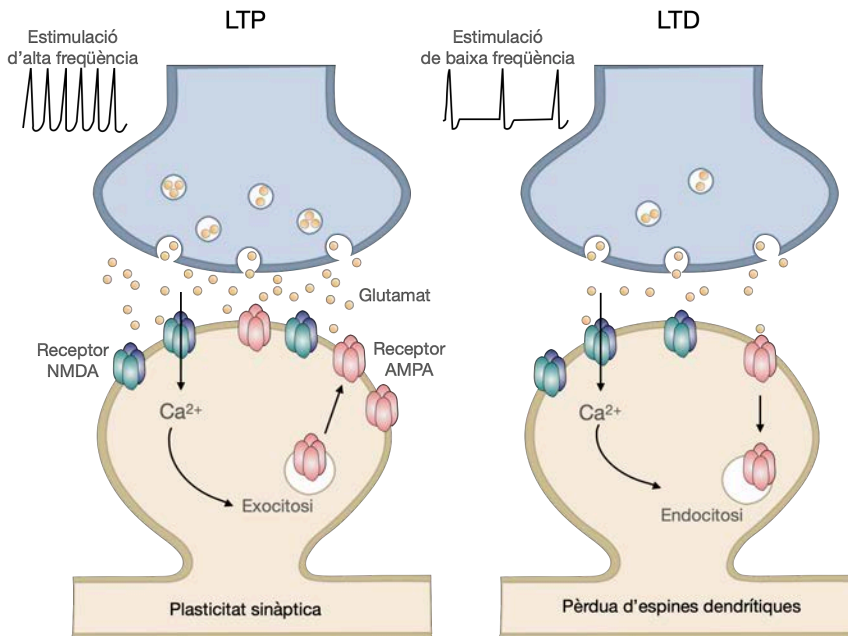


Figura 2. Els mecanismes d'LTP i LTD regulen la plasticitat sinàptica.

1.2.4 Fosforilació dels receptors NMDA

La part intracel·lular dels dominis carboxi-terminals de les subunitats dels receptors NMDA contenen múltiples zones per a les modificacions post-traduccionals i per a interaccions proteïna-proteïna. Aquests processos són rellevants per a la localització, trànsit i senyalització dels receptors. En concret, la fosforilació de les subunitats té un paper clau en la funcionalitat i localització dins les sinapsis dels receptors NMDA (Lussier, Sanz-Clemente, & Roche, 2015).

Regulació funcional dels receptors NMDA mitjançant la fosforilació de residus serina/treonina

Existeixen diferents zones de fosforilació serina/treonina dins els receptors NMDA, que són substrats per la proteïna quinasa cAMP-dependent (PKA, de l'anglès *protein kinase A*), la proteïna quinasa B (PKB, de l'anglès *protein kinase B*), la proteïna quinasa C (PKC de l'anglès *protein kinase C*), la proteïna quinasa dependent de calci/calmodulina II (CaMKII, de l'anglès *Calcium/calmodulin-dependent protein kinase II*), la quinasa ciclina-dependent 5 (Cdk5, de l'anglès

Cyclin dependent kinase 5) i la caseïna quinasa II (CKII). Aquestes quinases estan implicades en processos de plasticitat sinàptica, ja que regulen el trànsit intracel·lular i les propietats dels receptors NMDA (H.-K. Lee, 2006).

La subunitat GluN1, essencial per la conformació receptors NMDA, pot ser fosforilada per la quinasa PKC a la posició S890 i a la posició S896. Per una banda, la fosforilació de la posició S890 dona lloc a una alteració de la unió de la subunitat GluN1 amb el receptor (Tingley et al., 1997). Per altra banda, la fosforilació a la posició S896 conjuntament amb la fosforilació per part de la PKA a la posició S897, promou la localització del receptor NMDA a la superfície cel·lular (Scott, Blanpied, Swanson, Zhang, & Ehlers, 2001).

La fosforilació de cada subunitat GluN2, a diferència de la GluN1, aporta diferents propietats funcionals als receptors:

- La fosforilació de la subunitat GluN2A pot ser produïda per la PKC o per la Cdk5. La primera disminueix l'afinitat d'unió del receptor amb la CaMKII, modulant així de manera directa vies de senyalització intracel·lulars (Jones & Leonard, 2005; B.-S. Li et al., 2001). Per altra banda, la fosforilació produïda per la Cdk5 és responsable de l'augment de l'activitat del receptor (B.-S. Chen & Roche, 2007).
- La fosforilació de la subunitat GluN2B pot ser produïda per la PKC, la CaMKII i la CKII en diferents posicions. Curiosament, la fosforilació produïda per la CKII a la posició S1480 és la responsable de la disrupció de la interacció entre la subunitat GluN2B i la proteïna de densitat postsinàptica 95 (PSD95, de l'anglès *post synaptic density protein 95*) (Chung, Huang, Lau, & Huganir, 2004), que promou la internalització del receptor, i per tant l'alteració de l'estabilitat sinàptica (B.-S. Chen & Roche, 2007).

Regulació funcional dels receptors NMDA mitjançant la fosforilació de residus tirosina

Els receptors NMDA també poder estar fosforilats per les proteïnes tirosinquinases, especialment per les Src i les Fyn quinases (Y. T. Wang & Salter, 1994). La subunitat GluN2B és la subunitat principalment fosforilada per tirosinquinases, mentre que per exemple, la subunitat GluN1 sembla ser que no està regulada per aquest tipus de fosforilació (B.-S. Chen & Roche, 2007).

Existeixen tres llocs de fosforilació per tirosina quinases a la subunitat GluN2A (Y1292, Y1325 i Y1387), les quals són dianes de la quinasa Src (M. Yang & Leonard, 2001). Aquesta fosforilació potencia els corrents iònics a través del

canal. A més, la posició Y842 d'aquesta subunitat pot ser alhora fosforilada i desfosforilada, regulant així la interacció del receptor amb l'adaptador AP-2, que és part d'un complex proteic involucrat en la formació de vesícules endocítiques regulades per clatrina (Vissel, Krupp, Heinemann, & Westbrook, 2001).

La subunitat GluN2B conté tres llocs de fosforilació de tirosina (Y1252, Y1336 i Y1472) que són fosforilats per la quinasa Fyn. La posició Y1472 és el principal lloc de fosforilació, de la subunitat i quan es fosforila produeix la disrupció de la interacció entre el receptor NMDA i el complex endocític AP2-clatrina, estabilitzant el receptor a la superfície post-sinàptica, i inhibint l'endocitosi (B.-S. Chen & Roche, 2007). Curiosament, la posició Y1472 és molt a prop del lloc de fosforilació de la CKII (S1480). Aquests llocs de fosforilació tenen funcions oposades, mentre que la fosforilació a la posició Y1472 estabilitza la localització dels receptors a la membrana plasmàtica, la fosforilació de la posició S1480 la disminueix, a través de l'endocitosi (Lavezzari, McCallum, Lee, & Roche, 2003).

1.2.5 Localització sinàptica i extrasinàptica dels receptors

NMDA

De manera general, trobem els receptors NMDA a les zones post-sinàptiques de les espines dendrítiques, però també els podem trobar localitzats a zones extrasinàptiques. La ruta d'entrada del Ca^{2+} mitjançant receptors NMDA localitzats en zones sinàptiques o en zones extrasinàptiques, farà que s'activin una sèrie de cascades de senyalització o unes altres (Arispe, Rojas, & Pollard, 1993). Per explicar-ho existeixen dos models proposats, el model de localització i el model de composició de subunitats (Cai et al., 2006).

El model de localització postula que l'entrada de Ca^{2+} mitjançant aquells receptors localitzats a la zona extrasinàptica (ja sigui al coll sinàptic, eixos dendrítics o al soma) es relaciona amb l'activació de processos neurotòxics (Giles E Hardingham et al., 2010). Per altra banda, els receptors NMDA localitzats a zones postsinàptiques són normalment els encarregats de modular la plasticitat sinàptica, promovent l'activació de senyals de supervivència. Per tant, no seria l'augment d'entrada de Ca^{2+} l'únic factor determinant per la inducció de senyals neurotòxics sinó la localització per on es produeix l'entrada (G E Hardingham, Fukunaga, & Bading, 2002). L'altre model postula que la composició de subunitats de cada a receptor en determinarà el seu efecte. Per una banda, l'entrada de Ca^{2+} mitjançant receptors que continguin la subunitat GluN2A s'associa amb l'augment en la síntesi de factors involucrats en accions neuroprotectores (G E

Hardingham et al., 2002). Per altra banda, l'entrada de Ca^{2+} mitjançant receptors que contenen la subunitat GluN2B, poden induir diferents respostes segons la seva localització sinàptica o extra-sinàptica (McQuate & Barria, 2020). Els dos models no són excloents l'un de l'altre, ja que al cervell adult els receptors que contenen la subunitat GluN2A es troben majoritàriament a les sinapsis mentre que els receptors que contenen la subunitat GluN2B es localitzen majoritàriament a les zones extrasinàptiques.

L'activitat dels receptors NMDA sinàptics promou l'activació de mecanismes de neuroprotecció que es caracteritzen per tenir una durada més llarga que el temps d'activació del mateix receptor. A més a més, acostumen a comportar canvis sobre l'expressió gènica de diversos gens que participen en processos relacionats amb la millora de la funció mitocondrial, la potenciació de la defensa antioxidant i la supressió de l'activitat caspasa, implicada en processos apoptòtics (Giles E Hardingham et al., 2010). Altrament, existeixen vies inductores de la mort neuronal dependents dels receptors NMDA localitzats a zones extra-sinàptiques. En alguns casos, aquestes vies consisteixen en antagonitzar directament les vies de supervivència activades pels receptors NMDA sinàptics, mentre que en altres casos consisteixen en la iniciació de processos i/o activació de vies independents a les vies activades pels receptors NMDA sinàptics (Arundine & Tymianski, 2004) (**Figura 3**).

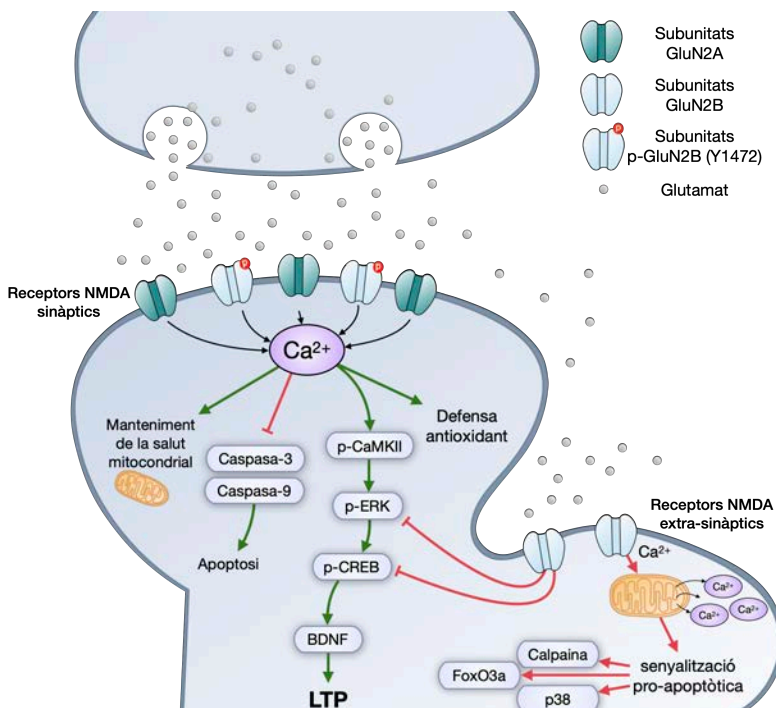


Figura 3. Efectes oposats de l'activació dels receptors NMDA sinàptics i extrasinàptics. (CaMKII: de l'anglès Calcium/calmodulin-dependent protein kinase II; ERK: de l'anglès extracellular signal-regulated kinase; CREB: de l'anglès cAMP response element-binding; BDNF: De l'anglès brain derived neurotrophic factor)

1.3 Envel·liment i deteriorament cognitiu

Al llarg de la vida, l'organisme pateix una sèrie de canvis funcionals que progressen amb l'edat. L'envelliment s'ha definit com la pèrdua progressiva de funcions genèriques acompanyada d'un augment de la mortalitat amb l'avanç de l'edat (Duncan, 2011). Aquest canvi natural associat a l'edat es denomina senescència i es produeix a diferents ritmes segons l'espècie, on existeixen variacions interindividuais i dins dels diferents teixits d'un individu. És un mecanisme irreversible i inevitable, que comporta l'aparició de dèficits cognitius, de la funció emocional i del comportament (Duncan, 2011).

López-Otín i col·laboradors (López-Otín, Blasco, Partridge, Serrano, & Kroemer, 2013) van identificar nou "marcadors de l'envelliment" i els van classificar en marcadors primaris, antagònics i integradors. Dins els marcadors primaris es troben la inestabilitat genòmica, el desgast dels telòmers, les alteracions epigenètiques i la pèrdua de proteostasi. La inestabilitat genòmica i el dany de l'ADN ja sigui causat per trencaments de la cadena simple o cadena doble de l'ADN, per insercions o delecions o per error de bases, es consideren una de les principals causes de l'envelliment i és l'eix central d'una de les teories dominants de l'envelliment (Chow & Herrup, 2015)(López-Otín et al., 2013). El dany a l'ADN no només genera inestabilitat genòmica, sinó que també inicia cascades de senyalització que s'estenen per tota la cèl·lula, per exemple promovent la senescència cel·lular i la inflamació, que en conjunt agreugen el procés neurodegeneratiu. Els telòmers s'escurcen a mesura que les cèl·lules es divideixen i, el deteriorament dels mecanismes que prevenen el seu l'escurçament en l'envelliment condueixen inevitablement a la senescència cel·lular (Kaushik et al., 2021; López-Otín et al., 2013). Finalment, les modificacions epigenètiques tals com la metilació i l'acetilació de l'ADN i de les histones influeixen l'estructura terciària de la cromatina, regulant així la seva activitat i funció en els processos de transcripció i de replicació, entre d'altres (Bradley-Whitman & Lovell, 2013). Així mateix, la pèrdua de la proteostasi es defineix com la pèrdua de l'equilibri entre la síntesi i la degradació de proteïnes. Per exemple, els processos autofàgics durant l'envelliment es veuen alterats, promovent-se així l'acumulació de restes cel·lulars, que dona lloc l'augment de secreció de citocines inflammatòries.

Els marcadors antagònics (disfunció mitocondrial, senescència cel·lular i desregulació de la detecció de nutrients) són respostes compensatòries o antagòniques al dany primari. En etapes inicials, aquestes respostes atenuen el dany, però amb el temps poden tornar-se nocives. Les neurones, com a cèl·lules metabòlicament molt actives presenten una gran demanda d'energia i són especialment sensibles a canvis de la funció mitocondrial. Per exemple, l'envelliment està implicat en l'augment de la secreció d'espècies reactives d'oxigen (ERO) per part de les mitocòndries danyades. Aquestes últimes alteren la biosíntesi de lípids, la senyalització de Ca^{2+} i l'apoptosi cel·lular, tots ells processos implicats en mecanismes neurodegeneratius (Johri & Beal, 2012). Per la seva part, la senescència cel·lular pot considerar-se com una resposta al dany que té com a objectiu mantenir la supervivència de les cèl·lules sanes i eliminar les danyades (James, 1988). Per últim, la desregulació de la detecció de nutrients i l'alteració del metabolisme s'associa de manera freqüent amb la disfunció mitocondrial i processos oxidatius (Babbar & Sheikh, 2013).

Finalment, els marcadors integradors (l'esgotament de les cèl·lules mare i l'alteració de la comunicació intracel·lular) són el resultat del dany acumulat induït pels marcadors primaris i antagònics i, en última instància, són els responsables del deteriorament funcional associat a l'envelliment (López-Otín et al., 2013). Les funcions i la capacitat proliferativa de les cèl·lules mare disminueix al llarg de la vida a causa de tots els processos mencionats anteriorment, per tant, dirigir noves teràpies a la regeneració de les cèl·lules mare envellides podria induir certes millores als processos degeneratius associats a l'edat (Hou et al., 2019; Oh, Lee, & Wagers, 2014). En últim lloc, cal destacar que el sistema immunitari és essencial per al desenvolupament del cervell i del sistema nerviós, però aquest canvia a mesura que s'envelleix i, per tant, pot haver una pèrdua de regulació de les respostes immunitàries que accelerin la neurodegeneració. La inflamació és un mecanisme de protecció que amb l'edat es troba regulat a l'alça, compromentent la supervivència cel·lular. La inflamació crònica, l'activació persistent de la micròglia i l'augment de l'estrès oxidatiu s'han relacionat d'una manera molt robusta amb l'aparició de malalties neurodegeneratives (Amor & Woodroffe, 2014; Currais, 2015).

Durant l'envelliment normal es produeixen una sèrie de canvis mesurables pel que fa a la cognició. Els canvis més importants es troben en les tasques cognitives que exigeixen processar o transformar ràpidament la informació per prendre una decisió, com la memòria de treball i la funció cognitiva (Morrison & Baxter, 2012). El coneixement acumulatiu i les habilitats relacionades amb l'experiència es mantenen fins a una edat avançada (Murman, 2015). De fet, canvis estructurals

i funcionals al cervell correlacionen amb aquests canvis cognitius relacionats amb l'edat, incloent-hi alteracions en l'estructura neuronal sense la presència de mort neuronal, la pèrdua de sinapsis i la disfunció de les xarxes neuronals (Pannese, 2011). Les malalties relacionades amb l'edat acceleren el ritme de la disfunció neuronal, la pèrdua de neurones, causant un deteriorament cognitiu suficientment greu per a afectar a les capacitats funcionals quotidianes, fenomen definit com a demència (Terry et al., 1991).

Tenint en compte, que l'envelliment s'ha descrit com el principal factor de risc en les malalties neurodegeneratives i que l'augment de l'esperança de vida va lligat a l'augment dels trastorns de salut relacionats amb l'edat, és important conèixer els mecanismes primaris de l'envelliment i el seu paper a l'inici i durant la seva progressió per tal de desenvolupar teràpies que permetin afrontar amb èxit els reptes de l'envelliment patològic (Carmona & Michan, 2016; Hou et al., 2019; Rose, 2009).

1.4 La malaltia d'Alzheimer

Alois Alzheimer va descriure per primera vegada la malaltia que portaria el seu nom fa més de cent anys (Alzheimer, Stelzmann, Schnitzlein, & Murtagh, 1995). La malaltia d'Alzheimer (MA) és una malaltia neurodegenerativa progressiva i irreversible que es caracteritza per un deteriorament inicial de la memòria i de l'aprenentatge, acompanyats de deteriorament cognitiu, que en última instància, pot afectar el comportament, la parla, l'orientació visuoespacial i el sistema motor (Aisen et al., 2017). S'estima que més de 47 milions de persones al món es veuen afectades per la demència avui en dia. Segons l'Organització Mundial de la Salut la MA és la principal causa de demència, representant entre el 60 i el 70% dels casos (World Health Organization, 2016). Les altres causes més comunes de demència inclouen la demència vascular, la demència de cossos de Lewy i la malaltia de Parkinson amb demència, i la pressió hidrocefàlica anormal representant cadascuna d'elles entre el 5 i el 10% dels casos; i d'aquestes, la demència vascular i la demència de cossos de Lewy s'associen més sovint amb la patologia mixta, incloent-hi la concurrència de la MA (Barker et al., 2002).

S'espera que aquestes malalties debilitants i devastadores augmentin a mitjans de segle, sent la previsió que més de 131 milions d'individus es vegin afectats l'any 2050 (Barker et al., 2002; 'World Alzheimer Report.', 2016). La prevalença s'estima sobre el 10% per a persones majors de 65 anys i el 40% per a persones majors de 80 anys (Alzheimer's Association, 2019; Matthews et al., 2013; Schrijvers et al., 2012). Els costos tant personals com econòmics fan necessari un

diagnòstic i tractament pre-clínic eficaç per a detenir la progressió de les malalties abans de l'inici simptomàtic.

1.4.1 Etiologia i factors de risc

La MA es pot classificar en funció del moment que es manifesta la malaltia i de si és o no hereditària. Per una banda, la MA d'inici precoç apareix abans dels 65 anys, mentre que la MA d'aparició tardana que representa més del 95% dels casos, es manifesta després dels 65 anys. Per altra banda, la MA familiar mostra una herència mendeliana dominant mentre que la MA esporàdica no mostra un vincle familiar simple. Pràcticament totes les formes de MA d'inici precoç són familiars, podent ser causades per mutacions a gens com el de la proteïna precursora amiloide (APP) i la presenilina (PSEN) 1 o 2. Aquestes formes familiars de la MA són rares, ja que representen menys de l'1% dels casos i es manifesten amb un curs agressiu (Mendez, 2017). La MA familiar pot arribar a presentar-se a partir dels 20 anys, amb una edat mitjana d'aparició als 46,2 anys (Ryman et al., 2014). De forma general totes les MA d'inici tardà són formes de MA esporàdica, encara que s'han identificat factors de risc genètics, destacant entre ells l'al·lel $\epsilon 4$ del gen l'apolipoproteïna E (*APOE*) (Lane, Hardy, & Schott, 2018). Concretament, existeixen tres al·lells: la presència de l'al·lel *APOE* $\epsilon 4$ suposa un augment del 50% de la susceptibilitat genètica a patir la MA, l'*APOE* $\epsilon 2$ s'ha vinculat a una funció protectora, mentre que l'*APOE* $\epsilon 3$ no incideix en la susceptibilitat de patir la MA. A més, s'han identificat altres factors de risc genètics per a la MA d'inici tardà, entre ells es troben els gens codificants pel receptor activador expressat a les cèl·lules mieloides 2 (*TREM2*, de l'anglès *Triggering receptor expressed on myeloid cells 2*), per la proteïna contenidora del domini desintegrina i metaloproteïna 10 (*ADAM10*, de l'anglès *A Disintegrin and metalloproteinase domain-containing protein 10*) i per la fosfolipasa D (*PLD*, de l'anglès *Phospholipase D*). Curiosament, no tots els gens identificats estan relacionats amb proteïnes directament involucrades amb la patofisiologia de la MA, sinó que també s'han identificat gens relacionats amb el metabolisme del colesterol, l'endocitosi o la resposta immunitària (Jansen et al., 2019).

A part dels factors de risc genètics també existeixen els factors de risc ambientals. Estudis epidemiològics coincideixen en demostrar que el baix nivell educacional està relacionat negativament amb l'aparició de la malaltia, així com els traumatismes cranioencefàlics repetits i els factors de risc cardiovasculars (Arundine & Tymianski, 2004; DeRidder et al., 2006; D. H. Lee et al., 2021). Per altra banda, també s'han trobat factors protectors com ara la dieta mediterrània,

l'entrenament cognitiu, l'activitat social i el consum de medicaments antiinflamatoris no esteroïdals (AINEs), ja que la seva administració de manera crònica per altres motius pot ajudar a disminuir els nivells de neuroinflamació característics de la malaltia (Rivers-Auty et al., 2020; Silva et al., 2019).

1.5 Neuropatologia de la malaltia d'Alzheimer

La MA va associada a efectes clínics, factors psicològics i característiques neuropatològiques com la pèrdua de massa cerebral, la pèrdua de cèl·lules neuronals, el dèficit de neurotransmissors, l'aparició de dipòsits del pèptid β -amiloide ($A\beta$) i l'acumulació intracel·lular de la proteïna tau hiperfosforilada (Figura 4).

Atròfia cerebral

Dins dels canvis a escala macroscòpica trobem que els cervells de pacients amb diagnòstic de la MA presenten en la majoria dels casos una atròfia cortical moderada, més marcada a les zones de l'escorça i les estructures del lòbul límbic. L'escorça frontal i temporal solen presentar els solcs ampliats amb atròfia als girs, mentre que l'escorça motora i la somatosensorial no solen estar (Perl, 2010). Com a conseqüència, normalment existeix un engrossiment de les astes frontals i temporals dels ventricles laterals, a més d'observar-se una disminució del pes del cervell. No obstant això, cap d'aquestes característiques macroscòpiques és específica de la MA, i les persones clínicament normals i no afectades per la MA poden presentar també una atròfia cortical moderada (Apostolova et al., 2012; Perl, 2010; Serrano-Pozo, Frosch, Masliah, & Hyman, 2011).

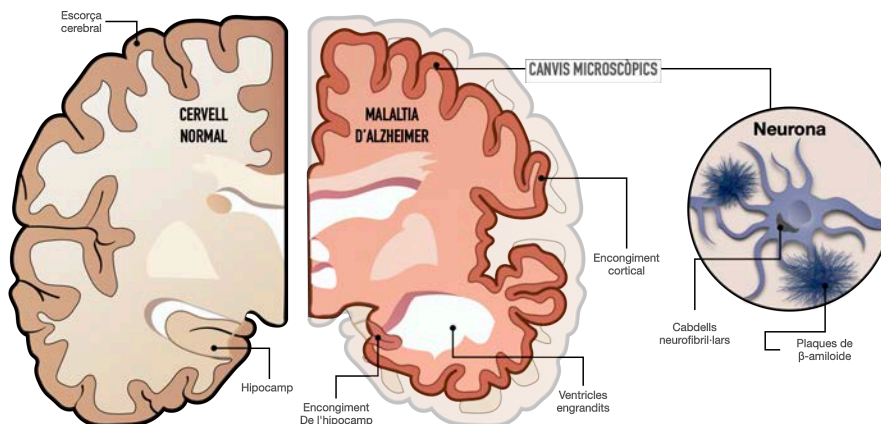


Figura 4. Canvis macroscòpics i microscòpics característics de la MA. Figura adaptada de (Drew, 2018).

Acumulació del pèptid β -amiloide ($A\beta$)

Les plaques senils amiloides estan formades per l'acumulació extracel·lular dels pèptids d' $A\beta$ (concretament els pèptids $A\beta_{40}$ i $A\beta_{42}$). Aquests pèptids es generen a partir de l'escissió, per part de proteases, de la proteïna APP. Fins ara, s'han proposat diverses funcions fisiològiques a aquesta proteïna: El domini extracel·lular de l'APP intervé en l'adhesió cèl·lula-cèl·lula per afavorir les connexions sinàptiques mentre que els homodímers d'APP poden funcionar com a receptors acoblats a proteïnes G (GPCR) regulant la senyalització neuronal i l'alliberació de neurotransmissors a través de l'activació de canals de Ca^{2+} (Ludewig & Korte, 2016; O'Brien & Wong, 2011). Els productes d'escissió d'APP, com les proteïnes precursors amiloides solubles (sAPP) α i β també tenen accions fisiològiques o patològiques. L'sAPP α té un paper important en la plasticitat i supervivència neuronal i s'ha demostrat que és protectora enfront de la toxicitat induïda pel pèptid $A\beta$ (Tackenberg & Nitsch, 2019).

El processament de l'APP depèn principalment de tres enzims proteolítics: l' α -, β - i γ -secretases. Les α -secretases inclouen l'ADAM9, 10 i 17. La proteïna precursora d'amiloide de lloc beta 1 (BACE1, de l'anglès *beta-site amyloid precursor protein cleaving enzyme 1*) és la β -secretasa, mentre que la γ -secretasa està formada per diversos components destacant la PSEN1 i la PSEN2 (Yun-wu Zhang, Thompson, Zhang, & Xu, 2011). Segons els productes d'escissió a partir del processament de l'APP, es poden distingir la via de processament amiloidogènica i no-amiloidogènica (**Figura 5**):

- La via no-amiloidogènica implica l'escissió de l'APP mitjançant l' α -secretasa, que allibera l'ectodomini sAPP α fora de la membrana cel·lular, retenint el fragment APP C-terminal dins de la membrana plasmàtica. Aquest domini que es manté a la membrana pot ser posteriorment escindit per la γ -secretasa alliberant un petit fragment a l'espai extracel·lular, mentre que la resta del domini intracel·lular de l'APP queda retingut al citoplasma (Yun-wu Zhang et al., 2011).
- La via amiloidogènica compren el tall proteolític de l'APP mitjançant la β -secretasa i el complex γ -secretasa. Després de l'escissió per part de la β -secretasa, s'allibera l'ectodomini sAPP β , i a la membrana cel·lular hi queda el fragment carboxi-terminal de l'APP de 99 aminoàcids (beta-CTF o C99). Aquest fragment retingut pot ser escindit posteriorment per la γ -secretasa, generant pèptids amiloides de diferents longituds de cadena ($A\beta_{37}$, $A\beta_{38}$, $A\beta_{39}$, $A\beta_{40}$, $A\beta_{42}$ i $A\beta_{43}$) (De Jonghe et al., 2001; Haass et al., 1995; Lanoiselée et al., 2017). Entre ells, els productes $A\beta_{40}$ i $A\beta_{42}$ són les principals espècies que es

troben al cervell, sent l' $A\beta_{40}$ la més abundant a les plaques amiloides. No obstant això, s'ha demostrat com un augment dels nivells d' $A\beta_{40}$ s'associen amb una disminució en l'acumulació d' $A\beta$ en forma de plaques. De fet, s'ha suggerit que les espècies $A\beta_{40}$ i $A\beta_{42}$ tenen efectes oposats pel que fa a l'acumulació d' $A\beta$: mentre que l' $A\beta_{42}$ en promou l'acumulació, l' $A\beta_{40}$ la inhibeix (Iwatsubo et al., 1994).

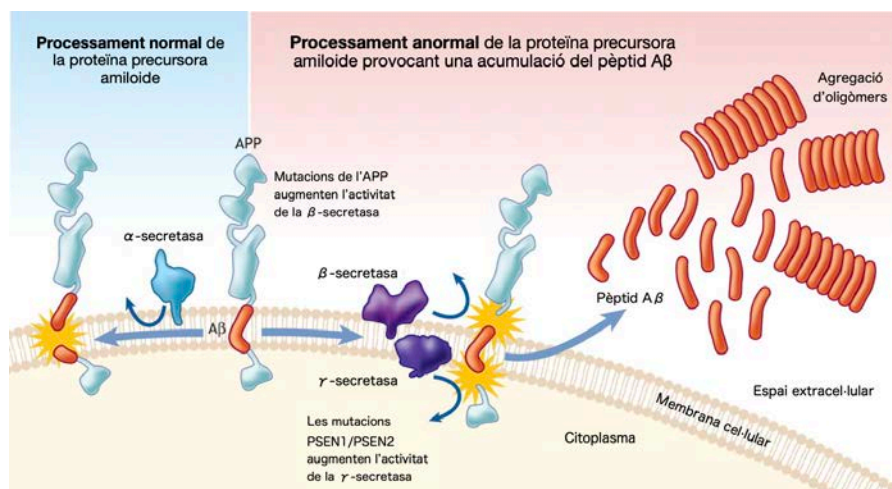


Figura 5. Vies de processament de la proteïna APP. Figura adaptada de (Patterson et al., 2008).

Les vies amiloidogènica i no-amiloidogènica competeixen i, s'ha suggerit que tant la potenciació de la via no-amiloidogènica com la reducció de l'activitat de la via amiloidogènica són estratègies terapèutiques viables per a la reducció de la generació d' $A\beta$ (Guo et al., 2020). Les mutacions PSEN1 són especialment predominants a la MA familiar, on s'han identificat 221 mutacions patogèniques. S'han descrit 32 mutacions a l'APP i 19 mutacions a la PSEN2 $A\beta$ (Lanoiselée et al., 2017). Cal remarcar, que no totes les mutacions a l'APP són patogèniques, de fet, existeix la mutació protectora (A673T) que és capaç de reduir el risc d'aparició de la MA mitjançant l'atenuació de la producció del pèptid (Eggert, Thomas, Kins, & Hermey, 2018).

Durant la patogènesi de la MA, les agregacions del pèptid $A\beta$ es formen a partir de monòmers, generant una varietat d'espècies oligomèriques inestables. Aquestes espècies oligomèriques s'agreguen després per formar protofibril·les curtes, flexibles i irregulars, que finalment s'allarguen en conjunts fibril·lars insolubles orientats perpendicularment a l'eix de la fibra (Walsh & Selkoe, 2007). Encara que, generalment es considera que els monòmers de $A\beta$ en concentracions fisiològiques no són tòxics, múltiples línies d'evidència suggereixen el contrari,

que els oligòmers d'A β són predominantment més neurotòxics que les fibril·les d'A β (U. Sengupta, Nilson, & Kaye, 2016).

Proteïna tau hiperfosforilada

La proteïna tau és un component d'unió a microtúbuls que promou la seva polimerització i estabilitza el citoesquelet de les neurones (Kadavath et al., 2015; Weingarten, Lockwood, Hwo, & Kirschner, 1975). S'expressa en gran part a les neurones i es localitza de manera predominant als axons com un regulador del transport axonal (Dixit, Ross, Goldman, & Holzbaur, 2008). A més, pot patir diferents tipus de modificacions post-traduccionals com la fosforilació, l'acetilació i la glicosilació, regulant la seva funció fisiològica i/o patològica com passa a la MA (Guo et al., 2020). La fosforilació de tau modula la unió als microtúbuls, mentre que la hiperfosforilació acaba promovent la dissociació de tau dels microtúbuls i n'augmenta la seva agregació convertint-se en el principal component dels cabdells neurofibril·lars (Grundke-Iqbal et al., 1986). A més, la fosforilació també modula la seva distribució dins les espines dendrítiques, pel que és important per mantenir la funcionalitat sinàptica (**Figura 6**).

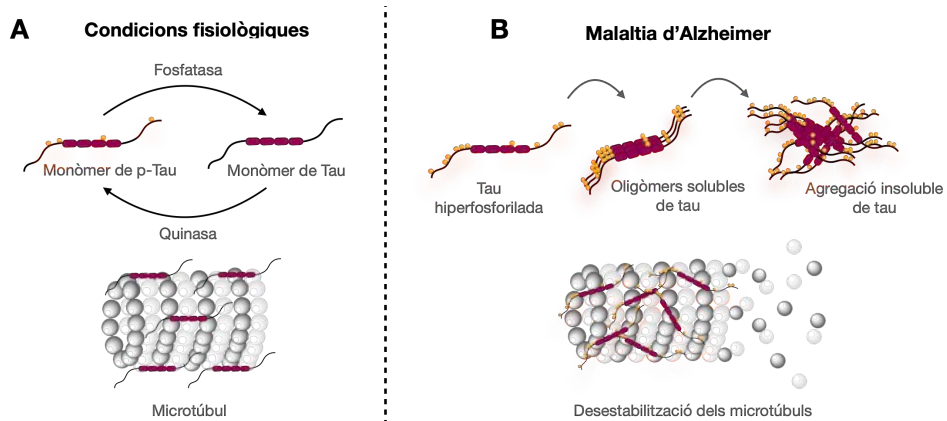


Figura 6. Funció estabilitzadora dels microtúbuls de tau (**A**). Desestabilització dels microtúbuls a causa de la hiperfosforilació i agregació insoluble de tau (**B**).

La proteïna tau hiperfosforilada es troba de manera general als filaments helicoidals aparellats del cervell de pacients amb la MA. La hiperfosforilació és un esdeveniment que succeeix durant les fases inicials de la malaltia, i s'ha correlacionat amb el deteriorament cognitiu. Per aquest motiu, se l'ha proposat com un biomarcador de diagnòstic de la MA (Andorfer et al., 2003; Medeiros, Baglietto-Vargas, & LaFerla, 2011). El procés de fosforilació està regulat per diverses quinases i fosfatases.

Dins la seqüència d'aminoàcids de la proteïna tau, s'han descrit al voltant de 85 llocs de fosforilació (Serina, treonina i tirosina) i cada fosforilació té un impacte diferent en la funció biològica de tau i en el seu paper patogènic (Mair et al., 2016). Un estudi quantitatiu *in vitro* va demostrar que la fosforilació de tau a les posicions S262, T231 i S235 inhibeix la seva unió als microtúbuls al voltant del 35%, 25% i 10%, respectivament (A. Sengupta et al., 1998). A més, s'ha suggerit que les posicions S199/S202/T205, T212, T231/S235, S262/S356, i S422 es troben entre els llocs crítics de fosforilació que converteixen la proteïna tau en una molècula inhibidora que segresta les proteïnes normals associades als microtúbuls (Alonso, Mederlyova, Novak, Grundke-Iqbal, & Iqbal, 2004) i, que per exemple, la fosforilació addicional a les posicions T231, S396 i S422 promou l'autoagregació de tau en filaments (Abraha et al., 2000). A més, de manera destacable, s'ha descrit com la fosforilació de les regions anomenades AT8 (S199/S202/T205) i PHF-1 (S396/S404) sembla que causen un plegament anormal i l'escissió de la proteïna tau, que de manera conjunta permetria l'acumulació de tau (Siddhartha Mondragón-Rodríguez, Basurto-Islas, Binder, & García-Sierra, 2009; Siddhartha Mondragón-Rodríguez et al., 2008).

Les tau quinases es poden distingir en dues categories: les Ser/Thr quinases com la Cdk5, la quinasa sintasa de glucògen 3β (GSK3 β , de l'anglès *glycogen synthase kinase* 3β), la proteïna quinasa activada per mitògens (MAPK, de l'anglès *mitogen-activated protein kinase*), la CaMKII, la PKA i la PKC i les tirosin-quinases que inclouen Fyn, Src, Syc i c-Abl (Tapia-Rojas et al., 2019). La hiperfosforilació de tau pot ser el resultat d'una activitat o expressió desequilibrada de les quinases i les fosfatases, de fet, s'ha observat un augment de l'expressió de GSK3 β i de l'activitat de Cdk5 a regions cerebrals específiques de pacients amb la MA (Pei et al., 1997; Tseng, Zhou, Shen, & Tsai, 2002).

1.6 Mecanismes bioquímics i cel·lulars de la malaltia d'Alzheimer

1.6.1 Excitotoxicitat

L'excitotoxicitat es defineix com un procés tòxic caracteritzat per l'estimulació continuada i sostinguda dels receptors d'aminoàcids excitadors. Aquest procés desencadena una sèrie de fenòmens tòxics que s'han caracteritzat en diferents models experimentals, com ara la sobreactivació de certes vies de senyalització nocives per la supervivència cel·lular, la disrupció de l'homeòstasi dels nivells de Ca^{2+} , i la producció d'ERO que en conjunt promouen l'aparició de l'estrès oxidatiu i finalment la mort cel·lular (X. Dong, Wang, & Qin, 2009).

A part dels efectes aguts, diferents estudis coincideixen demostrant la intervenció de l'excitotoxicitat durant la neurodegeneració d'evolució lenta (Ankarcrona et al., 1995; X. Dong et al., 2009; Rego & Oliveira, 2003; Sattler & Tymianski, 2001). En l'àmbit clínic, aquestes alteracions moleculars correlacionen amb el deteriorament progressiu de la cognició i la memòria i amb l'anatomia patològica del cervell característica dels malalts amb la MA (Wenk, 2006). Per tant, donada la importància dels receptors NMDA sobre la supervivència neuronal, el seu nivell d'activació o senyalització s'ha de mantenir en uns nivells suficients però no excessius per promoure la supervivència neuronal i evitar processos neurodegeneratius (R. Wang & Reddy, 2017).

Els principals factors que afecten la senyalització modulada pels receptors NMDA durant la MA inclouen la disponibilitat de glutamat i la modulació de la funció dels receptors NMDA (Masliah, Alford, DeTeresa, Mallory, & Hansen, 1996). La recaptació de glutamat i el seu sistema de reciclatge determinen la disponibilitat de glutamat i, durant la MA, aquest sistema es veu alterat, produint-se una disminució selectiva del transportador vesicular del glutamat (Kirvell, Esiri, & Francis, 2006; Masliah et al., 1996). De fet, diversos estudis assenyalen que la presència de pèptids d'A β en cultius cel·lulars neuronals provoca un augment de la disponibilitat de glutamat, a causa de l'alteració del sistema d'alliberació / recaptació del neurotransmissor (Fernández-Tomé, Brera, Arévalo, & de Ceballos, 2004). La integritat de la maquinària encarregada de l'alliberació del neurotransmissor, com la sinaptofisina, la syntaxina o la sinaptotagmina, també es veu afectada per la presència del pèptid A β , desencadenant una alliberació ineficient de neurotransmissors i l'alteració de les sinapsis (Jang, In, Choi, & Kim, 2014). Per altra banda, durant la MA, la funcionalitat dels receptors NMDA es

veu alterada per l'acció del pèptid A β : augmentant els senyals sinàptics regulades pels receptors NMDA i interactuant directa o indirectament amb els receptors NMDA a través de proteïnes sinàptiques com la proteïna PSD95, comproment-ne la localització a la superfície cel·lular o induint la sobreexpressió de D-serina (S.-Z. Wu et al., 2004). L'alteració de l'homeòstasi del Ca²⁺ intracel·lular produïda és la responsable d'afavorir l'aparició de processos com l'estrès oxidatiu, l'apoptosi i l'autofàgia (X. Dong et al., 2009).

1.6.1.1 Desregulació dels nivells de Ca²⁺ intracel·lular

S'ha suggerit que els canvis en la senyalització de Ca²⁺ durant la MA són causats per l'acció deletèria dels oligòmers d'A β a les neurones, per la disfunció mitocondrial i pels canvis moleculars patològics relacionats amb l'envelliment (Alzheimer's Association Calcium Hypothesis Workgroup & Khachaturian, 2017), i per això s'ha postulat com un dels factors desencadenants de la disfunció sinàptica i la neurodegeneració (Bezprozvanny, 2009; Tong, Wu, Li, & Cheung, 2018).

A conseqüència de la sobreactivació dels receptors NMDA, es produeix l'activació descontrolada d'una sèrie de proteïnes dependents de Ca²⁺, moltes d'elles relacionades amb la patologia de la MA. Per exemple, la Calcineurina (CaN) activada a través de la Calmodulina (CaM) inhibeix proteïnes fosfatases afavorint la hiperfosforilació de tau (Reese & Tagliatela, 2010), però alhora compromet la supervivència i creixement cel·lular, ja que regula la desfosforilació de proteïnes clau en la patogènesi de la malaltia tals com:

- L'element de resposta a l'AMPC (CREB, de l'anglès *cAMP response element-binding*) a la posició Ser133, que fosforilat afavoreix la transcripció de gens encarregats del manteniment i la formació sinàptica (Bito, Deisseroth, & Tsien, 1996).
- El factor nuclear de les cèl·lules T activades (NFAT, de l'anglès *nuclear factor of activated T-cells*) que es troba de manera normal a zones citoplasmàtiques en la seva forma fosforilada. Però, quan es desfosforila mitjançant l'acció de la CaN, s'indueix la seva translocació al nucli on finalment promou la transcripció de gens involucrats en la producció de citokines i factors proinflamatoris (Abdul et al., 2009).
- La desfosforilació de la proteïna de mort associada a Bcl-2 (BAD, de l'anglès *Bcl-2 associated agonist of cell death*) promou la translocació d'aquesta proteïna a la mitocondria, on forma dímers pro-apoptòtics amb la proteïna Bcl,

desencadenant l'alliberació del citocrom c i, iniciant així processos apoptòtics (Asai et al., 1999; H. G. Wang et al., 1999).

Per altra banda, el deteriorament del mecanisme encarregat de l'eliminació de proteïnes mal plegades i, en part responsable de l'acumulació dels oligòmers d'A β i dels cabdells neurofibril·lars també forma part de les conseqüències derivades de l'alteració dels nivells de Ca²⁺ neuronals (Nixon, 2007). Els mecanismes responsables d'aquestes alteracions a les neurones no es coneixen del tot, però, s'ha suggerit que probablement hi estan implicades proteïnes encarregades del control dels nivells de Ca²⁺, principalment localitzades en orgànuls i compartiments cel·lulars com el reticle endoplasmàtic, lisosomes i mitocondries (Popugaeva & Bezprozvanny, 2013). Com hem mencionat, la hipòtesi del pèptid A β i la hipòtesi de la proteïna tau són considerades com les principals causes de la malaltia, però és cert que la desregulació dels nivells de Ca²⁺ apareix molt abans que la deposició de les plaques i els cabdells (Etcheberrigaray et al., 1998). Per aquest motiu, compostos dirigits a corregir la desregulació del Ca²⁺ fa anys que es postulen com a una estratègia prometedora pel tractament de la MA (Arispe et al., 1993).

1.6.1.2 Estrès oxidatiu i disfunció mitocondrial

Les proteïnes, els lípids, els àcids nucleics i els carbohidrats són generalment sensibles a l'oxidació, afectant directament la seva funció (Cenini, Lloret, & Cascella, 2019). Les ERO es generen de manera natural a les cèl·lules dels organismes vius i són fonamentals per a mantenir l'homeòstasi cel·lular. Participen en processos com la resposta immunitària, la inflamació, la plasticitat sinàptica, la memòria i l'aprenentatge (Kishida & Klann, 2007). Però, la seva producció en excés pot ser nociva, produint modificacions oxidatives a components cel·lulars, principalment sobre les estructures mitocondrials (Rego & Oliveira, 2003).

L'estrès oxidatiu i la disfunció mitocondrial s'han relacionat amb la mort neuronal (Reynolds, Laurie, Lee Mosley, & Gendelman, 2007; Swerdlow, Burns, & Khan, 2010). La mitocondria té un paper fonamental en les funcions cel·lulars que influeixen l'excitabilitat neuronal incloent entre elles la producció d'adenosina trifosfat (ATP), l'oxidació d'àcids grassos, la biosíntesi de neurotransmissors i la regulació de l'homeòstasi del Ca²⁺ (Cenini et al., 2019). No obstant això, és el principal lloc de producció d'ERO (Halliwell, 2007). Durant la MA, s'han observat alteracions en la morfologia, nombre i transport de mitocondries, una menor activitat de la citocrom-oxidasa, deficiències en les proteïnes metabòliques,

canvis en el potencial de la membrana mitocondrial i un augment de l'estrès oxidatiu (Swerdlow et al., 2010).

L'augment de la producció neuronal d'ERO i l'acumulació de dany oxidatiu que es produeix amb l'edat, correlaciona d'una manera estreta amb la progressió de la neurodegeneració (Reynolds et al., 2007). De fet, la producció excessiva d'ERO i l'activitat insuficient de la maquinària antioxidant s'ha associat amb la patogènesi de malalties neurodegeneratives com l'esclerosi lateral amiotròfica, la malaltia de Parkinson, la MA i la malaltia de Huntington (J. Li, O, Li, Jiang, & Ghanbari, 2013). El sistema antioxidant cel·lular és l'encarregat de prevenir el dany als teixits i, està format per enzims antioxidants i altres compostos no enzimàtics amb capacitat de reduir les ERO (Uttara, Singh, Zamboni, & Mahajan, 2009). Aquest sistema s'encarrega de mantenir l'equilibri entre els agents prooxidants i antioxidants, i per tant, de reduir l'estrès oxidatiu (Agostinho, Cunha, & Oliveira, 2010). D'entre els principals enzims antioxidants es troben la superòxid dismutasa (SOD), la catalasa (CAT), la glutatió peroxidasa (GPx) i la glutatió reductasa (GR). La SOD és un dels principals mecanismes protectors enfront l'estrès oxidatiu, sent responsable de la conversió d' O_2^- a H_2O_2 i O_2 . Seguidament, el peròxid d'hidrogen generat és convertit en aigua i O_2 per part de la CAT. Per altra banda, també hem de considerar compostos com el glutatió, les tioredoxines, les vitamines A, E i C i el seleni (Kamat, Rai, Swarnkar, Shukla, & Nath, 2014). Durant la MA, els receptors NMDA en ser responsables de l'entrada massiva de Ca^{2+} , són també responsables d'estimular la generació d'ERO i, per tant, participen en la desregulació de les espècies oxidants i antioxidants, causant danys tant a les mitocondries com a les cèl·lules, especialment a les neurones (Kamat et al., 2014).

1.6.1.3 Mort neuronal i pèrdua sinàptica

Abans de la manifestació clínica de la MA es produeix una disminució de la densitat de població de les neurones, sobretot de l'hipocamp i l'escorça cerebrals, que en etapes més avançades de la malaltia correlaciona amb el grau de manifestació clínica (Gómez-Isla et al., 1997). S'ha demostrat que les proteïnes implicades en el trànsit de vesícules sinàptiques i el reciclatge de neurotransmissors, a més d'elements estructurals de les sinapsis es troben afectats durant la MA (Overk & Masliah, 2014): les espines dendrítiques es desestabilitzen per l'acumulació extracel·lular del pèptid $A\beta$, l'entrada massiva de Ca^{2+} a dins les neurones i l'activació microglial que acaben desencadenant la pèrdua sinàptica (Subramanian, Savage, & Tremblay, 2020).

La mort cel·lular induïda per l'excitotoxicitat s'associa a la mort apoptòtica característica del cervell dels mamífers (Loh, Huang, De Silva, Tan, & Zhu, 2006). Aquesta pèrdua neuronal massiva característica de la MA es troba principalment regulada pels receptors NMDA patològicament activats, i correlaciona de manera molt robusta amb l'aparició de la demència (Sturchio et al., 2021). En condicions no patològiques, l'equilibri entre els efectes proapoptòtics i els antiapoptòtics s'encarrega de mantenir la integritat mitocondrial i, per tant, de evitar la mort cel·lular. Els mediadors clàssics d'aquests processos són proteïnes com la p21, la p38, la MAPK, la quinasa c-Jun-NH₂-terminal, la p53, les caspases 2, 3, 8 i 9, la proteïna X associada a Bcl-2 (Bax, de l'anglès *BCL2 Associated X*) i la cèl·lula-B/linfoma 2 (Bcl-2, de l'anglès *B cell lymphoma 2*) (Friedlander, 2003; Gartel & Tyner, 2002; Tsujimoto, 1998; H. G. Wang et al., 1999; Yue & López, 2020). Com hem mencionat, la mort neuronal pot ser també potenciada per l'estrès oxidatiu (Zheng et al., 2009). En resum, els receptors NMDA són un factor clau en l'apoptosi neuronal que alhora influencia directament o indirectament la funció sinàptica (Kamat et al., 2016).

1.6.1.4 Alteracions en el procés autofàgic

L'autofàgia és un procés d'eliminació de proteïnes de rebuig, agregacions de proteïnes, orgànuls malmesos i de patògens invasors, és per això que es considera l'encarregada del manteniment de l'homeòstasi cel·lular. L'autofàgia és part necessària del desenvolupament i de l'envelliment, tenint un paper clau en el procés neurodegeneratiu (Nikoletopoulou & Tavernarakis, 2018). Donat que les sinapsis són regions amb un recanvi proteic ràpid i amb una alta demanda energètica, la síntesi i degradació coordinada de proteïnes és necessària per a dur a terme les modificacions morfològiques i funcionals durant els processos de plasticitat sinàptica (Nikoletopoulou & Tavernarakis, 2018).

Les primeres evidències que existeixen vinculant alteracions autofàgiques i la MA van descriure l'acumulació de grans quantitats de vesícules subcel·lulars (anomenades vacúols autofàgics) i acumulacions de la proteïna tau agregada a les neurites abans de l'aparició de les plaques d'A β (Suzuki & Terry, 1967). Aquestes acumulacions es van relacionar amb un defecte en el procés proteolític dels autofagolisosomes, que com a conseqüència comportava l'acumulació de l'A β i la proteïna tau pròpies de la MA (Cataldo et al., 2004). La disminució de la taxa d'iniciació de l'autofàgia, l'acumulació anormal d'autofagolisosomes i/o la digestió insuficient dels autofagosomas a través dels lisosomes són senyals d'alteracions del procés autofàgic durant la MA (Barnett & Brewer, 2011).

Durant el procés d'iniciació de l'autofàgia hi juga un paper essencial la proteïna beclina-1, que es troba disminuïda en pacients amb la MA (Liang et al., 1999; Pickford et al., 2008; Russo et al., 2011). La disminució dels nivells d'aquesta proteïna, s'ha suggerit que és deguda a l'activitat de la proteïna calpaïna-1 (Russo et al., 2011). La beclina-1 juntament amb la proteïna d'unió a ubiquitina p62, també anomenada p62 i la proteïna quinasa activadora de l'autofàgia unc-51 (ULK1, de l'anglès *Unc-51 like autophagy activating kinase*) (Pankiv et al., 2007; Zachari & Ganley, 2017) són les encarregades de la iniciació del procés autofàgic i de la formació dels vacúols autofàgics, que són transportats de manera retrògrada dels axons fins al soma. Durant la MA aquests dos passos de l'autofàgia es troben alterats degut a l'acumulació intracel·lular de la proteïna tau (Lim et al., 2001). Així mateix, diferents estudis han assenyalat que defectes dels lisosomes autofàgics poden comportar la formació dels oligòmers de tau i la seva agregació, mentre que un correcte funcionament de l'autofàgia o tractaments dirigits a millorar-lo, evitarien la formació de les agregacions d'aquest marcador neuropatològic de la MA (Hamano et al., 2008).

1.6.2 Neuroinflamació

La neuroinflamació es defineix com una resposta inflamatòria dins del SNC que pot ser causada per diverses agressions patològiques, com infeccions, traumatismes, isquèmia i toxines (Calsolaro & Edison, 2016). Aquest procés es caracteritza per la producció de citocines proinflamatòries com les interleucines IL-1 β , la IL-6, la IL-18 i el factor de necrosis tumoral (TNF, de l'anglès *tumor necrosis factor*), les quimiocines com el lligand de quimiocines amb motiu C-C 1 (CCL1, de l'anglès *Chemokine (C-C motif) ligand 1*), el CCL5 i el lligand de quimiocines amb motiu C-X-C 1 (CXCL1, de l'anglès *chemokine (C-X-C motif) ligand 1*), prostaglandines, òxid nítric (NO), i ERO per part de les cèl·lules immunitàries que, al cervell, són principalment la micròglia i els astròcits (Leng & Edison, 2021).

L'alliberació de molècules proinflamatòries pot contribuir a la disfunció sinàptica, la mort neuronal i la inhibició de la neurogènesi (Lyman, Lloyd, Ji, Vizcaychipi, & Ma, 2014). L'IL-1 β afavoreix la pèrdua sinàptica en augmentar la producció de prostaglandina E2, que condueix a l'alliberació presinàptica de glutamat i a l'activació dels receptors NMDA (A. Mishra, Kim, Shin, & Thayer, 2012). A més, el sistema del complement pot activar-se, augmentant la funció fagocítica de la micròglia, fet que podria alterar la funció normal de les sinapsis (Hong et al., 2016). Per altra banda, les citocines antiinflamatòries, com les interleucines IL-1,

la IL-4, la IL-10 i la IL-11, coexisteixen amb les molècules proinflamatòries durant els processos inflamatoris i formen part d'un mecanisme per evitar la inflamació excessiva (Calsolaro & Edison, 2016). Tanmateix, durant les malalties neurodegeneratives com la MA, la neuroinflamació tendeix a ser un procés crònic que no es resol per si sol i es considera un motor vital de la malaltia (Calsolaro & Edison, 2016).

Astròcits

Els astròcits són cèl·lules gials especialitzades del SNC (Sofroniew & Vinters, 2010). Dins les seves funcions trobem la regulació del flux sanguini cerebral, el manteniment de l'homeòstasi dels fluids i els neurotransmissors, la inducció de la formació de sinapsis i el subministrament metabòlic i neurotròfic de les neurones (Attwell et al., 2010; Pekny et al., 2016). Aquestes cèl·lules també formen canals perivasculars al SNC coneguts com sistema glinfàtic, que s'encarrega d'eliminar productes potencialment tòxics, com l'acumulació del pèptid A β i els cúmuls de proteïna tau hiperfosforilada (Jessen, Munk, Lundgaard, & Nedergaard, 2015). A més, responen a agressions patològiques mitjançant la gliosi reactiva (Pekny, Wilhelmsson, & Pekna, 2014). Els anomenats astròcits reactius són aquells astròcits activats que presenten processos hipertròfics i una regulació a l'alça de la proteïna àcida fibril·lar glial (GFAP, de l'anglès *Glial fibrillar acidic protein*) (Hol & Pekny, 2015). S'ha proposat també, l'existència de dos fenotips propis dels astròcits, el fenotip A1 i l'A2. El fenotip A1, a través de la via del potenciador del factor nuclear κ de cadena lleugera de les cèl·lules B activades (NF- κ B, de l'anglès *nuclear factor kappa-light-chain-enhancer of activated B cells*), promouria la secreció de factors proinflamatoris mentre que el fenotip A2 promouria la neuroprotecció mitjançant la secreció de factors neurotròfics (Liddelow & Barres, 2017).

Durant les fases inicials de la MA, els astròcits intenten recuperar l'homeòstasi als teixits cerebrals danyats. De fet, dins d'astròcits localitzats al voltant de plaques d'A β s'han observat grànuls que contenen el pèptid A β , el que suggereix un intent per part dels astròcits d'eliminar els dipòsits d'amiloide (Jo et al., 2014; Wyss-Coray et al., 2003). Tot i el paper beneficiós que tenen els astròcits intentant eliminar les plaques d'amiloide, també s'han descrit grans quantitats d'astròcits "tòxics" amb fenotip A1 al teixit cerebral *post mortem* de pacients amb la MA, el que implicaria un paper perjudicial per part d'aquestes cèl·lules (J. Chang et al., 2013). Per exemple, aquests astròcits reactius són capaços d'alliberar un excés de glutamat promovent així un entorn excitotòxic (Jo et al., 2014), fins i tot s'ha proposat que podrien afavorir la formació de les primeres plaques d'A β (Heneka

et al., 2005). Cal destacar que, els astròcits treballen de manera conjunta amb la micròglia i intervenen de manera rellevant en alguns mecanismes tòxics per part d'aquesta durant estadis avançats de la malaltia (Liddelow et al., 2017).

Micròglia

La micròglia són cèl·lules immunitàries de llinatge mieloide que es troben al SNC. Existeix una gran semblança entre la morfologia i marcadors de la superfície cel·lular de la micròglia activada i els fagòcits mononuclears (Harry, 2013). L'activitat microglial és present al SNC durant el desenvolupament, la maduració i la senescència, formant part de la regulació de l'apoptosi neuronal, el manteniment de la plasticitat sinàptica i la resposta immunitària (M. W. Salter & Stevens, 2017). S'ha observat que la micròglia ramificada és capaç de detectar danys en el SNC, activant una resposta microglial al lloc lesionat (Nimmerjahn, Kirchhoff, & Helmchen, 2005). No obstant això, en processos d'envelliment la micròglia presenta deficiències funcionals i és propensa a mantenir-se en un estat d'activació sostinguda, que podria contribuir a la patogènesi de malalties neurodegeneratives (Norden & Godbout, 2013).

Estudis transcriptòmics en models de ratolí de la MA han demostrat que la progressió de la malaltia és paral·lela a una transició gradual de la micròglia d'un estat homeostàtic a un estat patològic, associat a la malaltia (Keren-Shaul et al., 2017). Aquesta transició s'associa a la regulació a la baixa de gens homeostàtics i a la regulació a l'alça de gens associats a la MA com l'*APOE* i el gen *TREM2* (Keren-Shaul et al., 2017). El receptor *TREM2* al cervell s'expressa exclusivament a la micròglia, predominantment a l'hipocamp (Jay, von Saucken, & Landreth, 2017). Dins les seves funcions es troba el control de la proliferació de la micròglia, la inducció de la fagocitosis i la secreció de citocines, a més de regular el metabolisme i la supervivència microglial. Per tant, canvis funcionals de *TREM2* tenen un impacte tant en els efectes beneficiosos com perjudicials de la micròglia. De manera interessant s'ha descrit que la regulació gènica a l'alça de *TREM2* durant la MA forma part de mecanismes compensatoris per part de la micròglia com a resposta a l'acumulació d'A β i a l'augment de la demanda fagocítica (Jiang et al., 2014) i, s'ha proposat per aquest motiu, que la seva sobreexpressió en etapes primerenques de la malaltia és positiva, però quan es troba en un estat avançat l'efecte de *TREM2* és insuficient (Y. J. Tan et al., 2017).

Com en el cas dels astròcits s'han proposat dos fenotips propis de l'activació microglial, el fenotip M1 o fenotip "proinflamatori" i el fenotip M2 o fenotip "antiinflamatori" (Jurga, Paleczna, & Kuter, 2020; Q. Wang et al., 2021).

L'activació de la micròglia amb el fenotip M1 es considera un mecanisme agressiu que condueix a la citotoxicitat i a la inflamació immediata, mitjançant la qual s'alliberen citocines i quimiocines proinflamatòries com el TNF- α , la IL-6 o la IL-1 β . A més, un tret característic de la micròglia amb el fenotip M1 és la seva habilitat per produir ERO i espècies reactives de nitrogen (MacMicking, Xie, & Nathan, 1997). Un dels enzims clau associats a aquest procés és l'òxid nítric sintasa induïble (iNOS, de l'anglès *inducible nitric oxide synthase*), que utilitza l'arginina per la producció d'òxid nítric (Bagasra et al., 1995). No obstant això, encara que sembla senzill identificar les cèl·lules M1 basant-se en aquestes característiques, la seva classificació *in vivo* és més difícil degut a la naturalesa plàstica de la micròglia (L. Zhang, Zhang, & You, 2018). El fenotip M2 de la micròglia es distingeix per l'expressió de mediadors o receptors amb la capacitat de reparar o protegir el teixit cerebral reduint els processos inflamatoris (Varin & Gordon, 2009). Un dels marcadors més ben caracteritzats és l'enzim arginasa 1 (ARG1), que s'encarrega de convertir l'arginina en poliamines, prolines i ornitines, que contribueixen a la regeneració de les ferides (Munder, 2009). Curiosament, a l'utilitzar l'arginina que és el mateix substrat que utilitza l'iNOS, l'ARG1 hi competeix per contrarestar els seus efectes i regular a la baixa la producció d'òxid nítric (Corraliza, Soler, Eichmann, & Modolell, 1995). Un altre marcador utilitzat per identificar les cèl·lules M2 és la proteïna de tipus quitinasa 3, també anomenada YM1, que és una lectina d'unió a heparina que s'encarrega de prevenir la degradació dels components de la matriu extracel·lular (N. C. Chang et al., 2001).

Estudis d'imatge han demostrat la influència de la neuroinflamació en la correlació negativa entre l'activació microglial i la integritat estructural o l'activitat funcional del cervell durant la MA (Fan et al., 2015; Femminella et al., 2016). Curiosament, des d'una perspectiva clínica, existeix una relació inversa entre el rendiment cognitiu i l'activació microglial, però no amb la carrega d'amiloide cerebral (Leng & Edison, 2021).

De manera global, podem dir que la inflamació regulada tant pels astròcits com per la micròglia exerceix funcions tant beneficioses com perjudicials. La resposta dels astròcits i la micròglia a les agressions del SNC està regulada de manera dependent de l'alliberació de mediadors inflamatoris específics que dicten el seu fenotip funcional. Per exemple, mentre que l'activació glial prevé la progressió de la MA facilitant l'eliminació de les acumulacions d'A β al cervell (L'Episcopo et al., 2016; Y.-Y. Liu & Bian, 2010; Segura-Aguilar, 2015), una sobreactivació glial sostinguda augmenta la progressió de les patologies relacionades amb la MA

(Nagele, D'Andrea, Lee, Venkataraman, & Wang, 2003; Solito & Sastre, 2012; Wyss-Coray & Rogers, 2012) (**Figura 7**).

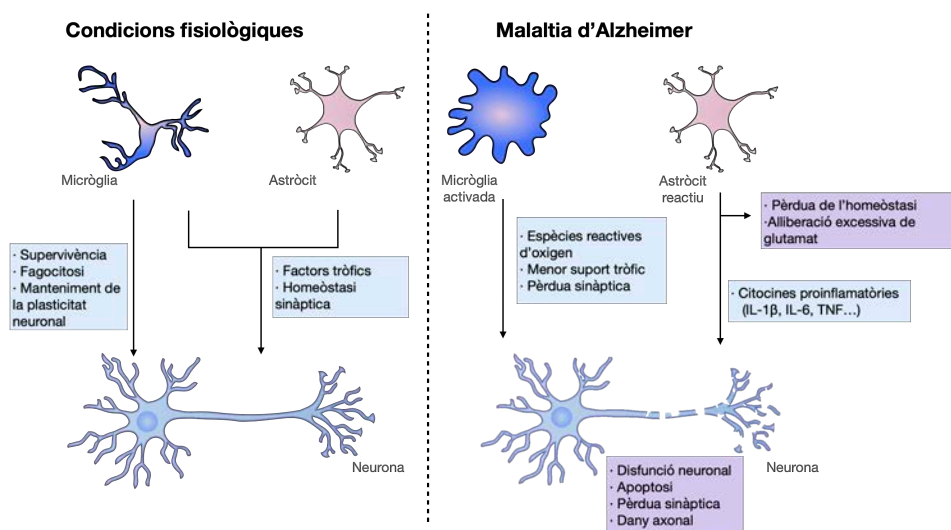


Figura 7. Funció de les cèl·lules inflammatòries en condicions fisiològiques i durant la MA.

1.7 Tractaments actuals per la malaltia d'Alzheimer

Actualment, el tractament de la MA és una necessitat mèdica no coberta, ja que només existeixen dos tipus de fàrmacs aprovats a Europa per l'Agència Europea de Medicaments (EMA, de l'anglès *European Medicine Agency*), i tres aprovats als Estats Units per l'FDA (de l'anglès *Food and Drug Administration*) que no són suficientment eficaços pel control de la malaltia. Entre ells es troben, tres inhibidors de l'acetilcolinesterasa, un antagonista del receptor NMDA, la combinació d'un inhibidor d'acetilcolinesterases i l'antagonista del receptor NMDA, i finalment el controvertit anticòs monoclonal dirigit al pèptid A β , l'aducamumab.

1.7.1 Inhibidors d'acetilcolinesterases

Durant la MA es redueixen els nivells de cèl·lules productores d'acetilcolina, causant una reducció de la transmissió colinèrgica al cervell i els tres inhibidors d'acetilcolinesterasa comercialitzats, actuen bloquejant les acetilcolinesterases i les butirilcolinesterases provocant l'augment dels nivells d'acetilcolina (**Figura 8**). Aquesta proposta terapèutica és capaç de millorar temporalment la funció cognitiva i neuronal a pacients diagnosticats amb la MA (Sharma, 2019).

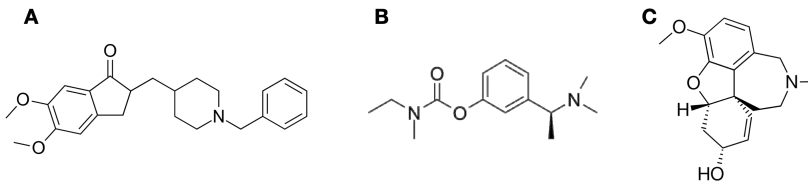


Figura 8. Estructura química dels inhibidors de l'acetilcolinesterasa. Donepezil (A), Rivastigmina (B) i Galantamina (C)

El donepezil és un derivat de la indanonebenzilpiperidina i es considera el principal fàrmac per la MA (Cacabelos, 2007). S'uneix a l'acetilcolinesterasa de forma reversible i inhibeix la hidròlisi de l'acetilcolina a les sinapsis. S'utilitza per tractar símptomes com el deteriorament cognitiu i les alteracions del comportament, però no és capaç de modificar la progressió de la malaltia (Cacabelos, 2007; Dooley & Lamb, 2000). La rivastigmina és un inhibidor pseudo-reversible i s'utilitza en estadis lleus i moderats de la MA. A més, és capaç de millorar funcions cognitives i activitats de la vida quotidiana però, la seva administració de forma oral s'associa a efectes adversos severes (Annicchiarico, Federici, Pettenati, & Caltagirone, 2007; Müller, 2007). La galantamina es considera un fàrmac de primera línia per a tots els casos lleus i moderats de la MA. El tractament amb aquest compost millora els símptomes conductuals, les activitats de la vida diària i la funció cognitiva d'una manera eficient i tolerable (Prvulovic, Hampel, & Pantel, 2010).

1.7.2 Antagonistes dels receptors NMDA

Molts dels trastorns neuropsiquiàtrics i neurodegeneratius estan relacionats amb defectes sinàptics i la disfunció dels receptors NMDA. No obstant això, fins la dècada dels 2000, els assajos clínics amb antagonistes competitius dels receptors NMDA, van fracassar degut als efectes secundaris causats per l'alta afinitat d'unió i la interacció amb els receptors d'altres neurotransmissors que acabaven provocant al·lucinacions, agitació, l'augment de la pressió arterial i anestèsia (Kornhuber & Weller, 1997; Sonkusare, Kaul, & Ramarao, 2005). Entre els antagonistes d'alta afinitat trobem la dizocilpina o MK-801, la fenciclidina i la ketamina (Doraiswamy, 2003). En canvi, els antagonistes no competitius tenen un millor perfil de seguretat i alguns d'ells són el que trobem en el mercat. Entre els antagonistes no competitius trobem els antagonistes de baixa afinitat o afinitat moderada com la memantina, el dextrometorfà i l'amantadina.

Memantina

La memantina (1-amino-3,5-dimetiladamantà) és un derivat aminoalquilciclohexà (**Figura 9**). Els aminoadamantans són compostos farmacològics atípics amb una estructura tricíclica no plana i tridimensional (Rogawski & Wenk, 2003) que representen una classe de fàrmacs que no produeixen els efectes secundaris característics d'altres antagonistes dels receptors NMDA, i que ja s'han utilitzat clínicament com agents antivirals, i antiparkinsonians (Chris G Parsons et al., 1999). Aquest fàrmac travessa la barrera hematoencefàlica de manera ràpida, i al cap de 30 minuts de la infusió intravenosa, es pot detectar al líquid cefaloraquídi (Kornhuber, Bormann, Hübers, Rusche, & Riederer, 1991) a més de presentar uns límits de seguretat i tolerabilitat adequats, mostrant un bon marge terapèutic.

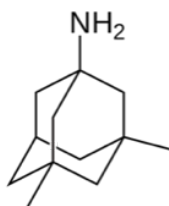


Figura 9. Estructura química de la memantina

La memantina es va sintetitzar per primer cop l'any 1960 i fins al 1980 no es va descobrir la seva funció d'antagonista dels receptor NMDA, sent comercialitzada al 2003 pel tractament de la MA (Reisberg et al., 2003). A avui en dia continua sent l'únic antagonista del receptor NMDA disponible al mercat. A causa de la seva baixa afinitat, bloqueja el receptor NMDA però és desplaçada ràpidament, i d'aquesta manera evita el bloqueig prolongat del receptor, evitant efectes secundaris greus (Doraiswamy, 2003). És capaç de blocar el canal de manera dependent de voltatge de manera que només ho fa quan aquest s'activa patològicament sota una concentració excessiva i constant de glutamat, com és el cas de la MA (C. G. Parsons, Danysz, & Quack, 1999). Durant els processos d'aprenentatge i memòria (alliberació transitòria elevada de glutamat) la memantina, en ser una antagonista no competitiu, abandona el receptor NMDA durant un breu període de temps, permetent l'activació d'aquest pel glutamat, produint un senyal que pot ser reconeguda i processada. Així, la memantina bloqueja la neurotoxicitat del glutamat sense interferir en les seves accions fisiològiques (Johnson & Kotermanski, 2006)(**Figura 10**).

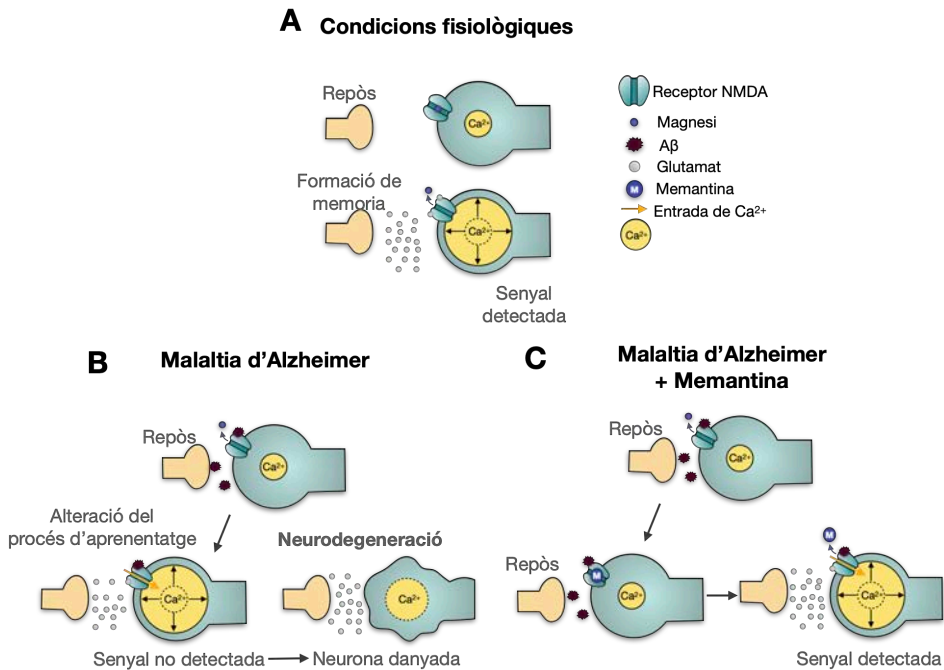


Figura 10. Mecanisme d'acció de la memantina. Procés d'entrada de Ca^{2+} a través dels receptors NMDA en condicions fisiològiques (A); Procés d'entrada de Ca^{2+} a través dels receptors NMDA durant la MA, on el Mg^{2+} deixa de bloquejar el canal degut a l'acció dels oligòmers d'A β (B); Mecanisme d'acció dependent de voltatge de la memantina, ocupant el lloc del Mg^{2+} , regulant la senyalització de Ca^{2+} (C). Figura adaptada de (Danysz & Parsons, 2012).

Adicionalment, la memantina presenta propietats antioxidants (Lupp, Kerst, & Karge, 2003) i és capaç d'augmentar els nivells del factor neurotròfic derivat del cervell (BDNF, de l'anglès *brain derived neurotrophic factor*), neurotrofina encarregada de millorar la transmissió sinàptica de l'hipocamp i d'induir l'expressió del seu receptor, el receptor de tropomiosina quinasa B (*TrkB*, de l'anglès *Tropomyosin receptor kinase B*) (Marvanová et al., 2001). D'aquesta manera, la regulació per part de la memantina d'aquests dos factors involucrats en mecanismes de neuroprotecció expliquen la seva millor efectivitat en la cognició (Marvanová et al., 2001). Adicionalment, un dels avantatges de la memantina respecte a altres antagonistes del receptor NMDA és la seva acció preferencial sobre les subunitats GluN2B respecte a les altres subunitats. Aquesta acció selectiva la situa com un tractament que és capaç d'evitar la senyalització tòxica induïda per aquestes subunitats (Xia, Chen, Zhang, & Lipton, 2010).

Els estudis clínics mostren que la memantina millora la cognició, els símptomes neuropsiquiàtrics i conductuals i l'evolució clínica en conjunt (Gauthier, Loft, & Cummings, 2008; Winblad & Poritis, 1999). Aquest efecte és clínicament

significatiu en els estadis moderats i greus de la MA (McShane et al., 2019; Tariot et al., 2004; Wilkinson & Andersen, 2007). El tractament combinat amb memantina i donepezil, també aprovat pels òrgans responsables, a pacients amb una MA de moderada a greu, millora significativament la cognició, les activitats quotidianes i el comportament (Tariot et al., 2004). Tanmateix, tot i els avantatges que aporta el tractament amb la memantina per als pacients amb la MA, tant el tractament amb memantina com la combinació de donepezil i memantina no són capaçs d'aturar la progressió ni de curar la malaltia.

S'han formulat diverses hipòtesis per explicar els efectes clínics de la memantina. Entre elles trobem la hipòtesi que assenyala que la seva efectivitat ve donada per capacitat d'inhibir de manera preferent els receptors NMDA extra-sinàptics (Giles E Hardingham et al., 2010). D'altres hipòtesis suggereixen que aquest efecte beneficiós sobre la malaltia pot estar associat a la inhibició preferent dels receptors NMDA que pateixen una dessensibilització dependent de Ca^{2+} després d'una exposició elevada al Ca^{2+} a nivell intracel·lular (Glasgow, Povysheva, Azofeifa, & Johnson, 2017).

1.7.3 Anticossos monoclonals

Durant anys s'han dut a terme la cerca de teràpies dirigides a disminuir l'acumulació de plaques d'A β i així poder modificar el curs de la MA. Dins de les estratègies dutes a terme, destaca la immunoteràpia usant anticossos monoclonals dirigits als pèptids d'A β (Panza, Lozupone, Logroscino, & Imbimbo, 2019).

El 7 de Juny del 2021 l'FDA va aprovar als Estats Units l'anticòs monoclonal aducanumab per al tractament de la MA (FDA, 2021), tot i que la seva comercialització es va qüestionar donat que els assaig clínics desenvolupats no van obtenir resultats clars d'eficàcia (Tagliavini, Tiraboschi, & Federico, 2021). Actualment, l'aducanumab està subjecte a un nou estudi post-comercialització per a demostrar la seva eficàcia clínica (Tagliavini et al., 2021)(Mullard, 2021). Pel que fa a Europa, l'EMA va comunicar el mes de Desembre del 2021 que no n'autoritza l'arribada al mercat europeu, basant-se en els resultats ambigus de la fase III d'assajos clínics, i afirmant que l'evidència científica no demostra de manera suficient que aquesta teràpia sigui efectiva per al tractament d'adults en fases inicials de la MA (EMA, 2021).

1.7.4 Recerca de nous tractaments

Durant l'última dècada s'han dut a terme molt pocs assaigs clínics sobre fàrmacs per la MA i tot ells amb resultats negatius, tot i que molts d'ells s'han centrat en els diferents mecanismes moleculars proposats de ser els causants de la MA, com per exemple la modulació del processament de la via de formació d'A β o de tau, la neuroinflamació o l'estrès oxidatiu (J. Cummings, Lee, Zhong, Fonseca, & Taghva, 2021). Per altra banda, cal assenyalar que existeixen diversos factors de risc modificables de la MA com ara els hàbits cardiovasculars, o l'estil de vida que poden ajudar a prevenir la malaltia sense la necessitat d'una intervenció farmacològica. De fet, existeixen estudis que afirmen que l'activitat física pot millorar la salut del cervell i reduir la possibilitat d'aparició de la MA, tot promovent mecanismes com la plasticitat sinàptica, la neurogènesi i reduint la neuroinflamació. A més, la dieta mediterrània, l'activitat intel·lectual i alt nivells d'educació (Reserva cognitiva) poden reduir la progressió de la malaltia (D. H. Lee et al., 2021; Scarmeas et al., 2009).

Cal tenir en compte però, que tots els mecanismes alterats durant la MA mencionats poden, i de fet, se solapen entre ells (J. Cummings et al., 2021). Per tant, la naturalesa complexa de la fisiopatologia de la MA i la manca de biomarcadors són els principals obstacles per a que el desenvolupament de nous fàrmacs pel tractament de la MA hagi progressat en paral·lel amb els esforços en recerca dedicats en les darreres dècades. No sols això, sinó que l'alta taxa de fracàs de molts fàrmacs en fases clíniques avançades fa que el procés de descobriment *de novo* sigui un procés molt car i amb una alta probabilitat de fracàs i per tant de descoratament de les grans companyies farmacèutiques (J. Cummings & Fox, 2017; L.-K. Huang, Chao, & Hu, 2020). Com a alternativa, el desenvolupament de nous fàrmacs basats en fàrmacs tradicionals representa una eina interessant a causa de la disminució de costos en comparació amb l'assaig de nous compostos dirigits a noves dianes. De fet, avui en dia existeixen diferents compostos que actuen sobre els receptors NMDA que s'han postulat com a candidats a ser utilitzats pel tractament de la MA:

- El compost JCC-02, N-(3,5-dimetiladamantan-1-il)-N'-(3-clorofenil) urea és un inhibidor del receptor NMDA, que és capaç de travessar la barrera hematoencefàlica i de millorar la funció cognitiva i la memòria (T. Yang et al., 2019).
- El compost DT-010 és un component extret de les plantes xines *Salvia miltiorrhiza* Bge i *Ligusticum chuanxiong* Hort que en assajos *in vitro* presenta

un efecte protector enfront l'excitotoxicitat, mitjançant el bloqueig del receptor NMDA (S. Hu et al., 2018).

- El compost rhynchophyllina extret de la planta xinesa *Uncaria rhynchophylla* va mostrar un efecte beneficiós sobre la funció cognitiva espacial en rates inhibint la sobre activació dels receptors NMDA extrasinàptics (Y. Yang et al., 2018).
- El compost AVP-78 que actua com a agonista del receptor σ -1 i alhora com a antagonista del receptor NMDA. Actualment es troba a la fase III d'assajos clínic per al tractament de l'agitació en pacients amb la MA (Garay & Grossberg, 2017).
- El compost MN-08 on s'ha incorporat el grup nitrat a la molècula de la memantina ha demostrat un efecte preventiu i terapèutic en models animals de la MA, pel que s'ha proposat com a compost candidat a ser avaluat en assajos clínics (L. Wu et al., 2021).

Així doncs, l'estratègia d'utilitzar un grup farmacològic eficaç per a la MA, com els antagonistes del receptor NMDA per a optimitzar-los quant a eficàcia, potència i seguretat, cobra especial rellevància. I, tenint en compte que la memantina és ben tolerada pels pacients amb la MA i la seva eficàcia clínica és limitada, s'han desenvolupat nous antagonistes del receptor NMDA, anàlegs de la memantina amb propietats farmacològiques similars, amb l'objectiu que presentin activitats addicionals a aquesta, per tal de millorar l'efectivitat terapèutica. En aquesta tesi doctoral caracteritzem farmacològicament dos d'aquests compostos, l'RL-208 i l'UB-ALT-EV.

1.7.4.1 RL-208

Leiva i col·laboradors van dissenyar, sintetitzar i caracteritzar noves amines policíclics com anàlegs de la memantina amb un perfil farmacològic millorat, entre ells el compost RL-208 (**Figura 11**). Es va determinar que les amines carbocíclics mostren afinitat pels receptors NMDA i que els grups metil de la memantina són crítics per a obtenir una potència òptima sobre els receptors NMDA (Leiva et al., 2018). Després d'avaluar el bloqueig en l'entrada de Ca^{2+} induïda per NMDA en cultius de cèl·lules granulars de rata i la capacitat funcional de bloqueig dels receptors NMDA per electrofisiologia, es va concloure que l'RL-208 presentava una dependència de voltatge i una potència comparable a la de la memantina i per tal se'l va seleccionar per la seva avaluació en models *in vivo* de la MA, esporàdica i familiar.

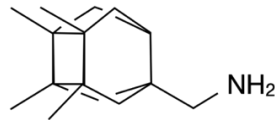


Figura 11. RL-208; (3,4,8,9-Tetrametiltetracido[4.4.0.0^{3,9}.0^{4,8}]dec-1-il)metilamina hidroclozur

1.7.4.2 UB-ALT-EV

Valverde i col·laboradors van dissenyar i sintetitzar nous anàlegs de la memantina basats en un nou anell benzopolicíclic. Es va avaluar el seu efecte sobre l'augment dels nivells de Ca²⁺ intracel·lular en cultius neuronals granulars de cerebel de rata induïts per NMDA. Els resultats van mostrar que el compost UB-ALT-EV presentava un valor d'IC₅₀ inferior al de l'amantadina a més d'exhibir una activitat similar a la de la memantina (**Figura 12**). La caracterització electrofisiològica i farmacodinàmica del compost UB-ALT-EV duta a terme pel grup de Química Terapèutica dirigida pel Dr. Vázquez està integrada en aquesta tesi (Leiva et al., 2018; Turcu et al., 2022).

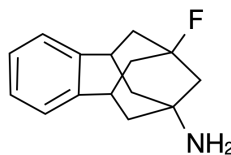


Figura 12. UB-ALT-EV; 9-Fluoro-5,6,8,9,10,11-hexahidro-7H-5,9:7,11-dimetanobenzo[9]annulè-7-amina hidroclozur

1.8 Models animals per l'estudi de la malaltia d'Alzheimer

Els models animals són essencials per a l'estudi de la patogènesis de la MA a més de ser necessaris pels assajos pre-clínic de nous tractaments. S'han desenvolupat diversos models per a l'estudi de la MA, incloent-hi el ratolí, la rata, el *Caenorhabditis elegans* (*C.elegans*), la *D. melanogaster* i les cèl·lules mare pluripotents humanes (Devi, Alldred, Ginsberg, & Ohno, 2010; Dosanjh, Brown, Rao, Link, & Luo, 2010; Link, 2005; Nagakura, Shitaka, Yarimizu, & Matsuoka, 2013; Takeda, 1997).

Pel fet que es desconeix l'etiologia de la MA, a la recerca s'utilitzen una gran varietat de models animals basats en la introducció de mutacions genètiques que provoquen canvis sobre la patologia amiloide i la patologia de tau, amb la

justificació que els esdeveniments posteriors al desencadenament inicial dels símptomes de la malaltia són iguals independentment de la causa inicial. Per aquest motiu, existeix controvèrsia sobre la validesa de confiar en models transgènics, sobretot degut a l'alta taxa de fracàs dels assajos clínics en teràpies per la MA (J. L. Cummings, Morstorf, & Zhong, 2014; Schneider et al., 2014). Tanmateix, els models genètics han estat de gran ajuda per a determinar mecanismes de la progressió de la MA i per a poder avaluar possibles teràpies. Cap dels models mostra tots els aspectes del gran espectre de la malaltia però cadascun d'ells permet analitzar en profunditat certs trets característics d'aquesta. Per aquest motiu, cal conèixer bé la neuropatologia de cada model per poder fer una correcta correlació amb la MA humana i poder interpretar els resultats amb una major precisió i així augmentar la probabilitat de traslladar els resultats dels estudis a humans (Drummond & Wisniewski, 2017).

1.8.1 El model *Caenorhabditis elegans*

El *C.elegans* és un nematode no parasitari de vida lliure que va ser proposat com a model per primera vegada per Sidney Brenner l'any 1963 (Brenner, 1974). És un cuc rodó, petit (1mm de longitud) i transparent, que té un cicle de vida curt de 3 dies des de l'ou fins que és adult. En condicions de creixement adequades, com a hermafrodites els cucs s'autofecunden, generant un gran nombre de cries. Aquest model animal es desenvolupa a través de quatre estadis larvaris (L1-L4), fins a arribar a adults amb un total de 959 cèl·lules somàtiques (Sulston & Horvitz, 1977). El cicle de vida dura entre 2 i 3 setmanes, el que facilita l'estudi de la seva biologia. La seqüenciació del seu genoma va demostrar que aproximadament el 38% dels seus gens tenen un ortòleg humà, entre ells es troben els gens que codifiquen per l'APP i tau (Shaye & Greenwald, 2011). Per aquests motius, el model *C. elegans* presenta molts avantatges com a model *in vivo* per a l'estudi de la MA i altres malalties neurodegeneratives. A més, és idoni per al cribratge de fàrmacs, ja que l'administració és conceptualment senzilla (s'afegeixen concentracions variables de fàrmacs candidats al medi de cultiu on després s'afegiran els cucs), podent-se generar corbes concentració-resposta i, per tant, determinar les efectives i les tòxiques (Lublin et al., 2011). De manera general a més, la toxicitat de compostos assajada en aquest model, coincideix amb la toxicitat observada en mamífers i per tant els compostos potencialment tòxics es poden eliminar en fases inicials del procés de desenvolupament de fàrmacs (Burns et al., 2010; Hunt, 2017). Tanmateix, encara que és poc probable que els models invertebrats puguin reproduir realment la patologia de la MA completament, s'han

desenvolupat múltiples soques transgèniques de *C.elegans* per modelar aspectes de la MA, com ara la neurotoxicitat del pèptid A β .

La soca CL2006 és la soca millor caracteritzada per l'estudi de la MA. Conté el transgen unc-54::A β^{1-42} que promou l'expressió del pèptid A β humà a les cèl·lules musculars i és el responsable del fenotip de la soca que presenta una paràlisi progressiva i una mort prematura potenciada per l'augment de temperatura. Aquesta soca és útil per avaluar els efectes de compostos seleccionats sobre la toxicitat induïda pel pèptid A β (Link, 1995). Per altra banda, la soca CL2355 és una soca que expressa de manera constitutiva i dependent de la temperatura, el pèptid A β_{1-42} a les cèl·lules neuronals (Bargmann, Hartwig, & Horvitz, 1993). És un altre model de *C. elegans* que permet i facilita el cribratge de fàrmacs a gran escala mitjançant l'anàlisi de l'índex quimiotàctic. La quimiotaxi és un comportament innat del model *C. elegans* regulat per les neurones sensorials i motores (Hobert & Bülow, 2003) mitjançant el qual els cucs poden detectar substàncies volàtils, que poden ser tant atraients com repel·lents (Bargmann et al., 1993). La soca CL2355 mostra una reducció de l'índex quimiotàctic després de l'augment de la temperatura en comparació amb la seva soca control, la CL2122, el que suggereix que l'expressió de l'A β neuronal és la responsable de l'alteració quimiotàctica. Aquest fenomen a més, s'ha associat amb el deteriorament de mecanismes d'aprenentatge propis de *C. elegans* (Dosanjh et al., 2010; Y. Wu et al., 2006).

1.8.2 Models de ratolí

La gran majoria de models animals utilitzats a la investigació de la MA són ratolins transgènics. La proteïna APP del ratolí salvatge presenta una homologia de seqüència del 97% amb l'APP humana. Tanmateix, les diferències de seqüència entre els ratolins i els humans inclouen aminoàcids localitzats dins de la seqüència del pèptid consistent (Tanzi et al., 1987; Xu et al., 2015). Aquestes diferències impedeixen la formació de les plaques amiloides als ratolins salvatge i, per tant, l'expressió de la proteïna APP humana és necessària per a la formació de plaques amiloides al cervell dels ratolins. Els primers models transgènics que es van generar expressaven la proteïna APP humana i, encara que tenien una major producció del pèptid amiloide, no mostraven una neuropatologia de la MA (Puzzo, Gulisano, Palmeri, & Arancio, 2015). Curiosament, l'expressió conjunta de la proteïna APP humana amb la inserció de mutacions associades a la MA familiar sí que donava lloc a una patologia amb presència de plaques amiloides. Per aquest motiu, s'han generat soques transgèniques en les quals el fenotip depèn de la

mutació que inclouen, el promotor utilitzat i de la soca base del ratolí (Drummond & Wisniewski, 2017). Cal destacar, però, que no només existeixen models de ratolí per la MA amb mutacions a la proteïna APP, sinó que també s'han generat soques transgèniques que indueixen la formació de cabdells neurofibril·lars (Andorfer et al., 2003). Aquestes mutacions que s'introdueixen a la proteïna tau per tal que els ratolins generin els cabdells neurofibril·lars no són característiques de la MA humana, per tant el posterior efecte que es produeixi mitjançant la interacció de la proteïna tau transgènica i el pèptid A β no serà característica de la MA, representant una limitació per l'estudi de la malaltia (Drummond & Wisniewski, 2017).

1.8.2.1 Ratolins 5XFAD

Oakley i col·laboradors van generar una soca de ratolins transgènics que co-expressen 5 mutacions de la MA familiar sota el promotor Thy1 (Oakley et al., 2006): el transgèn APP(695) que conté les mutacions *Swedish* (K670N i M671L), la mutació *Florida* (I716V) i la mutació *London* (V717I), i el transgèn PSEN1 que conté les mutacions de la MA familiar M146L i L286V. És una línia congènita de la soca C57BL/6J. Aquesta soca mostra una aparició de les plaques amiloides més ràpida que altres models, per la que se l'anomena una soca transgènica de la MA d'inici precoç. L'A β intraneuronal comença a acumular-se a partir del mes i mig de vida dels ratolins, i la deposició de plaques amiloides comença a partir dels dos mesos de vida. En primer lloc, les plaques apareixen en capes profundes de l'escorça cerebral i en els ratolins envellits les plaques ocupen gran part de l'escorça i l'hipocamp. A més s'ha descrit que els nivells d'A β ₄₂ al cap de sis mesos són més elevats que en altres soques transgèniques de la MA. Curiosament, els ratolins 5XFAD presenten els marcadors d'inflamació elevats i s'ha descrit que l'astrogliosi i la microgliosi comencen també al cap dels dos mesos de vida, havent-se correlacionat la seva aparició amb els nivells d'A β ₄₂. A més, diversos gens involucrats en l'activació microglial, que també estan alterats en pacients amb la MA, es troben alterats en aquests ratolins, el que dona consistència a la premissa que aquesta soca és un model vàlid per a estudiar la patogènesi de la MA i per a l'estudi de noves teràpies (Landel et al., 2014). A totes aquestes característiques s'hi suma la reducció dependent de l'edat de marcadors sinàptics com ara els nivells de sinaptofisina i de PSD95, a més de presentar una pèrdua selectiva de neurones noradrenèrgiques i colinèrgiques (Devi & Ohno, 2010; Kalinin et al., 2012). No obstant això, l'única característica neuropatològica d'aquest model que el distingeix de la MA humana és que no presenta la formació de cabdells neurofibril·lars (Oakley et al., 2006). Pel que fa a les característiques

cognitives aquesta soca a partir dels 4 mesos comença a presentar alteracions en la memòria espacial i la memòria de treball (Oakley et al., 2006) i a partir dels 9 mesos d'edat presenta una alteració del comportament social i alteracions motores (Flanigan, Xue, Kishan Rao, Dhanushkodi, & McDonald, 2014; O'Leary, Mantolino, Stover, & Brown, 2018).

1.8.2.2 Ratolins *SAMP8*

D'entre tots els models de ratolí de la MA, el model de ratolí propens a la senescència accelerada (*SAMP*, de l'anglès *Senescence Accelerated Mouse-Prone*) és àmpliament utilitzat i reconegut. Els ratolins *SAMP* i els ratolins resistents a la senescència (*SAMR*, de l'anglès *Senescence Accelerated Mouse Resistant*) van ser seleccionats pel professor Toshio Takeda, a través de la seva generació mitjançant encreuaments endogàmics i selecció fenotípica a partir de la soca *AKR/J* (Takeda et al., 1981). Es van generar un total de 12 línies de soques endogàmiques, les soques d'envelliment accelerat *SAMP1*, *SAMP2*, *SAMP3*, *SAMP6*, *SAMP7*, *SAMP8*, *SAMP9*, *SAMP10*, *SAMP11* amb una esperança de vida mitjana de 16 mesos i les soques resistents a l'envelliment *SAMR1*, *SAMR4* i *SAMR5* amb una esperança de vida de 10 mesos aproximadament (Akiguchi et al., 2017). Cada soca *SAMP* presenta fenotips de la malaltia específics associats a l'edat, que són similars als símptomes de l'envelliment en els humans, com ara l'amiloïdosi senil (*SAMP1*), l'osteoporosi senil (*SAMP6*) i alteracions de l'aprenentatge i la memòria dependent de l'edat (*SAMP8*) (Iino et al., 2007). El model de ratolí *SAMP8* es caracteritza per presentar un deteriorament de l'aprenentatge i la memòria, però també un envelliment de la pell, ansietat i pèrdua d'audició vida (Okouchi, Sakanoi, & Tsuduki, 2019).

Els ratolins *SAMP8* són un model animal d'envelliment espontani i accelerat. De manera característica desenvolupen dèficits d'aprenentatge i memòria al voltant dels 8 mesos d'edat, a més de presentar desordres emocionals com ara un comportament de tipus ansiós i depressiu i presenten una reducció de la seva esperança de vida (Miyamoto, Kiyota, Nishiyama, & Nagaoka, 1992). Els cervells d'aquests ratolins mostren una patologia associada a l'edat principalment a l'hipocamp, la hiperfosforilació de la proteïna tau, l'augment del dany oxidatiu (Butterfield & Poon, 2005), neuroinflamació, l'augment dels nivells de glutamat (Kitamura, Zhao, Ohnuki, Takei, & Nomura, 1992) i l'alteració de la funcionalitat dels receptors NMDA (Strong, Reddy, & Morley, 2003), una reducció de la densitat sinàptica neuronal i un augment de l'astrogliosi (Morley, Armbricht, Farr, & Kumar, 2012), i curiosament, produeixen en excés un component similar

al pèptid A β , encara que, les plaques amiloides apareixen de manera tardana, sobre els 20 mesos d'edat, fet que suggereix que les plaques, *per se* no estan implicades en la patogènesi de les alteracions de la memòria d'aquest model animal (Morley et al., 2000). Tots aquests trets característics del model el fan idoni per l'estudi de la MA i altres trastorns cognitius (Akiguchi et al., 2017; B. Liu, Liu, & Shi, 2020).

Capítol 2

Objectius

Actualment, l'augment de l'esperança de vida incrementa la incidència de malalties relacionades amb l'envelliment, incloent el deteriorament cognitiu i la MA, promovent que siguin un dels problemes més importants relacionats amb la salut. La MA és el tipus de demència majoritària al món i la seva prevenció i tractament és un dels majors reptes per la nostra societat, ja que no existeix cap fàrmac capaç de prevenir ni reduir la progressió de malaltia. La memantina, l'únic antagonista no competitiu del receptor NMDA utilitzat pel tractament de la MA, és capaç de millorar temporalment la funció cognitiva i les alteracions del comportament pròpies dels pacients amb la MA. Malauradament, encara que representa una de les millors opcions terapèutiques, la seva eficàcia està limitada perquè no és capaç de frenar la progressió de la malaltia. Com a conseqüència d'aquest fet, s'han sintetitzat nous antagonistes del receptors NMDA, anàlegs de la memantina, amb l'objectiu de que presentin activitats addicionals a aquesta per tal de millorar l'eficàcia terapèutica d'aquest grup farmacològic.

Per aquest motiu, l'objectiu principal d'aquesta tesi doctoral és l'estudi farmacològic de nous antagonistes del receptor NMDA (**RL-208** i **UB-ALT-EV**) en models *in vivo* de la MA. Concretament, ens hem centrat en avaluar l'efecte sobre el comportament i el deteriorament cognitiu, així com mecanismes involucrats en els processos neurodegeneratius que apareixen durant la progressió de la MA.

Per a assolir aquest objectiu, s'han establert diversos objectius específics:

1. Avaluar l'efecte neuroprotector del tractament crònic per via oral amb RL-208 en ratolins mascle SAMR1 i SAMP8 de 6 mesos d'edat.

- Determinar l'efecte del tractament amb RL-208 sobre la memòria de reconeixement, la memòria espacial i la conducta social dels ratolins.
- Identificar els canvis induïts pel tractament sobre marcadors d'activació apoptòtica i d'estrès oxidatiu.
- Investigar l'efecte del compost RL-208 sobre la síntesi i senyalització de factors tròfics implicats en la supervivència cel·lular.
- Avaluar l'efecte neuroprotector del tractament amb RL-208 a través de l'estudi de marcadors d'estabilitat sinàptica.

2. Avaluar l'efecte neuroprotector del tractament crònic per via oral amb UB-ALT-EV en models animals de MA, utilitzant un tractament amb memantina com a tractament de referència i identificar quins mecanismes subjacents podrien participar en aquest procés.

- Estudiar l'efecte neuroprotector de l'UB-ALT-EV en models transgènics de *C. elegans* per la MA, que presenten alteracions del comportament induïdes per l'expressió muscular i neuronal del pèptid A β .
- Analitzar l'efecte d'un tractament crònic per via oral amb UB-ALT-EV en ratolins femella 5XFAD de 6 mesos d'edat.
 - Determinar l'efecte del compost UB-ALT-EV sobre el deteriorament cognitiu i de la memòria.
 - Identificar l'efecte del compost UB-ALT-EV sobre els principals marcadors neuropatològics de la MA.
 - Investigar l'efecte del compost UB-ALT-EV sobre processos inductors de la neurodegeneració, mitjançant l'avaluació de marcadors de localització dels receptors NMDA, d'activació apoptòtica, del procés autofàgic.
 - Avaluar el paper del compost UB-EV-ALT i la memantina sobre la neuroinflamació, avaluant l'activació astrocítica i microglial.
 - Analitzar canvis en l'expressió gènica de gens associats a l'estrès oxidatiu després del tractament amb UB-EV-ALT.

Capítol 3

Mètodes i Resultats

3.1 Article 1

A novel NMDA receptor antagonist protects against cognitive decline presented by senescent mice

Companys-Aleman J.¹, Turcu A. L.², Bellver-Sanchis A.¹, Loza M. I.³, Brea J. M.³, Canudas A. M.¹, Leiva R.², Vázquez S.², Pallàs M.¹, Griñán-Ferré C.¹
Pharmaceutics, 2020;12(3),284.

doi: <https://doi.org/10.3390/pharmaceutics12030284>

JCR 2020 IF: 6,321

Afiliacions:

¹ Departament de Farmacologia, Toxicologia i Química Terapèutica. Facultat de Farmàcia i Ciències de l'Alimentació. Institut de Neurociències, Universitat de Barcelona (NeuroUB). Av. Joan XXIII 27-31, 08028 Barcelona, Espanya.

² Laboratori de Química Farmacèutica (Unitat Associada al CSIC), Departament de Farmacologia, Toxicologia i Química Terapèutica, Facultat de Farmàcia i Ciències de l'Alimentació, i Institut de Biomedicina (IBUB), Universitat de Barcelona, Av. Joan XXIII, 27-31, 08028 Barcelona, Espanya.

³ Innopharma screening platform. Biofarma research group. Centro de Investigación en Medicina Molecular y Enfermedades Crónicas (CIMUS). Universidad de Santiago de Compostela, Espanya.

RESUM

La memantina és un antagonista del receptor NMDA que s'utilitza per al tractament de la MA. Aquest fàrmac mostra una efecte consistent a nivell preclínic però la seva eficàcia a nivell clínic és limitada com a conseqüència de la seva incapacitat de frenar la progressió de la malaltia. Per tant, la síntesi i caracterització farmacològica de nous antagonistes del receptor NMDA és considera d'interès per a la cerca de noves teràpies més efectives per la MA.





En aquest estudi, es va caracteritzar l'efecte farmacològic *in vivo* d'un tractament crònic per via oral a una dosi baixa (5mg/Kg) del compost RL-208, un antagonista del receptor NMDA, estructuralment similar a la memantina. Per l'estudi es van emprar ratolins mascle de sis mesos d'edat d'una soca fenotípicament seleccionada pel seu envelliment accelerat, la soca SAMP8, que es considera un model de la MA d'aparició esporàdica. Els ratolins SAMR1 es van utilitzar com a soca control, degut a la seva resistència a la senescència.

Les millores observades després del tractament sobre la memòria de treball i memòria espacial, conjuntament amb la millora de la conducta social observada en els animals tractats va anar acompanyada de canvis positius a escala molecular. L'augment de la fosforilació (Y1472) de la subunitat GluN2B dels receptors NMDA va indicar de manera indirecta la inhibició de vies neurotòxiques. Aquest índex va ser posteriorment confirmat per la reducció dels nivells de marcadors proapoptòtics, com la calpaina-1, la caspasa-3, l'escissió de l' α -spectrina i de Bcl-2. L'RL-208 a més va afavorir la disminució en l'expressió de molècules prooxidants així com l'augment de marcadors antioxidants. Per altra banda, l'augment en l'expressió gènica de neurotrofines (*Bdnf*, *Tgf* i *Vgf*), la millora de senyalització de la via BDNF/TrkB, a més de l'augment dels nivells de proteïnes sinàptiques (SNAP25, Synaptophysin i PSD95) demostrava que el tractament amb RL-208 presentava efectes neuroprotectors. Finalment, es va demostrar com l'RL-208 era capaç de disminuir els nivells d'hiperfosforilació de la proteïna tau, un marcador neuropatològic de la MA.

En resum, les millores conductuals i de memòria, a més dels canvis moleculars induïts pel tractament amb RL-208 indiquen l'efecte neuroprotector d'aquest nou antagonista i el proposen com un bon candidat pel tractament de la MA.

Article

A Novel NMDA Receptor Antagonist Protects against Cognitive Decline Presented by Senescent Mice

Júlia Companys-Alemaný ¹, Andreea L. Turcu ², Aina Bellver-Sanchis ¹, Maria I Loza ³, José M. Brea ³, Anna M Canudas ¹, Rosana Leiva ², Santiago Vázquez ², Mercè Pallàs ^{1,*} and Christian Griñán-Ferré ¹

- ¹ Pharmacology Section, Department of Pharmacology, Toxicology and Therapeutic Chemistry, Faculty of Pharmacy and Food Sciences, Institute of Neuroscience, University of Barcelona (NeuroUB), Av. Joan XXIII 27-31, 08028 Barcelona, Spain; juliacompanyasalemany@gmail.com (J.C.-A.); abellver@gmail.com (A.B.-S.); canudas@ub.edu (A.M.C.); christian.grinan@ub.edu (C.G.-F.)
 - ² Laboratori de Química Farmacèutica (Unitat Associada al CSIC), Department de Farmacologia, Toxicologia i Química Terapèutica, Facultat de Farmàcia i Ciències de l'Alimentació, and Institute of Biomedicine (IBUB), Universitat de Barcelona, Av. Joan XXIII, 27-31, 08028 Barcelona, Spain; aturcu@ub.edu (A.L.T.); rosana.leiva58@gmail.com (R.L.); svazquez@ub.edu (S.V.)
 - ³ Innopharma Screening Platform, Biofarma Research Group, Centro de Investigación en Medicina Molecular y Enfermedades Crónicas (CIMUS), Universidad de Santiago de Compostela, 15701 Santiago de Compostela, Spain; Mabel.loza@usc.es (M.I.L.); pepo.brea@usc.es (J.M.B.)
- * Correspondence: pallas@ub.edu

Received: 20 February 2020; Accepted: 17 March 2020; Published: 22 March 2020



Abstract: Alzheimer's disease (AD) is the leading cause of dementia. Non-competitive N-Methyl-D-aspartate (NMDA) receptor antagonist memantine improved cognition and molecular alterations after preclinical treatment. Nevertheless, clinical results are discouraging. In vivo efficacy of the RL-208, a new NMDA receptor blocker described recently, with favourable pharmacokinetic properties was evaluated in Senescence accelerated mice prone 8 (SAMP8), a mice model of late-onset AD (LOAD). Oral administration of RL-208 improved cognitive performance assessed by using the three chamber test (TCT), novel object recognition test (NORT), and object location test (OLT). Consistent with behavioural results, RL-208 treated-mice groups significantly changed NMDAR2B phosphorylation state levels but not NMDAR2A. Calpain-1 and Caspase-3 activity was reduced, whereas B-cell lymphoma-2 (BCL-2) levels increased, indicating reduced apoptosis in RL-208 treated SAMP8. Superoxide Dismutase 1 (SOD1) and Glutathione Peroxidase 1 (GPX1), as well as a reduction of hydrogen peroxide (H₂O₂), was also determined in RL-208 mice. RL-208 treatment induced an increase in mature brain-derived neurotrophic factor (mBDNF), prevented Tropomyosin-related kinase B full-length (TrkB-FL) cleavage, increased protein levels of Synaptophysin (SYN) and Postsynaptic density protein 95 (PSD95). In whole, these results point out to an improvement in synaptic plasticity. Remarkably, RL-208 also decreased the protein levels of Cyclin-Dependent Kinase 5 (CDK5), as well as p25/p35 ratio, indicating a reduction in kinase activity of CDK5/p25 complex. Consequently, lower levels of hyperphosphorylated Tau (p-Tau) were found. In sum, these results demonstrate the neuroprotectant role of RL-208 through NMDAR blockade.

Keywords: NMDAR antagonist; cognitive decline; neurodegeneration; aging; Alzheimer's disease; oxidative stress; BDNF; apoptosis

1. Introduction

The prevalence of behavioural abnormalities associated with age-related cognitive decline is growing in older people [1]. Age is the most important risk factor for cognitive impairment and

dementia because of natural changes like neuronal death or functional impairments [2]. Alzheimer's disease (AD) is the most common type of dementia, affecting around 50 million people worldwide in 2018 [3]. A three-fold increase is estimated for the number of cases of AD to 131.5 million by 2050 [4,5]. The disease involves the degeneration of some areas of the brain, mainly the hippocampus, which results in behavioural changes, memory loss, and a decline in cognition functions [6]. Nevertheless, the causes of AD remain unknown, and no preventive or curative treatments are available.

The neuropathological hallmarks comprise the accumulation and deposition of β -amyloid ($A\beta$) in the senile plaques (SNPs). Likewise, the hyperphosphorylation of Tau protein is implicated in neurofibrillary tangles increase (NFTs) [7]. There are other important pathological processes under AD development. On one hand, oxidative stress (OS) [8], neuroinflammation [9], apoptosis [10], and synaptic abnormalities [11] play an essential role in the etiology of AD. On the other hand, there is accumulating evidence that several neurotransmitter pathways, such as acetylcholine, dopamine, glutamate, and serotonin [12] are involved in the pathological alterations of AD [13,14]. Indeed, glutamate-mediated toxicity is also one of the main processes responsible for memory impairment in AD.

Glutamate is the primary excitatory neurotransmitter in the central nervous system (CNS), and it plays a critical role in cognitive functions [15]. N-Methyl-D-aspartate receptor (NMDAR) is an important subtype of ionotropic glutamate receptors, essential for the normal function of the CNS [16]. Under normal conditions, extracellular Mg^{2+} that allows Ca^{2+} to move into the cell for the following physiological functions gates NMDAR. Hence, glutamatergic neurotransmission through NMDAR is critical for neuroplasticity [14], neuronal survival [17], and learning and memory formation [18]. However, excessive levels of glutamate lead to the overactivation of NMDAR and allow a higher amount of Ca^{2+} influx into the nerve cell, NMDAR overactivation being a feature present in several brain disorders [19]. This excessive activity causes excitotoxicity and promotes neuronal loss, OS production [20], neuroinflammation and increases p-Tau [21]. Indeed, several studies have demonstrated the association between changes in the NMDAR levels in the cerebral cortex and hippocampus, and cognitive deficits, including anxiety and fear behaviour [22]. In sum, a potential implication for NMDAR in different aspects of the cognitive decline occurred in AD [21].

Because of the importance of NMDAR, several uncompetitive antagonists have been tested both in animal studies and in clinical trials [23]. However, most of the compounds tested have failed due to reduced tolerance and efficacy [24,25]. One possibility for this high rate of attrition was because these compounds blocked the physiological activity of glutamate-mediated by NMDAR activation [26], producing unacceptable side effects, such as psychosis and nausea, among others [27].

Memantine is an uncompetitive and well-tolerated NMDAR antagonist, which has been used to treat moderate to severe AD [28]. However, memantine possesses limited clinical efficacy [29]. Considering this, new moderate-affinity NMDAR antagonists with similar but distinct pharmacological properties are of interest. Recently, we have developed a novel polycyclic amine, RL-208, a voltage-dependent, moderate-affinity, uncompetitive NMDAR blocker characterized pharmacologically and electrophysiologically through in vitro approaches [30].

In the current study, we aimed to have the in vivo proof of concept determining the beneficial effect of RL-208 treatment in behavioural abnormalities and cognitive decline in a mouse model of aging and AD, the senescence-accelerated mouse prone 8 (SAMP8). Several molecular pathways related to NMDAR activation, apoptosis, OS neurotrophic support, and tau pathology characteristic for SAMP8 were also studied.

2. Materials and Methods

2.1. Reagents

RL-208, (3,4,8,9-tetramethyltetracyclo [4.4.0.0^{3,9}.0^{4,8}]dec-1-yl)methylamine hydrochloride was synthesized as previously described [30].

2.2. Pharmacological Characterization of RL-208

2.2.1. Microsomal Stability in Human, Rat and Mice Microsomes

The human, rat, and mice microsomes employed were purchased from Tebu-Xenotech. The compound was incubated at 37 °C with the microsomes in a 50 mM phosphate buffer (pH = 7.4) containing 30 mM MgCl₂, 10 mM NADP, 100 mM glucose-6-phosphate and 20 U/mL glucose-6-phosphate-dehydrogenase. Samples (75 µL) were taken from each well at 0, 10, 20, 40, and 60 min and transferred to a plate containing 4 °C 75 µL acetonitrile. Then, 30 µL of 0.5% formic acid in water was added to improve the chromatographic conditions. The plate was centrifuged (46,000× g, 30 min) and supernatants were taken and analyzed in a UPLC-MS/MS (Xevo-TQD, Waters) by employing a BEH C18 column and an isocratic gradient of 0.1% formic acid in water: 0.1% formic acid acetonitrile (60:40) for 5 minutes and a flow of 0.25 mL/min. The metabolic stability of the compounds was calculated from the logarithm of remaining compounds at each time point studied.

2.2.2. Cytochrome Inhibition

To screen the inhibition potential of the compounds, recombinant human cytochrome P450 enzymes (CYP1A2, CYP2C9, CYP2C19, CYP2D6, and CYP3A4) and probe substrates were used with the fluorescent detection method.

Incubations were conducted in 200-µL volume 96 well microtiter plates (COSTAR 3915). Addition of cofactor-buffer mixture (KH₂PO₄ buffer, 1.3 mM NADP⁺, 3.3 mM MgCl₂, 3.3 mM Glucose-6-phosphate and 0.4 U/mL Glucose-6-phosphate Dehydrogenase), supersomes control, standard inhibitors (Furaflyline, Tranylpyromine, Ketoconazole, Sulfaphenazole, and Quinidine; from Sigma Aldrich), and test compounds to plates were carried out using a liquid handling station (Zephyr Caliper). The plate was then pre-incubated at 37 °C for 5 min, and the reaction initiated by the addition of pre-warmed enzyme/substrate (E/S) mix. The E/S mix contained buffer (KH₂PO₄), c-DNA-expressed P450 in insect cell microsomes, substrate (3-cyano-7-ethoxycoumarin (CEC) for CYP1A2 and CYP2C19, 7-methoxy-4-(trifluoromethyl)coumarin (7-MFC) for CYP2C9, 3-[2-(N,N-diethyl-N-methylammonium)ethyl]-7-methoxy-4-methylcoumarin (AMMC) for CYP2D6, 7-benzoyloxytrifluoromethyl coumarin (7-BFC) and Dibenzylfluorescein (DBF) for CYP3A4) to give the final assay concentrations in a reaction volume of 200 µL. Reactions were terminated after different incubation times, depending on each cytochrome, by the addition of STOP solution (ACN/TrisHCl 0.5M 80:20 and NaOH 2N for CYP3A4 (DBF) and ACN/TrisHCl 0.5M 80:20 for the other cytochromes).

Fluorescence per well was measured using a fluorescence plate reader (Tecan M1000 pro), and the percentage of inhibition was calculated.

2.3. Animals

SAMP8 is an inbred mouse strain that has been generated by selective inbreeding of the AKR/J strain of mice [31,32]. It displays a phenotype of accelerated aging with behavioural abnormalities [33,34], the age-related cognitive decline [35], and several AD hallmarks [2,36]. Overall, it is widely used as a feasible rodent model of cognitive dysfunction and late-onset AD (LOAD) [37]. Senescence-Accelerated Mouse Resistant 1 (SAMR1) mouse is used as a healthy control mouse model.

Male SAMR1 and SAMP8 mice (n = 41) with 20-weeks-old were used to carry out cognitive and molecular analysis. The animals were randomly divided into four groups: SAMR1 control (SR1 Ct) group (n = 11), SAMP8 control (SP8 Ct) group (n = 8), SAMR1 treated with RL-208 (SR1 RL-208 (5 mg/Kg)) group (n = 10) and SAMP8 treated with RL-208 (SP8 RL-208 (5 mg/Kg)) group (n = 12). Animals had free access to food and water, under standard temperature conditions (22±2°C) and 12h:12h light-dark cycles (300 lux/0 lux). RL-208, (3,4,8,9-tetramethyltetracyclo[4.4.0.0^{3,9}.0^{4,8}]dec-1-yl)-methylamine hydrochloride, (5 mg/kg/day) was administered through drinking water for four weeks before starting the cognitive test. RL-208 was administered up to euthanasia (Figure 1A). Water consumption was

controlled each week for each cage and strain. Afterwards, RL-208 concentration was adjusted accordingly to reach the optimal dose for each cage.

Studies were performed by the Institutional Guidelines for the Care and Use of Laboratory Animals established by the Animal Experimentation Ethics Committee (CEEA) at the University of Barcelona.

2.4. Behavioural and Cognitive Tests

2.4.1. Three-Chamber Test

The three-chamber test (TCT) was used to assess preference for social novelty (time spent with a novel intruder in contrast with a familiar one) and sociability (time spent with rodents) [38]. The apparatus consisted of a rectangular box with partitions separating the box into three chambers (Figure 1B). Each chamber was 15 × 15 × 20 cm with square openings. Testing occurs in a box with three equally dimensioned rooms. Each test consists of 15 minutes and is recorded with a camera. The animal is placed in the center of the box and allowed to explore the three chambers for 5 minutes. The time spent in each chamber was evaluated. Then, an intruder (same-sex and age) was added to one of the rooms in a metal cup, and behaviour is recorded for 10 minutes. The time spent in each chamber is evaluated as well as the time interacting with the intruder (e.g., sniffing, rears, entries in each chamber).

2.4.2. Object Location Test

The object location test (OLT) is a well-established task based on the spontaneous tendency of rodents to spend more time exploring a novel object location than a familiar object location, as well as to recognize when an object has been relocated [39]. The test was carried out for 3 days in a wooden box (50 × 50 × 25 cm), in which three walls were white except one that was black (Figure 1C). The first day, the box was empty, and the animals just habituated to the open field arena for 10 minutes. The second day, two objects were placed in front of the black wall, equidistant from each other and the wall. The objects were 10-cm high and identical. The animals were placed into the open field arena and allowed to explore both objects and surroundings for 10 minutes. Afterwards, animals were returned to their home cages, and the OLT apparatus was cleaned with 70% ethanol. On the third day, one object was moved in front of the white wall to test the spatial memory. Trials were recorded using a camera mounted above the open field area, and the total exploration time was determined by scoring the amount of time (seconds) spent sniffing the object in the new location (TN) and the object in the old location (TO). In order to evaluate the cognitive performance, the DI was calculated, which is defined as $(TN-TO)/(TN+TO)$.

2.4.3. Novel Object Recognition Test

The novel object recognition test (NORT) allows evaluating short- and long-term recognition memory involving cortical areas and the hippocampus [40,41]. The experimental apparatus used for this test was a 90°, two-arm, 25-cm-long, 20-cm-high, and a 5-cm-wide black maze of black polyvinyl chloride (Figure 1D). The walls could be removed for easy cleaning with 70% ethanol to eliminate olfactory cues, and light intensity in mid-field was 30 lux. The objects to be discriminated were made of plastic and chosen not to frighten mice and without any part likely to be bitten. Before performing the test, the mice were individually habituated to the apparatus for 10 min during 3 consecutive days. On day four the next day, the animals were allowed to explore freely a 10 min acquisition trial (First trial), during which they were placed in the maze in the presence of two identical novel objects (A+A' or B+B') at the end of each arm. The mouse was then removed from the apparatus and returned to its home cage. A 10 min retention trial (Second trial) was carried out two hours later. During this second trial, objects A and B were placed by to novel objects with different shapes and colors, and the mice were allowed to explore the maze for another 10 min. Twenty-four hours after the acquisition trial, the

mice were tested again, with a new object and an object identical to the new one in the previous trial (B+C). The time that mice explored the novel object (TN) and time that mice explored the old object (TO) were measured from the video recordings from each trial session. Exploration of an object was defined as pointing the nose towards the object at a distance ≤ 2 cms and/or touching it with the nose. Turning or sitting around the object was not considered exploration. To avoid object preference biases objects A and B were counterbalanced so that one-half of the animals in each experimental group were first exposed to object A and then to object B, whereas the other half first saw object B and then object A. To evaluate the cognitive performance, the discrimination index (DI) was calculated, which is defined as $(TN-TO)/(TN+TO)$.

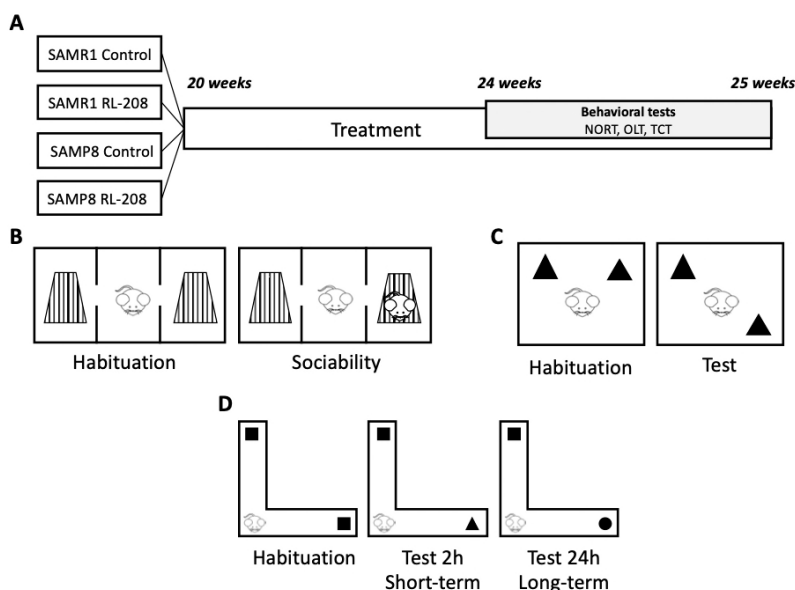


Figure 1. Scheme of experimental design (A), Scheme of Three Chamber Test (TCT) (B), Scheme of Object Location Test (OLT) (C), and scheme of Novel Object Recognition Test (NORT) (D).

2.5. Brain Processing

Three days after the behavioural and cognitive tests, mice were euthanized by cervical dislocation. Brains were immediately removed from the skull. The hippocampus and cortex were then isolated and frozen in powdered dry ice. They were maintained at -80 °C for further use. Tissue samples were homogenized in lysis buffer containing phosphatase and protease inhibitors (Cocktail II, Sigma). Total protein levels were obtained, and protein concentration was determined by the method of Bradford.

2.6. Protein Level Determination by Western Blotting

For Western blotting (WB), aliquots of 15 μ g of hippocampal protein extraction per sample were used. Protein samples were separated by Sodium dodecyl sulphate-Polyacrylamide gel electrophoresis (SDS-PAGE) (8–20%) and transferred onto Polyvinylidene difluoride (PVDF) membranes (Millipore). Afterwards, membranes were blocked in 5% non-fat milk in Tris-buffered saline (TBS) solution containing 0.1% Tween 20 TBS (TBS-T) for 1 hour at room temperature, followed by overnight incubation at a 4 °C with the primary antibodies listed in Table S1. Then, membranes were washed and incubated with secondary antibodies for 1 hour at room temperature. Immunoreactive proteins were viewed with the chemiluminescence-based detection kit, following the manufacturer's protocol (ECL Kit, Millipore), and digital images were acquired using ChemiDoc XRS+ System (BioRad). Semi-quantitative analyses were performed using ImageLab software (BioRad), and results were

expressed in arbitrary units (AU), considering control protein levels as 100%. Protein loading was routinely monitored by immunodetection of Glyceraldehyde-3-phosphate dehydrogenase (GAPDH).

2.7. Detection of Oxidative Stress in the Hippocampus

H₂O₂ levels from cortex samples were measured as an indicator of oxidative stress, and it was quantified using the Fluorimetric Hydrogen Peroxide Assay Kit (Sigma) according to the manufacturer's instructions.

2.8. RNA Extraction and Gene Expression Determination

Total RNA isolation from hippocampal samples was carried out using TRIsure™ reagent following the manufacturer's instructions (Bioline, Meridian Bioscience Inc., UK). The yield, purity, and quality of RNA were determined spectrophotometrically with a NanoDrop™ ND-1000 (Thermo Scientific, Wilmington, DE, USA) apparatus and an Agilent 2100B Bioanalyzer (Agilent Technologies, Palo Alto, CA, USA). RNAs with 260/280 ratios and RIN higher than 1.9 and 7.5, respectively, were selected. Reverse transcription-polymerase chain reaction (RT-PCR) was performed as follows: 2 µg of messenger RNA (mRNA) was reverse-transcribed using the High Capacity cDNA Reverse Transcription kit (Applied Biosystems, Foster City, CA, USA). Real-time quantitative PCR (qPCR) was used to quantify the mRNA expression of OS and synaptic plasticity genes listed in Table S2.

SYBR®Green real-time PCR was performed on a Step One Plus Detection System (Applied-Biosystems, Foster City, CA, USA) employing SYBR®Green PCR Master Mix (Applied-Biosystems, Foster City, CA, USA). Each reaction mixture contained 6.75 µL of complementary DNA (cDNA) (which concentration was 2 µg), 0.75 µL of each primer (which concentration was 100 nM), and 6.75 µL of SYBR®Green PCR Master Mix (2X).

Data were analyzed utilizing the comparative cycle threshold (Ct) method ($\Delta\Delta Ct$), where the housekeeping gene level was used to normalize differences in sample loading and preparation [42]. Normalization of expression levels was performed with β -actin for SYBR®Green-based real-time PCR results. Each sample was analyzed in duplicate, and the results represent the n-fold difference of the transcript levels among different groups.

2.9. Measurement of proBDNF and mBDNF Protein Levels in the Hippocampus

The hippocampal determination of pro-Brain-derived neurotrophic factor (proBDNF) and mature brain-derived neurotrophic factor (mBDNF) protein levels was performed using the enzyme-linked immunosorbent assay (ELISA) kit (Biosensis) according to the manufacturer's instructions.

2.10. Data Acquisition and Statistical Analysis

Behavioural analysis was performed blindly, the person who evaluated videos was different from the person who made the behavioural tests. Furthermore, videos are named with a blind code to avoid analysis bias. Data analysis was conducted using GraphPad Prism ver. 7 statistical software. Data are expressed as the mean \pm standard error of the mean (SEM) of at least 5 samples per group. Strain and treatment effects were compared using the two-way analysis of variance (ANOVA), followed by Tukey post-hoc analysis or two-tail student's t-test when it was necessary. Statistical significance was considered when p-values were <0.05. The statistical outliers were determined with Grubbs' test and when necessary were removed from the analysis.

3. Results

3.1. In Vitro Microsomal Stability and Cytochrome Inhibition

RL-208 was further studied in vitro for ascertaining their microsomal stability and CYP inhibition. RL-208 showed good microsomal stability in rat and mice microsomes, and did not inhibit in a

significant way cytochromes CYP2C9, $12 \pm 2\%$, CYP2D6 $10 \pm 3\%$; CYP1A2, $5 \pm 2\%$; CYP2C19, $23 \pm 1\%$; CYP3A4 (BFC), $35 \pm 4\%$; CYP3A4(DBF), $3 \pm 1\%$).

3.2. Improvement on Social Behaviour and Cognition after Treatment with RL-208

The TCT assess the general sociability in mice. In the sociability phase, in all experimental groups, the presence of an intruder increased significantly the time spent in the intruder chamber instead of the empty cup chamber (Figure 2A). Moreover, the time sniffing the intruder mouse was significantly higher in the SR1 Ct group compared to the SP8 Ct group, confirming the behavioural abnormalities described in the SAMP8 mouse model. After RL-208 treatment, the time sniffing the intruder was significantly augmented in SAMP8 strain, proving the beneficial effects on social behaviour (Figure 2B).

NORT evaluation confirmed the cognitive impairment of the SAMP8 mouse model in both short- and long-term recognition memories in comparison with the SAMR1 (Figure 2C,D). Strikingly, the SP8 RL-208 group exhibited a significant gain in both short- and long-term recognition memories compared to the SP8 Ct group, obtaining significant higher DI values (Figure 2C,D). Conversely, no significant changes in both short- and long-term DI values between SR1 groups were found. Regarding OLT evaluation, a significantly higher DI value in the SR1 Ct group compared to the SP8 Ct mice group was found (Figure 2E). Likewise, a better spatial memory in both treated mice groups was found, showing significant higher DI values after RL-208 treatment (Figure 2E).

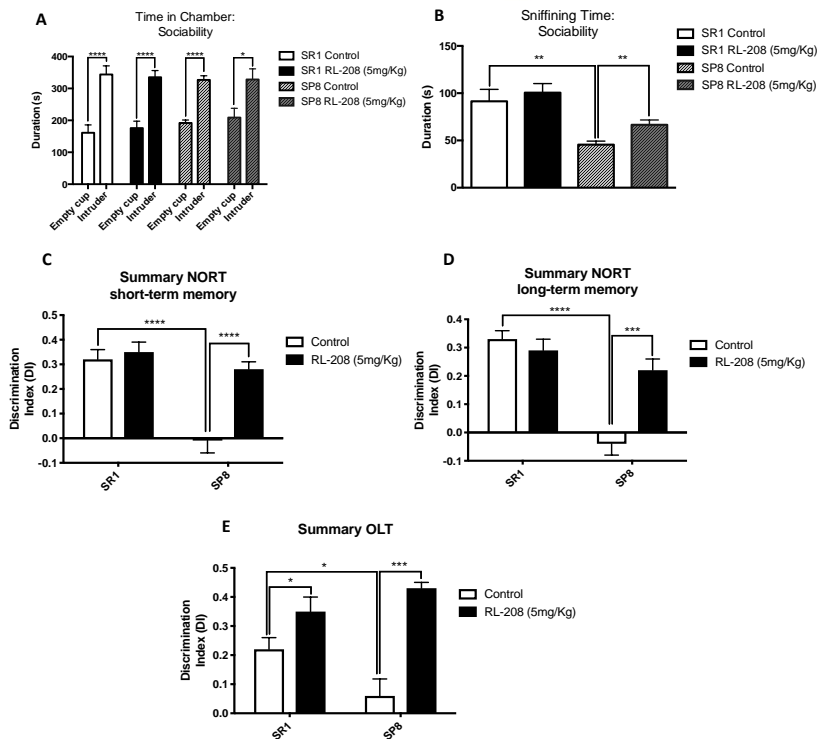


Figure 2. Results of Three Chamber Test (TCT), Object Location Test (OLT), and Novel Object Recognition Test (NORT) in male mice at 24-weeks-old SR1 and SP8 Ct mice groups and SR1 and SP8 treated with RL-208 (5 mg/Kg) mice groups. For TCT: Time spent in the chamber (A) and sniffing time: sociability with the intruder animal (B). For NORT: Summary of Discrimination Index (DI) from short-term memory (C), and summary of DI from long-term memory (D). For OLT: Summary of DI (E). Values represented are mean \pm Standard error of the mean (SEM); $n = 41$ (SR1 Ct $n = 11$; SP8 Ct $n = 8$; SR1 RL-208 $n = 10$; SP8 RL-208 $n = 12$). * $p < 0.05$; ** $p < 0.01$; *** $p < 0.001$; **** $p < 0.0001$.

3.3. Changes in NMDAR and Apoptotic Pathways Induced by RL-208

NMDAR changes and apoptotic markers were studied as a learning memory and synaptic plasticity activation. A significant decrease in NMDAR2A protein level was found in SP8 Ct compared to the SR1 Ct (Figure 3A), suggesting its participation in the cognitive decline presented by the SAMP8 mouse model. However, RL-208 treatment did not produce significant differences in the NMDAR2A protein levels neither in SR1 nor in SP8. Interestingly, RL-208 increased in a significant way p-NMDAR (Tyr1472) protein levels in both strains (Figure 3B), suggesting an improvement in neuronal functionality.

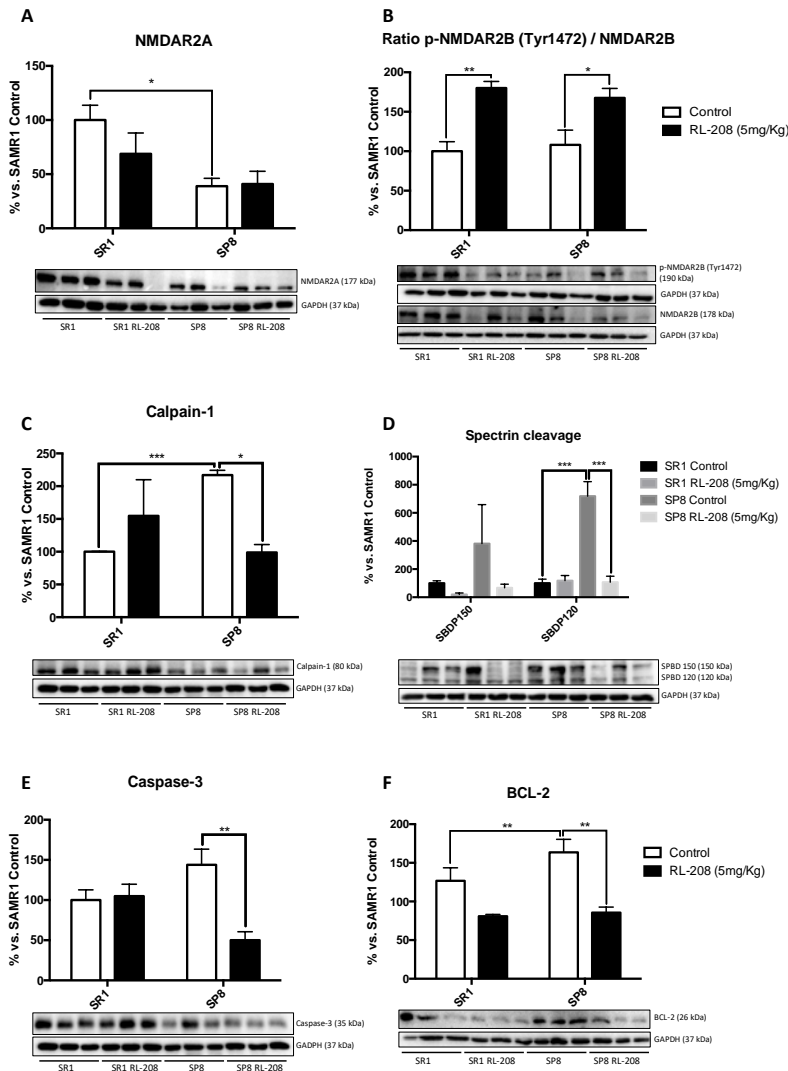


Figure 3. Representative Western Blot and quantifications for NMDAR2A (A), the ratio of p-NMDAR2B/NMDAR2B (B), Calpain-1 (C), ratio SBPD/Spectrin (D), Caspase-3 (E), BCL-2 (F). Values in bar graphs are adjusted to 100% for protein levels of the control SAMR1 (SR1 Ct). Values are the mean \pm Standard error of the mean (SEM); (n = 6 for each group). * $p < 0.05$; ** $p < 0.01$; *** $p < 0.001$.

Next, we evaluated the effects of RL-208 on the proteolytic processes that lead to apoptosis. Calpain-1 and 150 Spectrin Breakdown Products (SBDP) protein levels increased in SP8 Ct in comparison with the SR1 Ct group. RL-208 treatment reduced Calpain-1, Caspase-3 and 120BPD in the SP8 strain, not in SR1 (Figure 3C–E).

By contrast, B-cell lymphoma-2 (BCL-2) protein levels diminished, only reaching significance in the SP8 mouse model (Figure 3F).

3.4. Increased Neurotrophins and Synaptic Markers Protein Levels after Treatment with RL-208

A significant reduction in proBDNF protein levels in SP8 treated mice compared to the control group were found. Differences in SR1 strain were not significant (Figure 4A). Conversely, a significant augment in mature BDNF protein levels in RL-208 treated mice compared to control groups were found (Figure 4B). Tropomyosin-related kinase B full-length (TrkB-FL) protein levels increased significantly both in SR1 and SP8 treated with RL-208 (Figure 4C), whereas reduced TrkB intracellular fragment (TrkB-ICD) protein levels were observed (Figure 4D). TrkB signaling pathway regulates synaptosomal-associated protein 25 (SNAP25), a synaptic plasticity marker, and as expected, significant-high SNAP25 protein levels were found in SP8 RL-208 (Figure 4E).

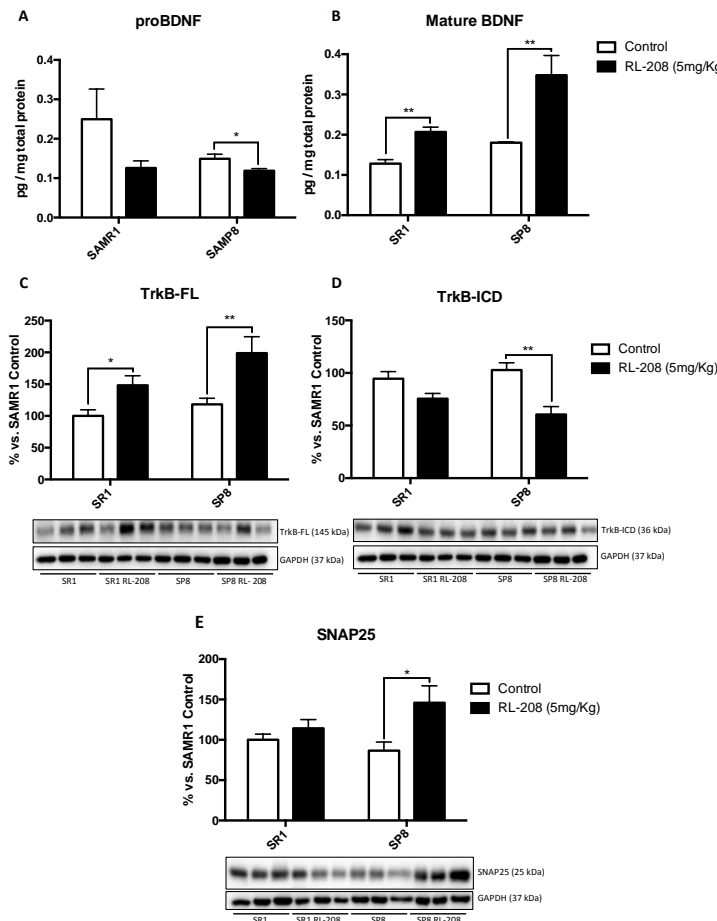


Figure 4. Protein levels of proBDNF (A), and mBDNF (B). Representative Western Blot and quantifications for TrkB-FL (C), TrkB-ICD (D) and SNAP25 (E). Values represented are mean \pm Standard error of the mean (SEM); (n = 6 for each group). * $p < 0.05$; ** $p < 0.01$; *** $p < 0.001$.

Deeping on synaptic plasticity markers, a significant increase in Synaptophysin (SYN) protein levels were found in RL-208 treated mice (Figure 5A). Postsynaptic density protein 95 (PSD95) protein levels were also augmented but did not reach significance in SP8 mice (Figure 5B). Regarding the neurotrophic factors, a significant gain in gene expression of the tumor growth factor (*Tgf*) in RL-208 treated mice groups, in comparison with the control groups, was observed (Figure 5C). Likewise, a significant increase in gene expression of VGF nerve growth factor inducible (*Vgf*) in SP8 RL-208 compared to the SP8 Ct group, but no changes between SR1 mice groups were found (Figure 5D).

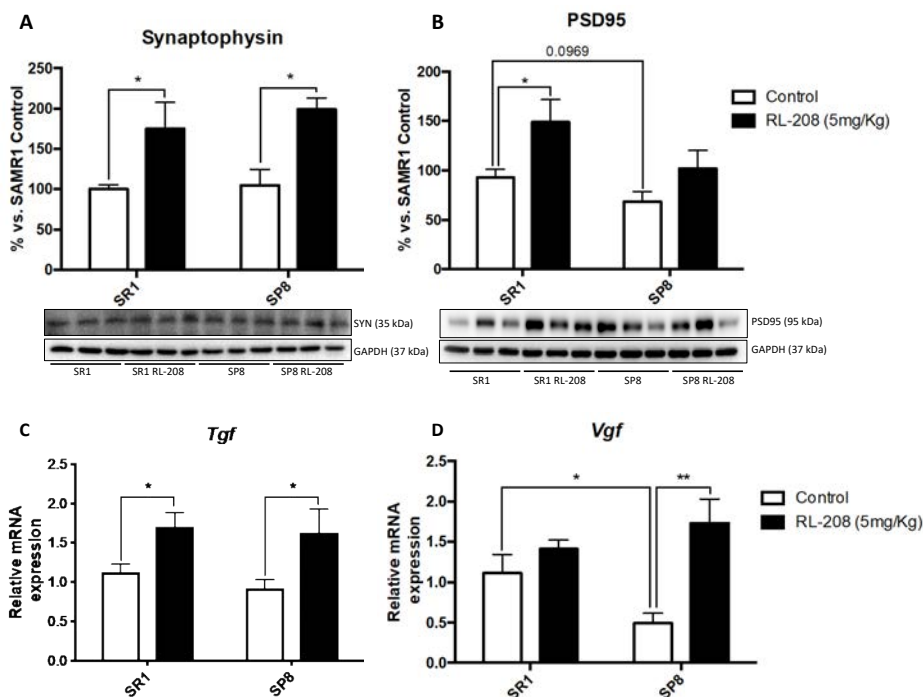


Figure 5. Representative Western Blot and quantifications for Synaptophysin (A), and PSD95 (B). Representative gene expression for *Tgf* (C), and *Vgf* (D). Values in bar graphs are adjusted to 100% for protein levels of the control SAMR1 (SR1 Ct). Gene expression levels were determined by real-time PCR. Values are the mean \pm Standard error of the mean (SEM); (n = 6 for each group). * $p < 0.05$; ** $p < 0.01$.

3.5. Changes in Protein Levels and Gene Expression of Antioxidant and Pro-oxidant Enzymes and ROS Levels after Treatment with RL-208

RL-208 increased, in a significant way, Superoxide Dismutase 1 (SOD1) and Glutathione Peroxidase 1 (GPX1), antioxidant protein levels SP8 mice, but not in SR1 mice (Figure 6A,B). Moreover, GPX1 protein levels tended to decrease in the SP8 Ct group compared to the SAMR1 Ct group was observed (Figure 6B). RL-208 elevated gene expression of Heme oxygenase decycling 1 (*Hmox1*), an important key enzyme in cellular antioxidant-defense in treated mice (Figure 6C). Conversely, RL-208 decreased gene expression of Cyclooxygenase-2 (*Cox2*) in treated mice groups in comparison with the control groups, being significant in the SP8 strain (Figure 6D). Finally, the evaluation of the hydrogen peroxide levels in the hippocampus showed a significant decrease in reactive oxygen species (ROS) levels in both RL-208 treated mice groups compared to the control groups (Figure 6E).

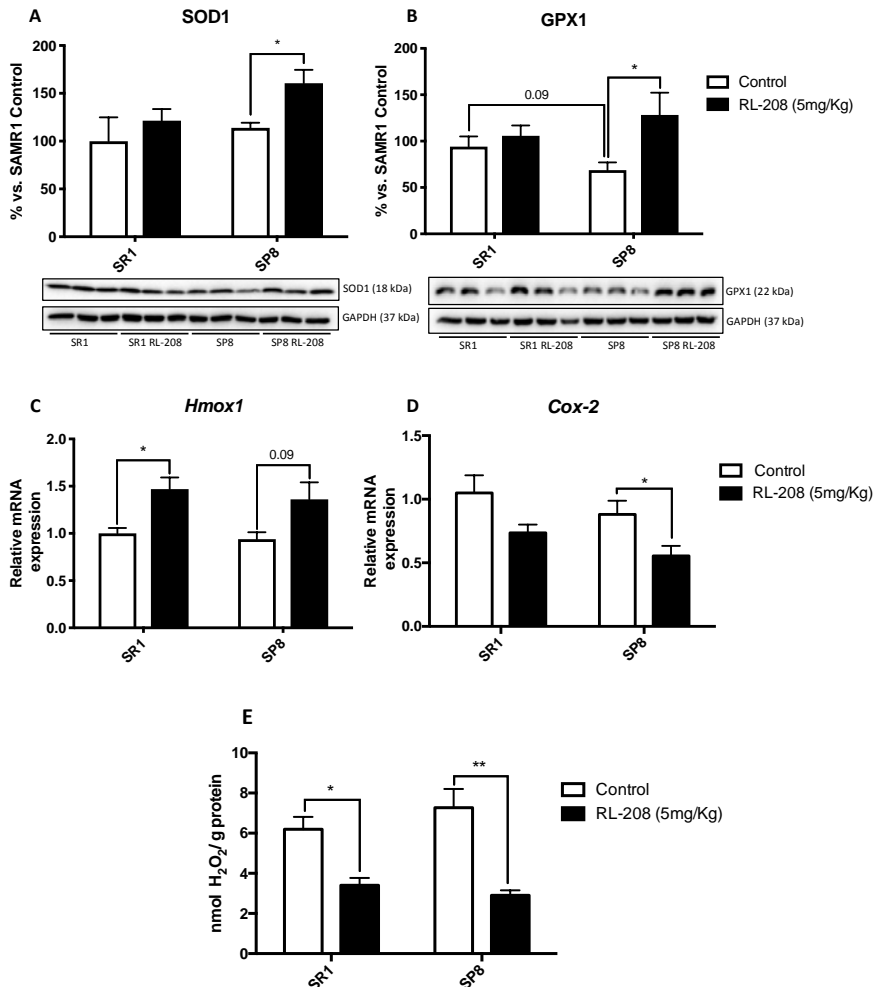


Figure 6. Representative Western Blot and quantifications of antioxidant enzymes for SOD1 (A), and GPX1 (B). Representative gene expression of the antioxidant enzyme for *Hmox1* (C), and pro-oxidant enzyme for *Cox2* (D). Representative OS measured as hydrogen peroxide concentration in homogenates of the hippocampus tissue (E). Values in bar graphs are adjusted to 100% for protein levels of the control SAMR1 (SR1 Ct). Gene expression levels were determined by real-time PCR. Values represented are mean \pm Standard error of the mean (SEM); (n = 6 for each group). * $p < 0.05$; ** $p < 0.01$.

3.6. Changes in CDK5/p25-35 Pathway Activation and Tau Phosphorylation after Treatment with RL-208

ADAM10 protein levels were diminished in SAMP8 in reference to SAMR1, and RL-208 prevented the loss of this secretase (Figure 7A). The Cyclin-Dependent Kinases 5 (CDK5)/p25-p35 and Tau phosphorylation were evaluated by WB (Figure 7B,C). We found a significant high p25/p35 ratio in the SP8 Ct compared to the SR1 Ct, accordingly with the increase in calpain activity described above. Likewise, CDK5 activation (measured by p-CDK5/CDK5 ratio) and p25/p35 ratio were significantly reduced in the SP8 RL-208 group compared to the control group (Figure 7B,C). Considering these results, we evaluated Tau hyperphosphorylation protein levels. A significant reduction in Tau phosphorylation in both treated mice groups was found, specifically for the Ser396 phosphorylation site (Figure 7D).

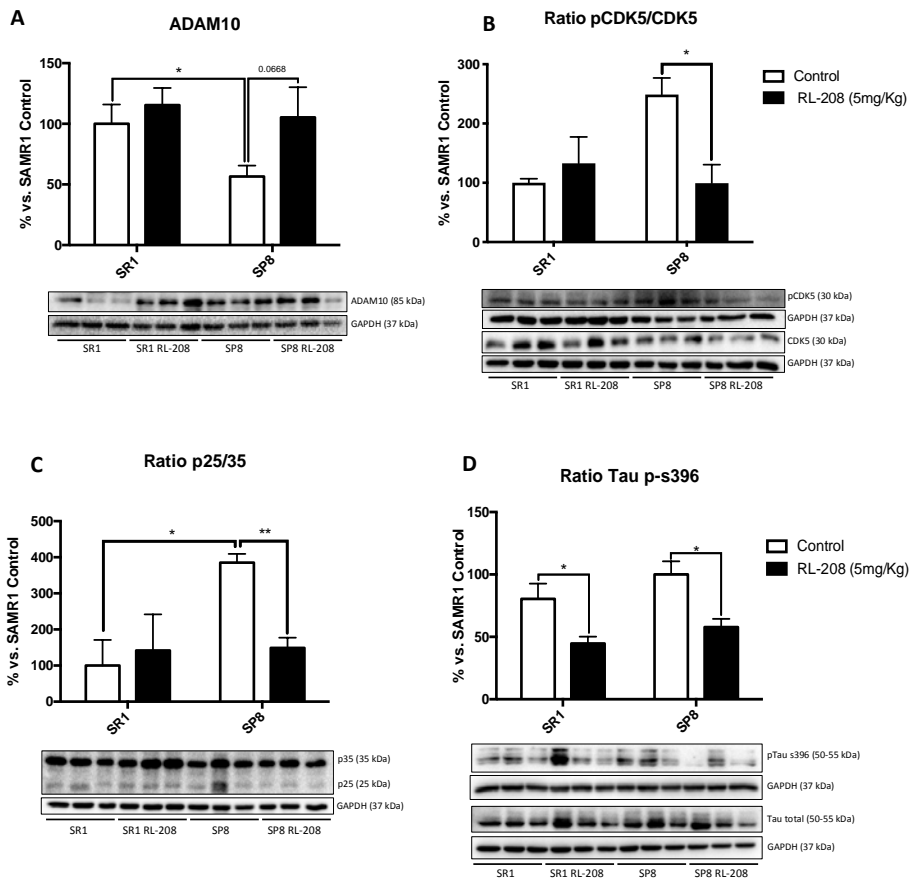


Figure 7. Representative Western Blot and quantifications for ADAM10 (A), ratio p-CDK5/CDK5 (B), ratio p25/p35 (C), and ratio Tau (p-s396) (D). Values in bar graphs are adjusted to 100% for protein levels of the control SAMR1 (SR1 Ct). Values represented are mean \pm Standard error of the mean (SEM); (n = 6 for each group). * $p < 0.05$; ** $p < 0.01$.

4. Discussion

As aforementioned, the alteration of NMDAR has been associated with neurodegenerative disorders, such as AD [43]. It has been well documented that competitive pharmacological blockade of NMDAR functions leads to cognitive disability [27] and impaired neuroplasticity [44], increasing apoptotic neuronal death [45]. However, memantine has demonstrated specific effects because its low-affinity, uncompetitive antagonist performance, and can block the NMDAR over-activation without affecting its normal activation [46,47]. The current study provides pieces of evidence demonstrating that the novel non-competitive NMDAR antagonist RL-208 can be a promising therapy for age-related cognitive and AD.

Early preclinical in vitro experiments indicated that RL-208 displays low IC_{50} , by 1 μ M [30], has low metabolism, and did not interact with cytochromes, having then a good druggable profile to test it in in vivo models and to reach the proof of concept of in vivo effectivity.

Several preclinical studies in different transgenic mice models of AD with NMDAR antagonists, including memantine, demonstrate beneficial cognitive activities [28,48–52]. In line with these findings, RL-208 treatment improved social behaviour and restoring cognitive impairment in SAMP8 animals, by using TCT and memory test (NORT and NOLT) respectively. As expected, we did not find any substantial improvements in behaviour and cognition in the control strain SAMR1 after RL-208

treatment, indicating that uncompetitive antagonist is effective in front overstimulation of NMDAR but not in physiological conditions.

The behavioural and cognitive changes induced by RL-208 were accompanied by changes in several molecular pathways associated with NMDAR functionality. RL-208 increased p-NMDAR2B (Tyr1472), which has been proved to play crucial roles in the induction of long-term potentiation (LTP), and the hippocampus-dependent memory formation [53]. There are several molecular pathways related to apoptosis that participated in cellular physiological and pathological processes, i.e., proteases as Calpain-1 and Caspase, or specific mediators as BCL-2. RL-208 decreased activation and protein levels of Calpain-1 and Caspase-3 proteases and decreased BCL-2 protein levels. Interestingly, Caspase-3 and BCL-2 changes were significant in SAMP8 treated with RL-208, confirming that RL-208 works under the overactivation of the NMDAR. Lack of effect in healthy conditions turn out in fewer side effects. To the best of our knowledge, there is only one report using memantine at a similar dose (4 mg/kg) which shows similar antiapoptotic effects related to NMDAR antagonism in the rats' hippocampus [54].

Previous studies have been described as the ability of NMDAR antagonists to modify synaptic plasticity [55–57]. In our hands, RL-208 treatment increased the majority of the synaptic plasticity markers such as SYN, PSD-95, and *Tgf* in the SAMP8 and SAMR1 hippocampus pointed out that the improvement in cognition under pathological conditions was associated with hippocampal plasticity. In the same line, neurotrophic signaling is severely impaired in AD, being BDNF/TrkB representative signaling pathway altered. BDNF/TrkB signaling pathway was ameliorated under RL-208 treatment, with significant increases in mBDNF, TrkB-FL, and SNAP25 protein levels. These results could indicate that RL-208 contributes to restoring cognition in SAMP8 mouse because of the increase in BDNF/TrkB signaling.

It has been reported that OS is involved in several neurodegenerative disorders, mediating neuronal death [58]. Several reports suggest that NMDAR activation mediated OS, causing synapse alterations [59–62]. Concretely, ROS leads to neuronal alterations and ultimately produce synaptic dysfunction, which is a critical factor of the age-related cognitive decline and AD [63]. RL-208 decrease hippocampal ROS levels in treated mice. In parallel, SOD1 and GPX1 protein levels and *Hmox1* gene expression increased, as well as *Cox-2* gene expression diminished in SAMP8 after RL-208 treatment. Then, in line with our findings, RL-208 delivered a significant diminution in OS because of its role as uncompetitive NMDAR antagonist.

Tau hyperphosphorylation is a characteristic histological mark in several neurodegenerative disorders. Tau phosphorylation levels are regulated by a complex network of protein kinases and phosphatases, such as CDK5 [64]. RL-208 reduced the activity of the CDK5 in SAMP8 mice, where CDK5 is overactivated. Furthermore, a significant reduction in the p25/p35 ratio in SP8 RL-208 group. Interestingly CDK5 co-activator p25 is cleaved by Calpain-1 from p35 peptide harbored in the cytoplasmic membrane, and as mentioned RL-208 reduced Calpain-1 proteolytic activity. Accordingly, significant diminution of p-Tau [Ser396] was found after RL-208 administration. To our knowledge, memantine is also described as able to reduce tau phosphorylation [65–67], linking the RL-208 antagonist action on NMDAR again with the neuroprotectant effectivity in SAMP8.

In sum, our in vivo study in SAMP8 demonstrated the therapeutic potential of RL-208, a novel NMDAR uncompetitive antagonist, for age-related cognitive decline, and AD. Because it is of interest to shed light on the underlying mechanisms by which NMDAR mediates neuroprotection and new pharmacological approaches are needed to fight devastating neurodegenerative diseases as AD, RL-208 beneficial effects described here, offer new clues to face the challenge in drug discovery (Figure 8). Noteworthy, more studies are needed to draw the complete landscape action for NMDAR antagonist, and in particular for RL-208 to proceed towards translational clinical application.

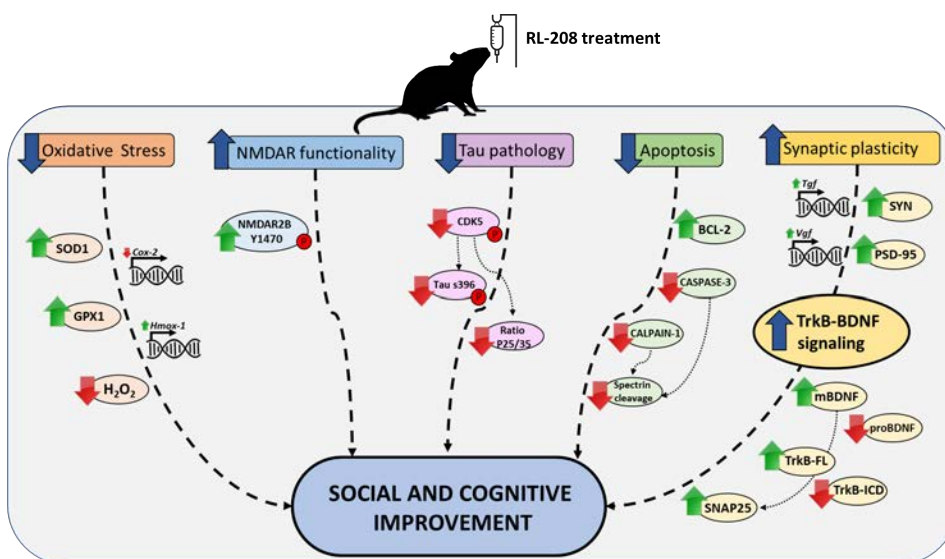


Figure 8. Illustrative cartoon of molecular and cognitive effects after RL-208 treatment.

Supplementary Materials: The following are available online at <http://www.mdpi.com/1999-4923/12/3/284/s1>, Table S1: Antibodies used in Western blot studies, Table S2: Primers used in qPCR studies.

Author Contributions: C.G.-F. carried out the experimental intervention and performed behaviour experiments. J.C.-A. and A.B.-S. performed Western blot analysis. J.C.-A. performed the RT-PCR experiments. C.G.-F., and M.P. analysed the data and drafted the manuscript. A.L.T. and S.V. synthesized and purified RL-208. J.M.B. and M.I.L. determined the ADMET parameters. C.G.-F. and M.P. designed the experiments and supervised the study. C.G.-F., J.C.-A., A.M.C., A.B.-S., A.L.T., S.V., R.L. and M.P. contributed to the writing the manuscript. All authors read and approved the final version of the manuscript.

Funding: This research was funded by *Ministerio de Economía, Industria y Competitividad* (Agencia Estatal de Investigación, AEI) and *Fondo Europeo de Desarrollo Regional* (MINECO-FEDER) (Projects SAF2017-82771-R, SAF2016-77703, SAF2015-68749 and SAF2017-90913), Xunta de Galicia (ED431C 2018/21) and Generalitat de Catalunya (2017 SGR 106).

Conflicts of Interest: The authors claim no financial conflict of interests.

References

- Chen, P.H.; Cheng, S.J.; Lin, H.C.; Lee, C.Y.; Chou, C.H. Risk factors for the progression of mild cognitive impairment in different types of neurodegenerative disorders. *Behav. Neurol.* **2018**, *2018*, 6929732. [[CrossRef](#)] [[PubMed](#)]
- Griñán-Ferré, C.; Corpas, R.; Puigoriol-Illamola, D.; Palomera-Ávalos, V.; Sanfeliu, C.; Pallàs, M. Understanding Epigenetics in the Neurodegeneration of Alzheimer's Disease: SAMP8 Mouse Model. *J. Alzheimers Dis.* **2018**, *62*, 943–963. [[CrossRef](#)] [[PubMed](#)]
- Alzheimer's Association. 2018 Alzheimer's Disease Facts and Figures. *Alzheimers Dement.* **2018**, *14*, 367–429. [[CrossRef](#)]
- Prince, M.J.; Wimo, A.; Guerchet, M.; Ali, G.C.; Wu, Y.-T.; Prina, M. World Alzheimer Report 2015: The Global Impact of Dementia: An Analysis of Prevalence. *Incid. Cost Trends* **2015**, *2017*.
- Prince, M.; Comas-Herrera, A.; Knapp, M.; Guerchet, M.; Karagiannidou, M. World Alzheimer report 2016: Improving healthcare for people living with dementia: Coverage, quality and costs now and in the future. *Alzheimer's Dis. Int. Lond.* **2016**, *1–40*.
- Peters, R. Ageing and the brain. *Postgrad. Med. J.* **2006**, *82*, 84–88. [[CrossRef](#)] [[PubMed](#)]
- Grill, J.D.; Cummings, J.L. Novel targets for Alzheimer's disease treatment. *Expert Rev Neurother.* **2010**, *10*, 711–728. [[CrossRef](#)]

8. Huang, W.J.; Zhang, X.; Chen, W.W. Role of oxidative stress in Alzheimer's disease. *Biomed. Rep.* **2016**, *4*, 519–522. [[CrossRef](#)]
9. Calsolaro, V.; Edison, P. Neuroinflammation in Alzheimer's disease: Current evidence and future directions. *Alzheimer's Dement.* **2016**, *12*, 719–732. [[CrossRef](#)]
10. Ehrnhoefer, D.E.; Wong, B.K.Y.; Hayden, M.R. Convergent pathogenic pathways in Alzheimer's and Huntington disease: Shared targets for drug development. *Nat. Rev. Drug Discov.* **2011**, *10*, 853–867. [[CrossRef](#)]
11. Kashyap, G.; Bapat, D.; Das, D.; Gowaikar, R.; Amritkar, R.E.; Rangarajan, G.; Ravindranath, V.; Ambika, G. Synapse loss and progress of Alzheimer's disease-A network model. *Sci. Rep.* **2019**, *9*, 6555. [[CrossRef](#)] [[PubMed](#)]
12. Xu, Y.; Yan, J.; Zhou, P.; Li, J.; Gao, H.; Xia, Y.; Wang, Q. Neurotransmitter receptors and cognitive dysfunction in Alzheimer's disease and Parkinson's disease. *Prog. Neurobiol.* **2012**, *97*, 1–13. [[CrossRef](#)] [[PubMed](#)]
13. Zhang, Y.; Li, P.; Feng, J.; Wu, M. Dysfunction of NMDA receptors in Alzheimer's disease. *Neurol. Sci.* **2016**, *37*, 1039–1047. [[CrossRef](#)] [[PubMed](#)]
14. Wang, R.; Reddy, P.H. Role of Glutamate and NMDA Receptors in Alzheimer's Disease. *J. Alzheimer's Dis.* **2017**, *57*, 1041–1048. [[CrossRef](#)] [[PubMed](#)]
15. Di Iorio, G.; Baroni, G.; Lorusso, M.; Montemitro, C.; Spano, M.C.; Di Giannantonio, M. Efficacy of Memantine in Schizophrenic Patients: A Systematic Review. *J. Amino Acids* **2017**, *2017*, 7021071. [[CrossRef](#)] [[PubMed](#)]
16. Chen, H.S.V.; Lipton, S.A. The chemical biology of clinically tolerated NMDA receptor antagonists. *J. Neurochem.* **2006**, *97*, 1611–1626. [[CrossRef](#)]
17. Hardingham, G.E.; Bading, H. Synaptic versus extrasynaptic NMDA receptor signalling: Implications for neurodegenerative disorders. *Nat. Rev. Neurosci.* **2010**, *11*, 682–696. [[CrossRef](#)] [[PubMed](#)]
18. Riedel, G.; Platt, B.; Micheau, J. Glutamate receptor function in learning and memory. *Behav. Brain Res.* **2003**, *140*, 1–47. [[CrossRef](#)]
19. Danysz, W.; Parsons, C.G. Alzheimer's disease, β -amyloid, glutamate, NMDA receptors and memantine-Searching for the connections. *Br. J. Pharmacol.* **2012**, *167*, 324–352. [[CrossRef](#)]
20. De Felice, F.G.; Velasco, P.T.; Lambert, M.P.; Viola, K.; Fernandez, S.J.; Ferreira, S.T.; Klein, W.L. A β oligomers induce neuronal oxidative stress through an N-methyl-D-aspartate receptor-dependent mechanism that is blocked by the Alzheimer drug memantine. *J. Biol. Chem.* **2007**, *282*, 11590–11601. [[CrossRef](#)]
21. Liu, J.; Chang, L.; Song, Y.; Li, H.; Wu, Y. The role of NMDA receptors in Alzheimer's disease. *Front. Neurosci.* **2019**, *13*, 43. [[CrossRef](#)] [[PubMed](#)]
22. Blundell, J.; Adamec, R. The NMDA receptor antagonist CPP blocks the effects of predator stress on pCREB in brain regions involved in fearful and anxious behavior. *Brain Res.* **2007**, *1136*, 59–76. [[CrossRef](#)] [[PubMed](#)]
23. Johnson, J.W.; Glasgow, N.G.; Povysheva, N.V. Recent insights into the mode of action of memantine and ketamine. *Curr. Opin. Pharmacol.* **2015**, *20*, 54–63. [[CrossRef](#)] [[PubMed](#)]
24. Ikonomidou, C.; Turski, L. Why did NMDA receptor antagonists fail clinical trials for stroke and traumatic brain injury? *Lancet Neurol.* **2002**, *1*, 383–386. [[CrossRef](#)]
25. Muir, K.W. Glutamate-based therapeutic approaches: Clinical trials with NMDA antagonists. *Curr. Opin. Pharmacol.* **2006**, *6*, 53–60. [[CrossRef](#)] [[PubMed](#)]
26. Lipton, S.A. Failures and Successes of NMDA Receptor Antagonists: Molecular Basis for the Use of Open-Channel Blockers like Memantine in the Treatment of Acute and Chronic Neurologic Insults. *NeuroRx* **2004**, *1*, 101–110. [[CrossRef](#)]
27. Olivares, D.; Deshpande, V.K.; Shi, Y.; Lahiri, D.K.; Greig, N.H.; Rogers, J.T.; Huang, X. N-Methyl D-Aspartate (NMDA) Receptor Antagonists and Memantine Treatment for Alzheimer's Disease, Vascular Dementia and Parkinson's Disease. *Curr. Alzheimer Res.* **2012**, *9*, 746–758. [[CrossRef](#)]
28. Liu, M.Y.; Wang, S.; Yao, W.F.; Zhang, Z.J.; Zhong, X.; Sha, L.; He, M.; Zheng, Z.H.; Wei, M.J. Memantine improves spatial learning and memory impairments by regulating NGF signaling in APP/PS1 transgenic mice. *Neuroscience* **2014**, *273*, 141–151. [[CrossRef](#)]
29. Matsunaga, S.; Kishi, T.; Iwata, N. Memantine monotherapy for Alzheimer's Disease: A systematic review and meta-analysis. *PLoS ONE* **2015**, *10*, e0123289. [[CrossRef](#)]
30. Leiva, R.; Phillips, M.B.; Turcu, A.L.; Gratacòs-Batlle, E.; León-García, L.; Sureda, F.X.; Soto, D.; Johnson, J.W.; Vázquez, S. Pharmacological and Electrophysiological Characterization of Novel NMDA Receptor Antagonists. *ACS Chem. Neurosci.* **2018**, *9*, 2722–2730. [[CrossRef](#)]

31. Pallàs, M. Senescence-Accelerated Mice P8: A Tool to Study Brain Aging and Alzheimer's Disease in a Mouse Model. *ISRN Cell Biol.* **2012**, *2012*, 917167. [[CrossRef](#)]
32. Takeda, T.; Hosokawa, M.; Takeshita, S.; Irino, M.; Higuchi, K.; Matsushita, T.; Tomita, Y.; Yasuhira, K.; Hamamoto, H.; Shimizu, K.; et al. A new murine model of accelerated senescence. *Mech Ageing Dev.* **1981**, *17*, 183–194. [[CrossRef](#)]
33. Yanai, S.; Endo, S. Early onset of behavioral alterations in senescence-accelerated mouse prone 8 (SAMP8). *Behav. Brain Res.* **2016**, *308*, 187–195. [[CrossRef](#)]
34. Griñan-Ferré, C.; Palomera-Ávalos, V.; Puigoriol-Illamola, D.; Camins, A.; Porquet, D.; Plá, V.; Aguado, F.; Pallàs, M. Behaviour and cognitive changes correlated with hippocampal neuroinflammation and neuronal markers in female SAMP8, a model of accelerated senescence. *Exp. Gerontol.* **2016**, *80*, 69. [[CrossRef](#)]
35. Butterfield, D.A.; Poon, H.F. The senescence-accelerated prone mouse (SAMP8): A model of age-related cognitive decline with relevance to alterations of the gene expression and protein abnormalities in Alzheimer's disease. *Exp. Gerontol.* **2005**, *40*, 774–783. [[CrossRef](#)] [[PubMed](#)]
36. Morley, J.E.; Armbrecht, H.J.; Farr, S.A.; Kumar, V.B. The senescence accelerated mouse (SAMP8) as a model for oxidative stress and Alzheimer's disease. *Biochim. Biophys. Acta-Mol. Basis Dis.* **2012**, *1822*, 650–656. [[CrossRef](#)]
37. Esquerda-Canals, G.; Montoliu-Gaya, L.; Güell-Bosch, J.; Villegas, S. Mouse Models of Alzheimer's Disease. *J. Alzheimer's Dis.* **2017**, *57*, 1171–1183. [[CrossRef](#)] [[PubMed](#)]
38. Griñan-Ferré, C.; Pérez-Cáceres, D.; Gutiérrez-Zetina, S.M.; Camins, A.; Palomera-Avalos, V.; Ortuño-Sahagún, D.; Rodrigo, M.T.; Pallàs, M. Environmental Enrichment Improves Behavior, Cognition, and Brain Functional Markers in Young Senescence-Accelerated Prone Mice (SAMP8). *Mol. Neurobiol.* **2016**, *53*, 2435–2450. [[CrossRef](#)]
39. Ennaceur, A.; Meliani, K. A new one-trial test for neurobiological studies of memory in rats. III. Spatial vs. non-spatial working memory. *Behav. Brain Res.* **1992**, *51*, 83–92. [[CrossRef](#)]
40. Ennaceur, A.; Delacour, J. A new one-trial test for neurobiological studies of memory in rats. 1: Behavioral data. *Behav. Brain Res.* **1988**, *31*, 47–59. [[CrossRef](#)]
41. Puigoriol-Illamola, D.; Griñan-Ferré, C.; Vasilopoulou, F.; Leiva, R.; Vázquez, S.; Pallàs, M. 11 β -HSD1 Inhibition by RL-118 Promotes Autophagy and Correlates with Reduced Oxidative Stress and Inflammation, Enhancing Cognitive Performance in SAMP8 Mouse Model. *Mol. Neurobiol.* **2018**, *55*, 8904–8915. [[CrossRef](#)] [[PubMed](#)]
42. Griñan-Ferré, C.; Sarroca, S.; Ivanova, A.; Puigoriol-Illamola, D.; Aguado, F.; Camins, A.; Sanfeliu, C.; Pallàs, M. Epigenetic mechanisms underlying cognitive impairment and Alzheimer disease hallmarks in 5XFAD mice. *Aging* **2016**, *8*, 664–684. [[CrossRef](#)] [[PubMed](#)]
43. Lakhan, S.E.; Caro, M.; Hadzimidichalis, N. NMDA receptor activity in neuropsychiatric disorders. *Front. Psychiatry* **2013**, *4*, 52. [[CrossRef](#)] [[PubMed](#)]
44. Lin, C.; Huang, Y.; Lin, C.; Lane, H.; Tsai, G. NMDA Neurotransmission Dysfunction in Mild Cognitive Impairment and Alzheimers Disease. *Curr. Pharm. Des.* **2014**, *20*, 5169–5179. [[CrossRef](#)]
45. Gao, S.; Yu, Y.; Ma, Z.Y.; Sun, H.; Zhang, Y.L.; Wang, X.T.; Wang, C.; Fan, W.M.; Zheng, Q.Y.; Ma, C.L. NMDAR-Mediated Hippocampal Neuronal Death is Exacerbated by Activities of ASIC1a. *Neurotox. Res.* **2015**, *28*, 122–137. [[CrossRef](#)]
46. Lipton, S.A. Paradigm shift in neuroprotection by NMDA receptor blockade: Memantine and beyond. *Nat. Rev. Drug Discov.* **2006**, *5*, 160–170. [[CrossRef](#)]
47. Johnson, J.W.; Kotermanski, S.E. Mechanism of action of memantine. *Curr. Opin. Pharmacol.* **2006**, *6*, 61–67. [[CrossRef](#)]
48. Martinez-Coria, H.; Green, K.N.; Billings, L.M.; Kitazawa, M.; Albrecht, M.; Rammes, G.; Parsons, C.G.; Gupta, S.; Banerjee, P.; LaFerla, F.M. Memantine improves cognition and reduces Alzheimer's-like neuropathology in transgenic mice. *Am. J. Pathol.* **2010**, *176*, 870–880. [[CrossRef](#)]
49. Minkeviciene, R.; Banerjee, P.; Tanila, H. Memantine improves spatial learning in a transgenic mouse model of Alzheimer's disease. *J. Pharmacol. Exp. Ther.* **2004**, *311*, 677–682. [[CrossRef](#)]
50. Nagakura, A.; Shitaka, Y.; Yarimizu, J.; Matsuoka, N. Characterization of cognitive deficits in a transgenic mouse model of Alzheimer's disease and effects of donepezil and memantine. *Eur. J. Pharmacol.* **2013**, *703*, 53–61. [[CrossRef](#)]

51. Nyakas, C.; Granic, I.; Halmy, L.G.; Banerjee, P.; Luiten, P.G.M. The basal forebrain cholinergic system in aging and dementia. Rescuing cholinergic neurons from neurotoxic amyloid- β 42 with memantine. *Behav. Brain Res.* **2011**, *221*, 594–603. [[CrossRef](#)] [[PubMed](#)]
52. Scholtzowa, H.; Wadghiri, Y.Z.; Douadi, M.; Sigurdsson, E.M.; Li, Y.S.; Quartermain, D.; Banerjee, P.; Wisniewski, T. Memantine leads to behavioral improvement and amyloid reduction in Alzheimer's-disease-model transgenic mice shown as by micromagnetic resonance imaging. *J. Neurosci. Res.* **2008**, *86*, 2784–2791. [[CrossRef](#)] [[PubMed](#)]
53. Li, Y.; Sun, W.; Han, S.; Li, J.; Ding, S.; Wang, W.; Yin, Y. IGF-1-Involved Negative Feedback of NR2B NMDA Subunits Protects Cultured Hippocampal Neurons Against NMDA-Induced Excitotoxicity. *Mol. Neurobiol.* **2017**, *54*, 684–696. [[CrossRef](#)] [[PubMed](#)]
54. Izumida, H.; Takagi, H.; Fujisawa, H.; Iwata, N.; Nakashima, K.; Takeuchi, S.; Iwama, S.; Namba, T.; Komatu, Y.; Kaibuchi, K.; et al. NMDA receptor antagonist prevents cell death in the hippocampal dentate gyrus induced by hyponatremia accompanying adrenal insufficiency in rats. *Exp. Neurol.* **2017**, *287*, 65–74. [[CrossRef](#)] [[PubMed](#)]
55. Volianskis, A.; France, G.; Jensen, M.S.; Bortolotto, Z.A.; Jane, D.E.; Collingridge, G.L. Long-term potentiation and the role of N-methyl-D-aspartate receptors. *Brain Res.* **2015**, *1621*, 5–16. [[CrossRef](#)] [[PubMed](#)]
56. Amidfar, M.; Kim, Y.K.; Wiborg, O. Effectiveness of memantine on depression-like behavior, memory deficits and brain mRNA levels of BDNF and TrkB in rats subjected to repeated unpredictable stress. *Pharmacol. Rep.* **2018**, *70*, 600–606. [[CrossRef](#)]
57. Hu, N.W.; Klyubin, I.; Anwyl, R.; Rowan, M.J. GluN2B subunit-containing NMDA receptor antagonists prevent A β -mediated synaptic plasticity disruption in vivo. *Proc. Natl. Acad. Sci. USA* **2009**, *106*, 20504–20509. [[CrossRef](#)]
58. Liu, Z.; Zhou, T.; Ziegler, A.C.; Dimitrion, P.; Zuo, L. Oxidative Stress in Neurodegenerative Diseases: From Molecular Mechanisms to Clinical Applications. *Oxid. Med. Cell. Longev.* **2017**, *2017*, 2525967. [[CrossRef](#)]
59. Kamat, P.K.; Kalani, A.; Rai, S.; Swarnkar, S.; Tota, S.; Nath, C.; Tyagi, N. Mechanism of Oxidative Stress and Synapse Dysfunction in the Pathogenesis of Alzheimer's Disease: Understanding the Therapeutics Strategies. *Mol. Neurobiol.* **2016**, *53*, 648–661. [[CrossRef](#)]
60. Lau, C.G.; Takeuchi, K.; Rodenas-Ruano, A.; Takayasu, Y.; Murphy, J.; Bennett, M.V.I.; Zukin, R.S. Regulation of NMDA receptor Ca²⁺ signalling and synaptic plasticity. *Biochem. Soc. Trans.* **2009**, *37*, 1369–1374. [[CrossRef](#)]
61. Reyes, R.C.; Brennan, A.M.; Shen, Y.; Baldwin, Y.; Swanson, R.A. Activation of neuronal NMDA receptors induces superoxide-mediated oxidative stress in neighboring neurons and astrocytes. *J. Neurosci.* **2012**, *32*, 12973–12978. [[CrossRef](#)] [[PubMed](#)]
62. Kamat, P.K.; Rai, S.; Swarnkar, S.; Shukla, R.; Nath, C. Mechanism of synapse redox stress in Okadaic acid (ICV) induced memory impairment: Role of NMDA receptor. *Neurochem. Int.* **2014**, *76*, 32–41. [[CrossRef](#)] [[PubMed](#)]
63. Tönnies, E.; Trushina, E. Oxidative Stress, Synaptic Dysfunction, and Alzheimer's Disease. *J. Alzheimers Dis.* **2017**, *57*, 1105–1121. [[CrossRef](#)] [[PubMed](#)]
64. Castro-Alvarez, J.F.; Uribe-Arias, A.; Raigoza, D.M.; Cardona-Gómez, G.P. Cyclin-dependent kinase 5, a node protein in diminished tauopathy: A systems biology approach. *Front. Aging Neurosci.* **2014**, *6*, 232. [[CrossRef](#)] [[PubMed](#)]
65. Liu, Y.; Cao, L.; Zhang, X.; Liang, Y.; Xu, Y.; Zhu, C. Memantine Differentially Regulates Tau Phosphorylation Induced by Chronic Restraint Stress of Varying Duration in Mice. *Neural Plast.* **2019**, *2019*, 4168472. [[CrossRef](#)] [[PubMed](#)]
66. Li, L.; Sengupta, A.; Haque, N.; Grundke-Iqbal, I.; Iqbal, K. Memantine inhibits and reverses the Alzheimer type abnormal hyperphosphorylation of tau and associated neurodegeneration. *FEBS Lett.* **2004**, *566*, 261–269. [[CrossRef](#)]
67. Wang, X.; Blanchard, J.; Grundke-Iqbal, I.; Iqbal, K. Memantine attenuates Alzheimer's disease-like pathology and cognitive impairment. *PLoS ONE* **2015**, *10*, e0145441. [[CrossRef](#)]



SUPPLEMENTARY MATERIAL

Table S1: Antibodies used in Western blot studies

Antibody	Host	Source/Catalog	WB dilution
NMDAR2A	Mouse	Santa Cruz/sc-515148	1:1000
NMDAR2B	Mouse	Santa Cruz/sc-365597	1:1000
p-NMDAR2B (Tyr1472)	Rabbit	Invitrogen/OPA1-04116	1:1000
Calpain-1	Mouse	BioRad/AHP2443	1:1000
Spectrin	Mouse	Millipore/MAB1622	1:1000
Caspase-3	Rabbit	BD Transduction Laboratories/C31720	1:1000
BCL-2	Rabbit	Cell Signaling/#2870	1:1000
SYN	Rabbit	Dako/CloneSY38	1:2000
PSD95	Rabbit	Abcam/ab18258	1:1000
TrkB	Rabbit	Santa Cruz/sc-8316	1:1000
SNAP25	Mouse	Santa Cruz/sc-20038	1:1000
SOD1	Mouse	Calbiochem/574597	1:1000
GPX1	Rabbit	Novus Biological/NBP1-33620	1:1000
p35/p25	Rabbit	Cell Signaling/#C64B10	1:1000
p-Tau Ser396	Rabbit	Invitrogen/44752G	1:1000
Tau total	Goat	Santa Cruz/sc-1995	1:1000
CDK5	Rabbit	Santa Cruz/sc-173	1:1000
p-CDK5	Rabbit	Abcam/ab63550	1:1000
GAPDH	Mouse	Millipore/MAB374	1:2000
Goat-anti-mouse HRP conjugated		BioRad/170-5047	1:2000
Goat-anti-rabbit HRP conjugated		BioRad/170-6515	1:2000
Donkey-anti-goat HRP conjugated		Santa Cruz/sc-2020	1:2000

Table S2: Primers used in qPCR studies.

Target	Product size (bp)	Forward primer (5'-3')	Reverse primer (5'-3')
<i>Hmox1</i>	177	TGACACCTGAGGTCAAGCAC	GTCTCTGCAGGGGCAGTATC
<i>Cox-2</i>	126	TGACCCCAAGGCTCAAATA	CCCAGGTCTCGCTTATGATC
<i>Vgf</i>	178	GTCAGACCCATAGCTCCC	CTCGGACTGAAATCTCGAAGTTC
<i>Tgf</i>	204	CAGGGTGAAGGGGAAAATC	AGTTCGGTCATTGAGTCTCGC
<i>β-Actin</i>	190	CAACGAGCGGTTCCGAT	GCCACAGGTTCCATACCA

Table S3: Parameters measured in the Three Chamber Test (TCT). (sec): Time in each chamber. Results are expressed as a mean ± Standard error of the mean (SEM). \$ p < 0.05 vs SR1 RL-208.

Time in Chamber:	SR1 Control	SR1 RL-208 (5mg/Kg)	SP8 Control	SP8 RL-208 (5mg/Kg)
Habituation				
Right zone	109.30 ± 20.05	86.72 ± 17.61	119.4 ± 8.48	149.10 ± 10.41 [§]
Left zone	110.09 ± 22.69	108.57 ± 23.52	119.21 ± 9.33	97.55 ± 9.68
Center zone	80.62 ± 11.20	104.71 ± 17.62	51.39 ± 2.13 [§]	53.35 ± 6.20

Table S4: Parameters measured in the Novel object recognition test (NORT). (sec): Time spent exploring each object during the familiarization phase. Results are expressed as a mean ± Standard error of the mean (SEM). *p < 0.05 vs SR1 Control.

Time spent exploring objects (sec):	SR1 Control	SR1 RL-208 (5mg/Kg)	SP8 Control	SP8 RL-208 (5mg/Kg)
Familiarization phase				
Left object	42.11 ± 4.25	39.88 ± 4.06	40.15 ± 3.55	39.63 ± 4.29
Right Object	40.56 ± 3.21	41.08 ± 2.56	42.36 ± 5.33	41.27 ± 3.07

Table S5: Parameters measured in the Object location test (OLT). (sec): Time spent exploring each object. Results are expressed as a mean ± Standard error of the mean (SEM). *p < 0.05 vs SR1 Control.

Time spent exploring objects (sec):	SR1 Control	SR1 RL-208 (5mg/Kg)	SP8 Control	SP8 RL-208 (5mg/Kg)
Habituation phase				
Object A1	28.01 ± 2.45	21.96 ± 1.96	33.35 ± 3.86	23.13 ± 2.09
Object A2	29.43 ± 2.43	25.78 ± 3.06	29.96 ± 4.23	26.47 ± 2.87

3.2 Article 2

Design, synthesis, and *in vitro* and *in vivo* characterization of new memantine analogs for Alzheimer's disease

Turcu A. L.^{1,2}, **Companys-Alemaný J.**³, Phillips M. B.⁴, Patel D. S.⁵, Griñán-Ferré C.³, Loza M. I.⁶, Brea J. M.⁶, Pérez B.⁷, Soto, D.^{2,8}, Sureda F. X.⁹, Kurnikova M. G.⁵, Johnson J. W.⁴, Pallàs M.³, Vázquez S.¹ *European Journal of Medicinal Chemistry*. 2022. 8;236:114354.

doi: <https://doi.org/10.1016/j.ejmech.2022.114354>

JCR 2020 IF: 6,51

Afiliacions:

¹ Laboratori de Química Farmacèutica (Unitat Associada al CSIC), Facultat de Farmàcia i Ciències de l'Alimentació i Institut de Biomedicina (IBUB), Universitat de Barcelona, Av. Joan XXIII, 27-31, 08028 Barcelona, Spain.

² Neurophysiology Laboratory, Physiology Unit, Department of Biomedicine, Medical School Universitat de Barcelona, August Pi i Sunyer Biomedical Research Institute (IDIBAPS), Barcelona, and Institut of Neurosciences, 08036 Barcelona, Spain.

³ Departament de Farmacologia, Toxicologia i Química Terapèutica. Facultat de Farmàcia i Ciències de l'Alimentació. Institut de Neurociències, Universitat de Barcelona (NeuroUB). Av. Joan XXIII 27-31, 08028 Barcelona, Espanya.

⁴ Department of Neuroscience and Center for Neuroscience, University of Pittsburgh, Pittsburgh, Pennsylvania 15260, United States.

⁵ Chemistry Department, Carnegie Mellon University, 4400 Fifth Ave, Pittsburgh, Pennsylvania 15213, United States.

⁶ Innopharma Screening Platform, Biofarma Research Group, Centro de Investigación en Medicina Molecular y Enfermedades Crónicas, Universidad de Santiago de Compostela, Edificio CIMUS, Av. Barcelona, S/N, E-15706 Santiago de Compostela, Spain.

⁷ Department of Pharmacology, Therapeutics and Toxicology, Autonomous University of Barcelona, E-08193 Bellaterra, Spain.

⁸ August Pi i Sunyer Biomedical Research Institute (IDIBAPS), Barcelona, Spain.

⁹ Pharmacology Unit, Faculty of Medicine and Health Sciences, Universitat Rovira i Virgili, C./ St. Llorenç 21, 43201 Reus, Tarragona, Spain.

RESUM

Donada la necessitat d'obtenir noves teràpies pel tractament de la MA, es van sintetitzar una nova sèrie de compostos anàlegs de la memantina amb una estructura de benzohomoadamantà. La majoria dels nous compostos eren capaços de bloquejar el receptor NMDA a escala micromolar.

L'anàlisi electrofisiològic i l'anàlisi de la dinàmica molecular van assenyalar el compost IIC (en aquesta tesi doctoral anomenat UB-ALT-EV) com el compost candidat ser utilitzat per a assajos *in vivo*. El nematode *C.elegans* va permetre avaluar, en primera instància, els efectes del compost IIC sobre fenotips associats a l'acumulació d'oligòmers d'A β . Tant la soca CL2006, que presenta acumulacions del pèptid A β a les cèl·lules musculars, com la soca CL2355 que expressa el pèptid A β a les neurones van mostrar una millora del seu fenotip després del tractament amb el compost IIC. Així mateix, es va dur a terme l'avaluació de l'efecte farmacològic del compost IIC en un model de ratolí transgènic de la MA, el 5XFAD, mitjançant un tractament crònic per via oral. L'avaluació cognitiva, mitjançant el test de reconeixement de l'objecte nou (NORT), tal com s'esperava, va indicar una millora la memòria de treball dels animals 5XFAD femella tractats durant un mes per via oral. A més, l'estudi molecular va permetre demostrar l'activació de vies de supervivència neuronal, a través de l'avaluació de la fosforilació de la subunitat GluN2B del receptor NMDA a la posició Y1472 i de Fyn, la quinasa encarregada d'aquesta fosforilació, l'expressió proteica de PSD95 i de la translocació al nucli de del factor de transcripció CREB.

En resum aquests resultats van indicar l'efecte neuroprotector induït pel tractament amb el compost IIC, assenyalant-lo com el compost líder de la sèrie (del terme en anglès *lead compound*) i com un potencial nou agent terapèutic per al tractament de la MA.

En aquest treball la meua participació ha estat la determinació de la caracterització farmacològica del compost IIC en els models *in vivo* *C.elegans* i 5XFAD.



ELSEVIER

Contents lists available at ScienceDirect

European Journal of Medicinal Chemistry

journal homepage: <http://www.elsevier.com/locate/ejmech>Design, synthesis, and *in vitro* and *in vivo* characterization of new memantine analogs for Alzheimer's disease

Andreea L. Turcu^{a, b}, Júlia Companys-Aleman^c, Matthew B. Phillips^d, Dhilon S. Patel^e, Christian Griñán-Ferré^c, M. Isabel Loza^f, José M. Brea^f, Belén Pérez^g, David Soto^{b, h}, Francesc X. Suredaⁱ, Maria G. Kurnikova^e, Jon W. Johnson^d, Mercè Pallàs^c, Santiago Vázquez^{a, *}

^a Laboratori de Química Farmacèutica (Unitat Associada al CSIC), Facultat de Farmàcia i Ciències de l'Alimentació i Institut de Biomedicina (IBUB), Universitat de Barcelona, Av. Joan XXIII, 27-31, 08028, Barcelona, Spain

^b Neurophysiology Laboratory, Department of Biomedicine, Faculty of Medicine and Health Sciences, Institute of Neurosciences, University of Barcelona, 08036, Barcelona, Spain

^c Pharmacology Section, Department of Pharmacology, Toxicology and Therapeutic Chemistry, Faculty of Pharmacy and Food Sciences, Institute of Neurosciences (NeuroUB), Universitat de Barcelona, Av. Joan XXIII 27-31, 08028, Barcelona, Spain

^d Department of Neuroscience and Center for Neuroscience, University of Pittsburgh, Pittsburgh, PA, 15260, USA

^e Chemistry Department, Carnegie Mellon University, 4400 Fifth Ave, Pittsburgh, PA, 15213, USA

^f Inopharma Screening Platform, Biofarma Research Group, Centro de Investigación en Medicina Molecular y Enfermedades Crónicas, Universidad de Santiago de Compostela, Edificio CIMUS, Av. Barcelona, S/N, E, 15706, Santiago de Compostela, Spain

^g Department of Pharmacology, Therapeutics and Toxicology, Autonomous University of Barcelona, E-08193, Bellaterra, Spain

^h August Pi i Sunyer Biomedical Research Institute (IDIBAPS), Barcelona, Spain

ⁱ Pharmacology Unit, Faculty of Medicine and Health Sciences, Universitat Rovira i Virgili, C/ St. Llorenç 21, 43201, Reus, Tarragona, Spain

ARTICLE INFO

Article history:

Received 27 February 2022

Received in revised form

31 March 2022

Accepted 1 April 2022

Available online 8 April 2022

Keywords:

Alzheimer's disease
Benzohomoadamantane
Caenorhabditis elegans
Electrophysiology
5XFAD
Memantine analogs

ABSTRACT

Currently, of the few accessible symptomatic therapies for Alzheimer's disease (AD), memantine is the only *N*-methyl-*D*-aspartate receptor (NMDAR) blocker approved by the FDA. This work further explores a series of memantine analogs featuring a benzohomoadamantane scaffold. Most of the newly synthesized compounds block NMDARs in the micromolar range, but with lower potency than previously reported hit **11c**, results that were supported by molecular dynamics simulations. Subsequently, electrophysiological studies with the more potent compounds allowed classification of **11c**, a low micromolar, uncompetitive, voltage-dependent, NMDAR blocker, as a memantine-like compound. The excellent *in vitro* DMPK properties of **11c** made it a promising candidate for *in vivo* studies in *Caenorhabditis elegans* (*C. elegans*) and in the 5XFAD mouse model of AD. Administration of **11c** or memantine improved locomotion and rescues chemotaxis behavior in *C. elegans*. Furthermore, both compounds enhanced working memory in 5XFAD mice and modified NMDAR and CREB signaling, which may prevent synaptic dysfunction and modulate neurodegenerative progression.

© 2022 The Authors. Published by Elsevier Masson SAS. This is an open access article under the CC BY-NC-ND license (<http://creativecommons.org/licenses/by-nc-nd/4.0/>).

1. Introduction

Alzheimer's disease (AD) is a major and rising public health concern due to not only its increasing global prevalence, but also the lack of effective treatment options [1–3]. To date, only four drugs have approval for treating AD. Unfortunately, these drugs only improve cognitive and behavioral symptoms without

modifying the course of the disease. Despite intensive efforts to develop new AD pharmacotherapeutics [4], progress has been slow and difficult. For example, a new drug, aducanumab [5], has recently been approved by the Food and Drug Administration (FDA). However, its approval is mired in controversy due to risk of severe side effects and conflicting reports of efficacy [6–9].

The first drugs developed for AD, the acetylcholinesterase inhibitors (AChEIs), aim to revert the cholinergic deficit responsible for the cognitive impairment of patients [10]. In addition to currently available AChEIs (donepezil, rivastigmine and

* Corresponding author.

E-mail address: svazquez@ub.edu (S. Vázquez).

galantamine), multiple AChEIs have been developed over the last few years. However, few novel AChEIs have reached clinical trials and none have arrived at the market [11–16].

Another drug approved by the FDA is memantine, a *N*-methyl-*D*-aspartate receptors (NMDAR) uncompetitive antagonist [17,18]. Memantine acts as an open channel blocker that is thought to prevent NMDAR overactivation and glutamate-mediated neurotoxicity in the pathogenesis of AD [19,20]. It has better therapeutic tolerability and favorable safety relative to other NMDAR channel blockers because of its ability to preferentially block extrasynaptic NMDARs, which have been associated with activation of cell death pathways [21]. Memantine is characterized by faster blocking/unblocking kinetics, strong voltage dependency, and moderate affinity for NMDAR [22]. Due to its excellent drug profile, numerous companies and academic groups have developed new analogs of memantine. Although only neramexane has reached clinical trials [23], much effort is still ongoing for developing new NMDAR open channel blockers with pharmacological profiles similar to memantine for use as potential therapies for AD and other neurodegenerative diseases [24–34]. In addition, other NMDAR open channel blockers are also currently being developed for the treatment of tinnitus and as a new class of drugs with fast-onset antidepressant effects [35–41].

Recently, our research group has synthesized new memantine analogs based on a novel benzopolycyclic ring (Fig. 1). First, compounds with the general structure **I** were synthesized, but they were found to be less potent than memantine (e.g., **Ia** and **Ib**) [42,43]. Interestingly, the replacement of the oxygen atom at the C8 position of **Ia** ($IC_{50} = 98 \pm 26 \mu M$) by a methylene unit led to the seven-fold more potent amine **IIa** ($IC_{50} = 13.6 \pm 3.4 \mu M$). Thereafter, further variations at the C9 position in the general structure **II** generated compounds with promising potency, in the low-moderate micromolar range. Indeed, three of these derivatives displayed potencies very similar to (**IIc** and **IIg**) or even stronger than (**IIb**) memantine (Fig. 1) [44].

In our endeavor to find novel analogs of memantine, herein we report further structure-activity relationships (SAR) on the

benzohomoadamantane scaffold, i.e., derivatives of general structure **III**, in order to select a proper candidate for additional *in vitro* pharmacokinetic studies, and subsequently perform an *in vivo* study in a 5XFAD murine model of AD.

2. Results and discussion

2.1. Design and synthesis of new NMDAR channel blockers

First, to explore alternative substituents at the C9 position, we synthesized **2** (Scheme 1). It is known that H/D bioisosteric replacement may lead to compounds with the same activity and selectivity [45–47]. Furthermore, considering that the C9 position is susceptible to being metabolized, the presence of deuterium may be a good strategy to avoid rapid metabolization and prolong the pharmacokinetic stability of the compound [48]. The approach followed for the synthesis of **2** was similar to that previously applied to the preparation of **IIb** [44]. Thus, the reaction of known alcohol **1** [44] with thionyl bromide followed by radical dehalogenation of the unstable bromo intermediate, generated the amine **2** in moderate overall yield (Scheme 1).

We have previously reported that the NMDAR antagonist activities of amantadine and its ring-contracted analogs are of the same order of magnitude [49]. Consequently, we also designed the ring-contracted analog **6**, by removing a methylene group from **IIb** and bonding positions C7 and C9 (Scheme 1). The synthesis of amine **6** involved four steps: a) reaction of known alcohol **3** [50] with mesyl chloride; b) reaction of the corresponding mesylate with NaI in the presence of H_3PO_3 to furnish iodide **4**; c) radical photochemical carboxylation of **4** to carboxylic acid **5**; and, d) Curtius rearrangement of **5** to generate primary amine **6**.

We have previously synthesized and described several derivatives of **I** and **II**, but, so far, we have not explored the impact of introducing substituents on the aromatic ring of the benzohomoadamantane scaffold. Although **IIb** ($IC_{50} = 0.70 \pm 0.12 \mu M$), **IIc** ($IC_{50} = 1.93 \pm 0.21 \mu M$) and **2** ($IC_{50} = 1.2 \pm 0.1 \mu M$) are more potent NMDAR antagonists than **IIa** ($IC_{50} = 13.6 \pm 3.40 \mu M$, see below), we

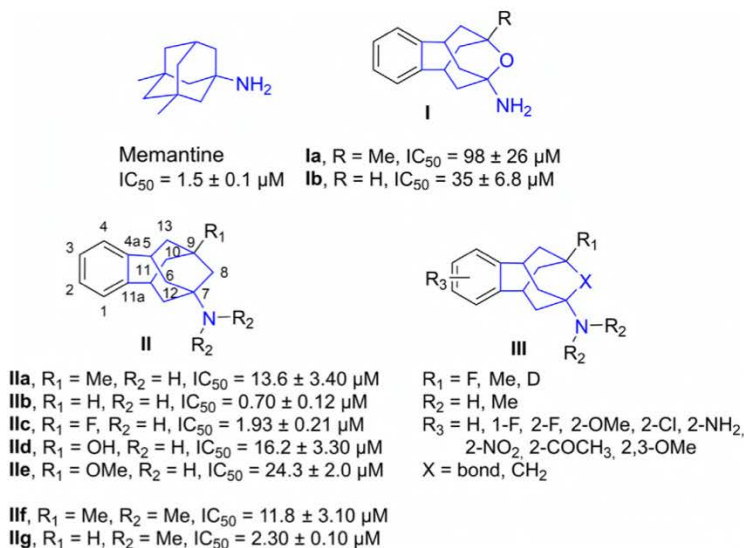
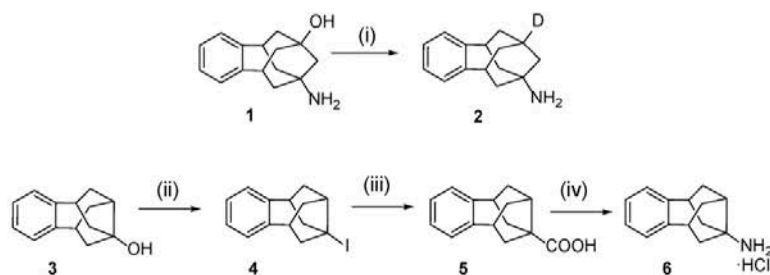


Fig. 1. Structures of memantine, previously studied polycycles **Ia-b** and **IIa-g**, and the new series **III**. IC_{50} values for memantine and polycycles **Ia-b** and **IIa-g** are provided under each structure.



Scheme 1. Synthesis of series III amines **2** ($R_1 = D$, $X = CH_2$) and **6** ($R_1 = H$, $X = bond$). Reagent and conditions: (i) 1) $SOBr_2$, toluene, rt, 1.5 h; 2) Bu_3SnD , AIBN, anh toluene, $95^\circ C$, 4 h, 40% overall yield. (ii) 1) Methanesulfonyl chloride, pyridine, $120^\circ C$, 5 h; 2) H_3PO_3 , NaI, $150^\circ C$, 6 h, 76% overall yield. (iii) 1) bis(tributyltin), methyl oxalyl chloride, anh toluene, hv, 20 h; 2) MeOH, Et_3N ; 3) KOH/MeOH 40%, 2 h; 4) H_2O , reflux, 3 h, 37% overall yield. (iv) DPPA, Et_3N , toluene, reflux, 3 h; 2) HCl 6 N, reflux, 24 h; 3) HCl/MeOH, 39% overall yield.

first decided to screen the NMDAR blocking activity of benzene-substituted derivatives based on **IIa**, because this amine shows an excellent compromise between acceptable potency as NMDAR channel blocker and better synthetic availability. Therefore, we prepared a series of ten derivatives of general structure III ($R_1 = Me$, $X = CH_2$) which are analogs of **IIa**, by introducing a variety of electron-withdrawing and electron-donating group on the aromatic ring. The key introduction of the substituents in the aromatic ring was accomplished using two alternative procedures (Schemes 2–4).

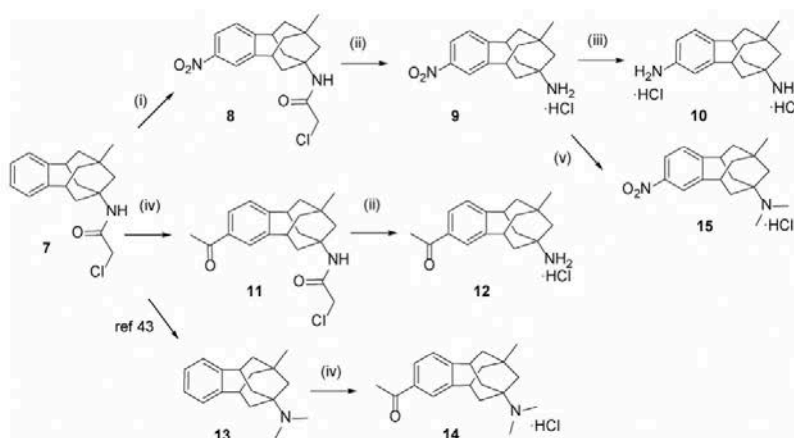
In the first approach, electrophilic aromatic substitution reactions on known chloroacetamide **7** [43] or acetamide **16** [51] were carried out for the synthesis of **9**, **10**, **12**, **14**, **15** and **20**. Thus, from the known chloroacetamide **7**, following a classical approach that involved aromatic nitration and cleavage of the chloroacetyl group, amine **9** was obtained. Catalytic hydrogenation of **9** furnished aniline **10**. Additionally, Friedel–Crafts acylation of **7**, followed by deprotection afforded amine **12** in good yield. A Friedel–Crafts reaction of the known **13** [43] led to amine **14** and a reductive alkylation of **9** provided amine **15** (Scheme 2).

A first attempt to obtain amine **20**, through catalytic hydrogenation of **8** followed by a classical Sandmeyer reaction and removal of the chloroacetamide group, met with failure. Thus, **20** was

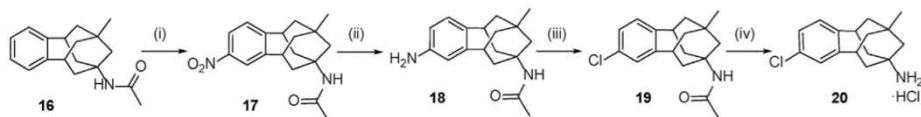
prepared from the known acetamide **16** [51] through a four-step process that involved aromatic nitration, catalytic hydrogenation, Sandmeyer reaction, and hydrolysis (Scheme 3).

A different synthetic strategy was undertaken for the synthesis of the aromatic substituted compounds **37–40**, which involved the construction of the benzohomoadamantane scaffold starting from a suitably mono- or disubstituted *o*-phthalaldehyde (Scheme 4). Thus, once the substituted *o*-phthalaldehydes **21** [52], **22** [53], **23** [54], and **24** [55] were obtained via procedures previously reported, a synthetic route that included a Weiss-Cook condensation [56], hydrolysis, decarboxylation, and dehydration led to the corresponding diketones **25–28**. Subsequently, the treatment of these ketones under Wittig olefination and Ritter-type transannular cyclization conditions furnished the chloroacetamides **33–36** that after deprotection provided the desired amines **37–40**.

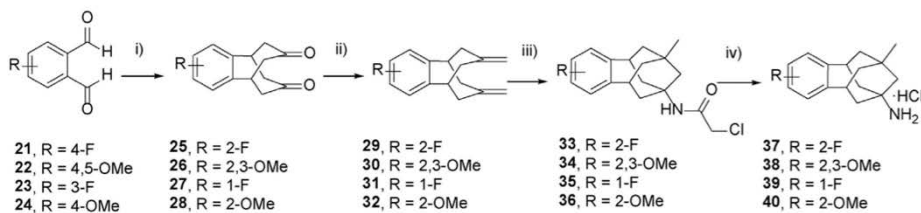
In order to determine the effects of different aromatic substituents on NMDAR block, the potency of the new benzohomoadamantane substituted amines **9–10**, **12**, **14–15**, **20** and **37–40** was tested (see below) and compared with that of the unsubstituted **IIa** (Table 1). Briefly, the introduction of substituents in the aromatic ring resulted in a decrease in the potency as NMDAR blockers for the majority of compounds regardless of the position, size or electronic character of the substituent (**9**, $IC_{50} = 164 \mu M$; **10**,



Scheme 2. Synthesis of amines **9**, **10**, **12**, **14** and **15** (compounds from series III with $R_1 = Me$ and $X = CH_2$). Reagent and conditions: (i) fuming HNO_3 , Ac_2O , AcOH, $0^\circ C$ to rt, overnight, 85% yield. (ii) 1) thiourea, glacial AcOH, abs. ethanol, reflux, overnight; 2) HCl/ Et_2O , 74% overall yield for **9** and 52% overall yield for **12**. (iii) 1) H_2 , Pd/C, MeOH, 1 atm, rt, 48 h; 2) HCl/MeOH, quant. overall yield. (iv) CH_3COCl , $AlCl_3$, DCM, rt, 1 h, 54% yield for **11** and 40% yield for **14** as hydrochloride salt obtained with HCl/ Et_2O . (v) 1) formalin 37%, $NaBH_3CN$, glacial AcOH, MeOH, rt, overnight; 2) HCl/ Et_2O , 74% overall yield.



Scheme 3. Synthesis of amine **20** (compound from series **III** with $R_1 = \text{Me}$ and $X = \text{CH}_2$). Reagent and conditions: (i) fuming HNO_3 , Ac_2O , AcOH , 0°C to rt, overnight, 60% yield. (ii) H_2 , PtO_2 , EtOH , 1 atm, rt, 4 h, 68% yield. (iii) 1) $\text{NaNO}_2/\text{conc. HCl}$, $<5^\circ\text{C}$; 2) $\text{CuCl}/\text{conc. HCl}$, 60°C , 90 min, 21% overall yield. (iv) 1) conc. $\text{HCl}/2$ -propanol, 6 days, reflux; 2) $\text{HCl}/\text{Et}_2\text{O}$, 19% overall yield.



Scheme 4. Synthesis of amines **37–40** (compounds from series **III** with $R_1 = \text{Me}$ and $X = \text{CH}_2$). Reagent and conditions: (i) 1) dimethyl-1,3-acetonedicarboxylate, Et_2NH , MeOH , reflux, 1.5 h; 2) glacial AcOH , conc. HCl , reflux, 12 h; 3) Toluene, reflux, 13% overall yield for **25**, 30% for **26**, 51% for **27**, 65% for **28**. (ii) $\text{Ph}_3\text{PCH}_3\text{I}$, NaH , anh DMSO , 90°C , overnight, 60% yield for **29**, 23% for **30**, 69% for **31**, 38% for **32**. (iii) ClCH_2CN , conc. H_2SO_4 , AcOH , 0°C to rt, overnight, 48% yield for **33**, 75% yield for **34**, 68% yield for **35**, 57% for **36**. (iv) 1) thiourea, glacial AcOH , abs. ethanol, reflux, overnight; 2) $\text{HCl}/\text{Et}_2\text{O}$, 36% overall yield for **37**, 81% for **38**, 84% for **39**, 81% for **40**.

Table 1

IC_{50} values (μM) of the new series **III** of benzohomoadamantane derivatives as NMDAR channel blockers and of references **IIa–c** and memantine.^a

Comp.	IC_{50} (μM)
2	1.16 ± 0.07
6	111 ± 18.8
9	164 ± 4.48
10	NA ^b
12	323 ± 89.2
14	566 ± 186
15	309 ± 120
20	34.7 ± 5.98
37	30.9 ± 4.70
38	517 ± 54.7
39	13.2 ± 1.07
40	77.4 ± 13.5
44	29.0 ± 11.9
IIa ^c	13.6 ± 3.40
IIb ^d	0.70 ± 0.12
IIc ^d	1.93 ± 0.21
Memantine	1.5 ± 0.1

^a Functional data were obtained from primary cultures of cerebellar granule neurons using the method described in the experimental section by measuring the intracellular calcium concentration. Cells were challenged with NMDA as indicated. Data shown are means \pm SEM of at least three separate experiments carried out on three different batches of cultured cells.

^b NA, non-active.

^c See ref. 43.

^d See ref. 44.

IC_{50} = not active; **12**, IC_{50} = $323 \mu\text{M}$; **14**, IC_{50} = $566 \mu\text{M}$; **15**, IC_{50} = $309 \mu\text{M}$; **20**, IC_{50} = $34.7 \mu\text{M}$; **37**, IC_{50} = $30.9 \mu\text{M}$; **38**, IC_{50} = $517 \mu\text{M}$; **39**, IC_{50} = $13.2 \mu\text{M}$; **40**, IC_{50} = $77.4 \mu\text{M}$ (see below and Table 1). An exception to this trend is amine **39**, with a fluorine atom at the C1 position, the potency of which (IC_{50} = $13.2 \mu\text{M}$) was similar to that of **IIa** (IC_{50} = $13.6 \mu\text{M}$). Thus, once this screening was completed with derivatives of **IIa**, and considering the electrophysiological studies carried out with **IIb**, **IIc** and **2** (see below), amine **44** was envisaged as a promising compound. **44** contains two fluorine atoms at C1 and C9 and was synthesized starting from

the diketone **27**, through a four-step sequence that involved a selective mono-Wittig olefination, followed by a Ritter-type transannular cyclization, substitution of the hydroxyl group by a fluorine atom and final removal of the chloroacetamide group (Scheme 5).

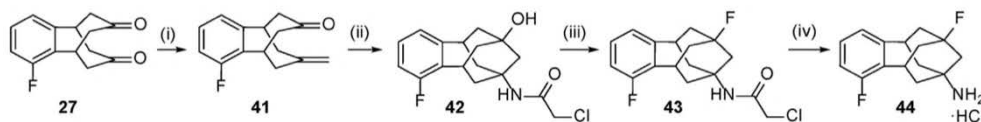
The new amines, **2**, **6**, **9–10**, **12**, **14–15**, **20**, **37–40**, and **44**, were fully characterized as hydrochlorides through their spectroscopic data and elemental analyses or HPLC/UV (see Experimental Section and supporting information for further details).

2.2. NMDAR blockers activities and SAR

To evaluate whether the synthesized compounds were able to block NMDARs, we measured their effect on increases in intracellular calcium evoked by $100 \mu\text{M}$ NMDA (in the presence of $10 \mu\text{M}$ of glycine) on rat cultured cerebellar granule neurons using a previously reported Fura 2 assay (Table 1) [57].

As expected, the substitution of the hydrogen atom at C9 in **IIb** by a deuterium atom did not affect the biological potency of **2** (IC_{50} = $0.70 \pm 0.12 \mu\text{M}$ for **IIb** vs IC_{50} = $1.16 \pm 0.07 \mu\text{M}$ for **2**). However, the ring contraction from **IIb** to **6** resulted in a dramatic drop in potency (IC_{50} = $0.70 \pm 0.12 \mu\text{M}$ for **IIb** vs IC_{50} = $111 \pm 18.8 \mu\text{M}$ for **6**).

Regarding the aromatic substitution, it can be concluded that the functionalization of the aromatic ring is highly deleterious for the compound's NMDAR channel blocking potency (Table 1), regardless of the electron donor or acceptor character of the substituent (compare **IIa** vs **9**, **10**, **12**, **20**, **37–40**). However, size and substitution position exerted a certain influence on potency. Small size substituents such as chlorine (**20**) and fluorine (**37**) at C2 were less deleterious for potency than bigger substituents such as a nitro (**9**) or an acetyl (**12**) group. More importantly, the introduction of a fluorine atom at C1, as in **39** (IC_{50} = $13.2 \pm 1.07 \mu\text{M}$) does not alter the IC_{50} value in respect to the unsubstituted **IIa** (IC_{50} = $13.6 \pm 3.4 \mu\text{M}$), unlike **37** (IC_{50} = $30.9 \pm 4.70 \mu\text{M}$) which possesses the fluorine atom at C2. Overall, within this series of new amines featuring a methyl group at C9, **39**, with its fluorine atom at C1, emerged as the most interesting derivative. Due to the effect of the C1 fluorine atom and our finding that the replacement of **IIa**'s methyl group at C9 with a fluorine atom, as in **IIc**, resulted in a



Scheme 5. Synthesis of amine **44** (compound from series **III** with $R_1 = F$ and $X = CH_2$). Reagent and conditions: (i) Ph_3PCH_3 , NaH, anh DMSO, 90 °C, overnight, 46% yield. (ii) $ClCH_2CN$, conc. H_2SO_4 , DCM, 0 °C to rt, overnight, 32% yield. (iii) diethylaminosulfur trifluoride (DAST), DCM, -30 °C to rt, overnight, 69% yield. (iv) 1) thiourea, glacial AcOH, abs. ethanol, reflux, overnight; 2) HCl/Et_2O , 79% yield.

remarkable increase of potency, we synthesized amine **44**. Unexpectedly, **44** ($IC_{50} = 29.0 \pm 11.9 \mu M$) was a less potent NMDAR channel blocker than **IIc** ($IC_{50} = 1.93 \pm 0.21 \mu M$).

Finally, within this new series of benzohomoadamantane derivatives, tertiary amines were clearly less potent than the corresponding primary amines (**9** vs **15** and **12** vs **14**), in contrast to the trend observed in reference compounds **IIa** and **IIb**.

Overall, with the sole exception of the deuterated amine **2** ($IC_{50} = 1.16 \pm 0.07 \mu M$), all the amines herein reported were less potent as NMDAR channel blockers than the previously described amines **IIb** ($IC_{50} = 0.70 \pm 0.12 \mu M$) and **IIc** ($IC_{50} = 1.93 \pm 0.21 \mu M$). Particularly striking is the marked decrease in potency when going from **IIb** to its ring-contracted analog **6** ($IC_{50} = 111 \pm 18.8 \mu M$).

2.3. Molecular dynamics (MD) simulations

Electrophysiological studies (see discussion below in electrophysiology section) confirmed NMDAR channel blocking ability for compounds investigated in this study. However, to better understand molecular mechanisms of how these channel blockers occlude ion permeation and to rationalize the differential binding affinities of these benzohomoadamantane derivatives caused by ring contraction, the exchange of substituent at the C9 position, or introduction of different groups on the aromatic ring, we used molecular dynamic (MD) simulations. We have developed a computational structural model of the NMDAR (GluN1/2A) trans-membrane domain with a closed gate. We selected four compounds, **IIa**, **IIb**, **IIc** and **6**, to generate initial docking-based protein-ligand complex structures for NMDAR-**IIa**, NMDAR-**IIb**, NMDAR-**IIc** and NMDAR-**6**. The complexes then were embedded in a POPC lipid bilayer and solvated in water and 0.15 M NaCl solution. 200 ns molecular dynamics simulations were carried out for each of the structures to allow for equilibration of the ligand in the channel in native-like conditions. From these simulations we obtained atomic level insights on binding modes and their stabilities to analyze how their structural and dynamic features correlate with the reported difference in the binding affinities of these compounds.

During MD simulations, all compounds showed stable binding in a “flipped down” conformation (Fig. 2) with the NH_3^+ groups facing the intracellular side of the membrane. In this flipped down conformation the NH_3^+ groups formed H-bond interactions with the asparagine (ASN) clusters at the tips of the M2 helices of GluN1 (N616) and GluN2A (N614) subunits. The hydrophobic aromatic core of the compounds stabilized between the protein channel sub-pockets created by the hydrophobic side chains of L642 and A643 of GluN2A, and V644, A645 and M641 of GluN1 inside the channel (Fig. 2A–C). Similar flipped down binding modes were reported for memantine and MK-801 in the GluN1/2B NMDAR channel [58].

For all compounds that stabilized in flipped down conformations, we observed mobility of the blocker’s hydrophobic core in the plane of its phenyl ring. This mobility allowed for different binding pose occupancies within the sub-pockets created between M3 helices of GluN1 and GluN2A (Fig. 3). Similar flexible orientations were reported in MD simulations of MK-801 in the GluN1/2B

NMDAR channel [58]. Orientationally different poses are indeed stable in flipped down binding conformations (Fig. S1) and could easily block ion conduction by physical occlusion of the permeation pathway.

Comparing MD simulation results provided further insights into binding differences among **IIa**, **IIb** and **IIc**. For example, very close contact of the methyl at C9 in **IIa** (Fig. 2A) with the side chain hydroxyl groups of the threonines (T648 – GluN1 and T647 – GluN2A) inside the channel cavity may cause an energetic penalty on binding, which could explain the reduced binding affinity of **IIa** in comparison to **IIb** (Fig. 2B). In contrast, due to the smaller size of the fluorine at this position in **IIc**, there is no steric clash with threonine side chains, which may explain the more similar potencies of **IIb** and **IIc** (Fig. 2C). These observations also suggest that any substitution larger than hydrogen or fluorine will result in a steric clash with the hydrophobic wall and would require a wider channel opening to accommodate such a compound. Furthermore, the simulations showed that heavy atoms of the protein side chains are within 4 Å of the phenyl ring (Fig. 2). This suggests that any substitution on the aromatic ring will negatively affect binding since it will clash with the hydrophobic wall. Indeed, consistent with simulations, only unsubstituted derivatives of the phenyl ring (**IIa–g** and **2**) and their fluorinated analogs (**37**, **39** and **44**) showed acceptable potency (Fig. 1 and Table 1).

Finally, MD simulations performed with **6** showed a flipped down binding mode similar to **IIa**, **IIb** and **IIc** where the NH_3^+ of **6** maintains H-bonding interaction to ASN cluster through the majority of the MD simulation time (Fig. 2D). However, we observed a slight instability of the flipped down conformation. This could be explained by the presence of water molecules in the channel cavity between the hydrophobic core of compound **6** and the hydrophobic residues of the channel, which is likely due to the smaller size of the ring-contracted **6** (Fig. 2D). Considering that hydrophobic residues in the NMDAR channel cavity play an important role in the binding of channel blockers [59], the loss of the interaction between **6** and hydrophobic channel residues provides an explanation for the reduction of the potency of this amine.

2.4. Functional block of NMDAR by benzohomoadamantane derivatives **IIb**, **IIc**, and **2** compared with memantine

We next selected compounds with similar potency to memantine (**IIb**, **IIc** and **2**) and measured functional block of NMDAR. To measure the properties of the newly synthesized amines, we performed whole-cell patch-clamp recordings from tsA201 cells transfected with expression plasmids codifying for rat GluN1 and GluN2A subunits [28,60].

Fig. 4A shows representative current traces obtained using a protocol that allowed us to quickly screen NMDAR inhibition by the compounds of interest at two membrane potentials. While clamping the cell at -60 mV, NMDAR currents were elicited with 100 μM NMDA plus 10 μM glycine. After NMDA-mediated currents had reached a steady state, a blocking compound (either memantine, **IIb**, **IIc** or **2**) was applied for 40 s in the presence of agonist.

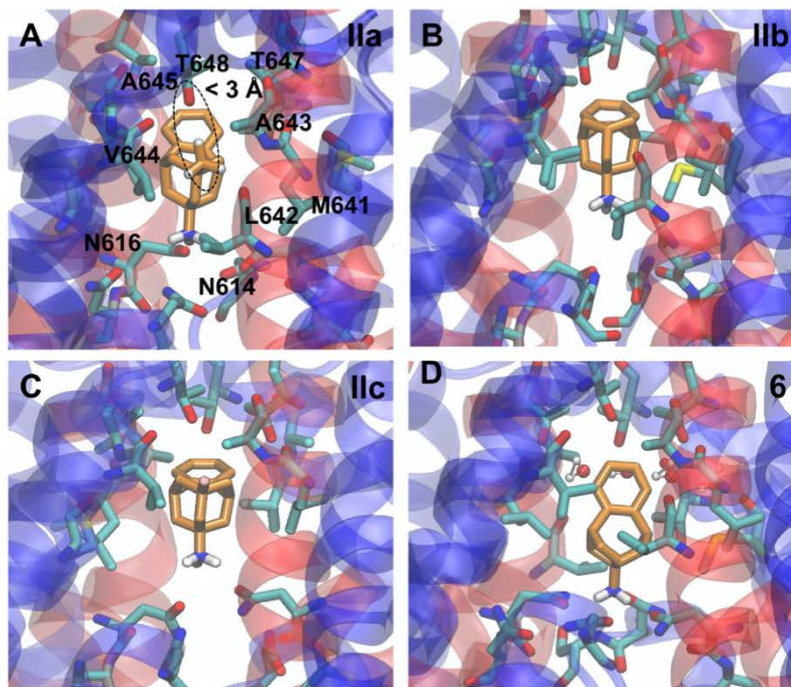


Fig. 2. Representative conformational orientation of **Ila** (A), **I Ib** (B), **I Ic** (C), and **6** (D). **A.** **Ila** shown with hydrophobic channel residues and ASN cluster residues also the methyl of **Ila** showed a minor clash (dotted circle) with threonine side chains from the cavity that may decrease its potency. **B.** **I Ib** shows similar interactions as **Ila** but no clash with threonine. **C.** **I Ic** shows similar interactions as **Ila**. **D.** **6** is shown surrounded by water molecules that may prevent it from interacting with the receptor binding pocket in the NMDA channel during MD simulations. In all panels GluN1 subunit is depicted as blue ribbons; GluN2A subunit is depicted as red ribbons; side chains of channel residues within 4 Å of compounds are shown in stick representations.

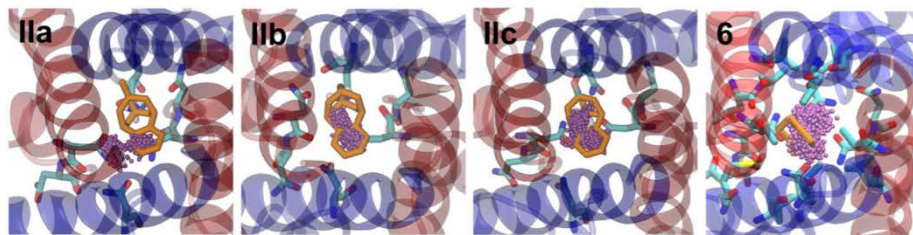


Fig. 3. Top view of the hydrophobic core orientation flexibility for **Ila**, **I Ib**, **I Ic** and **6** in XY plane with respect to phenyl ring inside the channel. Center of mass occupancies of phenyl rings are shown as purple balls.

During blocker application, the membrane voltage was jumped to +60 mV for 5 s and returned to −60 mV. Blocker then was removed to allow blocker unbinding and recovery of the current from inhibition, during which another 5 s jump to +60 mV was performed before returning to −60 mV and subsequent removal of agonists.

Although memantine, **I Ib**, and **2** show a similar degree of NMDAR inhibition, inhibition by **I Ic** was noticeably weaker ($69.1 \pm 1.2\%$ for **I Ic** vs. $86.2 \pm 1.4\%$ for memantine $p < 0.0001$; one-way ANOVA with Bonferroni's multiple comparison test; Fig. 4B). While no differences were observed in percentage of block for **2** in comparison to memantine ($89.3 \pm 3.1\%$; $p > 0.05$), **I Ib** appeared to

block slightly more efficiently than memantine ($94.1 \pm 1.4\%$; $p < 0.05$). Regarding blocking kinetics (measured as the time needed to reach approximately 2/3 of the maximal block; τ_{weighted} (weighted time constant) in seconds; see experimental section), all compounds tested presented values similar to memantine (around 1 s), although development of block by **I Ic** was faintly slower (Fig. 4C).

Inhibition by all known NMDAR channel blockers depends on membrane voltage, with potency increasing as membrane voltage is hyperpolarized. We assessed the voltage dependence of the compounds tested by applying two positive voltage steps to +60 mV in the presence of the blocker or after blocker washout

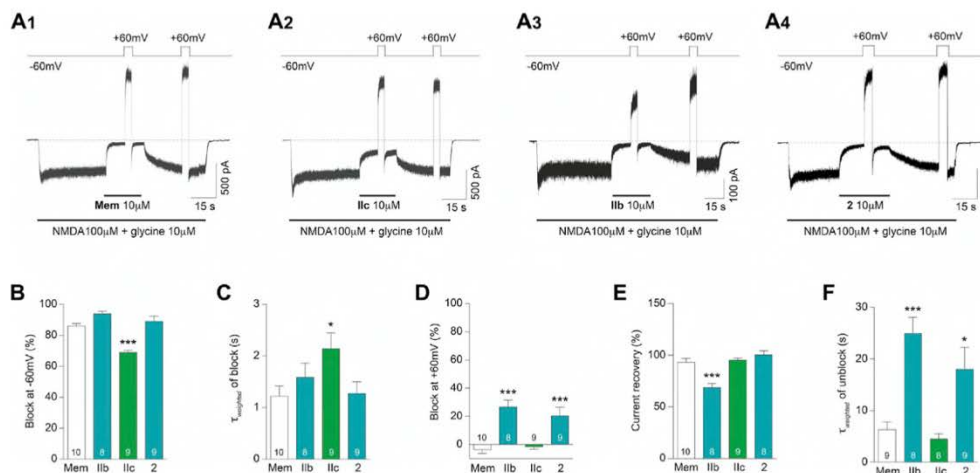


Fig. 4. Block, unbinding, voltage dependence, and blocking and unblocking kinetics of memantine (Mem), Ilb, Ilc and 2. **A.** Examples of whole-cell currents evoked by bath application of 100 μ M NMDA plus 10 μ M glycine onto tsA201 cells expressing GluN1/2A NMDARs. Compounds were rapidly applied with a piezoelectric device at 10 μ M in the presence of the agonists. **B.** Blocking percentage at the holding potential of -60 mV. Numbers inside bars denote the number of experiments. **C.** Blocking kinetics expressed in time constant (s). Numbers inside bars denote the number of experiments. **D.** Percentage of block at $+60$ mV ($n = 10, 8, 9$ and 9 for memantine, Ilb, Ilc and 2, respectively). **E.** Degree of unbinding, measured as the percentage of current recovery after removal of the blocker. Numbers inside bars denote the number of experiments. **F.** Unblocking kinetics expressed in time constant (s). Numbers inside bars denote the number of experiments. Asterisks identify mean values with statistically significant differences from the value for memantine: **** $p < 0.0001$, *** $p < 0.001$, ** $p < 0.01$, * $p < 0.05$.

(Equation (1)). We observed that Ilc showed strong voltage dependent block similar to that of memantine (Fig. 4D). Ilb and 2 showed weaker apparent voltage dependence of block: % block at $+60$ mV was $26.9 \pm 4.7\%$ for Ilb and $20.6 \pm 5.9\%$ for 2 compared to $-3.9 \pm 2.5\%$ for memantine ($p < 0.001$ for both compounds vs. memantine). It is likely that these results reveal that Ilb and 2 exhibit both weaker voltage dependence, and slower unblocking kinetics (Fig. 4F), than memantine or Ilc.

Importantly, a potential memantine-like compound should have similar unbinding kinetics. Therefore, we calculated the percentage of current recovery 40 s after removal of the blocker for the selected compounds and we compared it with that of memantine ($93.6 \pm 3.3\%$ recovery of current). Note that, because of the interposed depolarization, current recovery will depend on the drugs' unblocking kinetics both at -60 and at $+60$ mV. Ilb showed less current recovery than memantine ($69.0 \pm 3.6\%$ recovery; $p < 0.0001$ vs. memantine), whereas current recovery for Ilc and 2 was similar to memantine (Fig. 4E). The lower current recovery after 40 s observed for Ilb suggested that its unbinding kinetics are slower than memantine's, a conclusion supported by the observed unblocking kinetics (quantified as $\tau_{unblock}$; see experimental section; $\tau_{unblock} = 18.1 \pm 4.2$ s for Ilb vs. 6.4 ± 1.4 s for memantine; $p > 0.001$; Fig. 4F).

Since our main aim was to select the best memantine analog for an *in vivo* study, Ilb and 2 were discarded as candidates due to their relatively weak voltage dependence, despite their high potency. Although Ilc did not block to the same degree as memantine, it showed a similar electrophysiological profile and IC_{50} value, making it a suitable candidate for additional *in vitro* experiments and a subsequent *in vivo* study.

2.5. Characteristics of NMDAR inhibition by Ilc

We next further quantified the potency and voltage dependence of NMDAR inhibition by Ilc using whole-cell patch-clamp recordings from tsA201 cells expressing GluN1/2A receptors.

Inhibition by Ilc was measured as a function of drug concentration (Fig. 5A) and used to calculate the Ilc IC_{50} in cells held at -65 mV. The IC_{50} of Ilc was found to be 4.40 ± 0.15 μ M (Fig. 5B and C), well within the range of therapeutically beneficial NMDAR antagonists (e.g. ketamine $IC_{50} \sim 1$ μ M; memantine $IC_{50} \sim 1-2$ μ M; amantadine $IC_{50} \sim 40-75$ μ M) [28,61-68]. This IC_{50} value slightly differs from the Ilc IC_{50} measured using intracellular Ca^{2+} measurements from cerebellar granule neurons (1.93 ± 0.21 μ M; Table 1), consistent with previous similar comparisons of NMDAR channel blocker IC_{50} s [28]. The discrepancy may result from differences in recording technique and/or from expression of GluN2 subunits other than GluN2A by cerebellar granule neurons [69-71].

NMDAR channel blockers share overlapping binding sites in the NMDAR channel [72-75]. Thus, many organic NMDAR channel blockers (e.g. amantadine, memantine, and ketamine) show competitive binding with the endogenous blocker Mg^{2+} [68,74,76-78]. To ascertain whether Ilc inhibits NMDARs via channel block, we tested the effect of extracellular Mg^{2+} on Ilc potency. As predicted, the inclusion of 0.2 mM Mg^{2+} in the recording solution led to a substantial rightward shift in the Ilc IC_{50} curve and a significant increase in Ilc IC_{50} ($IC_{50} = 4.40 \pm 0.15$ μ M in 0 Mg^{2+} vs 21.41 ± 0.56 μ M in 0.2 mM Mg^{2+} ; $p < 0.0001$, two-sample Student t-test, $n = 10$ and 6, respectively; Fig. 5B and C). This roughly 5-fold decrease in Ilc potency suggests a competitive interaction between Mg^{2+} and Ilc in the NMDAR channel.

We next determined the voltage dependence of inhibition by 10 μ M (~ 2 -fold IC_{50} at -65 mV) Ilc. As predicted of a positively charged channel blocker, inhibition by Ilc was markedly weaker at depolarized potentials (Fig. 5D-F). Equations (3) and (4) were used to quantify V_0 , the change in voltage (in mV) that results in an e-fold change in the IC_{50} of a drug, and δ , an estimate of the fraction of the total transmembrane voltage field felt by the blocker at its binding site [79]. Inhibition of GluN1/2A receptors by Ilc is strongly voltage-dependent, as reflected by the drug's small V_0 (25.43 ± 0.54 mV) and large δ (1.01 ± 0.02). The Ilc V_0 and δ values are similar to previously reported values for monovalent organic channel

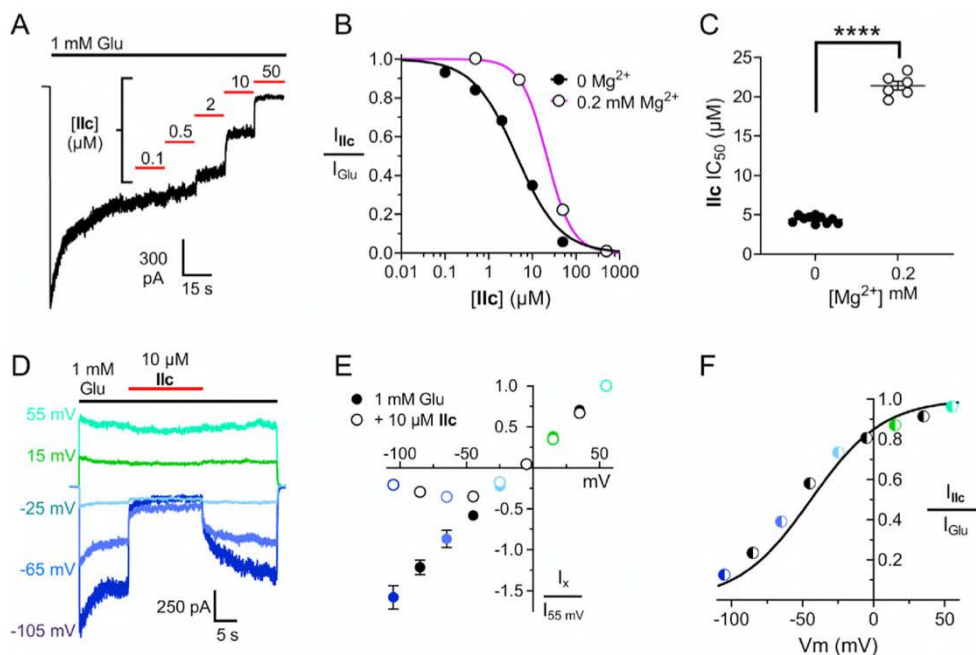


Fig. 5. Characteristics of GluN1/2A receptor channel block by Ilc. **A.** Representative current trace from one cell depicting inhibition of GluN1/2A receptors by Ilc at -65 mV. Current evoked by application of 1 mM glutamate (Glu; black bars) was reduced as concentration of Ilc (red bars) increased. **B.** Concentration-inhibition relation for Ilc in 0 Mg^{2+} (black line, filled symbols) and in 0.2 mM Mg^{2+} (purple line, open symbols). Symbols represent means, error bars are smaller than symbols. Lines show best fits of Equation (2) to data. **C.** Comparison of IC_{50} values in 0 and 0.2 mM Mg^{2+} . 0.2 mM Mg^{2+} greatly reduces Ilc potency ($p < 0.0001$, two-sample Student t -test, $n = 10$ and 6 , respectively). Data shown as individual values, line and error bars depict mean \pm SEM. **D.** Representative current traces from one cell depicting the voltage dependence of inhibition by 10 μM Ilc. For clarity, traces from only five of the tested membrane potentials are displayed. **E.** Current-voltage relation for GluN1/2A receptors in 1 mM Glu (filled symbols) and 1 mM Glu + 10 μM Ilc (open symbols). Current at each voltage (I_x) was normalized to current at 55 mV (I_{55} mV) for each cell. Symbols represent means, error bars represent SEM; some error bars are smaller than symbols. **F.** Mean current-voltage relation data replotted as fractional current in the presence of 10 μM Ilc. Solid line shows best fit of Equation (3) to estimate V_0 (25.43 ± 0.54 mV; $n = 7$). V_0 was subsequently used to calculate δ (1.01 ± 0.02 ; $n = 7$) with Equation (4). Error bars in F are smaller than symbols. Colored symbols in E and F correspond to example traces in D; black symbols represent measurements at voltages not shown in D.

blockers (e.g. $V_0 \sim 26$ – 30 mV, $\delta \sim 0.8$ – 1.0 for memantine, ketamine, and recently synthesized polycyclic amines) [28,63,68,80,81]. The profound dependence of Ilc inhibition on $[Mg^{2+}]$ and on membrane potential strongly supports the conclusion that Ilc inhibits NMDARs by binding in and blocking the NMDAR channel.

2.6. In vitro DMPK profile, hERG safety and cytotoxicity of Ilc

This compound was characterized in terms of microsomal stability (human and mouse species), hERG (human ether-a-go-go-related gene) inhibition, cytochrome P450 (CYP) inhibition, Caco-2 and predicted brain permeability (PAMPA-BBB assay), to confirm its suitability as a candidate for *in vivo* studies in *Caenorhabditis elegans* (*C. elegans*) and in the 5XFAD mouse model. Results from these measurements are given in Table 2.

Ilc showed high metabolic stability in human and mice liver microsomes, which are widely used to determine the likely degree of primary metabolic clearance in the liver. Next, cytochrome P450 (CYP) inhibition was evaluated through a fluorescence-detection method using human recombinant cytochrome P450 enzymes CYP1A2, CYP2C19, CYP2C9, CYP2D6, and CYP3A4. Pleasantly, the compound did not significantly inhibit the evaluated cytochromes. hERG channel is an ion channel which is commonly used as an important toxicology screen because of its known association with cardiotoxicity. Interestingly, Ilc, at 10 μM , did not significantly

inhibit hERG. The Caco-2 cell permeability model was used to evaluate the permeability of the compound. Apparent permeability values (P_{app}) were determined from the amount permeated through the Caco-2 cell membranes in both apical-basolateral (A-B) and basolateral-apical (B-A) directions. Satisfactorily, Ilc showed good permeability. Any AD drug should cross the blood-brain-barrier (BBB), so we used the PAMPA-BBB assay to predict the ability of Ilc to permeate BBB. Ilc had a positive predicted BBB permeability. Next, the cytotoxicity of Ilc was tested using the MTT assay in Neuro2a cells. Interestingly, the selected compounds did not show cytotoxic at the highest concentration tested (100 μM) (see section 4.7. for further details).

Overall, Ilc has low micromolar activity, an excellent electrophysiological profile as a NMDA receptor blocker, favorable DMPK properties, and non-cytotoxicity. Thus, Ilc was deemed a suitable candidate for the *in vivo* studies [82].

2.7. In vivo efficacy studies

To evaluate the effectivity of Ilc to ameliorate cognitive impairment through the modulation of NMDAR-mediated neurodegenerative pathways, we performed a series of *in vivo* studies in *C. elegans* and in the 5XFAD mouse model.

It has been reported that memory in *C. elegans* is mediated by NMDA-type ionotropic glutamate receptors [83]. This nematode

Table 2
Microsomal stability, cytochrome and hERG inhibition, Caco-2 and PAMPA-BBB of **IIc**.

Microsomal stability ^a		CYP inhibition ^b						hERG inhibition ^b	Caco-2 Papp (nm/s) ^c			PAMPA-BBB
h	m	1A2	2C19	2C9	2D6	3A4 ^d	3A4 ^e		A - B	B - A	ER	
96	77	9 ± 2	21 ± 2	9 ± 3	15 ± 1	4 ± 2	10 ± 2	13 ± 1	310 ± 41	208 ± 12	0.7 ± 0.1	CNS+

^a Percentage of remaining compound after 60 min of incubation with human (h) and mouse (m) microsomes in the presence of NADPH at 37 °C.

^b Percentage of inhibition at 10 μM.

^c The efflux ratio (ER) was calculated as ER = (Papp B→A)/(Papp A→B).

^d Using benzyloxytrifluoromethylcoumarin (BFC) as substrate.

^e Using dibenzylfluorescein (DBF) as substrate. See methods for further details.

expresses two NMDA-type subunits, NMR-1 and NMR-2, homologous to mammalian GluN1 and GluN2A subunits, respectively [84]. Thus, *C. elegans* has been described as a suitable model for the study of NMDAR-mediated neurotoxicity [85,86]. The 5XFAD mouse model, which displays altered NMDAR function [87], is one of the most used AD mouse models to evaluate pharmacological interventions [88].

Considering that **IIc** has proven to be a memantine analog in terms of potency and electrophysiological behavior, we incorporated memantine as a standard to analyze if these analogies persist in the *in vivo* efficacy studies. Of note, just a single study has been published on the effects of memantine in *C. elegans*, using the transgenic strain CL2006 [84], and only two studies have been published describing effects of memantine on 5XFAD mice [89,90].

2.7.1. Concentration-response effect of memantine and **IIc** on paralysis induced by Aβ expression in CL2006

The analysis of locomotor deficits has been traditionally used to discriminate between N2 wild-type (WT) and CL2006 mutant *C. elegans*. Herein, the N2 WT strain was used as a positive control and CL2006 worms, which constitutively expresses human Aβ₁₋₄₂, served as an AD model [91]. As expected, CL2006 worms presented paralysis (measured as defective locomotion) compared to N2 WT, which exhibited a significantly lower percentage of defective locomotion (Fig. 6A). After treatments, we found that memantine and **IIc** reduced defective locomotion over a range of concentrations (0.1–10 μM) in CL2006 nematodes (Fig. 6A–B). These initial results in nematodes showed the capability of **IIc**, as well as memantine, to rescue the motor deficits in an AD model.

2.7.2. Treatment with NMDAR channel blockers rescues chemotaxis behavior of CL2355 nematodes disrupted by Aβ expression

The impressive chemotaxis behavior of *C. elegans* is well known as a suitable model to evaluate the neuroprotective effects of new compounds. To evaluate the effect of NMDAR antagonists on the chemotaxis behavior of *C. elegans*, the transgenic strain CL2355, which shows Aβ aggregates as well as deficits in chemotaxis, and CL2122, a positive control strain, were used [91]. Therefore, we performed a chemotaxis assay as previously described [92]. As expected, CL2355 showed disrupted chemotaxis behavior and a reduced chemotaxis index (CI) in comparison to CL2122. Interestingly, both memantine and **IIc** treatments significantly reversed the disrupted chemotaxis behavior, suggesting that **IIc** might protect against Aβ toxicity-related neuronal dysfunction in a fashion similar to memantine (Fig. 6C).

2.7.3. NMDA channel blockers memantine and **IIc** rescue working memory impairment in 5XFAD

To determine the effects of the administration of memantine and **IIc** on AD-like symptoms, 5XFAD mice, a model of familial AD, were treated with either memantine or **IIc** at 5 mg/day for 4 weeks.

A novel object recognition test (NORT) was used to evaluate short- and long-term working memories in 5XFAD mice. As described previously [88,93], 6-month-old 5XFAD mice presented robust cognitive deficits compared to WT (Fig. 7). We found that memantine treatment resulted in the recovery of cognitive function by increasing the discrimination index (DI) in both short-term (Fig. 7A) and long-term (Fig. 7B) memory tests. Importantly, **IIc** also enhanced working memory function in 5XFAD mice, with treated mice showing a significant DI increase at both tests (Fig. 7).

2.7.4. NMDAR molecular alterations in 5XFAD mouse model after **IIc** treatment

NMDARs are heterotetramers composed of two GluN1 subunits and typically two GluN2 subunits, of which there are four subtypes (GluN2A–D). In the adult forebrain, GluN2A and GluN2B are the two predominant subtypes. GluN2A subunits, incorporated into synaptic NMDARs, mediate long-term synaptic plasticity and their activation is associated with neuroprotective pathways. Therefore, selective activation of NMDARs containing GluN2A subunits would have a beneficial effect on AD pathology [94,95].

Western-blot analysis showed that 5XFAD mice exhibit less GluN2A protein levels than control mice, and interestingly, **IIc** treatment was able to rescue GluN2A to control levels (Fig. 8A–B).

Extrasynaptic NMDARs are enriched in GluN2B subunits and are believed to promote neuronal death, as occurring in neurodegenerative diseases. The activation of NDMARs containing the GluN2B subunit may be increased by Aβ, contributing to neurodegenerative and apoptotic pathways [96]. Memantine preferentially blocks extrasynaptic NMDARs over those located at the synaptic cleft, contributing to the clinical tolerability of this drug [21,97,98]. Additionally, GluN2B-subunit-containing NMDARs may induce synaptic NMDAR internalization after dephosphorylation, disrupting normal synaptic function [99]. Furthermore, phosphorylated Fyn kinase (p-Fyn) is responsible for phosphorylation of GluN2B at tyrosine 1472, which prevents GluN2B endocytosis and maintains NMDARs at the synaptic surface, preventing neuronal death [100]. To evaluate GluN2B subunit and Fyn kinase phosphorylation in control mice and the effects of memantine and **IIc** on 5XFAD mice, the p-GluN2B(Tyr1472)/GluN2B and p-Fyn/Fyn ratios (Figures 8A, 8C–D) were determined. Of note, we found that treatment of 5XFAD mice with memantine or **IIc** increased Fyn phosphorylated levels and correspondingly elevated GluN2B phosphorylation at Tyr1472. These findings support the literature relating GluN2B-subunit phosphorylation at Tyr1472 and the prevention of NMDAR internalization, which may prevent synaptic dysfunction [101,102].

2.7.5. **IIc** treatment modifies CREB pathways leading to synaptic improvements

Fyn activity is related to proteins implicated in cell-survival, such as cAMP response element binding protein (CREB) [103]. Therefore, we evaluated p-CREB protein levels in cytosol and nuclei.

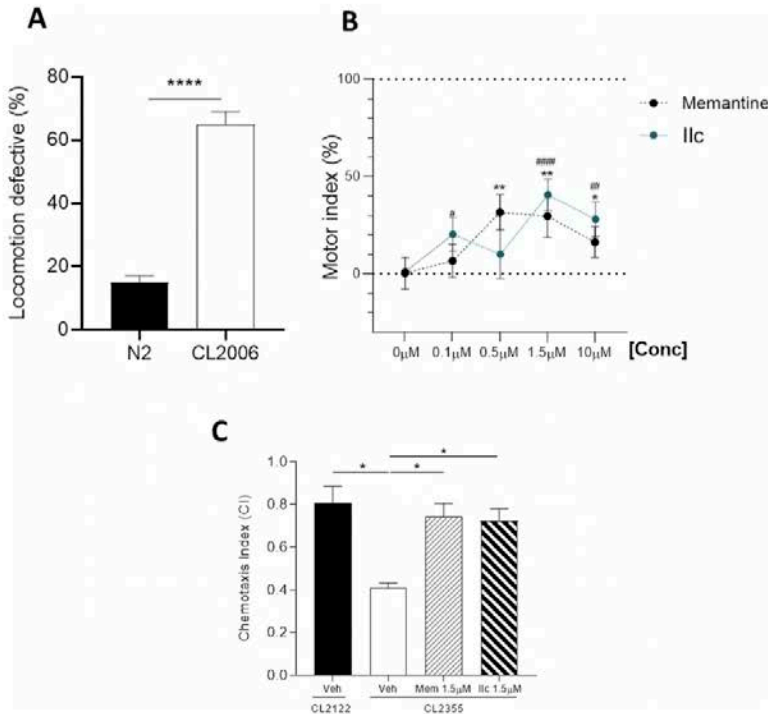


Fig. 6. A. Locomotion defective (%) of N2 WT vs CL2006 strains. B. Motor index (%) calculated in CL2006 worms treated with the indicated memantine or Ilc concentrations. C. Chemotaxis index (CI) for CL2122 and CL2355 worms treated with vehicle (Veh), memantine (Mem) and Ilc. Values are depicted as mean ± Standard error of the mean (SEM). ****p < 0.0001 for N2 vs CL2006; *p < 0.05, **p < 0.01 for memantine 0.5 μM, 1.5 μM and 10 μM vs memantine 0 μM; #p < 0.05, ##p < 0.01, ###p < 0.0001 for Ilc 0.5 μM, 1.5 μM and 10 μM vs Ilc 0 μM; *p < 0.05 for CL2355 Veh vs other groups.

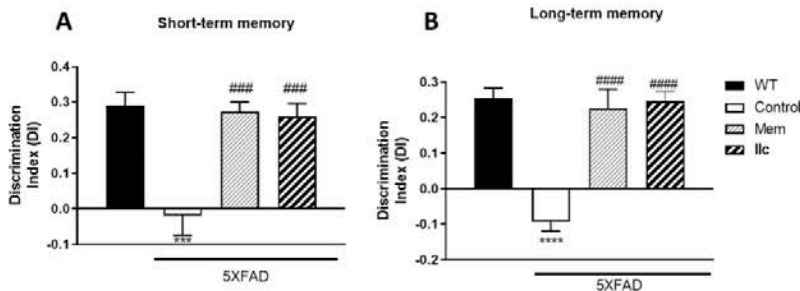


Fig. 7. A. Discrimination index (DI) calculated by using exploration time for novel and familiar object in the short-term (2 h) memory test. B. DI in the long-term memory test session (24 h). Values are the mean ± Standard error of the mean (SEM); (n = 14 for WT, n = 8 for 5XFAD control groups, n = 11 for memantine (Mem, 5 mg/kg) and n = 10 for Ilc (5 mg/kg) groups). ***p < 0.001; ****p < 0.0001 for WT vs 5XFAD control. ###p < 0.001; ####p < 0.0001 for memantine (Mem, 5 mg/kg) or Ilc (5 mg/kg) vs 5XFAD control.

p-CREB levels were found to be dysregulated in 5XFAD compared to WT. p-CREB protein in the nucleus was reduced in 5XFAD mice compared to the WT group, whereas treatment with memantine or Ilc significantly increased p-CREB protein levels in the nucleus compared to untreated 5XFAD mice. The enhanced p-CREB translocation to the nucleus of the treated groups (Fig. 9A and B) indicated a beneficial effect of NMDAR antagonists by modulating signaling pathways involved in cell survival.

To further evaluate the effect of memantine and Ilc on AD-

related proteins, the calcium-dependent protein calbindin was evaluated. Calbindin D-28K is a Ca²⁺ binding protein and an important regulator of Ca²⁺ homeostasis found to be dysregulated in AD animal models [104]. Remarkably, we found a significant, unprecedented dysregulation of calbindin protein levels in 5XFAD mice (Fig. 9A and C), suggesting the important role of calbindin in the Aβ pathology presented by this transgenic mouse model. We also demonstrated that treatment with memantine or Ilc reverts calbindin D-28K protein levels to WT levels (Fig. 9A and C).

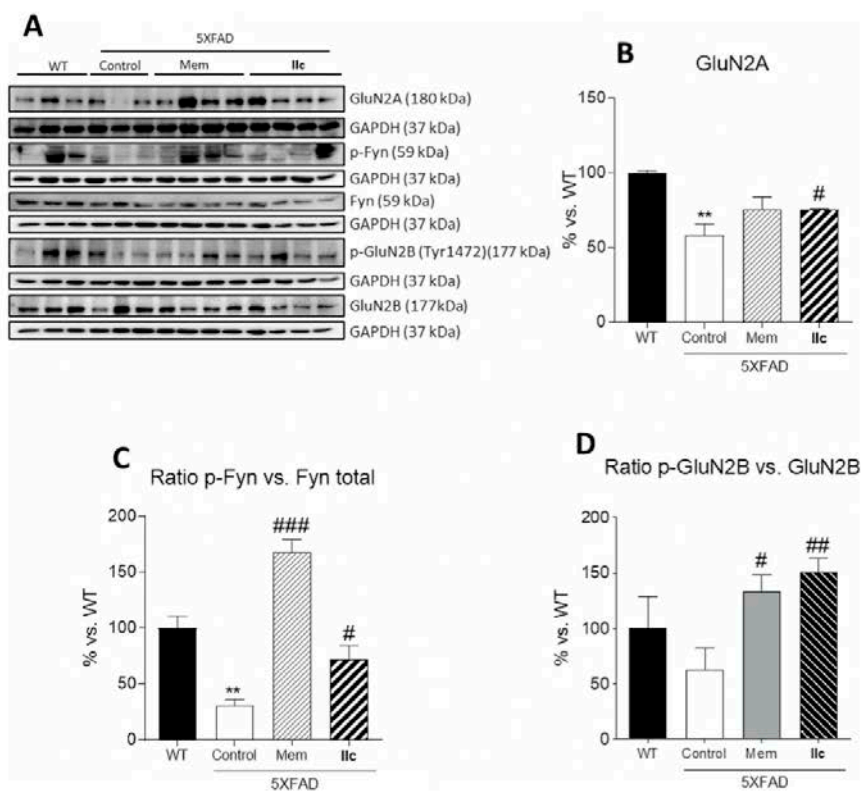


Fig. 8. A. Representative Western Blots and quantification. B. GluN2A. C. Ratio p-Fyn/Fyn. D. Ratio p-GluN2B (Tyr1472)/GluN2B. Values plotted in bar graphs are adjusted to 100% for protein levels of wild type (WT). Values are the mean \pm Standard error of the mean (SEM); (n = 3 for WT and 5XFAD Control groups and n = 4 for memantine (Mem, 5 mg/kg) and Ilc (5 mg/kg) groups. **p < 0.01 for WT vs 5XFAD Control. #p < 0.05; ###p < 0.01; ####p < 0.001 for memantine (Mem, 5 mg/kg) or Ilc (5 mg/kg) vs 5XFAD Control.

It is noteworthy that p-CREB is a transcription factor that increases the expression of several proteins implicated in neuroprotection and neuronal signaling [105]. Interestingly, we found that treatment with memantine or Ilc rescues expression of post-synaptic density protein (PSD) 95 in 5XFAD mice (Fig. 9D). Together, these data may explain the improvement in working memory observed in 5XFAD after treatment with NMDAR channel blockers.

Overall, we provide promising evidence that Ilc treatment rescues Fyn-GluN2B-CREB signaling and PSD95 expression in 5XFAD mice. Our results suggest a mechanism by which Ilc may improve cell survival and synaptic function in AD through increasing the activity of cell-survival signaling pathways and preventing internalization of synaptic NMDARs. Thus, Ilc could be a feasible candidate for further testing as a new clinically therapeutic NMDAR channel blocker.

3. Conclusions

Despite scientific efforts to develop new clinically useful NMDAR blockers, memantine remains the only noncholinergic drug approved for symptomatic AD treatment. Therefore, we further explored the benzohomoadamantane scaffold with the main aim to develop new memantine analogs. Although most of the changes in the chemical structure of benzohomoadamantane negatively impact potency at NMDARs, **2**, **IIa** and **IIc** showed low micromolar

potencies. Furthermore, these results were rationalized and strongly supported by MD simulations. Subsequently, of the most active derivatives, **IIc** was found to possess electrophysiological characteristics similar to memantine, including similar potencies, voltage dependencies, and blocking sites. Additionally, our DMPK studies (microsomal stability, cytochrome and hERG inhibition, Caco-2 and PAMPA assays) revealed that **IIc** was a good candidate for *in vivo* studies. The administration of **IIc** to both *C. elegans* and the 5XFAD mouse model of AD reverted the condition of the animals to that of controls, both at the behavioral and the biochemical levels. The effect observed was comparable with that produced by memantine, demonstrating that **IIc** could be a feasible and promising candidate for a new clinically therapeutic NMDAR blocker.

4. Experimental part

4.1. Chemistry. General methods

Commercially available reagents and solvents were used without further purification unless stated otherwise. Preparative normal phase chromatography was performed on a CombiFlash Rf 150 (Teledyne Isco) with pre-packed RediSep Rf silica gel cartridges. Thin-layer chromatography was performed with aluminum-backed sheets with silica gel 60 F254 (Merck, ref 1.05554), and spots were visualized with UV light and 1% aqueous solution of KMnO_4 .

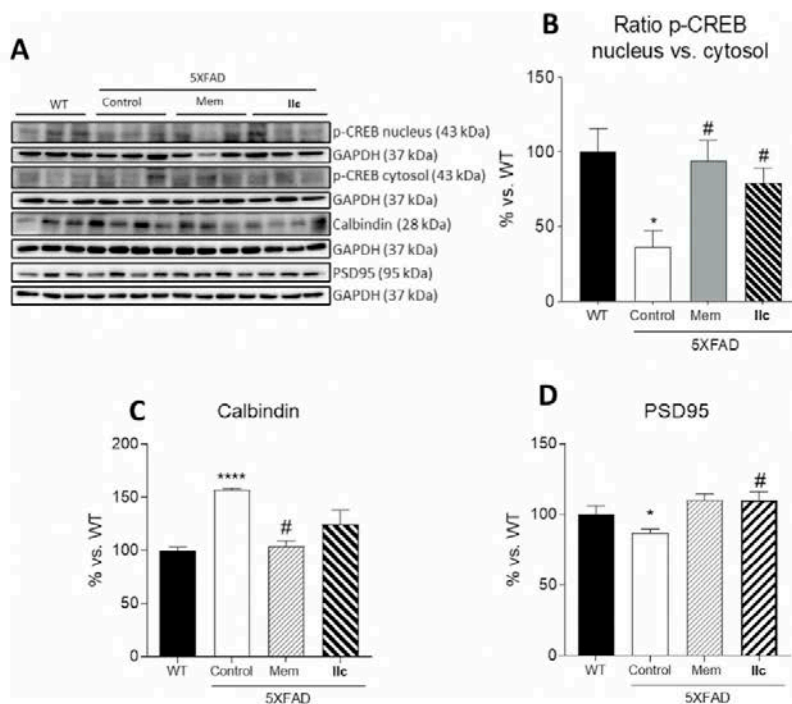


Fig. 9. A. Representative Western Blot and quantifications for B. Ratio of p-CREB in the nucleus vs in the cytosol C. Calbindin D. PSD95. Values in bar graphs are adjusted to 100% for protein levels of the wild type (WT). Values are the mean \pm Standard error of the mean (SEM); (n = 3 for WT and 5XFAD Control groups and n = 4 for memantine (Mem, 5 mg/kg) and Ilc (5 mg/kg) groups. *p < 0.05; ****p < 0.0001 for WT vs 5XFAD Control. #p < 0.05; ##p < 0.01 for memantine (Mem, 5 mg/kg) or Ilc (5 mg/kg) vs 5XFAD Control.

Melting points were determined in open capillary tubes with a MFB 595010 M Gallenkamp. 400 MHz ^1H and 100.6 MHz ^{13}C NMR spectra were recorded on a Varian Mercury 400 or on a Bruker 400 Avance III spectrometers. The chemical shifts are reported in ppm (δ scale) relative to internal tetramethylsilane, and coupling constants are reported in Hertz (Hz). Assignments given for the NMR spectra of selected new compounds have been carried out on the basis of COSY $^1\text{H}/^{13}\text{C}$ (gHSQC) experiments. IR spectra were run on Perkin-Elmer Spectrum RX I, Perkin-Elmer Spectrum TWO or Nicolet Avatar 320 FT-IR spectrophotometers. Absorption values are expressed as wavenumbers (cm^{-1}); only significant absorption bands are given. High-resolution mass spectrometry (HRMS) analyses were performed with an LC/MSD TOF Agilent Technologies spectrometer. The elemental analyses were carried out in a Flash 1112 series ThermoFinnigan elemental microanalyzer (A5) to determine C, H, N. HPLC/MS were determined with a HPLC Agilent 1260 Infinity II LC/MSD coupled to a photodiode array and mass spectrometer. 5 μL of sample 0.5 mg/mL in methanol: acetonitrile were injected, using an Agilent Poroshell 120 EC-C18, 2.7 μm , 50 mm \times 4.6 mm column at 40 $^\circ\text{C}$. The mobile phase was a mixture of A = water with 0.05% formic acid and B = acetonitrile with 0.05% formic acid, with the method described as follows: flow 0.6 mL/min, 5% B-95% A 3 min, 100% B 4 min, 95% B-5% A 1 min. Purity is given as % of absorbance at 210 or 275 nm. The structure of all new compounds was confirmed by elemental analysis and/or accurate mass measurement, IR, ^1H NMR and ^{13}C NMR. The analytical samples of all the new compounds, which were subjected to pharmacological evaluation, possessed purity >95% as evidenced by their elemental analyses or HPLC-UV.

4.1.1. 5,6,8,9,10,11-Hexahydro-7H-5,9:7,11-dimethanobenzo[9]annulen-9-d-7-amine (2)

- 9-bromo-6,7,8,9,10,11-hexahydro-9-methyl-5,7:9,11-dimethano-5H-benzocyclonon-7-amine hydrochloride. Thionyl bromide (6.5 mL, $\delta = 2.68$, 83.8 mmol) was added to a solution of amine **1** (500 mg, 2.81 mmol) in toluene (17 mL) containing a few drops of DMF. The resulting red solution was stirred at rt for 1.5 h. The reaction mixture was concentrated to dryness *in vacuo*. Toluene (50 mL) was added, and the resulting solution concentrated *in vacuo*. The procedure was repeated five times more until an orange solid was obtained. The crude was partitioned between DCM (15 mL) and saturated aq NaHCO_3 solution (15 mL) and the phases were separated. The aq layer was extracted with further dichloromethane (100 mL) and the combined organic extracts were dried over anhydrous Na_2SO_4 , filtered and concentrated *in vacuo* to give a colourless oil (530 mg, 83% yield) that was used in the next step without further purification.
- 5,6,8,9,10,11-hexahydro-7H-5,9:7,11-dimethanobenzo[9]annulen-9-d-7-amine. To a suspension of 9-bromo-6,7,8,9,10,11-hexahydro-9-methyl-5,7:9,11-dimethano-5H-benzocyclonon-7-amine hydrochloride (prepared from the addition of an excess of $\text{HCl}/\text{Et}_2\text{O}$ to the compound) (250 mg, 0.76 mmol) in anhydrous and deoxygenated toluene (3 mL) under Ar atmosphere were added tributylstannane-*d* (372 μL , 1.37 mmol) and AIBN (16 mg, 0.10 mmol). The resulting solution was heated to 95 $^\circ\text{C}$ for 4 h adding more AIBN (16 mg, 0.10 mmol) each 60 min. Saturated aq Na_2CO_3 solution was added until pH = 12 and then

the aq layer was extracted with 10% MeOH/EtOAc (3 × 15 mL). All organic layers were joined, dried over anhydrous Na₂SO₄, filtered and concentrated *in vacuo*. The resulting crude was purified by Biotage® purification system in silica gel using a MeOH/NH₃ 0.7 M in DCM mixture (0.4/9.6) to obtain **2** as a pale-yellow solid (100 mg, 61% yield). Its hydrochloride was obtained by adding an excess of HCl/Et₂O in DCM, followed by filtration of the resulting white precipitate. mp 72–73 °C. IR (ATR) ν : 2906, 2838, 1653, 1560, 1490, 1439, 1352, 1115, 1047, 990, 933, 914, 874, 826, 755, 702, 610 cm⁻¹. ¹H NMR (400 MHz, CD₃OD) δ : 1.66–1.72 [complex signal, 6H, 6(12)-H_a, 10(13)-H₃ and 8-H₂], 1.85 [m, 2H, 6(12)-H_b], 1.92 [dd, J = 12.8 Hz, J' = 6.0 Hz, 2H, 10(13)-H_b], 3.03 [tt, J = 6.0, J' = 1.5 Hz, 2H, 5(11)-H], 7.02 (br s, 4H, Ar-H). ¹³C NMR (100.6 MHz, CD₃OD) δ : 32.7 (t, J_{C-D} = 20.0 Hz, C9), 35.4 [CH₂, C10(13)], 42.9 [CH, C5(11)], 44.1 [CH₂, C6(12)], 45.0 (CH₂, C8), 48.8 (C, C7), 127.3 [CH, C2(C3)], 129.0 [CH, C1(C4)], 148.0 [C, C4a(C11a)]. HRMS-ESI + m/z [M+H]⁺ calcd for [C₁₅H₁₉DN]⁺: 215.1658, found: 215.1653.

4.1.2. 7-Iodo-5,6,7,8,9,10-hexahydro-5,8:7,10-dimethanobenzo[8]annulene (**4**)

- a) 5,8,9,10-tetrahydro-5,8:7,10-dimethanobenzo[8]annulene-7(6H)-yl methanesulfonate. To a solution of 5,8,9,10-tetrahydro-5,8:7,10-dimethanobenzo[8]annulene-7(6H)-ol (1.19 g, 5.40 mmol) in pyridine (9 mL), methanesulfonyl chloride (2.32 mL, δ = 1.48, 29.9 mmol) was added slowly with stirring at rt. The mixture was then heated at 120 °C for 5 h. After cooling, crushed ice (100 g) was added and the mixture was extracted with DCM (5 × 40 mL). The combined organic phase was washed with 2 N HCl solution (2 × 40 mL), H₂O (2 × 40 mL), saturated aq NaHCO₃ solution (2 × 40 mL) and dried over anhydrous Na₂SO₄. The crude mesylate was obtained after filtration and removal of the solvent under reduced pressure as a dark oil that was used in the next step without further purification (1.32 g, 80% yield). HRMS-ESI + m/z [M+H]⁺ calcd for [C₁₅H₁₈O₂S + NH₄]⁺: 296.1315, found: 296.1318.
- b) 7-iodo-5,6,7,8,9,10-hexahydro-5,8:7,10-dimethanobenzo[8]annulene. In an RBF equipped with a reflux condenser, H₃PO₃ (99%, 135 g), mesylate (1.32 g, 4.75 mmol) and NaI (63 g, 42.0 mmol) were added. The mixture was stirred at 150 °C for 6 h. After cooling, H₂O (150 mL) was added slowly to the mixture. The resulting red solution was extracted with DCM (4 × 80 mL) and the combined organic phase was washed with saturated aq sodium thiosulfate solution (1 × 100 mL), dried over anhydrous Na₂SO₄, then filtered and concentrated under vacuum to give **4** as a white solid (1.39 g, 95% yield). mp 132–133 °C (dec.). IR (NaCl disk) ν : 3052, 3013, 2950, 2892, 2852, 1490, 1447, 1304, 1278, 1232, 1215, 1095, 1046, 1032, 967, 830, 778, 755 cm⁻¹. ¹H NMR (400 MHz, CDCl₃) δ : 1.59 [dd, J = 12.4 Hz, J' = 2.4 Hz, 2H, 9(12)-H_a], 2.01 [dd, J = 11.6 Hz, J' = 2.4 Hz, 2H, 6(11)-H_a], 2.24 [m, 2H, 6(11)-H_b], 2.39 [m, 2H, 9(12)-H_b], 2.55 (t, J = 8.8 Hz, 1H, 8-H), 3.23 [t, J = 6.0 Hz, 2H, 5(10)-H], 7.08 [m, 2H, 1(4)-H or 2(3)-H], 7.13 [m, 2H, 2(3)-H or 1(4)-H]. ¹³C NMR (100.6 MHz, CDCl₃) δ : 42.8 [CH₂, C9(12)], 48.3 [CH, C5(10)], 49.6 (CH, C8), 51.0 [CH₂, C6(11)], 90.5 (C, C7), 126.2 [CH, C1(4) or C2(3)], 129.5 [CH, C2(3) or C1(4)], 145.3 [C, C4a(10a)]. GC-MS (EI), t_r = 17.8 min: 310 [(M)⁺, 2], 183 [(M-1)⁺, 100], 141 (73), 129 (23), 128 (15).

4.1.3. 5,8,9,10-Tetrahydro-5,8:7,10-dimethanobenzo[8]annulene-7(6H)-carboxylic acid (**5**)

To a solution of 7-iodo-5,6,7,8,9,10-hexahydro-5,8:7,10-dimethanobenzo[8]annulene (2.03 g, 6.54 mmol) in dry and

degassed toluene (20 mL), methyl oxalyl chloride (1.8 mL, δ = 1.33, 19.5 mmol) and bis(tributyltin) (4.55 g, 7.85 mmol) were added. The mixture was irradiated in a quartz reactor under argon atmosphere with a 125 W Hg lamp for 20 h. Then, DCM (15 mL), methanol (0.6 mL) and triethylamine (1.2 mL) were successively added to the reaction mixture at 0 °C and it was concentrated under vacuum to give a dark oil (3.99 g). A solution of this oil in a 40% methanol solution of KOH (50 mL) was heated to reflux for 2 h. H₂O (50 mL) was added, and the reaction was refluxed for 3 h. The reaction mixture was allowed to cool to rt and the methanol was removed under vacuum. H₂O (40 mL) was added to the residue and the aq layer was washed with DCM (4 × 50 mL). After that, the aq phase was acidified with conc. HCl until pH = 1 and extracted with DCM (4 × 50 mL). The organic extracts were dried over anhydrous Na₂SO₄, filtered and concentrated under reduced pressure to give the acid as a brown solid (555 mg, 37% overall yield). An analytical sample of the acid was obtained by crystallization from DCM/Pentane, mp 188–189 °C. IR (NaCl disk) ν : 3300–2800 (3065, 3011, 2946, 2858), 1690, 1488, 1450, 1410, 1318, 1290, 1231, 1218, 1092, 1052, 1038, 941 cm⁻¹. ¹H NMR (400 MHz, CDCl₃) δ : 1.71 [dd, J = 12.8 Hz, J' = 2.4 Hz, 2H, 9(12)-H_a], 1.89 [dd, J = 12.4 Hz, J' = 2.4 Hz, 2H, 6(11)-H_a], 2.23 [m, 2H, 9(12)-H_b], 2.57 [dm, J = 12.4 Hz, 2H, 6(11)-H_b], 3.20 (t, J = 8.8 Hz, 1H, 8-H), 3.27 [t, J = 6 Hz, 2H, 5(10)-H], 7.08 [m, 2H, 1(4)-H or 2(3)-H], 7.15 [m, 2H, 2(3)-H or 1(4)-H]. ¹³C NMR (100.6 MHz, CDCl₃) δ : 43.3 [CH₂, C9(12)], 46.4 [CH₂, C6(11)], 49.4 [CH, C5(10)], 49.9 (CH, C8), 59.9 (C, C7), 126.2 [CH, C1(4) or C2(3)], 129.5 [CH, C2(3) or C1(4)], 145.4 [C, C4a(10a)], 184.1 (C, C7-COOH). HRMS-ESI + m/z [M - H]⁻ calcd for [C₁₅H₁₅O₂]⁻: 227.1078, found: 227.1078.

4.1.4. 5,8,9,10-Tetrahydro-5,8:7,10-dimethanobenzo[8]annulene-7(6H)-amine hydrochloride (**6**)

To a solution of 5,8,9,10-tetrahydro-5,8:7,10-dimethanobenzo[8]annulene-7(6H)-carboxylic acid (90 mg, 0.39 mmol) in toluene (1.2 mL), Et₃N (73 μ L, 0.53 mmol) and diphenylphosphoryl azide (159 mg, 0.58 mmol) were added and the mixture was heated at reflux for 3 h. The mixture was cooled and washed with 1 N HCl solution (2 × 10 mL). Thereafter, to the organic layer was added 6 N HCl solution (1.6 mL) and the suspension was heated at reflux for 24 h. The reaction mixture was then cooled to rt and the two phases were separated. The aq phase was extracted with ethyl acetate (3 × 3 mL). The combined organic phases were washed with 5 N NaOH solution (3 × 10 mL), dried over anhydrous Na₂SO₄, filtered and concentrated under vacuum to give **6**. Its hydrochloride was obtained by adding an excess of HCl/methanol to a solution of the amine in methanol. The methanol was removed under reduced pressure yielding **6** as a brown solid (35 mg, 38% yield). An analytical sample was obtained by crystallization from MeOH/Et₂O, mp > 250 °C. IR (KBr disk) ν : 3100–2500 (2943, 2881, 2665), 2043, 1622, 1598, 1501, 1448, 1336, 1246, 1175, 1089, 1057, 1028, 952, 769, 749, 614 cm⁻¹. ¹H NMR (400 MHz, MeOD) δ : 1.67 [dd, J = 12.4 Hz, J' = 2.4 Hz, 2H, 9(12)-H_a], 2.02 [dd, J = 12.0 Hz, J' = 2.4 Hz, 2H, 6(11)-H_a], 2.30 [m, 2H, 6(11)-H_b], 2.42 [m, 2H, 9(12)-H_b], 2.80 (t, J = 8.8 Hz, 1H, 8-H), 3.33 [t, J = 6.0 Hz, 2H, 5(10)-H], 7.08 [m, 2H, 1(4)-H or 2(3)-H], 7.15 [m, 2H, 2(3)-H or 1(4)-H]. ¹³C NMR (100.6 MHz, MeOD) δ : 43.4 [CH₂, C9(12)], 48.2 [CH₂, C6(11)], 49.1 (CH, C8), 49.4 [CH, C5(10)], 70.6 (C, C7), 127.6 [CH, C1(4) or C2(3)], 130.5 [CH, C2(3) or C1(4)], 145.3 [C, C4a(10a)]. HRMS-ESI + m/z [M+H]⁺ calcd for [C₁₄H₁₈N]⁺: 200.1434, found: 200.1432.

4.1.5. 2-Chloro-N-(9-methyl-2-nitro-5,6,8,9,10,11-hexahydro-7H-5,9:7,11-dimethanobenzo[9]annulene-7-yl)acetamide (**8**)

To a cold (0 °C) solution of chloroacetamide **7** (3.0 g, 9.87 mmol) in acetic anhydride (10 mL), glacial acetic acid (1.6 mL) and fuming nitric acid (1.9 mL) were carefully added. The mixture was allowed

to reach rt and left stirring overnight. The obtained yellow solution was then poured into ice-water (20 mL) and extracted with DCM (3 × 40 mL). The combined organic extracts were washed with 2 N NaOH solution (1 × 40 mL), H₂O (1 × 40 mL) and brine (1 × 40 mL). The organic layer was dried over anhydrous Na₂SO₄, filtered and concentrated under vacuum to give a yellow residue. Purification by CombiFlash® in silica gel using as eluent a gradient from hexane to ethyl acetate/hexane mixture (1/9) gave **8** as a white solid (2.92 g, 85% yield), mp 174–176 °C. IR (ATR) ν : 3269, 3233, 3080, 2951, 2922, 2903, 2846, 1670, 1563, 1518, 1460, 1405, 1362, 1346, 1336, 1303, 1279, 1226, 1166, 1138, 1083, 884, 839, 794, 739, 708, 667 cm⁻¹. ¹H NMR (400 MHz, CDCl₃) δ : 0.96 (s, 3H, 9-CH₃), 1.50–1.58 [complex signal, 2H, 10(13)-H_a], 1.67–1.76 [complex signal, 2 H, 10(13)-H_b], 1.81 (dm, *J* = 12.0 Hz, 1H, 8-H_a), 1.87 (dm, *J* = 12.0 Hz, 1H, 8-H_b), 2.10–2.23 [complex signal, 4H, 6(12)-H₂], 3.19–3.25 [complex signal, 2H, 5(11)-H], 3.93 (s, 2H, CH₂Cl), 6.34 (broad s, 1H, NH), 7.21 (d, *J* = 8.8 Hz, 1 H, 4-H), 7.94 (dd, *J* = 8.8 Hz, *J*' = 2.4 Hz, 1 H, 3-H), 7.95 (d, *J* = 2.4 Hz, 1H, 1-H). ¹³C NMR (100.6 MHz, CDCl₃) δ : 32.1 (CH₃, C9–CH₃), 33.8 (C, C9), 38.0 (CH₂) and 38.3 (CH₂) (C6 and C12), 40.5 (CH₂) and 40.7 (CH₂) (C10 and C13), 40.88 (CH) and 40.90 (CH) (C5 and C11), 43.0 (CH₂, CH₂Cl), 46.9 (CH₂, C8), 54.6 (C, C7), 121.9 (CH) and 123.1 (CH) (C1 and C3), 129.2 (CH, C4), 146.6 (C, C11a), 147.6 (C, C2), 153.8 (C, C4a), 164.9 (C, CO). HRMS-ESI + *m/z* [M+H]⁺ calcd for [C₁₈H₂₂ClN₂O₃]⁺: 349.1313, found: 349.1313.

4.1.6. 9-Methyl-2-nitro-5,6,8,9,10,11-hexahydro-7H-5,9,7,11-dimethanobenzo[9]annulen-7-amine hydrochloride (**9**)

Thiourea (177 mg, 2.33 mmol) and glacial acetic acid (1 mL) were added to a solution of chloroacetamide **8** (677 mg, 1.94 mmol) in abs. ethanol (33 mL) and the mixture was heated at reflux overnight. The resulting suspension was then tempered to rt, H₂O (20 mL) was added and the pH adjusted to 12 with 5 N NaOH solution. DCM (40 mL) was added, the phases were separated, and the aqueous phase was extracted with further DCM (2 × 40 mL). The combined organic layers were dried over anhydrous Na₂SO₄, then filtered and concentrated *in vacuo* to give **9** as a light brown solid. Its hydrochloride was obtained by adding an excess of HCl/Et₂O to a solution of the amine in ethyl acetate, followed by filtration of the resulting white precipitate (443 mg, 74% yield), mp > 225 °C (dec). IR (ATR) ν : 3381, 3100–2800 (2997, 2927, 2856), 2065, 1613, 1520, 1486, 1350, 1329, 1305, 1286, 1138, 1033, 896, 837, 801, 762, 736 cm⁻¹. ¹H NMR (400 MHz, MeOD) δ : 1.02 (s, 3H, CH₃), 1.55–1.63 [complex signal, 2H, 10(13)-H_a], 1.71–1.75 (complex signal, 1H, 8-H₂), 1.73–1.81 [complex signal, 2 H, 10(13)-H_b], 1.85–1.94 [complex signal, 2H, 6(12)-H_a], 2.07–2.14 [complex signal, 2H, 6(12)-H_b], 3.36–3.42 [complex signal, 2H, 5(11)-H], 7.37 (d, *J* = 8.4 Hz, 1H, 4-H), 7.99 (dd, *J* = 8.2 Hz, *J*' = 2.4 Hz, 1H, 3-H), 8.02 (d, *J* = 2.4 Hz, 1H, 1-H). ¹³C NMR (100.6 MHz, MeOD) δ : 32.0 (CH₃, C9–CH₃), 34.7 (C, C9), 38.5 (CH₂) and 38.7 (CH₂) (C6 and C12), 40.8 (CH₂) and 41.0 (CH₂) (C10 and C13), 41.3 (CH) and 41.4 (CH) (C5 and C11), 46.8 (CH₂, C8), 55.2 (C, C7), 123.0 (CH, C3), 124.0 (CH, C1), 130.6 (CH, C4), 148.1 (C, C11a), 148.3 (C, C2), 154.2 (C, C4a). HRMS-ESI + *m/z* [M+H]⁺ calcd for [C₁₆H₂₁N₂O₂]⁺: 273.1598, found: 273.1604.

4.1.7. 9-Methyl-5,6,8,9,10,11-hexahydro-7H-5,9,7,11-dimethanobenzo[9]annulene-2,7-diamine dihydrochloride (**10**)

To a solution of amine **9**·HCl (200 mg, 0.65 mmol) in methanol (25 mL), Pd on charcoal (20 mg, ca. 10% Pd) was added and the resulting suspension was hydrogenated at 1 atm of H₂ at rt for 48 h. The black suspension was filtered, and the solvent removed by concentration *in vacuo* to give **10** as a brown solid. Its hydrochloride was obtained by addition of an excess of HCl/MeOH to a solution of the amine in methanol followed by evaporation to obtain a brown solid (204 mg, quant. yield), mp 294–295 °C. IR (KBr disk) ν : 3200–2500 (3024, 2912, 2847, 2588), 1994, 1598, 1502, 1454, 1381,

1365, 1303, 1261, 1173, 1131, 1021, 957, 877, 827, 576, 473 cm⁻¹. ¹H NMR (400 MHz, MeOD) δ : 1.01 (s, 3H, CH₃), 1.50–1.60 [complex signal, 2H, 10(13)-H_a], 1.68–1.80 [complex signal, 2H, 10(13)-H_b], 1.72 (broad s., 2H, 8-H₂), 1.84–1.94 (complex signal, 2H, 6-H_a, 12-H_a), 2.03–2.14 (complex signal, 2H, 6-H_b, 12-H_b), 3.26–3.29 [complex signal, 5(11)-H], 7.16 (m, 1H, 3-H), 7.18 (d, *J* = 2.0 Hz, 1H, 1-H), 7.29 (m, 1H, 4-H). ¹³C NMR (100.6 MHz, MeOD) δ : 32.1 (CH₃, C9–CH₃), 34.7 (C, C9), 38.7 (CH₂) and 38.8 (CH₂) (C6 and C12), 41.1 (CH₂) and 41.15 (CH₂) (C10 and C13), 41.21 (CH₂) and 41.4 (CH₂) (C5 and C11), 46.8 (CH₂, C8), 55.3 (C, C7), 122.2 (CH) and 123.7 (CH) (C1 and C3), 130.4 (C, C4a), 131.1 (CH, C4), 147.1 (C) and 148.9 (C) (C2 and C11a). HRMS-ESI + *m/z* [M+H]⁺ calcd for [C₁₆H₂₃N₂]⁺: 243.1856, found: 243.1856.

4.1.8. N-(2-acetyl-9-methyl-5,6,8,9,10,11-hexahydro-7H-5,9,7,11-dimethanobenzo[9]annulen-7-yl)-2-chloroacetamide (**11**)

A solution of **7** (557 mg, 1.83 mmol) and acetyl chloride (1.31 mL, 18.4 mmol) were dissolved in DCM (14 mL) and treated with aluminium trichloride (1.22 g, 9.15 mmol). The resulting black mixture was stirred for 60 min then poured over a mixture of ice and saturated aq Na₂CO₃ solution (10 mL). After stirring 20 min the mixture was extracted with DCM (3 × 30 mL). The organic layer was dried over anhydrous Na₂SO₄, filtered and concentrated *in vacuo* to give a yellow solid. Purification by CombiFlash® in silica gel using as eluent a gradient from hexane to ethyl acetate/hexane mixture (2/8) gave **11** as a white solid (340 mg, 54% yield), mp 186–187 °C. IR (ATR) ν : 3276, 3083, 2959, 2916, 2845, 1670, 1603, 1562, 1456, 1419, 1405, 1364, 1336, 1281, 1271, 1249, 1238, 1228, 1166, 1108, 1051, 1013, 966, 948, 842, 795, 704, 689, 643 cm⁻¹. ¹H NMR (400 MHz, CDCl₃) δ : 0.95 (s, 3H, CH₃), 1.50–1.58 [complex signal, 2H, 10(13)-H_a], 1.66–1.74 [complex signal, 2H, 10(13)-H_b], 1.82 (dm, *J* = 12.0 Hz, 1H, 8-H_a), 1.87 (dm, *J* = 12.0 Hz, 1H, 8-H_b), 2.08–2.22 [complex signal, 4H, 6(12)-H₂], 2.57 (s, 3H, COCH₃), 3.13–3.23 [complex signal, 2H, 5-(11)-H], 3.92 (s, 2H, CH₂Cl), 6.32 (broad s., 1H, NH), 7.15 (d, *J* = 7.8 Hz, 1H, 4-H), 7.67 (m, 1H, 3-H), 7.69 (d, *J* = 1.6 Hz, 1H, 1-H). ¹³C NMR (100.6 MHz, CDCl₃) δ : 26.7 (CH₃, CH₃CO), 32.2 (CH₃, C9–CH₃), 33.8 (C, C9), 38.3 (CH₂) and 38.6 (CH₂) (C6 and C12), 40.8 (CH₂) and 40.97 (CH₂) (C10 and C13), 41.0 (CH) (C5 and C11), 43.1 (CH₂, CH₂Cl), 46.9 (CH₂, C8), 54.8 (C, C7), 127.1 (CH, C1), 128.0 (CH, C3), 128.6 (CH, C4), 135.7 (C) and 146.5 (C) (C2 and C11a), 151.9 (C, C4a), 164.8 (C, NHCO), 198.1 (C, COCH₃). HRMS-ESI + *m/z* [M+H]⁺ calcd for [C₂₀H₂₅ClNO₂]⁺: 346.1568, found: 346.1570.

4.1.9. 1-(7-Amino-9-methyl-6,7,8,9,10,11-hexahydro-5H-5,9,7,11-dimethanobenzo[9]annulen-2-yl)ethan-1-one hydrochloride (**12**)

Thiourea (233 mg, 3.06 mmol) and glacial acetic acid (1.6 mL) were added to a solution of chloroacetamide **11** (845 mg, 2.44 mmol) in abs. ethanol (42 mL) and the mixture was heated at reflux overnight. The resulting suspension was then tempered to rt, then H₂O (20 mL) was added and the pH was adjusted to 12 with 5 N NaOH solution. DCM (40 mL) was added, the phases were separated, and the aq phase was extracted with further dichloromethane (2 × 40 mL). The combined organic layers were dried over anhydrous Na₂SO₄, filtered and concentrated *in vacuo* to give a light brown solid. Purification by CombiFlash® in silica gel using as eluent a gradient from hexane to ethyl acetate/hexane mixture (3/7) gave **12** as a white solid. Its hydrochloride was obtained by adding an excess of HCl/Et₂O to a solution of the amine in ethyl acetate, followed by filtration of the resulting white precipitate (385 mg, 52% yield), mp > 200 °C (dec.). IR (ATR) ν : 3000–2400 (2988, 2904, 2858), 1678, 1603, 1508, 1451, 1428, 1362, 1272, 1256, 1207, 1135, 1115, 1031, 1002, 949, 912, 835, 827, 649, 640 cm⁻¹. ¹H NMR (400 MHz, MeOD) δ : 1.01 (s, 3H, CH₃), 1.53–1.61 [complex signal, 2H, 10(13)-H_a], 1.70 (broad s., 2H, 8-H₂), 1.70–1.80 [complex signal, 2 H, 10(13)-H_b], 1.82–1.92 [complex signal, 2H, 6(12)-H_a], 2.03–2.12 [complex

signal, 2H, 6(12)-H_b], 2.57 (s, 3H, COCH₃), 3.33–3.35 [complex signal, 2H, 5(11)-H], 7.26 [d, *J* = 7.6 Hz, 1H, 4-H), 7.75–7.78 (complex signal, 2H, 1-H, 3-H). ¹³C NMR (100.6 MHz, MeOD) δ: 26.7 (CH₃, CH₃CO), 32.1 (CH₃, C9–CH₃), 34.7 (C, C9), 38.8 (CH₂) and 39.1 (CH₂) (C6 and C12), 41.1 (CH₂) and 41.4 (CH₂) (C10 and C13), 41.5 (CH) and 41.6 (CH) (C5 and C11), 47.0 (CH₂, C8), 55.3 (C, C7), 128.5 (CH) and 129.2 (CH) (C1 and C3), 129.8 (CH, C4), 137.2 (C) and 147.0 (C) (C2 and C11a), 152.3 (C, C4a), 200.2 (C, CO). HRMS-ESI + *m/z* [M+H]⁺ calcd for [C₁₈H₂₄NO]⁺: 270.1852, found: 270.1858.

4.1.10. 1-(7-(dimethylamino)-9-methyl-6,7,8,9,10,11-hexahydro-5H-5,9,7,11-dimethanobenzo[9]annulen-2-yl)ethan-1-one hydrochloride (**14**)

AlCl₃ (419 mg, 3.14 mmol) was added to a solution of **13** (161 mg, 0.63 mmol) and AcCl (0.45 mL, 6.31 mmol) in DCM (5 mL). The resulting mixture was stirred for 60 min and then poured over a mixture of ice and saturated aq Na₂CO₃ solution (10 mL). After stirring 20 min the mixture was extracted with DCM (3 × 10 mL). The organic layer was dried over anhydrous Na₂SO₄, filtered and concentrated *in vacuo* to give **14** as a yellow solid. Its hydrochloride was obtained by adding an excess of HCl/Et₂O to a solution of the amine in ethyl acetate, followed by filtration of the resulting light brown precipitate (83 mg, 44% yield), mp 180–181 °C. IR (ATR) ν: 3300–2400 (3221, 2947, 2928, 2903, 2850), 1666, 1657, 1651, 1646, 1518, 1505, 1460, 1399, 1363, 1355, 1285, 1277, 1258, 1245, 1211, 1190, 1158, 1133, 1124, 1091, 1082, 1025, 1006, 960, 900, 864, 813, 803, 740, 708, 689 cm⁻¹. ¹H NMR (400 MHz, MeOD) δ: 1.04 (s, 3H, CH₃), 1.52–1.61 [complex signal, 2H, 10(13)-H_a], 1.71–1.81 [complex signal, 2H, 10(13)-H_b], 1.81 (broad s, 2H, 8-H₂), 1.97–2.07 [complex signal, 2H, 6(12)-H_a], 2.10–2.21 [complex signal, 2H, 6(12)-H_b], 2.57 (s, 3H, COCH₃), 2.83 [s, 6H, N(CH₃)₂], 3.41 [complex signal, 2H, 5(11)-H], 7.27 (d, *J* = 8.0 Hz, 1H, 4-H), 7.75–7.80 (complex signal, 1-H, 3-H). ¹³C NMR (100.6 MHz, MeOD) δ: 26.7 (CH₃, CH₃CO), 32.3 (CH₃, C9–CH₃), 34.0 (CH₂) and 34.2 (CH₂) (C6 and C12), 35.5 (C, C9), 37.3 [CH₃, N(CH₃)₂], 40.9 (CH₂) and 41.2 (CH₂) (C10 and C13), 41.5 (CH) and 41.6 (CH) (C5 and C11), 44.2 (CH₂, C8), 67.0 (C, C7), 128.6 (CH) and 129.2 (CH) (C1 and C3), 129.8 (CH, C4), 137.2 (C, C2), 146.9 (C, C11a), 152.2 (C, C4a), 200.1 (C, CO). HRMS-ESI + *m/z* [M+H]⁺ calcd for [C₂₀H₂₈NO]⁺: 298.2165, found: 298.2176.

4.1.11. N,N,9-trimethyl-2-nitro-5,6,8,9,10,11-hexahydro-7H-5,9,7,11-dimethanobenzo[9]annulen-7-amine hydrochloride (**15**)

To a solution of **9-HCl** (222 mg, 0.72 mmol) in MeOH (7 mL), NaBH₃CN (129 mg, 2.05 mmol), AcOH (0.3 mL) and formaldehyde (0.22 mL, 37% in H₂O solution, 2.16 mmol) were added and the mixture was stirred at rt for 8 h. An additional portion of NaBH₃CN (129 mg, 2.05 mmol) and formaldehyde (0.22 mL, 37% in H₂O solution, 2.16 mmol) were added, then the mixture was stirred at rt for 18 h and subsequently was concentrated *in vacuo* to dryness. H₂O (20 mL) was added to the residue, then the suspension was basified with 1 N NaOH solution (10 mL) and was extracted with ethyl acetate (4 × 15 mL). The combined organic extracts were washed with brine (2 × 10 mL), dried with anhydrous Na₂SO₄, then filtered and concentrated *in vacuo* to give **15** as a yellow oil. Its hydrochloride was obtained by adding an excess of HCl/Et₂O to a solution of the amine in ethyl acetate, followed by filtration of the white solid precipitate (180 mg, 74% yield), mp 168–169 °C. IR (ATR) ν: 3452, 3411, 2947, 2906, 2860, 2655, 2631, 2601, 1514, 1484, 1460, 1445, 1348, 1309, 1281, 1174, 1123, 1108, 1088, 1000, 982, 905, 896, 833, 801, 766, 736 cm⁻¹. ¹H NMR (400 MHz, MeOD) δ: 1.05 (s, 3H, CH₃), 1.55–1.62 [complex signal, 2H, 10(13)-H_a], 1.75–1.82 [complex signal, 2H, 10(13)-H_b], 1.82–1.85 (complex signal, 2H, 8-H₂), 2.01–2.11 [complex signal, 2H, 6(12)-H_a], 2.14–2.22 [complex signal, 2H, 6(12)-H_b], 2.84 [s, 6H, N(CH₃)₂], 3.44–3.50 [complex signal, 2H, 5(11)-H], 7.39 (d, *J* = 8.0 Hz, 1H, 4-H), 8.00 (dd, *J* = 8.0 Hz,

J' = 2.4 Hz, 1H, 3-H), 8.04 (d, *J* = 2.4 Hz, 1H, 1-H). ¹³C NMR (100.6 MHz, MeOD) δ: 32.2 (CH₃, C9–CH₃), 33.6 (CH₂) and 33.9 (CH₂) (C6 and C12), 35.5 (C, C9), 37.3 [CH₃, N(CH₃)₂], 40.6 (CH₂) and 40.8 (CH₂) (C10 and C13), 41.3 (CH) and 41.4 (CH) (C5 and C11), 44.0 (CH₂, C8), 66.8 (C, C7), 123.0 (CH, C3), 124.0 (CH, C1), 130.6 (CH, C4), 148.1 (C) and 148.2 (C) (C2 and C11a), 154.1 (C, C4a). HRMS-ESI + *m/z* [M+H]⁺ calcd for [C₁₈H₂₅N₂O₂]⁺: 301.1911, found: 301.1916.

4.1.12. N-(9-methyl-2-nitro-5,6,8,9,10,11-hexahydro-7H-5,9,7,11-dimethanobenzo[9]annulen-7-yl)acetamide (**17**)

To a cold (0 °C) solution of **16** (2.68 g, 9.95 mmol) in acetic anhydride (10.6 mL), glacial acetic acid (1.6 mL) and fuming nitric acid (1.9 mL) were carefully added. The mixture was allowed to react at rt and left stirring overnight. The obtained yellow solution was then poured into ice–water (20 mL) and extracted with DCM (3 × 40 mL). The combined organic extracts were washed with 2 N NaOH solution (1 × 40 mL), H₂O (1 × 40 mL) and brine (1 × 40 mL). The organic layer was dried over anhydrous Na₂SO₄, filtered and concentrated *in vacuo* to give a yellow residue. Purification by Combiflash® in silica gel using as eluent a gradient from hexane to ethyl acetate/hexane mixture (3/7) gave **17** as a white solid (1.87 g, 60% yield), mp 174–176 °C. IR (NaCl disk) ν: 3398, 3307, 3201, 3063, 2943, 2917, 2863, 1653, 1588, 1523, 1455, 1346, 1322, 1304, 1268, 1245, 1214, 1166, 1141, 1124, 1081, 1037, 1010, 945, 893, 865, 838, 798, 763, 740, 701, 645 cm⁻¹. ¹H NMR (400 MHz, CDCl₃) δ: 0.93 (s, 3H, CH₃), 1.52 [complex signal, 2H, 10(13)-H_a], 1.67–1.73 [complex signal, 2H, 10(13)-H_b], 1.76 (dt, *J* = 12.0 Hz, *J'* = 2.0 Hz, 2H, 8-H₂), 1.84 (dt, *J* = 12.0 Hz, *J'* = 2.0 Hz, 2H, 8-H₂), 1.90 (s, CH₃, CH₃CO), 2.06–2.19 [complex signal, 4H, 6(12)-H₂], 3.17–3.21 [complex signal, 2H, 5(11)-H], 5.27 (broad s, 1H, NH), 7.20 (d, *J* = 8.8 Hz, 1H, 4-H), 7.91–7.94 (complex signal, 2H, 1-H, 3-H). ¹³C NMR (100.6 MHz, CDCl₃) δ: 24.8 (CH₃, CH₃CO), 32.2 (CH₃, C9–CH₃), 33.7 (C, C9), 38.2 (CH₂, C6 or C12), 38.7 (CH₂, C12 or C6), 40.6 (CH₂, C10 or C13), 40.8 (CH₂, C13 or C10), 40.98 (CH, C5 or C11) and 41.00 (CH, C11 or C5), 47.2 (CH₂, C8), 54.1 (C, C7), 121.8 (CH, C1 or C3), 123.1 (CH, C3 or C1), 129.2 (CH, C4), 146.5 (C2 or C11a), 147.8 (C, C11a or C2), 154.1 (C, C4a), 169.5 (C, NHCO). HRMS-ESI + *m/z* [M – H]⁺ calcd for [C₁₈H₂₃N₂O₃]⁺: 315.1703, found: 315.1714.

4.1.13. N-(2-amino-9-methyl-5,6,8,9,10,11-hexahydro-7H-5,9,7,11-dimethanobenzo[9]annulen-7-yl)acetamide (**18**)

To a solution of acetamide (2.65 g, 8.43 mmol) in abs. ethanol (140 mL), PtO₂ (190 mg, 0.84 mmol) was added, and the resulting suspension was hydrogenated at 1 atm of H₂ at rt for 4 h. The black suspension was filtered, and the solvent removed by concentration *in vacuo* to give a dark solid. Purification by Combiflash® in silica gel using as eluent a gradient from hexane to ethyl acetate/hexane mixture (5/5) gave **18** as a white solid (1.63 g, 68% yield), mp 113 °C. IR (NaCl disk) ν: 3432, 3324, 3224, 3056, 3004, 2938, 2903, 2856, 2835, 1651, 1618, 1546, 1507, 1447, 1362, 1344, 1300, 1262, 1194, 1164, 1136, 1065, 862, 818, 735, 701 cm⁻¹. ¹H-RMN (400 MHz, CDCl₃) δ: 0.89 (s, 3H, CH₃), 1.45–1.54 [complex signal, 2H, 10(13)-H_a], 1.59–1.65 [complex signal, 2H, 10(13)-H_b], 1.76 (dm, *J* = 12.0 Hz, 1H, 8-H_a), 1.85 (dm, *J* = 12.0 Hz, 1H, 8-H_b), 1.89 (s, 3H, CH₃CO), 1.90 (m, 1H, 6-H_a or 12-H_a), 1.96 (broad d, *J* = 12.0 Hz, 1H, 12-H_a or 6-H_a), 2.09 (ddd, *J* = 12.8 Hz, *J'* = 6.4 Hz, *J''* = 2.4 Hz, 2H, 6-H_b or 12-H_b), 2.17 (ddd, *J* = 12.8 Hz, *J'* = 6.4 Hz, *J''* = 2.4 Hz, 2H, 12-H_b or 6-H_b), 2.90 (t, *J* = 6.0 Hz, 1H, 5-H or 11-H), 2.96 (t, *J* = 6.0 Hz, 1H, 11-H or 5-H), 5.21 (broad s, 1H, NH), 6.40 (dd, *J* = 8.0 Hz, *J'* = 2.2 Hz, 1H, 3-H), 6.42 (d, *J* = 2.2 Hz, 1H, 1-H), 6.83 (d, *J* = 8.0 Hz, 1H, 4-H). ¹³C NMR (100.6 MHz, CDCl₃) δ: 25.0 (CH₃, CH₃CO), 32.4 (CH₃, C9–CH₃), 33.6 (C, C9), 39.1 (CH₂, C12 or C6), 39.9 (CH₂, C6 or C12), 40.2 (CH, C11 or C5), 41.2 (CH, C5 or C11), 41.3 (CH₂, C10 or C13), 41.9 (CH₂, C13 or C10), 47.3 (CH₂, C8), 54.6 (C, C7), 112.6 (CH, C3), 115.4 (CH, C1), 129.1 (CH, C4), 136.9 (C, C4a), 144.6 (C, C11a), 147.5 (C, C2), 169.3 (C,

NHCO). HRMS-ESI + m/z [M - H]⁺ calcd for [C₁₈H₂₅N₂O]⁺: 285.1961, found: 285.1972.

4.1.14. *N*-(2-chloro-9-methyl-5,6,8,9,10,11-hexahydro-7H-5,9:7,11-dimethanobenzo[9]annulen-7-yl)acetamide (**19**)

18-HCl (1.04 g, 3.24 mmol) was dissolved in H₂O (6 mL) and conc. HCl solution (6 mL) then cooled to 0 °C and treated with a solution of sodium nitrite (448 mg, 6.49 mmol) in H₂O (2 mL) dropwise. To the resulting solution was added a CuCl (691 mg, 6.98 mmol) in conc. HCl solution (3 mL) and over 10 min gas was observed. The resulting solution was warmed to 60 °C for 90 min, then was cooled to rt, diluted in H₂O (60 mL) and extracted with DCM (4 × 90 mL). The combined organic extracts were washed with saturated aq NaHCO₃ solution, brine and were dried over anhydrous Na₂SO₄, filtered and concentrated *in vacuo* to give a dark green solid. Purification by CombiFlash® in silica gel using as eluent a gradient from hexane to ethyl acetate/hexane mixture (1/9) gave **19** as a white solid (210 mg, 21% yield), mp 190–191 °C. IR (NaCl disk) ν : 3301, 3196, 3071, 2921, 2855, 1651, 1594, 1549, 1487, 1454, 1414, 1364, 1343, 1308, 1281, 1263, 1211, 1139, 1109, 1012, 950, 875, 820 cm⁻¹. ¹H NMR (400 MHz, CDCl₃) δ : 0.91 (s, 3H, CH₃), 1.46–1.54 [complex signal, 2H, 10(13)-H_a], 1.60–1.68 [complex signal, 2H, 10(13)-H_b], 1.78–1.81 [complex signal, 2H, 8-H₂], 1.90 (s, 3H, CH₃CO), 1.98–2.06 [complex signal, 2H, 6(12)-H_a], 2.09–2.16 [complex signal, 2H, 6(12)-H_b], 3.00 (tm, $J = 6.0$ Hz, 1H, 5-H or 11-H), 3.04 (tm, $J = 6.0$ Hz, 1H, 11-H or 5-H), 5.19 (broad s, 1H, NH), 6.97 (dd, $J = 7.2$ Hz, $J' = 1.6$ Hz, 1H, 3-H), 7.02–7.04 [complex signal, 2H, 1(4)-H]. ¹³C NMR (100.6 MHz, CDCl₃) δ : 24.9 (CH₃, CH₃CO), 32.3 (CH₃, C9–CH₃), 33.7 (C, C9), 38.9 (CH₂, C12 or C6), 39.0 (CH₂, C6 or C12), 40.5 (CH, C11 or C5), 40.9 (CH, C5 or C11), 41.1 (CH₂, C10 or C13), 41.2 (CH₂, C13 or C10), 47.3 (CH₂, C8), 54.4 (C, C7), 126.2 (CH, C1 or C4), 128.1 (CH, C4 or C1), 129.6 (CH, C3), 131.6 (C, C2), 144.6 (C, C4a), 148.2 (C, C11a), 169.3 (C, NHCO). HRMS-ESI + m/z [M - H]⁺ calcd for [C₁₈H₂₃ClNO]⁺: 304.1463, found: 304.1460.

4.1.15. 2-Chloro-9-methyl-5,6,8,9,10,11-hexahydro-7H-5,9:7,11-dimethanobenzo[9]annulen-7-amine hydrochloride (**20**)

To a solution of acetamide **19** (190 mg, 0.63 mmol) in 2-propanol (6 mL), H₂O (8 mL) and conc. HCl (4 mL) were added, and the mixture was stirred under reflux for 6 days. The solution was cooled and washed with ethyl acetate (3 × 4 mL). The aq phase was basified with 1 N NaOH solution (10 mL) and extracted with ethyl acetate (4 × 15 mL). The combined organic layers were dried over anhydrous Na₂SO₄, filtered and concentrated *in vacuo* to give **20** as a light brown solid. Its hydrochloride was obtained by adding an excess of HCl/Et₂O to a solution of the amine in ethyl acetate, followed by filtration of the resulting white precipitate (36 mg, 19% yield). The analytical sample was obtained by crystallization from MeOH/Et₂O, mp > 250 °C. IR (KBr disk) ν : 3200–2500 (2990, 2950, 2916, 2861), 2058, 1597, 1570, 1509, 1488, 1454, 1416, 1380, 1365, 1302, 1256, 1217, 1155, 1133, 1110, 1093, 1032, 1000, 948, 875, 820, 771, 673 cm⁻¹. ¹H NMR (400 MHz, MeOD) δ : 1.00 (s, 3H, CH₃), 1.52–1.60 [complex signal, 2H, 10(13)-H_a], 1.65–1.68 [complex signal, 2H, 8-H₂], 1.68–1.74 [complex signal, 2H, 10(13)-H_b], 1.82–1.90 [complex signal, 2H, 6(12)-H_a], 1.99–2.07 [complex signal, 2H, 6(12)-H_b], 3.18 (tm, $J = 6.0$ Hz, 1H, 5-H or 11-H), 3.22 (tm, $J = 6.0$ Hz, 1H, 11-H or 5-H), 7.09–7.102 [complex signal, 2H, 3(4)-H], 7.14 (broad signal, 1H, 1-H). ¹³C NMR (100.6 MHz, MeOD) δ : 32.2 (CH₃, C9–CH₃), 34.7 (C, C9), 39.0 (CH₂, C12 or C6), 39.1 (CH₂, C6 or C12), 41.0 (CH, C11 or C5), 41.3 (CH, C5 or C11 and CH₂, C10 or C13), 41.4 (CH₂, C13 or C10), 47.0 (CH₂, C8), 55.3 (C, C7), 127.7 (CH, C3 or C4), 129.1 (CH, C1), 130.9 (CH, C4 or C3), 133.2 (C, C2), 145.2 (C, C4a), 148.5 (C, C11a). HRMS-ESI + m/z [M+]⁺ calcd for [C₁₆H₂₁ClN]⁺: 262.1357, found: 262.1359.

4.1.16. 2-Fluoro-5,6,8,9-tetrahydro-7H-5,9-propanobenzo[7]annulene-7,11-dione (**25**)

a) 4-fluorophthalaldehyde (1 g, 6.57 mmol) was dissolved in methanol (18 mL) then dimethyl-1,3-acetonedicarboxylate (2.33 g, 13.4 mmol) and diethylamine (2 drops) were added. The yellow solution was brought to reflux for 1.5 h. The solution was allowed to cool to rt and more diethylamine (2 drops) was added. The solution was left at 4 °C overnight and then the solid was filtered off, obtaining the tetraester as a white solid (675 mg, 22% yield). Crude was used in the next step without further purification.

b) The aforementioned tetraester (675 mg, 1.45 mmol) was mixed with conc. HCl (1 mL) and glacial acetic acid (4 mL). The yellow solution was heated to reflux for 12 h. The solvent was removed under vacuum and the solid residue was diluted with hot diethyl ether (10 mL) over 15 min and the solution was stored at 4 °C overnight. The residue was filtered off obtaining a white solid (250 mg) that was constituted by a mixture of diketone **25** and its hydrate in an approximate ratio of 1:2. The pure diketone was obtained as a white solid using 7 mL of toluene as a solvent in a Dean-Stark apparatus for 24 h (200 mg, 59% yield), mp 105–107 °C. IR (NaCl disk) ν : 2923, 2848, 1710, 1607, 1593, 1490, 1428, 1380, 1346, 1253, 1208, 1153, 1119, 1074, 985, 944, 865, 806 cm⁻¹. ¹H NMR (400 MHz, CDCl₃) δ : 2.68–2.78 [complex signal, 4H, 6(12)-H_a, 8(10)-H_a], 2.84–2.93 [complex signal, 4H, 6(12)-H_b, 8(10)-H_b], 3.31 (tt, $J = J' = 4.4$ Hz, 1H, 5-H or 9-H), 3.37 (tt, $J = J' = 4.4$ Hz, 1H, 9-H or 5-H), 7.01 (td, $J = 8.0$ Hz, $J' = 2.8$ Hz, 1H, 3-H), 7.06 (dd, $J = 9.2$ Hz, $J' = 2.8$ Hz, 1H, 1-H), 7.29 (dd, $J = 8.0$ Hz, $J' = 5.6$ Hz, 1H, 4-H). ¹³C NMR (100.6 MHz, CDCl₃) δ : 37.3 (CH) and 38.1 (CH), (C5 and C9), 49.0 (CH₂) and 49.3 (CH₂) [C6(12) and C8(10)], 115.0 (CH, d, $J_{C-F} = 21$ Hz, C3), 115.8 (CH, d, $J_{C-F} = 22$ Hz, C1), 130.7 (CH, d, $J_{C-F} = 8.0$ Hz, C4), 138.9 (C, C4a), 145.2 (C, d, $J_{C-F} = 7.1$ Hz, C9a), 162.4 (C, d, $J_{C-F} = 247.3$ Hz, C2), 208.4 [C, C7(11)-CO]. HRMS-ESI + m/z [M+]⁺ calcd for [C₁₄H₁₄FO₂]⁺: 233.0972, found: 233.0967.

4.1.17. 2,3-Dimethoxy-5,6,8,9-tetrahydro-7H-5,9-propanobenzo[7]annulene-7,11-dione (**26**)

a) 4,5-dimethoxyphthalaldehyde (6.54 g, 33.7 mmol) was dissolved in methanol (130 mL) then dimethyl-1,3-acetonedicarboxylate (11.7 g, 67.4 mmol) and diethylamine (19 drops) were added. The brown solution was brought to reflux for 1.5 h. The brown suspension was allowed to cool to rt and more diethylamine (19 drops) was added. The suspension was left at 4 °C over the weekend and was then filtered under vacuum. The white residue was dried under vacuum (6.84 g, 40% yield) and was used in the next step without further purification.

b) The aforementioned tetraester (6.84 g, 13.5 mmol) was mixed with conc. HCl (10 mL) and glacial acetic acid (35 mL). The yellow paste was heated to reflux for 24 h. The resulting orange suspension was allowed to cool to rt and was then concentrated under vacuum. The brown solid was dissolved in toluene and the brown solution was heated to reflux in a Dean-Stark set up for 24 h. The yellow solution was allowed to cool to rt and was then concentrated under vacuum. The resulting brown solid was washed twice with hot methanol and was dried again to obtain diketone **26** as a brown solid (2.80 g, 76% yield), mp 236–237 °C. IR (NaCl disk) ν : 2952, 2840, 1698, 1605, 1516, 1467, 1451, 1416, 1355, 1336, 1254, 1221, 1192, 1162, 1025, 1002, 880, 811 cm⁻¹. ¹H NMR (400 MHz, CDCl₃) δ : 2.73 [dd, $J = 15.2$ Hz, $J' = 4.0$ Hz, 4H, 6(8,10,12)-H_a], 2.85 [dd, $J = 15.2$ Hz, $J' = 4.4$ Hz, 4H, 6(8,10,12)-

H_b], 3.27 [tt, *J* = 4.8 Hz, *J'* = 3.6 Hz, 2H, 5(9)-H], 3.90 (s, 6H, OCH₃), 6.82 [s, 2H, 1(4)-H]. ¹³C NMR (100.6 MHz, CDCl₃) δ: 37.7 [CH, C5(9)], 49.4 [CH₂, C6(8,10,12)], 56.3 [CH₃, OCH₃], 112.4 [CH, C1(4)], 135.2 [C, C4a(9a)], 148.5 [C, C2(3)], 209.1 [C, C7(11)]. HRMS-ESI + *m/z* [M+H]⁺ calcd for [C₁₆H₁₉O₄]⁺: 275.1278, found: 275.1279.

4.1.18. 1-Fluoro-5,6,8,9-tetrahydro-7H-5,9-propanobenzo[7]annulene-7,11-dione (**27**)

a) 3-fluorophthalaldehyde (11.2 g, 73.6 mmol) was dissolved in methanol (220 mL) then dimethyl-1,3-acetonedicarboxylate (25.6 g, 147 mmol) and diethylamine (33 drops) were added. The yellow solution was brought to reflux for 1.5 h. The solution was allowed to cool to rt and more diethylamine (33 drops) was added. The solution was left at 4 °C overnight and was then filtered under vacuum. The white crystals were dried under vacuum and the tetraester was used in the next step without further purification (18.5 g, 54% yield).

b) The aforementioned tetraester (18.5, 39.9 mmol) was mixed with conc. HCl (31 mL) and glacial acetic acid (103 mL). The yellow solution was heated to reflux for 24 h. The pale-yellow solution was allowed to cool to rt and was then concentrated under vacuum. The off-white solid was dissolved in toluene and the yellow solution was heated to reflux in a Dean-Stark set up for 24 h. The yellow solution was allowed to cool to rt and was then concentrated under vacuum to give **27** as an off-white solid (8.73 g, 94% yield), mp > 150 °C. IR (NaCl disk) *ν*: 2940, 2908, 1701, 1619, 1585, 1468, 1421, 1370, 1304, 1245, 1222, 1203, 1072, 1052, 988, 931, 897, 789, 746 cm⁻¹. ¹H NMR (400 MHz, CDCl₃) δ: 2.69 [dd, *J* = 15.6 Hz, *J'* = 3.6 Hz, 2H, 8(10)-H_a], 2.75 [dd, *J* = 15.6 Hz, *J'* = 4.0 Hz, 2H, 6(12)-H_a], 2.90 [dd, *J* = 15.6 Hz, *J'* = 4.8 Hz, 4H, 6(12)-H_b, 8(10)-H_b], 3.42 (m, 1H, 5-H), 4.00 (tt, *J* = 4.4 Hz, *J'* = 4.0 Hz, 1H, 9-H), 7.08–7.15 [complex signal, 2H, 2(4)-H], 7.29 (m, 1H, 3-H). ¹⁹F NMR (376 MHz, CDCl₃) δ: 117.3 (t, *J* = 7.52 Hz). ¹³C NMR (100.6 MHz, CDCl₃) δ: 26.4 (CH, d, *J*_{C-F} = 6.4 Hz, C9), 37.9 (CH, d, *J*_{C-F} = 2.5 Hz, C5), 48.6 [CH₂, C8(10)], 49.0 [CH₂, C6(12)], 115.1 (CH, d, *J*_{C-F} = 24.1 Hz, C2), 124.3 (CH, d, *J*_{C-F} = 3.2 Hz, C4), 129.3 (CH, d, *J*_{C-F} = 9.2 Hz, C3), 130.0 (C, d, *J*_{C-F} = 13.8 Hz, C9a), 146.0 (C, d, *J*_{C-F} = 1.9 Hz, C4a), 159.5 (C, d, *J*_{C-F} = 245.8 Hz, C1), 208.5 (C, CO). HRMS-ESI + *m/z* [M+H]⁺ calcd for [C₁₄H₁₄FO₂]⁺: 233.0972, found: 233.0976.

4.1.19. 2-Methoxy-5,6,8,9-tetrahydro-7H-5,9-propanobenzo[7]annulene-7,11-dione (**28**)

a) 4-methoxyphthalaldehyde (10.2 g, 62.1 mmol) was dissolved in methanol (380 mL) then dimethyl-1,3-acetonedicarboxylate (21.6 g, 124 mmol) and diethylamine (28 drops) were added. The dark red solution was brought to reflux for 1.5 h. The solution was allowed to cool to rt and more diethylamine (22 drops) was added. The solution was left at 4 °C over 5 days and was then filtered under vacuum. The red residue was dried under vacuum (19.4 g, 66% yield) and was used in the next step without further purification.

b) The aforementioned tetraester (250 mg, 0.53 mmol) was mixed with conc. HCl (0.4 mL) and glacial acetic acid (1.4 mL). The white suspension was heated to reflux for 24 h. The dark red solution was allowed to cool to rt and was then concentrated under vacuum. The red oil was dissolved in toluene and the red solution was heated to reflux in a Dean-Stark set up for 24 h. The red solution was allowed to cool to rt and was then concentrated under vacuum to give **28** as a red solid (125 mg, 98% yield), mp

157–158 °C. IR (NaCl disk) *ν*: 2941, 2910, 2837, 1701, 1610, 1585, 1504, 1431, 1414, 1370, 1321, 1300, 1266, 1166, 1094, 1033, 989 cm⁻¹. ¹H NMR (400 MHz, CDCl₃) δ: 2.68–2.78 [complex signal, 4H, 6(12)-H_a, 8(10)-H_a], 2.82–2.91 [complex signal, 4H, 6(12)-H_b, 8(10)-H_b], 3.27 (tt, *J* = 4.4 Hz, *J'* = 4.0 Hz, 1H, 9-H), 3.32 (tt, *J* = 4.4 Hz, *J'* = 4.0 Hz, 1H, 5-H), 3.84 (s, 3H, OCH₃), 6.83 (dd, *J* = 8.4 Hz, *J'* = 2.8 Hz, 1H, 3-H), 6.87 (d, *J* = 2.8 Hz, 1H, 1-H), 7.23 (d, *J* = 8.4 Hz, 1H, 4-H). ¹³C NMR (100.6 MHz, CDCl₃) δ: 37.2 (CH, C5), 38.4 (CH, C9), 49.2 (CH₂) and 49.6 (CH₂), C6(12) and C8(10), 55.5 (CH₃, OCH₃), 112.9 (CH, C3), 114.7 (CH, C1), 130.2 (CH, C4), 135.2 (C, C4a), 144.2 (C, C9a), 160.0 (C, C2), 209.1 [C, C7(11)-CO]. HRMS-ESI + *m/z* [M+H]⁺ calcd for [C₁₅H₁₇O₃]⁺: 245.1172, found: 245.1180.

4.1.20. 2-Fluoro-7,11-dimethylene-6,7,8,9-tetrahydro-5H-5,9-propanobenzo[7]annulene (**29**)

A suspension of sodium hydride, 60% dispersion in mineral oil (85 mg, 2.13 mmol), in anhydrous DMSO (2 mL) was heated to 90 °C for 45 min under N₂ atmosphere. After the reaction mixture was tempered, a solution of triphenylmethylphosphonium iodide (1.48 g, 3.66 mmol) in anhydrous DMSO (3.5 mL) was added, and the resulting yellow solution was stirred at rt for 20 min. Then a suspension of diketone (200 mg, 0.86 mmol) in anhydrous DMSO (2 mL) was added and the obtained solution was heated to 90 °C overnight. The resulting black solution was allowed to cool to rt and then poured into H₂O (20 mL). Hexane (20 mL) was added and the phases were separated. The aq phase was extracted with further hexane (4 × 20 mL) and the combined organic phases were washed with brine (20 mL), dried over anhydrous Na₂SO₄, filtered and concentrated *in vacuo*. The crude was purified by Combiflash® in silica gel using 100% hexane to give diene **29** as a white solid (118 mg, 60% yield), mp 108–109 °C. IR (NaCl disk) *ν*: 3072, 2985, 2921, 2844, 1639, 1612, 1592, 1494, 1451, 1444, 1363, 1246, 1162, 1135, 1095, 1048, 974, 951, 930, 887, 820, 716, 658, 638, 598, 528 cm⁻¹. ¹H NMR (400 MHz, CDCl₃) δ: 2.41–2.51 [complex signal, 4H, 6(12)-H_a, 8(10)-H_a], 2.55–2.62 [complex signal, 4H, 6(12)-H_b, 8(10)-H_b], 3.04 (tt, *J* = *J'* = 4.4 Hz, 1H, 5-H or 9-H), 3.09 (tt, *J* = *J'* = 4.4 Hz, 1H, 9-H or 5-H), 4.68 [s, 4H, 7(11)-CH₂], 6.75–6.82 [complex signal, 2H, 1(3)-H], 7.02 (m, 1H, 4-H). ¹³C NMR (100.6 MHz, CDCl₃) δ: 40.7 (CH₂) and 40.9 (CH₂) [C6(12) and C8(10)], 40.9 (CH) and 41.6 (CH) (C5 and C9), 112.8 (CH, d, *J*_{C-F} = 20 Hz, C1), 115.4 [complex signal, C7(11) = CH₂, C3], 130.0 (CH, d, *J*_{C-F} = 8.0 Hz, C4), 137.1 (C, C4a), 146.3 [C, C7(11)], 162.8 (C, C2). The signal from C9a was not observed.

4.1.21. 2,3-Dimethoxy-7,11-dimethylene-6,7,8,9-tetrahydro-5H-5,9-propanobenzo[7]annulene (**30**)

In a flame dried 3-necked round bottom flask, sodium hydride 60% in mineral oil (1.67 g, 41.8 mmol) was added under N₂ and was dissolved in anhydrous DMSO (22 mL). The grey suspension was heated to 75 °C for 45 min and was then cooled to rt. Methyltriphenylphosphonium iodide (16.9 g, 41.8 mmol) dissolved in anhydrous DMSO (36 mL) and diketone **29** (2.80 g, 10.2 mmol) dissolved in anhydrous DMSO (23 mL) were sequentially added under N₂. The brown solution was stirred and heated to 90 °C overnight. The black solution was allowed to cool to rt and it was then poured into H₂O (200 mL). The H₂O was extracted with hexane (4 × 200 mL) and the organic layer was dried over anhydrous Na₂SO₄, filtered and concentrated under vacuum. The crude was purified by Combiflash® in silica gel using a solvent system of 100% hexane. Diene **30** was isolated as a yellow solid (633 mg, 23% yield), mp 74–75 °C. IR (NaCl disk) *ν*: 3068, 2977, 2913, 2832, 1639, 1606, 1515, 1464, 1450, 1429, 1414, 1358, 1342, 1293, 1261, 1240, 1225, 1191, 1173, 1103, 1023, 956, 931, 889, 804, 656, 634 cm⁻¹. ¹H NMR (400 MHz, CDCl₃) δ: 2.48 [dd, *J* = 14.0 Hz, *J'* = 5.2 Hz, 4H, 6(8,10,12)-H_a], 2.59 [dd, *J* = 14.0 Hz, *J'* = 4.4 Hz, 4H,

6(8,10,12)-H_b], 3.00 [tt, *J* = 4.8 Hz, *J'* = 4.4 Hz, 2H, 5(9)-H], 3.86 (s, 6H, OCH₃), 4.67 (s, 4H, 7(11)-C=CH₂), 6.63 [s, 2H, 1(4)-H]. ¹³C NMR (100.6 MHz, CDCl₃) δ: 41.1 [CH₂, C6(8,10,12)], 41.3 [CH, C5(9)], 56.1 [CH₃, OCH₃], 112.7 [CH, C1(4)], 115.1 [CH₂, C=CH₂], 136.8 [C, C4a(9a)], 146.8 [C, C7(11)], 148.5 [C, C2(3)]. HRMS-ESI + *m/z* [M+H]⁺ calcd for [C₁₈H₂₃O₂]⁺: 271.1693, found: 271.1688.

4.1.22. 1-Fluoro-7,11-dimethylene-6,7,8,9-tetrahydro-5H-5,9-propanobenzo[7]annulene (31)

In a flame dried 3-necked round bottom flask, sodium hydride 60% dispersion in mineral oil (2.82 g, 70.5 mmol) was added under N₂ and was dissolved in anhydrous DMSO (34.8 mL). The grey suspension was heated to 75 °C for 45 min, yielding a green suspension, and was then cooled to rt. To the green suspension, methyltriphenylphosphonium iodide (28.5 g, 70.5 mmol) diluted in anhydrous DMSO (75 mL) and the diketone **27** (4.00 g, 17.2 mmol) diluted in anhydrous DMSO (38 mL) were added sequentially. The resulting mixture was heated at 90 °C overnight. The resulting black solution was allowed to cool to rt and it was then poured into H₂O (200 mL). The H₂O was extracted with hexane (4 × 200 mL) and the organic layer was dried over anhydrous Na₂SO₄, filtered and concentrated under vacuum. The crude was purified by Combiflash® using as eluent a gradient from pure hexane to ethyl acetate/hexane mixture (1/9). Diene **31** was isolated as a colourless oil (2.69 g, 69% yield). IR (NaCl disk) *ν*: 3071, 3033, 2981, 2921, 2838, 1639, 1614, 1583, 1464, 1446, 1429, 1365, 1248, 1155, 1046, 991, 935, 919, 895 cm⁻¹. ¹H NMR (400 MHz, CDCl₃) δ: 2.43–2.56 [complex signal, 4H, 6(12)-H_a, 8(10)-H_a], 2.64 [dd, *J* = 14.4 Hz, *J'* = 4.2 Hz, 4H, 6(12)-H_b, 8(10)-H_b], 3.19 (m, 1H, 5-H), 3.79 (tt, *J* = *J'* = 4.8 Hz, 1H, 9-H), 4.72 [d, *J* = 0.8 Hz, 4H, 7(11)-CH₂], 6.88–6.96 [complex signal, 2H, 2-H, 4-H], 7.08 (m, 1H, 3-H). ¹⁹F NMR (376 MHz, CDCl₃) δ: -119.9 (t, *J* = 4.89 Hz). ¹³C NMR (100.6 MHz, CDCl₃) δ: 29.5 (CH, d, *J*_{C-F} = 5 Hz, C9), 40.2 (CH₂) and 40.6 (CH₂), C6(12) and C8(10), 41.7 (CH, d, *J*_{C-F} = 2.0 Hz, C5), 113.7 (CH, d, *J*_{C-F} = 24 Hz, C2), 115.5 [CH₂, C7(11)-CH₂], 124.1 (CH, d, *J*_{C-F} = 3.0 Hz, C4), 127.4 (CH, d, *J*_{C-F} = 9.1 Hz, C3), 131.0 (C, d, *J*_{C-F} = 13.1 Hz, C9a), 146.2 [C, C7(11)], 147.6 (C, d, *J*_{C-F} = 2.5 Hz, C4a), 159.7 (C, d, *J*_{C-F} = 242.4 Hz, C1). HRMS-ESI + *m/z* [M+H]⁺ calcd for [C₁₆H₁₈F]⁺: 229.1387, found: 229.1392.

4.1.23. 2-Methoxy-7,11-dimethylene-6,7,8,9-tetrahydro-5H-5,9-propanobenzo[7]annulene (32)

In a flame dried 3-necked round bottom flask, sodium hydride 60% in mineral oil (2.68 g, 67.0 mmol) was added under N₂ and was dissolved in anhydrous DMSO (35 mL). The grey suspension was heated to 75 °C for 45 min and was then cooled to rt. Methyltriphenylphosphonium iodide (27.1 g, 67.0 mmol) dissolved in anhydrous DMSO (57 mL) and **28** (4.00 g, 16.4 mmol) dissolved in anhydrous DMSO (38 mL) were sequentially added under N₂. The brown solution was stirred and heated to 90 °C overnight. The black solution was allowed to cool to rt and it was then poured into H₂O (200 mL). The H₂O was extracted with hexane (4 × 200 mL) and the organic layer was dried over anhydrous Na₂SO₄, filtered and concentrated under vacuum. The crude was purified by Combiflash® in silica gel using a solvent system of 100% hexane. Diene **32** was isolated as a yellow waxy oil (1.50 g, 38% yield), mp 68–69 °C. IR (NaCl disk) *ν*: 3068, 2979, 2911, 2833, 1639, 1609, 1580, 1501, 1464, 1449, 1431, 1363, 1313, 1260, 1203, 1172, 1152, 1109, 1034, 955, 929, 889, 809, 661, 613 cm⁻¹. ¹H NMR (400 MHz, CDCl₃) δ: 2.43–2.53 [complex signal, 4H, 6(12)-H_a, 8(10)-H_a], 2.55–2.64 [complex signal, 4H, 6(12)-H_b, 8(10)-H_b], 3.03 (tt, *J* = 4.8 Hz, *J'* = 4.4 Hz, 1H, 5-H), 3.07 (tt, *J* = 4.8 Hz, *J'* = 4.4 Hz, 9-H), 3.79 (s, 3H, CH₃), 4.68 [s, 4H, 7(11)-CH₂], 6.65 (dd, *J* = 8.0 Hz, *J'* = 2.8 Hz, 1H, 3-H), 6.66 (d, *J* = 2.8 Hz, 1H, 1-H), 7.00 (d, *J* = 8.0 Hz, 1H, 4-H). ¹³C NMR (100.6 MHz, CDCl₃) δ: 40.7 (CH,

C9), 40.9 (CH₂) and 41.2 (CH₂) C6(8,10,12), 41.9 (CH, C5), 55.2 (CH₃, OCH₃), 110.8 (CH, C3), 114.9 (CH, C1), 115.1 [CH₂, C7(11)-CH₂], 129.6 (CH, C4), 136.9 (C, C4a), 146.0 (C, C9a), 146.7 [C, C7(11)], 158.3 (C, C2). HRMS-ESI + *m/z* [M+H]⁺ calcd for [C₁₇H₂₁O]⁺: 241.1587, found: 241.1588.

4.1.24. 2-Chloro-N-(2-fluoro-9-methyl-5,6,8,9,10,11-hexahydro-7H-5,9:7,11-dimethanobenzo[9]annulene-7-yl)acetamide (33)

Chloroacetonitrile (84 μL, δ = 1.19, 1.32 mmol) was added to a solution of 2-fluoro-7,11-dimethylene-6,7,8,9-tetrahydro-5H-5,9-propanobenzo[7]annulene (75 mg, 0.32 mmol) in acetic acid (0.25 mL) and the mixture was cooled to 0–5 °C with an ice bath. Conc. H₂SO₄ (0.11 mL, δ = 1.84, 1.97 mmol) was added dropwise (<10 °C). After the addition, the mixture was allowed to reach rt and was stirred overnight. The solution was added to ice (2 g) and the mixture was stirred at rt for a few minutes. DCM (5 mL) was added, the phases were separated, and the aq phase was extracted with further DCM (2 × 5 mL). The combined organic layers were dried over anhydrous Na₂SO₄, then filtered and evaporated *in vacuo* to give **33** as a yellow solid (50 mg, 48% yield), mp 141–144 °C. IR (NaCl disk) *ν*: 3399, 3313, 3067, 2944, 2920, 2851, 1657, 1607, 1591, 1518, 1498, 1451, 1361, 1345, 1252, 1179, 1145, 1086, 1049, 1009, 966, 963, 863, 820 cm⁻¹. ¹H NMR (400 MHz, CDCl₃) δ: 0.94 (s, 3H, 9-CH₃), 1.49–1.59 [complex signal, 2H, 10(13)-H_a], 1.62–1.70 [complex signal, 2 H, 10(13)-H_b], 1.81 (m, 1H, 8-H_a), 1.84 (m, 1H, 8-H_b), 2.05–2.19 [complex signal, 4H, 6(12)-H₂], 3.03 (m, 1H, 5-H or 11-H), 3.09 (m, 1H, 11-H or 5-H), 3.93 (s, 2H, CH₂Cl), 6.30 (broad s, 1H, NH), 6.73 (dd, *J* = 8.4 Hz, *J'* = 2.8 Hz, 1H, 1-H), 6.76 (m, 1H, 3-H), 7.00 (dd, *J* = 8.0 Hz, *J'* = 6.0 Hz, 1 H, 4-H). ¹³C NMR (100.6 MHz, CDCl₃) δ: 32.2 (CH₃, C9–CH₃), 33.7 (C, C9), 38.5 (CH₂) and 38.9 (CH₂) (C6 and C12), 40.3 (CH, C11), 40.93 (CH, C5), 40.97 (CH₂) and 41.26 (CH₂) (C10 and C13), 43.1 (CH₂, CH₂Cl), 47.0 (CH₂, C8), 55.0 (C, C7), 112.5 (CH, d, *J*_{C-F} = 20 Hz, C1), 115.0 (CH, d, *J*_{C-F} = 21 Hz, C3), 129.6 (CH, d, *J*_{C-F} = 8 Hz, C4), 141.9 (C, d, *J*_{C-F} = 3 Hz, C4a), 148.2 (C, d, *J*_{C-F} = 6.9 Hz, C11a), 161.4 (C, d, *J*_{C-F} = 244 Hz, C2), 164.7 (C, NHCO). HRMS-ESI + *m/z* [M+H]⁺ calcd for [C₁₈H₂₂ClFNO]⁺: 322.1368, found: 322.137.

4.1.25. 2-Chloro-N-(2,3-dimethoxy-9-methyl-5,6,8,9,10,11-hexahydro-7H-5,9:7,11-dimethanobenzo[9]annulene-7-yl)acetamide (34)

Diene **30** (498 mg, 1.84 mmol) was dissolved in glacial acetic acid (1.6 mL) and chloroacetonitrile (467 μL, δ = 1.19, 7.38 mmol) was added. The solution was cooled to 0 °C and conc. H₂SO₄ (601 μL, δ = 1.84, 11.0 mmol) was added dropwise with care not to raise above 10 °C. The solution was allowed to warm to rt and was left stirring overnight, then it was poured over ice (2 g) and extracted with DCM (3 × 10 mL). The organic layer was dried over anhydrous Na₂SO₄, then filtered and concentrated under vacuum. The crude was crystallized from DCM to obtain **34** as a white solid (501 mg, 75% yield), mp 204–205 °C. IR (NaCl disk) *ν*: 3306, 2941, 2907, 2861, 2838, 1666, 1605, 1516, 1467, 1452, 1415, 1381, 1361, 1345, 1293, 1252, 1231, 1191, 1168, 1092, 1021, 948, 861, 802 cm⁻¹. ¹H NMR (400 MHz, CDCl₃) δ: 0.93 (s, 3H, 9-CH₃), 1.55 [d, *J* = 13.2 Hz, 2H, 10(13)-H_a], 1.65 [dd, *J* = 13.2 Hz, *J'* = 6 Hz, 2H, 10(13)-H_b], 1.83 (s, 2H, 8-H₂), 2.07 [d, *J* = 12.8 Hz, 2H, 6(12)-H_a], 2.15 [ddd, *J* = 12.8 Hz, *J'* = 6.4 Hz, *J''* = 2.0 Hz, 2H, 6(12)-H_b], 3.00 [t, *J* = 6.4 Hz, 2H, 5(11)-H], 3.84 (s, 6H, OCH₃), 3.93 (s, 2H, CH₂-Cl), 6.29 (broad s, 1H, NH), 6.60 [s, 2H, 1(4)-H]. ¹³C NMR (100.6 MHz, CDCl₃) δ: 32.3 (CH₃, C9–CH₃), 33.7 (C, C9), 39.0 [CH₂, C6(12)], 40.7 [CH, C5(11)], 41.4 [CH₂, C10(13)], 43.1 (CH₂, CH₂-Cl), 47.1 (CH₂, C8), 55.1 (C, C7), 56.2 (CH₃, OCH₃), 112.4 [CH, C1(4)], 138.4 [C, C4a(11a)], 146.8 [C, C2(3)], 164.7 (C, NHCO). HRMS-ESI + *m/z* [M+H]⁺ calcd for [C₂₀H₂₇ClNO₃]⁺: 364.1674, found: 364.1674.

4.1.26. 2-Chloro-N-(1-fluoro-9-methyl-5,6,8,9,10,11-hexahydro-7H-5,9,7,11-dimethanobenzo[9]annulen-7-yl)acetamide (**35**)

Chloroacetonitrile (2.7 mL, $\delta = 1.19$, 42.7 mmol) was added to a solution of diene **31** (2.37 g, 10.4 mmol) in acetic acid (7 mL) and the mixture was cooled to 0–5 °C with an ice bath. Conc. H₂SO₄ (3.4 mL, $\delta = 1.84$, 63.8 mmol) was added dropwise (<10 °C). After the addition, the mixture was allowed to reach rt and stirred overnight. The solution was added to ice (10 g) and the mixture was stirred at rt for few minutes. DCM (100 mL) was added, the phases were separated, and the aqueous phase was extracted with further DCM (2 × 100 mL). The combined organic layers were dried over anhydrous Na₂SO₄, filtered and evaporated *in vacuo* to give **35** as a white solid (2.28 g, 68% yield), mp 154–155 °C. IR (NaCl disk) ν : 3402, 3308, 3073, 2947, 2911, 2863, 2840, 1660, 1613, 1583, 1529, 1463, 1363, 1348, 1312, 1242, 1186, 1155, 1069, 1053, 979, 875, 798, 748 cm⁻¹. ¹H-NMR (400 MHz, CDCl₃) δ : 0.93 (s, 3H, 9-CH₃), 1.45–1.61 (complex signal, 2H, 10-H_a, 13-H_a), 1.63–1.71 (complex signal, 2H, 10-H_b, 13-H_b), 1.80 (dt, $J = 12.0$ Hz, $J' = 2.0$ Hz, 1H, 8-H_a), 1.87 (dt, $J = 12.0$ Hz, $J' = 2.0$ Hz, 1H, 8-H_b), 2.08–2.11 (complex signal, 2H, 6-H₂ or 12-H₂), 2.14–2.17 (complex signal, 2H, 12-H₂, 6-H₂), 3.13 (m, 1H, 5-H), 3.73 (tm, $J = 6.0$ Hz, 1H, 11-H), 3.93 (s, 2H, CH₂Cl), 6.31 (broad s, 1H, NH), 6.84 (d, $J = 8.0$ Hz, 1H, 4-H), 6.86 (dd, $J = 8.4$ Hz, $J' = 1.2$ Hz, 1H, 2-H) 7.01 (m, 1H, 3-H). ¹³C NMR (100.6 MHz, CDCl₃) δ : 28.6 (CH, d, $J_{C-F} = 5.7$ Hz, C11), 32.2 (CH₃, C9–CH₃), 33.81 (C, C9), 38.3 (CH₂) and 38.4 (CH₂) (C6 and C12), 40.6 (CH₂) and 40.96 (CH₂) (C10 and C13), 41.03 (CH, d, $J = 2.3$ Hz, C5), 43.1 (CH₂, CH₂Cl), 47.0 (CH₂, C8), 55.0 (C, C7), 113.5 (CH, d, $J_{C-F} = 24.8$ Hz, C2), 123.6 (CH, d, $J_{C-F} = 3.1$ Hz, C4), 127.2 (CH, d, $J_{C-F} = 9.3$ Hz, C3), 132.6 (CH, d, $J_{C-F} = 13.2$ Hz, C11a), 149.3 (C, d, $J_{C-F} = 2.2$ Hz, C4a), 159.3 (C, d, $J_{C-F} = 243.5$ Hz, C1), 164.7 (C, NHCO). HRMS-ESI + m/z [M+H]⁺ calcd for [C₁₈H₂₂ClFN]⁺: 322.1368, found: 322.1374.

4.1.27. 2-Chloro-N-(2-methoxy-9-methyl-5,6,8,9,10,11-hexahydro-7H-5,9,7,11-dimethanobenzo[9]annulen-7-yl)acetamide (**36**)

Diene **32** (1.50 g, 6.24 mmol) was dissolved in glacial acetic acid (4.8 mL) and chloroacetonitrile (1.58 mL, $\delta = 1.19$, 24.9 mmol) was added. The solution was cooled to 0 °C and conc. H₂SO₄ (2.00 mL, $\delta = 1.84$, 37.5 mmol) was added dropwise with care not to raise above 10 °C. The dark red solution was allowed to warm to rt and was left stirring overnight. The dark red solution was poured over ice (5 g) and it was then extracted with DCM (3 × 20 mL). The organic layer was washed with 10 N NaOH solution (1 × 20 mL), dried over anhydrous Na₂SO₄, then filtered and concentrated under vacuum to give a brown solid (1.18 g, 57% yield), mp 144–145 °C. IR (NaCl disk) ν : 3403, 3304, 3062, 2997, 2945, 2905, 2860, 2838, 1662, 1609, 1582, 1528, 1499, 1454, 1382, 1361, 1311, 1267, 1242, 1198, 1180, 1154, 1043, 1013, 955, 873 cm⁻¹. ¹H NMR (400 MHz, CDCl₃) δ : 0.93 (s, 3H, 9-CH₃), 1.48–1.59 (complex signal, 2H, 10(13)-H_a), 1.61–1.70 [complex signal, 2H, 10(13)-H_b], 1.82 (dm, $J = 12.0$ Hz, 1H, 8-H_a), 1.86 (dm, $J = 12.0$ Hz, 1H, 8-H_b), 2.00–2.10 [complex signal, 2H, 6(12)-H_a], 2.10–2.21 [complex signal, 2H, 6(12)-H_b], 2.99–3.09 [complex signal, 2H, 5(11)-H], 3.77 (s, 3H, OCH₃), 3.92 (s, 2H, CH₂-Cl), 6.60 (dd, $J = 8.0$ Hz, $J' = 2.8$ Hz, 1H, 3-H), 6.63 (d, $J = 2.8$ Hz, 1-H), 6.97 (d, $J = 8.0$ Hz, 1H, 4-H). ¹³C NMR (100.6 MHz, CDCl₃) δ : 32.3 (CH₃, C9–CH₃), 33.7 (C, C9), 38.8 (CH₂) and 39.2 (CH₂) (C6 and C12), 40.1 (CH) and 41.2 (CH) (C5 and C11), 41.2 (CH₂) and 41.6 (CH₂) (C10 and C13), 43.0 (CH₂, CH₂-Cl), 47.0 (CH₂, C8), 54.8 (C, C7), 55.3 (CH₃, OCH₃), 110.6 (CH, C3), 114.3 (CH, C1), 129.2 (CH, C4), 138.5 (C, C4a), 147.5 (C, C11a), 158.1 (C, C2), 164.6 (C, NHCO). HRMS-ESI + m/z [M+H]⁺ calcd for [C₁₉H₂₅ClNO]⁺: 334.1568, found: 334.1569.

4.1.28. 2-Fluoro-9-methyl-5,6,8,9,10,11-hexahydro-7H-5,9,7,11-dimethanobenzo[9]annulen-7-amine hydrochloride (**37**)

Thiourea (15 mg, 0.20 mmol) and glacial acetic acid (0.1 mL) were added to a solution of **33** (50 mg, 0.16 mmol) in absolute

ethanol (3 mL) and the mixture was heated at reflux overnight. The resulting suspension was then tempered to rt and concentrated under vacuum. Crude was partitioned in H₂O (2 mL) and DCM (3 mL) and the phases were separated. Then the pH of the aq phase was adjusted to 12 with 5 N NaOH solution and extracted with further DCM (3 × 3 mL). The combined organic layers were dried over anhydrous Na₂SO₄, filtered and concentrated *in vacuo* to obtain amine **37**. Its hydrochloride was obtained by adding an excess of HCl/Et₂O to a solution of the amine in ethyl acetate, followed by filtration of the resulting white precipitate (16 mg, 36% yield), mp > 300 °C (dec.). IR (KBr disk) ν : 3200–2500 (2983, 2945, 2917, 2867), 2059, 1612, 1595, 1501, 1456, 1444, 1431, 1379, 1364, 1302, 1283, 1256, 1246, 1186, 1157, 1143, 1132, 1030, 1004, 962, 863, 814 cm⁻¹. ¹H NMR (400 MHz, MeOD) δ : 1.0 (s, 3H, 9-CH₃), 1.51–1.61 [complex signal, 2H, 10(13)-H_a], 1.68 (s, 2H, 8-H₂), 1.68–1.75 [complex signal, 2H, 10(13)-H_b], 1.82–1.91 [complex signal, 2H, 6(12)-H_a], 2.00–2.08 [complex signal, 4H, 6(12)-H_b], 3.18 (tm, $J = 6.2$ Hz, 1H, 5-H or 11-H), 3.23 (tm, $J = 6.2$ Hz, 1H, 11-H or 5-H), 6.81 (td, $J = 8.4$ Hz, $J' = 2.8$ Hz, 3-H), 6.87 (dd, $J = 9.4$ Hz, $J' = 2.8$ Hz, 1-H), 7.11 (dd, $J = 8.4$ Hz, $J' = 5.6$ Hz, 1H, 4-H). ¹³C NMR (100.6 MHz, MeOD) δ : 32.2 (CH₃, C9–CH₃), 34.7 (C, C9), 39.0 (CH₂) and 39.3 (CH₂) (C6 and C12), 40.8 (CH) and 41.4 (CH) (C5 and C11), 41.3 (CH₂) and 41.6 (CH₂) (C10 and C13), 47.1 (CH₂, C8), 55.3 (C, C7), 113.8 (CH, d, $J_{C-F} = 20$ Hz, C3), 115.9 (CH, d, $J_{C-F} = 22$ Hz, C1), 131.0 (CH, d, $J_{C-F} = 8.1$ Hz, C4), 142.5 (C, d, $J_{C-F} = 3$ Hz, C4a), 148.8 (C, d, $J_{C-F} = 7.1$ Hz, C11a), 162.9 (C, d, $J_{C-F} = 243$ Hz, C2). HRMS-ESI + m/z [M+H]⁺ calcd for [C₁₆H₂₁FN]⁺: 246.1653, found: 246.1649.

4.1.29. 2,3-Dimethoxy-9-methyl-5,6,8,9,10,11-hexahydro-7H-5,9,7,11-dimethanobenzo[9]annulen-7-amine hydrochloride (**38**)

Chloroacetamide **34** (436 mg, 1.20 mmol) was dissolved in abs. ethanol (23 mL) and glacial acetic acid (0.75 mL). Thiourea (109 mg, 1.44 mmol) was added, and the solution was left stirring overnight at reflux. The yellow solution was concentrated under vacuum and the solid was dissolved in MeOH (10 mL). HCl/Et₂O was added, and the solution was concentrated to dryness. The off-white solid was washed with DCM (2 × 3 mL). The combined supernatants were concentrated under vacuum to obtain the hydrochloride of **38** as a white solid (315 mg, 81% yield), mp > 200 °C (dec.). IR (KBr disk) ν : 3200–2500 (2993, 2918, 2831), 2047, 1701, 1606, 1517, 1451, 1416, 1386, 1365, 1327, 1310, 1291, 1252, 1237, 1192, 1174, 1131, 1098, 1031, 973, 950, 863, 798, 586, 543 cm⁻¹. ¹H NMR (400 MHz, CDCl₃) δ : 0.95 (s, 3H, 9-CH₃), 1.55 [d, $J = 13.6$ Hz, 2H, 10(13)-H_a], 1.63 [dd, $J = 13.6$ Hz, $J' = 6.0$ Hz, 2H, 10(13)-H_b], 1.80 (s, 2H, 8-CH₂), 2.04 [d, $J = 12.6$ Hz, 2H, 6(12)-H_a], 2.15 [dd, $J = 12.6$ Hz, $J' = 6.0$ Hz, 2H, 6(12)-H_b], 3.01 [t, $J = 5.2$ Hz, 2H, 5(11)-H], 3.83 (s, 6H, OCH₃), 6.58 [s, 2H, 1(4)-H], 8.38 (broad s, 3H, 7C–NH₃⁺). ¹³C NMR (100.6 MHz, CDCl₃) δ : 31.9 (CH₃, C9–CH₃), 33.9 (C, C9), 38.6 [CH₂, C6(12)], 40.1 [CH, C5(11)], 40.7 [CH₂, C10(13)], 46.5 (CH₂, C8), 55.7 (C, C7), 56.2 (CH₃, OCH₃), 112.5 [CH, C1(4)], 137.4 [C, C4a(11a)], 147.1 [C, 2(3)]. HRMS-ESI + m/z [M+H]⁺ calcd for [C₁₈H₂₆NO₂]⁺: 288.1958, found: 288.1954.

4.1.30. 1-Fluoro-9-methyl-5,6,8,9,10,11-hexahydro-7H-5,9,7,11-dimethanobenzo[9]annulen-7-amine hydrochloride (**39**)

Thiourea (284 mg, 3.73 mmol) and glacial acetic acid (2 mL) were added to a solution of **35** (1.00 g, 3.11 mmol) in abs. ethanol (54 mL) and the mixture was heated at reflux overnight. The resulting suspension was then tempered to rt and concentrated under vacuum. Crude was partitioned in H₂O (40 mL) and DCM (30 mL) and the phases were separated. Then the pH of the aq phase was adjusted to 12 with 5 N NaOH solution and extracted with further DCM (3 × 30 mL). The combined organic layers were dried over anhydrous Na₂SO₄, then filtered and concentrated *in vacuo*. The hydrochloride of **39** was obtained by adding an excess of HCl/Et₂O

to a solution of the amine in ethyl acetate followed by filtration of the resulting white precipitate (732 mg, 84% yield). The analytical sample was obtained by crystallization from methanol, mp > 200 °C (dec.). IR (KBr disk) ν : 3200–2500 (2945, 2717, 2586), 2060, 1677, 1608, 1584, 1511, 1464, 1380, 1366, 1317, 1303, 1248, 1214, 1199, 1165, 1132, 1071, 1052, 1032, 1000, 977, 946, 885, 877, 854, 798, 747, 623 cm⁻¹. ¹H NMR (400 MHz, MeOD) δ : 1.0 (s, 3H, CH₃), 1.50 [d, *J* = 14.0 Hz, 1H, 10-H_a or 13-H_a], 1.57 (d, *J* = 14.0 Hz, 1H, 13-H_a or 10-H_a), 1.72 (s, 2H, 8-H₂), 1.68–1.75 [complex signal, 2H, 10(13)-H_b], 1.79 (d, *J* = 12.8 Hz, 1H, 6-H_a or 12-H_a) 1.86 (d, *J* = 12.8 Hz, 1H, 12-H_a or 6-H_a), 2.00–2.08 (complex signal, 2H, 6-H_b, 12-H_b), 3.27 (m, 1H, 5-H), 3.80 (t, *J* = 6.2 Hz, 11-H), 6.90 (ddd, *J* = 8.4 Hz, *J'* = 8.0 Hz, *J''* = 1.4 Hz, 1H, 2-H), 6.92 (m, 1H, 4-H), 7.09 (ddd, *J* = 8.4 Hz, *J'* = 7.6 Hz, *J''* = 5.6 Hz, 1H, 3-H). ¹³C NMR (100.6 MHz, MeOD) δ : 29.5 (CH, d, *J*_{C-F} = 6 Hz, C11), 32.7 (CH₃, C9–CH₃), 34.7 (C, C9), 38.6 (CH₂) and 39.0 (CH₂) (C6 and C12), 40.9 (CH₂) and 41.3 (CH₂) (C10 and C13), 41.6 (CH, d, *J*_{C-F} = 3 Hz, C5), 47.0 (CH₂, C8), 55.3 (C, C7), 114.7 (CH, d, *J*_{C-F} = 25 Hz, C2), 125.2 (CH, d, *J*_{C-F} = 4 Hz, C4), 129.1 (CH, d, *J*_{C-F} = 10 Hz, C3), 132.8 (CH, d, *J*_{C-F} = 14.1 Hz, C11a), 149.7 (C, d, *J*_{C-F} = 2 Hz, C4a), 160.4 (C, d, *J*_{C-F} = 24.2 Hz, C1). HRMS-ESI + *m/z* [M+H]⁺ calcd for [C₁₆H₂₁FN]⁺: 246.1653, found: 246.1649.

4.1.31. 2-Methoxy-9-methyl-5,6,8,9,10,11-hexahydro-7H-5,9,7,11-dimethanobenzo[9]annulen-7-amine hydrochloride (**40**)

Chloroacetamide **36** (1.10 g, 3.29 mmol) was dissolved in abs. ethanol (60 mL) and glacial acetic acid (2.2 mL). Thiourea (300 mg, 3.94 mmol) was added and the orange solution was left stirring overnight. The orange solution was concentrated under vacuum and the solid was dissolved in MeOH (10 mL). HCl/Et₂O was added, the solution was concentrated, and the off-white solid was extracted with DCM (2 × 3 mL). The combined supernatants were concentrated under vacuum to obtain **40** as a brown solid that was crystallized from DCM/pentane (779 mg, 81% yield), mp > 200 °C (dec.). IR (KBr disk) ν : 3200–2500 (2985, 2942, 2908), 2056, 1735, 1609, 1582, 1499, 1449, 1379, 1364, 1334, 1305, 1268, 1252, 1205, 1170, 1132, 1103, 1040, 1001, 954, 869, 849, 815, 756, 692 cm⁻¹. ¹H NMR (400 MHz, CD₃OD) δ : 0.99 (s, 3H, 9-CH₃), 1.50–1.59 [complex signal, 2H, 10(13)-H_a], 1.65 (s, 2H, 8-CH₂), 1.65–1.73 [complex signal, 2H, 10(13)-H_b], 1.79–1.89 [complex signal, 2H, 6(12)-H_a], 1.97–2.06 [complex signal, 2H, 6(12)-H_b], 3.10–3.18 [complex signal, 2H, 5(11)-H], 3.74 (s, 3H, OCH₃), 6.64 (dd, *J* = 8.0 Hz, *J'* = 2.8 Hz, 1H, 3-H), 6.67 (d, *J* = 2.8 Hz, 1H, 1-H), 7.00 (d, *J* = 8.0 Hz, 4-H). ¹³C NMR (100.6 MHz, CD₃OD) δ : 32.3 (CH₂, 9-CH₃), 34.6 (C, C9), 39.3 (CH₂) and 39.6 (CH₂) (C6 and C12), 40.8 (CH) and 41.6 (CH) (C5 and C11), 41.7 (CH₂) and 42.0 (CH₂) (C10 and C13), 47.2 (CH₂, C8), 55.5 (C, C7), 55.7 (CH₃, OCH₃) 112.1 (CH, C3), 115.2 (CH, C1), 130.3 (CH, C4), 138.6 (C, C4a), 147.7 (C, C11a), 159.9 (C, C2). HRMS-ESI + *m/z* [M+H]⁺ calcd for [C₁₇H₂₄NO]⁺: 258.1852, found: 258.1862.

4.1.32. 1-Fluoro-11-methylene-6,7,8,9-tetrahydro-5H-5,9-propanobenzo[7]annulen-7-one (**41**)

In a flame dried 3-necked round bottom flask, sodium hydride 60% dispersion in mineral oil (1.01 g, 25.2 mmol) was added under N₂ and was dissolved in anh DMSO (50 mL). The grey suspension was heated to 90 °C for 45 min and was then cooled to rt. After the reaction mixture was tempered, a solution of triphenylmethylphosphonium iodide (10.6 g, 26.2 mmol) in anh DMSO (58 mL) was added and the resulting yellow solution was stirred at rt for 20 min. Then a suspension of diketone **27** (4.72 g, 20.3 mmol) in anh DMSO (50 mL) was added and the obtained solution was heated to 90 °C overnight. The resulting black solution was allowed to cool to rt and then poured into H₂O (200 mL). The H₂O was extracted with hexane (4 × 200 mL) and the organic layer was dried over anh Na₂SO₄,

filtered and concentrated under vacuum. The crude was purified by Combiflash® using as eluent a gradient from pure hexane to an ethyl acetate/hexane mixture (2.5/7.5). The product **41** was isolated as a yellow solid (2.16 g, 46% yield), mp 96 °C. IR (ATR) ν : 2928, 2913, 2895, 2849, 1688, 1612, 1583, 1462, 1432, 1406, 1366, 1247, 1196, 1104, 1049, 1034, 1002, 970, 921, 911, 883, 819, 789, 749, 657 cm⁻¹. ¹H NMR (400 MHz, CDCl₃) δ : 2.39 (d, *J* = 13.2 Hz, 1H, 10-H_a or 12-H_a), 2.46 (d, *J* = 12.4 Hz, 1H, 10-H_a or 12-H_a), 2.48–2.62 [complex signal, 2H, 6(8)-H_a], 2.64–2.72 [complex signal, 2H, 10(12)-H_b], 2.83–2.91 [complex signal, 2H, 6(8)-H_b], 3.22 (m, 1H, 5-H), 3.80 (m, 1H, 9-H), 4.96 (complex signal, C=CH₂), 6.97 (ddd, *J* = 8.4 Hz, *J'* = 1.6 Hz, 1H, 2-H), 6.99 (d, *J* = 8.0 Hz, 4-H), 7.15 (ddd, *J* = 8.4 Hz, *J'* = 7.6 Hz, *J''* = 5.6 Hz, 1H, 3-H). ¹³C NMR (100.6 MHz, CDCl₃) δ : 28.3 (CH, d, *J*_{C-F} = 5 Hz, C9), 40.4 (CH, d, *J*_{C-F} = 3 Hz, C5), 41.4 (CH₂) and 41.7 (CH₂) (C10 and C12), 48.1 (CH₂) and 48.5 (CH₂) (C6 and C8), 114.3 (CH, d, *J*_{C-F} = 24 Hz, C2), 120.3 (CH₂, 11-CH₂), 124.1 (CH, d, *J*_{C-F} = 3 Hz, C4), 128.3 (CH, d, *J*_{C-F} = 9 Hz, C3), 131.2 (C, d, *J*_{C-F} = 14.1 Hz, C9a), 143.4 (C, C11), 147.5 (C, d, *J*_{C-F} = 3 Hz, C4a), 159.5 (C, d, *J*_{C-F} = 244.5 Hz, C1), 211.2 [C, C7–CO]. HRMS-ESI + *m/z* [M+H]⁺ calcd for [C₁₅H₁₆FO]⁺: 231.1180, found: 231.1180.

4.1.33. 2-Chloro-N-(1-fluoro-9-hydroxy-5,6,8,9,10,11-hexahydro-7H-5,9,7,11-dimethanobenzo[9]annulen-7-yl)acetamide (**42**)

Chloroacetonitrile (0.62 mL, δ = 1.19, 9.77 mmol) was added to a solution of **41** (2.06 g, 8.94 mmol) in DCM (21 mL) and the mixture was cooled to 0–5 °C with an ice bath. Conc. H₂SO₄ (0.75 mL, δ = 1.84, 14.1 mmol) was added dropwise (<10 °C). After the addition, the mixture was allowed to reach rt and stirred overnight. The solution was added to ice (10 g) and the mixture was stirred at rt for a few minutes. DCM (15 mL) was added, the phases were separated, and the aq phase was extracted with further DCM (2 × 15 mL). The combined organic layers were dried over anh Na₂SO₄, then filtered and evaporated *in vacuo* to give **42** as a white solid (921 mg, 32% yield), mp 150 °C. IR (ATR) ν : 3406, 3272, 3217, 3075, 2926, 2905, 2850, 1661, 1585, 1561, 1466, 1443, 1428, 1409, 1362, 1341, 1311, 1298, 1243, 1218, 1158, 1105, 1037, 991, 974, 891, 884, 791, 744, 734, 679, 625 cm⁻¹. ¹H NMR (400 MHz, CDCl₃) δ : 1.67–1.80 [complex signal, 2H, 10(13)-H_a], 1.93–2.00 [complex signal, 2H, 10(13)-H_b], 2.02–2.22 [complex signal, 4H, 6(12)-H₂], 3.24 (m, 1H, 5-H), 3.84 (t, *J* = 6.8 Hz, 1H, 11-H), 3.93 (s, 2H, CH₂Cl), 6.38 (broad s, 1H, NH), 6.86–6.91 [complex signal, 2 H, 2(4)-H], 7.05 (ddd, *J* = 8.2 Hz, *J'* = 7.6 Hz, *J''* = 5.6 Hz, 1H, 3-H). ¹³C NMR (100.6 MHz, CDCl₃) δ : 27.8 (CH, d, *J*_{C-F} = 6 Hz, C11), 37.9 (CH₂) and 38.0 (CH₂) (C6 and C12), 39.9 (CH, d, *J* = 3 Hz, C5), 41.9 (CH₂) and 42.2 (CH₂) (C10 and C13), 43.0 (CH₂, CH₂Cl), 48.0 (CH₂, C8), 57.4 (C, C7), 70.8 (C, C9), 113.8 (CH, d, *J*_{C-F} = 24 Hz, C2), 123.7 (CH, d, *J*_{C-F} = 3 Hz, C4), 127.6 (CH, d, *J*_{C-F} = 9 Hz, C3), 131.6 (CH, d, *J*_{C-F} = 13.1 Hz, C11a), 148.2 (C, d, *J*_{C-F} = 2 Hz, C4a), 159.2 (C, d, *J*_{C-F} = 243.5 Hz, C1), 164.9 (C, NHCO). HRMS-ESI + *m/z* [M+H]⁺ calcd for [C₁₇H₂₀ClFNO₂]⁺: 324.1161, found: 324.1162.

4.1.34. 2-Chloro-N-(1,9-difluoro-5,6,8,9,10,11-hexahydro-7H-5,9,7,11-dimethanobenzo[9]annulen-7-yl)acetamide (**43**)

A solution of chloroacetamide **42** (611 mg, 1.89 mmol) in DCM (10 mL) was cooled to –30 °C. Then, DAST (2.8 mL, 1 M solution in DCM, 2.8 mmol) was added and the reaction mixture was stirred at rt overnight. To the resulting solution was added H₂O (10 mL) and the pH adjusted to 12 with 5 N NaOH solution. The phases were separated, and the aq phase was extracted with further DCM (3 × 10 mL), and the combined organic layers were dried over anh Na₂SO₄, then filtered and concentrated *in vacuo*. The crude was purified by Combiflash® in silica gel using as eluent a gradient from pure hexane to ethyl acetate/hexane mixture (6/4) to give **43** as a white solid (420 mg, 69% yield), mp 180 °C. IR (ATR) ν : 3276, 3075, 2964, 2940, 2901, 2858, 1671, 1650, 1584, 1552, 1463, 1442, 1360,

1337, 1331, 1317, 1282, 1242, 1219, 1175, 1143, 1104, 1018, 1066, 1018, 1004, 979, 901, 887, 865, 799, 746, 737, 696, 662 cm^{-1} . ^1H NMR (400 MHz, CDCl_3) δ : 1.85–1.92 [complex signal, 2H, 6(12)- H_a], 2.01–2.12 [complex signal, 2H, 10(13)- H_a], 2.13–2.24 [complex signal, 4H, 6(10,12,13)- H_b], 2.24–2.35 (complex signal, 2H, 8- H_2), 3.31 (m, 1H, 5-H), 3.90 (m, 1H, 11-H), 3.94 (s, 2H, CH_2Cl), 6.40 (broad s., 1H, NH), 6.88 (m, 1H, 4-H), 6.93 (ddd, $J = 8.8$ Hz, $J' = 8.4$ Hz, $J'' = 1.6$ Hz, 1H, 2-H), 7.07 (ddd, $J = 8.4$ Hz, $J' = 7.2$ Hz, $J'' = 5.2$ Hz, 1H, 3-H). ^{13}C NMR (100.6 MHz, CDCl_3) δ : 27.4 (CH, dd, $J_{\text{C-F}} = 13.6$ Hz, $J'_{\text{C-F}} = 6.4$ Hz, C11), 37.8 (CH_2 , d, $J_{\text{C-F}} = 1.1$ Hz, C6 or C12), 37.9 (CH_2 , d, $J_{\text{C-F}} = 1.0$ Hz, C12 or C6), 39.4 (CH, dd, $J_{\text{C-F}} = 13.3$ Hz, $J'_{\text{C-F}} = 2.4$ Hz, C5), 39.7 (CH_2 , d, $J_{\text{C-F}} = 19.5$ Hz, C10 or C13), 39.8 (CH_2 , d, $J_{\text{C-F}} = 20.4$ Hz, C13 or C10), 43.0 (CH_2 , CH_2Cl), 45.7 (CH_2 , d, $J_{\text{C-F}} = 19$ Hz, C8), 58.1 (C, d, $J_{\text{C-F}} = 11$ Hz, C7), 93.0 (C, d, $J_{\text{C-F}} = 178.1$ Hz, C9), 114.1 (CH, d, $J_{\text{C-F}} = 24.8$ Hz, C2), 123.8 (CH, d, $J_{\text{C-F}} = 3.2$ Hz, C4), 127.9 (CH, d, $J_{\text{C-F}} = 9.3$ Hz, C3), 131.2 (CH, d, $J_{\text{C-F}} = 13.4$ Hz, C11a), 147.7 (C, d, $J_{\text{C-F}} = 2.1$ Hz, C4a), 159.2 (C, d, $J_{\text{C-F}} = 244.1$ Hz, C1), 164.9 (C, NHCO). HRMS-ESI + m/z [$\text{M}+\text{H}$] $^+$ calcd for $[\text{C}_{17}\text{H}_{19}\text{ClF}_2\text{NO}]^+$: 326.1118, found: 326.1116.

4.1.35. 1,9-Difluoro-5,6,8,9,10,11-hexahydro-7H-5,9,7,11-dimethanobenzo[9]annulen-7-amine hydrochloride (**44**)

Thiourea (56 mg, 0.74 mmol) and glacial acetic acid (0.46 mL) were added to a solution of **43** (240 mg, 0.74 mmol) in absolute ethanol (14 mL) and the mixture was heated at reflux overnight. The resulting suspension was then tempered to rt and concentrated under vacuum. Crude was partitioned in H_2O (30 mL) and DCM (30 mL) and the phases were separated. Then the pH of the aq phase was adjusted to 12 with 5 N NaOH solution and extracted with further DCM (3 \times 40 mL). The combined organic layers were dried over anhydrous Na_2SO_4 , then filtered and concentrated *in vacuo*. The hydrochloride of **44** was obtained by adding an excess of HCl/Et $_2$ O to a solution of the amine in ethyl acetate, followed by filtration of the resulting white precipitate (167 mg, 79% yield). The analytical sample was obtained by crystallization from methanol, mp > 200 $^\circ\text{C}$ (dec.) IR (ATR) ν : 3000–2700 (2981, 2950, 2911, 2867, 2831), 2063, 1611, 1588, 1509, 1465, 1445, 1363, 1321, 1246, 1194, 1105, 1095, 1008, 1002, 988, 967, 903, 888, 860, 801, 743, 673 cm^{-1} . ^1H -RMN (400 MHz, MeOD) δ : 1.74–1.96 [complex signal, 4 H, 6(10,12,13)- H_a], 2.07–2.15 [complex signal, 4H, 6(12)- H_b and 8- H_2], 2.15–2.26 [complex signal, 2H, 10(13)- H_b], 3.48 (broad s, 1H, 5-H), 3.99 (t, $J = 5.6$ Hz, 1H, 11-H), 6.98 (ddd, $J = 8.8$ Hz, $J' = 8.0$ Hz, $J'' = 1.2$ Hz, 1H, 2-H), 7.00 (m, 1H, 4-H), 7.17 (ddd, $J = 8.4$ Hz, $J' = 8.0$ Hz, $J'' = 5.6$ Hz, 1H, 3-H). ^{13}C NMR (100.6 MHz, MeOD) δ : 28.4 (CH, dd, $J_{\text{C-F}} = 13.4$ Hz, $J'_{\text{C-F}} = 6.9$ Hz, C11), 38.0 (CH_2 , C6 or C12), 38.4 (CH_2 , C12 or C6), 39.8 (CH_2 , d, $J_{\text{C-F}} = 21.0$ Hz, C10 or C13), 40.0 (CH, dd, $J_{\text{C-F}} = 13.1$ Hz, $J'_{\text{C-F}} = 2.1$ Hz, C5), 40.2 (CH_2 , d, $J_{\text{C-F}} = 20.8$ Hz, C13 or C10), 45.8 (CH_2 , d, $J_{\text{C-F}} = 20.6$ Hz, C8), 58.0 (C, d, $J_{\text{C-F}} = 11.1$ Hz, C7), 93.9 (C, d, $J_{\text{C-F}} = 179.9$ Hz, C9), 115.2 (CH, d, $J_{\text{C-F}} = 25$ Hz, C2), 125.2 (CH, d, $J_{\text{C-F}} = 4$ Hz, C4), 129.6 (CH, d, $J_{\text{C-F}} = 9$ Hz, C3), 131.7 (CH, d, $J_{\text{C-F}} = 13$ Hz, C11a), 148.3 (C, C4a), 160.3 (C, d, $J_{\text{C-F}} = 243.4$ Hz, C1). HRMS-ESI + m/z [$\text{M}+\text{H}$] $^+$ calcd for $[\text{C}_{15}\text{H}_{18}\text{F}_2\text{N}]^+$: 250.1402, found: 250.1401.

4.2. Intracellular calcium-based determination of IC_{50} of NMDAR channel blockers

A functional assay of antagonist activity at NMDA receptors was performed using primary cultures of rat cerebellar granule neurons that were prepared according to established protocols [49]. Cells were grown on 10 mm poly-L-lysine coated round glass cover slips and used for the experiments after 6–9 days *in vitro*. Cells were loaded with 6 μM Fura-2 AM (ThermoFisher) for 30 min. After loading, a coverslip was mounted on a quartz cuvette containing a Mg^{2+} -free Locke-HEPES buffer using a specialized holder.

Measurements were performed using a PerkinElmer LS-55 fluorescence spectrometer equipped with a fast filter accessory, under mild agitation and at 37 $^\circ\text{C}$. Analysis from each sample was recorded real-time over 1600 s. After stimulation with NMDA (100 μM , in the presence of 10 μM glycine), increasing concentrations of the compound to be tested were added after signal stabilization. The percentage of inhibition at every tested concentration was analyzed using non-linear regression curve fitting (variable slope) using the software Prism 5.04 (GraphPad Software Inc.).

4.3. Molecular docking and MD simulations

To understand structural aspects of ligand binding using molecular docking and MD simulations, we used an MD-refined computational structural model of the NMDAR (GluN1/2A) transmembrane domain with the channel gate closed. Simulations of receptor-bound **IIa**, **IIb**, **IIc** and **6** were initiated with the compounds in their protonated forms docked into the channel oriented in a “flipped down” conformation such that their amines were interacting with the asparagine (ASN) cluster on the tip of M2 helices. Docking was performed in AutoDock Vina [106], which predicts interactions between small molecules and proteins. Protein and ligand coordinate files were converted to pdbqt format using AutoDock Tools, where non-polar hydrogen atoms were merged to the bonded heavy atoms. The active site of the protein was designated as a box with size of 26 \times 26 \times 40 Å at 1 Å grid spacing.

Docked receptor-ligand complexes of NMDAR-**IIa**, NMDAR-**IIb**, NMDAR-**IIc** and NMDAR-**6** were built and assembled with POPC membrane using CHARMM-GUI Membrane Builder [107,108]. All systems were solvated with TIP3P water and neutralized by adding Na^+ and Cl^- ions to the bulk solution until the salt concentration was 0.15 M, leading to a total system size of approximately 169,070 atoms and box size of 127 \times 127 \times 101 Å . All initial membrane-protein-ligand complex model systems for MD equilibration simulations were built with tleap program in AMBERTOOLS18 [109]. FF14SB force field parameters were used for the protein [110]; Amber Lipid14 FF for POPC lipid [111] and general AMBER force field [112] (GAFF) was used for all four ligands. To confirm convergence in binding stability of ligands, we used two replicates for each of NMDAR-**IIa**, NMDAR-**IIb**, NMDAR-**IIc** and NMDAR-**6** systems.

All 8 initial membrane-protein-ligand complex model systems were energy minimized for 500 cycles of each steepest-descent and conjugate gradient algorithm while keeping restraints on the protein $\text{C}\alpha$ atoms. Water and ions were equilibrated at constant volume as the temperature was gradually increased from 0 to 300K with restraints of 40 kcal/mol/ Å on all protein and lipid heavy atoms. This was followed by equilibration for 20 ns at 1 atm and 300 K with a time step of 2 fs using the pmemd.cuda program of the AMBER18 molecular dynamics package [109]. The restraints on the protein residues were gradually reduced from 20 to 0.5 kcal/mol/ Å . For each system, MD production runs without any restraints using AMBER18 were performed for 200 ns. The NPT equilibration and production MD simulations were performed with an integration time step of 2 fs while pressure and temperature of the simulated system were maintained at 1 bar and 300 K respectively. We used Langevin thermostat with damping coefficient of 1 ps^{-1} and a semi-isotropic pressure scaling algorithm as implemented in AMBER18, with pressure relaxation time of 5 ps. During whole simulations, hydrogen bonds were constrained via the SHAKE algorithm [113]. Periodic boundary conditions and all atom wrapping were employed in all simulations as implemented in AMBER18. Long range electrostatics were calculated using the Particle Mesh Ewald method [114] where Non-bonded Lennard-Jones and Coulombic interactions were truncated at 8 Å . Results were viewed and analyzed with VMD [115] and CPPTRAJ tools [116].

4.4. Cell culture, transfection, recording, and analysis for electrophysiology experiments

Electrophysiological characterization of memantine-like compounds for Fig. 4 was carried out using tsA201 cells transiently transfected with plasmids codifying for NMDAR subunits. tsA201 (Sigma catalog #85120602) is a cell line derived from HEK293 cells stably expressing the temperature sensitive gene for SV40 T-antigen to allow plasmid replication using the SV40 origin and thus enabling high levels of recombinant proteins. Cells were maintained in DMEM supplemented with 10% fetal bovine serum and 1% streptomycin/penicillin as described [60]. Prior to transfection, cells were plated at 1×10^6 cells/cover slip in glass coverslips previously coated with poly D-lysine (0.1 mg/ml). 24 h after plating, cells were transiently transfected with 1 μ g total cDNAs using PEI transfection reagent (1 mg/ml) in a 3:1 ratio (PEI:DNA). Cells were transfected with plasmids encoding the rat GluN1 subunit, rat GluN2A subunit and enhanced green fluorescent protein (eGFP) for identification of transfected cells. cDNA ratios of 0.5 eGFP: 1 GluN1: 1 GluN2A were used. Culture medium was supplemented with the competitive NMDAR antagonist D,L-2-amino-5-phosphonopentanoate (dl-APV, Sigma, 200 μ M) at the time of transfection to prevent NMDAR-mediated cell death.

Whole-cell voltage-clamp recordings were obtained on tsA201 cells 18–30 h after transfection. Pipettes were pulled from borosilicate capillary tubing (OD = 1.5 mm, ID = 0.86 mm; Harvard Apparatus) using a P-97 electrode puller (Sutter Instruments) and subsequently fire-polished to a resistance of 2–5 M Ω using a MF-830 forge (Narishige). Intracellular pipette solution contained (in mM): 140 CsCl, 10 HEPES, 5 EGTA, 4 Na₂ATP and 0.1 Na₃GTP with pH adjusted to 7.25 with CsOH. Extracellular recording solution contained (in mM): 140 NaCl, 5 KCl, 1 CaCl₂, 10 HEPES and 10 glucose, adjusted to pH 7.42 with NaOH.

Whole-cell currents were recorded using an Axopatch 200B patch-clamp amplifier (Molecular Devices). Current signal was low-pass filtered at 1 kHz, and sampled at 2 kHz in pClamp 10 (Molecular Devices). Solutions containing agonists (100 μ M NMDA and 10 μ M glycine) or blockers (10 μ M) were applied by piezoelectric translation (P-601.30; Physik Instrumente) of a theta-barrel application tool made from borosilicate glass (1.5 mm o.d.; Sutter Instruments). All recordings were performed at rt.

The percentage of channel block, unblock, and recovery were measured with the following protocol: At a holding of –60 mV, NMDA (100 μ M) and glycine (10 μ M) were applied until current reached a clear steady-state. Then, **I_{IIb}**, **I_{IIc}** or **2** were rapidly applied by piezo control (1 ms solution exchange) for 30 s as described [28]. During the application of the blocker, a 5 s jump to +60 mV was performed to study the voltage dependence of channel block. Blockers were then removed in the presence of the agonists to allow recovery of the current. During this period (around 1 min) a second jump (5 s duration) to +60 mV was performed. Finally, agonists were removed. Percentage of block was calculated by dividing steady state current in the presence of the blocker by steady state current in the absence of the blocker. Percentage of unblock was calculated by dividing the steady state current after blocker removal by the steady state current before blocker application. Finally, the voltage dependence (% of block at +60 mV) was calculated by using Equation 1:

$$\% \text{ of block} = 100 \left(1 - \frac{I_{+60}(\text{Drug})}{I_{+60}(\text{Agonist})} \right)$$

where $I_{+60}(\text{Drug})$ is the current after 5 s at the holding voltage of +60 mV in the presence of the blocker and $I_{+60}(\text{Agonist})$ is the

current after 5 s at +60 mV in the absence of the blocker. The kinetics of blocking and unblocking of NMDAR responses were fitted according to a double-exponential function to calculate the weighted time constant (τ_{weighted}):

$$\tau_{\text{weighted}} = \tau_f \left(\frac{A_f}{A_f + A_s} \right) + \tau_s \left(\frac{A_s}{A_f + A_s} \right)$$

where A_f and τ_f are the amplitude and time constant of the fast component of recovery and A_s and τ_s are the amplitude and time constant of the slow component.

For Fig. 5, cells were maintained as previously described [117]. Briefly, tsA201 cells (European Collection of Authenticated Cell Cultures) were cultured and plated in DMEM supplemented with 10% fetal bovine serum and 1% GlutaMAX (Thermo Fisher Scientific). 18–24 h after plating, the cells were transfected using FuGENE 6 (Promega) with cDNA coding for enhanced green fluorescent protein (eGFP), WT rat GluN1-1a (GluN1; GenBank X63255), and GluN2A (GenBank M91561 in pcDNA1). GluN1-1a and eGFP were expressed using a plasmid containing cDNA encoding eGFP inserted between the promoter and the GluN1 open reading frame [118]. dl-APV was added to the medium at the time of transfection to prevent NMDAR-mediated cell death.

For Fig. 5, all whole-cell voltage-clamp recordings were performed at rt 18–30 h after transfection. Pipettes were fabricated from borosilicate capillary tubing (OD = 1.5 mm, ID = 0.86 mm) using a Flaming Brown P-97 electrode puller (Sutter Instruments) and fire-polished to a resistance of 3.0–4.0 M Ω . The intracellular pipette solution contained (in mM): 130 CsCl, 10 HEPES, 10 BAPTA, and 4 MgATP; adjusted to pH 7.2 \pm 0.05 with CsOH. Pipette solution osmolality was 275 \pm 10 mOsm. Extracellular recording solutions contained (in mM): 140 NaCl, 2.8 KCl, 1 CaCl₂, 10 HEPES, 0.01 EDTA, and 0.1 glycine; adjusted to pH 7.2 \pm 0.05 with NaOH and to osmolality 290 \pm 10 mOsm with sucrose. Concentrated stocks of glutamate, MgCl₂, and/or **I_{IIc}** were diluted in extracellular solution on the day of experiments (glutamate stock = 1 M; MgCl₂ stock = 1 M; **I_{IIc}** stock = 10 mM in 140 mM NaCl and 2% DMSO, maximum [DMSO] = 0.075%). Extracellular solutions were applied to the patched cell via an in-house built fast perfusion system [117]. Whole-cell currents were recorded and digitized using an Axopatch 200A patch-clamp amplifier and Digidata 1440A digitizer (Molecular Devices). The current signal was low-pass filtered at 5 kHz and sampled at 20 kHz using pClamp 10.7 (Molecular Devices). Series resistance was compensated 85–90% in all experiments. An empirically determined –6 mV liquid junction potential between the internal and external solutions was corrected in all experiments.

Concentration-inhibition relations were measured using the protocol shown in Fig. 5A. Glutamate (1 mM) was applied until current reached steady-state, then sequentially increasing concentrations of **I_{IIc}** were applied for 10 s in the presence of glutamate. Glutamate alone was reapplied for 80 s following **I_{IIc}** application to allow recovery from inhibition. Cells in which current did not recover to 90% of steady-state current during the initial glutamate application were excluded from analysis to prevent underestimation of potency. We estimated IC₅₀ by fitting Equation 2 to concentration-inhibition data:

$$\frac{I_{IIc}}{I_{Glu}} = \frac{1}{1 + \left(\frac{[IIc]}{IC_{50}} \right)^{n_H}}$$

where I_{IIc} is mean current steady state current during application of **I_{IIc}**, I_{Glu} is the average of the mean steady state currents before and after application of **I_{IIc}** and n_H is the Hill coefficient. IC₅₀ and n_H

were free parameters during fitting. I_{IIC} and I_{Clu} were measured as the mean current over the final 1 s of each application. Baseline current was subtracted from all current measurements. For Mg^{2+} competition experiments, I_{IC} IC_{50} s were measured in the constant presence of extracellular 0.2 mM Mg^{2+} .

We measured the voltage dependence of block by **IIC** using the protocol shown in Fig. 5D. Inhibition by **IIC** was measured in each cell at nine voltages ranging from -105 to $+55$ mV. During each voltage step, the cell was exposed to: 5 s in extracellular solution following the voltage step; a 10 s application of 1 mM glutamate; a 15 s application of **IIC** with 1 mM glutamate; a second application of 1 mM glutamate for 15 s to allow drug unbinding; application of extracellular solution for 2 s to allow a return to baseline current. Voltage was then returned to -65 mV for 3 s before the next voltage jump was made. Voltage dependence of block was quantified using Equation 3:

$$\frac{I_{IIC}}{I_{Clu}} = \frac{1}{1 + \frac{[IIC]}{(IC_{50}^{-65 \text{ mV}}) e^{\frac{V_m - 65}{V_0}}}}$$

where $IC_{50}^{-65 \text{ mV}}$ is the IC_{50} at -65 mV (calculated from concentration-inhibition experiments), V_m represents the holding potential, and V_0 represents the change in voltage (in mV) that results in an e-fold change in the IC_{50} of the drug. I_{IIC} and I_{Clu} were measured as in analysis of concentration-inhibition data. V_0 was the only free parameter during fitting. The fraction of the total membrane voltage field felt by the blocker at its binding site (δ) [119] was estimated using Equation 4:

$$\delta = \frac{RT}{V_0 zF}$$

where R is the ideal gas constant, T is the absolute temperature, z represents the valence of the blocker, and F is the Faraday constant. Note that while δ is useful for comparing voltage dependence of blockers, permeant ions influence the voltage dependence of NMDAR channel block [120]. Therefore, δ only provides a rough estimate of the location of a channel blocker's binding site in the voltage field.

4.5. In vitro DMPK

4.5.1. Microsomal stability

The human, rat, and mouse pooled microsomes employed were purchased from Tebu-Xenotech. The compound was incubated at 37°C with the microsomes in a 50 mM phosphate buffer (pH = 7.4) containing 3 mM $MgCl_2$, 1 mM NADP, 10 mM glucose-6-phosphate and 1 U/mL glucose-6-phosphate-dehydrogenase. Samples (75 μL) were taken from each well at 0, 10, 20, 40 and 60 min and transferred to 4°C in a plate containing 75 μL acetonitrile and 30 μL of 0.5% formic acid in water, which were added to improve the chromatographic conditions. The plate was centrifuged (46000 g, 30 min) and supernatants were taken and analyzed in a UPLC-MS/MS (Xevo-TQD, Waters) using a BEH C18 column and an isocratic gradient of 0.1% formic acid in water: 0.1% formic acid acetonitrile (60:40). The metabolic stability of the compounds was calculated from the logarithm of the remaining compounds at each time point studied.

4.5.2. Permeability

The Caco-2 cells were cultured to confluency, trypsinized and seeded onto a 96-filter transwell insert (Corning) at a density of $\sim 10,000$ cells/well in DMEM cell culture medium supplemented with 10% fetal bovine serum, 2 mM L-Glutamine and 1% penicillin/

streptomycin. Confluent Caco-2 cells were subcultured at passages 58–62 and grown in a humidified atmosphere of 5% CO_2 at 37°C . Following an overnight attachment period (24 h after seeding), the cell medium was replaced with fresh medium in both the apical and basolateral compartments every other day. The cell monolayers were used for transport studies 21 days post seeding. The monolayer integrity was checked by measuring the transepithelial electrical resistance (TEER), obtaining values $\geq 500 \Omega/\text{cm}^2$. On the day of the study, after the TEER measurement, the medium was removed and the cells were washed twice with pre-warmed (37°C) Hank's Balanced Salt Solution (HBSS) buffer to remove traces of medium. Stock solutions were made in DMSO, and further diluted in HBSS (final DMSO concentration 1%). Each compound and reference compounds (Colchicine, E3S) were tested at a final concentration of 10 μM . For A \rightarrow B directional transport, the donor working solution was added to the apical (A) compartment and the transport media as receiver working solution was added to the basolateral (B) compartment. For B \rightarrow A directional transport, the donor working solution was added to the basolateral (B) compartment and transport media as receiver working solution was added to the apical (A) compartment. The cells were incubated at 37°C for 2 h with gentle stirring.

At the end of the incubation, samples were taken from both donor and receiver compartments and transferred into 384-well plates and analyzed by UPLC-MS/MS. Detection was performed using an ACQUITY UPLC/Xevo TQD system. After the assay, Lucifer yellow (LY) was used to further validate the cell monolayer integrity, cells were incubated with LY 10 μM in HBSS for 1 h at 37°C , obtaining permeability (Papp) values for LY of ≤ 10 nm/s confirming the well-established Caco-2 monolayer.

4.5.3. Cytochrome P450 inhibition assay

The objective of this study was to screen the inhibition potential of the compound using recombinant human cytochrome P450 enzymes (CYP1A2, CYP2C9, CYP2C19, CYP2D6, CYP3A4 (BFC) and CYP3A4 (DBF)) and probe substrates with fluorescent detection. Incubations were conducted in a 200 μL volume in 96-well microtiter plates (COSTAR 3915). The addition of the mixture buffer-cofactor (KH_2PO_4 buffer, 1.3 mM NADP, 3.3 mM $MgCl_2$, 3.3 mM glucose-6-phosphate and 0.4 U/mL glucose-6-phosphate dehydrogenase), control supersomes, standard inhibitors (furfurylamine, tranlylpyromine, ketoconazole, sulfaphenazole and quinidine; Sigma Aldrich), and previously diluted compound to plates was carried out by a liquid handling station (Zephyr Caliper). The plate was then preincubated at 37°C for 5 min, and the reaction was initiated by the addition of prewarmed enzyme/substrate (E/S) mix. The E/S mix contained buffer (KH_2PO_4), c-DNA-expressed cytochrome P450 enzymes in insect cell microsomes, substrate (3-cyano-7-ethoxycoumarin, for CYP1A2 and CYP2C19; 7-methoxy-4-(trifluoromethyl)coumarin for CYP2C9; 3-[2-(*N,N*-diethyl-*N*-methylammonium)ethyl]-7-methoxy-4-methylcoumarin for CYP2D6; and 7-benzoyloxytrifluoromethyl coumarin (7-BFC) and dibenzylfluorescein (DBF) for CYP3A4) in a reaction volume of 200 μL . Reactions were terminated after various times (a specific time for each cytochrome) by addition of STOP solution (ACN/TrisHCl 0.5 M 80:20 or 2 N NaOH). Fluorescence per well was measured using a fluorescence plate reader (Tecan Infinity M1000 pro) and percentage of inhibition was calculated.

4.5.4. hERG inhibition assay

The assay was carried out on a CHO cell line transfected with the hERG potassium channel. 72 h before the assay, 2500 cells were seeded on a 384 well black plate (Greiner 781091). Cells were maintained at 37°C in a 5% CO_2 atmosphere for 24 h and at 30°C in a 5% CO_2 atmosphere for 48 h plus. hERG activity was measured by

using the Fluxor™ Potassium Ion Channel Assay Kit (Thermo Fisher F10016). Medium was replaced for 20 μ L Loading Buffer and the cells were incubated for 60 min at RT, protected from direct light. After incubation, Loading Buffer was replaced with Assay buffer and the compounds were incubated for 30 min at RT. 5 μ L of Stimulus Buffer was added to each well and the fluorescence was read ($\lambda_{\text{exc}} = 490$ nm, $\lambda_{\text{em}} = 525$ nm) using imaging plate reader system (FDSS7000EX, Hamamatsu®) every second after the establishment of a baseline line. Astemizole ($IC_{50} = 152$ nM) was used to validate the assay.

4.5.5. Parallel artificial membrane permeation assays-blood-brain barrier (PAMPA-BBB)

To evaluate the brain penetration of the compounds, a parallel artificial membrane permeation assay for blood-brain barrier was used, following the method described by Di et al. [121] The *in vitro* permeability (P_e) of fourteen commercial drugs through lipid extract of porcine brain membrane together with the test compounds were determined. Commercial drugs and assayed compounds were tested using a mixture of PBS:EtOH (70:30). The assay was validated by comparing experimental and reported P_e values of a set of fourteen commercial drugs (Table S2), and the following correlation was obtained: P_e (exp) = 1.6662 P_e (lit) - 1.4174 ($R^2 = 0.9334$). On the basis of this equation and the limits established for BBB permeation [119], the threshold for high BBB permeation (CNS+) was set at P_e (10^{-6} cm s^{-1}) > 5.247; low BBB permeation (CNS-) was set at P_e (10^{-6} cm s^{-1}) < 1.915; and the range for uncertain BBB permeation (CNS \pm) at 5.247 > P_e (10^{-6} cm s^{-1}) > 1.915. Three different experiments, each performed in triplicate, were carried out for each compound.

4.6. In vivo evaluation of **IIc** and memantine

4.6.1. Worm strains, maintenance, and general methods

Strains used are listed in Table S3. Standard methods were used for culturing and examination *C. elegans* [92]. Wild-type strains were cultured at 20 °C, while transgenic strains were cultured at 16 °C in a temperature-controlled incubator on solid nematode growth medium (NGM) seeded with *Escherichia coli* (*E. coli*) OP50 strain as a food source. To collect age synchronized populations of eggs, adults were treated with alkaline hypochlorite solution (0.5 M NaOH, ~2.6% NaCl) for 5–7 min. Fertilized eggs were re-suspended in S-medium for 12 h, and L1 larvae were incubated to hatch overnight in the absence of food.

4.6.2. Compound preparation and treatment

The compounds were dissolved in 100% DMSO. Each concentration was then dissolved in MilliQ purified water to achieve a final concentration between 100 mg/L and 16 mg/L in 1% DMSO in well. For the locomotion assay, treatments were carried out in liquid culture for 4 days at 20 °C. Each well contained a final volume of 60 μ L, consisting of 25–30 animals in the L1 stage, compounds under study at the appropriate doses, and OP50 inactivated by freeze-thaw cycles and incubated in S-medium complete to a final optical density of 595 (OD595) of 0.9–0.8 measured in the microplate reader. For the chemotaxis assay synchronized CL2355 and CL2122 strains were treated with DMSO or compounds on NGM plates seeded with inactivated *E. coli* (OP50). They were cultured at 16 °C for 36 h, and then at 23 °C for 36 h.

4.6.3. Locomotion assay

A locomotion assay of NMDA receptor channel blockers was run to obtain a dose-response profile and evaluate their effects on motor function of the CL2006 transgenic strain. The animals were synchronized by alkaline hypochlorite treatment, and the OP50

bacteria OD595 was adjusted to 0.9 to perform the assay. WT strain (N2), and the transgenic strain (CL2006) were treated in liquid media for 4 days at 20 °C with continuous shaking at 180 rpm, starting at the L1 stage. On day 5 of age, the nematodes were moved from the 96-well plates to an unseeded NGM plate for 45 min before starting the trial, allowing the plate to dry. Locomotion assays were conducted in 30 mm NGM plates, where the entire plate was covered by OP50. 5 to 10 adult nematodes were positioned in the center of a circle (1 cm diameter) in seeded 30 mm NGM plates. After 1 min, the number of animals remaining inside the circle were considered locomotor defective. A locomotor defective score (LD) was calculated by dividing the number of worms inside the circle by the total number of worms on the plate. Motor behavior assays were run with a total of at least 200 animals tested per compound concentration. The motor index score ranges from 0% (animals that exhibit the same motor defect as untreated CL2006 animals) to 100% (animals that exhibit motor behavior comparable to WT animals). All results included in the figures are calculated using the following formula:

$$\text{Motor index(\%)} = \frac{LD \text{ CL2006}_{\text{vehicle}} - LD \text{ CL2006}_{\text{drug}}}{LD \text{ CL2006}_{\text{vehicle}} - LD \text{ WT}_{\text{vehicle}}} \times 100$$

4.6.4. Chemotaxis assay

Nematodes were sampled after the treatments with memantine and **IIc** and washed with M9 buffer (3 g/L KH_2PO_4 , 6 g/L Na_2HPO_4 , 5 g/L NaCl, 1 mL/L 1 mM $MgSO_4$, 800 mL/L ddH_2O). In brief, the assay was performed in 100 mm NGM plates. 10 μ L of odorant (0.025% benzaldehyde in 96% ethanol) was added to the "attractant" spot, and on the opposite side of the NGM, 10 μ L of control odorant (96% ethanol) was added. Then, 70–80 worms were positioned in the center of the plate. Assay plates were incubated at 23 °C for 1 h and were scored according to the chemotaxis index (CI) as follows: $CI = (\text{number of worms at attractant} - \text{number of worms at control}) / (\text{number of worms at attractant spot} + \text{number of worms at control spot})$. Two trials were performed in triplicate. In each experiment, at least 250 worms from each group were analyzed.

4.6.5. 5XFAD mice

The 5XFAD strain is a well-established and suitable transgenic AD mouse model expressing five familial mutations of human AD. 5XFAD mice also exhibit early-onset cognitive impairment and A β pathology [88]. Six months old female Wild Type (WT) and 5XFAD mice (n = 43) were randomly divided into four groups: WT (n = 14), 5XFAD Control (Control) (n = 8), 5XFAD treated with memantine (Mem) (n = 11) and 5XFAD treated with **IIc** (**IIc**) (n = 10). Animals had free access to food and water under standard temperature conditions (22 ± 2 °C) and were maintained on 12 h: 12 h light-dark cycles (300 lux/0 lux). Water consumption was controlled each week; drug concentrations were adjusted accordingly to reach the appropriate dose for each cage. Memantine and **IIc** were dissolved in 1.8% 2-hydroxypropyl- β -cyclodextrin and administered at 5 mg/kg/day through drinking water for four weeks and up to euthanasia. Studies were approved by the Animal Experimentation Ethics Committee (CEEA) at the University of Barcelona. All efforts were made to reduce the number of animals used and their suffering.

4.6.6. Novel object recognition test (NORT)

NORT is a cognitive test used to assess short- and long-term recognition memories. The apparatus used consisted of a 90°, two-arm, 25-cm-long, 20-cm-high, and a 5-cm-wide black maze of

black polyvinyl chloride. The objects to be discriminated were made of plastic and chosen not to frighten mice and without any part likely to be bitten. The test was performed over 5 days. On the first three days, animals were individually habituated to the apparatus for 10 min each day. On the fourth day, the animals were individually exposed during 10 min to the apparatus and were allowed to freely explore the zone inside the apparatus (First trial/Familiarization) where we had placed two identical novel objects (A + A' or B + B') at the end of each arm. After 10 min, the animals were removed and returned to their home cage, and 2 h later the retention trial (second trial) was performed. In this second trial, objects A' and B' were swapped (A + B' or A'+B) and the mice were allowed to explore the maze for 10 min. Twenty-four hours after the first trial, animals were exposed again to the apparatus, and in this case, objects A' and B' were substituted by two new objects with different shapes and colours (A + C or B + C'), and animals were allowed to explore them for 10 min. The time exploring the novel object (TN) and the old object (TO) were measured and recorded using a camera. Exploration of an object was defined as pointing the nose towards the object at a distance ≤ 2 cm and/or touching it with the nose. Turning or sitting around the object was not considered exploration. To avoid object preference biases objects A and B were counterbalanced so that one-half of the animals in each experimental group were first exposed to object A and then to object B, whereas the other half first saw object B and then object A. Finally, to quantify cognitive performance, the Discrimination Index (DI) was calculated, which is defined as $(TN-TO)/(TN + TO)$.

4.6.7. Brain tissue preparation

Mice groups were euthanized by cervical dislocation and brains were immediately removed from the skull. For molecular experiments, the hippocampus was isolated and frozen in powdered dry ice. Hippocampi were maintained at -80 °C for further use for protein extraction, RNA and DNA isolation. For thioflavin-S staining, mice were anesthetized (ketamine 100 mg/kg and xylazine 10 mg/kg, intraperitoneally) and then perfused with 4% paraformaldehyde (PFA) diluted in 0.1 M phosphate buffer solution intracardially. Brains were removed and postfixed in 4% PFA overnight at 4 °C. Afterwards, brains were changed to PFA +15% sucrose. Finally, the brains were frozen on powdered dry ice and stored at -80 °C until sectioning. Brain coronal sections of 30 μ m were obtained (Leica Microsystems CM 3050S cryostat, Wetzlar, Germany) and kept in a cryoprotectant solution at -20 °C until use.

4.6.8. Protein level determination by Western Blotting

For Western Blotting (WB), aliquots of 15 μ g of hippocampal protein extraction per sample were used. In brief, tissues were homogenized in lysis buffer containing phosphatase and protease inhibitors (Cocktail II, Sigma-Aldrich). Total protein levels were obtained, and protein concentration was determined by the Bradford method. Protein samples were separated by Sodium dodecyl sulphate-Polyacrylamide gel electrophoresis (SDS-PAGE) (8–20%) and transferred onto Polyvinylidene difluoride (PVDF) membranes (Millipore). Afterwards, membranes were blocked in 5% non-fat milk in Tris-buffered saline (TBS) solution containing 0.1% Tween 20 TBS (TBS-T) for 1 h at rt, followed by overnight incubation at 4 °C with the primary antibodies listed in Table S4. Then, membranes were washed and incubated with secondary antibodies for 1 h at RT. Immunoreactive proteins were viewed with the chemiluminescence-based detection kit, following the manufacturer's protocol (ECL Kit, Millipore), and digital images were acquired using ChemiDoc XRS + System (BioRad). Semi-quantitative analyses were done using ImageLab software (BioRad), and results were expressed in Arbitrary Units (AU), considering control protein levels as 100%. Protein loading was routinely monitored by

immunodetection of Glyceraldehyde-3-phosphate dehydrogenase (GAPDH).

4.6.9. Data Acquisition and statistical analysis

Data analysis was conducted using GraphPad Prism ver. 6 statistical software. Data are expressed as the mean \pm standard error of the mean (SEM) of at least 3 samples per group. Statistical analysis was performed by way of two-tail Student's t-test or one-way analysis of variance (ANOVA) followed by Tukey post-hoc analysis. Statistical significance was defined as p-value < 0.05 . Statistical outliers were determined with Grubbs' test and, when necessary, were removed from the analysis. The cognitive analysis was performed blindly: an experimenter unaware of the treatment groups performed the tests and recorded the number of animals. Another experimenter analyzed the videos and the behavioral scoring.

4.7. Cytotoxicity

The cytotoxicity of **11c** was measured in Neuro2A cells. Cells were plated in 96-well plates at a density of 40,000 cells/well and grown under conventional conditions (0.2 mL per well in RPMI medium 10%FBS and supplemented with pyruvate and antibiotics). The day after, cells were exposed during 24 h to 1, 10 or 100 μ M EV-19. Afterwards, cell viability was assessed using the MTT method. Briefly, 20 μ L of a solution of 5 mg/ml of 3-(4,5-dimethyl-2-thiazolyl)-2,5-diphenyl-2H-tetrazolium bromide in PBS was added in each well and after 1 h in the cell incubator the supernatant was discarded and cells lysed with 200 μ L DMSO. After shaking, absorbance was measured at 595 nm in a Biotek PowerWave HT plate reader. Assays were performed in triplicate and no difference was found between controls and drug-treated cells at any concentration.

Contributions

A.L.T. and J.C.-A. contributed equally. S.V. conceived the idea. A.L.T. synthesized and chemically characterized the compounds. F.X.S. performed the intracellular calcium-based determination of the IC₅₀s in cells. A.L.T., M.B.P., D.S. and J.W.J. designed and carried out electrophysiological studies. D.S.P. and M.G.K. designed and performed MD calculations. M.L.L., J.M.B. and B.P. carried out DMPK studies. J.C.-A., C.G.-F. and M.P. designed and carried out the *in vivo* experiments. A.L.T. wrote the first draft of the manuscript. A.L.T., D.S., M.B.P., J.W.J., D.S.P., M.G.K., J.C.-A., C.G.-F., M.P. and S.V. wrote the definitive manuscript with feedback from all the authors. All authors have given approval to the final version of the manuscript.

Declaration of competing interest

The authors declare that they have no known competing financial interests or personal relationships that could have appeared to influence the work reported in this paper.

Acknowledgements

This research was funded by the Spanish *Ministerio de Economía, Industria y Competitividad* (Grant SAF2017-82771-R to S.V. and PID2019-106285RB-I00 to M.P.), the *María de Maeztu Unit of Excellence* (Institute of Neurosciences, Universitat de Barcelona, MDM-2017-0729, to M.P. and D.S.), and 2017SGR106 (AGAUR, Catalonia to S.V. and M.P.), the Spanish *Ministerio de Ciencia e Innovación* (Grant PID2020-119932 GB-I00/AEI /10.13039/5011000011033 to D.S.), the European Regional Development Fund (ERDF), the *Xunta de Galicia* (ED431G 2019/02 and ED431C 2018/

21), and the United States National Institutes of Health (Grant R01AG065594 to J.W.J., M.G.K., and S.V.; Grant F31NS113477 to M.B.P.). J.C.-A acknowledges the Spanish *Ministerio de Ciencia e Innovación* for a FPI fellowship (MDM-2017-0729-19-2). A.L.T. acknowledges a PhD fellowship (FPU grant) from the Spanish *Ministerio de Educación, Cultura y Deporte* and the Spanish Society of Medicinal Chemistry (SEQT) and Enantia S. L. for an "Award for Novel Researchers in the Discovery and Development of New Drugs". Computational work used the Extreme Science and Engineering Discovery Environment (XSEDE) Bridges 2 at Pittsburgh Supercomputing Center, allocation to M.G.K. TG-MCB180173, which is supported by the United States National Science Foundation grant number ACI-1548562.

Appendix A. Supplementary data

Supplementary data to this article can be found online at <https://doi.org/10.1016/j.ejmech.2022.114354>.

References

- [1] M.W. Bondi, E.C. Edmonds, D.P. Salmon, Alzheimer's disease: past, present, and future, *J. Int. Neuropsychol. Soc.* 23 (2017) 818–831.
- [2] Alzheimer's Disease International, *Alzheimer's Disease International*, London, 2019.
- [3] GBD 2016 Dementia Collaborators, Global, regional, and national burden of Alzheimer's disease and other dementias, 1990–2016: a systematic analysis for the Global Burden of Disease Study 2016, *Lancet Neurol.* 18 (2019) 88–106.
- [4] M. Vaz, S. Silvestre, Alzheimer's disease: recent treatment strategies, *Eur. J. Pharmacol.* 887 (2020), 173554.
- [5] J. Sevigny, P. Chiao, T. Bussière, P.H. Weinreb, L. Williams, M. Maier, R. Dunstan, S. Salloway, T. Chen, Y. Ling, J. O'Gorman, F. Qian, M. Arastu, M. Li, S. Chollate, M.S. Brennan, O. Quintero-Monzon, R.H. Scannevin, H.M. Arnold, T. Engber, K. Rhodes, J. Ferrero, Y. Hang, A. Mikulskis, J. Grimm, C. Hock, R.M. Nitsch, A. Sandrock, The antibody aducanumab reduces A β plaques in Alzheimer's disease, *Nature* 537 (2016) 50–56.
- [6] S. Jaffe, USA FDA defends approval of Alzheimer's disease drug, *Lancet* 398 (2021) 32.
- [7] L.A. Hershey, R. Tarawneh, Clinical efficacy, drug safety and surrogate endpoints: has aducanumab met all of its expectations? *Neurology* 97 (2021) 517–518.
- [8] S. Salloway, J. Cummings, Aducanumab, amyloid lowering, and slowing of Alzheimer disease, *Neurology* 97 (2021) 543–544.
- [9] D.S. Knopman, J.S. Perlmutter, Prescribing aducanumab in the face of meager efficacy and real risks, *Neurology* 97 (2021) 545–547.
- [10] G. Marucci, M. Buccioni, D.D. Ben, C. Lambertucci, R. Volpini, F. Amenta, Efficacy of acetylcholinesterase inhibitors in Alzheimer's disease, *Neuropharmacology* 190 (2021), 108352.
- [11] J.M. López-Arrieta, L. Schneider, Metrifonate for Alzheimer's disease, *Cochrane Database Syst. Rev.* 2 (2006), CD003155.
- [12] Klein, J. Phenserine, *Expert Opin. Invest. Drugs* 16 (2007) 1087–1097.
- [13] O. Weinreb, T. Amit, O. Bar-Am, M.B. Youdim, A novel anti-Alzheimer's disease drug, ladostigil neuroprotective, multimodal brain-selective monoamine oxidase and cholinesterase inhibitor, *Int. Rev. Neurobiol.* 100 (2011) 191–215.
- [14] M. Son, C. Park, S. Rampogu, A. Zeb, K.W. Lee, Discovery of novel netylcholinesterase inhibitors as potential candidates for the treatment of Alzheimer's Disease, *Int. J. Mol. Sci.* 20 (2019) 1000.
- [15] M. Saxena, R. Dubey, Target enzyme in Alzheimer's disease: acetylcholinesterase inhibitors, *Curr. Top. Med. Chem.* 19 (2019) 264–275.
- [16] M. Bortolami, D. Rocco, A. Messori, R. Di Santo, R. Costi, V.N. Madia, L. Scipione, F. Pandolfi, Acetylcholinesterase inhibitors for the treatment of Alzheimer's disease – a patent review (2016–present), *Expert Opin. Ther. Pat.* 31 (2021) 399–420.
- [17] T. Kishi, S. Matsunaga, K. Oya, I. Nomura, T. Ikuta, N. Iwata, Memantine for Alzheimer's disease: an updated systematic review and meta-analysis, *J. Alzheimers Dis.* 60 (2017) 401–425.
- [18] S. Matsunaga, T. Kishi, I. Nomura, K. Sakuma, M. Okuya, T. Ikuta, N. Iwata, The efficacy and safety of memantine for the treatment of Alzheimer's disease, *Expert Opin. Drug Saf.* 17 (2018) 1053–1061.
- [19] C.G. Parsons, A. Stoffer, W. Danysz, Memantine: a NMDA receptor antagonist that improves memory by restoration of homeostasis in the glutamatergic system—too little activation is bad, too much is even worse, *Neuropharmacology* 53 (2007) 699–723.
- [20] W. Danysz, C.G. Parsons, Alzheimer's disease, β -amyloid, glutamate, NMDA receptors and memantine—searching for the connections, *Br. J. Pharmacol.* 167 (2012) 324–352.
- [21] P. Xia, H.-S.V. Chen, D. Zhang, S.A. Lipton, Memantine preferentially blocks extrasynaptic over synaptic NMDA receptor currents in hippocampal autapses, *J. Neurosci.* 30 (2010) 11246–11250.
- [22] K.E. Gilling, C. Jatzke, M. Hechenberger, C.G. Parsons, Potency, voltage-dependency, agonist concentration-dependency, blocking kinetics and partial untrapping of the uncompetitive N-methyl-D-aspartate (NMDA) channel blocker memantine at human NMDA (GluN1/GluN2A) receptors, *Neuropharmacology* 56 (2009) 866–875.
- [23] Rammes, G. Neramexane, A moderate-affinity NMDA receptor channel blocker: new prospects and indications, *Expert Rev. Clin. Pharmacol.* 2 (2009) 231–238.
- [24] Y. Wang, J. Eu, M. Washburn, T. Gong, H.S.V. Chen, W.L. James, S.A. Lipton, J.S. Stamler, G.T. Went, S. Porter, The pharmacology of aminoamantane nitrates, *Curr. Alzheimer Res.* 3 (2006) 201–204.
- [25] Y. Wang, J. Eu, M. Washburn, T. Gong, H.S. Chen, W.L. James, S.A. Lipton, J.S. Stamler, G.T. Went, S. Porter, Memantine-sulfur containing antioxidant conjugates as potential prodrugs to improve the treatment of Alzheimer's disease, *Eur. J. Pharmacol.* 49 (2013) 187–198.
- [26] H. Takahashi, P. Xia, J. Cui, M. Talantova, K. Bodhinathan, W. Li, S. Saleem, E.A. Holland, G. Tong, J. Piña-Crespo, D. Zhang, N. Nakanishi, J.W. Larrick, S.R. McKercher, T. Nakamura, Y. Wang, S.A. Lipton, Pharmacologically targeted NMDA receptor antagonism by nitromemantine for cerebrovascular disease, *Sci. Rep.* 5 (2016) 14781.
- [27] S.O. Bachurin, E.F. Shevtsova, G.F. Makhaeva, V.V. Grigoriev, N.P. Boltneva, N.V. Kovaleva, S.V. Lushchekina, P.N. Shevtsov, M.E. Neganova, O.M. Redkozubova, E.V. Bovina, A.V. Gabrelyan, V.P. Fisenko, V.B. Sokolov, A.Y. Aksinenko, V. Echeverria, G.E. Barreto, G. Aliev, Novel conjugates of aminoamantanes with carbazole derivatives as potential multitarget agents for AD treatment, *Sci. Rep.* 30 (2017) 45627.
- [28] R. Leiva, M.B. Phillips, A.L. Turcu, E. Gratacós-Batlle, L. León-García, F.X. Sureda, D. Soto, J.W. Johnson, S. Vázquez, Pharmacological and electrophysiological characterization of novel NMDA receptor antagonists, *ACS Chem. Neurosci.* 9 (2018) 2722–2730.
- [29] T. Kumamoto, M. Nakajima, R. Uga, N. Ihayazaka, H. Kashihara, K. Katakawa, T. Ishikawa, R. Saiki, K. Nishimura, K. Igarashi, Design, synthesis, and evaluation of polyamine-memantine hybrids as NMDA channel blockers, *Bioorg. Med. Chem.* 26 (2018) 603–608.
- [30] S. Sestito, S. Daniele, D. Pietrobono, V. Citi, L. Bellusi, G. Chiellini, V. Calderone, C. Martini, S. Rapposelli, Memantine prodrug as a new agent for Alzheimer's disease, *Sci. Rep.* 9 (2019) 4612.
- [31] L. Wu, X. Zhou, Y. Cao, S.H. Mak, L. Zha, N. Li, Z. Su, Y. Han, Y. Wang, M.P. Man Hot, Y. Sun, G. Zhang, Z. Zhang, X. Yang, Therapeutic efficacy of novel memantine nitrate MN-08 in animal models of Alzheimer's disease, *Aging Cell* 20 (2021), e13371.
- [32] S. Couly, M. Denus, M. Bouchet, G. Rubinstenn, T. Maurice, Anti-amnesic and neuroprotective effects of fluoroethylnormemantine in a pharmacological mouse model of Alzheimer's disease, *Int. J. Neuropsychopharmacol.* 24 (2021) 142–157.
- [33] <http://www.rest-therapeutics.com/> (accessed 2021-12-29).
- [34] <https://eumentistx.com/> (accessed 2021-12-29).
- [35] G. Bernstein, K. Davis, C. Mills, L. Wang, M. McDonnell, J. Oldenhof, C. Inturrisi, P.L. Manfredi, O.V. Vitolo, Characterization of the safety and pharmacokinetic profile of d-methadone, a novel N-Methyl-D-Aspartate receptor antagonist in healthy, opioid-naïve subjects: results of two phase 1 studies, *J. Clin. Psychopharmacol.* 39 (2019) 226–237.
- [36] <https://www.relmada.com/product-development> (accessed 2021-12-29).
- [37] D. Vandame, G. Desmadyl, J. Becerril Ortega, M. Teigell, N. Crouzin, A. Buisson, A. Privat, H. Hirbec, Comparison of the pharmacological properties of GK11 and MK801, two NMDA receptor antagonists: towards an explanation for the lack of intrinsic neurotoxicity of GK11, *J. Neurochem.* 103 (2007) 1682–1696.
- [38] <https://www.otonomy.com/pipeline/> (accessed 2021-08-26).
- [39] <https://www.nrxpharma.com/> (accessed 2021-08-26).
- [40] R.S. Duman, G.K. Aghajanian, G. Sanacora, J.H. Krystal, Synaptic plasticity and depression: new insights from stress and rapid-acting antidepressants, *Nat. Med.* 22 (2016) 238–249.
- [41] <https://aurismedical.com/science/inner-ear-therapeutics> (accessed 2021-08-27).
- [42] M.D. Duque, P. Camps, E. Torres, E. Valverde, F.X. Sureda, M. López-Querol, A. Camins, S.R. Prathalingam, J.M. Kelly, S. Vázquez, New oxapolycyclic cage amines with NMDA receptor antagonist and trypanocidal activities, *Bioorg. Med. Chem.* 18 (2010) 46–57.
- [43] T. Torres, M.D. Duque, M. López-Querol, M.C. Taylor, N. Naesens, C. Ma, L.H. Pinto, F.X. Sureda, J.M. Kelly, S. Vázquez, Synthesis of benzopolycyclic cage amines: NMDA receptor antagonist, trypanocidal and antiviral activities, *Bioorg. Med. Chem.* 20 (2012) 942–948.
- [44] E. Valverde, F.X. Sureda, S. Vázquez, Novel benzopolycyclic amines with NMDA receptor antagonist activity, *Bioorg. Med. Chem.* 22 (2014) 2678–2683.
- [45] R.D. Tung, Deuterium medicinal chemistry comes of age, *Future Med. Chem.* 8 (2016) 491–494.
- [46] T. Piralì, M. Serafini, S. Cargini, A.A. Genazzani, Applications of deuterium in medicinal chemistry, *J. Med. Chem.* 62 (2019) 5276–5297.
- [47] J.F. Liu, S.L. Harbeson, C.L. Brummel, R. Tung, R. Silverman, D. Dolter, A decade of deuteration in medicinal chemistry, *Annu. Rep. Med. Chem.* 50 (2017)

- 519–542.
- [48] S. Carginin, M. Serafini, T. Piralì, A primer of deuterium in drug design, *Future Med. Chem.* 11 (2019) 2039–2042.
- [49] P. Camps, M.D. Duque, S. Vázquez, L. Naesens, E. De Clercq, F.X. Sureda, M. López-Querol, A. Camins, M. Pallàs, S.R. Prathalingam, J.M. Kelly, V. Romero, D. Ivorra, D. Cortés, Synthesis and pharmacological evaluation of several ring-contracted amantadine analogs, *Bioorg. Med. Chem.* 16 (2008) 9925–9936.
- [50] R.A. Bishop, The intramolecular cyclization of unsaturated benzo derivatives of Bicyclo[3.3.2]decane, *Aust. J. Chem.* 36 (1983) 2465–2472.
- [51] R. Bishop, G. Burgess, Ritter reactions. II. Reductive deamidation of N-bridgehead amides, *Tetrahedron Lett.* 28 (1987) 1585–1588.
- [52] E. Sánchez-Larios, J.M. Holmes, C.L. Daschner, M. Gravel, NHC-Catalyzed spiro bis-indane formation via domino Stetter-Aldol-Michael and Stetter-Aldol-Aldol reactions, *Org. Lett.* 12 (2010) 5772–5775.
- [53] C.J. Moody, G.J. Warreilow, Vinyl azides in heterocyclic synthesis. Part 10. Synthesis of the isoindolobenzazepine alkaloid lennoxamine, *J. Chem. Soc. Perkin Trans. 1* (1990) 2929–2936.
- [54] O. Farooq, Oxidation of aromatic 1,2-dimethanols by activated dimethyl sulfoxide, *O. Synthesis* 10 (1994) 1035–1036.
- [55] J.J. Pappas, W.P. Keaveney, M. Berger, R.V. Rush, Directional effects of substituents in the ozonolysis of naphthalenes. Synthesis of o-phthalaldehydes, *J. Org. Chem.* 33 (1968) 787–792.
- [56] A.K. Gupta, X. Fu, J.P. Snyder, J.M. Cook, General approach for the synthesis of polyquinines via the Weiss reaction, *Tetrahedron* 47 (1991) 3665–3710.
- [57] A.M. Canudas, D. Pubill, F.X. Sureda, E. Verdagué, P. Camps, D. Muñoz-Torero, A. Jiménez, A. Camins, M. Pallàs, Neuroprotective effects of (+/-)-huprine Y on in vitro and in vivo models of excitotoxicity damage, *Exp. Neurol.* 180 (2003) 123–130.
- [58] X. Song, M.O. Jensen, V. Jogini, R.A. Stein, C.-H. Lee, H.S. Mchaourab, D.E. Shaw, E. Gouaux, Mechanism of NMDA receptor channel block by MK-801 and memantine, *Nature* 556 (2018) 515–519.
- [59] W. Limapichat, W.Y. Yu, E. Branigan, H.A. Lester, D.A. Dougherty, Key binding interactions for memantine in the NMDA receptor, *ACS Chem. Neurosci.* 4 (2013) 255–260.
- [60] E. Gratacós-Batlle, N. Yefimenko, H. Cascos-García, D. Soto, AMPAR interacting protein CPT1C enhances surface expression of GluA1-containing receptors, *Front. Cell. Neurosci.* 8 (2015) 469.
- [61] I. Bresink, T.A. Benke, V.J. Collett, A.J. Seal, C.G. Parsons, J.M. Henley, G.L. Collingridge, Effects of memantine on recombinant rat NMDA receptors expressed in HEK 293 cells, *Br. J. Pharmacol.* 119 (1996) 195–204.
- [62] C.G. Parsons, V.A. Panchenko, V.O. Pinchenko, A.Y. Tsyndrenko, O.A. Krishtal, Comparative patch-clamp studies with freshly dissociated rat hippocampal and striatal neurons on the NMDA receptor antagonistic effects of amantadine and memantine, *Eur. J. Neurosci.* 8 (1996) 446–454.
- [63] T.A. Blanpied, F.A. Boeckman, E. Aizenman, J.W. Johnson, Trapping channel block of NMDA-activated responses by amantadine and memantine, *J. Neurophysiol.* 77 (1997) 309–323.
- [64] T.A. Blanpied, R.J. Clarke, J.W. Johnson, Amantadine inhibits NMDA receptors by accelerating channel closure during channel block, *J. Neurosci.* 25 (2005) 3312–3322.
- [65] C.G. Parsons, A. Stöffler, W. Danysz, Memantine: a NMDA receptor antagonist that improves memory by restoration of homeostasis in the glutamatergic system—too little activation is bad, too much is even worse, *Neuropharmacology* 53 (2007) 699–723.
- [66] C.G. Parsons, K. Gilling, Memantine as an example of a fast, voltage-dependent, open channel N-methyl-D-aspartate receptor blocker, *Methods Mol. Biol.* 403 (2007) 15–36.
- [67] S.E. Kotermanski, J.W. Johnson, Mg²⁺ imparts NMDA receptor subtype selectivity to the Alzheimer's drug memantine, *J. Neurosci.* 29 (2009) 2774–2779.
- [68] H.J. Otton, A. Lawson McLean, M.A. Pannozzo, C.H. Davies, D.J. Wyllie, Quantification of the Mg²⁺-induced potency shift of amantadine and memantine voltage-dependent block in human recombinant GluN1/GluN2A NMDARs, *Neuropharmacology* 60 (2011) 388–396.
- [69] M.L. Vallano, B. Lambalez, E. Audinat, J. Rossier, Neuronal activity differentially regulates NMDA receptor subunit expression in cerebellar granule cells, *J. Neurosci.* 16 (1996) 631–639.
- [70] M. Llansola, A. Sánchez-Pérez, O. Cauli, V. Felipe, Modulation of NMDA receptors in the cerebellum. 1. Properties of the NMDA receptor that modulate its function, *Cerebellum* 4 (2005) 154–161.
- [71] L. Cathala, C. Misra, S. Cull-Candy, Developmental profile of the changing properties of NMDA receptors at cerebellar mossy fiber-granule cell synapses, *J. Neurosci.* 20 (2000) 5899–5905.
- [72] N. Burnashev, H. Monyer, P.H. Seeburg, B. Sakmann, Divalent ion permeability of AMPA receptor channels is dominated by the edited form of a single subunit, *Neuron* 8 (1992) 189–198.
- [73] H. Mori, H. Masaki, T. Yamakura, M. Mishina, Identification by mutagenesis of a Mg(2+)-block site of the NMDA receptor channel, *Nature* 358 (1992) 673–675.
- [74] K. Kashiwagi, T. Masuko, C.D. Nguyen, T. Kuno, I. Tanaka, K. Igarashi, K. Williams, Channel blockers acting at N-methyl-D-aspartate receptors: differential effects of mutations in the vestibule and ion channel pore, *Mol. Pharmacol.* 61 (2002) 533–545.
- [75] H.S. Chen, S.A. Lipton, Pharmacological implications of two distinct mechanisms of interaction of memantine with N-methyl-D-aspartate-gated channels, *J. Pharmacol. Exp. Therapeut.* 314 (2005) 961–971.
- [76] J.F. MacDonald, M.C. Bartlett, I. Mody, P. Papatil, J.N. Reynolds, M.W. Salter, J.H. Schneiderman, P.S. Pennefather, Actions of ketamine, memantine, MK-801 on NMDA receptor currents in cultured mouse hippocampal neurons, *J. Physiol.* 432 (1991) 483–508.
- [77] M.V. Nikolaev, L.G. Magazankin, D.B. Tikhonov, Influence of external magnesium ions on the NMDA receptor channel block by different types of organic cations, *Neuropharmacology* 62 (2012) 2078–2085.
- [78] N.G. Glasgow, M.R. Wilcox, J.W. Johnson, Effects of Mg²⁺ on recovery of NMDA receptors from inhibition by memantine and ketamine reveal properties of a second site, *Neuropharmacology* 137 (2018) 344–358.
- [79] A.M. Woodhull, Ionic blockage of sodium channels in nerve, *J. Gen. Physiol.* 61 (1973) 687–708.
- [80] C.G. Parsons, W. Danysz, G. Quack, Memantine is a clinically well tolerated N-methyl-D-aspartate (NMDA) receptor antagonist—a review of preclinical data, *Neuropharmacology* 38 (1999) 735–767.
- [81] K.E. Gilling, C. Jatzke, M. Hechenberger, C.G. Parsons, Potency, voltage-dependency, agonist concentration-dependency, blocking kinetics and partial untrapping of the uncompetitive N-methyl-D-aspartate (NMDA) channel blocker memantine at human NMDA (GluN1/GluN2A) receptors, *Neuropharmacology* 56 (2009) 866–875.
- [82] Oral Administration of Ilc (5 Mg/kg) to Mice Led to its Fast Absorption from the Gastrointestinal Tract, Reaching a Maximum Plasma Concentration (C_{max}) of 1.12 ± 0.76 MM after 45 Min. Interestingly, a Much Higher Concentration of UB-ALT-EV Was Found in Brain as Compared to Plasma, Indicating a Fast and Very High BBB Penetration. A C_{max} of 17.10 ± 6.06 μM Was Determined in Brain Which Was Reached after about 1 H (T_{max} = 56 Min). Thus, the C_{max} in Brain Was 15-fold Higher than that in Plasma. A Brain/Plasma Ratio of 32 Was Observed after 1 H at C_{max} (Brain). Companys-Aleman, J.; Turcu, A. L.; Schneider, M.; Müller, C. E.; Vázquez, S.; Grinán-Ferré, C.; Pallàs, M. NMDA Receptor Antagonists Reduce Amyloid-β Deposition by Modulating Calpain-1 Signaling and Autophagy, Rescuing Cognitive Impairment in 5XFAD Mice, Unpublished Results.
- [83] W.A.M. de Almeida, J.P. de Andrade, D.S. Chacon, C.R. Lucas, E. Mariana, L. de Santis Ferreira, T. Guaratini, E.G. Barbosa, J.A. Zuanazzi, F. Hallwass, W. de Souza Borges, R. de Paula Oliveira, R.B. Giordani, Isoquinoline alkaloids reduce beta-amyloid peptide toxicity in *Caenorhabditis elegans*, *Nat. Prod. Res.* (2020) 1–5.
- [84] T. Limana da Silveira, M. Lopes Machado, F. Bicca Obetina Baptista, D. Farina Gonçalves, D. Duarte Hartmann, L. Marafija Cordeiro, A. Franzen da Silva, C. Lenz Dalla Corte, M. Aschner, F.A. Antunes Soares, *Caenorhabditis elegans* as a model for studies on quinolinic acid-induced NMDAR-dependent glutamatergic disorders, *Brain Res. Bull.* 175 (2021) 90–98.
- [85] T. Kano, P.J. Brockie, T. Sassa, H. Fujimoto, Y. Kawahara, Y. Lino, J.E. Melleme, D.M. Madsen, R. Hosono, A.V. Maricq, Memory in *Caenorhabditis elegans* is mediated by NMDA-type ionotropic glutamate receptors, *Curr. Biol.* 18 (2008) 1010–1015.
- [86] P.J. Brockie, A.V. Maricq, Ionotropic glutamate receptors in *Caenorhabditis elegans*, *Neurosignals* 12 (2003) 108–125.
- [87] M.K. Back, S. Ruggieri, E. Jacobi, J. von Engelhardt, Amyloid beta-mediated changes in synaptic function and spine number of neocortical neurons depend on NMDA receptors, *Int. J. Mol. Sci.* 22 (2021) 6298.
- [88] S.D. Girard, M. Jacquet, K. Baranger, M. Migliorati, G. Escoffier, A. Bernard, M. Khrestchatsky, F. Féron, S. Rivera, F.S. Roman, E. Marchetti, Onset of hippocampus-dependent memory impairments in 5XFAD transgenic mouse model of Alzheimer's disease, *Hippocampus* 24 (2014) 762–772.
- [89] L. Devi, M. Ohno, Cognitive benefits of memantine in Alzheimer's 5XFAD model mice decline during advanced disease stages, *Pharmacol. Biochem. Behav.* 144 (2016) 60–66.
- [90] M. Jürgenson, T. Zharkovskaja, A. Noortoots, M. Morozova, A. Beniashvili, M. Zapolski, A. Zharkovskiy, Effects of the drug combination memantine and melatonin on impaired memory and brain neuronal deficits in an amyloid-predominant mouse model of Alzheimer's disease, *J. Pharm. Pharmacol.* 71 (2019) 1695–1705.
- [91] X. Chen, J.W. Barclay, R.D. Burgoyne, A. Morgan, Using *C. elegans* to discover therapeutic compounds for ageing-associated neurodegenerative diseases, *Chem. Cent. J.* 9 (2015) 65.
- [92] C. Grinán-Ferré, A. Bellver-Sanchis, M. Olivares-Martín, O. Bañuelos-Hortigüela, M. Pallàs, Synergistic neuroprotective effects of a natural product Mixture against AD hallmarks and cognitive decline in *Caenorhabditis elegans* and an SAMP8 mice model, *Nutrients* 13 (2021) 2411.
- [93] A.L. Oblak, P.B. Lin, K.P. Kotredes, R.S. Pandey, D. Garceau, H.M. Williams, A. Uyar, R. O'Rourke, S. O'Rourke, C. Ingraham, D. Bednarczyk, M. Belanger, Z.A. Cope, G.J. Little, S.G. Williams, C. Ash, A. Bleckert, T. Ragan, B.A. Logsdon, L.M. Mangravite, S.J. Sukoff Rizzo, P.R. Territo, G.W. Carter, G.R. Howell, M. Sasner, B.T. Lamb, Comprehensive evaluation of the 5XFAD mouse model for preclinical testing applications: a MODEL-AD study, *Front. Aging Neurosci.* 13 (2021), 713726.
- [94] G.E. Hardingham, H. Bading, Synaptic versus extrasynaptic NMDA receptor signaling: implications for neurodegenerative disorders, *Nat. Rev. Neurosci.* 11 (2010) 682–696.
- [95] Y. Liu, T.P. Wong, M. Aarts, A. Rooyackers, L. Liu, T.W. Lai, D.C. Wu, J. Lu, M. Tymianski, A.M. Craig, Y.T. Wang, NMDA receptor subunits have differential roles in mediating excitotoxic neuronal death both *in vitro* and *in vivo*,

- J. Neurosci. 27 (2007) 2846–2857.
- [96] D.T. Proctor, E.J. Coulson, P.R. Dodd, Post-synaptic scaffolding protein interactions with glutamate receptors in synaptic dysfunction and Alzheimer's disease, *Prog Neurobiol* 93 (2011) 509–521.
- [97] Z. Liu, C. Lv, W. Zhao, Y. Song, D. Pei, T. Xu, NR2B-containing NMDA receptors expression and their relationship to apoptosis in hippocampus of Alzheimer's disease-like rats, *Neurochem. Res.* 37 (2012) 1420–1427.
- [98] Y.-N. Wu, S.W. Johnson, Memantine selectively blocks extrasynaptic NMDA receptors in rat substantia nigra dopamine neurons, *Brain Res.* 1603 (2015) 1–7.
- [99] R. Wang, P.H. Reddy, Role of glutamate and NMDA receptors in Alzheimer's Disease, *J. Alz. Dis.* 57 (2017) 1041–1048.
- [100] F.J. Carvajal, R.G. Mira, M. Rovegno, A.N. Minniti, W. Cerpa, Age-related NMDA signaling alterations in SOD2 deficient mice, *Biochim. Biophys. Acta (BBA) - Mol. Basis Dis.* 1864 (2018) 2010–2020.
- [101] R. Knox, C. Zhao, D. Miguel-Perez, S. Wang, J. Yuan, D. Ferriero, X. Jiang, Enhanced NMDA receptor tyrosine phosphorylation and increased brain injury following neonatal hypoxia-ischemia in mice with neuronal Fyn overexpression, *Neurobiol. Dis.* 51 (2013) 113–119.
- [102] K. Prybylowski, K. Chang, N. Sans, L. Kan, S. Vicini, R.J. Wenthold, The synaptic localization of NR2B-containing NMDA receptors is controlled by interactions with PDZ proteins and AP-2, *Neuron* 47 (2005) 845–857.
- [103] M. Xie, Y. Li, S.H. Wang, Q.T. Yu, X. Meng, X.M. Liao, The involvement of NR2B and tau protein in MG132-induced CREB dephosphorylation, *J. Mol. Neurosci.* 62 (2017) 154–162.
- [104] M. Amidfar, J. de Oliveira, E. Kucharska, J. Budni, Y.-K. Kim, The role of CREB and BDNF in neurobiology and treatment of Alzheimer's disease, *Life Sci.* 257 (2020), 118020.
- [105] S.L. Angulo, T. Henzi, S.A. Neymotin, M.D. Suarez, W.W. Lytton, B. Schwaller, H. Moreno, Amyloid pathology-produced unexpected modifications of calcium homeostasis in hippocampal subicular dendrites, *Alzheimer's Dementia* 16 (2020) 251–261.
- [106] O. Trott, A.J. Olson, AutoDock Vina, Improving the speed and accuracy of docking with a new scoring function, efficient optimization and multithreading, *J. Comput. Chem.* 31 (2010) 455–461.
- [107] S. Jo, T. Ki, V.G. Iyer, W. Im, CHARMM-GUI: a web-based graphical user interface for CHARMM, *J. Comput. Chem.* 29 (2008) 1859–1865.
- [108] E.L. Wu, S. Jo, H. Rui, K.C. Song, E.M. Dávila-Contreras, Y. Qi, J. Lee, V. Monje-Galvan, R.M. Venable, J.B. Klauda, W. Im, CHARMM-GUI *Membrane Builder* toward realistic biological membrane simulations, *J. Comput. Chem.* 35 (2014) 1997–2004.
- [109] D.A. Case, I.Y. Ben-Shalom, S.R. Brozell, D.S. Cerutti, T.E.I. Cheatham, V.W.D. Cruzeiro, T.A. Darden, R.E. Duke, D. Ghoreishi, M.K. Gilson, H. Gohlke, A.W. Goetz, D. Greene, R. Harris, N. Homeyer, S. Izadi, A. Kovalenko, T. Kurtzman, T.S. Lee, S. LeGrand, P. Li, C. Lin, J. Liu, T. Luchko, R. Luo, D.J. Mermelstein, K.M. Merz, Y. Miao, G. Monard, C. Nguyen, H. Nguyen, I. Omelyan, A. Onufriev, F. Pan, R. Qi, D.R. Roe, A. Roitberg, C. Sagui, S. Schott-Verdugo, J. Shen, C.L. Simmerling, J. Smith, R. Salomon-Ferrer, J. Swails, R.C. Walker, J. Wang, H. Wei, R.M. Wolf, X. Wu, L. Xiao, D.M. York, P.A. Kollman, AMBER 2018, University of California, San Francisco, 2018.
- [110] J.A. Maier, C. Martinez, K. Kasavajhala, L. Wickstrom, K.E. Hauser, C. Simmerling, ff14SB: improving the accuracy of protein side chain and backbone parameters from ff99SB, *J. Chem. Theor. Comput.* 11 (2015) 3696–3713.
- [111] C.J. Dickson, B.D. Madej, A.A. Skjevik, R.M. Betz, K. Teigen, I.R. Gould, R.C. Walker, Lipid14: the Amber lipid force field, *J. Chem. Theor. Comput.* 10 (2014) 865–879.
- [112] J. Wang, R.M. Wolf, J.W. Caldwell, P.A. Kollman, D.A. Case, Development and testing of a general amber force field, *J. Comput. Chem.* 25 (2004) 1157–1174.
- [113] J.-P. Ryckaert, G. Cicotti, H.J.C. Berendsen, Numerical integration of the cartesian equations of motion of a system with constraints: molecular dynamics of *n*-alkanes, *J. Comp. Phys.* 23 (1977) 327–341.
- [114] T. Darden, D. York, L. Pedersen, Particle mesh Ewald: an N-log(N) method for Ewald sums in large systems, *J. Chem. Phys.* 98 (1993) 10089–10092.
- [115] W. Humphrey, A. Dalke, K. Schulten, VMD: visual molecular dynamics, *J. Mol. Graph.* 14 (1996) 33–38.
- [116] D.R. Roe, T.E. Cheatham III, PTRAJ and CPPTRAJ: software for processing and analysis of molecular dynamics trajectory data, *J. Chem. Theor. Comput.* 9 (2013) 3084–3095.
- [117] N.G. Glasgow, J.W. Johnson, Whole-cell patch-clamp analysis of recombinant NMDA receptor pharmacology using brief glutamate applications, *Methods Mol. Biol.* 1183 (2014) 23–41.
- [118] F. Yi, S. Bhattacharya, C.M. Thompson, S.F. Traynelis, K.B. Hansen, Functional and pharmacological properties of trimeric GluN1/2B/2D NMDA receptors, *J. Physiol.* 597 (2019) 5495–5514.
- [119] A.M. Woodhull, Ionic blockage of sodium channels in nerve, *J. Gen. Physiol.* 61 (1973) 687–708.
- [120] S.M. Antonov, V.E. Gmiro, J.W. Johnson, Binding sites for permeant ions in the channel of NMDA receptors and their effects on channel block, *Nat. Neurosci.* 1 (1998) 451–461.
- [121] L. Di, E.H. Kerns, K. Fan, O.J. McConnell, G.T. Carter, High throughput artificial membrane permeability assay for blood-brain barrier, *Eur. J. Med. Chem.* 38 (2003) 223–232.

3.3 Article 3

NMDA receptor antagonists reduce amyloid- β deposition by modulating calpain-1 signaling and autophagy, rescuing cognitive impairment in 5XFAD mice

**Companys-Aleman J.¹, Turcu A. L.², Schneider M.³, Müller C. E.³,
Vázquez S.², Griñán-Ferré C.¹, Pallàs M.¹**

Cellular and Molecular Life Sciences 2022, en procés de revisió

JCR 2020 IF: 9,261

Afiliacions:

¹ Departament de Farmacologia, Toxicologia i Química Terapèutica. Facultat de Farmàcia i Ciències de l'Alimentació. Institut de Neurociències, Universitat de Barcelona (NeuroUB). Av. Joan XXIII 27-31, 08028 Barcelona, Espanya.

² Laboratory of Medicinal Chemistry (CSIC Associated Unit), Department of Pharmacology, Toxicology, and Therapeutic Chemistry. Faculty of Pharmacy and Food Sciences and Institute of Biomedicine (IBUB), University of Barcelona, Av. Joan XXIII, 27-31, E-08028 Barcelona, Spain.

³ PharmaCenter Bonn, Pharmaceutical Institute, Pharmaceutical & Medicinal Chemistry, University of Bonn, 53121 Bonn, Germany.

RESUM

Els antagonistes del receptor NMDA són capaços de modular la sobreactivació d'aquests durant la MA alleugerint, així, els símptomes clínics de la malaltia. En aquest estudi es va proposar estudiar l'efecte d'un nou antagonista dels receptors NMDA, l'UB-ALT-EV sobre mecanismes involucrats en processos neurodegeneratius en el model transgènic de la MA, 5XFAD, utilitzant un tractament amb memantina com a tractament de referència.

Primer, es va demostrar la biodisponibilitat del compost UB-ALT-EV al cervell després de la seva administració per via oral. Seguidament, després d'un tractament crònic per via oral a ratolins femella de 6 mesos d'edat, es va demostrar una millora de la memòria espacial i la reducció de conductes de tipus ansiós pròpies dels animals 5XFAD. A escala molecular, es va poder descriure com el tractament amb UB-ALT-EV va promoure una reducció de l'activitat de la calpaina-1 i dels seus efectes en processos apoptòtics i en la fosforilació de tau, sumat a la reducció de marcadors proapoptòtics com les proteïnes Bcl-2, Bax i caspasa-3. A més, es va demostrar una reducció en l'acumulació d'A β a l'escorça i a l'hipocamp cerebrals gràcies a la reducció del processament amiloidogènic de la proteïna APP. Finalment, els canvis moleculars induïts pel tractament amb UB-ALT-EV en marcadors autofàgics, van suggerir una inducció del flux autofàgic que ajudaria a explicar en part la reducció del nombre de plaques d'A β .

En conjunt, els resultats evidencien un potencial efecte neuroprotector per part del compost UB-ALT-EV, reduint l'activació de mecanismes apoptòtics relacionats amb la sobreactivació del receptor NMDA, reduint la formació i acumulació d'A β , i augmentant l'autofàgia que finalment acaben col·laborant en la millora cognitiva observada en els ratolins tractats.

Cellular and Molecular Life Sciences

NMDA receptor antagonists reduce amyloid- β deposition by modulating calpain-1 signaling and autophagy, rescuing cognitive impairment in 5XFAD mice --Manuscript Draft--

Manuscript Number:	CMLS-D-22-00883	
Full Title:	NMDA receptor antagonists reduce amyloid- β deposition by modulating calpain-1 signaling and autophagy, rescuing cognitive impairment in 5XFAD mice	
Article Type:	Original Article	
Corresponding Author:	Mercè Pallàs, PhD University of Barcelona: Universitat de Barcelona SPAIN	
Corresponding Author Secondary Information:		
Corresponding Author's Institution:	University of Barcelona: Universitat de Barcelona	
Corresponding Author's Secondary Institution:		
First Author:	Júlia Companys-Alemany	
First Author Secondary Information:		
Order of Authors:	Júlia Companys-Alemany Andreea L Turcu Marion Schneider Christa E Müller Santiago Vázquez, PhD Christian Griñán-Ferré Mercè Pallàs, PhD	
Order of Authors Secondary Information:		
Funding Information:	Ministerio de Economía y Competitividad (PID2019-106285RB)	Dr. Mercè Pallàs
	Ministerio de Economía y Competitividad (MDM-2017-0729)	Not applicable
	Agència de Gestió d'Ajuts Universitaris i de Recerca (2017SGR106)	Dr. Mercè Pallàs
	Ministerio de Ciencia Tecnología y Telecomunicaciones (PDC2021-121096)	Dr. Mercè Pallàs
Abstract:	<p>Overstimulation of N-methyl-D-aspartate receptors (NMDARs) is the leading cause of brain excitotoxicity and often contributes to neurodegenerative diseases such as Alzheimer's Disease (AD), the most common form of dementia. This study aimed to evaluate a new NMDA receptor antagonist (UB-ALT-EV) and memantine in 6-month-old female 5XFAD mice that were exposed orally to a chronic low-dose treatment. Behavioural and cognitive tests confirmed better cognitive performance in both treated groups. Calcium-dependent protein calpain-1 reduction was found after UB-ALT-EV treatment but not after memantine. Changes in spectrin breakdown products (SBDP) and the p25/p35 ratio confirmed diminished calpain-1 activity. Amyloid β ($A\beta$) production and deposition was evaluated in 5XFAD mice and demonstrated a robust effect of NMDAR antagonists on reducing $A\beta$ deposition and the number and size of plaques. Furthermore, glycogen synthase kinase 3β (GSK3β) active form and phosphorylated tau (AT8) levels were diminished after UB-ALT-EV treatment, revealing tau pathology improvement. Because calpain-1 is involved in autophagy activation, autophagic proteins were studied. Strikingly, results showed changes in the protein</p>	

	<p>levels of unc-51-like kinase (ULK1), beclin-1, microtubule-associated protein 1A/1B-light chain 3(LC3B-II)/LC3B-I ratio and lysosomal-associated membrane protein 1 (LAMP1) after NMDAR antagonist treatments, suggesting an accumulation of autophagolysosomes in 5XFAD mice, reversed by UB-ALT-EV. Likewise, treatment with UB-ALT-EV recovered a WT mice profile in apoptosis markers Bcl-2, Bax, and caspase-3. In conclusion, our results revealed the potential neuroprotective effect of UB-ALT-EV by attenuating NMDA-mediated apoptosis and reducing Aβ deposition and deposition jointly with the autophagy rescue to finally reduce cognitive alterations in a mice model of familial AD</p>
<p>Suggested Reviewers:</p>	<p>Ana Coto Universidad de Oviedo acoto@uniovi.es She is an expert in autophagy</p> <p>Gemma Casadesus University of Florida College of Medicine gcasadesus@ufl.edu She is an expert in Alzheimer's disease</p> <p>Ferdinando Nicoletti Universita degli Studi di Roma La Sapienza Ferdinando.nicoletti@uniroma1.it He is an expert in neurodegeneration</p>
<p>Opposed Reviewers:</p>	<p>Cheera Maarouf</p> <p>She does not use animals models for AD studies</p> <p>Antonio Currais Salk Institute: Salk Institute for Biological Studies</p>

NMDA receptor antagonists reduce amyloid- β deposition by modulating calpain-1 signaling and autophagy, rescuing cognitive impairment in 5XFAD mice

Júlia Companys-Aleman^{*}, Andreea L. Turcu[†], Marion Schneider^{††}, Christa E. Müller^{††}, Santiago Vázquez[†], Christian Griñán-Ferré^{*} and Mercè Pallàs^{*}

^{*}Pharmacology Section, Department of Pharmacology, Toxicology, and Therapeutic Chemistry. Faculty of Pharmacy and Food Sciences, Institut de Neurociències, Universitat de Barcelona (NeuroUB), Av. Joan XXIII 27-31, 08028 Barcelona, Spain.

[†]Laboratory of Medicinal Chemistry (CSIC Associated Unit), Department of Pharmacology, Toxicology, and Therapeutic Chemistry. Faculty of Pharmacy and Food Sciences and Institute of Biomedicine (IBUB), University of Barcelona, Av. Joan XXIII, 27-31, E-08028 Barcelona, Spain.

^{††}PharmaCenter Bonn, Pharmaceutical Institute, Pharmaceutical & Medicinal Chemistry, University of Bonn, 53121 Bonn, Germany.

Co-corresponding author:

Mercè Pallàs, PhD.

Christian Griñán-Ferré, PhD

Pharmacology Section in Pharmacology, Toxicology, and Therapeutic Chemistry Department, Faculty of Pharmacy and Food Sciences, Universitat de Barcelona, Av. Joan XXIII 27-31, 08028 Barcelona, Spain.

e-mail: pallas@ub.edu; christian.grinan@ub.edu

Running title: NMDA receptor antagonists reduce neurodegeneration and cognitive impairment in 5XFAD mice.

Summary

Overstimulation of N-methyl-D-aspartate receptors (NMDARs) is the leading cause of brain excitotoxicity and often contributes to neurodegenerative diseases such as Alzheimer's Disease (AD), the most common form of dementia. This study aimed to evaluate a new NMDA receptor antagonist (UB-ALT-EV) and memantine in 6-month-old female 5XFAD mice that were exposed orally to a chronic low-dose treatment. Behavioural and cognitive tests confirmed better cognitive performance in both treated groups. Calcium-dependent protein calpain-1 reduction was found after UB-ALT-EV treatment but not after memantine. Changes in spectrin breakdown products (SBDP) and the p25/p35 ratio confirmed diminished calpain-1 activity. Amyloid β ($A\beta$) production and deposition was evaluated in 5XFAD mice and demonstrated a robust effect of NMDAR antagonists on reducing $A\beta$ deposition and the number and size of plaques. Furthermore, glycogen synthase kinase 3 β (GSK3 β) active form and phosphorylated tau (AT8) levels were diminished after UB-ALT-EV treatment, revealing tau pathology improvement. Because calpain-1 is involved in autophagy activation, autophagic proteins were studied. Strikingly, results showed changes in the protein levels of unc-51-like kinase (ULK1), beclin-1, microtubule-associated protein 1A/1B-light chain 3(LC3B-II)/LC3B-I ratio and lysosomal-associated membrane protein 1 (LAMP1) after NMDAR antagonist treatments, suggesting an accumulation of autophagolysosomes in 5XFAD mice, reversed by UB-ALT-EV. Likewise, treatment with UB-ALT-EV recovered a WT mice profile in apoptosis markers Bcl-2, Bax, and caspase-3. In conclusion, our results revealed the potential neuroprotective effect of UB-ALT-EV by attenuating NMDA-mediated apoptosis and reducing $A\beta$ deposition and deposition jointly with the autophagy rescue to finally reduce cognitive alterations in a mice model of familial AD.

Keywords: Alzheimer's Disease; NMDA receptor; NMDAR antagonist; neurodegeneration; amyloid plaques; p-tau; autophagy; apoptosis

1. INTRODUCTION

N-methyl-D-aspartate receptors (NMDARs) are ionotropic glutamate receptors that play an essential role in the central nervous system (CNS), fundamentally in synaptic transmission and plasticity [1]. Nevertheless, the overactivation of NMDARs is a crucial factor that promotes the increase of intracellular Ca^{2+} levels leading to synaptic dysfunction and neuronal loss [2]. Hence, NMDARs dysfunction were associated with neurodegenerative disorders such as Alzheimer's Disease (AD), supporting the rationale of memantine in AD therapy [3,4].

AD is still an insufficiently understood progressive and neurodegenerative age-related disease and is the most common form of dementia, and is predicted to become a global epidemic by 2050 [5–7]. Neuropathologically, the extracellular accumulation of the amyloid- β ($\text{A}\beta$) protein and the intracellular accumulation of hyperphosphorylated tau (p-tau) protein are defined as the main characteristic hallmarks of the disease followed by synaptic loss mainly in the hippocampus [8,9]. In this regard, it is interesting to note that activation of glycogen synthase kinase 3 β (GSK3 β) has a role in the hyperphosphorylation of tau at most of its sites, promoting neurofibrillary tangles (NTFs) and neuronal dysfunction [10].

Several lines of evidence showed that the overactivation of NMDARs in AD is responsible for the expression alteration of several proteins such as calpains, Ca^{2+} /calmodulin-dependent protein kinase II (CaMKII), GSK3 β , among others, all of them having important roles in apoptosis and neurodegeneration [11–14]. Therefore, the modulation of NMDARs led to changes in different apoptotic proteins such as calpain and caspase proteases [15].

Autophagy processes eliminate intracellular organelles and can remove damaged aggregated proteins such as $\text{A}\beta$. Defective autophagy has been implicated in AD pathogenesis [16]. Both $\text{A}\beta$ and tau accumulations can be eliminated by autophagy, suggesting that potentiation of this lysosomal process could be a treatment for AD[17–19]. Furthermore, neuronal autophagy also participates in neurotransmitter release, presynaptic assembly, axonal growth, and dendritic spine density formation [16]. Thus, the optimization of autophagy could potentially improve synaptic signaling in AD.

Memantine is an uncompetitive low-affinity NMDAR antagonist and is one of the few symptomatic treatments approved by Drug Administrations (EMA/FDA) [20]. The reduction of NMDARs overactivation, and the blockade of extrasynaptic NMDARs in front of synaptic ones by memantine, demonstrated the capacity to rescue memory deficits as well as protect neurons from $\text{A}\beta$ pathology

[21,22]. Besides, many other processes involved in AD have been described to be influenced by the action of memantine, such as tau hyperphosphorylation or apoptosis [11–13]. This treatment strategy has shown much effectiveness in AD pathology in different animal models [3,23–25], even though clinical trials do not show the same potential effects seen in preclinical studies [26,27]. Nonetheless, a growing body of evidence suggests that targeting NMDARs could help prevent or slow AD progression. Consequently, in recent years, increasing attention has been paid to identifying new NMDAR antagonists to enhance the effects of memantine [28,29]. Recently, we have designed and characterized by *in vitro* and *in vivo* experiments a novel polycyclic amine, UB-ALT-EV, a voltage-dependent, moderate-affinity (IC_{50} : 1.9 μ M), uncompetitive NMDAR antagonist [30].

The 5XFAD strain is a well-established and suitable transgenic AD mouse model expressing five familial mutations of human AD. It also exhibits early-onset cognitive impairment, starting at 3-month-old, including emotional disturbances. Moreover, A β plaque formation and gliosis starting at 2-month-old [31] have been described. Those events are accompanied by tau hyperphosphorylation and synaptic dysfunction starting at 4- and 6-month-old, respectively [32]. Likewise, NMDARs dysfunction in the 5XFAD model has been described, correlating with cognitive impairment and A β accumulation [33,34]. However, the effects of memantine or other NMDAR antagonists on neurodegenerative markers in 5XFAD mice are poorly described [23,35]. It should be noted that the incidence of AD is higher in women than in men, so the study of a new treatment in female mouse models is mandatory to focus on the therapeutic usefulness in this sex. [36]. Thus, the current work aimed to further evaluate the effects of chronic oral treatment of a new NMDAR antagonist, UB-ALT-EV (9-fluoro-5,6,8,9,10,11-hexahydro-7H-5,9:7,11-dimethanobenzo[9]annulen-7-amine hydrochloride), compared to memantine (**Fig. 1a**), in female 5XFAD mice. In addition, we focus on unveiling the molecular pathways modified by blocking NMDARs signaling beyond calcium entry blockade.

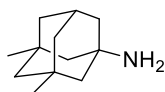
2. MATERIALS AND METHODS

2.1. Animals and treatment

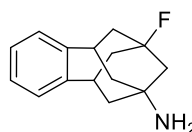
Female Wild Type (WT) and 5XFAD mice (n = 43) at 6 months of age were used to perform the cognitive tests followed by molecular analysis. The animals were randomly divided into four groups: Wild Type (**WT**) group (n = 14), 5XFAD Control group (**Control**) (n = 8), 5XFAD treated with memantine groups (**Mem**) (n = 11) and 5XFAD treated with UB-ALT-EV group (**UB-ALT-EV**) (n = 10). The sample size for the intervention was chosen following previous studies in our laboratory and using one of the available interactive tools (<http://www.biomath.info/power/index.html>) designed to estimate the required sample size to achieve adequate power. Animals had free access to food and water under standard temperature conditions (22 ± 2 °C) and 12h:12h light-dark cycles (300 lux/0 lux).

The experimental design is shown in (**Fig. 1b**) Memantine and UB-ALT-EV were dissolved in aqueous 1.8% 2-hydroxypropyl- β -cyclodextrin and administered at 5 mg/kg/day through drinking water for four weeks and during the behavioural tests. The doses of the compounds were recalculated weekly by considering the daily water consumption in each cage and by monitoring the body weight of the animals weekly. The average daily water consumption per animal was 5 mL/day, and no differences were found between the groups. Also, the body weight of the animals was not significantly different during the whole treatment period (Figure S1). The dosage of NMDAR antagonists was chosen based on published studies using AD mouse models [28,37,38]. Studies were performed by the Institutional Guidelines for the Care and Use of Laboratory Animals established by (European Communities Council Directive 2010/63/EU and Guidelines for the Care and Use of Mammals in Neuroscience and Behavioural Research, National Research Council 2003) and were approved by the Animal Experimentation Ethics Committee (CEEA) at the University of Barcelona. All efforts were made to reduce the number of animals and their suffering.

a



Memantine
 $IC_{50} = 1.5 \pm 0.1 \mu M$



UB-ALT-EV
 $IC_{50} = 1.9 \pm 0.2 \mu M$

volume of administration was 10 mL/kg and the required volume was calculated before each administration according to animal weight. Mice were anesthetized and sacrificed by cervical dislocation and blood samples (0.5–0.8 mL) were collected from animals at different time points (0 h, 0.5 h, 1 h, 2 h, 3 h, 4 h, 6 h, 10 h and 24 h after drug administration) in tubes with serum gel and clotting activator (Sarstedt Micro tube 1.1 mL Z-Gel). Blood samples were centrifuged at 10,000 rpm for 5 min to obtain plasma that was stored at $-20\text{ }^{\circ}\text{C}$ until analysis. Experimental procedures were in line with the Directive 2010/63/EU and approved by the Institutional Animal Care and Generalitat de Catalunya (#10291, 1/28/2018). Frozen plasma samples were defrosted, and 50 μL of cold acetonitrile containing 0.1% formic acid was added to 50 μL of plasma sample. After homogenization, followed by centrifugation (15 min at 15000 rpm), the supernatant was transferred to an HPLC vial, and 4 μL were injected. Frozen brain samples were weighed after thawing. Then, 1 mL of acetonitrile containing 0.1% formic acid was added to each brain sample. The mixture was treated in a TissueLyser (Qiagen, Germany) at 50 Hz for 5 min, followed by centrifugation for 15 min at 15000 rpm. Then, 200 μL of each sample were transferred into HPLC vials, and 2.8 μL of the sample were injected. Calibration samples were run before, during and after the actual samples, injecting a volume of 2 μL . Mass spectra were recorded on a QTrap 6500+ (Sciex, Darmstadt, Germany) with an ESI-source coupled to an HPLC 1290 Infinity (Agilent, Waldbronn, Germany) using a Kinetex C18 PolarRP column (Phenomenex). The column temperature was $30\text{ }^{\circ}\text{C}$. An HPLC gradient was run starting with 98% water containing 0.1% formic acid and 2% acetonitrile containing 0.1% formic acid to 100% acetonitrile containing 0.1% formic acid within 2.2 min followed by flushing the column with acetonitrile containing 0.1% formic acid for 1.3 min and subsequent equilibration for 1.5 min. Sample solutions (2 μL each) were injected applying a flow rate of 0.6 mL/min. Dihydrocodeine tartrate was used as an internal standard (100 nM). Multiple reaction monitoring (MRM) was applied for quantification. Two different methods were employed: (i) MRM 232 \rightarrow 155, (ii) MRM 232 \rightarrow 215 (internal standard, MRM 302 \rightarrow 199). Both methods yielded comparable results, and all determined data were included in the calculations.

2.3. Cognitive Tests

2.3.1. Open Field Test

In brief, the open field test (OFT) was performed using a wall-enclosed area as previously described [39]. The ground was divided into two defined as the center and peripheral areas. Behaviour was evaluated with SMART® ver.3.0 software,

and each test was recorded for later evaluation using a camera located above the apparatus. Mice were located at the center and allowed to explore the white plywood box (50x50x25cm) for 5 minutes. Then, the animals were returned to their home cages, and the OFT apparatus was cleaned with 70% ethanol (EtOH). The parameters measured included center time duration, rearings, defecations, and locomotor activity, calculated as the sum of global distance moved in the arena for 5 minutes.

2.3.2. Morris Water Maze

The Morris water maze (MWM) is a cognitive procedure extensively used to study spatial memory and learning [40]. An open circular pool (100 cm x 50 cm) of opaque water, which contains white latex paint (temperature maintained at 24 °C \pm 1), and an escape platform submerged 1.5 cm below the water level (in the middle of one quadrant). The task was performed across 7 consecutive days. On the first day, the platform was not present in the pool to allow the mice to swim and explore the pool for 60 seconds. The learning phase was conducted from the second day until day 6th, and each group was trained in 5 daily trials of 60 seconds. Each trial placed the animal in the water in 5 different starting points (set at NE, E, SE, S and SW) and allowed the animal to swim until it found the platform. When the animal found the platform, the investigator left the animal to remain on the platform for 30 seconds to allow for spatial orientation. If the animal could not reach the platform in 60 seconds the investigator guided the animal until the platform and left the animal for 30 seconds on it. One minute was allowed between trials, and every trial started from different locations in the pool. On the 7th day, the memory test was performed, the platform was removed from the pool and only one trial of 60 seconds was conducted. The animals swimming paths patterns were recorded by a camera located above the pool, and data were analyzed with SMART v 3.0 software from Panlab. The parameters measured were the mean distance travelled to the platform during the learning phase, the mean distance travelled to the platform zone the trial day and the number of entries in the platform quadrant.

2.4. Brain Tissue Preparation

After three days of the cognitive and memory tests, all mice groups were euthanized by cervical dislocation and brains were immediately removed from the skull. For molecular experiments, the hippocampi were isolated and frozen in powdered dry ice. They were maintained at -80°C for further use for protein extraction and RNA isolation. For protein extraction, tissue samples were homogenized in lysis buffer (50-mM Tris-HCl pH 7.4, 150-mM NaCl, 5-mM

EDTA and 1% Triton X-100) containing phosphatase and protease inhibitors cocktails (Cocktail II, Sigma-Aldrich, St. Louis, MO, USA). Total protein levels were obtained, and protein concentration was determined by the method of Bradford. For thioflavin-S staining, mice were anesthetized (ketamine 100 mg/kg and xylazine 10 mg/kg, intraperitoneally) and then perfused with 4% paraformaldehyde (PFA) diluted in 0.1 M phosphate buffer solution intracardially. Brains were removed and postfixed in 4% PFA overnight at 4°C. Afterwards, brains were changed to PFA + 15% sucrose. Finally, the brains were frozen on powdered dry ice and stored at -80°C until sectioning. Brain coronal sections of 30 µm were obtained (Leica Microsystems CM 3050S cryostat, Wetzlar, Germany) and kept in a cryoprotectant solution at -20°C until use.

2.5. Protein Level Determination by Western Blotting

For Western Blotting (WB), aliquots of 15 µg of hippocampal protein extraction per sample were used. Protein samples were separated by Sodium dodecyl sulphate-Polyacrylamide gel electrophoresis (SDS-PAGE) (8-20%) and transferred onto Polyvinylidene difluoride (PVDF) membranes (Millipore). Afterwards, membranes were blocked in 5% non-fat milk in Tris-buffered saline (TBS) solution containing 0.1% Tween 20 TBS (TBS-T) for 1 hour at room temperature (RT), followed by overnight incubation at a 4°C with the primary antibodies listed in Table S1. Then, membranes were washed and incubated with secondary antibodies for 1 hour at RT. Immunoreactive proteins were viewed with the chemiluminescence-based detection kit, following the manufacturer's protocol (ECL Kit, Millipore), and digital images were acquired using ChemiDoc XRS+ System (BioRad). Semi-quantitative analyses were done using ImageLab software (BioRad), and results were expressed in Arbitrary Units (AU), considering control protein levels as 100%. Protein loading was routinely monitored by immunodetection of Glyceraldehyde-3-phosphate dehydrogenase (GAPDH).

2.6. Thioflavin-S staining

β-amyloid plaques were stained with Thioflavin-S using three animals per group. Three brain sections per animal were first rehydrated at room temperature by 5 minutes incubation in PBS. Next, brain sections were washed 1 minute each in 50%, 70% and 80% ethanol and incubated with 0.3% Thioflavin-S (Sigma-Aldrich) solution for 10 minutes at RT in the dark. Subsequently, these samples were submitted to washes in 1 minutes series of 80%, 70% and 50% and finally, one last wash of 5 min in PBS. Then, slides were mounted with Fluoromount-GTM (EMS, Hatfield, NJ, USA) and allowed to dry overnight. Image acquisition

was performed with a fluorescence laser microscope (Olympus BX51, Germany) using 4X and 20X objectives, and images were analysed by using ImageJ software. Similar and comparable histological areas were selected for plaque quantification, focusing on the adjacent positioning of the whole cortical area and the hippocampus. Each image was converted to 8-bit greyscale, thresholded to a linear scale, and the number of particles and the percentage of area covered by thioflavin-S were calculated and then averaged from three different sections from each animal.

2.7. Amyloid- β protein levels quantification by ELISA

A β_{40} and A β_{42} protein levels were analyzed by ELISA with the human amyloid- β_{40} ELISA Kit (Invitrogen, #KHB3481; Thermo Fisher) and the human amyloid- β_{42} Ultrasensitive ELISA Kit (Invitrogen, #KHB3441), respectively. All procedures followed the manufacturer's instructions.

2.8. Data Acquisition and Statistical Analysis

Data analysis was conducted using GraphPad Prism ver. 8 statistical software. Data are expressed as the mean \pm standard error of the mean (SEM) of at least 3 samples per group. One-way analysis of variance (ANOVA) was followed by Tukey post-hoc analysis or two-tail Student's t-test when necessary. In case of MWM learning curve, repeated-measures ANOVA was performed. Statistical significance was considered when p-values were <0.05 . The statistical outliers were determined with Grubbs' test and, when necessary, were removed from the analysis. The cognitive analysis was performed blindly. An experimenter unaware of the treatment groups performed the tests and recorded the number of animals. Another experimenter analyzed the videos and the behavioural scoring.

3. RESULTS

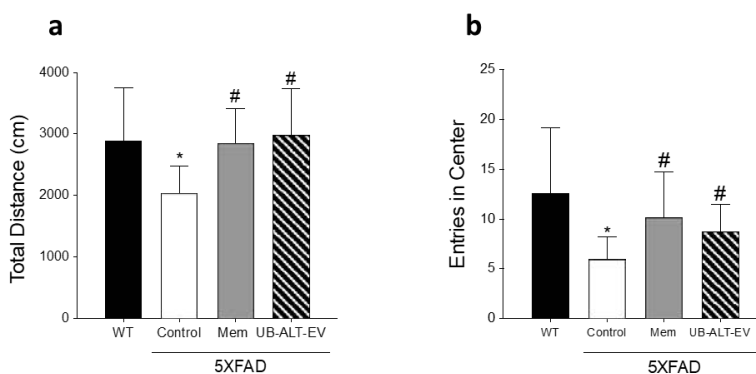
3.1 Pharmacokinetic properties of UB-ALT-EV in mice.

To characterize the pharmacokinetic profile of UB-ALT-EV after oral administration, its bioavailability (plasma and brain levels) was assessed in mice. Following a single oral administration of UB-ALT-EV (5 mg/Kg), absorption of UB-ALT-EV from the gastrointestinal tract was fast, reaching a maximum plasma concentration (C_{\max}) of $1.12 \pm 0.76 \mu\text{M}$ after 45 min. Interestingly, a much higher concentration of UB-ALT-EV was found in the brain (**Fig.1c** inset) compared to plasma, indicating a fast and very high blood brain barrier (BBB) penetration. A C_{\max} of $17.10 \pm 6.06 \mu\text{M}$ was determined in the brain, which was reached after about 1 h ($T_{\max} = 56$ min). Thus, the C_{\max} in the brain was 15-fold higher than that

in plasma. A brain/plasma ratio of 32 was observed after 1 h at C_{\max} (brain) (**Fig. 1c**).

3.2. Improvement in locomotion, anxiety-like behaviour and spatial memory after treatment with UB-ALT-EV

OFT evaluation revealed an improvement of locomotor activity in treated groups compared to the 5XFAD Control group via the analysis of the total distance (**Fig. 2a**). The analysis of the entries in the OFT center zone, as evaluation of anxiety-like behavior, showed significantly fewer entries for 5XFAD Control group in comparison with WT group (**Fig. 2b**). Interestingly, both NMDAR antagonists treated groups increased center entries (**Fig. 2b**). The MWM is used to assess spatial memory. After the training period, the learning curve (**Fig. 2c**) revealed that all groups learned the platform's location except the 5XFAD Control group, suggesting a learning deficits recovery after NMDAR antagonist treatment. On the trial day, the 5XFAD Control group, when the distance to the platform was evaluated, only 5XFAD control group did travel significantly more distance when compared to other groups (**Fig. 2c**). Moreover, WT group, memantine, and UB-ALT-EV groups showed significantly more entries into the platform quadrant than the 5XFAD Control group (**Fig. 2d**). The swimming paths were recorded, and each group's representative swimming path pattern is shown (**Fig. 2e**). This figure revealed that WT group, jointly with memantine and UB-ALT-EV treated groups, spent most of the time trying to find the platform in the correct quadrant, while the 5XFAD Control group showed an erratic swim-pattern (**Fig. 2f**). These results suggest that memantine and UB-ALT-EV protected against impairments in spatial memory caused by the 5XFAD mutations.



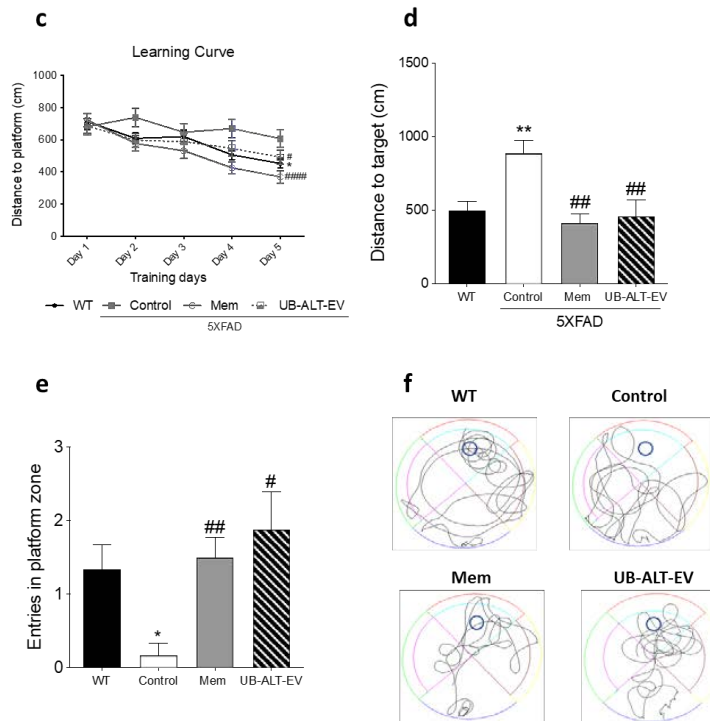


Fig. 2. Results of OF: Total distance (a), Entries in center zone (b). For Morris water maze: Learning curve (c), distance to target of the test day (d), entries in platform quadrant during the test (e) and representative swim paths patterns for each group (f). Values are the mean \pm standard error of the mean (SEM); (n = 14 for WT, n = 8 for Control, n = 11 for Mem and n = 10 for UB-ALT-EV). For WT vs. 5XFAD Control groups data was analyzed using a two-tail Student's t-test, and for 5XFAD groups a standard one-way ANOVA followed by Tukey post-hoc analysis was performed. * $p < 0.05$; ** $p < 0.01$ for WT vs. Control. # $p < 0.05$; ## $p < 0.01$; for Mem or UB-ALT-EV vs. Control.

3.3. Chronic administration UB-ALT-EV prevented calcium dependent proteins activation

Considering the relationship between intracellular calcium levels and NMDAR dysfunction, calcium-dependent proteins CaMKII and calpain-1 were evaluated. Regarding the CaMKII activation, we found significantly increased p-CaMKII levels in 5XFAD; both memantine and UB-ALT-EV treatments reduced p-CaMKII levels (Fig. 3a, b). Likewise, compared to WT mice, the 5XFAD Control group showed significant higher calpain-1 protein levels that were significantly reduced after UB-ALT-EV treatment, but not in the case of memantine treated group (Fig. 3a, c).

Pursuing the UB-ALT-EV effects on calpain-1 protein levels, we evaluated α -spectrin breakdown products (SBDP), a target of this protease. Accordingly, results revealed that 5XFAD Control mice presented significant higher protein levels of SBDP 150 kDa fragment, a marker of calpain activation, when compared to WT mice group, being diminished by UB-ALT-EV treatment (**Fig. 3a, e**). In addition, when the calpain target p35 was evaluated through the p25/35 ratio, 5XFAD mice exhibited significantly higher levels when compared to WT (**Fig. 3a, f**), further indicating a calpain-1 activation. Interestingly, UB-ALT-EV, but not memantine, reduced SBDP 150 kDa and p25/p35 ratio compared to 5XFAD control mice (**Fig. 3a, d-f**). All these findings agree with the hypothesis by reducing NMDAR overactivation, and all the calcium-dependent proteins would reduce their overactivity, then contributing to stopping the neurodegenerative process.

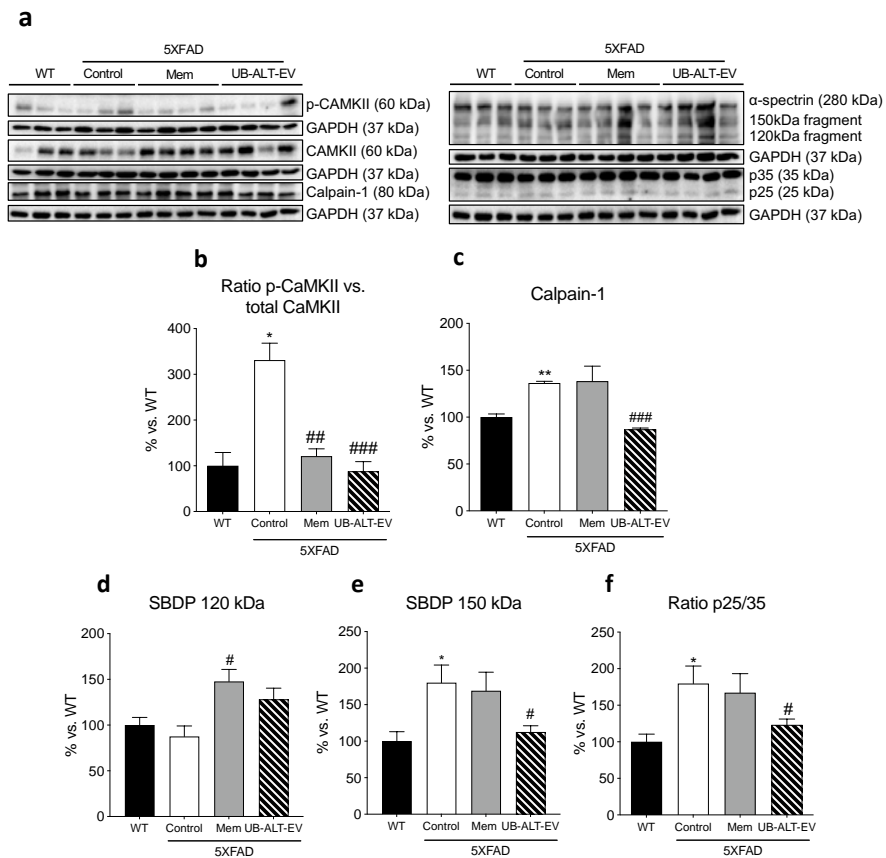


Fig. 3. Representative Western Blot (**a**) and quantifications for ratio p-CAMKII vs. total CAMKII (**b**), Calpain-1 (**c**), SBDP 120kDa (**d**) SBDP 150kDa (**e**) and ratio p25/35 (**f**). Values in bar graphs are adjusted to 100% for protein levels of the wild type (WT). Values are the mean \pm Standard error

of the mean (SEM); (n = 3 for WT and Control groups and n = 4 for Mem and UB-ALT-EV groups. For WT vs. 5XFAD Control groups data was analyzed using a two-tail Student's t-test, and for 5XFAD groups a standard one-way ANOVA followed by Tukey post-hoc analysis was performed. *p<0.05; **p<0.01; for WT vs. Control. #p<0.05; ###p<0.01; ####p<0.001 for Mem or UB-ALT-EV vs. Control.

3.4. Reduced APP protein processing and tau kinases activation promotes a diminution in tau pathology and increases synapsin I level in 5XFAD mice after UB-ALT-EV treatment

Since A β formation is a hallmark of AD, several APP protein processing proteins were studied. Significant higher protein levels of β -site amyloid precursor protein cleaving enzyme 1 (BACE1) were found in the 5XFAD Control group compared to the WT group. Strikingly, only UB-ALT-EV treated mice were able to significantly reduce their protein levels compared to the 5XFAD Control group (**Fig. 4a, b**). Moreover, protein levels of soluble amyloid precursor protein α fragment (sAPP α), a non-amyloidogenic pathway marker, were significantly increased in both treated groups compared to the 5XFAD Control group reaching similar levels of WT mice (**Fig. 4a, c**). In addition, when the c-terminal fragments (CTFs) were analyzed, the ratio CTFs/pre-APP results significantly higher in the case of 5XFAD Control group compared to the WT group. Likewise, a significant reduction of the ratio CTFs/pre-APP only was observed in UB-ALT-EV treated animals compared to the 5XFAD Control group (**Fig. 4a, d**). Those results suggest that after treatment with NMDAR antagonist, an amelioration of the amyloidogenic formation pathway and fostering non-amyloidogenic pathway.

Since the hyperphosphorylation of tau is a hallmark of AD, several protein levels related to tau pathology were evaluated. We mentioned above an increase in p25 (a coactivator of cyclin-dependent-kinase 5 (CDK5) tau kinase) and its diminution after UB-ALT-EV treatment (**Fig. 3a, f**). Pursuing tau kinases activity, we evaluated GSK3 β quantifying the ratio p-GSK3 β Tyr216/GSK3 β and, remarkably, we only found a significant reduction in the UB-ALT-EV treated group in comparison with the 5XFAD Control group (**Fig. 4a, e**). Accordingly, only the UB-ALT-EV treatment significantly reduced protein levels of phosphorylated AT8 tau (Ser202, Th205) compared to the 5XFAD Control group (**Fig. 4a, f**). Besides, p-Tau (Ser396) protein was reduced after UB-ALT-EV but did not reach significance (**Fig. 4a, g**). All of the above results suggest that UB-ALT-EV prevented tau hyper-phosphorylation.

Synapsin I is a synaptic vesicle-associated protein downregulated in AD [41], and also It has been associated with tau [42]. Indeed, synapsin I was found in

significantly lower levels in the 5XFAD mice compared to the WT group (**Fig. 4a, h**). Interestingly our results indicated that synapsin I protein levels were increased after treatment with UB-ALT-EV, but not with memantine (**Fig. 4a, h**).

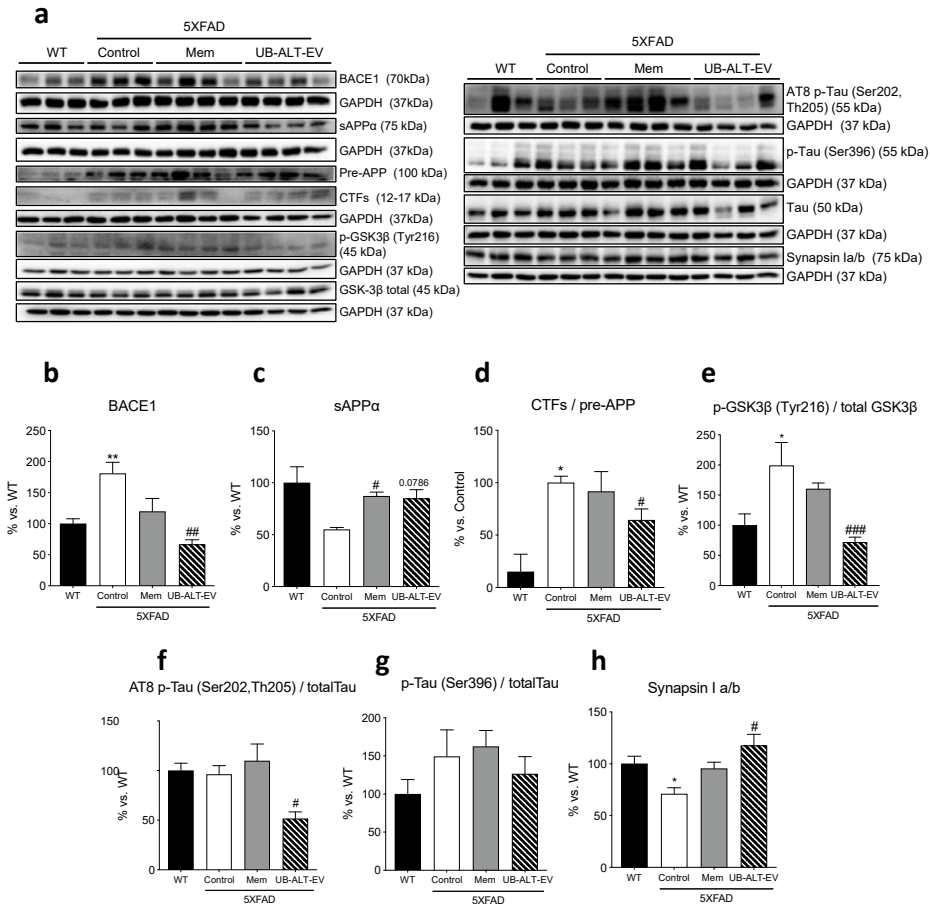


Fig. 4. Representative Western Blot (**a**) and quantifications for BACE1 (**b**) sAPP α (**c**), ratio CTFs/pre-APP (**d**) ratio p-GSK3 β (Tyr216)/GSK3 β (**e**), ratio AT8 p-Tau (Ser202, Th205)/Tau (**f**), ratio p-Tau/Tau (Ser396) (**g**) and Synapsin I a/b (**h**). Values in bar graphs are adjusted to 100% for protein levels of the wild type (WT). Values are the mean \pm Standard error of the mean (SEM); (n = 3 for WT and Control groups and n = 4 for Mem and UB-ALT-EV groups. For WT vs. 5XFAD Control groups data was analyzed using a two-tail Student's t-test, and for 5XFAD groups a standard one-way ANOVA followed by Tukey post-hoc analysis was performed. *p<0.05; **p<0.01 for WT vs. Control. #p<0.05; ##p<0.01; ###p<0.001 for Mem or UB-ALT-EV vs. Control.

3.5. Reduced Amyloid- β deposition induced by NMDAR antagonists

Amyloid- β plaques were quantified by Thioflavin-S staining (**Fig. 5a**) in 5XFAD mice hippocampus and cortex. Results highlighted the ability of the NMDAR antagonists treatments to reduce the amyloid burden compared to the 5XFAD Control group (**Fig. 5b, c**). Remarkably, we found that treated animals with memantine or UB-ALT-EV presented smaller size plaques compared to the 5XFAD Control group (**Fig. 5d**). Interestingly, our results showed a significant increase of $A\beta_{40}$ levels in 5XFAD mice treated with NMDA receptor antagonist, whereas no changes occurred for $A\beta_{42}$ (**Fig. 5e, f**). Therefore, $A\beta_{42}/A\beta_{40}$ ratios were significantly decreased after treatment compared with control group (**Fig. 5g**). These results highlighted the neuroprotective role of NMDAR antagonists in reducing an important hallmark of AD.

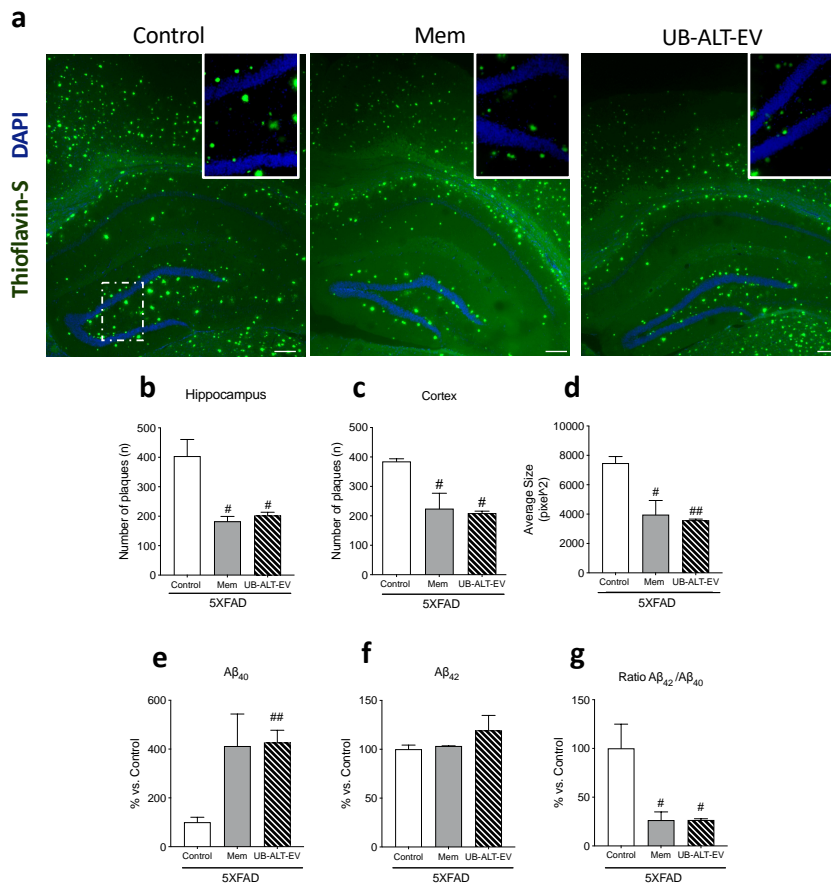


Fig. 5. Thioflavin-S-positive staining (green) and DAPI (blue) in the 5XFAD hippocampus and cerebral cortex for Control, Mem and UB-ALT-EV. Scale bar: 200 μ m. **(a)**. Quantification of the number of $A\beta$ plaques in 5XFAD mice hippocampus **(b)** and cortex **(c)**. Average Size of $A\beta$ plaques

measurement (d). Levels of amyloid- β_{40} levels (e). Levels of amyloid- β_{42} (f). Ratio of amyloid- β_{42} /amyloid- β_{40} (g). Values are the mean \pm Standard error of the mean (SEM); (n = 3 for each group). A standard one-way ANOVA followed by Tukey post-hoc analysis was performed. #p<0.05; ##p<0.01 for Mem or UB-ALT-EV vs. Control.

3.6. NMDAR antagonist UB-ALT-EV treatment in 5XFAD mice induced changes in apoptosis and the autophagic process

To further evaluate the neuroprotective effects of NMDAR antagonists in 5XFAD mice, the levels of apoptosis-related proteins were determined. Caspase-3 was evaluated as a critical apoptotic protein, being protein levels significantly higher in 5XFAD Control mice than in the WT group. UB-ALT-EV treated 5XFAD mice showed a significant diminution in caspase-3 protein levels compared to the 5XFAD Control group (Fig. 6a, b). By contrast, the SBDP 120kDa fragment (a marker of caspase-3 activation) increased in a significant way in memantine-treated group compared to 5XFAD Control mice (Fig. 3a-d). Surprisingly, the anti-apoptotic protein B-cell lymphoma 2 (Bcl-2) increased in 5XFAD Control mice, but after NMDAR antagonists treatment, Bcl-2 protein levels reached WT mice levels (Fig. 6a, c). By contrast, the pro-apoptotic protein Bax was found increased in 5XFAD Control mice, and after NMDAR antagonist treatment was reestablished to the WT levels (Fig. 6a, d). These findings indicated decreased apoptotic process in 5XFAD by NMDAR antagonist treatment.

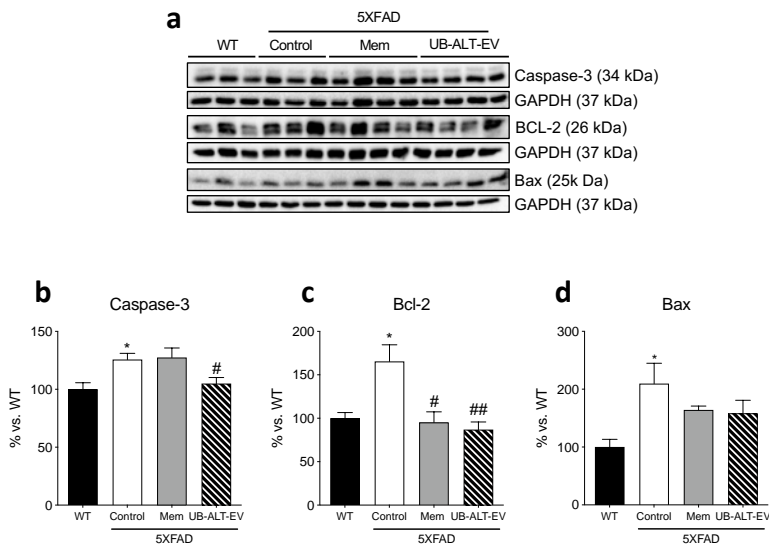


Fig. 6. Representative Western Blot (a) and quantifications for Caspase-3 (b) Bcl-2 (c) and Bax (d). Values in bar graphs are adjusted to 100% for protein levels of the wild type (WT). Values are the

mean \pm Standard error of the mean (SEM); (n = 3 for WT and Control groups and n = 4 for Mem and UB-ALT-EV groups. For WT vs. 5XFAD Control groups data was analyzed using a two-tail Student's t-test, and for 5XFAD groups a standard one-way ANOVA followed by Tukey post-hoc analysis was performed. *p<0.05 for WT vs. Control. #p<0.05; ##p<0.01 for Mem or UB-ALT-EV vs. Control.

Additionally, autophagic markers were evaluated. Unc-51-like kinase (ULK1) and Beclin-1 are initiation markers of the autophagic process. A significant decrease in unc-51-like kinase and beclin-1 protein levels in 5XFAD compared with WT was demonstrated, therefore revealing a dysfunctional autophagy process. UB-ALT-EV and memantine treatments prevented those changes (**Fig. 7a, b, e**). However, p62, a protein necessary for phagophore generation, was unmodified throughout the experimental groups (data not shown). Then, microtubule-associated protein 1A/1B light chain 3 I and II (LC3B-I and LC3B-II), a well-known essential actor for autophagy, was evaluated. Usually, LC3B-II correlates with the number of autophagosomes. However, ratio LC3B-II/LC3B-I, was increased in transgenic mice and was partially diminished in UB-ALT-EV treated mice (**Fig. 7a, c**). Lysosomal-associated membrane protein 1 (LAMP-1) was also studied as a marker for autophagolysosome formation. Our results showed a significant decrease in LAMP-1 protein levels in 5XFAD Control mice in front of the WT mice, which were recovered to WT mice levels in 5XFAD mice treated with UB-ALT-EV. On the whole, results suggested that treatment increases autophagic flux in 5XFAD mice (**Fig. 7a, d**).

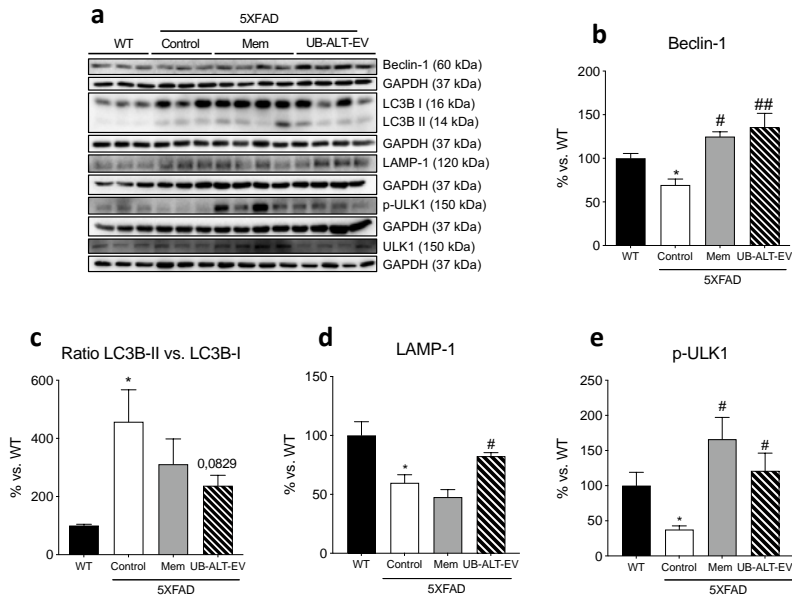


Fig. 7. Representative Western Blot **(a)** and quantifications for Beclin-1 **(b)**, ratio LC3B-II vs. LC3B-I **(c)**, LAMP-1 **(d)** and ULK1 **(e)**. Values in bar graphs are adjusted to 100% for protein levels of the wild type (WT). Values are the mean \pm Standard error of the mean (SEM); (n = 3 for WT and Control groups and n = 4 for Mem and UB-ALT-EV groups. For WT vs. 5XFAD Control groups data was analyzed using a two-tail Student's t-test, and for 5XFAD groups a standard one-way ANOVA followed by Tukey post-hoc analysis was performed. *p<0.05 for WT vs. Control. #p<0.05; ##p<0.01 for Mem or UB-ALT-EV vs. Control.

4. DISCUSSION

More effective pharmacological treatments or disease-modifying agents are urgently needed to slow down or prevent the progression of AD. Since memantine was approved in 2003 to treat patients with dementia and moderate to severe AD, no other drug has successfully passed clinical trials [43,44]. Only very recently the disease-modifying agent, aducanumab, has been conditionally approved by the FDA based on its presumed efficacy [45]. In any case, it is worth noting that nowadays symptomatic drugs, such as memantine, are still essential to treat the behavioral and cognitive alterations that appear during the disease.

Notwithstanding, growing evidence suggesting that targeting NMDARs could protect against excitotoxicity and may also alter other signaling cascades, promoting indirect neuroprotective effects that have not previously been studied. Therefore, the field may benefit from developing new NMDAR antagonists with an improved pharmacological profile and reduced side effects or neurotoxicity. Furthermore, the development of new antagonists has also been described in several *in vitro* and *in vivo* published reports carried out over the last decade in various AD mouse models, demonstrating the potential to target NMDARs [38,46–48].

The present study was conducted to demonstrate the efficacy of UB-ALT-EV, a new BBB penetrant optimized NMDAR antagonist, to ameliorate cognitive impairment through the modulation of NMDAR-mediated neurodegenerative pathways promoted by A β pathology in the 5XFAD mouse model. In addition, we incorporate memantine as a gold standard to compare to the new compound, UB-ALT-EV. Of note, only two studies have been published describing the effects of memantine on 5XFAD mice, and to the best of our knowledge, none of them provides results about the effects of chronic low-dose memantine treatment on cognition, apoptosis and autophagy in 5XFAD mice [23,35].

First, we demonstrated the oral bioavailability for UB-ALT-EV and its ability to cross BBB when applied orally at a 5 mg/Kg dose, confirming that it can reach the target in the brain in a sufficiently high concentration. As we expected,

NMDAR antagonist's treatment improved behavioral tasks, showing higher locomotor activity, and reducing alterations associated with anxiety-like behavior. In addition, we confirmed a firmly cognitive recovery for spatial memory deficits in 5XFAD mice treated with both NMDAR antagonists, confirming our results in working memory in 5XFAD mice model treated with UB-ALT-EV and memantine [49]. Thus, in line with those results, it has been described that NMDAR antagonist strategy displayed better cognitive performance, including behavioral abnormalities in AD mice [23–25,35]

Regarding the mechanisms of action, it is assumed that NMDARs are pathologically overactivated in AD. Resulting in elevated intracellular levels of Ca^{2+} , which activate a variety of downstream signaling pathways that promote neurodegeneration [50]. However, the presence of NMDAR2A subunit rather than NMDAR2B on NMDARs complex has been described to mediate neuroprotective pathways [51,52]. We recently showed that NMDAR2A levels in 5XFAD mice were lower than WT, and UB-ALT-EV treatment was able to increase NMDAR2A subunit protein levels slightly but significantly [49]. Besides, we found that UB-ALT-EV, in a more effective way than memantine, increased tyrosine phosphorylation of NMDAR2B subunits. This event is known to prevent NMDARs internalization, and consequently fostering cell-survival, synaptic function and cognitive improvement.

Another possible mechanism by which NMDAR antagonists could mediate neuroprotection is by reducing the calcium influx impacting the activity of calcium-dependent proteins [53]. In fact, NMDAR antagonists are known to modulate the calcium-mediated pathways related to neurodegenerative disorders like AD [54]. Then, we delve further into the modulation of calcium-dependent proteins by UB-ALT-EV and memantine in 5XFAD mice. Our experiments demonstrated that UB-ALT-EV significantly reduced calpain-1 levels and, importantly, its activation, as can be deduced by p25/p35 ratio decrease, pointing out a potent effect of this new NMDAR antagonist and suggesting a reduction of calcium signaling. The calpain-1 inhibition after UB-ALT-EV treatment was confirmed by the reduction of the α -spectrin SBDP 150 fragment protein levels in UB-ALT-EV treated animals but not memantine-treated ones. This is consistent with a previous work that demonstrated a reduction in calpain activation after the treatment with NDMARs antagonists [55].

Moreover, we found that after NMDAR antagonist treatment, CaMKII, other calcium-dependent protein, phosphorylation levels decreased, supporting the decrease in calcium entry through NMDARs, and subsequently, CaMKII

activation. Interestingly, it has been demonstrated that the decreased autophosphorylation of CaMKII recovered cognitive symptoms of dementia in mice by the use of memantine or donepezil [56]. Thus, the data support the hypothesis that calpain-1 and CaMKII activity modulation by UB-ALT-EV treatment might improve cell signaling and finally lead to reduced cognitive deficits presented by 5XFAD mice. Furthermore, we found increased levels of synapsin I, a synaptic vesicle-associated protein [57], after UB-ALT-EV treatment, that may explain partially the amelioration on 5XFAD mice cognitive status. Consistent with these findings, *Syn1^{-/-}* mice showed spatial and emotional abnormalities through different behavioral and cognitive tests [58]. Furthermore, UB-EV-ALT treatment increased levels of postsynaptic density protein 95 (PSD95) in 5XFAD [49]. In whole, those findings suggested that UB-EV-ALT treatment mediates synapse improvement.

Of note, CaMKII activation coincides with pathological phosphorylation of tau in AD brains and is also activated by the disruption of calcium homeostasis [59] like it occurs in 5XFAD mice. As mentioned, tau pathology is associated with a complex modulatory network of proteins, in which CDK5 and GSK3 β are the most prominent tau kinases [60]. Then, we evaluated the activity of GSK3 β through the ratio of p-GSK3 β Tyr216/total GSK3 β as well as tau phosphorylation levels. Our results showed that UB-ALT-EV, but not memantine, caused a diminution in GSK3 β activity and AT8 levels in 5XFAD. These results reflect the modulation of this AD mark by UB-ALT-EV, linking GSK3 β activity to NMDARs functionality which differs from that of classical NMDAR antagonists [25]. Moreover, we found that both treatments, UB-ALT-EV and memantine, ameliorated A β pathology in treated 5XFAD mice, as demonstrated by a reduction in the number and size of A β plaques, and also by the reduction of the A β ₄₂/A β ₄₀ ratio [61]. Likewise, we found about 4x increased levels of A β ₄₀ in both treated groups. Of note, it is well established that this amyloid fragment inhibits A β deposition *in vivo* [62], suggesting in part the mechanism by which A β deposition might be reduced after both treatments. Furthermore, the improvement of amyloidogenic pathology after treatment with UB-ALT-EV was accompanied by beneficial effects on APP processing as evidenced by protein levels for BACE1, sAPP α and the CTFs/pre-APP ratio. Those results, support the hypothesis that disease progression in 5XFAD mice is modified by NMDAR antagonists treatment.

The calpain protease system and autophagy are strongly interconnected, and modifications in calpain expression induce changes in autophagic processes. Concretely, it is known that calpains can cleave proteins involved in autophagy

[63]. In 5XFAD, autophagy was impaired by altered levels of ULK-1, beclin-1, LC3B, and LAMP-1 proteins, indicating that the autophagic process was unfinished. Interestingly, calpain-1 is implicated in the proteolytic cleavage of beclin-1, impeding the initiation of autophagosome formation [64]. In this line of evidence, treatment of 5XFAD mice with UB-ALT-EV increased beclin-1 protein levels probably due to the decreased calpain-1 proteolytic activity. Both phenomena allowed the initiation of the beclin-1-mediated autophagosome formation and continuation of the autophagic process induced by increased protein levels of ULK-1, which plays a critical role during the early stages of autophagy. In the next step of autophagy, 5XFAD mice revealed an accumulation of LC3B-II, a promoter of phagophore formation and low levels of LAMP-1, that plays an important role in lysosome biogenesis, indicating a defect in the autophagosome degradation. Interestingly, the reduced levels of LC3B-II vs. LC3B-I ratio observed in the 5XFAD-treated groups could be identified as an amelioration of the autophagosome accumulation. Moreover, UB-ALT-EV treatment increased LAMP-1 protein levels, enhancing the autophagolysosome generation and allowing the completion of effective and proper autophagy process that would improve cell function by removing cellular debris such as aberrant protein accumulation. Likewise, these findings are in accordance with the reduced A β plaques deposition results. Overall, it was reported that autophagy enhancement can drive a reduction in A β levels and apoptosis, thereby inhibiting apoptosis [17–19,65]. Our results suggested that UB-ALT-EV would regulate apoptosis and autophagic process supporting its neuroprotective effect through NMDAR antagonism beyond memantine.

Remarkably, the cross-talk between calpain-caspase-3 apoptotic signaling pathways has been related to AD through NMDARs overactivation [66]. Caspase-3 protein levels were slightly modified in 5XFAD mice and decreased under UB-ALT-EV treatment, but no changes in SBDP 120 kDa fragments were determined; however, it must be kept in mind that activation of caspase-3 is not directly associated with calcium increases. Furthermore, it was demonstrated that apoptosis could be promoted by autophagy in AD patients [67,68], whereby the reduced levels of caspase-3 found here could be explained by the increased autophagic process induced by UB-ALT-EV treatment. Supporting those results, it was found that memantine could attenuate cell apoptosis by inhibiting the calpain-caspase-3 after ischemic stroke intervention [15].

Regarding the Bcl-2, increased levels are well described in AD brains [69], and previous reports demonstrated high levels of Bcl-2 in mice models of AD that were reduced after treatment with neuroprotective drugs [28,70]. Accordingly,

Bcl-2 expression after treatment confirmed the influence of NMDAR antagonists on regulating the apoptotic process.

5. Conclusions

Based on our results, it can be concluded that chronic treatment with UB-ALT-EV resulted in neuroprotective effects on 5XFAD mice, ameliorating the tau and amyloid pathology, as well as cognitive improvements (**Fig. 8**). Together with those recently reported, these findings propose new NMDAR antagonist drug research opportunities on more effective treatments for fighting against cognitive impairment and AD.

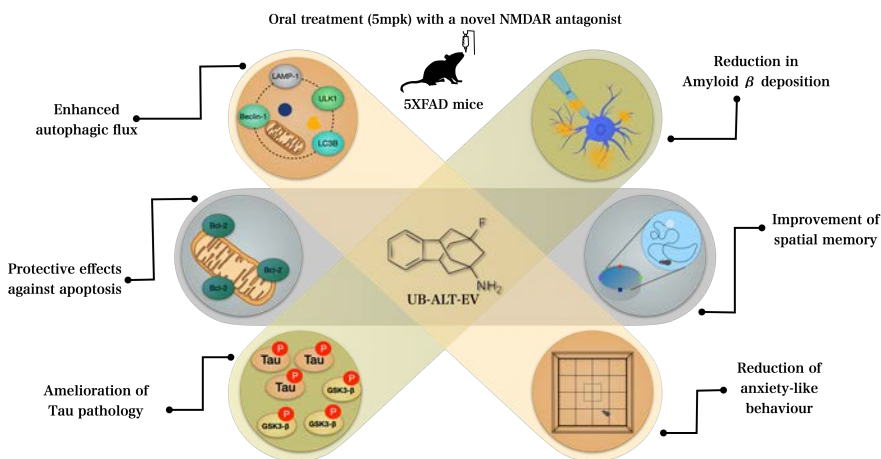


Fig. 8. Illustrative cartoon of effects of UB-ALT-EV in 6-months-old 5XFAD mice.

References

1. Parsons CG, Danysz W, Quack G. Memantine is a clinically well tolerated N-methyl-D-aspartate (NMDA) receptor antagonist - A review of preclinical data. *Neuropharmacology*. Pergamon; 1999;38:735-67.
2. Zhang Y, Li P, Feng J, Wu M. Dysfunction of NMDA receptors in Alzheimer's disease. *Neurol Sci*. Springer-Verlag Italia s.r.l.; 2016;37:1039-47.
3. Filali M, Lalonde R, Rivest S. Subchronic memantine administration on spatial learning, exploratory activity, and nest-building in an APP/PS1 mouse model of Alzheimer's disease. *Neuropharmacology*. *Neuropharmacology*; 2011;60:930-6.
4. Kumar A. NMDA receptor function during senescence: Implication on cognitive performance. *Front Neurosci*. 2015;9:1-15.

5. Wittenauer BR, Smith L. Priority Medicines for Europe and the World " A Public Health Approach to Innovation " Update on 2004 Background Paper. Who. 2013.
6. Mattson MP. Pathways towards and away from Alzheimer's disease. *Nature*. NIH Public Access; 2004;430:631-9.
7. World Health Organization. WHO | Dementia: a public health priority. World Heal. Organ. World Health Organization; 2016.
8. Viola KL, Klein WL. Amyloid β oligomers in Alzheimer's disease pathogenesis, treatment, and diagnosis. *Acta Neuropathol*. Springer Verlag; 2015;129:183-206.
9. Dickson DW. Neuropathological diagnosis of Alzheimer's disease: A perspective from longitudinal clinicopathological studies. *Neurobiol Aging*. 1997;18:S21-6.
10. L'Episcopo F, Drouin-Ouellet J, Tirolo C, Pulvirenti A, Giugno R, Testa N, et al. GSK-3 β -induced Tau pathology drives hippocampal neuronal cell death in Huntington's disease: involvement of astrocyte–neuron interactions. *Cell Death Dis*. Nature Publishing Group; 2016;7:e2206.
11. Lv X, Li Q, Mao S, Qin, L, Dong P. The protective effects of memantine against inflammation and impairment of endothelial tube formation induced by oxygen-glucose deprivation/reperfusion. *Aging (Albany NY)*. Impact Journals LLC; 2020;12:21469-80.
12. Song G, Li Y, Lin L, Cao Y. Anti-autophagic and anti-apoptotic effects of memantine in a SH-SY5Y cell model of Alzheimer's disease via mammalian target of rapamycin-dependent and -independent pathways. *Mol Med Rep*. Spandidos Publications; 2015;12:7615-22.
13. Pietá Dias C, Martins de Lima MN, Presti-Torres J, Dornelles A, Garcia VA, Siciliani Scalco F, et al. Memantine reduces oxidative damage and enhances long-term recognition memory in aged rats. *Neuroscience*. Neuroscience; 2007;146:1719-25.
14. Ndountse LT, Chan HM. Role of N-methyl-D-aspartate receptors in polychlorinated biphenyl mediated neurotoxicity. *Toxicol Lett*. Elsevier; 2009;184:50-5.
15. Chen B, Wang G, Li W, Liu W, Lin R, Tao J, et al. Memantine attenuates cell apoptosis by suppressing the calpain-caspase-3 pathway in an experimental model of ischemic stroke. *Exp Cell Res*. Exp Cell Res; 2017;351:163-72.
16. Shen H, Zhu H, Panja D, Gu Q, Li Z. Autophagy controls the induction and developmental decline of NMDAR-LTD through endocytic recycling. *Nat Commun*. Nature Publishing Group; 2020;11:2979.
17. Spilman P, Podlutskaya N, Hart MJ, Debnath J, Gorostiza O, Bredesen D, et

- al. Inhibition of mTOR by rapamycin abolishes cognitive deficits and reduces amyloid- β levels in a mouse model of alzheimer's disease. *PLoS One*. *PLoS One*; 2010;5.
18. Tan CC, Yu JT, Tan MS, Jiang T, Zhu XC, Tan L. Autophagy in aging and neurodegenerative diseases: Implications for pathogenesis and therapy. *Neurobiol Aging*. *Neurobiol Aging*; 2014;35:941-57.
 19. Zhu XC, Yu JT, Jiang T, Tan L. Autophagy modulation for alzheimer's disease therapy. *Mol. Neurobiol*. Humana Press Inc.; 2013.
 20. Kishi T, Matsunaga S, Oya K, Nomura I, Ikuta T, Iwata N. Memantine for Alzheimer's Disease: An Updated Systematic Review and Meta-analysis. *J Alzheimer's Dis*. IOS Press; 2017;60:401-25.
 21. Liu M, Wang S, Yao W, Zhang Z, Zhong X, L S, et al. Memantine improves spatial learning and memory impairments by regulating NGF signaling in APP/PS1 transgenic mice. *Neuroscience*. *Neuroscience*; 2014;273.
 22. Wang X, Blanchard J, Grundke-Iqbal I, Iqbal K. Memantine attenuates Alzheimer's disease-like pathology and cognitive impairment. *PLoS One*. Public Library of Science; 2015;10.
 23. Jürgenson M, Zharkovskaja T, Noortoots A, Morozova M, Beniashvili A, Zapolski M, et al. Effects of the drug combination memantine and melatonin on impaired memory and brain neuronal deficits in an amyloid-predominant mouse model of Alzheimer's disease. *J Pharm Pharmacol*. Blackwell Publishing Ltd; 2019;71:1695-705.
 24. Scholtzova H, Wadghiri YZ, Douadi M, Sigurdsson EM, Li Y-S, Quartermain D, et al. Memantine leads to behavioral improvement and amyloid reduction in Alzheimer's-disease-model transgenic mice shown as by micromagnetic resonance imaging. *J Neurosci Res*. *J Neurosci Res*; 2008;86:2784-91.
 25. Martinez-Coria H, Green KN, Billings LM, Kitazawa M, Albrecht M, Rammes G, et al. Memantine improves cognition and reduces Alzheimer's-like neuropathology in transgenic mice. *Am J Pathol*. Elsevier Inc.; 2010;176:870-80.
 26. Briggs R, Kennelly SP, O'Neill D. Drug treatments in Alzheimer's disease. *Clin Med J R Coll Physicians London*. 2016;16:247-53.
 27. Mufson EJ, Counts SE, Perez SE, Ginsberg SD. Cholinergic system during the progression of Alzheimer's disease: Therapeutic implications. *Expert Rev Neurother*. 2008;8:1703-18.
 28. Companys-Aleman J, Turcu AL, Bellver-Sanchis A, Loza MI, Brea JM, Canudas AM, et al. A Novel NMDA Receptor Antagonist Protects against Cognitive Decline Presented by Senescent Mice. *Pharmaceutics*. Multidisciplinary Digital Publishing Institute; 2020;12:284.

29. Leiva R, Phillips MB, Turcu AL, Gratacòs-Batlle E, León-García L, Sureda FX, et al. Pharmacological and Electrophysiological Characterization of Novel NMDA Receptor Antagonists. *ACS Chem Neurosci*. American Chemical Society; 2018;9:2722-30.
30. Valverde E, Sureda FX, Vázquez S. Novel benzopolycyclic amines with NMDA receptor antagonist activity. *Bioorganic Med Chem*. Elsevier Ltd; 2014;22:2678-83.
31. Girard SD, Jacquet M, Baranger K, Migliorati M, Escoffier G, Bernard A, et al. Onset of hippocampus-dependent memory impairments in 5XFAD transgenic mouse model of Alzheimer's disease. *Hippocampus*. John Wiley and Sons Inc.; 2014;24:762-72.
32. Griñán-Ferré C, Sarroca S, Ivanova A, Puigoriol-Illamola D, Aguado F, Camins A, et al. Epigenetic mechanisms underlying cognitive impairment and Alzheimer disease hallmarks in 5XFAD mice. *Aging (Albany NY)*. 2016;8:664-84.
33. Lazic D, Tesic V, Jovanovic M, Brkic M, Milanovic D, Zlokovic B V., et al. Every-other-day feeding exacerbates inflammation and neuronal deficits in 5XFAD mouse model of Alzheimer's disease. *Neurobiol Dis*. Academic Press; 2020;136:104745.
34. Li N, Li Y, Li L-J, Zhu K, Zheng Y, Wang X-M. Glutamate receptor delocalization in postsynaptic membrane and reduced hippocampal synaptic plasticity in the early stage of Alzheimer's disease. *Neural Regen Res*. Wolters Kluwer -- Medknow Publications; 2019;14:1037-45.
35. Devi L, Ohno M. Cognitive benefits of memantine in Alzheimer's 5XFAD model mice decline during advanced disease stages. *Pharmacol Biochem Behav*. Elsevier Inc.; 2016;144:60-6.
36. J V, A L. Why women have more Alzheimer's disease than men: gender and mitochondrial toxicity of amyloid-beta peptide. *J Alzheimers Dis*. *J Alzheimers Dis*; 2010;20:527-33.
37. Zhou X, Wang L, Xiao W, Su Z, Zheng C, Zhang Z, et al. Memantine improves cognitive function and alters hippocampal and cortical proteome in triple transgenic mouse model of Alzheimer's disease. *Exp Neurol*. Korean Society for Neurodegenerative Disease; 2019;28:390-403.
38. Liu MY, Wang S, Yao WF, Zhang ZJ, Zhong X, Sha L, et al. Memantine improves spatial learning and memory impairments by regulating NGF signaling in APP/PS1 transgenic mice. *Neuroscience*. Elsevier Ltd; 2014;273:141-51.
39. Seibenhener ML, Wooten MC. Use of the Open Field Maze to Measure Locomotor and Anxiety-like Behavior in Mice. *J Vis Exp*. MyJoVE

- Corporation; 2015;e52434.
40. Nunez J. Morris water maze experiment. *J Vis Exp*. MyJoVE Corporation; 2008;
 41. Marsh J, Bagol SH, Williams RSB, Dickson G, Alifragis P. Synapsin I phosphorylation is dysregulated by beta-amyloid oligomers and restored by valproic acid. *Neurobiol Dis*. United States; 2017;106:63-75.
 42. Robbins M, Clayton E, Kaminski Schierle GS. Synaptic tau: A pathological or physiological phenomenon? *Acta Neuropathol Commun*. 2021;9:149.
 43. Muir KW. Glutamate-based therapeutic approaches: clinical trials with NMDA antagonists. *Curr Opin Pharmacol*. Elsevier; 2006;6:53-60.
 44. Ikonomidou C, Turski L. Why did NMDA receptor antagonists fail clinical trials for stroke and traumatic brain injury? *Lancet Neurol*. Elsevier; 2002;1:383-6.
 45. Mahase E. FDA approves controversial Alzheimer's drug despite uncertainty over effectiveness. *BMJ*. British Medical Journal Publishing Group; 2021;373:n1462.
 46. Nagakura A, Shitaka Y, Yarimizu J, Matsuoka N. Characterization of cognitive deficits in a transgenic mouse model of Alzheimer's disease and effects of donepezil and memantine. *Eur J Pharmacol*. *Eur J Pharmacol*; 2013;703:53-61.
 47. Sun D, Chen J, Bao X, Cai Y, Zhao J, Huang J, et al. Protection of Radial Glial-Like Cells in the Hippocampus of APP/PS1 Mice: a Novel Mechanism of Memantine in the Treatment of Alzheimer's Disease. *Mol Neurobiol*. Humana Press Inc.; 2015;52:464-77.
 48. Zhou X, Wang L, Xiao W, Su Z, Zheng C, Zhang Z, et al. Memantine Improves Cognitive Function and Alters Hippocampal and Cortical Proteome in Triple Transgenic Mouse Model of Alzheimer's Disease. *Exp Neurobiol*. Korean Society for Brain and Neural Science; 2019;28:390.
 49. Turcu AL, Companys-Aleman J, Phillips MB, Patel DS, Griñán-Ferré C, Loza MI, et al. Design, synthesis, and in vitro and in vivo characterization of new memantine analogs for Alzheimer's Disease. *Eur J Med Chem*. 2022; <https://doi.org/10.1016/j.ejmech.2022.114354>
 50. Liu J, Chang L, Song Y, Li H, Wu Y. The role of NMDA receptors in Alzheimer's disease. *Front Neurosci*. Frontiers Media S.A.; 2019;13:43.
 51. Proctor DT, Coulson EJ, Dodd PR. Post-synaptic scaffolding protein interactions with glutamate receptors in synaptic dysfunction and Alzheimer's disease. *Prog Neurobiol*. Elsevier Ltd; 2011;93:509-21.
 52. Chen M, Lu TJ, Chen XJ, Zhou Y, Chen Q, Feng XY, et al. Differential roles of NMDA receptor subtypes in ischemic neuronal cell death and ischemic

- tolerance. *Stroke*. 2008;39:3042-8.
53. Mahaman YAR, Huang F, Afewerky HK, Maibouge TMS, Ghose B, Wang X. Involvement of calpain in the neuropathogenesis of Alzheimer's disease. *Med Res Rev*. John Wiley & Sons, Ltd; 2019;39:608-30.
 54. Wang R, Reddy PH. Role of Glutamate and NMDA Receptors in Alzheimer's Disease. *J Alzheimer's Dis*. 2017;57:1041-8.
 55. Tanqueiro SR, Ramalho RM, Rodrigues TM, Lopes L V., Sebastião AM, Diógenes MJ. Inhibition of NMDA Receptors Prevents the Loss of BDNF Function Induced by Amyloid β . *Front Pharmacol*. Frontiers Media SA; 2018;9:237.
 56. Yabuki Y, Matsuo K, Hirano K, Shinoda Y, Moriguchi S, Fukunaga K. Combined Memantine and Donepezil Treatment Improves Behavioral and Psychological Symptoms of Dementia-Like Behaviors in Olfactory Bulbectomized Mice. *Pharmacology*. S. Karger AG; 2017;99:160-71.
 57. Sudhof T, Czernik A, Kao H, Takei K. Synapsins: mosaics of shared and individual domains in a family of synaptic vesicle phosphoproteins. *Science* (80-). 1989;245:1474-80.
 58. Corradi A, Zanardi A, Giacomini C, Onofri F, Valtorta F, Zoli M, et al. Synapsin-I- and synapsin-II-null mice display an increased age-dependent cognitive impairment. *J Cell Sci*. England; 2008;121:3042-51.
 59. Oka M, Fujisaki N, Maruko-Otake A, Ohtake Y, Shimizu S, Saito T, et al. Ca^{2+} /calmodulin-dependent protein kinase II promotes neurodegeneration caused by tau phosphorylated at Ser262/356 in a transgenic *Drosophila* model of tauopathy. *J Biochem*. Oxford University Press; 2017;162:335-42.
 60. Lauretti E, Dincer O, Praticò D. Glycogen synthase kinase-3 signaling in Alzheimer's disease. *Biochim Biophys Acta Mol Cell Res*. *Biochim Biophys Acta Mol Cell Res*; 2020;1867.
 61. Oakley H, Cole SL, Logan S, Maus E, Shao P, Craft J, et al. Intraneuronal beta-amyloid aggregates, neurodegeneration, and neuron loss in transgenic mice with five familial Alzheimer's disease mutations: potential factors in amyloid plaque formation. *J Neurosci*. 2006;26:10129-40.
 62. Kim J, Onstead L, Randle S, Price R, Smithson L, Zwizinski C, et al. A β 40 inhibits amyloid deposition in vivo. *J Neurosci*. 2007;27:627-33.
 63. Weber JJ, Pereira Sena P, Singer E, Nguyen HP. Killing Two Angry Birds with One Stone: Autophagy Activation by Inhibiting Calpains in Neurodegenerative Diseases and beyond. *Biomed Res*. Int. Hindawi Limited; 2019.
 64. Russo R, Berliocchi L, Adornetto A, Varano G, Cavaliere F, Nucci C, et al. Calpain-mediated cleavage of Beclin-1 and autophagy deregulation following

- retinal ischemic injury in vivo. *Cell Death Dis.* *Cell Death Dis*; 2011;2.
65. Caccamo A, Majumder S, Richardson A, Strong R, Oddo S. Molecular interplay between mammalian target of rapamycin (mTOR), amyloid- β , and Tau: Effects on cognitive impairments. *J Biol Chem.* *J Biol Chem*; 2010;285:13107-20.
66. Carvajal FJ, Mattison HA, Cerpa W. Role of NMDA Receptor-Mediated Glutamatergic Signaling in Chronic and Acute Neuropathologies. Kang KD, editor. *Neural Plast.* Hindawi Publishing Corporation; 2016;2016:2701526.
67. Louneva N, Cohen JW, Han LY, Talbot K, Wilson RS, Bennett DA, et al. Caspase-3 is enriched in postsynaptic densities and increased in Alzheimer's disease. *Am J Pathol.* American Society for Investigative Pathology Inc.; 2008;173:1488-95.
68. Nixon RA, Wegiel J, Kumar A, Yu WH, Peterhoff C, Cataldo A, et al. Extensive involvement of autophagy in Alzheimer disease: An immunoelectron microscopy study. *J Neuropathol Exp Neurol.* Lippincott Williams and Wilkins; 2005;64:113-22.
69. Callens M, Kraskovskaya N, Derevtsova K, Annaert W, Bultynck G, Bezprozvanny I, et al. The role of Bcl-2 proteins in modulating neuronal Ca²⁺ signaling in health and in Alzheimer's disease. *Biochim Biophys Acta - Mol Cell Res.* 2021;1868:118997.
70. Vasilopoulou F, Griñán-Ferré C, Rodríguez-Arévalo S, Bagán A, Abás S, Escolano C, et al. I2 imidazoline receptor modulation protects aged SAMP8 mice against cognitive decline by suppressing the calcineurin pathway. *GeroScience.* Springer Science and Business Media Deutschland GmbH; 2021;43:965-83.

Statements and Declarations

Ethics approval: This study was performed in line with the principles of the Declaration of Helsinki, according to European Community Council Directive 86/609/EEC and were approved by the Institutional Animal Care and Use Committee of the University of Barcelona (670/14/8102, approved at 14 November 2014) and by Generalitat de Catalunya, Spain (10291, approved at 28 January 2018).

Consent for publication: Not applicable

Availability of data and material: The datasets generated during and/or analysed during the current study are not publicly available due to are standard raw data for

RT-PCR, Western blot and ICH image quantification etc. but are available from the corresponding author on reasonable request

Competing Interests: The authors have no relevant financial or non-financial interests to disclose.

Fundings: This study was supported by Ministerio de Economía y Competitividad of Spain and FEDER (PID2019-106285RB; PDC2021-121096), María de Maeztu Unit of Excellence (Institute of Neurosciences, University of Barcelona) MDM-2017-0729 and 2017SGR106 (AGAUR, Catalonia).

Author Contributions: C.G-F, S.V. and M.P. conceived the idea. A.L.T synthesized and chemically characterized the compounds. J.C.-A. and C.G.-F. designed and carried out the in vivo experiments. C.G-F, M.S. and C-E. M. carried out DMPK studies. The first draft of the manuscript was written by J.C-A. C. G-F and M.P. wrote the definitive manuscript with feedback from all the authors and all authors commented on previous versions of the manuscript.

Acknowledgements: J.C.-A. acknowledge Ministry of Economy and Competitiveness (MINECO) for her FPI (MDM-2017-0729) fellowship. A.L.T. thanks the Spanish *Ministerio de Educación, Cultura y Deporte* for a PhD fellowship (FPU program).

Financial interests: Authors declare they have no financial interests

Table S1: Antibodies used for Western blotting experiments.

Antibodies	Host	Source	Dilution
α-Spectrin alpha chain	Mouse	Millipore/MAB1622	1:1000
APP C terminal fragment	Mouse	Covance / SIG-39152	1:1000
BACE	Rabbit	Cell Signaling / #5606	1:1000
Bax	Rabbit	Cell Signaling / #2772	1:1000
BCL-2	Rabbit	Cell Signaling / #2870	1:1000
Beclin-1	Rabbit	Cell Signaling / #3495	1:1000
Calpain-1	Rabbit	Bio-Rad / AHP2443	1:1000
CaMKII	Rabbit	Abcam / ab52476	1:1000
CaMKII (Phospho-Thr286)	Rabbit	Signalway Antibody / #11287	1:1000
Caspase-3	Rabbit	BD Transduction Laboratories / C31720	1:1000
GAPDH	Mouse	Millipore / #MAB374	1:5000
GSK3β	Rabbit	Cell Signaling / #9315	1:1000
GSK3β (Phospho-Y216)	Rabbit	Abcam / ab75745	1:1000
LAMP1	Mouse	Santa Cruz Biotechnology / sc-19992	1:500
LC3B	Rabbit	Cell Signaling / #2775	1:1000
p25/35	Rabbit	Cell Signaling / #2680	1:1000
Tau Total	Rabbit	GeneTex/GTX112981	1:1000
Tau (phospho-Ser396)	Rabbit	Invitrogen/#44-752G	1:1000
Tau (phosphor-Ser202, Thr205)(AT8)	Mouse	Invitrogen/ #MN1020	1:1000
sAPPα	Rabbit	Covance / SIG-39139-005	1:1000
Synapsin Ia	Mouse	Santa Cruz Biotechnology / sc-136086	1:500
ULK1	Mouse	Santa Cruz Biotechnology / sc-390904	1:500
ULK1 (Phospho-Ser757)	Rabbit	Cell Signaling / #6888	1:1000
anti-mouse HRP conjugated	Goat	Bio-Rad / 170-5047	1:2000
anti-rabbit HRP conjugated	Goat	Bio-Rad / 170-6515	1:2000

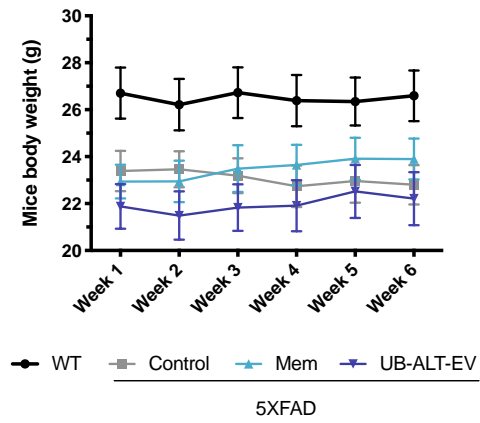


Fig. S1. Body weight measurement over the last six weeks of the study for WT and 5XFAD mice.

3.4 Article 4

Glial cell activation and oxidative stress prevention in Alzheimer's disease mice model by an optimized NMDA receptor antagonist

**Comanys-Aleman J.¹, Turcu A. L.², Vázquez S.², Pallàs M.¹,
Griñán-Ferré C.¹**

Scientific Reports, enviat a la revista (1.05.2022)

JCR 2020 IF: 4,38

Afiliacions:

¹ Departament de Farmacologia, Toxicologia i Química Terapèutica. Facultat de Farmàcia i Ciències de l'Alimentació. Institut de Neurociències, Universitat de Barcelona (NeuroUB). Av. Joan XXIII 27-31, 08028 Barcelona, Espanya.

² Laboratory of Medicinal Chemistry (CSIC Associated Unit), Department of Pharmacology, Toxicology, and Therapeutic Chemistry. Faculty of Pharmacy and Food Sciences and Institute of Biomedicine (IBUB), University of Barcelona, Av. Joan XXIII, 27-31, E-08028 Barcelona, Spain.

RESUM

Durant la MA els alts nivells de glutamat afavoreixen l'aparició de l'excitotoxicitat desencadenant l'aparició de la neuroinflamació, l'estrès oxidatiu i finalment provocant la mort neuronal. Tenint en compte que la memantina ha demostrat modular aquests processos relacionats amb la neurodegeneració, aquest estudi es va centrar en avaluar l'efecte del tractament crònic per via oral amb UB-ALT-EV, un antagonista del receptor NMDA optimitzat, en ratolins transgènics de la MA de 6 mesos d'edat.

Els canvis obtinguts en la via CaN/NFATc1 després del tractament indiquen una disminució de l'activitat inflamatòria, que posteriorment es va confirmar observant la reducció de l'activació astroglià i microglial, avaluades mitjançant els marcadors GFAP i Iba-1. A més, la disminució de l'expressió gènica de *Trem2* induïda pel tractament amb UB-ALT-EV, però no per la memantina feia indicar una modulació de l'activitat fagocítica de la microglia diferents entre els dos compostos. En aquest sentit, després de l'avaluació dels nivells d'expressió gènica de marcadors proinflamatoris i antiinflamatoris associats a la microglia, es va comprovar com el compost UB-ALT-EV i memantina els regulen de forma diferencial. A més a més, l'UB-ALT-EV va reduir els nivells d'expressió gènica d'*iNOS*, un marcador que indica el vincle entre l'activitat microglial i l'estrès oxidatiu. Per aquest motiu, es va dur a terme l'anàlisi de 84 gens associats a l'estrès oxidatiu, mitjançant l'ús un bioxip (del terme en anglès *array*) per tal d'identificar vies d'activitat oxidativa modulades pel compost. L'anàlisi bioinformàtic, va identificar l'acció del compost UB-ALT-EV sobre vies implicades en l'activitat generadora de superòxid, l'activitat antioxidant i l'acció de citoquines.

En conjunt, els resultats suggereixen una activitat moduladora de processos inflamatoris i oxidatius per part del compost UB-ALT-EV diferent a la de la memantina. Aquests resultats suggereixen que el procés d'optimització de la molècula de la memantina té un alt potencial en el camp de desenvolupament de noves teràpies per la MA.

Glial cell activation and oxidative stress prevention in Alzheimer's disease mice model by an optimized NMDA receptor antagonist

Júlia Companys-Aleman^{*}, Andreea L. Turcu[†], Santiago Vázquez[†], Mercè Pallàs^{*} and Christian Griñán-Ferré^{*}

^{*}Pharmacology Section, Department of Pharmacology, Toxicology, and Therapeutic Chemistry. Faculty of Pharmacy and Food Sciences, Institut de Neurociències, Universitat de Barcelona (NeuroUB), Av. Joan XXIII 27-31, 08028 Barcelona, Spain.

[†]Laboratory of Medicinal Chemistry (CSIC Associated Unit), Department of Pharmacology, Toxicology, and Therapeutic Chemistry. Faculty of Pharmacy and Food Sciences and Institute of Biomedicine (IBUB), University of Barcelona, Av. Joan XXIII, 27-31, 08028 Barcelona, Spain

Co-corresponding author:
Christian Griñán-Ferré, PhD
Mercè Pallàs, PhD.

Pharmacology Section in Pharmacology, Toxicology, and Therapeutic Chemistry Department, Faculty of Pharmacy and Food Sciences, Universitat de Barcelona, Av. Joan XXIII 27-31, 08028 Barcelona, Spain.
e-mail: pallas@ub.edu; christian.grinan@ub.edu

ABSTRACT

In Alzheimer's disease pathology, several neuronal processes are dysregulated by excitotoxicity including neuroinflammation and oxidative stress (OS). New therapeutic agents capable of modulating such processes are needed to foster neuroprotection. Here, the effect of an optimised NMDA receptor antagonist, UB-ALT-EV and memantine, as a gold standard, have been evaluated in 5XFAD mice. Following treatment with UB-ALT-EV, nor memantine, changes in the calcineurin (CaN)/NFAT pathway were detected. UB-ALT-EV increased neurotrophic factors (*Bdnf*, *Vgf* and *Ngf*) gene expression. Treatments reduced astrocytic and microglial activation as revealed by GFAP and Iba-1 quantification. Interestingly, only UB-ALT-EV was able to reduce gene expression of *Trem2*, a marker of microglial activation and NF-κB. Pro-inflammatory M1-microglial phenotype (*Il-1β*, *Ifn-γ*, *Ccl2* and *Ccl3*) markers were down-regulated in UB-ALT-EV-treated mice but not in memantine-treated mice. Interestingly, the anti-inflammatory markers of the M2-microglial phenotype, *chitinase-like 3* (*Ym1*) and *Arginase-1* (*Arg1*), were up-regulated after treatment with UB-ALT-EV. Since iNOS gene expression decreased after UB-ALT-EV treatment, a qPCR array containing 84 OS-related genes was performed. We found changes in *Il-19*, *Il-22*, *Gpx6*, *Ncf1*, *Aox1* and *Vim* gene expression after UB-ALT-EV. In sum, our results reveal a robust effect on neuroinflammation and OS processes after UB-ALT-EV treatment, surpassing the memantine effect in 5XFAD.

Keywords: NMDA antagonist, neuroinflammation, neurotrophins, oxidative stress, calcineurin, NFAT1c

1. INTRODUCTION

N-Methyl-d-Aspartate receptors (NMDARs) and aberrant post-synaptic calcium signalling have been implicated in neurodegenerative conditions, including Alzheimer's Disease (AD)¹. However, the physiological activity of NMDARs is necessary to mediate some aspects of development, synaptic transmission and normal neuronal function^{2,3}. In AD, high levels of glutamate can be released from glial cells favouring excitotoxicity and leading to a massive influx of Ca²⁺ mediated by NMDARs⁴, promoting cell death⁵, oxidative stress (OS)⁶, and neuroinflammation⁷. Thus, the activation of several inflammatory signalling pathways promotes the synthesis of many proinflammatory mediators, including cytokines as well as other immune mediators such as reactive oxygen species (ROS), fostering a chronic neuroinflammatory state triggered by glial reactivity (especially microglia and astrocytes)^{7,8}.

Considering these facts, it is important to note that inflammatory response, glial activation and OS are three associated mechanisms that emerge as main factors for AD progression⁹. Pursuing this vicious cycle between ROS and glial activation, the inflammatory regulatory signalling molecules, which are directly activated by calcineurin (CaN), nuclear factor of activated T-cells (NFAT) and the nuclear factor kappa-light-chain-enhancer of activated B cell (NF- κ B), can be modulated by ROS increase¹⁰⁻¹². Thus, in AD, both signalling pathways can feed a forward cycle in which cytokine production increases amyloid- β (A β) and neurofibrillary tangles (NFTs) production that mediates the release of more cytokines and maintain a continuous environment of inflammation and gliosis¹³. Moreover, a balance between ROS production and the antioxidant defence is essential for neuronal synaptic functionality¹⁴; when this equilibrium is inadequate, the accumulation of ROS triggers a deleterious response in the brain¹⁵. In AD, there is an unbalanced activity of the antioxidant enzymatic machinery¹⁶. Indeed, a link between ROS and neuroinflammation has been widely described via nitric oxide synthase (iNOS)¹⁷. iNOS activity and expression are tightly regulated by cytokines. Therefore, inflammatory process control directly impacts OS, resulting in a deleterious effect on neuronal functionality¹⁸.

For decades AD treatment has included memantine, a non-competitive NMDAR antagonist, combined with acetylcholinesterase inhibitors¹⁹. Although these drugs' effectiveness has been seriously questioned in Alzheimer's patients in advanced stages^{20,21}, they are the only clinical option available, as the efficacy of the recently amyloid β -directed monoclonal antibody aducanumab is still controversial^{22,23}. It is well-known that memantine reduces neuronal damage and ameliorates memory and learning dysfunction^{24,25}. All these beneficial effects could induce a reduction in neuroinflammation and consequently a cerebral function improvement. Furthermore, several pathways modulated by NMDAR blockade have been implicated in neuroprotection against excitotoxicity, in addition to those directly activated by calcium dysregulation²⁶. All these beneficial effects could induce a reduction of neuroinflammation and OS, and consequently a cerebral function improvement, reinforcing the idea of targeting NMDARs to reduce neuroinflammation in AD. Nevertheless, as mentioned, clinical trials have shown that memantine displays a lack of effectivity in severe AD²⁷. Therefore, new NMDAR antagonists with a higher capability to modulate glutamate signalling are needed.

We have developed an optimized NMDAR antagonist, UB-ALT-EV, with an excellent compromise between potency as an NMDAR channel blocker and druggable properties²⁸. Strikingly, the compound UB-ALT-EV exhibits better

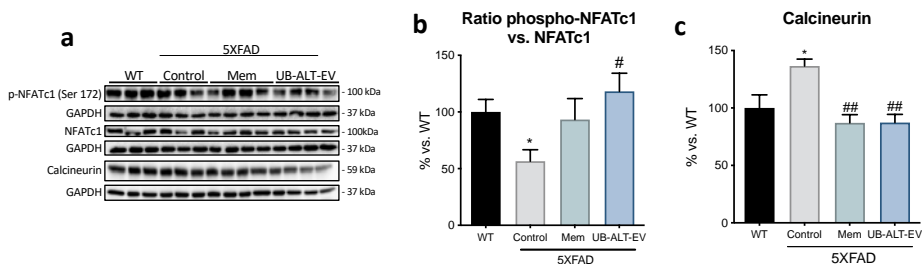
neuroprotective effects than memantine in 5XFAD mice²⁸. The 5XFAD transgenic mouse model is well-established for describing the molecular alterations in AD associated with A β accumulation, co-expressing five familial AD mutations²⁹. Importantly, 5XFAD also showed an association between cognitive impairment, chronic neuroinflammation and OS markers suggesting the contribution of glial activation and OS in AD pathology²⁹.

In the present study, we delved into the modulation of signalling pathways exerted by UB-ALT-EV compared to memantine, focusing on glial activation, neuroinflammatory response, and OS by using the 5XFAD mouse model. Therefore, we evaluated several inflammatory pathways, including their cytokines, as well as we determined changes in gene expression of OS markers related to the triggering of neuroinflammation following memantine and UB-ALT-EV treatments in 5XFAD mice.

2. RESULTS

2.1. NMDAR antagonists treatments modified CaN/NFATc1 signaling pathway in 5XFAD mice.

Alterations in CaN/NFAT activity have been associated with glial activation and excitotoxicity in 5XFAD³⁰. In this regard, it would be interesting to evaluate the ability of NMDAR antagonists to modulate CaN/NFAT pathway. Strikingly, we found that the phosphorylated NFATc1 was significantly reduced in 5XFAD mice compared to the WT group. Intriguingly, we found that UB-ALT-EV, but not memantine, increased phosphorylated NFATc1 levels, thereby preventing nuclear translocation (Fig. 1a, b). Considering these results, CaN, a calcium-dependent protein with phosphatase activity, revealed higher protein levels in the 5XFAD group compared to the WT group. Conversely, in both treated groups, CaN protein levels were decreased compared to the 5XFAD control group (Fig. 1a, c). Collectively, these results suggest a role of both NMDAR antagonists in modulating CaN/NFAT signaling pathway, by reducing Ca²⁺ entry and its downstream mediators.



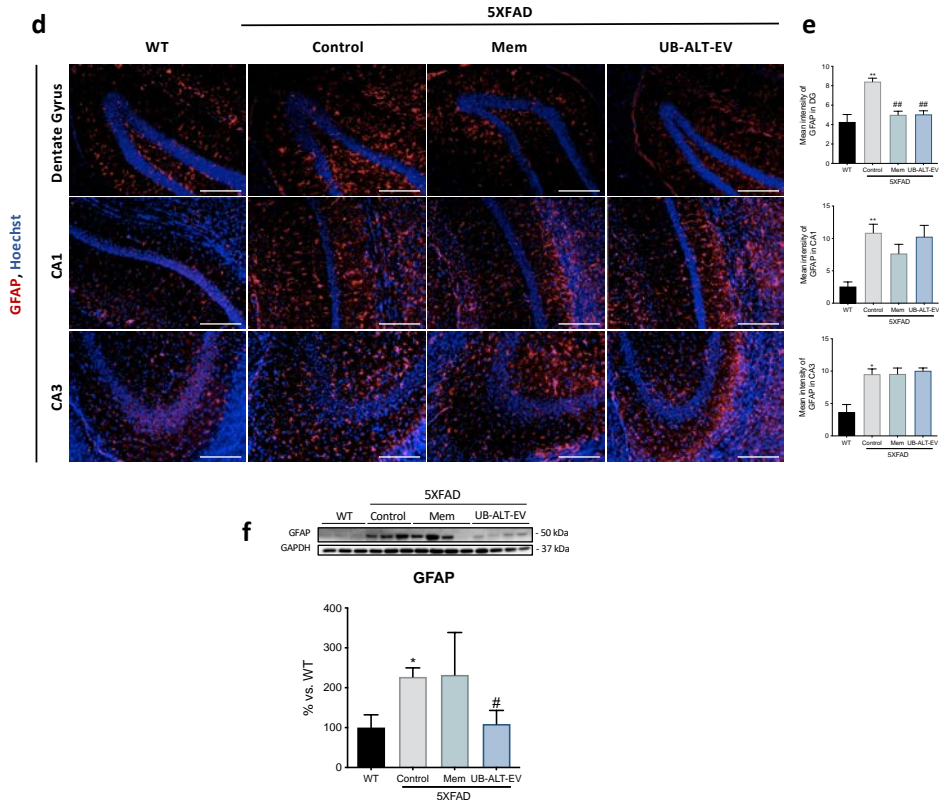


Fig. 1. Treatment with UB-ALT-EV changed the protein expression of inflammatory and astrocytic activation markers and in 5XFAD mice. Representative Western Blot (a) and quantifications for ratio phospho-NFATc1 vs. NFATc1 (b) and CaN (c). Values in bar graphs are adjusted to 100% for protein levels of the wild type (WT). Representative GFAP (Red) and Hoechst (Blue) positive staining in dentate gyrus, CA1 and CA3 hippocampal areas (d). Scale bars: 200 μ m. Mean intensity of GFAP staining in dentate gyrus, CA1 region, and CA3 region (e). Representative Western Blot and quantification for GFAP (f). Values are the mean \pm Standard error of the mean (SEM); (n = 3 for WT and Control groups and n = 4 for Mem and UB-ALT-EV groups. For WT vs. 5XFAD Control groups data was analyzed using a two-tail Student's t-test, and for 5XFAD groups a standard one-way ANOVA followed by Tukey post-hoc analysis was performed. * $p < 0.05$; ** $p < 0.01$ for WT vs. Control. # $p < 0.05$; ### $p < 0.01$ for Mem or UB-ALT-EV vs. Control.

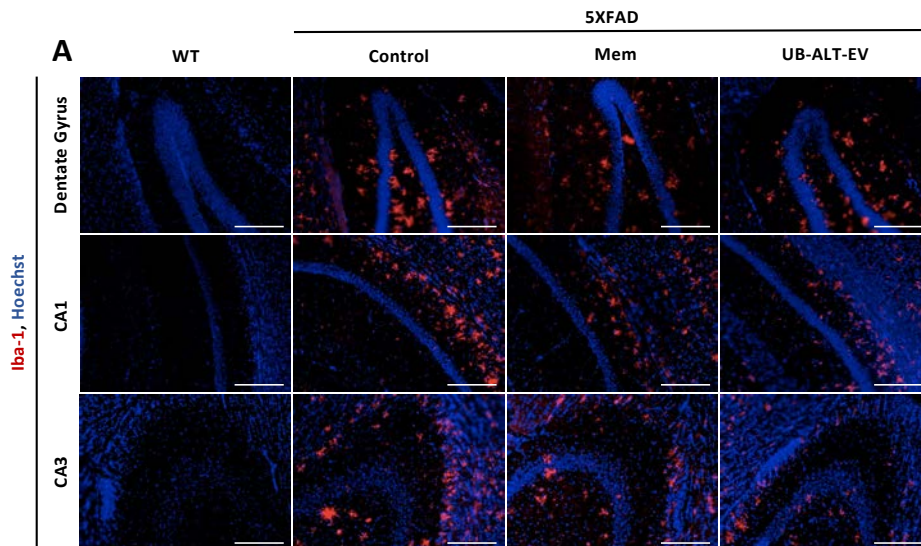
2.2. UB-ALT-EV and memantine treatments reduced hippocampal astroglia in 5XFAD mice.

Next, we assessed the impact of NMDAR antagonists on astroglia performing an immunofluorescence assay against GFAP (Fig. 1d). The results revealed significantly higher GFAP immunostaining in 5XFAD mice compared to WT mice in the dentate gyrus, CA1 and CA3 regions. UB-ALT-EV and memantine treatments reduced astroglia in the dentate gyrus but not in CA1 and CA3 brain

regions (**Fig. 1d,e**). Besides, total GFAP protein expression was evaluated by western blot analysis. As expected, 5XFAD showed significantly higher total protein levels when compared to WT and UB-ALT-EV, but not memantine, treatment reduced significantly GFAP protein levels compared to the 5XFAD control group (**Fig. 1f**).

2.3. Differential expression levels of microglial markers after UB-ALT-EV or memantine treatment in 5XFAD mice.

Signs of microglial activation have been established in the AD brains, indicating a prominent role of neuroinflammation in the pathogenesis of AD ¹³. 5XFAD microglial activation was evaluated by immunofluorescence analysis of Iba-1 protein and *Trem2* gene expression. Higher levels of Iba-1 protein were determined in 5XFAD mice compared to WT mice in CA1, CA3 regions and dentate gyrus (**Fig. 2a**). NMDAR antagonist treatments reduced Iba-1 immunostaining in dentate gyrus and CA3 regions, but not in CA1 (**Fig. 2a, b**). Accordingly, *Trem2* gene expression analysis revealed increased expression in 5XFAD mice when compared to WT mice. Interestingly, only UB-ALT-EV treatment was able to significantly reduce gene expression of *Trem2* in 5XFAD mice (**Fig. 2c**). These results demonstrated that UB-ALT-EV reduced microglial markers better than memantine.



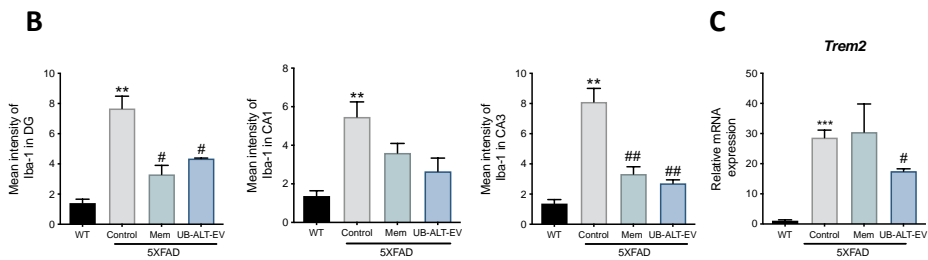


Fig. 2. Treatment-induced changes in the expression of microglial activation markers with NMDA receptor antagonists in 5XFAD of 6 months of age. Representative Iba-1 (Red) and Hoechst (Blue) positive staining in dentate gyrus, CA1 and CA3 hippocampal areas (a). Scale bars: 200 μ m. Mean intensity of Iba-1 staining in dentate gyrus, CA1 region, and CA3 region (b). Representative gene expression for *Trem2* (c). Values are the mean \pm Standard error of the mean (SEM); (n = 3 for WT and Control groups and n = 4 for Mem and UB-ALT-Ev groups. For WT vs. 5XFAD Control groups data was analyzed using a two-tail Student's t-test, and for 5XFAD groups a standard one-way ANOVA followed by Tukey post-hoc analysis was performed. **p<0.01; ***p<0.001 for WT vs. Control. #p<0.05; ##p<0.01 for Mem or UB-ALT-EV vs. Control.

2.4. UB-ALT-EV treatment changed the expression of proinflammatory (M1) phenotype microglial markers in 5XFAD mice

Microglial cells can show a damaging "M1 proinflammatory" phenotype or an "M2 anti-inflammatory", neuroprotective phenotype depending on the released mediators. The transcription factor NF- κ B promotes the release of inflammatory cytokines/chemokines associated with an M1 phenotype³¹. Assessment of NF- κ B protein levels revealed significantly higher levels in the 5XFAD group compared to WT. Interestingly, while the memantine group significantly increased NF- κ B protein levels, UB-ALT-EV treatment in 5XFAD mice significantly reduced protein levels of this transcription factor, compared to the 5XFAD control group (Fig. 3a). To decipher the precise role of NMDARs on inflammation, we carried out an exhaustive gene expression evaluation of proinflammatory (M1) phenotype microglial markers. Then, we evaluated *Interleukin-6 (Il-6)*, *interleukin-1 β (Il-1 β)*, *Interferon-gamma (Ifn- γ)*, *tumor necrosis factor α (Tnf- α)*, *monocyte chemoattractant protein-1 (Ccl2)*, *C-C chemokine ligand 3 (Ccl3)* and *C-C Chemokine ligand 12 (Ccl12)*. All the proinflammatory markers evaluated revealed significantly higher expression in 5XFAD mice compared to WT mice (Fig. 3b,c,d,e,h). Interestingly, memantine treatment produced no change compared to 5XFAD control group, but the UB-ALT-EV group showed a significant diminution in *Il-1 β* , *Ifn- γ* , *Ccl2* and *Ccl3* gene expression compared to 5XFAD Control group (Fig. 3c,d,e,f,g). Taken together, these data suggest that

UB-ALT-EV treatment reduces microglial activation, unlike memantine treatment, by reducing the NF- κ B signaling pathway.

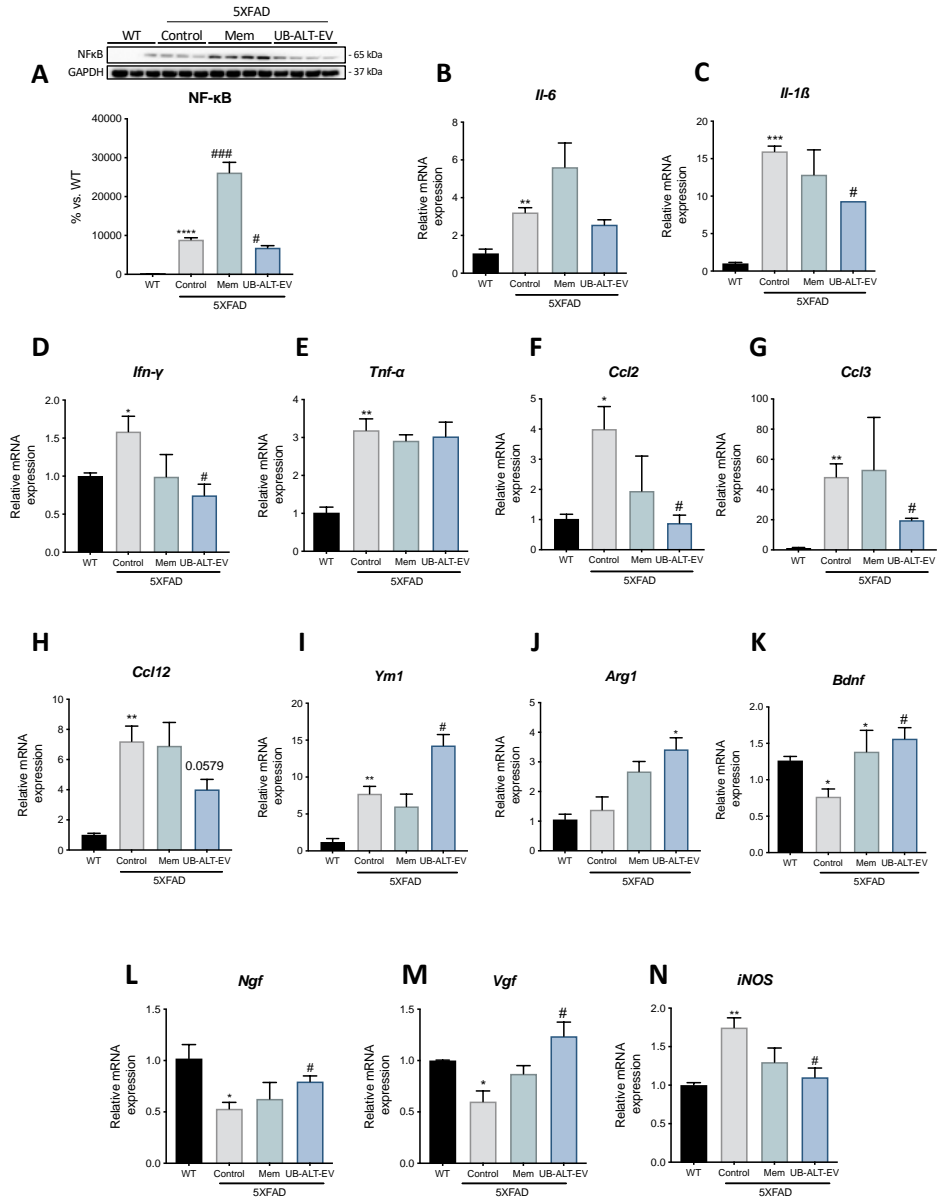


Fig. 3. Differential effect of UB-ALT-EV treatment over memantine treatment on gene expression of pro-inflammatory and anti-inflammatory microglial markers in 5XFAD mice. Representative Western Blot and quantification for NF- κ B (a). Values in bar graphs are adjusted to 100% for protein levels of the wild type (WT). Representative gene expression for *Il-6* (b), *Il-1 β* (c), *Ifn- γ* (d), *Tnf- α* (e), *Ccl2* (f), *Ccl3* (g), *Ccl12* (h), *Ym1* (i), *Arg1* (j), *Bdnf* (k), *Ngf* (l), *Vgf* (m) and

iNOS (n). Values are the mean \pm Standard error of the mean (SEM); (n = 3 for WT and Control groups and n = 4 for Mem and UB-ALT-EV groups. For WT vs. 5XFAD Control groups data was analyzed using a two-tail Student's t-test, and for 5XFAD groups a standard one-way ANOVA followed by Tukey post-hoc analysis was performed. *p<0.05; **p<0.01; ***p<0.001; ****p<0.0001 for WT vs. Control. #p<0.05; ###p<0.001 for Mem or UB-ALT-EV vs. Control.

2.5. UB-ALT-EV treatment increased gene expression of microglial markers (M2 phenotype) together with neurotrophins and reduced *iNOS* gene expression in 5XFAD mice

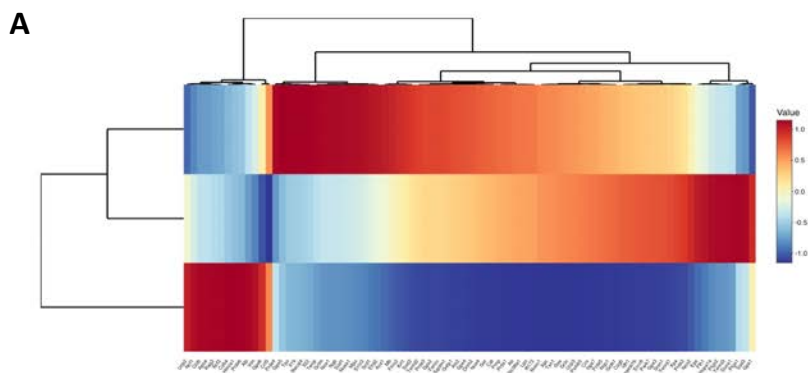
To further assess microglial activation, we measured anti-inflammatory (M2) markers of the microglial phenotype such as *chitinase-like 3* (*Ym1*), *Arginase-1* (*Arg1*), and neurotrophins gene expression. Interestingly, 5XFAD mice showed higher expression levels of *Ym1* compared to WT mice, which may indicate a possible compensatory mechanism (**Fig. 3i**). Besides, results revealed a significant anti-inflammatory effect after UB-ALT-EV treatment in 5XFAD mice, whereas memantine treatment did not induce changes (**Fig. 3i,j**). Furthermore, microglial cells could affect neuronal plasticity by releasing neurotrophic factors³². Thus, we found that after UB-ALT-EV administration, *Bdnf*, *Ngf* and *Vgf* gene expression in 5XFAD increased significantly, being like the levels exhibited by WT mice, whereas for memantine, only *Bdnf* gene expression was increased (**Fig. 3k,l,m**). These results revealed the robust neuroprotective efficacy of UB-ALT-EV compared to memantine. Finally, we investigated the association between microglial activation and OS through *iNOS* gene expression. Interestingly, we observed that only the UB-ALT-EV treated group could reduce *iNOS* gene expression (**Fig. 3n**).

2.6. UB-ALT-EV treatment regulates genes associated with OS response in 5XFAD mice

We then sought further to investigate the OS response following treatment with UB-ALT-EV. First, we determined the expression profile of OS-associated genes in the UB-ALT-EV-treated 5XFAD mice, whereby we carried out a qPCR array containing 84 OS-related genes. Clustering analysis revealed three gene clusters (**Fig. 4a**). After function and process pathway analysis by using the GO database, we found that cluster 1 functional enrichment is mainly associated with superoxide activity (GO:0016175), and oxidoreductase activity (GO:0016491) (Table 1, and **Supplementary Fig. 1**). Likewise, the process enrichment is associated with superoxide processes and response to OS (**Supplementary Fig. 1**). The changes in *Aox1* and *Gpx6* gene expression found were also validated for

UB-ALT-EV group but nor for memantine (**Fig. 4b,c,d**). Cluster 2 is functional associated with antioxidant (GO:0016209), oxidoreductase (GO:0016491) and peroxidase (GO:0004601) activities (Table 2, and **Supplementary Fig. 1**), partially validated through *Ncf1* and *Vim* for both NMDAR antagonist treatments (**Fig. 4e,f,g**). Besides, the GO enrichment process showed modulation associated with response to OS, stress and ROS metabolic process (**Supplementary Fig. 1**). Finally, cluster 3 is associated with cytokine activity (GO:0005125) in functional enrichment analysis and mainly associated with ROS metabolic as well as IL-6 production in process enrichment (Table 3, and **Supplementary Fig. 1**), and it was only validated through *Il-19* and *Il-22* in UB-ALT-EV treated mice group (**Fig. 4h,i,j**). Additionally, KEGG analysis for cluster 1 demonstrated alterations in the phagosome, and AD pathways, among others. Regarding KEGG analysis for cluster 2, we found enrichment associated with tyrosine and glutathione metabolisms, longevity regulating pathway, among others (**Supplementary Fig. 1**). By last, KEGG analysis for cluster 3 demonstrated the association with cytokine-cytokine receptor interaction and some inflammatory pathways (**Supplementary Fig. 1**).

On the other hand, using the TRRUST database, we found that some genes present in cluster 1, 2 and 3 can be regulated by NF-kB and REL (**Supplementary Table 2**), two subunits of the transcription factor NF-kB, suggesting that NF-kB modulates the neuroinflammatory process in the 5XFAD model after UB-ALT-EV treatment. Therefore, these results suggest that treatment with UB-ALT-EV in 5XFAD reverses the OS process, affecting the neuroinflammation and vice versa in a better way than memantine treatment.



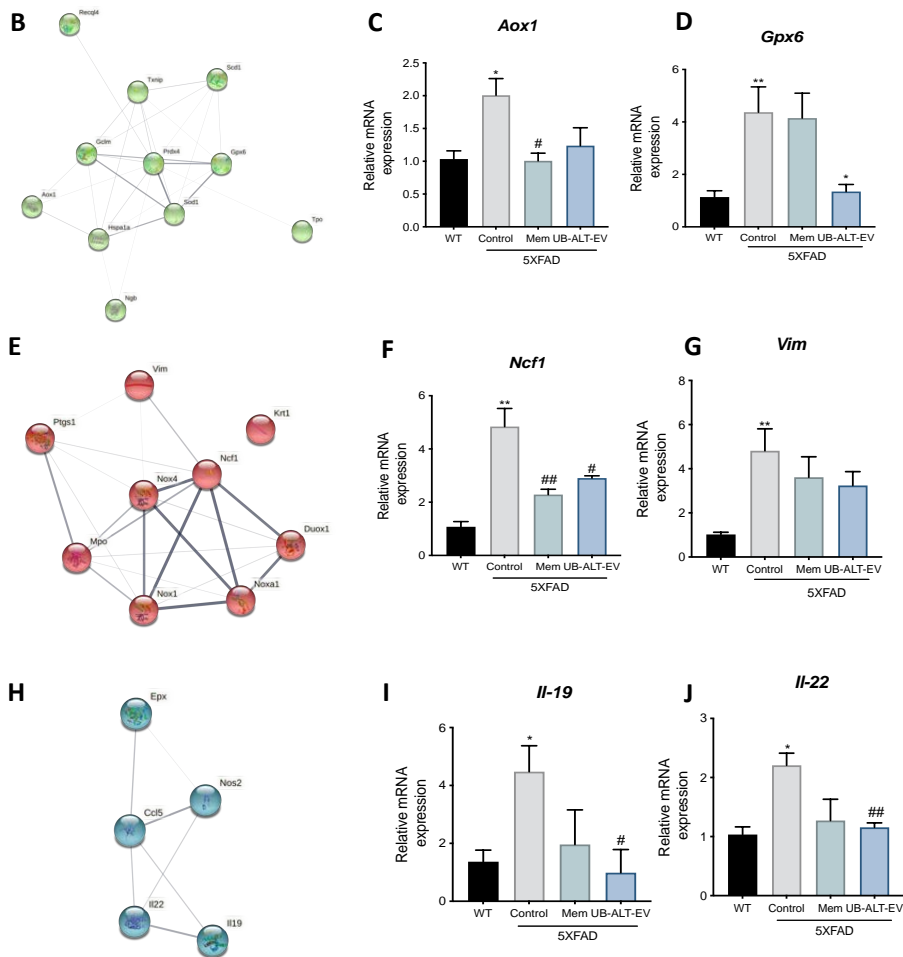


Fig. 4. qPCR analysis of 84 OS-related gene expression after a treatment with NMDA receptor antagonists in 6-month-old 5XFAD mice. Hierarchical clustering of the qPCR array in WT and 5XFAD mice treated with UB-ALT-EV (a). The predicted protein-protein interactions analysis are shown (b,e,h). Validation of representative subset of genes. Gene expression of *Aox1* (a), *Gpx6* (b), *Ncf1* (f), *Vim* (g), *Il-19* (i), and *Il-22* (j) in the hippocampus of WT and 5XFAD mice groups. Gene expression were determined by qPCR. Values are the mean \pm Standard error of the mean (SEM); (n = 3 for WT and Control groups and n = 4 for Mem and UB-ALT-EV groups). For WT vs. 5XFAD Control groups data was analyzed using a two-tail Student's t-test, and for 5XFAD groups a standard one-way ANOVA followed by Tukey post-hoc analysis was performed. * $p < 0.05$; ** $p < 0.01$; *** $p < 0.001$; **** $p < 0.0001$ for WT vs. Control. # $p < 0.05$; ### $p < 0.001$ for Mem or UB-ALT-EV vs. Control.

3. DISCUSSION

Based on our previous studies demonstrating the promising role of UB-ALT-EV, an NMDA antagonist, against neurodegeneration²⁸, we hypothesized that this new compound could have an additional therapeutic role in neuroinflammation, a relevant key mechanism in the onset of AD, apart from the canonical calcium signaling regulation mediated by NMDA antagonists. We found that UB-ALT-EV promoted neuroprotection by modifying neuroinflammation, reducing glial activation via microglial response modulation. Moreover, UB-ALT-EV exhibited a relevant role in the reduction of the OS state, due to the up-regulation of anti-inflammatory mediators in an AD mouse model (5XFAD).

Brain inflammation is a defense mechanism with a neuroprotective effect against injury and infection, and in early degenerative stages, there is a balance between proinflammatory and anti-inflammatory responses³³. However, there appears to be a shift from resting microglia to classically activated microglia in AD, impairing the cytokine balance that ultimately leads to a chronic neuroinflammatory environment³⁴. Otherwise, there are several pathways by which Ca^{2+} dysregulation can be linked to releasing cytokines that promote neuroinflammation. In particular, the CaN/NFAT pathway has been associated with Ca^{2+} dysregulation and glial activation³⁵. The increase in the dephosphorylated form of the transcription factor NFATc1 reflects an increase in its nuclear translocation and fosters a chronic inflammatory state, synapse dysfunction and glutamate dysregulation³⁶. CaN, as a phosphatase, can dephosphorylate NFAT allowing its nuclear translocation and the activation of cytokines transcription. These observations are consistent with several published reports showing high CaN and NFAT protein levels in 5XFAD³⁰. However, to our knowledge, the effect of NMDAR blockage on CaN/NFAT pathway remains unknown. In our study, we found that both NMDAR antagonists tested, memantine and UB-ALT-EV reduced CaN protein levels but only UB-ALT-EV significantly increased p-NFATc1/NFAT protein level ratio. Therefore, these results suggest the implication of UB-ALT-EV in preventing the production of several proinflammatory cytokines regulated by CaN/NFAT signaling pathway, and likewise a diminution in gliosis phenomena.

In the light of our findings, we further explored astrocyte activation by evaluating GFAP protein levels in the hippocampus. As expected, an up-regulation of GFAP protein was observed in the hippocampus of 5XFAD mice³⁷⁻³⁹. Memantine significantly reduced GFAP protein levels in the dentate gyrus, while UB-ALT-EV delivered similar results. In addition, UB-ALT-EV treatment significantly

reduced total GFAP protein content, probably because the reduction in global astroglial activation was greater after UB-ALT-EV treatment than with memantine.

Microglial activation is known to be divided into two phenotypic profiles: the proinflammatory (M1) and the anti-inflammatory (M2)⁴⁰. In AD, there is an altered homeostasis between the two microglial phenotypes, and a cytokine-dominated inflammatory landscape occurs, enhancing the shift to the M1 phenotype over M2⁴¹. Therefore, to pursue the inflammatory process accounting in 5XFAD mice model, the microglial status was evaluated through Iba-1 and *Trem2*. According to the literature, increases in Iba-1 were found in 5XFAD mice³⁷. Strikingly, we observed a reduction in Iba-1 staining in 5XFAD hippocampus treated with NMDAR antagonists, specifically in the CA3 region^{26,42}. TREM2, a cell surface receptor that is mainly expressed in microglial cells⁴³, is relevant in the phagocytic role of microglia, constituting a key mediator against A β deposition⁴⁴. As a consequence of glial activation in 5XFAD mice, an up-regulation of the *Trem2* gene expression accounted³⁷. Interestingly, we found that UB-ALT-EV but not memantine induced changes in *Trem2* gene expression, suggesting a novel anti-inflammatory effect of UB-ALT-EV by preventing microglial activation. In line with our results, a recent study in microglial cells demonstrated that TREM2 levels were unchanged after memantine pretreatment⁴⁵.

NF- κ B is also a CaN-sensitive transcription factor implicated in the proinflammatory phenotype (M1) of glial activation⁴⁶. Recent studies reported the NF- κ B inhibition by memantine indicating that NF- κ B signaling can be regulated after NMDARs^{47,48}. Here, we found an unexpected up-regulation of NF- κ B in the 5XFAD memantine-treated group, being downregulated in the case of UB-ALT-EV treatment, accordingly with arrays results by the TRRUST analysis. Thus, these results indicated a different modulation of the inflammatory process by the two NMDARs antagonist tested.

To delve further into these findings, several proinflammatory cytokines associated with M1 phenotype were evaluated. Interestingly, *Ifn- γ* , *Il-1 β* , *Ccl2* and *Ccl3* gene expression was reduced only by UB-ALT-EV in the 5XFAD group correlating with reduced NF- κ B protein levels. Of note, the anti-inflammatory activated microglia (M2) phenotype can contribute to neuronal plasticity by also expressing neurotrophic factors^{40,41,46}. Here, when M2 microglial state was assessed in 5XFAD mice, UB-ALT-EV treatment induced not only up-regulation of *Ym1* and *Arg1* gene expression but also the up-regulation of several neurotrophins such as

Bdnf, *Ngf* and *Vgf*, involved in neuroprotection⁴⁹, whereas memantine only induced the expression of *Bdnf*, indicating the improved capacity of UB-ALT-EV to promote neuroprotective effects. Consistent with these findings, we previously demonstrated improvements in the reduction of A β deposition, tau hyperphosphorylation, and autophagic processes after UB-ALT-EV treatment compared to the memantine group²⁸.

Lastly, we found that *iNOS* gene expression was modulated in a significant way by UB-ALT-EV, and weakly by memantine. iNOS is an enzyme implicated both in the control of inflammatory mediators' release, but also in the generation of ROS that contributes to neuronal damage and AD progression¹⁷. Besides, it is well-established that neuroinflammation can induce OS, and vice versa, by activating multiple pathways. Then, we evaluated the implication of OS modulation in the neuroprotective effects of UB-ALT-EV by using a qPCR array determination of the 84 genes associated with OS signaling pathways. After analysis, we found that UB-ALT-EV changed the gene expression of 24 genes in 5XFAD, generating three hierarchical clusters based on the enrichment heatmap. Remarkably, our results showed alterations in GO enrichment analysis in processes associated with superoxide-generating NADPH oxidase activity (Cluster 1), cytokine activity (Cluster 2), and antioxidant activity (Cluster 3), among others. KEGG pathways are also related to OS and inflammation, among others. Furthermore, we were able to validate that the gene expression of *Il-19*, *Il-22*, *Gpx6*, and *Ncf1* were significantly reduced in 5XFAD treated mice, and a clear tendency was observed for *Aox1* and *Vim*. Gene array validation indicated a better modulation of UB-ALT-EV than memantine, for both OS and inflammatory pathways, thus demonstrating optimization of the efficacy of the NMDAR antagonist.

Overall, our results highlighted that the treatment with UB-ALT-EV changes the inflammatory landscape in 5XFAD mice, suggesting an attenuation of M1 phenotype activated microglia. Besides, anti-inflammatory effects were accompanied by OS changes. These beneficial effects were not so clear in 5XFAD treated with memantine, indicating additional pharmacological activities of UB-ALT-EV, which were also found in previous studies²⁸. Thus, the optimized NMDARs antagonist, UB-ALT-EV, offers a new opportunity for the treatment of AD, showing novel neuroprotective mechanisms including the reduction of proinflammatory microglial markers and the amelioration of astrocyte activation, additionally to calcium entry blockage (**Fig. 5**).

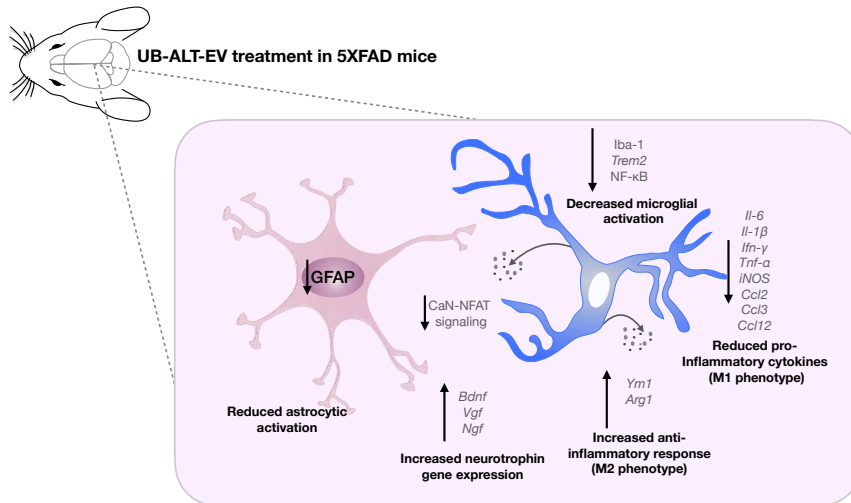


Fig. 5. Illustrative cartoon of effects of UB-ALT-EV in 6-months-old 5XFAD mice in oxidative and neuroinflammatory pathology.

4. MATERIALS AND METHODS

4.1. Animals and treatment

Six-month-old female 5XFAD mice ($n = 29$) and wild type (WT) ($n = 14$) mice were randomly allocated to experimental groups and divided into four groups: WT control and 5XFAD control, administrated with vehicle ((2-hydroxypropyl)- β -cyclodextrin 1.8 %) and 5XFAD treated with memantine, or UB-ALT-EV (5mg/kg/day) dissolved in vehicle. The sample size for the intervention was chosen following previous studies in our laboratory and using one of the available interactive tools (<http://www.biomath.info/power/index.html>) that is designed to estimate the required sample size to achieve adequate power. Compounds were administered through drinking water for 4 weeks and the doses of each cage were weekly re-calculated taking into account the daily water consumption in each cage and monitoring the body weight of the animals. Animals had free access to food and water and were maintained under standard temperature conditions (22 ± 2 °C) and 12 h: 12 h light-dark cycles (300 lux/0 lux). Water consumption was monitored weekly, and both NMDAR antagonist concentrations were adjusted in the tap water bottle to achieve the precise dose.

Research was conducted in accordance with the Institutional Guidelines for the Care and Use of Laboratory Animals established by (European Communities Council Directive 2010/63/EU and Guidelines for the Care and Use of Mammals

in Neuroscience and Behavioural Research, National Research Council 2003) and approved by the Ethics Committee for Animal Experimentation (CEEA) of the University of Barcelona. All experimental procedures with mice followed the recommendations in the ARRIVE guidelines. All possible efforts were taken to reduce the number of animals and their suffering.

4.2. RNA extraction and gene expression determination

Mice were euthanized by cervical dislocation after the treatment period. The brains were immediately removed from the skulls, and the hippocampus were dissected, frozen and maintained at $-80\text{ }^{\circ}\text{C}$. Total RNA isolation from hippocampal samples was performed using the TRIzol[®] reagent according to the manufacturer's instructions (Bioline Reagent). The yield, purity and quality of RNA were determined spectrophotometrically with a NanoDrop[™]ND-1000 apparatus (Thermo Scientific) and an Agilent 2100B Bioanalyzer (Agilent Technologies). RNA samples with 260/280 ratios higher than 1.9 were selected. Reverse Transcription-Polymerase Chain Reaction (RT-PCR) was performed. Briefly, 1 μg and 2 μg of messenger RNA (mRNA) was reverse transcribed using a high-capacity cDNA reverse transcription kit (Applied Biosystems) for PCR Array performance and q-PCR validation, respectively. Genes are listed in **Supplementary Table 1**.

SYBR[®] Green real-time PCR was performed on a Step One Plus Detection System (Applied-Biosystems) employing SYBR[®] Green PCR Master Mix (Applied-Biosystems). Each reaction mixture contained 6.75 μL of complementary DNA (cDNA) (which concentration was 2 μg), 0.75 μL of each primer (which concentration was 100 nM), and 6.75 μL of SYBR[®] Green PCR Master Mix (2X). Data were analyzed utilizing the comparative Cycle threshold (Ct) method ($\Delta\Delta\text{Ct}$), where the housekeeping gene level was used to normalize differences in sample loading and preparation. Normalization of expression levels was performed with *β -actin* for SYBR[®] Green-based real-time PCR results. Each sample was analyzed in duplicate, and the results represent the n-fold difference of the transcript levels among different groups.

4.3. Real-time quantitative PCR Array

Real-time quantitative PCR array containing 84 oxidative stress-related genes (qPCR Sign Arrays 96 system, AnyGenes, Paris, France) was used for screening according to the instructions of the manufacturer. Briefly, 2 μL of diluted cDNA pooled samples (n=3-4) (2 μg cDNA diluted at the 1/12 from Reverse

Transcription (20 μ L) performed with 1 μ g of RNA) was mixed with 10 μ l of 2X Perfect Master Mix SYBR Green and 8 μ L Ultra-pure H₂O and added to each well, being consequently the total reaction volume 20 μ L per well. After 20 μ L of the reaction mix was in each well of the 96-well plate, the plate was centrifuged and then the qPCR run was performed using a Step One Plus Detection System (Applied-Biosystems), following the manufacturer's recommendations and protocols. PCR reaction conditions were 95 °C, 10 min; 95 °C, 5 s and 60 °C, 30 s, \times 40 cycles. After completion of the reaction, the melting curve was analyzed, 95 °C, 10 s, 65 °C-95 °C, 30 s.

4.4. Hierarchical clustering

Hierarchical clustering was carried out with the genes screened on the qPCR Sign Arrays 96 system to assess the expression profile among the study groups. Genes were grouped into three clusters based on the expression profile using the R package pheatmap. Expression data were then clustered by Euclidean distances between genes and by applying the complete hierarchical clustering method.

4.5. Protein-protein interaction network and functional annotation

We conducted protein-protein interaction networks using the STRING database⁵⁰. A PPI enrichment p-value <0.001 was taken as statistically significant, indicating that proteins are at least partially biologically connected. To establish the functional annotation of the three groups, we identified the Gene Ontology (GO) and undertook pathway analysis with the Kyoto Encyclopedia of Genes and Genomes (KEGG), by using the Database for Annotation, Visualisation and Integrated Discovery (DAVID)⁵¹. GO terms and KEGG pathways with an adjusted p-value <0.05 were taken as statistically significant. We used the KEGG mapping tool to show downregulated (green) and up-regulated (red) genes in the KEGG pathway maps⁵². To assess transcriptional regulatory interactions between the three gene clusters and mouse transcriptional factors (TFs), we used the TRRUST database⁵³. TRRUST identifies potential TFs involved in the regulation of genes of interest. TFs with an adjusted p-value<0.05 were considered statistically significant.

4.6. Protein Level Determination by Western Blotting

For western blot analyses, mice were euthanized by cervical dislocation and the brains were removed immediately from the skull. The hippocampus was then excised and frozen in powdered dry ice. They were kept at -80 °C for subsequent

use in protein extraction. For protein extraction, tissue samples were homogenized in lysis buffer containing phosphatase and protease inhibitors (Cocktail II, Sigma-Aldrich). Total protein levels were extracted, protein concentration was determined by Bradford's method and 15 µg samples were separated by sodium dodecyl sulphate-polyacrylamide dodecyl sulphate gel electrophoresis (SDS-PAGE) (8-20%). After transfer to polyvinylidene difluoride (PVDF) membranes (Millipore), the membranes underwent blocking in 5% nonfat milk in Tris-buffered saline (TBS) containing 0.1% Tween 20 TBS (TBS-T) for 1 hour at room temperature (RT), which was followed by overnight incubation at 4°C with the primary antibodies: NFATc1 (St John's/STJ24751) diluted 1:1000; p-NFAT (Ser172) (Invitrogen/PA5-64696) diluted 1:500; Calcineurin (BioRad/VPA00329) diluted 1:1000; Glyceraldehyde-3-Phosphate Dehydrogenase (Millipore/MAB374) diluted 1:5000; GFAP (Gene Tex/GTX100850) diluted 1:1000; NF-κB (Cell signaling/8242S) diluted 1:1000; Goat-anti-mouse HRP conjugated (Biorad Lab 170-5047) diluted 1:6000 and Goat-anti-rabbit HRP conjugated (Biorad Lab/170-6515) diluted 1:6000. The membranes were then washed and incubated with secondary antibodies for 1 hour at RT. Immunoreactive proteins were imaged with the chemiluminescence-based detection kit, following the manufacturer's protocol (ECL Kit, Millipore), and digital images were then acquired using the ChemiDoc XRS+ system (BioRad). Semi-quantitative analyses were conducted using ImageLab software (BioRad), and results were extracted in arbitrary units (AU), considering control protein levels as 100%. Protein loading was routinely controlled by immunodetection of glyceraldehyde-3-phosphate dehydrogenase (GAPDH).

4.7. Immunofluorescence assay

For immunofluorescence, mice were anesthetized (ketamine 100 mg/kg and xylazine 10 mg/kg, intraperitoneally) and then intracardially perfused with 4% paraformaldehyde (PFA) diluted in 0.1 M phosphate buffer solution. The brains were removed and post-fixed in 4% PFA overnight at 4 °C. Thereafter, the brains were changed to PFA + 15% sucrose. Finally, brains were frozen in powdered dry ice and stored at -80°C until sectioning. Coronal brain sections of 30 µm were obtained (Leica Microsystems CM 3050S cryostat, Wetzlar, Germany) and stored in cryoprotective solution at -20°C until used.

Free-floating brain slices were washed 5 min in PBS and blocked and permeabilized in PBS, BSA 1% and 0,3% Triton X-100 solution for 20 min. After two washes of 5 min with PBS (0,1M), primary antibody (GFAP (Dako/Z0334) or Iba-1 (Abcam/ab48050) , were incubated over-night at 4°C at a dilution of

1:400. The following day, after two washes with PBS, the secondary antibody (Alexa Fluor[®] 594, Abcam/ab150080) was incubated at room temperature for 1h in the dark at a dilution of 1:400. Later, sections were co-incubated with 1mg/ml Hoechst (Sigma[®]) staining solution for 5 min in the dark at room temperature and washed twice for 5 min in PBS. Finally, the slices were mounted with Fluoromount G (EMS, USA).

4.8. Image acquisition and analysis

Acquisition of images was conducted with a fluorescence laser microscope (Olympus BX51, Germany). At least 3 images from 4 different individuals per group were analyzed with ImageJ/Fiji software from the National Institutes of Health available online. For the acquisition of glial fibrillary acidic protein (GFAP) and Iba-1 images, a fixed exposure was maintained for all samples in all the experiments. Fluorescence intensity of GFAP and Iba-1 positive cells was measured in different areas of the hippocampus (CA1, CA3 and dentate gyrus) and the quantification was then averaged from each subject's three different sections.

4.9. Data Acquisition and Statistical Analysis

Data analysis was conducted using GraphPad Prism ver. 9 statistical software. Data are expressed as the mean \pm standard error of the mean (SEM) of at least 3 samples per group. Strain was compared using the two tail Student's t-test to evaluate differences between WT vs. 5XFAD control group. For 5XFAD mice One-way analysis of variance (ANOVA) was followed by Tukey post-hoc analysis or two-tail Student's t-test when necessary. Statistical significance was considered when p-values were <0.05 . The statistical outliers were determined with Grubbs' test and, when necessary, were removed from the analysis.

5. REFERENCES

1. Wang, R. & Reddy, P. H. Role of Glutamate and NMDA Receptors in Alzheimer's Disease. *J. Alzheimer's Dis.* **57**, 1041–1048 (2017).
2. Bliss, T. V. P. & Collingridge, G. L. A synaptic model of memory: long-term potentiation in the hippocampus. *Nature* **361**, 31–39 (1993).
3. Cotman, C. W., Geddes, J. W., Bridges, R. J. & Monaghan, D. T. N-methyl-D-aspartate receptors and Alzheimer's disease. *Neurobiol. Aging* **10**, 603–620 (1989).

4. Talantova, M. *et al.* A β induces astrocytic glutamate release, extrasynaptic NMDA receptor activation, and synaptic loss. *Proc. Natl. Acad. Sci. U. S. A.* **110**, E2518-27 (2013).
5. Sattler, R. & Tymianski, M. Molecular mechanisms of glutamate receptor-mediated excitotoxic neuronal cell death. *Mol. Neurobiol.* **24**, 107–129 (2001).
6. Uttara, B., Singh, A. V, Zamboni, P. & Mahajan, R. T. Oxidative stress and neurodegenerative diseases: a review of upstream and downstream antioxidant therapeutic options. *Curr. Neuropharmacol.* **7**, 65–74 (2009).
7. Vesce, S., Rossi, D., Brambilla, L. & Volterra, A. Glutamate Release from Astrocytes in Physiological Conditions and in Neurodegenerative Disorders Characterized by Neuroinflammation. in *Neuroinflammation in Neuronal Death and Repair* **82**, 57–71 (Academic Press, 2007).
8. Reynolds, A., Laurie, C., Lee Mosley, R. & Gendelman, H. E. Oxidative Stress and the Pathogenesis of Neurodegenerative Disorders. in *Neuroinflammation in Neuronal Death and Repair* **82**, 297–325 (Academic Press, 2007).
9. Kinney, J. W. *et al.* Inflammation as a central mechanism in Alzheimer's disease. *Alzheimer's Dement. (New York, N. Y.)* **4**, 575–590 (2018).
10. Sompol, P. & Norris, C. M. Ca²⁺, Astrocyte Activation and Calcineurin/NFAT Signaling in Age-Related Neurodegenerative Diseases. *Front. Aging Neurosci.* **10**, (2018).
11. Kraner, S. D. & Norris, C. M. Astrocyte Activation and the Calcineurin/NFAT Pathway in Cerebrovascular Disease. *Front. Aging Neurosci.* **10**, 287 (2018).
12. Singh, S. & Singh, T. G. Role of Nuclear Factor Kappa B (NF- κ B) Signalling in Neurodegenerative Diseases: An Mechanistic Approach. *Curr. Neuropharmacol.* **18**, 918–935 (2020).
13. Leng, F. & Edison, P. Neuroinflammation and microglial activation in Alzheimer disease: where do we go from here? *Nat. Rev. Neurol.* **17**, 157–172 (2021).
14. Ray, P. D., Huang, B.-W. & Tsuji, Y. Reactive oxygen species (ROS) homeostasis and redox regulation in cellular signaling. *Cell. Signal.* **24**, 981–990 (2012).
15. Kim, T.-S. *et al.* Decreased plasma antioxidants in patients with Alzheimer's disease. *Int. J. Geriatr. Psychiatry* **21**, 344–348 (2006).
16. Schipper, H. M. *et al.* Glial heme oxygenase-1 expression in Alzheimer disease and mild cognitive impairment. *Neurobiol. Aging* **27**, 252–261 (2006).

17. Galea, E., Feinstein, D. L. & Reis, D. J. Induction of calcium-independent nitric oxide synthase activity in primary rat glial cultures. *Proc. Natl. Acad. Sci. U. S. A.* **89**, 10945–10949 (1992).
18. Ramos-González, E. J., Bitzer-Quintero, O. K., Ortiz, G., Hernández-Cruz, J. J. & Ramírez-Jirano, L. J. Relationship between inflammation and oxidative stress and its effect on multiple sclerosis. *Neurología* (2021). doi:<https://doi.org/10.1016/j.nrl.2021.10.003>
19. Owen, R. T. Memantine and donepezil: a fixed drug combination for the treatment of moderate to severe Alzheimer's dementia. *Drugs Today (Barc)*. **52**, 239–248 (2016).
20. Raina, P. *et al.* Effectiveness of Cholinesterase Inhibitors and Memantine for Treating Dementia: Evidence Review for a Clinical Practice Guideline. *Ann. Intern. Med.* **148**, 379–397 (2008).
21. Martorana, A., Esposito, Z. & Koch, G. Beyond the Cholinergic Hypothesis: Do Current Drugs Work in Alzheimer's Disease? *CNS Neurosci. Ther.* **16**, 235–245 (2010).
22. Tagliavini, F., Tiraboschi, P. & Federico, A. Alzheimer's disease: the controversial approval of Aducanumab. *Neurol. Sci.* **42**, 3069–3070 (2021).
23. Mahase, E. FDA approves controversial Alzheimer's drug despite uncertainty over effectiveness. *BMJ* **373**, n1462 (2021).
24. Cosman, K. M., Boyle, L. L. & Porsteinsson, A. P. Memantine in the treatment of mild-to-moderate Alzheimer's disease. *Expert Opin. Pharmacother.* **8**, 203–214 (2007).
25. Matsunaga, S. *et al.* The efficacy and safety of memantine for the treatment of Alzheimer's disease. *Expert Opin. Drug Saf.* **17**, 1053–1061 (2018).
26. Wu, H.-M. *et al.* Novel neuroprotective mechanisms of memantine: increase in neurotrophic factor release from astroglia and anti-inflammation by preventing microglial activation. *Neuropsychopharmacol. Off. Publ. Am. Coll. Neuropsychopharmacol.* **34**, 2344–2357 (2009).
27. Reisberg, B. *et al.* Memantine in moderate-to-severe Alzheimer's disease. *N. Engl. J. Med.* **348**, 1333–1341 (2003).
28. Turcu, A. L. *et al.* Design, synthesis, and in vitro and in vivo characterization of new memantine analogs for Alzheimer's Disease. *Eur. J. Med. Chem.* **236**, 114354 (2022).
29. Oakley, H. *et al.* Intraneuronal β -amyloid aggregates, neurodegeneration, and neuron loss in transgenic mice with five familial Alzheimer's disease mutations: Potential factors in amyloid plaque formation. *J. Neurosci.* **26**, 10129–10140 (2006).
30. Sompol, P. *et al.* Calcineurin/NFAT Signaling in Activated Astrocytes

- Drives Network Hyperexcitability in A β -Bearing Mice. *J. Neurosci.* **37**, 6132 LP – 6148 (2017).
31. Akhtar, F. *et al.* Acute maternal oxidant exposure causes susceptibility of the fetal brain to inflammation and oxidative stress. *J. Neuroinflammation* **14**, 195 (2017).
 32. Wadhwa, M. *et al.* Inhibiting the microglia activation improves the spatial memory and adult neurogenesis in rat hippocampus during 48 h of sleep deprivation. *J. Neuroinflammation* **14**, 222 (2017).
 33. Kwon, H. S. & Koh, S.-H. Neuroinflammation in neurodegenerative disorders: the roles of microglia and astrocytes. *Transl. Neurodegener.* **9**, 42 (2020).
 34. Wang, Q. *et al.* Microglia Polarization in Alzheimer's Disease: Mechanisms and a Potential Therapeutic Target. *Front. Aging Neurosci.* **13**, 772717 (2021).
 35. Furman, J. L. & Norris, C. M. Calcineurin and glial signaling: Neuroinflammation and beyond. *J. Neuroinflammation* **11**, 1–12 (2014).
 36. Reese, L. C. & Taglialetela, G. Neuroimmunomodulation by calcineurin in aging and Alzheimer's disease. *Aging Dis.* **1**, 245–253 (2010).
 37. Vasilopoulou, F. *et al.* Disease-modifying treatment with I₂ imidazoline receptor ligand LSL60101 in an Alzheimer's disease mouse model: a comparative study with donepezil. *Br. J. Pharmacol.* **178**, 3017–3033 (2021).
 38. Belaya, I. *et al.* Astrocyte remodeling in the beneficial effects of long-term voluntary exercise in Alzheimer's disease. *J. Neuroinflammation* **17**, 271 (2020).
 39. Iram, T. *et al.* Astrocytes from old Alzheimer's disease mice are impaired in A β uptake and in neuroprotection. *Neurobiol. Dis.* **96**, 84–94 (2016).
 40. Zhang, L., Zhang, J. & You, Z. Switching of the Microglial Activation Phenotype Is a Possible Treatment for Depression Disorder. *Front. Cell. Neurosci.* **12**, 306 (2018).
 41. Cherry, J. D., Olschowka, J. A. & O'Banion, M. K. Neuroinflammation and M2 microglia: the good, the bad, and the inflamed. *J. Neuroinflammation* **11**, 98 (2014).
 42. Qiu, L.-L. *et al.* Dysregulation of BDNF/TrkB signaling mediated by NMDAR/Ca(2+)/calpain might contribute to postoperative cognitive dysfunction in aging mice. *J. Neuroinflammation* **17**, 23 (2020).
 43. Guerreiro, R. J. *et al.* Using exome sequencing to reveal mutations in TREM2 presenting as a frontotemporal dementia-like syndrome without bone involvement. *JAMA Neurol.* **70**, 78–84 (2013).
 44. Wang, Y. *et al.* TREM2 lipid sensing sustains the microglial response in an

- Alzheimer's disease model. *Cell* **160**, 1061–1071 (2015).
45. Murakawa-Hirachi, T., Mizoguchi, Y., Ohgidani, M., Haraguchi, Y. & Monji, A. Effect of memantine, an anti-Alzheimer's drug, on rodent microglial cells in vitro. *Sci. Rep.* **11**, 6151 (2021).
 46. Huang, M. *et al.* Paraquat modulates microglia M1/M2 polarization via activation of TLR4-mediated NF- κ B signaling pathway. *Chem. Biol. Interact.* **310**, 108743 (2019).
 47. Alomar, S. Y. *et al.* Novel Mechanism for Memantine in Attenuating Diabetic Neuropathic Pain in Mice via Downregulating the Spinal HMGB1/TRL4/NF- κ B Inflammatory Axis. *Pharmaceuticals* **14**, (2021).
 48. Wang, F. *et al.* Regulation of Human Brain Microvascular Endothelial Cell Adhesion and Barrier Functions by Memantine. *J. Mol. Neurosci.* **62**, 123–129 (2017).
 49. Skaper, S. D. The neurotrophin family of neurotrophic factors: an overview. *Methods Mol. Biol.* **846**, 1–12 (2012).
 50. Szklarczyk, D. *et al.* The STRING database in 2021: customizable protein-protein networks, and functional characterization of user-uploaded gene/measurement sets. *Nucleic Acids Res.* **49**, D605–D612 (2021).
 51. Dennis, G. *et al.* DAVID: Database for Annotation, Visualization, and Integrated Discovery. *Genome Biol.* **4**, R60 (2003).
 52. Dai, Z. *et al.* Gene expression profiles and pathway enrichment analysis of human osteosarcoma cells exposed to sorafenib. *FEBS Open Bio* **8**, 860–867 (2018).
 53. Han, H. *et al.* TRRUST v2: an expanded reference database of human and mouse transcriptional regulatory interactions. *Nucleic Acids Res.* **46**, D380–D386 (2018).

Acknowledgements

This study was supported by Ministerio de Economía y Competitividad of Spain and FEDER (PID2019-106285RB; PDC2021-121096), María de Maeztu Unit of Excellence (Institute of Neurosciences, University of Barcelona) MDM-2017-0729 and 2017SGR106 (AGAUR, Catalonia). J.C.-A. acknowledge Ministry of Economy and Competitiveness (MINECO) for her FPI (MDM-2017-0729) fellowship. A.L.T. acknowledges a PhD fellowship (FPU grant) from the *Spanish Ministerio de Educación, Cultura y Deporte*.

Author contributions

C.G.-F. and M.P. conceived the idea. J.C.-A. and C.G.-F. designed the experiments. A.L.T. and S.V. synthesized and purified the compounds. J.C.-A.

carried out the experiments. J.C.-A. and C.G.-F. analysed the data. The first draft of the manuscript was written by J.C.-A. C.G.-F., M.P. and J.C.-A. wrote the definitive manuscript with feedback from all the authors and all authors commented on previous versions of the manuscript. All authors read and approved the final version of the manuscript.

Table 1. Function and process pathway analysis by using the GO data base of cluster 1

#term ID	description	observed gene count	background gene count	strength	false discovery rate	matching proteins in your network (IDs)	matching proteins in your network (labels)
GO:0016175	Superoxide-generating nad(ph) oxidase activity	3	8	2.96	4.04e-05	10090.ENSMUSP00000016094, 10090.ENSMUSP00000032781, 10090.ENSMUSP00000033610	<i>Ncf1, Nox4, Nox1</i>
GO:0016176	Superoxide-generating nadph oxidase activator activity	2	8	2.79	0.0070	10090.ENSMUSP00000016094, 10090.ENSMUSP00000037423	<i>Ncf1, Noxa1</i>
GO:0016491	Oxidoreductase activity	5	710	1.24	0.0070	10090.ENSMUSP00000016094, 10090.ENSMUSP00000020779, 10090.ENSMUSP00000032781, 10090.ENSMUSP00000033610, 10090.ENSMUSP00000059977	<i>Ncf1, Mpo, Nox4, Nox1, Ptgs1</i>
GO:0016174	NAD(P)H oxidase H2O2-forming activity	2	9	2.74	0.0071	10090.ENSMUSP00000032781, 10090.ENSMUSP00000033610	<i>Nox4, Nox1</i>
GO:0006801	Superoxide metabolic process	5	33	2.57	2.53e-08	10090.ENSMUSP00000016094, 10090.ENSMUSP00000020779, 10090.ENSMUSP00000032781, 10090.ENSMUSP00000033610, 10090.ENSMUSP00000037423	<i>Ncf1, Mpo, Nox4, Nox1, Noxa1</i>
GO:0042554	Superoxide anion generation	4	13	2.88	2.66e-07	10090.ENSMUSP00000016094, 10090.ENSMUSP00000032781, 10090.ENSMUSP00000033610, 10090.ENSMUSP00000037423	<i>Ncf1, Nox4, Nox1, Noxa1</i>
GO:0006952	Defense response	7	1133	1.18	0.00014	10090.ENSMUSP00000016094, 10090.ENSMUSP00000020779, 10090.ENSMUSP00000023790, 10090.ENSMUSP00000028062, 10090.ENSMUSP00000032781, 10090.ENSMUSP00000033610, 10090.ENSMUSP00000059977	<i>Ncf1, Mpo, Krt1, Vim, Nox4, Nox1, Ptgs1</i>
GO:0042743	Hydrogen peroxide metabolic process	3	33	2.35	0.0012	10090.ENSMUSP00000016094, 10090.ENSMUSP00000020779, 10090.ENSMUSP00000033610	<i>Ncf1, Mpo, Nox1</i>
GO:0002679	Respiratory burst involved in defense response	2	5	2.99	0.0091	10090.ENSMUSP00000016094, 10090.ENSMUSP00000020779	<i>Ncf1, Mpo</i>
GO:0006979	Response to oxidative stress	4	395	1.39	0.0309	10090.ENSMUSP00000016094, 10090.ENSMUSP00000020779, 10090.ENSMUSP00000033610, 10090.ENSMUSP00000059977	<i>Ncf1, Mpo, Nox1, Ptgs1</i>
GO:0001878	Response to yeast	2	14	2.54	0.0310	10090.ENSMUSP00000016094, 10090.ENSMUSP00000020779	<i>Ncf1, Mpo</i>

Table 2. Function and process pathway analysis by using the GO data base of cluster 2.

#term ID	term description	observed gene count	background gene count	Strength	false discovery rate	Matching proteins in your network (IDs)	matching proteins in your network (labels)
GO:0016209	Antioxidant activity	4	70	2.06	0.00020	10090.ENSMUSP00000004453,10090.ENSMUSP00000021005,10090.ENSMUSP00000023707,10090.ENSMUSP00000026328	<i>Gpx6,Tpo,Sod1,Prdx4</i>
GO:0016491	Oxidoreductase activity	6	710	1.23	0.0012	10090.ENSMUSP00000001027,10090.ENSMUSP00000004453,10090.ENSMUSP00000021005,10090.ENSMUSP00000023707,10090.ENSMUSP00000026328,10090.ENSMUSP000000036936	<i>Aox1,Gpx6,Tpo,Sod1,Prdx4,Scd1</i>
GO:0004601	Peroxidase activity	3	40	2.18	0.0020	10090.ENSMUSP00000004453,10090.ENSMUSP00000021005,10090.ENSMUSP00000026328	<i>Gpx6,Tpo,Prdx4</i>
GO:0006979	Response to oxidative stress	6	395	1.48	0.00026	10090.ENSMUSP00000004453,10090.ENSMUSP00000021005,10090.ENSMUSP00000023707,10090.ENSMUSP00000026328,10090.ENSMUSP00000029769,10090.ENSMUSP00000102710	<i>Gpx6,Tpo,Sod1,Prdx4,Gclm,Txnip</i>
GO:0006950	Response to stress	9	3045	0.77	0.0023	10090.ENSMUSP00000004453,10090.ENSMUSP00000021005,10090.ENSMUSP00000023707,10090.ENSMUSP00000026328,10090.ENSMUSP00000029769,10090.ENSMUSP000000036936,10090.ENSMUSP00000044363,10090.ENSMUSP00000084586,10090.ENSMUSP00000102710	<i>Gpx6,Tpo,Sod1,Prdx4,Gclm,Scd1,Recq14,Hspa1a,Txnip</i>
GO:0072593	Reactive oxygen species metabolic process	3	101	1.77	0.0318	10090.ENSMUSP00000021005,10090.ENSMUSP00000023707,10090.ENSMUSP00000026328	<i>Tpo,Sod1,Prdx4</i>

Table 3. Function and process pathway analysis by using the GO data base of cluster 3.

#term ID	term description	observed gene count	background gene count	strength	false discovery rate	matching proteins in your network (IDs)	matching proteins in your network (labels)
GO:005125	Cytokine activity	3	215	1.79	0.0491	10090.ENSMUSP00000039600,10090.ENSMUSP00000094449,10090.ENSMUSP0000108084	<i>Ccl5,Il22,Il19</i>
GO:072593	Reactive oxygen species metabolic process	4	101	2.24	4.23e-05	10090.ENSMUSP00000018610,10090.ENSMUSP00000050497,10090.ENSMUSP00000094449,10090.ENSMUSP0000108084	<i>Nos2,Epx,Il22,Il19</i>
GO:032635	interleukin-6 production	2	12	2.87	0.0327	10090.ENSMUSP00000018610,10090.ENSMUSP00000108084	<i>Nos2,Il19</i>
GO:072677	Eosinophil migration	2	18	2.69	0.0455	10090.ENSMUSP00000039600,10090.ENSMUSP00000050497	<i>Ccl5,Epx</i>

Supplementary Table 1. Primers used in qPCR studies.

Target	Forward primer (5'-3')	Reverse primer 5'-3'
<i>Trem2</i>	CCTGAAGAAGCGGAATGGG	CCTGATTCTGGAGGTGCT
<i>Il-6</i>	ATCCAGTTGCCTCTTGGGACTGA	TAAGCCTCCGACTTGTGAAGTGGT
<i>Il-18</i>	ACAGAATATCAACCAACAAGTGATATTCTC	GATTCTTTCCTTTGAGGCCCA
<i>Ifn-γ</i>	CCTTCTTCAGCAACAGCAAGGCG	CTTGGCGCTGGACCTGTGGG
<i>Tnf-α</i>	TCGGGGTGATCGGTCCCAA	TGGTTTGTACGACGTGGGCT
<i>Ccl2</i>	CCAGCAAGATGATCCAATG	CTTCTTGGGGTCAGCACAGA
<i>Ccl3</i>	TGACCCCAAGGCTCAAATA	CCCAGGTCCTCGTTATGATC
<i>Ccl12</i>	ACACTGGTTCCTGACTCCTCT	ACCTGAGGACTGATGGTGGT
<i>Ym1</i>	GACAGGGCTCCTTTCAGGAC	GCCAAGGTTAAAGCCACTGC
<i>Arg1</i>	GTGGAGAAAGACATTCCAAGGC	CAGTTCAGGGATCCTGTACCCA
<i>Bdnf</i>	GGGAAATCTCCTGAGCCGAG	AGCTTTCTCAACGCCTGTCA
<i>Ngf</i>	GGAGCGCATCGAGTGACTT	CCTCACTGCGGCCAGTATAG
<i>Vgf</i>	GTCAGACCCATAGCCTCCC	CTCGGACTGAAATCTCGAAGTTC
<i>iNOS</i>	GGCAGCCTGAGAGACCTTTG	GGAAGCGTTTTCGGGATCTGAA
<i>Il-19</i>	CACACAAGCTCACTTGCACT	GCAAGAATCTGAGAGGCCGA
<i>Il-22</i>	<i>GTGCGATCTCTGATGGCTGT</i>	GACGATGTATGGCTGCTGGA
<i>Aox1</i>	CATAGGCGGCCAGGAACATT	TCCTCGTCCAGAATGCAGC
<i>Gpx6</i>	GTCACGGTTTTGGGCTTTCC	CTGGTGACCGAGTGAACAA
<i>Ncf1</i>	<i>TGGAGGGCAGAGACAATCCA</i>	AGGGATAGGAGCCGTCTAGG
<i>Vim</i>	GCAGTATGAAAGCGTGGCTG	CTCCAGGGACTCGTTAGTGC
β - <i>Actin</i>	CAACGAGCGTCCGAT	GCCACAGGTTCCATACCCA

Supplementary Table 2. TRRUST database, analysis for cluster 1, 2 and 3

Key TF	Description	# of overlapped genes	P value	Q value	List of overlapped genes
Nfkb1	Nuclear factor of kappa light polypeptide gene enhancer in B cells 1, p105	5	3.95e-06	3.42e-05	<i>Nos2, Ptgs1, Ccl5, Gclm, Ngb</i>
Rel	reticuloendotheliosis oncogene	3	5.26e-06	3.42e-05	<i>Nos2, Ccl5, Ngb</i>
Ep300	E1A binding protein p300	3	5.36e-05	0.000232	<i>Txnip, Nos2, Scd1</i>
Mlxipl	MLX interacting protein-like	2	0.000151	0.00049	<i>Txnip, Scd1</i>
Irf8	Interferon regulatory factor 8	2	0.000361	0.000797	<i>Nos2, Ccl5</i>
Irf1	Interferon regulatory factor 1	2	0.000427	0.000797	<i>Ccl5, Nos2</i>
Rela	v-rel reticuloendotheliosis viral oncogene homolog A (avian)	3	0.000429	0.000797	<i>Ngb, Ccl5, Nos2</i>
Hdac1	Histone deacetylase 1	2	0.000537	0.000873	<i>Nos2, Ccl5</i>
Spi1	Spleen focus forming virus (SFFV) proviral integration oncogene	2	0.0011	0.00159	<i>Ccl5, Nef1</i>
E2f1	E2F transcription factor 1	2	0.00165	0.00214	<i>Nox4, Nos2</i>
Fos	FBJ osteosarcoma oncogene	2	0.00214	0.00253	<i>Nos2, Ccl5</i>
Jun	Jun proto-oncogene	2	0.0112	0.0121	<i>Ccl5, Nos2</i>
Sp1	Trans-acting transcription factor 1	2	0.0431	0.0431	<i>Ptgs1, Ngb</i>

Capítol 4

Discussió

Els esforços dedicats durant les últimes dues dècades per a desxifrar la gran complexitat de la MA han permès conèixer millor la patogènia de la malaltia, i identificar noves dianes terapèutiques (J. Cummings, Feldman, & Scheltens, 2019; J. Cummings, Lee, Zhong, Fonseca, & Taghva, 2021; Vaz & Silvestre, 2020). Malauradament, des de que la memantina es va aprovar per l'ús clínic, l'any 2003 (Marder, 2004), només un nou agent terapèutic ha estat capaç de superar la fase III d'assajos clínics, l'anticòs monoclonal aducanumab, encara que amb certa controvèrsia (Mahase, 2021).

Clínicament, la MA s'inicia presentant dèficits cognitius que van acompanyats d'una sèrie de símptomes neurològics i psiquiàtrics que augmenten a mesura que la malaltia progressa. Alguns d'ells s'han associat a un deteriorament cognitiu funcional més ràpid (Becker, Boiler, Lopez, Saxton, & McGonigle, 1994; López & DeKosky, 2008). Els fàrmacs disponibles pel tractament de la MA (sense tenir en compte l'aducanumab) es basen en la substitució o modulació de neurotransmissors per finalment produir un benefici simptomàtic de la malaltia (Dooley & Lamb, 2000; Müller, 2007; Parsons, Danysz, & Quack, 1999). Entre ells, la memantina és capaç de millorar el comportament i la funció cognitiva en estadis de la malaltia moderats i greus (Kishi et al., 2017). Tot i això, s'assumeix que el seu benefici clínic es manté durant un any i es necessiten sis mesos de tractament addicional per determinar si segueix havent un benefici clínic o cal abandonar el tractament (Gagnon, Rive, Hux, & Guilhaume, 2007). Per aquest motiu el tractament amb memantina es considera molt poc efectiu i, és imperatiu avançar en el desenvolupament de noves molècules que facin front de manera més eficaç a la MA.

Una de les estratègies que s'està imposant amb força en el camp de desenvolupament de noves teràpies per la MA, és la de posicionar de nou els fàrmacs ja en ús pel tractament de la MA, al centre de la recerca, optimitzant-los per aconseguir una eficàcia major. Gràcies a la col·laboració establerta entre el nostre grup d'investigació i el grup de Química Farmacèutica de la Facultat de Farmàcia i Ciències de l'Alimentació de la Universitat de Barcelona, vam tenir la possibilitat de participar en la caracterització farmacològica de nous compostos antagonistes dels receptors de NMDA. Així doncs, aquesta tesi doctoral ha abordat l'avaluació farmacològica de dos nous antagonistes del receptor NMDA, seleccionats per la seva activitat optimitzada sobre aquest receptor en estudis *in vitro*, les seves característiques farmacocinètiques i electrofisiològiques i perfil de seguretat. Concretament, hem estudiat una amina policíclica (**RL-208**) (**Figura**

11) i un compost amb un nou anell benzopolicíclic força diferent químicament de la memantina (**UB-ALT-EV**) (**Figura 12**).

En el primer estudi es va dur a terme la prova de concepte dels efectes de l'antagonista **RL-208** sobre la MA esporàdica, utilitzant ratolins SAMR1 i SAMP8. Es va avaluar la funció cognitiva i els canvis moleculars produïts pel tractament; entre ells, marcadors d'apoptosi, estabilitat sinàptica, estrès oxidatiu i fosforilació de tau, a més de l'avaluació de la via BDNF/TrkB implicada en la supervivència neuronal. Posteriorment, en vista dels bons i prometedors resultats obtinguts amb el compost **RL-208** ens vam proposar avaluar farmacològicament l'**UB-ALT-EV**, que presenta unes millors característiques farmacocinètiques que el compost **RL-208** i, es va assenyalar com el compost més atractiu per la seva avaluació *in vivo*. En primer lloc, es va avaluar farmacològicament el compost **UB-ALT-EV** en el model *C. elegans*, amb la finalitat d'avaluar en un model *in vivo* senzill els efectes del nou compost sobre el comportament. Tot seguit, en vista dels resultats obtinguts es va avaluar l'efecte neuroprotector de l'**UB-ALT-EV** en ratolins 5XFAD, soca transgènica per la MA familiar. En aquesta segona fase vam afegir la memantina com a tractament de referència (del terme en anglès *gold standard*). Aquest estudi es pot considerar també una prova de principi (del terme en anglès *proof-of-principle*), ja que no existeixen articles publicats utilitzant un tractament crònic amb antagonistes del receptor NMDA a una dosi baixa, en el model 5XFAD. En aquest cas, es van avaluar l'efecte dels dos antagonistes sobre la cognició, els marcadors histopatològics de la MA, i vies moleculars associades a la neurodegeneració. Finalment, considerant els resultats previs i l'idea assenyalada per diversos autors, que associa la neuroinflamació i l'estrès oxidatiu com mecanismes directament implicats en el procés neurodegeneratiu, es va dur a terme un estudi dirigit a avaluar l'efecte del tractament amb el compost **UB-ALT-EV** sobre aquests processos moleculars.

4.1 Efecte de nous compostos antagonistes del receptor NMDA sobre la funció cognitiva

La pèrdua de memòria és una característica bàsica i definitòria de la MA (Perry, Watson, & Hodges, 2000; Welsh, Butters, Hughes, Mohs, & Heyman, 1991). Es manifesta de manera típica com alteracions de la memòria episòdica, la memòria semàntica (Greene & Hodges, 1996; Lambon Ralph, Patterson, Graham, Dawson, & Hodges, 2003; Salmon, Heindel, & Lange, 1999) i la memòria de treball (Baddeley, Logie, Bressi, Sala, & Spinnler, 1986; Morris & Baddeley, 1988). Els receptors NMDA participen en la transmissió i la plasticitat sinàptica, processos

considerats com la base de l'aprenentatge i la memòria (Kodis, Choi, Swanson, Ferreira, & Bloom, 2018; Paoletti, Bellone, & Zhou, 2013). Però, l'activació patològica d'aquests receptors durant la MA, suposa una pèrdua gradual de la funció sinàptica i la mort de les cèl·lules neuronals, que correlaciona clínicament amb el deteriorament progressiu de les funcions cognitives (Danysz & Parsons, 2003; R. Wang & Reddy, 2017; Wenk, 2006). Per aquest motiu, es considera una estratègia viable l'ús d'antagonistes del receptor NMDA com a tractament neuroprotector per a la MA. Tenint en compte que la memantina és un agent terapèutic eficaç pel tractament de les alteracions de la memòria i els desordres cognitius característics de pacients amb la MA es van avaluar els efectes sobre la memòria dels nous antagonistes del receptor NMDA seleccionats.

L'avaluació de l'efecte del tractament amb l'**UB-ALT-EV** i amb memantina en models de patologia amiloidogènica de *C. elegans* ens va permetre aportar una primera evidència sobre el paper dels antagonistes del receptor NMDA sobre la cognició dels nematodes. Tant el test de motilitat com el de la quimiotaxi en dues soques diferents que expressen el pèptid A β en cèl·lules motores (soca CL2006) i neuronals (soca CL2355) van permetre demostrar el potencial terapèutic dels compostos, atès que van modular l'alteració locomotora i en van revertir l'alteració quimiotàctica.

Seguidament, atès que la progressió de la MA s'associa amb el deteriorament progressiu de l'hipocamp, una estructura cerebral essencial per la consolidació de la informació de la memòria i per les funcions cognitives (Jahn, 2013), es van dur a terme una sèrie de tests cognitius que avaluen diferents tipus de memòria dependent de l'hipocamp, en els ratolins SAMP8 i 5XFAD: El test de reconeixement de l'objecte nou (NORT, de l'anglès *Novel Object Recognition Test*), el test de localització d'objecte (OLT, de l'anglès *Object Location Test*) i el test de laberint d'aigua de Morris (MWM, de l'anglès *Morris Water Maze*). El tractament crònic amb l'antagonista **RL-208** a ratolins SAMP8 o el tractament amb el compost **UB-ALT-EV** a ratolins 5XFAD de sis mesos d'edat va millorar tant la memòria de reconeixement a curt i a llarg termini com la memòria espacial dels animals tractats, de manera anàloga a la memantina. Els resultats obtinguts indiquen que el tractament amb els antagonistes del receptor NMDA amb una estructura modificada respecte a la de la memantina continua sent una estratègia terapèutica eficaç pel tractament del deteriorament cognitiu de la MA. A més, ja que els dos models utilitzats representen dues etiologies diferents de la MA, la millora de la memòria produïda pels nous compostos indica una acció neuroprotectora sobre la memòria, independentment del seu origen.

Per altra banda, durant la MA, a part de les alteracions de la memòria, existeixen una sèrie de símptomes neuropsiquiàtrics que s'han anomenat símptomes conductuals i psicològics associats a la demència (del terme en anglès *behavioral and psychological symptoms of dementia*) (Petrovic et al., 2007). Aquests símptomes són tan rellevants des del punt de vista clínic com els símptomes cognitius, ja que presenten una forta associació amb el grau de deteriorament funcional present en els pacients amb la MA (Petrovic et al., 2007). Entre ells, hi trobem l'agitació, les alteracions motores, l'ansietat, la irritabilitat, la depressió o els dèficits en la sociabilitat (Monastero, Mangialasche, Camarda, Ercolani, & Camarda, 2009). De fet, s'ha demostrat de manera repetida en diferents estudis amb rosegadors que l'aïllament social promou el dèficit de memòria en models animals de la MA (Ali, Khalil, Elariny, & Abu-Elfotuh, 2017; Leser & Wagner, 2015). Així mateix, l'aïllament social es considera la principal font d'estrès mental i psicosocial que contribueix a l'augment de la prevalença de les malalties neurològiques, a més d'augmentar el risc d'aparició de molts trastorns neuropsicològics (Friedler, Crapser, & McCullough, 2015; O'Keefe et al., 2014). De la mateixa manera, el comportament de tipus ansiós és un símptoma freqüentment diagnosticat en pacients amb la MA, que es relaciona amb un deteriorament ràpid de la funció cognitiva (Geda et al., 2008; Wilson et al., 2003).

Diversos autors han descrit com el tractament amb memantina és capaç de revertir alteracions en la sociabilitat i el comportament de tipus ansiós en rosegadors, indicant una relació entre els desajustos dels nivells de Ca^{2+} i aquest tipus de símptomes característics de la demència (Almahozzi, Radhi, Alzayer, & Kamal, 2019; Bagewadi, Ak, & Shivaramgowda, 2015; Chez et al., 2007; Kumar & Sharma, 2016; Meeker, Chadman, Heaney, & Carp, 2013). Per aquest motiu es va avaluar en primera instància l'alteració de la conducta social després del tractament crònic amb **RL-208** en els animals SAMP8, mitjançant el test de les tres cambres (TCT, de l'anglès *Three Chamber Test*). Gràcies als paràmetres avaluats, vam demostrar que el tractament amb **RL-208** en ratolins SAMP8, era capaç de modificar positivament la conducta social dels rosegadors. Així doncs, considerant que l'alteració de la conducta social dels pacients amb MA és molt habitual i que aquest fenomen pot empitjorar la progressió de la malaltia, aquests resultats són d'especial rellevància (Hsiao, Chang, & Gean, 2018). Per aquest motiu, i, tenint en compte que s'ha associat positivament l'aïllament social amb l'aparició de comportaments de tipus ansiós (Kumari, Singh, Baghel, & Thakur, 2016), es van avaluar paràmetres de comportament de tipus ansiós en el model de ratolí 5XFAD després del tractament amb el compost **UB-ALT-EV** o memantina. En aquest cas, el test del camp obert (OF, de l'anglès *Open Field*) ens va permetre

demostrar com el tractament amb **UB-ALT-EV**, anàlogament a la memantina, era capaç de modificar paràmetres característics d'una conducta de tipus ansiós en els animals 5XFAD.

Fins ara, tots els treballs publicats on s'avalua el deteriorament cognitiu en aquestes soques utilitzen dosis de memantina superiors a 10mg/Kg (J. Dong, Zhou, Wu, Du, & Wang, 2012; J. Wang et al., 2017). Globalment, vam demostrar per primer cop els efectes beneficiosos d'un tractament crònic a una dosi baixa de memantina i amb antagonistes optimitzats del receptor NMDA (5mg/Kg) en els models de ratolí SAMP8 i 5XFAD tant a nivell cognitiu com conductual.

4.2 Efecte dels nous antagonistes del receptor NMDA sobre la neuropatologia de la malaltia d'Alzheimer

4.2.1 Producció i acumulació del pèptid A β

L'acumulació d'oligòmers d'A β , de la mateixa manera que el glutamat, pot activar els receptors NMDA i, per tant, contribuir a l'augment de l'entrada de Ca²⁺ (Ferreira et al., 2012; Parameshwaran, Dhanasekaran, & Suppiramaniam, 2008). L'acumulació d'oligòmers d'A β s'ha associat amb l'alteració de processos com l'LTD dependent dels receptors NMDA a les sinapsis de la regió CA1 i al gir dentat de l'hipocamp (Danysz & Parsons, 2012). Aquesta alteració de l'LTD està lligada també, a l'activació de proteases com la calpaïna, mitjançant l'entrada de Ca²⁺ a través dels receptors NMDA extrasinàptics, associats a l'activació de processos neuro tòxics (Li et al., 2011).

La memantina, ha demostrat de manera repetida els seus efectes beneficiosos sobre la patologia amiloidogènica, no només prevenint la formació de les agregacions d'A β sinó també afavorint la seva disgregació en rosegadors (Ito et al., 2017; Martinez-Coria et al., 2010; Scholtzova et al., 2008; Takahashi-Ito, Makino, Okado, & Tomita, 2017). Com ja hem mencionat, l'avaluació de l'efecte del tractament amb l'**UB-ALT-EV** en el model *C. elegans* ens va permetre aportar una primera evidència sobre el paper d'aquest compost en la patologia amiloidogènica en els models transgènics de *C. elegans*, de la mateixa manera que ho va fer la el tractament amb memantina. Així mateix, l'avaluació dels nous antagonistes del receptor NMDA en els models de ratolí SAMP8 i 5XFAD va mostrar en ambdós casos un augment de l'activació de la via no amiloidogènica en detriment de la via amiloidogènica. A més, de manera destacable, el tractament crònic amb el compost **UB-ALT-EV** a ratolins 5XFAD va modificar significativament marcadors característics del processament de la proteïna APP,

d'una manera més robusta que el tractament amb memantina. En vista dels resultats obtinguts en els animals SAMP8, ens vam proposar aprofundir més en l'estudi de la patologia amiloidogènica, avaluant els nivells d'A β i la seva acumulació. Aquesta avaluació la vam dur a terme només en els ratolins 5XFAD, ja que existeix certa controvèrsia amb el fet de si en el model SAMP8 presenta o no deposició d'oligòmers del pèptid A β (Akiguchi et al., 2017; Del Valle et al., 2010). Així doncs, en el model 5XFAD, vam confirmar la reducció del ratio A β_{42} /A β_{40} i la disminució de plaques d'amiloide tant a l'escorça cerebral com a l'hipocamp després del tractament amb **UB-ALT-EV** i amb memantina. Cal remarcar però, que actualment existeix certa controvèrsia sobre si la reducció de l'acumulació d'A β té un impacte directe sobre la millora de la cognició (Ackley et al., 2021; Martinez-Coria et al., 2010; Scholtzova et al., 2008). És cert però, que la seva reducció, afavorida en el nostre cas a través del tractament amb el compost **UB-ALT-EV**, alleugera la patologia de la MA, prevenint l'activació de processos implicats en la neurodegeneració.

Particularment, s'ha suggerit que l'efecte antiagregant de la memantina podria ser degut a mecanismes independents de la seva funció sobre el receptor NMDA, ja que l'amantadina, un antagonista del receptor NMDA estructuralment similar a la memantina no té efectes sobre l'agregació del pèptid A β (Takahashi-Ito et al., 2017). En el nostre cas, el tractament amb memantina o **UB-ALT-EV** va modificar de manera significativa la ratio A β_{42} /A β_{40} incrementant els nivells d'A β_{40} de manera significativa. Aquest resultat és rellevant considerant que la producció de l'espècie A β_{40} s'ha associat amb una funció antiagregant dels oligòmers d'A β (Kim et al., 2007). Per tant el seu augment després del tractament amb memantina o **UB-ALT-EV** recolzaria la hipòtesi que aquest fos el mecanisme d'acció pel qual es reduís l'acumulació de plaques d'A β . En conjunt, els nostres resultats aporten una evidència consistent que demostra com el compost **UB-ALT-EV** de la mateixa manera que la memantina, és capaç de reduir l'agregació amiloidogènica i la formació de plaques sent un efecte addicional als ja descrits pel bloqueig de l'entrada de Ca²⁺.

4.2.2 Hiperfosforilació de la proteïna tau

La formació de cabdells neurofibril·lars correlaciona d'una manera més estreta amb el deteriorament cognitiu, en comparació amb l'acumulació d'oligòmers d'A β (Nelson et al., 2012). Durant la MA la fosforilació de la proteïna tau, pas previ a la formació de cabdells neurofibril·lars, es troba significativament augmentada (Iqbal et al., 1986; Köpke et al., 1993). Aquest fenomen es produeix a diferents residus de serina, treonina i tirosina a causa de l'alteració de l'equilibri

de l'activitat pròpia de les tau-quinases i tau-fosfatases (Medeiros, Baglietto-Vargas, & LaFerla, 2011). Tenint en compte que l'augment de l'entrada de Ca^{2+} mitjançant els receptors NMDA s'ha relacionat amb l'activació de tau-quinases com la Cdk5 i la GSK-3 β , de forma directa o a través de l'activació de proteases depenents de Ca^{2+} com la calpaïna (Cao, Guan, Liang, Huang, & Wang, 2019), ens vam proposar estudiar aquestes vies després del tractament amb **RL-208** i **UB-EV-19** en els dos models de ratolí de la MA.

La calpaïna-1 és una proteasa involucrada en la mort cel·lular i en l'augment de la fosforilació de tau, que es troba de forma sobreactivada durant la MA a causa de l'augment dels nivells de Ca^{2+} (Jin et al., 2015; Saito, Elce, Hamos, & Nixon, 1993). Precisament, la calpaïna-1 és la responsable de generar el fragment p25, que actua com a coactivador de la tau-quinasa Cdk5 (M. S. Lee et al., 2000). El compost **RL-208** va disminuir els nivells tant de calpaïna-1 com de p25, que van anar acompanyats d'una disminució de l'expressió de Cdk5 en els ratolins mascle SAMP8. Com a conseqüència es va determinar una reducció significativa de la fosforilació de tau en determinats epítops fonamentals per la formació dels cabdells neurofibril·lars (Mondragón-Rodríguez, Perry, Luna-Muñoz, Acevedo-Aquino, & Williams, 2014). Anàlogament, el tractament amb l'**UB-ALT-EV** en ratolins femella 5XFAD, però no el tractament amb memantina, va reduir els nivells de fosforilació de tau després de la conseqüent reducció dels nivells de la calpaïna-1, del fragment p25, així com de la forma activada de la GSK-3 β . Així doncs, indicant que la millora cognitiva dels rosegadors SAMP8 i 5XFAD després dels tractaments amb **RL-208** i **UB-EV-19** respectivament, esta relacionada amb la reducció en l'activació de vies relacionades amb la hiperfosforilació de tau.

Tenint en compte l'absència d'efecte en la regulació de vies implicades en la fosforilació de tau, de la memantina no ens va sorprendre observar la manca d'efecte d'aquest compost sobre els marcadors d'hiperfosforilació de tau en els ratolins 5XFAD, tot i que estaven descrits en altres models animals o bé en cultius cel·lulars (X. Liu et al., 2017; Z. Song et al., 2021). Considerant que hi ha estudis que demostren que la memantina pot regular els nivells de fosforilació de tau, la manca d'efecte mesurable en el nostre cas podria explicar-se per la dosi utilitzada (com hem mencionat és el primer treball on s'administra memantina en 5XFAD a una dosi baixa) o pel temps de tractament. En qualsevol cas, el fet que l'**UB-ALT-EV** presenti efectes beneficiosos en el procés d'hiperfosforilació de tau, és indicatiu de la seva millor efectivitat respecte la memantina.

4.3 Efecte del tractament amb nous antagonistes del receptor NMDA sobre vies moleculars implicades en el procés neurodegeneratiu

Com ja hem mencionat, en condicions patològiques, la sobreactivació dels receptors NMDA és responsable de la iniciació de processos apoptòtics i de l'alteració del flux autofàgic, a més de provocar la disfunció mitocondrial i l'acumulació d'ERO que acaba desencadenant l'estrès oxidatiu (De Felice et al., 2007; X. Dong, Wang, & Qin, 2009; Ghavami et al., 2014; Hamano et al., 2008; Rego & Oliveira, 2003). Per tant, el bloqueig dels receptors per part d'antagonistes pot donar lloc a la restauració d'aquestes alteracions contribuint de forma diferencial en l'efecte neuroprotector. A continuació, es discuteixen els resultats obtinguts després del tractament de models de ratolí de la MA amb els compostos **RL-208** i **UB-ALT-EV**. En el cas del model 5XFAD, també es comentaran els resultats obtinguts en el tractament amb memantina.

4.3.1 Efectes sobre l'expressió dels receptors NMDA

La disfunció neuronal en estadis inicials de la MA, induïda per l'acumulació d'A β es troba regulada per l'activació dels receptors NMDA que contenen la subunitat GluN2B (Rönicke et al., 2011). Curiosament, els nivells d'ARN missatger (ARNm) de la subunitat GluN1 són significativament més baixos durant la MA i, els nivells d'expressió de les subunitats GluN2A i GluN2B es troben reduïts en les regions més vulnerables del cervell humà, com l'hipocamp i el l'escorça cerebral (Mishizen-Eberz et al., 2004). Com les subunitats GluN2A han estat implicades en rutes neuroprotectores, mentre que les subunitats GluN2B semblen augmentar la vulnerabilitat neuronal, teràpies que promoguin l'expressió de la subunitat GluN2A i la disminució de l'expressió de la subunitat GluN2B representen una estratègia terapèutica viable per reduir la disfunció neuronal induïda per la presència d'A β (Y. Liu et al., 2007).

En aquesta tesi doctoral mostrem com el tractament amb el compost **UB-ALT-EV**, però no el tractament amb memantina, sobre els ratolins 5XFAD va ser capaç de promoure d'una manera subtil l'augment de l'expressió de la subunitat "neuroprotectora" GluN2A. Pel que fa la subunitat GluN2B, es va estudiar la seva expressió però també el grau de fosforilació que modula la seva activitat neuroprotectora o neurotòxica. Els receptors NMDA que contenen la subunitat GluN2B requereixen de la fosforilació a la posició Y1472, a través de tirosinquinases com Fyn, per tal d'evitar l'activació de vies neurotòxiques (Trepanier,

Jackson, & MacDonald, 2012). La fosforilació en aquesta posició s'encarrega de l'enfortiment de la interacció entre el receptor i la proteïna PSD95 a la regió postsinàptica i promou l'activitat fisiològica del receptor (Goebel-Goody, Davies, Alvestad Linger, Freund, & Browning, 2009; Vissel, Krupp, Heinemann, & Westbrook, 2001; Yu, Askalan, Keil, & Salter, 1997). En primer lloc, es va veure un increment de la fosforilació de la subunitat GluN2B a la posició Y1472 després dels tractaments amb **RL-208** i **UB-ALT-EV** en els animals SAMP8 i 5XFAD, respectivament. Curiosament, el tractament amb el compost **RL-208** va mostrar un augment de la fosforilació de GluN2B també a la soca SAMR1. Aquest efecte beneficiós de l'**RL-208** indica que l'antagonista podria estar modulant la incipient disfunció dels receptors donada l'edat dels animals tot i no repercutir en la cognició. A més, considerant l'associació establerta entre l'augment dels nivells de fosforilació de la subunitat GluN2B a la posició Y1472 i la millora de la memòria espacial en ratolins envellits, els resultats obtinguts en aquest sentit encara cobren més rellevància (Zamzow, Elias, Acosta, Escobedo, & Magnusson, 2016).

A més, en el segon estudi, vam profunditzar més en l'avaluació d'aquesta fosforilació i, tal i com s'esperava, es va confirmar l'increment de l'activitat quinasa Fyn després del tractament dels 5XFAD amb **UB-ALT-EV** i amb memantina. Malgrat tot, Fyn és també una quinasa de tau i moduladora de la neuroinflamació micròglia, i s'estan desenvolupant inhibidors de Fyn pel tractament del deteriorament cognitiu, proposant-los com a moduladors de la neuroinflamació (Nygaard, van Dyck, & Strittmatter, 2014; Tang et al., 2020). Aquests desenvolupaments haurien de tenir present aquesta acció beneficiosa de l'activació de Fyn modificant l'acció neurotòxica de GluN2B, per establir aquests antagonistes com a noves teràpies en MA o en malalties neurodegeneratives amb un clar component excitotòxic.

Aquests resultats, conjuntament amb l'augment dels nivells de la proteïna PSD-95 produït pels tractaments amb l'**RL-208** i l'**UB-ALT-EV** indiquen que s'afavoreix l'expressió dels receptors NMDA a les zones sinàptiques amb un clar component neuroprotector (Delint-Ramírez, Salcedo-Tello, & Bermudez-Rattoni, 2008; Goebel-Goody et al., 2009). Aquest fenomen per tant, seria responsable d'afavorir la senyalització glutamatèrgica, inhibint vies neurotòxiques relacionades amb l'activació dels receptors NMDA extrasinàptics (Pallas-Bazarra, Draffin, Cuadros, Antonio Esteban, & Avila, 2019).

4.3.2 Efectes produïts sobre la desregulació dels nivells de Ca^{2+} intracel·lular

El ió Ca^{2+} és un segon missatger imprescindible en la funció dels circuits de les cèl·lules nervioses del cervell. Entre les seves funcions hi trobem la regulació de funcions neuronals com el creixement neuronal, l'exocitosi de neurotransmissors, la plasticitat sinàptica i la funció cognitiva (Ferreiro, Oliveira, & Pereira, 2004; Zhao et al., 2013). Durant la MA, es produeix una alteració de la seva homeòstasi a causa de la sobreactivació dels receptors NMDA, que implica greus alteracions en les funcions cerebrals que són la base de la neuropatologia de la malaltia, la pèrdua de memòria i la disfunció cognitiva (Chakroborty, Goussakov, Miller, & Stutzmann, 2009; Stutzmann & Mattson, 2011). En concret, s'ha demostrat com els nivells de Ca^{2+} es troben incrementats en aquelles neurones properes a les acumulacions d' $\text{A}\beta$ (Kuchibhotla et al., 2008).

En estudis d'electrofisiologia, tant amb el compost **RL-208** com l'**UB-ALT-EV**, van mostrar que són capaços d'inhibir l'entrada de Ca^{2+} a través de receptor NMDA de manera tant eficaç ($88.3 \pm 3.7 \%$, i $69.1 \pm 1.2 \%$ respectivament) com la memantina ($86.2 \pm 1.4 \%$) (Leiva et al., 2018; Valverde, Sureda, & Vázquez, 2014). Per aquest motiu, el tractament amb els dos antagonistes feia preveure que s'observarien canvis en els mecanismes intracel·lulars que precisen de Ca^{2+} en el ratolins SAMP8 i 5XFAD.

Ja hem mencionat que l'activitat de la calpaïna-1, depèn dels nivells de Ca^{2+} intracel·lular (M. S. Lee et al., 2000) i que participa en l'activació de la Cdk5, però a més, aquesta proteasa també participa en l'escissió de proteïnes sinàptiques (Ahmad et al., 2018; B. Chen et al., 2017). La reducció dels nivells d'expressió de calpaïna-1, així com de la seva activitat mitjançant l'avaluació de la fragmentació de la proteïna α -spectrina després del tractament amb **RL-208** sembla indicar una relació l'augment de l'expressió de les proteïnes sinàptiques avaluades com la proteïna associada als sinaptosomes, 25 (SNAP25), la sinaptofisina o la PSD95 en els animals SAMP8.

Seguint els indicis del primer treball, durant l'avaluació farmacològica del compost **UB-ALT-EV** vam profunditzar més en l'avaluació de proteïnes dependents de Ca^{2+} . Les proteïnes CaMKII i CaN tenen un paper regulador clau sobre la plasticitat sinàptica, la formació de la memòria i la supervivència cel·lular (Asai et al., 1999; Yan et al., 2016). En condicions patològiques la seva sobreactivació pot induir processos neurodegeneratius, influint de manera directa sobre la patologia de tau, donat que la primera pot fosforilar-la i la CaN inhibeix l'activitat de diferents fosfatases (Goto et al., 1985; Oka et al., 2017; Reese &

Tagliatalata, 2010). El tractament dels ratolins 5XFAD amb **UB-ALT-EV**, de la mateixa manera que la memantina, va disminuir els nivells de CaMKII i de CaN que es trobaven significativament incrementats en el ratolins transgènics en comparació amb els *wild type*. D'acord amb els resultats presentats prèviament on l'**UB-ALT-EV** era capaç de reduir els nivells de fosforilació de tau, la reducció dels nivells de la CaMKII i de la CaN per aquest compost resultaria en un efecte addicional a la modulació de les tau kinases Cdk5 i GSK3 que hem descrit anteriorment.

D'altra banda, l'acumulació de la proteïna tau hiperfosforilada s'ha associat amb la desfosforilació de CREB, reduint la translocació al nucli d'aquest factor de transcripció i per tant evitant la seva acció sobre la supervivència neuronal (Teich et al., 2015). I, d'acord amb aquesta evidència, els tractaments amb **UB-ALT-EV** i amb memantina van produir l'increment dels nivells de CREB fosforilat al nucli, efecte que se sumaria als ja descrits per a prevenir la neurodegeneració en el model 5XFAD.

4.3.3 Efectes sobre la pèrdua sinàptica i neuronal

Com hem esmentat, la sobreactivació dels receptors NMDA està relacionada amb processos neurotòxics principalment amb l'activació de vies apoptòtiques i de mort cel·lular durant la MA (Flanigan, Xue, Kishan Rao, Dhanushkodi, & McDonald, 2014; Jang, In, Choi, & Kim, 2014; J. Liu, Chang, Song, Li, & Wu, 2019). I, tenint en compte aquesta relació, s'ha assenyalat que l'efecte antiapoptòtic de la memantina formaria part de la seva acció neuroprotectora (G. Song, Li, Lin, & Cao, 2015). Com hem esmentat anteriorment, diversos autors han descrit un augment de les calpaïnes durant la MA, que són responsables de l'activació de quinases com la Cdk5, GSK3 β , o la CaMKII, però també existeix un augment de l'activitat caspasa durant la MA, ambdues vinculades a processos apoptòtics (Mahaman et al., 2019; Roth, 2001; Shimokawa & Trindade, 2010). La seva activació no només s'ha associat a l'alteració de processos de memòria, sinó també a processos implicats en la generació dels cabdells neurofibril·lars i la producció dels pèptids A β ₄₀ i A β ₄₂ (M. S. Lee et al., 2000; Louneva et al., 2008). En aquesta tesi doctoral demostrem com els tractaments crònics a una dosi baixa amb els antagonistes **RL-208**, **UB-ALT-EV** o memantina regulen l'expressió de marcadors d'apoptosi característics de la MA com ara la caspasa-3, Bax o Bcl-2. Tots aquests marcadors es van avaluar en models de ratolí de la MA familiar i de la MA esporàdica i, tenint en compte que l'origen de la neurodegeneració en ambdós models de ratolí és diferent, l'efecte antiapoptòtic demostrat pels tractaments amb **RL-208** i **UB-ALT-EV** segueixen la línia d'evidència fins ara

mostrada per la memantina, indicant el paper regulador de l'apoptosi per part dels receptors NMDA (B. Chen et al., 2017; Izumida et al., 2017; G. Song et al., 2015).

Els factors neurotròfics, per altra banda, són reguladors essencials pel desenvolupament, manteniment i supervivència cel·lular, i per tant tenen un paper important en processos cognitius i en la formació i emmagatzematge de la memòria (Hellweg & Jockers-Scherübl, 1994). Durant la MA s'ha observat una disminució dels nivells de BDNF (Gezen-Ak et al., 2013; Peng, Wu, Mufson, & Fahnstock, 2005; Yasutake, Kuroda, Yanagawa, Okamura, & Yoneda, 2006), així com de l'expressió del seu receptor, TrkB, veient-se així alterada la funció normal de la neurotrofina (Allen, Wilcock, & Dawbarn, 1999; Ferrer et al., 1999; Phillips et al., 1991). A més aquestes alteracions es sumen a l'alteració del transport axonal del BDNF des l'escorça entorrinal, on es sintetitza, fins a l'hipocamp, en concret a les àrees CA3 i CA1, a causa de la presència de cabdells neurofibril·lars (Adalbert, Gilley, & Coleman, 2007). Per tant, la taupatia causa l'alteració dels nivells de BDNF, degut a la desregulació de la seva síntesi, la pèrdua de funció deguda a la fragmentació dels seu receptor i l'alteració del seu transport s'associa a símptomes clínics de la MA com alteracions de la cognició i de la memòria (Schindowski, Belarbi, & Buée, 2008). És també rellevant el fet que la regulació a la baixa de BDNF s'ha associat a alteracions del comportament social (Hsiao et al., 2018), tal i com vam demostrar mitjançant l'ús del test de les tres cambres.

Diversos autors han demostrat que la memantina regula a l'alça la síntesi de BDNF (Marvanová et al., 2001; Meisner et al., 2008). De la mateixa manera, el tractament amb **RL-208** en va augmentar els nivells proteics, i el tractament amb **UB-ALT-EV** o memantina van demostrar afavorir l'expressió gènica de BDNF. A més, de manera significativa, el tractament amb el compost **RL-208** no només va regular a l'alça l'expressió de BDNF madur i en va disminuir la seva forma tòxica (proBDNF) (F. Wang et al., 2017), sinó que també en van evitar la pèrdua de funció mitjançant la inhibició de la fragmentació de TrkB (Qiu et al., 2020). A més, tot semblaria indicar que la disminució dels nivells d'hiperfosforilació de tau després dels tractaments amb **RL-208** i **UB-ALT-EV**, estaria prevenint l'alteració en el transport axonal del BDNF (Jerónimo-Santos et al., 2015). Així doncs, els resultats obtinguts indiquen que tractaments amb **RL-208** o **UB-ALT-EV** milloren la senyalització del BDNF, afavorint el manteniment de la cognició i de la sociabilitat. Cal destacar també que el tractament dels animals 5XFAD amb **UB-ALT-EV**, però no amb memantina, va augmentar l'expressió d'altres neurotrofines com el factor de creixement nerviós induïble (*Vgf*, de l'anglès *Nerve*

growth factor inducible) i el factor de creixement nerviós (*Ngf*, de l'anglès *Nerve growth factor*).

L'administració de neurotrofines pel tractament de la MA no és possible donat que són proteïnes que es degraden ràpidament i que pràcticament no travessen la barrera hematoencefàlica, però, establir estratègies que n'indueixin l'expressió de manera endògena poden ser una teràpia alternativa per a les malalties neurodegeneratives (Tuszynski et al., 2005). Per aquest motiu el fet que tant el compost **RL-208** com l'**UB-ALT-EV** siguin capaços d'estimular l'expressió o la funcionalitat de les neurotrofines, els assenjala com una alternativa viable per prevenir o modular la seva desregulació, ja que aquests efectes beneficiosos sobre els factors neurotròfics podrien ser subsidiaris a la reducció dels nivells d'A β i de l'hiperfosforilació de tau.

Adicionalment, s'ha demostrat com la pèrdua sinàptica és el factor que millor correlaciona amb la demència (DeKosky, Scheff, & Styren, 1996; Masliah, Hansen, Albright, Mallory, & Terry, 1991), indicant una connexió directa entre la patologia de les sinapsis i l'activitat de l'oligòmer A β durant la MA (Figueiredo et al., 2013). L'activació dels receptors NMDA extrasinàptics i la conseqüent activació de caspases i calpaines són responsables de la reducció de l'expressió de proteïnes de manteniment sinàptic, posant en risc l'estabilitat sinàptica (Louneva et al., 2008). Existeixen evidències que demostren que tractaments amb memantina augmenten els nivells de proteïnes sinàptiques, i que aquesta correlaciona amb la millora cognitiva (B. Chen et al., 2017; Z.-Z. Chen et al., 2016). En aquest sentit, tant l'**RL-208** com l'**UB-ALT-EV**, però no la memantina, han estat capaços de disminuir l'activitat caspasa i calpaïna dels animals SAMP8 i 5XFAD respectivament, reduint també l'acumulació del pèptid A β . Aquest fenomen conduiria a la millora de l'estabilitat sinàptica, demostrada a través de l'increment de l'expressió de proteïnes pre- i postsinàptiques, com la SNAP25, la PSD95, la sinaptofisina i la syntaxina. De manera significativa, en el cas de la memantina, les proteïnes sinàptiques avaluades en l'estudi no es van veure augmentades després del tractament amb el fàrmac, així com tampoc es va veure una disminució de l'activitat calpaïna. Aquests resultats confirmen una bona optimització dels compostos en quant al seu efecte estabilitzador de les sinapsis.

4.3.4 Efectes del tractament amb UB-ALT-EV sobre l'autofàgia

La patogènesi de malalties neurodegeneratives com la MA, s'ha associat amb alteracions en el procés autofàgic donada la seva relació amb l'acumulació excessiva de proteïnes, que en última instància causen la mort neuronal (J. Cheng

et al., 2018; C. C. Tan et al., 2014; Zhu, Yu, Jiang, & Tan, 2013). L'autofàgia s'ha descrit com un element regulador de l'eliminació dels oligòmers d'A β i de la proteïna tau (Nilsson et al., 2015), que ha demostrat ser un mecanisme neuroprotector per fer front a aquestes acumulacions pròpies de la MA (Harris & Rubinsztein, 2011). No obstant això, durant la MA s'han descrit alteracions durant la maduració dels autofagolisosomes que contribueixen a l'acumulació excessiva de vacúols autofàgics a les neurones (J.-H. Lee et al., 2010; Yamazaki et al., 2010). En aquest sentit, s'ha demostrat com l'ús de compostos activadors de l'autofàgia per tal de promoure la reducció de les acumulacions de proteïnes aberrants, afavoreix la millora dels dèficits cognitius, a nivell pre-clínic (Di Meco et al., 2017; Morgan et al., 2015). La memantina per la seva banda, s'ha assenyalat com un agent inductor del flux autofàgic, ja que promou l'eliminació de proteïnes propenses a l'agregació en diversos models neuronals (Hirano et al., 2019). No obstant això, s'ha postulat que aquest efecte per part de la memantina no depèn de l'antagonisme del receptor NMDA, sinó d'un mecanisme independent (Hirano et al., 2019). Recentment, s'ha suggerit que la inducció de l'estrès de reticle endoplasmàtic per part de la memantina, seria la responsable d'activar el mecanisme autofàgic a través de l'activació de la beclina-1 (Kataura et al., 2021; Ogata et al., 2006).

Considerant els efectes beneficiosos de la memantina sobre el procés autofàgic i la disminució en l'acumulació d'A β induïda pel tractament amb **UB-ALT-EV** en els animals 5XFAD ens vam proposar avaluar si aquest nou compost participa en la modulació de l'activitat autofàgica. La beclina-1 és una proteïna necessària per a l'inici del procés autofàgic. Però, l'activació de l'activitat calpaïna a causa de l'activació dels receptors NMDA és responsable de l'escissió de la beclina-1 i, per tant, impedeix l'inici de l'autofàgia. El tractament amb antagonistes del receptor NMDA ha demostrat ser capaç de prevenir l'escissió de la beclina-1 (Russo et al., 2011). En aquest sentit, després del tractament amb **UB-ALT-EV** a ratolins 5XFAD, donada la disminució dels nivells i de l'activitat calpaïna es va observar un augment de l'expressió proteica de la beclina-1. A més, el tractament va augmentar la fosforilació de la proteïna quinasa activadora de l'autofàgia de tipus Unc-51, (ULK1, de l'anglès *Unc-51 like autophagy activating kinase*) demostrant una inducció de la iniciació del procés autofàgic (Russo et al., 2011). La memantina va mostrar resultats similars, tot i que s'ha descrit que no incrementa la fosforilació d'ULK en cultius neuronals (Hirano et al., 2019). A més, el tractament amb **UB-ALT-EV**, però no amb memantina, va potenciar la degradació lisosomal dels autofagosomes reduint els nivells d'acumulació de la proteïna associada als microtúbuls 1A/1B de cadena lleugera 3 (LC3B-II, de

l'anglès *Microtubule-associated proteins 1A/1B light chain 3*) i augmentant els nivells proteics de la proteïna de membrana associada a lisosomes 1 (LAMP-1, de l'anglès *Lysosomal-associated membrane protein 1*) (X.-T. Cheng et al., 2018; Y.-K. Lee & Lee, 2016). En resum, després de la caracterització farmacològica del compost **UB-ALT-EV** respecte el seu efecte en el procés autofàgic, els nostres resultats suggereixen que el nou compost presenta una activitat millorada en comparació als efectes produïts per la memantina, i que aquest efecte podria ser responsable en part de la disminució de les acumulacions de les plaques d'A β observades a l'escorça cerebral i a l'hipocamp, conjuntament amb l'efecte antiagregant del pèptid A β ₄₀.

4.3.5 Efectes sobre l'estrès oxidatiu

La sobreactivació dels receptors NMDA provoca una desregulació de l'equilibri entre les molècules prooxidants i antioxidants al cervell, fenomen que acaba donant lloc a l'estrès oxidatiu (Ankarcona et al., 1995; Murphy & Baraban, 1990). L'estrès oxidatiu representa doncs, un factor que contribueix al procés d'envelliment i a la progressió de malalties neurodegeneratives, com la MA (Beal, 2005; Trushina & McMurray, 2007). Donada aquesta relació entre els receptors NMDA i la desregulació de l'homeòstasi oxidativa, el tractament amb antagonistes del receptor NMDA representa una estratègia viable pel modular aquest aspecte de la malaltia. De fet, el tractament amb memantina és capaç de protegir les neurones del dany oxidatiu, freqüentment associat a la producció de radicals lliures (De Felice et al., 2007; Pietá Dias et al., 2007).

El tractament crònic de ratolins SAMP8 amb el compost **RL-208**, en primera instància va indicar la regulació a l'alça de proteïnes amb efectes antioxidants com la superòxid dismutasa 1 (SOD1) i la glutatió peroxidasa 1 (GPX1) així com, l'augment de l'expressió gènica de l'enzim antioxidant hemo oxigenasa 1 (*Hmox1*, de l'anglès *Heme oxygenase 1*). A més, aquest efecte antioxidant va anar acompanyat de la reducció dels nivells de peròxid d'hidrogen a l'hipocamp dels rosegadors. Cal destacar, que la presència dels pèptids d'A β presenta una forta associació amb la generació d'ERO, concretament amb la generació de peròxid d'hidrogen (Huang et al., 1999), pel que els resultats obtinguts indiquen que la reducció d'aquesta important espècie oxidant podria venir donada per l'acció conjunta de les proteïnes amb efecte antioxidant i la reducció de la patologia amiloidogènica evidenciant l'efecte protector del tractament amb **RL-208** enfront l'estrès oxidatiu en els ratolins SAMP8. A més, durant la MA la producció neuronal d'NO i d'O₂⁻ es considera un pas clau que relaciona l'activació dels receptors NMDA amb la mort cel·lular (Forder & Tymianski, 2009; Girouard et

al., 2009; Lafon-Cazal, Pietri, Culcasi, & Bockaert, 1993). En aquest sentit, la reducció dels nivells d'ARNm d'*iNOS* induïda pel tractament amb **UB-ALT-EV** en ratolins 5XFAD però no per la memantina, indica l'optimització de l'acció farmacològica respecte al fàrmac de referència. Estudis previs en cultius cel·lulars i estimulació amb estreptozocina van observar que la memantina reduïa l'expressió d'*iNOS*, però els nostres resultats són força més rellevants en usar un model de rosegador de la MA (Kelestemur et al., 2016; Mishra, Hidau, & Rai, 2021).

En vista dels resultats tan favorables vers la patologia oxidativa, es va decidir dur a terme l'anàlisi de l'expressió de 84 gens relacionats amb l'estrès oxidatiu a través d'un bioxip (del terme en anglès *array*) en ratolins 5XFAD tractats amb **UB-ALT-EV** per tal d'identificar vies d'activitat oxidativa modulades pel compost. En aquest mateix sentit, els resultats van mostrar que 24 dels 84 gens analitzats es trobaven alterats entre els animals *wild-type* i els 5XFAD i, després de l'anàlisi bioinformàtic dels resultats vam trobar com aquests gens estaven implicats envies moleculars associades a l'activitat generadora de superòxid, l'activitat antioxidant i a l'acció de citoquines. Més endavant, la validació dels gens assenyalats per l'anàlisi de l'*array* separats en tres subgrups (*clusters*) en base a la seva funció, va indicar un efecte reductor de l'expressió gènica d'aquests gens per part del tractament amb **UB-ALT-EV** indicant una disminució de l'activitat oxidant i per tant, reduint l'estrès oxidatiu. En aquesta anàlisi a més, els resultats obtinguts després del tractament amb memantina, van demostrar una vegada més una acció millorada per part de l'**UB-ALT-EV** ja que per exemple l'expressió gènica d' *Il-19*, *Il-22* i *Gpx6* va estar regulada pel nou antagonista i no per la memantina.

En conjunt, els resultats de l'avaluació farmacològica dels nous antagonistes sobre la patologia oxidativa durant la MA indiquen una regulació favorable de l'homeòstasi oxidativa després del tractament crònic per via oral. Particularment, destaca l'efecte millorat per part del compost **UB-ALT-EV** en comparació amb l'efecte produït per la memantina, mostrant una vegada més, com en el camp de desenvolupament de noves teràpies per la MA, el procés d'optimització de la molècula de la memantina té un alt potencial.

4.4 Efectes produïts sobre la neuroinflamació mitjançant el tractament amb UB-ALT-EV

Estudis epidemiològics, genòmics, funcionals i bioinformàtics fets durant els últims anys indiquen de manera inequívoca que les respostes inflamatòries al

cervell contribueix de manera decisiva a la patogènesi i progressió de la MA (Heppner, Ransohoff, & Becher, 2015; VanItallie, 2017). En condicions fisiològiques els astròcits, donada la seva morfologia altament ramificada, tenen un contacte estret amb les neurones que els fa participants del manteniment de la funció neuronal actuant com una primera línia de defensa (Osborn, Kamphuis, Wadman, & Hol, 2016). Són els encarregats d'alliberar molècules antioxidants i de recaptar l'excés de glutamat (P.-C. Chen et al., 2009). Durant la MA, l'acumulació d'oligòmers d'A β es considera el principal factor responsable de l'activació glial, que acabarà produint una resposta en forma de cascada degenerativa mitjançant l'alliberació de factors inflamatoris, contribuint al deteriorament cognitiu (Osborn et al., 2016; Serrano-Pozo et al., 2011). L'activació astrocítica o astrogliosi és una característica de la MA que comprèn una àmplia gamma de canvis tan moleculars com funcionals en els astròcits (Sofroniew, 2009). Els astròcits reactius durant la MA mostren una regulació a l'alça de proteïnes com la GFAP, la vimentina o la nestina i una hipertrofia morfològica (Hol & Pekny, 2015). De fet, els astròcits activats durant la MA envolten les plaques senils arribant a penetrar el nucli de cada placa, servint com a barreres protectores per a les neurones (Kamphuis et al., 2014; Wegiel, Wang, Tarnawski, & Lach, 2000)

La via CaN/NFAT, és una via implicada en la neuroinflamació, la desregulació de glutamat, la patologia amiloidogènica i la sinaptotoxicitat (Canellada, Ramirez, Minami, Redondo, & Cano, 2008; Fernandez, Fernandez, Carrero, Garcia-Garcia, & Torres-Aleman, 2007; Pérez-Ortiz et al., 2008). Concretament, està descrit que la sobreactivació de la via CaN/NFAT genera un fenotip d'astròcits neuro tòxics, que afavoreix la producció de citoquines proinflamatòries i la inducció de l'expressió de BACE1 (Sompol et al., 2017). D'aquesta manera, l'augment de la producció d'oligòmers d'A β , iniciaria un cicle viciós, promovent una major desregulació dels receptors NMDA i, per tant, un augment de l'activació d'aquesta via de senyalització. En els ratolins 5XFAD es produeix un increment de l'astrogliosi, que va lligada a un increment de citoquines proinflamatòries, la formació de plaques d'amiloide (Oakley et al., 2006). El tractament amb antagonistes del receptor NMDA va reduir l'atrogliosi, reduint els nivells proteics de GFAP, especialment l'**UB-ALT-EV**. A més, el tractament amb l'**UB-ALT-EV** o amb memantina va produir una reducció dels nivells proteics de CaN. En el cas de l'**UB-ALT-EV** també va disminuir l'activitat de la fosfatasa, donat que es va incrementar la forma fosforilada del factor de transcripció NFAT1c. L'NFAT1c pot regular l'expressió de citoquines antiinflamatòries i també la de diversos factors neurotròfics (Fernandez et al., 2007; Pérez-Ortiz et al., 2008;

Sompol et al., 2017), de manera que l'acció neuroprotectora observada després del tractament amb **UB-ALT-EV**, derivaria de la modulació de la via CaN/NFAT, que en el cas del tractament amb memantina no va ser modificada, suggerint una millora en l'efecte neuroprotector del compost **UB-ALT-EV** en comparació a la memantina. Així mateix, cal destacar doncs, que el tractament crònic amb **UB-ALT-EV** en ratolins 5XFAD ha aportat la primera evidència que els antagonistes del receptor NMDA poden modular la aquesta via moduladora de la inflamació.

Durant la MA, la micròglia és la responsable de l'alliberació de citokines proinflamatòries en resposta a la presència d'A β , que promou alhora l'activació dels astròcits. És en aquest moment, quan els astròcits inicien també la producció de citokines com l'IL-1 β i el TNF α (Heneka et al. 2010). Aquest altre cicle viciós és un tret característic de la MA que s'ha associat amb un estat inflamatori crònic del cervell durant la malaltia i, que s'ha associat amb un augment de l'entrada Ca²⁺ a les neurones postsinàptiques (Bezzi et al., 2001). A dia d'avui, es coneix que la memantina és capaç de reduir els nivells de micròglia activada durant processos de neuroinflamació crònica (Rosi et al., 2006). Aquest resultat es van reproduir en les nostres mans perquè el tractament amb memantina dels ratolins 5XFAD va reduir la micròglia activada mesurada per immunohistoquímica d'Iba-1. De manera anàloga, l'administració d'**UB-ALT-EV** a ratolins 5XFAD va reduir dels nivells de Iba-1 a l'hipocamp, especialment a la regió CA1 i al gir dentat (Jay, von Saucken, & Landreth, 2017; Jurga, Paleczna, & Kuter, 2020; Y. Wang et al., 2015).

El marcador Trem2 s'expressa a la superfície microglial i constitueix un mediador clau en el procés fagocític dels oligòmers d'A β (Jay et al., 2017; Y. J. Tan et al., 2017). La disminució de la seva expressió gènica en els ratolins 5XFAD després del tractament amb **UB-ALT-EV** suggereix una menor activació de la micròglia com a conseqüència de la reducció de la patologia amiloidogènica. En concordança amb estudis publicats anteriorment (Murakawa-Hirachi, Mizoguchi, Ohgidani, Haraguchi, & Monji, 2021), la memantina no va modificar l'expressió gènica d'aquest marcador microglial. Aquest resultat de nou apunta a que l'**UB-ALT-EV** presenta una activitat optimitzada respecte la seva eficàcia en comparació amb la memantina.

Finalment, però no menys important, ens vam centrar en l'avaluació dels dos perfils de la micròglia, el "proinflamatori" o l'M1 i l'"antiinflamatori" o l'M2. Curiosament, les ERO i la via de l'NF- κ B, un marcador del fenotip M1, juguen un paper important sobre la regulació de l'activitat dels receptors NMDA, formant part d'un cicle que involucra l'apoptosi, l'estrès oxidatiu, i la resposta inflamatòria

(Ma, Cheng, Chen, Luo, & Feng, 2020). De manera anàloga als resultats de l'expressió de *Trem2*, l'**UB-ALT-EV** va reduir els nivells d'expressió proteica de l'NF- κ B i d'expressió gènica de citoquines proinflamatòries relacionades amb el fenotip M1, com l'interferó γ (*Ifn- γ*), l' *Il-1 β* , el lligand 2 de quimiocina (*Ccl2*, de l'anglès *chemokine (C-C motif) ligand 2*) i el lligand 3 de quimiocina (*Ccl3*, de l'anglès *chemokine (C-C motif) ligand 3*), mentre que va incrementar l'expressió gènica d'*Ym1* i *Arg1*, marcadors típics del fenotip M2.

En definitiva, tot i que s'ha descrit que la memantina podia regular el procés inflamatori (Lv, Li, Mao, Qin, L, & Dong, 2020; Mishra et al., 2021; Rosi et al., 2006), els resultats obtinguts en els ratolins 5XFAD després del tractament amb el compost **UB-ALT-EV** evidencien que l'acció antiinflamatoria d'aquest antagonista és molt més consistent que la de la memantina, i per tant demostra la millora terapèutica d'aquest compost front, com a mínim a la modulació de la neuroinflamació. Aquesta nova via de modulació de l'antagonista **UB-ALT-EV** obre un nou camí d'estudi, sent un repte dilucidar els mecanismes precisos pels quals es disminueix l'activació astroglià i microglial de manera molt més eficaç que amb memantina. A més, considerant que durant les últimes dècades més de 30 fàrmacs desenvolupats pel tractament de la neuroinflamació durant la MA han fracassat donada la seva incapacitat d'endarrerir ni tan sols millorar els símptomes de pacients amb la MA (Fu, Wang, & Ip, 2019), els resultats obtinguts amb el compost **UB-ALT-EV** cobren encara més rellevància.

4.5 Consideracions finals

Encara que durant l'última dècada, una gran part de la recerca en el desenvolupament de noves teràpies per la MA s'ha centrat en el desenvolupament de nous agents terapèutics dirigits a l'acumulació del pèptid A β , fins ara l'eficàcia d'aquestes teràpies ha demostrat no ser una estratègia viable (J. L. Cummings, Morstorf, & Zhong, 2014; J. Cummings et al., 2021; Schneider et al., 2014; Sevigny et al., 2016). Per aquest motiu, s'ha proposat que el tractament de la MA no s'ha d'abordar d'una manera dirigida únicament als marcadors neuropatològics sinó des d'una perspectiva més global, incloent tots els processos moleculars alterats que participen en la patogènesi de la malaltia.

Tenint en compte l'efecte neuroprotector de la memantina, i la seva capacitat d'actuar no només reduint l'activitat glutamatergic, sinó modulant també processos com l'estrès oxidatiu, la inflamació i l'autofàgia entre d'altres l'ús de teràpies més efectives basades en la modulació dels receptors NMDA sobreactivats ja s'havia postulat com una estratègia modificadora de la MA

prometedora (Emadeldin et al., 2017; Rogawski & Wenk, 2003; Van Dam & De Deyn, 2006). En aquesta tesi doctoral hem mostrat com la recerca de nous antagonistes del receptor NMDA pot donar lloc a compostos optimitzats que mantenen les accions beneficioses de la memantina, millorant-les i potenciant-les (**Figura 13**) i fins hi tot que intervenen en noves vies de neuroprotecció, com l'eix CaN/NFAT, que permetrien l'abordatge de la MA de forma més eficaç per finalment poder ser considerats com a modificadors de la MA, i no només com a tractaments simptomàtics. Tot així, el desenvolupament dels compostos estudiats en aquesta tesi fins a fases clíniques encara requereix d'un treball específic, centrat no només en la eficàcia sinó també en la seguretat, la toxicitat i altres aspectes relacionats amb l'administració a essers humans.

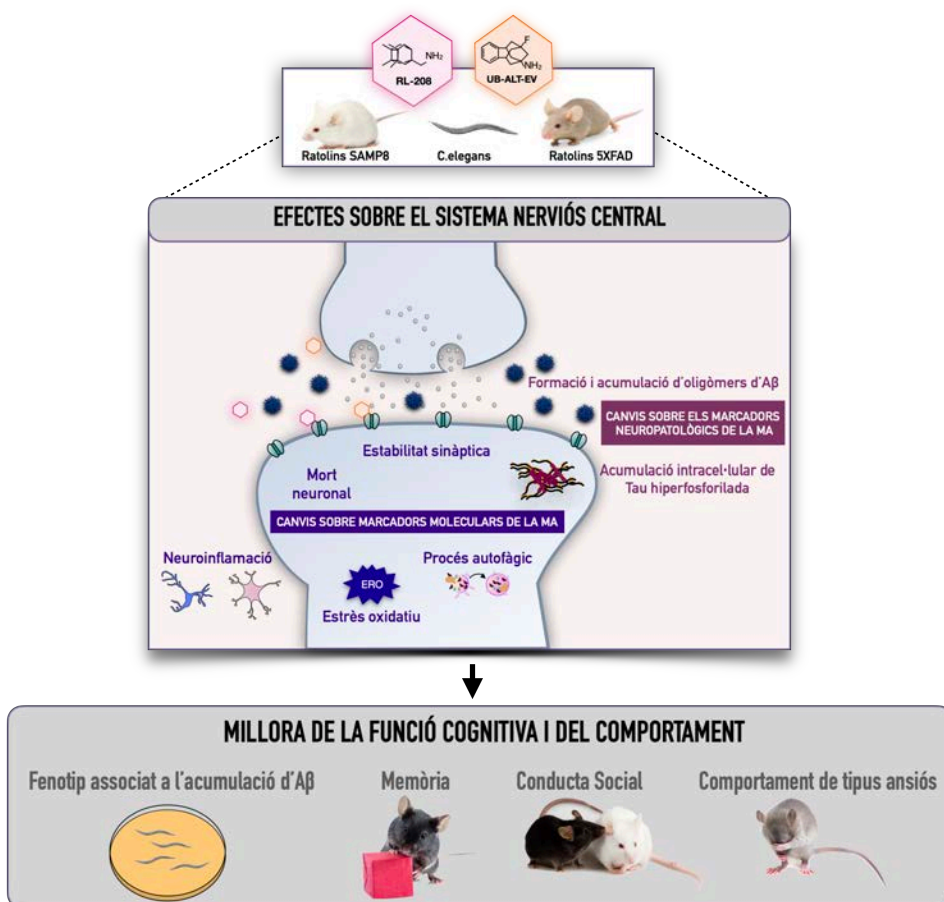


Figura 13. Representació esquemàtica de les vies moleculars del SNC modificades per l'acció dels nous antagonistes del receptor NMDA optimitzats respecte la memantina, i dels efectes a nivell cognitiu i del comportament.

Capítol 5

Conclusions

La conclusió general dels estudis duts a terme en aquesta tesi doctoral és que hi ha marge de millora per a la cerca i desenvolupament de nous antagonistes del receptor NMDA, sent l'optimització de l'estructura molecular de la memantina una estratègia viable per al tractament de la MA. De manera remarcable, el compost **UB-ALT-EV** ha demostrat ser capaç de promoure una acció neuroprotectora que implica mecanismes addicionals als de la memantina, i que podria representar un agent terapèutic amb efectes addicionals a aquesta.

De manera específica, les principals conclusions que deriven d'aquesta tesi doctoral son les següents:

1. El tractament amb **UB-ALT-EV** és capaç de millorar el fenotip associat a l'acumulació del pèptid A β en les soques transgèniques específiques del nematode *C.elegans*. Aquest efecte el va assenyalar com a agent candidat a ser avaluat *in vivo* en un model animal més complex.
2. Els tractaments orals crònics amb els diferents compostos **RL-208** i **UB-ALT-EV** milloren la memòria espacial i de reconeixement a curt i a llarg termini, a més de millorar les alteracions sobre el comportament dels ratolins SAMP8 i 5XFAD, models de la MA esporàdica i familiar respectivament.
3. Els compostos **RL-208** i **UB-ALT-EV** prevenen l'aparició dels marcadors neuropatològics de la MA en models de ratolí de la malaltia participant en la modulació del processament amiloidogènic de la proteïna APP i en la regulació de la fosforilació de la proteïna tau. Addicionalment, l'**UB-ALT-EV** és capaç de reduir l'acumulació de plaques d'A β i la ratio A β_{42} /A β_{40} en ratolins 5XFAD de 6 mesos d'edat, sent aquest últim un possible indicador d'una acció antiagregant.
4. El tractament oral crònic a ratolins SAMP8 i 5XFAD amb l'**RL-208** i l'**UB-ALT-EV** afavoreix la fosforilació (Y1472) de la subunitat GluN2B del receptor NMDA, implicada en la inhibició de vies de senyalització neurotòxiques durant la MA. L'efecte neuroprotector del tractament oral crònic amb els compostos **RL-208** i **UB-ALT-EV** es veuria en part donat per l'increment en la síntesi i senyalització de factors neurotròfics a l'hipocamp dels ratolins SAMP8 i 5XFAD, i per l'augment de l'expressió de proteïnes d'estabilitat sinàptica.

5. Els compostos **RL-208** i **UB-ALT-EV** redueixen l'expressió de marcadors d'apoptosi en ratolins SAMP8 i 5XFAD després d'un tractament per via oral durant 4 setmanes, exhibint la seva acció neuroprotectora, prevenint la mort neuronal.
6. L'**UB-ALT-EV** administrat per via oral a ratolins 5XFAD de 6 mesos d'edat modula el flux autofàgic, contribuint així a la reducció en l'acumulació de proteïnes característica de la MA, millor que la memantina.
7. L'**UB-ALT-EV** i la memantina regulen de manera diferent el procés d'activació astrocítica i microglial en ratolins 5XFAD després d'un tractament crònic. Aquest fet assenyalaria un nou mecanisme amb potencial terapèutic de l'**UB-ALT-EV** respecte a la memantina.
8. Els antagonistes del receptor NMDA, **RL-208** i **UB-ALT-EV** promouen una regulació a l'alça de mediadors antioxidants, així com una reducció de la producció d'ERO en models murins de la MA.

Referències

- Abdul, H. M., Sama, M. A., Furman, J. L., Mathis, D. M., Beckett, T. L., Weidner, A. M., ... Norris, C. M. (2009). Cognitive decline in Alzheimer's disease is associated with selective changes in calcineurin/NFAT signaling. *The Journal of Neuroscience: The Official Journal of the Society for Neuroscience*, 29(41), 12957-12969. <https://doi.org/10.1523/JNEUROSCI.1064-09.2009>
- Abraha, A., Ghoshal, N., Gamblin, T. C., Cryns, V., Berry, R. W., Kuret, J., & Binder, L. I. (2000). C-terminal inhibition of tau assembly in vitro and in Alzheimer's disease. *Journal of Cell Science*, 113 Pt 21, 3737-3745. <https://doi.org/10.1242/jcs.113.21.3737>
- Ackley, S. F., Zimmerman, S. C., Brenowitz, W. D., Tchetgen Tchetgen, E. J., Gold, A. L., Manly, J. J., ... Glymour, M. M. (2021). Effect of reductions in amyloid levels on cognitive change in randomized trials: instrumental variable meta-analysis. *BMJ*, 372. <https://doi.org/10.1136/bmj.n156>
- Adalbert, R., Gilley, J., & Coleman, M. P. (2007). Abeta, tau and ApoE4 in Alzheimer's disease: the axonal connection. *Trends in Molecular Medicine*, 13(4), 135-142. <https://doi.org/10.1016/j.molmed.2007.02.004>
- Agostinho, P., Cunha, R. A., & Oliveira, C. (2010). Neuroinflammation, oxidative stress and the pathogenesis of Alzheimer's disease. *Current pharmaceutical design*, 16(25), 2766-2778.
- Ahmad, F., Das, D., Kommaddi, R. P., Diwakar, L., Gowaikar, R., Rupanagudi, K. V., ... Ravindranath, V. (2018). Isoform-specific hyperactivation of calpain-2 occurs presymptotically at the synapse in Alzheimer's disease mice and correlates with memory deficits in human subjects. *Scientific Reports*, 8(1), 13119. <https://doi.org/10.1038/s41598-018-31073-6>
- Aisen, P. S., Cummings, J., Jack, C. R. J., Morris, J. C., Sperling, R., Frölich, L.,

- ... Dubois, B. (2017). On the path to 2025: understanding the Alzheimer's disease continuum. *Alzheimer's Research & Therapy*, 9(1), 60. <https://doi.org/10.1186/s13195-017-0283-5>
- Akiguchi, I., Pallàs, M., Budka, H., Akiyama, H., Ueno, M., Han, J., ... Hosokawa, M. (2017). SAMP8 mice as a neuropathological model of accelerated brain aging and dementia: Toshio Takeda's legacy and future directions. *Neuropathology: Official Journal of the Japanese Society of Neuropathology*, 37(4), 293-305. <https://doi.org/10.1111/neup.12373>
- Ali, A. A., Khalil, M. G., Elariny, H. A., & Abu-Elfotuh, K. (2017). Study on social isolation as a risk factor in development of Alzheimer's disease in rats. *Brain Disord Ther*, 6(230), 2.
- Allen, S. J., Wilcock, G. K., & Dawbarn, D. (1999). Profound and selective loss of catalytic TrkB immunoreactivity in Alzheimer's disease. *Biochemical and Biophysical Research Communications*, 264(3), 648-651. <https://doi.org/10.1006/bbrc.1999.1561>
- Almahazi, A., Radhi, M., Alzayer, S., & Kamal, A. (2019). Effects of Memantine in a Mouse Model of Postoperative Cognitive Dysfunction. *Behavioral Sciences (Basel, Switzerland)*, 9(3). <https://doi.org/10.3390/bs9030024>
- Alonso, A. del C., Mederlyova, A., Novak, M., Grundke-Iqbal, I., & Iqbal, K. (2004). Promotion of hyperphosphorylation by frontotemporal dementia tau mutations. *The Journal of Biological Chemistry*, 279(33), 34873-34881. <https://doi.org/10.1074/jbc.M405131200>
- Alzheimer's Association. (2019). 2019 Alzheimer's disease facts and figures. *Alzheimer's & Dementia*, 15(3), 321-387. <https://doi.org/https://doi.org/10.1016/j.jalz.2019.01.010>
- Alzheimer's Association Calcium Hypothesis Workgroup, & Khachaturian, Z. S. (2017). Calcium Hypothesis of Alzheimer's disease and brain aging: A framework for integrating new evidence into a comprehensive theory of pathogenesis. *Alzheimer's & Dementia*, 13(2), 178-182.e17. <https://doi.org/https://doi.org/10.1016/j.jalz.2016.12.006>
- Alzheimer, A., Stelzmann, R. A., Schnitzlein, H. N., & Murtagh, F. R. (1995). An English translation of Alzheimer's 1907 paper, «Über eine eigenartige Erkrankung der Hirnrinde». *Clinical Anatomy (New York, N.Y.)*, 8(6), 429-431. <https://doi.org/10.1002/ca.980080612>
- Amor, S., & Woodroffe, M. N. (2014, març). Innate and adaptive immune responses in neurodegeneration and repair. *Immunology*. <https://doi.org/10.1111/imm.12134>
- Andorfer, C., Kress, Y., Espinoza, M., de Silva, R., Tucker, K. L., Barde, Y.-A., ... Davies, P. (2003). Hyperphosphorylation and aggregation of tau in mice

- expressing normal human tau isoforms. *Journal of Neurochemistry*, 86(3), 582-590. <https://doi.org/10.1046/j.1471-4159.2003.01879.x>
- Ankarcrona, M., Dypbukt, J. M., Bonfoco, E., Zhivotovsky, B., Orrenius, S., Lipton, S. A., & Nicotera, P. (1995). Glutamate-induced neuronal death: a succession of necrosis or apoptosis depending on mitochondrial function. *Neuron*, 15(4), 961-973. [https://doi.org/10.1016/0896-6273\(95\)90186-8](https://doi.org/10.1016/0896-6273(95)90186-8)
- Annicchiarico, R., Federici, A., Pettenati, C., & Caltagirone, C. (2007). Rivastigmine in Alzheimer's disease: Cognitive function and quality of life. *Therapeutics and Clinical Risk Management*, 3(6), 1113-1123.
- Apostolova, L. G., Green, A. E., Babakchanian, S., Hwang, K. S., Chou, Y.-Y., Toga, A. W., & Thompson, P. M. (2012). Hippocampal atrophy and ventricular enlargement in normal aging, mild cognitive impairment (MCI), and Alzheimer Disease. *Alzheimer Disease and Associated Disorders*, 26(1), 17-27. <https://doi.org/10.1097/WAD.0b013e3182163b62>
- Arispe, N., Rojas, E., & Pollard, H. B. (1993). Alzheimer disease amyloid beta protein forms calcium channels in bilayer membranes: blockade by tromethamine and aluminum. *Proceedings of the National Academy of Sciences*, 90(2), 567-571.
- Arundine, M., & Tymianski, M. (2004). Molecular mechanisms of glutamate-dependent neurodegeneration in ischemia and traumatic brain injury. *Cellular and Molecular Life Sciences: CMLS*, 61(6), 657-668. <https://doi.org/10.1007/s00018-003-3319-x>
- Asai, A., Qiu, J. h, Narita, Y., Chi, S., Saito, N., Shinoura, N., ... Kirino, T. (1999). High level calcineurin activity predisposes neuronal cells to apoptosis. *The Journal of Biological Chemistry*, 274(48), 34450-34458. <https://doi.org/10.1074/jbc.274.48.34450>
- Attwell, D., Buchan, A. M., Charpak, S., Lauritzen, M., Macvicar, B. A., & Newman, E. A. (2010). Glial and neuronal control of brain blood flow. *Nature*, 468(7321), 232-243. <https://doi.org/10.1038/nature09613>
- Babbar, M., & Sheikh, M. S. (2013). Metabolic Stress and Disorders Related to Alterations in Mitochondrial Fission or Fusion. *Molecular and Cellular Pharmacology*, 5(3), 109-133.
- Baddeley, A., Logie, R., Bressi, S., Sala, S. Della, & Spinnler, H. (1986). Dementia and working memory. *The Quarterly Journal of Experimental Psychology Section A*, 38(4), 603-618.
- Bagasra, O., Michaels, F. H., Zheng, Y. M., Bobroski, L. E., Spitsin, S. V, Fu, Z. F., ... Koprowski, H. (1995). Activation of the inducible form of nitric oxide synthase in the brains of patients with multiple sclerosis. *Proceedings of the National Academy of Sciences of the United States of America*, 92(26),

- 12041-12045. <https://doi.org/10.1073/pnas.92.26.12041>
- Bagewadi, H. G., Ak, A. K., & Shivaramgowda, R. M. (2015). An Experimental Study to Evaluate the Effect of Memantine in Animal Models of Anxiety in Swiss Albino Mice. *Journal of Clinical and Diagnostic Research : JCDR*, 9(8), FF01-5. <https://doi.org/10.7860/JCDR/2015/13233.6287>
- Bargmann, C. I., Hartweg, E., & Horvitz, H. R. (1993). Odorant-selective genes and neurons mediate olfaction in *C. elegans*. *Cell*, 74(3), 515-527. [https://doi.org/10.1016/0092-8674\(93\)80053-h](https://doi.org/10.1016/0092-8674(93)80053-h)
- Barker, W. W., Luis, C. A., Kashuba, A., Luis, M., Harwood, D. G., Loewenstein, D., ... Duara, R. (2002). Relative frequencies of Alzheimer disease, Lewy body, vascular and frontotemporal dementia, and hippocampal sclerosis in the State of Florida Brain Bank. *Alzheimer Disease and Associated Disorders*, 16(4), 203-212. <https://doi.org/10.1097/00002093-200210000-00001>
- Barnett, A., & Brewer, G. J. (2011). Autophagy in aging and Alzheimer's disease: pathologic or protective? *Journal of Alzheimer's Disease : JAD*, 25(3), 385-394. <https://doi.org/10.3233/JAD-2011-101989>
- Beal, M. F. (2005). Oxidative damage as an early marker of Alzheimer's disease and mild cognitive impairment. *Neurobiology of Aging*, 26(5), 585-586. <https://doi.org/10.1016/j.neurobiolaging.2004.09.022>
- Becker, J. T., Boiler, F., Lopez, O. L., Saxton, J., & McGonigle, K. L. (1994). The natural history of Alzheimer's disease: description of study cohort and accuracy of diagnosis. *Archives of neurology*, 51(6), 585-594.
- Benveniste, M., & Mayer, M. L. (1991). Kinetic analysis of antagonist action at N-methyl-D-aspartic acid receptors. Two binding sites each for glutamate and glycine. *Biophysical Journal*, 59(3), 560-573. [https://doi.org/10.1016/S0006-3495\(91\)82272-X](https://doi.org/10.1016/S0006-3495(91)82272-X)
- Berger, A. J., Dieudonné, S., & Ascher, P. (1998). Glycine uptake governs glycine site occupancy at NMDA receptors of excitatory synapses. *Journal of Neurophysiology*, 80(6), 3336-3340. <https://doi.org/10.1152/jn.1998.80.6.3336>
- Bezprozvanny, I. (2009). Calcium signaling and neurodegenerative diseases. *Trends in molecular medicine*, 15(3), 89-100.
- Bezzi, P., Domercq, M., Brambilla, L., Galli, R., Schols, D., De Clercq, E., ... Meldolesi, J. (2001). CXCR4-activated astrocyte glutamate release via TNF α : amplification by microglia triggers neurotoxicity. *Nature neuroscience*, 4(7), 702-710.
- Bito, H., Deisseroth, K., & Tsien, R. W. (1996). CREB phosphorylation and dephosphorylation: a Ca(2+)- and stimulus duration-dependent switch for

- hippocampal gene expression. *Cell*, 87(7), 1203-1214. [https://doi.org/10.1016/s0092-8674\(00\)81816-4](https://doi.org/10.1016/s0092-8674(00)81816-4)
- Blanke, M. L., & VanDongen, A. M. J. (2009). Activation Mechanisms of the NMDA Receptor. En A. M. Van Dongen (Ed.). Boca Raton (FL).
- Bradley-Whitman, M. A., & Lovell, M. A. (2013). Epigenetic changes in the progression of Alzheimer's disease. *Mechanisms of Ageing and Development*, 134(10), 486-495. <https://doi.org/10.1016/j.mad.2013.08.005>
- Brenner, S. (1974). The genetics of *Caenorhabditis elegans*. *Genetics*, 77(1), 71-94. <https://doi.org/10.1093/genetics/77.1.71>
- Burns, A. R., Wallace, I. M., Wildenhain, J., Tyers, M., Giaever, G., Bader, G. D., ... Roy, P. J. (2010). A predictive model for drug bioaccumulation and bioactivity in *Caenorhabditis elegans*. *Nature Chemical Biology*, 6(7), 549-557. <https://doi.org/10.1038/nchembio.380>
- Butterfield, D. A., & Poon, H. F. (2005). The senescence-accelerated prone mouse (SAMP8): A model of age-related cognitive decline with relevance to alterations of the gene expression and protein abnormalities in Alzheimer's disease. *Experimental Gerontology*, 40(10), 774-783. <https://doi.org/10.1016/j.exger.2005.05.007>
- Cacabelos, R. (2007). Donepezil in Alzheimer's disease: From conventional trials to pharmacogenetics. *Neuropsychiatric Disease and Treatment*.
- Cai, B., Chang, S. H., Becker, E. B. E., Bonni, A., Xia, Z., Köhr, G., ... Quintanilla, R. A. (2006). NMDA receptor function: subunit composition versus spatial distribution. *Cell and Tissue Research*, 326(2), 439-446. <https://doi.org/10.1007/s00441-006-0273-6>
- Calsolaro, V., & Edison, P. (2016). Neuroinflammation in Alzheimer's disease: Current evidence and future directions. *Alzheimer's & Dementia: The Journal of the Alzheimer's Association*, 12(6), 719-732. <https://doi.org/10.1016/j.jalz.2016.02.010>
- Canellada, A., Ramirez, B. G., Minami, T., Redondo, J. M., & Cano, E. (2008). Calcium/calcineurin signaling in primary cortical astrocyte cultures: Rcan1-4 and cyclooxygenase-2 as NFAT target genes. *Glia*, 56(7), 709-722. <https://doi.org/10.1002/glia.20647>
- Cao, L.-L., Guan, P.-P., Liang, Y.-Y., Huang, X.-S., & Wang, P. (2019). Calcium Ions Stimulate the Hyperphosphorylation of Tau by Activating Microsomal Prostaglandin E Synthase 1. *Frontiers in Aging Neuroscience*, 11, 108. <https://doi.org/10.3389/fnagi.2019.00108>
- Carmona, J. J., & Michan, S. (2016). Biology of Healthy Aging and Longevity. *Revista de Investigacion Clinica; Organo Del Hospital de Enfermedades de La Nutricion*, 68(1), 7-16.

- Cataldo, A. M., Peterhoff, C. M., Schmidt, S. D., Terio, N. B., Duff, K., Beard, M., ... Nixon, R. A. (2004). Presenilin mutations in familial Alzheimer disease and transgenic mouse models accelerate neuronal lysosomal pathology. *Journal of Neuropathology and Experimental Neurology*, 63(8), 821-830. <https://doi.org/10.1093/jnen/63.8.821>
- Cenini, G., Lloret, A., & Cascella, R. (2019). Oxidative Stress in Neurodegenerative Diseases: From a Mitochondrial Point of View. *Oxidative Medicine and Cellular Longevity*, 2019, 2105607. <https://doi.org/10.1155/2019/2105607>
- Chakroborty, S., Goussakov, I., Miller, M. B., & Stutzmann, G. E. (2009). Deviant ryanodine receptor-mediated calcium release resets synaptic homeostasis in presymptomatic 3xTg-AD mice. *The Journal of Neuroscience: The Official Journal of the Society for Neuroscience*, 29(30), 9458-9470. <https://doi.org/10.1523/JNEUROSCI.2047-09.2009>
- Chang, J., Liu, F., Lee, M., Wu, B., Ting, K., Zara, J. N., ... Wang, C.-Y. (2013). NF- κ B inhibits osteogenic differentiation of mesenchymal stem cells by promoting β -catenin degradation. *Proceedings of the National Academy of Sciences of the United States of America*, 110(23), 9469-9474. <https://doi.org/10.1073/pnas.1300532110>
- Chang, N. C., Hung, S. I., Hwa, K. Y., Kato, I., Chen, J. E., Liu, C. H., & Chang, A. C. (2001). A macrophage protein, Ym1, transiently expressed during inflammation is a novel mammalian lectin. *The Journal of Biological Chemistry*, 276(20), 17497-17506. <https://doi.org/10.1074/jbc.M010417200>
- Chatterton, J. E., Awobuluyi, M., Premkumar, L. S., Takahashi, H., Talantova, M., Shin, Y., ... Zhang, D. (2002). Excitatory glycine receptors containing the NR3 family of NMDA receptor subunits. *Nature*, 415(6873), 793-798. <https://doi.org/10.1038/nature715>
- Chen, B.-S., & Roche, K. W. (2007). Regulation of NMDA receptors by phosphorylation. *Neuropharmacology*, 53(3), 362-368. <https://doi.org/10.1016/j.neuropharm.2007.05.018>
- Chen, B., Wang, G., Li, W., Liu, W., Lin, R., Tao, J., ... Wang, Y. (2017). Memantine attenuates cell apoptosis by suppressing the calpain-caspase-3 pathway in an experimental model of ischemic stroke. *Experimental cell research*, 351(2), 163-172. <https://doi.org/10.1016/j.yexcr.2016.12.028>
- Chen, P.-C., Vargas, M. R., Pani, A. K., Smeyne, R. J., Johnson, D. A., Kan, Y. W., & Johnson, J. A. (2009). Nrf2-mediated neuroprotection in the MPTP mouse model of Parkinson's disease: Critical role for the astrocyte. *Proceedings of the National Academy of Sciences*, 106(8), 2933-2938.
- Chen, Z.-Z., Yang, D.-D., Zhao, Z., Yan, H., Ji, J., & Sun, X.-L. (2016).

- Memantine mediates neuroprotection via regulating neurovascular unit in a mouse model of focal cerebral ischemia. *Life Sciences*, *150*, 8-14. <https://doi.org/10.1016/j.lfs.2016.02.081>
- Cheng, J., North, B. J., Zhang, T., Dai, X., Tao, K., Guo, J., & Wei, W. (2018). The emerging roles of protein homeostasis-governing pathways in Alzheimer's disease. *Aging Cell*, *17*(5), e12801. <https://doi.org/10.1111/acel.12801>
- Cheng, X.-T., Xie, Y.-X., Zhou, B., Huang, N., Farfel-Becker, T., & Sheng, Z.-H. (2018). Revisiting LAMP1 as a marker for degradative autophagy-lysosomal organelles in the nervous system. *Autophagy*, *14*(8), 1472-1474. <https://doi.org/10.1080/15548627.2018.1482147>
- Chez, M. G., Burton, Q., Dowling, T., Chang, M., Khanna, P., & Kramer, C. (2007). Memantine as adjunctive therapy in children diagnosed with autistic spectrum disorders: an observation of initial clinical response and maintenance tolerability. *Journal of Child Neurology*, *22*(5), 574-579. <https://doi.org/10.1177/0883073807302611>
- Chow, H., & Herrup, K. (2015). Genomic integrity and the ageing brain. *Nature Reviews. Neuroscience*, *16*(11), 672-684. <https://doi.org/10.1038/nrn4020>
- Chung, H. J., Huang, Y. H., Lau, L.-F., & Huganir, R. L. (2004). Regulation of the NMDA receptor complex and trafficking by activity-dependent phosphorylation of the NR2B subunit PDZ ligand. *The Journal of Neuroscience: The Official Journal of the Society for Neuroscience*, *24*(45), 10248-10259. <https://doi.org/10.1523/JNEUROSCI.0546-04.2004>
- Corraliza, I. M., Soler, G., Eichmann, K., & Modolell, M. (1995). Arginase induction by suppressors of nitric oxide synthesis (IL-4, IL-10 and PGE2) in murine bone-marrow-derived macrophages. *Biochemical and Biophysical Research Communications*, *206*(2), 667-673. <https://doi.org/10.1006/bbrc.1995.1094>
- Cull-Candy, S., Brickley, S., & Farrant, M. (2001). NMDA receptor subunits: diversity, development and disease. *Current Opinion in Neurobiology*, *11*(3), 327-335. [https://doi.org/10.1016/s0959-4388\(00\)00215-4](https://doi.org/10.1016/s0959-4388(00)00215-4)
- Cull-Candy, S. G., & Leszkiewicz, D. N. (2004). Role of distinct NMDA receptor subtypes at central synapses. *Science's STKE: Signal Transduction Knowledge Environment*, *2004*(255), re16. <https://doi.org/10.1126/stke.2552004re16>
- Cummings, J., Feldman, H. H., & Scheltens, P. (2019). The «rights» of precision drug development for Alzheimer's disease. *Alzheimer's Research and Therapy*, *11*(1). <https://doi.org/10.1186/s13195-019-0529-5>
- Cummings, J., & Fox, N. (2017). Defining disease modifying therapy for

- Alzheimer's disease. *The journal of prevention of Alzheimer's disease*, 4(2), 109.
- Cummings, J. L., Morstorf, T., & Zhong, K. (2014). Alzheimer's disease drug-development pipeline: few candidates, frequent failures. *Alzheimer's Research & Therapy*, 6(4), 37. <https://doi.org/10.1186/alzrt269>
- Cummings, J., Lee, G., Zhong, K., Fonseca, J., & Taghva, K. (2021). Alzheimer's disease drug development pipeline: 2021. *Alzheimer's & Dementia: Translational Research & Clinical Interventions*, 7(1), e12179. <https://doi.org/https://doi.org/10.1002/trc2.12179>
- Currais, A. (2015). Ageing and inflammation - A central role for mitochondria in brain health and disease. *Ageing Research Reviews*, 21, 30-42. <https://doi.org/10.1016/j.arr.2015.02.001>
- Danysz, W., & Parsons, C. G. (2003). The NMDA receptor antagonist memantine as a symptomatological and neuroprotective treatment for Alzheimer's disease: preclinical evidence. *International journal of geriatric psychiatry*, 18(S1), S23-S32.
- Danysz, W., & Parsons, C. G. (2012). Alzheimer's disease, β -amyloid, glutamate, NMDA receptors and memantine--searching for the connections. *British Journal of Pharmacology*, 167(2), 324-352. <https://doi.org/10.1111/j.1476-5381.2012.02057.x>
- De Felice, F. G., Velasco, P. T., Lambert, M. P., Viola, K., Fernandez, S. J., Ferreira, S. T., & Klein, W. L. (2007). A β oligomers induce neuronal oxidative stress through an N-methyl-D-aspartate receptor-dependent mechanism that is blocked by the Alzheimer drug memantine. *The Journal of Biological Chemistry*, 282(15), 11590-11601. <https://doi.org/10.1074/jbc.M607483200>
- De Jonghe, C., Esselens, C., Kumar-Singh, S., Craessaerts, K., Serneels, S., Checler, F., ... De Strooper, B. (2001). Pathogenic APP mutations near the gamma-secretase cleavage site differentially affect A β secretion and APP C-terminal fragment stability. *Human Molecular Genetics*, 10(16), 1665-1671. <https://doi.org/10.1093/hmg/10.16.1665>
- Deisseroth, K., Mermelstein, P. G., Xia, H., & Tsien, R. W. (2003). Signaling from synapse to nucleus: the logic behind the mechanisms. *Current Opinion in Neurobiology*, 13(3), 354-365. [https://doi.org/10.1016/s0959-4388\(03\)00076-x](https://doi.org/10.1016/s0959-4388(03)00076-x)
- DeKosky, S. T., Scheff, S. W., & Styren, S. D. (1996). Structural correlates of cognition in dementia: quantification and assessment of synapse change. *Neurodegeneration: A Journal for Neurodegenerative Disorders, Neuroprotection, and Neuroregeneration*, 5(4), 417-421.

- <https://doi.org/10.1006/neur.1996.0056>
- Del Valle, J., Duran-Vilaregut, J., Manich, G., Casadesús, G., Smith, M. A., Camins, A., ... Vilaplana, J. (2010). Early amyloid accumulation in the hippocampus of SAMP8 mice. *Journal of Alzheimer's disease : JAD*, *19*(4), 1303-1315. <https://doi.org/10.3233/JAD-2010-1321>
- Delint-Ramírez, I., Salcedo-Tello, P., & Bermudez-Rattoni, F. (2008). Spatial memory formation induces recruitment of NMDA receptor and PSD-95 to synaptic lipid rafts. *Journal of Neurochemistry*, *106*(4), 1658-1668. <https://doi.org/10.1111/j.1471-4159.2008.05523.x>
- DeRidder, M. N., Simon, M. J., Siman, R., Auberson, Y. P., Raghupathi, R., & Meaney, D. F. (2006). Traumatic mechanical injury to the hippocampus in vitro causes regional caspase-3 and calpain activation that is influenced by NMDA receptor subunit composition. *Neurobiology of disease*, *22*(1), 165-176. <https://doi.org/10.1016/j.nbd.2005.10.011>
- Devi, L., Alldred, M. J., Ginsberg, S. D., & Ohno, M. (2010). Sex- and brain region-specific acceleration of β -amyloidogenesis following behavioral stress in a mouse model of Alzheimer's disease. *Molecular Brain*, *3*(1), 34. <https://doi.org/10.1186/1756-6606-3-34>
- Devi, L., & Ohno, M. (2010). Phospho-eIF2 α level is important for determining abilities of BACE1 reduction to rescue cholinergic neurodegeneration and memory defects in 5XFAD mice. *PloS one*, *5*(9), e12974.
- Di Meco, A., Li, J.-G., Blass, B. E., Abou-Gharbia, M., Lauretti, E., & Praticò, D. (2017). 12/15-Lipoxygenase Inhibition Reverses Cognitive Impairment, Brain Amyloidosis, and Tau Pathology by Stimulating Autophagy in Aged Triple Transgenic Mice. *Biological Psychiatry*, *81*(2), 92-100. <https://doi.org/10.1016/j.biopsych.2016.05.023>
- Dixit, R., Ross, J. L., Goldman, Y. E., & Holzbaur, E. L. F. (2008). Differential regulation of dynein and kinesin motor proteins by tau. *Science (New York, N.Y.)*, *319*(5866), 1086-1089. <https://doi.org/10.1126/science.1152993>
- Dong, J., Zhou, M., Wu, X., Du, M., & Wang, X. (2012). Memantine combined with environmental enrichment improves spatial memory and alleviates Alzheimer's disease-like pathology in senescence-accelerated prone-8 (SAMP8) mice. *Journal of Biomedical Research*, *26*(6), 439-447. <https://doi.org/10.7555/JBR.26.20120053>
- Dong, X., Wang, Y., & Qin, Z. (2009). Molecular mechanisms of excitotoxicity and their relevance to pathogenesis of neurodegenerative diseases. *Acta Pharmacologica Sinica*, *30*(4), 379-387. <https://doi.org/10.1038/aps.2009.24>
- Dooley, M., & Lamb, H. M. (2000). Donepezil: a review of its use in Alzheimer's

- disease. *Drugs & Aging*, 16(3), 199-226. <https://doi.org/10.2165/00002512-200016030-00005>
- Doraiswamy, P. M. (2003). Alzheimer's disease and the glutamate NMDA receptor. *Psychopharmacology bulletin*, 37(2), 41-49.
- Dosanjh, L. E., Brown, M. K., Rao, G., Link, C. D., & Luo, Y. (2010). Behavioral phenotyping of a transgenic *Caenorhabditis elegans* expressing neuronal amyloid- β . *Journal of Alzheimer's Disease*, 19(2), 681-690.
- Drew, L. (2018). An age-old story of dementia. *Nature*, 559(7715), S2-S3. <https://doi.org/10.1038/d41586-018-05718-5>
- Drummond, E., & Wisniewski, T. (2017). Alzheimer's disease: experimental models and reality. *Acta Neuropathologica*, 133(2), 155-175. <https://doi.org/10.1007/s00401-016-1662-x>
- Duncan, G. W. (2011). The aging brain and neurodegenerative diseases. *Clinics in Geriatric Medicine*, 27(4), 629-644. <https://doi.org/10.1016/j.cger.2011.07.008>
- Eggert, S., Thomas, C., Kins, S., & Hermeijer, G. (2018). Trafficking in Alzheimer's Disease: Modulation of APP Transport and Processing by the Transmembrane Proteins LRP1, SorLA, SorCS1c, Sortilin, and Calsyntenin. *Molecular Neurobiology*, 55(7), 5809-5829. <https://doi.org/10.1007/s12035-017-0806-x>
- EMA. (2021). EMA. Refusal of the marketing authorisation for Aduhelm (aducanumab). Recuperat 11 febrer 2022, de <https://www.ema.europa.eu/en/medicines/human/summaries-opinion/aduhelm>
- Emadeldin, D., Ramadan, A., Fala, S. Y., Sadik, M., Sadik, F., Bahbah, E. I., ... Negida, A. (2017). Disease modifying efficacy of memantine in Alzheimer's disease; a pooled analysis of 13 randomized controlled trials. *Journal of the Neurological Sciences*, 381, 767. <https://doi.org/10.1016/j.jns.2017.08.2166>
- Endele, S., Rosenberger, G., Geider, K., Popp, B., Tamer, C., Stefanova, I., ... Kutsche, K. (2010). Mutations in GRIN2A and GRIN2B encoding regulatory subunits of NMDA receptors cause variable neurodevelopmental phenotypes. *Nature Genetics*, 42(11), 1021-1026. <https://doi.org/10.1038/ng.677>
- Etcheberrigaray, R., Hirashima, N., Nee, L., Prince, J., Govoni, S., Racchi, M., ... Alkon, D. L. (1998). Calcium responses in fibroblasts from asymptomatic members of Alzheimer's disease families. *Neurobiology of Disease*, 5(1), 37-45. <https://doi.org/10.1006/nbdi.1998.0176>
- Fan, Z., Aman, Y., Ahmed, I., Chetelat, G., Landeau, B., Ray Chaudhuri, K., ...

- Edison, P. (2015). Influence of microglial activation on neuronal function in Alzheimer's and Parkinson's disease dementia. *Alzheimer's & Dementia : The Journal of the Alzheimer's Association*, 11(6), 608-21.e7. <https://doi.org/10.1016/j.jalz.2014.06.016>
- FDA. (2021). FDA's decision to approve new treatment for Alzheimer's disease. Recuperat 11 febrer 2021, de <https://www.fda.gov/drugs/news-events-human-drugs/fdas-decision-approve-new-treatment-alzheimers-disease>
- Femminella, G. D., Ninan, S., Atkinson, R., Fan, Z., Brooks, D. J., & Edison, P. (2016). Does Microglial Activation Influence Hippocampal Volume and Neuronal Function in Alzheimer's Disease and Parkinson's Disease Dementia? *Journal of Alzheimer's Disease: JAD*, 51(4), 1275-1289. <https://doi.org/10.3233/JAD-150827>
- Fernández-Tomé, P., Brera, B., Arévalo, M.-A., & de Ceballos, M. L. (2004). Beta-amyloid25-35 inhibits glutamate uptake in cultured neurons and astrocytes: modulation of uptake as a survival mechanism. *Neurobiology of Disease*, 15(3), 580-589. <https://doi.org/10.1016/j.nbd.2003.12.006>
- Fernandez, A. M., Fernandez, S., Carrero, P., Garcia-Garcia, M., & Torres-Aleman, I. (2007). Calcineurin in reactive astrocytes plays a key role in the interplay between proinflammatory and anti-inflammatory signals. *The Journal of Neuroscience: The Official Journal of the Society for Neuroscience*, 27(33), 8745-8756. <https://doi.org/10.1523/JNEUROSCI.1002-07.2007>
- Ferreira, I. L., Bajouco, L. M., Mota, S. I., Auberson, Y. P., Oliveira, C. R., & Rego, A. C. (2012). Amyloid beta peptide 1-42 disturbs intracellular calcium homeostasis through activation of GluN2B-containing N-methyl-d-aspartate receptors in cortical cultures. *Cell Calcium*, 51(2), 95-106. <https://doi.org/10.1016/j.ceca.2011.11.008>
- Ferreiro, E., Oliveira, C. R., & Pereira, C. (2004). Involvement of endoplasmic reticulum Ca²⁺ release through ryanodine and inositol 1,4,5-triphosphate receptors in the neurotoxic effects induced by the amyloid-beta peptide. *Journal of Neuroscience Research*, 76(6), 872-880. <https://doi.org/10.1002/jnr.20135>
- Ferrer, I., Marín, C., Rey, M. J., Ribalta, T., Goutan, E., Blanco, R., ... Martí, E. (1999). BDNF and full-length and truncated TrkB expression in Alzheimer disease. Implications in therapeutic strategies. *Journal of Neuropathology and Experimental Neurology*, 58(7), 729-739. <https://doi.org/10.1097/00005072-199907000-00007>
- Figueiredo, C. P., Clarke, J. R., Ledo, J. H., Ribeiro, F. C., Costa, C. V., Melo, H. M., ... Ferreira, S. T. (2013). Memantine Rescues Transient Cognitive

- Impairment Caused by High-Molecular-Weight A β Oligomers But Not the Persistent Impairment Induced by Low-Molecular-Weight Oligomers. *Journal of Neuroscience*, 33(23), 9626-9634. <https://doi.org/10.1523/JNEUROSCI.0482-13.2013>
- Flanigan, T. J., Xue, Y., Kishan Rao, S., Dhanushkodi, A., & McDonald, M. P. (2014). Abnormal vibrissa-related behavior and loss of barrel field inhibitory neurons in 5xFAD transgenics. *Genes, Brain, and Behavior*, 13(5), 488-500. <https://doi.org/10.1111/gbb.12133>
- Forder, J. P., & Tymianski, M. (2009). Postsynaptic mechanisms of excitotoxicity: Involvement of postsynaptic density proteins, radicals, and oxidant molecules. *Neuroscience*, 158(1), 293-300. <https://doi.org/10.1016/j.neuroscience.2008.10.021>
- Friedlander, R. M. (2003). Apoptosis and Caspases in Neurodegenerative Diseases. *New England Journal of Medicine*, 348(14), 1365-1375. <https://doi.org/10.1056/NEJMra022366>
- Friedler, B., Crapser, J., & McCullough, L. (2015). One is the deadliest number: the detrimental effects of social isolation on cerebrovascular diseases and cognition. *Acta Neuropathologica*, 129(4), 493-509. <https://doi.org/10.1007/s00401-014-1377-9>
- Fu, W.-Y., Wang, X., & Ip, N. Y. (2019). Targeting Neuroinflammation as a Therapeutic Strategy for Alzheimer's Disease: Mechanisms, Drug Candidates, and New Opportunities. *ACS Chemical Neuroscience*, 10(2), 872-879. <https://doi.org/10.1021/acscemneuro.8b00402>
- Gagnon, M., Rive, B., Hux, M., & Guilhaume, C. (2007). Cost-effectiveness of memantine compared with standard care in moderate-to-severe Alzheimer disease in Canada. *Canadian Journal of Psychiatry. Revue Canadienne de Psychiatrie*, 52(8), 519-526. <https://doi.org/10.1177/070674370705200810>
- Garay, R. P., & Grossberg, G. T. (2017). AVP-786 for the treatment of agitation in dementia of the Alzheimer's type. *Expert Opinion on Investigational Drugs*, 26(1), 121-132. <https://doi.org/10.1080/13543784.2017.1267726>
- Gartel, A. L., & Tyner, A. L. (2002). The role of the cyclin-dependent kinase inhibitor p21 in apoptosis. *Molecular Cancer Therapeutics*, 1(8), 639-649.
- Gauthier, S., Loft, H., & Cummings, J. (2008). Improvement in behavioural symptoms in patients with moderate to severe Alzheimer's disease by memantine: a pooled data analysis. *International journal of geriatric psychiatry*, 23(5), 537-545.
- Geda, Y. E., Roberts, R. O., Knopman, D. S., Petersen, R. C., Christianson, T. J. H., Pankratz, V. S., ... Rocca, W. A. (2008). Prevalence of neuropsychiatric symptoms in mild cognitive impairment and normal cognitive aging:

- population-based study. *Archives of General Psychiatry*, 65(10), 1193-1198. <https://doi.org/10.1001/archpsyc.65.10.1193>
- Gezen-Ak, D., Dursun, E., Hanağası, H., Bilgiç, B., Lohman, E., Araz, Ö. S., ... Yilmazer, S. (2013). BDNF, TNF α , HSP90, CFH, and IL-10 serum levels in patients with early or late onset Alzheimer's disease or mild cognitive impairment. *Journal of Alzheimer's Disease: JAD*, 37(1), 185-195. <https://doi.org/10.3233/JAD-130497>
- Ghavami, S., Shojaei, S., Yeganeh, B., Ande, S. R., Jangamreddy, J. R., Mehrpour, M., ... Łos, M. J. (2014). Autophagy and apoptosis dysfunction in neurodegenerative disorders. *Progress in Neurobiology*. Elsevier Ltd. <https://doi.org/10.1016/j.pneurobio.2013.10.004>
- Girouard, H., Wang, G., Gallo, E. F., Anrather, J., Zhou, P., Pickel, V. M., & Iadecola, C. (2009). NMDA receptor activation increases free radical production through nitric oxide and NOX2. *The Journal of Neuroscience: The Official Journal of the Society for Neuroscience*, 29(8), 2545-2552. <https://doi.org/10.1523/JNEUROSCI.0133-09.2009>
- Glasgow, N. G., Povysheva, N. V., Azofeifa, A. M., & Johnson, J. W. (2017). Memantine and Ketamine Differentially Alter NMDA Receptor Desensitization. *Journal of Neuroscience*, 37(40), 9686-9704. <https://doi.org/10.1523/JNEUROSCI.1173-17.2017>
- Goebel-Goody, S. M., Davies, K. D., Alvestad Linger, R. M., Freund, R. K., & Browning, M. D. (2009). Phospho-regulation of synaptic and extrasynaptic N-methyl-d-aspartate receptors in adult hippocampal slices. *Neuroscience*, 158(4), 1446-1459. <https://doi.org/10.1016/j.neuroscience.2008.11.006>
- Goldberg, J. H., Yuste, R., & Tamas, G. (2003). Ca²⁺ imaging of mouse neocortical interneurone dendrites: Contribution of Ca²⁺-permeable AMPA and NMDA receptors to subthreshold Ca²⁺ dynamics. *The Journal of physiology*, 551(1), 67-78.
- Gómez-Isla, T., Hollister, R., West, H., Mui, S., Growdon, J. H., Petersen, R. C., ... Hyman, B. T. (1997). Neuronal loss correlates with but exceeds neurofibrillary tangles in Alzheimer's disease. *Annals of Neurology*, 41(1), 17-24. <https://doi.org/10.1002/ana.410410106>
- Goto, S., Yamamoto, H., Fukunaga, K., Iwasa, T., Matsukado, Y., & Miyamoto, E. (1985). Dephosphorylation of microtubule-associated protein 2, tau factor, and tubulin by calcineurin. *Journal of Neurochemistry*, 45(1), 276-283. <https://doi.org/10.1111/j.1471-4159.1985.tb05504.x>
- Greene, J. D. W., & Hodges, J. R. (1996). Identification of famous faces and famous names in early Alzheimer's disease: Relationship to anterograde episodic and general semantic memory. *Brain*, 119(1), 111-128.

- Grundke-Iqbal, I., Iqbal, K., Tung, Y.-C., Quinlan, M., Wisniewski, H. M., & Binder, L. I. (1986). Abnormal phosphorylation of the microtubule-associated protein tau (tau) in Alzheimer cytoskeletal pathology. *Proceedings of the National Academy of Sciences*, *83*(13), 4913-4917.
- Guo, T., Zhang, D., Zeng, Y., Huang, T. Y., Xu, H., & Zhao, Y. (2020). Molecular and cellular mechanisms underlying the pathogenesis of Alzheimer's disease. *Molecular Neurodegeneration*, *15*(1), 40. <https://doi.org/10.1186/s13024-020-00391-7>
- Haass, C., Lemere, C. A., Capell, A., Citron, M., Seubert, P., Schenk, D., ... Selkoe, D. J. (1995). The Swedish mutation causes early-onset Alzheimer's disease by beta-secretase cleavage within the secretory pathway. *Nature Medicine*, *1*(12), 1291-1296. <https://doi.org/10.1038/nm1295-1291>
- Hackos, D. H., & Hanson, J. E. (2017). Diverse modes of NMDA receptor positive allosteric modulation: Mechanisms and consequences. *Neuropharmacology*, *112*(Pt A), 34-45. <https://doi.org/10.1016/j.neuropharm.2016.07.037>
- Halliwell, B. (2007). Biochemistry of oxidative stress. *Biochemical society transactions*, *35*(5), 1147-1150.
- Hamano, T., Gendron, T. F., Causevic, E., Yen, S.-H., Lin, W.-L., Isidoro, C., ... Ko, L. (2008). Autophagic-lysosomal perturbation enhances tau aggregation in transfectants with induced wild-type tau expression. *The European Journal of Neuroscience*, *27*(5), 1119-1130. <https://doi.org/10.1111/j.1460-9568.2008.06084.x>
- Hansen, K. B., Yi, F., Perszyk, R. E., Furukawa, H., Wollmuth, L. P., Gibb, A. J., & Traynelis, S. F. (2018). Structure, function, and allosteric modulation of NMDA receptors. *Journal of General Physiology*, *150*(8), 1081-1105. <https://doi.org/10.1085/jgp.201812032>
- Hardingham, G E, Fukunaga, Y., & Bading, H. (2002). Extrasynaptic NMDARs oppose synaptic NMDARs by triggering CREB shut-off and cell death pathways. *Nature Neuroscience*, *5*(5), 405-414. <https://doi.org/10.1038/nn835>
- Hardingham, Giles E, Bading, H., Subramanian, J., Savage, J. C., Tremblay, M.-È., Overk, C. R., ... Volpicelli, F. (2010). Synaptic versus extrasynaptic NMDA receptor signalling: implications for neurodegenerative disorders. *Nature Reviews Neuroscience*, *11*(10), 682-696. <https://doi.org/10.3390/ijms21207777>
- Harris, H., & Rubinsztein, D. C. (2011). Control of autophagy as a therapy for neurodegenerative disease. *Nature Reviews. Neurology*, *8*(2), 108-117. <https://doi.org/10.1038/nrneurol.2011.200>

- Harry, G. J. (2013). Microglia during development and aging. *Pharmacology & Therapeutics*, *139*(3), 313-326. <https://doi.org/10.1016/j.pharmthera.2013.04.013>
- Hellweg, R., & Jockers-Scherübl, M. (1994). Neurotrophic factors in memory disorders. *Life Sciences*, *55*(25-26), 2165-2169. [https://doi.org/10.1016/0024-3205\(94\)00397-1](https://doi.org/10.1016/0024-3205(94)00397-1)
- Heneka, M. T., O'Banion, M. K., Terwel, D., & Kummer, M. P. (2010). Neuroinflammatory processes in Alzheimer's disease. *Journal of neural transmission*, *117*(8), 919-947.
- Heneka, M. T., Sastre, M., Dumitrescu-Ozimek, L., Dewachter, I., Walter, J., Klockgether, T., & Van Leuven, F. (2005). Focal glial activation coincides with increased BACE1 activation and precedes amyloid plaque deposition in APP[V717I] transgenic mice. *Journal of Neuroinflammation*, *2*, 22. <https://doi.org/10.1186/1742-2094-2-22>
- Henson, M. A., Roberts, A. C., Pérez-Otaño, I., & Philpot, B. D. (2010). Influence of the NR3A subunit on NMDA receptor functions. *Progress in Neurobiology*, *91*(1), 23-37. <https://doi.org/10.1016/j.pneurobio.2010.01.004>
- Heppner, F. L., Ransohoff, R. M., & Becher, B. (2015). Immune attack: the role of inflammation in Alzheimer disease. *Nature Reviews. Neuroscience*, *16*(6), 358-372. <https://doi.org/10.1038/nrn3880>
- Hirano, K., Fujimaki, M., Sasazawa, Y., Yamaguchi, A., Ishikawa, K.-I., Miyamoto, K., ... Hattori, N. (2019). Neuroprotective effects of memantine via enhancement of autophagy. *Biochemical and Biophysical Research Communications*, *518*(1), 161-170. <https://doi.org/10.1016/j.bbrc.2019.08.025>
- Hobert, O., & Bülow, H. (2003). Development and maintenance of neuronal architecture at the ventral midline of *C. elegans*. *Current Opinion in Neurobiology*, *13*(1), 70-78. [https://doi.org/10.1016/s0959-4388\(03\)00002-3](https://doi.org/10.1016/s0959-4388(03)00002-3)
- Hol, E. M., & Pekny, M. (2015). Glial fibrillary acidic protein (GFAP) and the astrocyte intermediate filament system in diseases of the central nervous system. *Current opinion in cell biology*, *32*, 121-130.
- Hong, S., Beja-Glasser, V. F., Nfonoyim, B. M., Frouin, A., Li, S., Ramakrishnan, S., ... Stevens, B. (2016). Complement and microglia mediate early synapse loss in Alzheimer mouse models. *Science (New York, N.Y.)*, *352*(6286), 712-716. <https://doi.org/10.1126/science.aad8373>
- Hou, Y., Dan, X., Babbar, M., Wei, Y., Hasselbalch, S. G., Croteau, D. L., & Bohr, V. A. (2019). Ageing as a risk factor for neurodegenerative disease.

- Nature Reviews Neurology*, 15(10), 565-581.
<https://doi.org/10.1038/s41582-019-0244-7>
- Hsiao, Y.-H., Chang, C.-H., & Gean, P.-W. (2018). Impact of social relationships on Alzheimer's memory impairment: mechanistic studies. *Journal of Biomedical Science*, 25(1), 3. <https://doi.org/10.1186/s12929-018-0404-x>
- Hu, C., Chen, W., Myers, S. J., Yuan, H., & Traynelis, S. F. (2016). Human GRIN2B variants in neurodevelopmental disorders. *Journal of Pharmacological Sciences*, 132(2), 115-121.
<https://doi.org/10.1016/j.jphs.2016.10.002>
- Hu, S., Hu, H., Mak, S., Cui, G., Lee, M., Shan, L., ... Han, Y. (2018). A Novel Tetramethylpyrazine Derivative Prophylactically Protects against Glutamate-Induced Excitotoxicity in Primary Neurons through the Blockage of N-Methyl-D-aspartate Receptor. *Frontiers in Pharmacology*, 9, 73.
<https://doi.org/10.3389/fphar.2018.00073>
- Huang, L.-K., Chao, S.-P., & Hu, C.-J. (2020). Clinical trials of new drugs for Alzheimer disease. *Journal of biomedical science*, 27(1), 1-13.
- Huang, X., Atwood, C. S., Hartshorn, M. A., Multhaup, G., Goldstein, L. E., Scarpa, R. C., ... Bush, A. I. (1999). The A β Peptide of Alzheimer's Disease Directly Produces Hydrogen Peroxide through Metal Ion Reduction. *Biochemistry*, 38(24), 7609-7616. <https://doi.org/10.1021/bi990438f>
- Hunt, P. R. (2017). The *C. elegans* model in toxicity testing. *Journal of Applied Toxicology : JAT*, 37(1), 50-59. <https://doi.org/10.1002/jat.3357>
- Husi, H., Ward, M. A., Choudhary, J. S., Blackstock, W. P., & Grant, S. G. (2000). Proteomic analysis of NMDA receptor-adhesion protein signaling complexes. *Nature Neuroscience*, 3(7), 661-669.
<https://doi.org/10.1038/76615>
- Iino, M., Nomura, T., Tamaki, Y., Yamada, Y., Yoneyama, K., Takeuchi, Y., ... Yokota, T. (2007). Progesterone: its occurrence in plants and involvement in plant growth. *Phytochemistry*, 68(12), 1664-1673.
<https://doi.org/10.1016/j.phytochem.2007.04.002>
- Iqbal, K., Grundke-Iqbal, I., Zaidi, T., Merz, P. A., Wen, G. Y., Shaikh, S. S., ... Winblad, B. (1986). Defective brain microtubule assembly in Alzheimer's disease. *Lancet (London, England)*, 2(8504), 421-426.
[https://doi.org/10.1016/s0140-6736\(86\)92134-3](https://doi.org/10.1016/s0140-6736(86)92134-3)
- Ito, K., Tatebe, T., Suzuki, K., Hirayama, T., Hayakawa, M., Kubo, H., ... Makino, M. (2017). Memantine reduces the production of amyloid- β peptides through modulation of amyloid precursor protein trafficking. *European Journal of Pharmacology*, 798(January), 16-25.
<https://doi.org/10.1016/j.ejphar.2017.02.001>

- Iwatsubo, T., Odaka, A., Suzuki, N., Mizusawa, H., Nukina, N., & Ihara, Y. (1994). Visualization of A beta 42(43) and A beta 40 in senile plaques with end-specific A beta monoclonals: evidence that an initially deposited species is A beta 42(43). *Neuron*, 13(1), 45-53. [https://doi.org/10.1016/0896-6273\(94\)90458-8](https://doi.org/10.1016/0896-6273(94)90458-8)
- Izumida, H., Takagi, H., Fujisawa, H., Iwata, N., Nakashima, K., Takeuchi, S., ... Sugimura, Y. (2017). NMDA receptor antagonist prevents cell death in the hippocampal dentate gyrus induced by hyponatremia accompanying adrenal insufficiency in rats. *Experimental Neurology*, 287(Pt 1), 65-74. <https://doi.org/10.1016/j.expneurol.2016.08.007>
- Jahn, H. (2013). Memory loss in Alzheimer's disease. *Dialogues in Clinical Neuroscience*, 15(4), 445-454. <https://doi.org/10.31887/DCNS.2013.15.4/hjahn>
- James, W. H. (1988, setembre). Parental coital rates and Down syndrome. *American Journal of Medical Genetics*. United States. <https://doi.org/10.1002/ajmg.1320310121>
- Jang, B. G., In, S., Choi, B., & Kim, M.-J. (2014). Beta-amyloid oligomers induce early loss of presynaptic proteins in primary neurons by caspase-dependent and proteasome-dependent mechanisms. *Neuroreport*, 25(16), 1281-1288. <https://doi.org/10.1097/WNR.0000000000000260>
- Jansen, I. E., Savage, J. E., Watanabe, K., Bryois, J., Williams, D. M., Steinberg, S., ... Posthuma, D. (2019). Genome-wide meta-analysis identifies new loci and functional pathways influencing Alzheimer's disease risk. *Nature Genetics*, 51(3), 404-413. <https://doi.org/10.1038/s41588-018-0311-9>
- Jay, T. R., von Saucken, V. E., & Landreth, G. E. (2017). TREM2 in Neurodegenerative Diseases. *Molecular Neurodegeneration*, 12(1), 56. <https://doi.org/10.1186/s13024-017-0197-5>
- Jerónimo-Santos, A., Vaz, S. H., Parreira, S., Rapaz-Lérias, S., Caetano, A. P., Buée-Scherrer, V., ... Diógenes, M. J. (2015). Dysregulation of TrkB Receptors and BDNF Function by Amyloid- β Peptide is Mediated by Calpain. *Cerebral Cortex (New York, N.Y. : 1991)*, 25(9), 3107-3121. <https://doi.org/10.1093/cercor/bhu105>
- Jessen, N. A., Munk, A. S. F., Lundgaard, I., & Nedergaard, M. (2015). The Glymphatic System: A Beginner's Guide. *Neurochemical Research*, 40(12), 2583-2599. <https://doi.org/10.1007/s11064-015-1581-6>
- Jiang, T., Tan, L., Zhu, X.-C., Zhang, Q.-Q., Cao, L., Tan, M.-S., ... Yu, J.-T. (2014). Upregulation of TREM2 ameliorates neuropathology and rescues spatial cognitive impairment in a transgenic mouse model of Alzheimer's disease. *Neuropsychopharmacology: Official Publication of the American*

- College of Neuropsychopharmacology*, 39(13), 2949-2962.
<https://doi.org/10.1038/npp.2014.164>
- Jin, N., Yin, X., Yu, D., Cao, M., Gong, C.-X., Iqbal, K., ... Liu, F. (2015). Truncation and activation of GSK-3 β by calpain I: a molecular mechanism links to tau hyperphosphorylation in Alzheimer's disease. *Scientific Reports*, 5, 8187. <https://doi.org/10.1038/srep08187>
- Jo, S., Yarishkin, O., Hwang, Y. J., Chun, Y. E., Park, M., Woo, D. H., ... Lee, C. J. (2014). GABA from reactive astrocytes impairs memory in mouse models of Alzheimer's disease. *Nature Medicine*, 20(8), 886-896. <https://doi.org/10.1038/nm.3639>
- Johnson, J. W., & Kotermanski, S. E. (2006). Mechanism of action of memantine. *Current Opinion in Pharmacology*, 6(1), 61-67. <https://doi.org/10.1016/j.coph.2005.09.007>
- Johri, A., & Beal, M. F. (2012). Mitochondrial dysfunction in neurodegenerative diseases. *The Journal of Pharmacology and Experimental Therapeutics*, 342(3), 619-630. <https://doi.org/10.1124/jpet.112.192138>
- Jones, M. L., & Leonard, J. P. (2005). PKC site mutations reveal differential modulation by insulin of NMDA receptors containing NR2A or NR2B subunits. *Journal of neurochemistry*, 92(6), 1431-1438.
- Jurga, A. M., Paleczna, M., & Kuter, K. Z. (2020). Overview of General and Discriminating Markers of Differential Microglia Phenotypes. *Frontiers in Cellular Neuroscience*, 14. <https://doi.org/10.3389/fncel.2020.00198>
- Kadavath, H., Hofele, R. V., Biernat, J., Kumar, S., Tepper, K., Urlaub, H., ... Zweckstetter, M. (2015). Tau stabilizes microtubules by binding at the interface between tubulin heterodimers. *Proceedings of the National Academy of Sciences of the United States of America*, 112(24), 7501-7506. <https://doi.org/10.1073/pnas.1504081112>
- Kalinin, S., Polak, P. E., Lin, S. X., Sakharkar, A. J., Pandey, S. C., & Feinstein, D. L. (2012). The noradrenaline precursor L-DOPS reduces pathology in a mouse model of Alzheimer's disease. *Neurobiology of aging*, 33(8), 1651-1663.
- Kamat, P. K., Kalani, A., Rai, S., Swarnkar, S., Tota, S., Nath, C., & Tyagi, N. (2016). Mechanism of Oxidative Stress and Synapse Dysfunction in the Pathogenesis of Alzheimer's Disease: Understanding the Therapeutics Strategies. *Molecular Neurobiology*, 53(1), 648-661. <https://doi.org/10.1007/s12035-014-9053-6>
- Kamat, P. K., Rai, S., Swarnkar, S., Shukla, R., & Nath, C. (2014). Mechanism of synapse redox stress in Okadaic acid (ICV) induced memory impairment: Role of NMDA receptor. *Neurochemistry International*, 76, 32-41.

- <https://doi.org/10.1016/j.neuint.2014.06.012>
- Kamphuis, W., Middeldorp, J., Kooijman, L., Sluijs, J. A., Kooi, E.-J., Moeton, M., ... Hol, E. M. (2014). Glial fibrillary acidic protein isoform expression in plaque related astrogliosis in Alzheimer's disease. *Neurobiology of aging*, 35(3), 492-510.
- Káradóttir, R., Cavelier, P., Bergersen, L. H., & Attwell, D. (2005). NMDA receptors are expressed in oligodendrocytes and activated in ischaemia. *Nature*, 438(7071), 1162-1166.
- Kataura, T., Tashiro, E., Nishikawa, S., Shibahara, K., Muraoka, Y., Miura, M., ... Imoto, M. (2021). A chemical genomics-aggrephagy integrated method studying functional analysis of autophagy inducers. *Autophagy*, 17(8), 1856-1872. <https://doi.org/10.1080/15548627.2020.1794590>
- Kaushik, S., Tasset, I., Arias, E., Pampliega, O., Wong, E., Martinez-Vicente, M., & Cuervo, A. M. (2021). Autophagy and the hallmarks of aging. *Ageing Research Reviews*, 72, 101468. <https://doi.org/10.1016/j.arr.2021.101468>
- Kelestemur, T., Yulug, B., Caglayan, A. B., Beker, M. C., Kilic, U., Caglayan, B., ... Kilic, E. (2016). Targeting different pathophysiological events after traumatic brain injury in mice: Role of melatonin and memantine. *Neuroscience Letters*, 612, 92-97. <https://doi.org/10.1016/j.neulet.2015.11.043>
- Keren-Shaul, H., Spinrad, A., Weiner, A., Matcovitch-Natan, O., Dvir-Szternfeld, R., Ulland, T. K., ... Amit, I. (2017). A Unique Microglia Type Associated with Restricting Development of Alzheimer's Disease. *Cell*, 169(7), 1276-1290.e17. <https://doi.org/10.1016/j.cell.2017.05.018>
- Kim, J., Onstead, L., Randle, S., Price, R., Smithson, L., Zwizinski, C., ... McGowan, E. (2007). A β 40 Inhibits Amyloid Deposition In Vivo. *Journal of Neuroscience*, 27(3), 627-633. <https://doi.org/10.1523/JNEUROSCI.4849-06.2007>
- Kirvell, S. L., Esiri, M., & Francis, P. T. (2006). Down-regulation of vesicular glutamate transporters precedes cell loss and pathology in Alzheimer's disease. *Journal of Neurochemistry*, 98(3), 939-950. <https://doi.org/10.1111/j.1471-4159.2006.03935.x>
- Kishi, T., Matsunaga, S., Oya, K., Nomura, I., Ikuta, T., & Iwata, N. (2017). Memantine for Alzheimer's Disease: An Updated Systematic Review and Meta-analysis. *Journal of Alzheimer's Disease*, 60(2), 401-425. <https://doi.org/10.3233/JAD-170424>
- Kishida, K. T., & Klann, E. (2007). Sources and targets of reactive oxygen species in synaptic plasticity and memory. *Antioxidants & Redox Signaling*, 9(2), 233-244. <https://doi.org/10.1089/ars.2007.9.ft-8>

- Kitamura, Y., Zhao, X.-H., Ohnuki, T., Takei, M., & Nomura, Y. (1992). Age-related changes in transmitter glutamate and NMDA receptor/channels in the brain of senescence-accelerated mouse. *Neuroscience letters*, *137*(2), 169-172.
- Kleckner, N. W., & Dingledine, R. (1988). Requirement for glycine in activation of NMDA-receptors expressed in *Xenopus* oocytes. *Science (New York, N.Y.)*, *241*(4867), 835-837. <https://doi.org/10.1126/science.2841759>
- Kodis, E. J., Choi, S., Swanson, E., Ferreira, G., & Bloom, G. S. (2018). N-methyl-D-aspartate receptor-mediated calcium influx connects amyloid- β oligomers to ectopic neuronal cell cycle reentry in Alzheimer's disease. *Alzheimer's & Dementia*, *14*(10), 1302-1312.
- Köpke, E., Tung, Y. C., Shaikh, S., Alonso, A. C., Iqbal, K., & Grundke-Iqbal, I. (1993). Microtubule-associated protein tau. Abnormal phosphorylation of a non-paired helical filament pool in Alzheimer disease. *The Journal of Biological Chemistry*, *268*(32), 24374-24384.
- Kornhuber, J., Bormann, J., Hübers, M., Rusche, K., & Riederer, P. (1991). Effects of the 1-amino-adamantanes at the MK-801-binding site of the NMDA-receptor-gated ion channel: a human postmortem brain study. *European Journal of Pharmacology: Molecular Pharmacology*, *206*(4), 297-300.
- Kornhuber, J., & Weller, M. (1997). Psychotogenicity and N-methyl-D-aspartate receptor antagonism: implications for neuroprotective pharmacotherapy. *Biological psychiatry*, *41*(2), 135-144.
- Kuchibhotla, K. V., Goldman, S. T., Lattarulo, C. R., Wu, H.-Y., Hyman, B. T., & Bacskai, B. J. (2008). Abeta plaques lead to aberrant regulation of calcium homeostasis in vivo resulting in structural and functional disruption of neuronal networks. *Neuron*, *59*(2), 214-225. <https://doi.org/10.1016/j.neuron.2008.06.008>
- Kumar, H., & Sharma, B. (2016). Memantine ameliorates autistic behavior, biochemistry & blood brain barrier impairments in rats. *Brain Research Bulletin*, *124*, 27-39. <https://doi.org/https://doi.org/10.1016/j.brainresbull.2016.03.013>
- Kumari, A., Singh, P., Baghel, M. S., & Thakur, M. K. (2016). Social isolation mediated anxiety like behavior is associated with enhanced expression and regulation of BDNF in the female mouse brain. *Physiology & Behavior*, *158*, 34-42. <https://doi.org/10.1016/j.physbeh.2016.02.032>
- L'Episcopo, F., Drouin-Ouellet, J., Tirolo, C., Pulvirenti, A., Giugno, R., Testa, N., ... Marchetti, B. (2016). GSK-3 β -induced Tau pathology drives hippocampal neuronal cell death in Huntington's disease: involvement of

- astrocyte–neuron interactions. *Cell Death & Disease*, 7(4), e2206. <https://doi.org/10.1038/CDDIS.2016.104>
- Lafon-Cazal, M., Pietri, S., Culcasi, M., & Bockaert, J. (1993). NMDA-dependent superoxide production and neurotoxicity. *Nature*, 364(6437), 535-537. <https://doi.org/10.1038/364535a0>
- Lalo, U., Pankratov, Y., Kirchhoff, F., North, R. A., & Verkhratsky, A. (2006). NMDA receptors mediate neuron-to-glia signaling in mouse cortical astrocytes. *Journal of Neuroscience*, 26(10), 2673-2683.
- Lambon Ralph, M. A., Patterson, K., Graham, N., Dawson, K., & Hodges, J. R. (2003). Homogeneity and heterogeneity in mild cognitive impairment and Alzheimer's disease: a cross-sectional and longitudinal study of 55 cases. *Brain*, 126(11), 2350-2362.
- Landel, V., Baranger, K., Virard, I., Loriod, B., Khrestchatsky, M., Rivera, S., ... Féron, F. (2014). Temporal gene profiling of the 5XFAD transgenic mouse model highlights the importance of microglial activation in Alzheimer's disease. *Molecular neurodegeneration*, 9(1), 1-18.
- Lane, C. A., Hardy, J., & Schott, J. M. (2018). Alzheimer's disease. *European Journal of Neurology*, 25(1), 59-70. <https://doi.org/10.1111/ene.13439>
- Lanoiselée, H.-M., Nicolas, G., Wallon, D., Rovelet-Lecrux, A., Lacour, M., Rousseau, S., ... Champion, D. (2017). APP, PSEN1, and PSEN2 mutations in early-onset Alzheimer disease: A genetic screening study of familial and sporadic cases. *PLoS Medicine*, 14(3), e1002270. <https://doi.org/10.1371/journal.pmed.1002270>
- Lavezzari, G., McCallum, J., Lee, R., & Roche, K. W. (2003). Differential binding of the AP-2 adaptor complex and PSD-95 to the C-terminus of the NMDA receptor subunit NR2B regulates surface expression. *Neuropharmacology*, 45(6), 729-737. [https://doi.org/10.1016/s0028-3908\(03\)00308-3](https://doi.org/10.1016/s0028-3908(03)00308-3)
- Lee, C.-H., Lü, W., Michel, J. C., Goehring, A., Du, J., Song, X., & Gouaux, E. (2014). NMDA receptor structures reveal subunit arrangement and pore architecture. *Nature*, 511(7508), 191-197. <https://doi.org/10.1038/nature13548>
- Lee, D. H., Seo, S. W., Roh, J. H., Oh, M., Oh, J. S., Oh, S. J., ... Jeong, Y. (2021). Effects of Cognitive Reserve in Alzheimer's Disease and Cognitively Unimpaired Individuals. *Frontiers in Aging Neuroscience*, 13, 784054. <https://doi.org/10.3389/fnagi.2021.784054>
- Lee, H.-K. (2006). Synaptic plasticity and phosphorylation. *Pharmacology & Therapeutics*, 112(3), 810-832. <https://doi.org/10.1016/j.pharmthera.2006.06.003>
- Lee, J.-H., Yu, W. H., Kumar, A., Lee, S., Mohan, P. S., Peterhoff, C. M., ...

- Nixon, R. A. (2010). Lysosomal proteolysis and autophagy require presenilin 1 and are disrupted by Alzheimer-related PS1 mutations. *Cell*, *141*(7), 1146-1158. <https://doi.org/10.1016/j.cell.2010.05.008>
- Lee, M. S., Kwon, Y. T., Li, M., Peng, J., Friedlander, R. M., & Tsai, L. H. (2000). Neurotoxicity induces cleavage of p35 to p25 by calpain. *Nature*, *405*(6784), 360-364. <https://doi.org/10.1038/35012636>
- Lee, Y.-K., & Lee, J.-A. (2016). Role of the mammalian ATG8/LC3 family in autophagy: differential and compensatory roles in the spatiotemporal regulation of autophagy. *BMB Reports*, *49*(8), 424-430. <https://doi.org/10.5483/bmbrep.2016.49.8.081>
- Leiva, R., Phillips, M. B., Turcu, A. L., Gratacòs-Batlle, E., León-García, L., Sureda, F. X., ... Vázquez, S. (2018). Pharmacological and Electrophysiological Characterization of Novel NMDA Receptor Antagonists. *ACS Chemical Neuroscience*, *9*(11), 2722-2730. <https://doi.org/10.1021/acschemneuro.8b00154>
- Leng, F., & Edison, P. (2021). Neuroinflammation and microglial activation in Alzheimer disease: where do we go from here? *Nature Reviews Neurology*, *17*(3), 157-172. <https://doi.org/10.1038/s41582-020-00435-y>
- Leser, N., & Wagner, S. (2015). The effects of acute social isolation on long-term social recognition memory. *Neurobiology of Learning and Memory*, *124*, 97-103. <https://doi.org/10.1016/j.nlm.2015.07.002>
- Li, B.-S., Sun, M.-K., Zhang, L., Takahashi, S., Ma, W., Vinade, L., ... Pant, H. C. (2001). Regulation of NMDA receptors by cyclin-dependent kinase-5. *Proceedings of the National Academy of Sciences*, *98*(22), 12742-12747.
- Li, J., O, W., Li, W., Jiang, Z.-G., & Ghanbari, H. A. (2013). Oxidative stress and neurodegenerative disorders. *International Journal of Molecular Sciences*, *14*(12), 24438-24475. <https://doi.org/10.3390/ijms141224438>
- Li, S., Jin, M., Koeglsperger, T., Shepardson, N. E., Shankar, G. M., & Selkoe, D. J. (2011). Soluble A β oligomers inhibit long-term potentiation through a mechanism involving excessive activation of extrasynaptic NR2B-containing NMDA receptors. *The Journal of Neuroscience: The Official Journal of the Society for Neuroscience*, *31*(18), 6627-6638. <https://doi.org/10.1523/JNEUROSCI.0203-11.2011>
- Liang, X. H., Jackson, S., Seaman, M., Brown, K., Kempkes, B., Hibshoosh, H., & Levine, B. (1999). Induction of autophagy and inhibition of tumorigenesis by beclin 1. *Nature*, *402*(6762), 672-676. <https://doi.org/10.1038/45257>
- Liddelw, S. A., & Barres, B. A. (2017). Reactive Astrocytes: Production, Function, and Therapeutic Potential. *Immunity*, *46*(6), 957-967. <https://doi.org/10.1016/j.immuni.2017.06.006>

- Liddelw, S. A., Guttenplan, K. A., Clarke, L. E., Bennett, F. C., Bohlen, C. J., Schirmer, L., ... Barres, B. A. (2017). Neurotoxic reactive astrocytes are induced by activated microglia. *Nature*, *541*(7638), 481-487. <https://doi.org/10.1038/nature21029>
- Lim, F., Hernández, F., Lucas, J. J., Gómez-Ramos, P., Morán, M. A., & Avila, J. (2001). FTDP-17 mutations in tau transgenic mice provoke lysosomal abnormalities and Tau filaments in forebrain. *Molecular and Cellular Neurosciences*, *18*(6), 702-714. <https://doi.org/10.1006/mcne.2001.1051>
- Link, C. D. (1995). Expression of human beta-amyloid peptide in transgenic *Caenorhabditis elegans*. *Proceedings of the National Academy of Sciences of the United States of America*, *92*(20), 9368-9372. <https://doi.org/10.1073/pnas.92.20.9368>
- Link, C. D. (2005). Invertebrate models of Alzheimer's disease. *Genes, Brain, and Behavior*, *4*(3), 147-156. <https://doi.org/10.1111/j.1601-183X.2004.00105.x>
- Liu, B., Liu, J., & Shi, J.-S. (2020). SAMP8 Mice as a Model of Age-Related Cognition Decline with Underlying Mechanisms in Alzheimer's Disease. *Journal of Alzheimer's Disease*, *75*, 385-395. <https://doi.org/10.3233/JAD-200063>
- Liu, J., Chang, L., Song, Y., Li, H., & Wu, Y. (2019). The role of NMDA receptors in Alzheimer's disease. *Frontiers in Neuroscience*, *13*, 43. <https://doi.org/10.3389/fnins.2019.00043>
- Liu, X., Ou, S., Yin, M., Xu, T., Wang, T., Liu, Y., ... Chen, Y. (2017). N-methyl-D-aspartate receptors mediate epilepsy-induced axonal impairment and tau phosphorylation via activating glycogen synthase kinase-3 β and cyclin-dependent kinase 5. *Discovery Medicine*, *23*(127), 221-234.
- Liu, Y.-Y., & Bian, J.-S. (2010). Hydrogen sulfide protects amyloid- β induced cell toxicity in microglia. *Journal of Alzheimer's Disease: JAD*, *22*(4), 1189-1200. <https://doi.org/10.3233/JAD-2010-101002>
- Liu, Y., Wong, T. P., Aarts, M., Rooyackers, A., Liu, L., Lai, T. W., ... Craig, A. M. (2007). NMDA receptor subunits have differential roles in mediating excitotoxic neuronal death both in vitro and in vivo. *Journal of Neuroscience*, *27*(11), 2846-2857.
- Loh, K. P., Huang, S. H., De Silva, R., Tan, B. K. H., & Zhu, Y. Z. (2006). Oxidative stress: apoptosis in neuronal injury. *Current Alzheimer Research*, *3*(4), 327-337. <https://doi.org/10.2174/156720506778249515>
- López-Otín, C., Blasco, M. A., Partridge, L., Serrano, M., & Kroemer, G. (2013). The hallmarks of aging. *Cell*, *153*(6), 1194-1217. <https://doi.org/10.1016/j.cell.2013.05.039>

- López, O. L., & DeKosky, S. T. B. T.-H. of C. N. (2008). Clinical symptoms in Alzheimer's disease. En *Dementias* (Vol. 89, p. 207-216). Elsevier. [https://doi.org/https://doi.org/10.1016/S0072-9752\(07\)01219-5](https://doi.org/https://doi.org/10.1016/S0072-9752(07)01219-5)
- Louneva, N., Cohen, J. W., Han, L.-Y. Y., Talbot, K., Wilson, R. S., Bennett, D. A., ... Arnold, S. E. (2008). Caspase-3 is enriched in postsynaptic densities and increased in Alzheimer's disease. *American Journal of Pathology*, *173*(5), 1488-1495. <https://doi.org/10.2353/ajpath.2008.080434>
- Lublin, A., Isoda, F., Patel, H., Yen, K., Nguyen, L., Hajje, D., ... Mobbs, C. (2011). FDA-approved drugs that protect mammalian neurons from glucose toxicity slow aging dependent on cbp and protect against proteotoxicity. *PLoS One*, *6*(11), e27762. <https://doi.org/10.1371/journal.pone.0027762>
- Ludewig, S., & Korte, M. (2016). Novel Insights into the Physiological Function of the APP (Gene) Family and Its Proteolytic Fragments in Synaptic Plasticity. *Frontiers in Molecular Neuroscience*, *9*, 161. <https://doi.org/10.3389/fnmol.2016.00161>
- Lupp, A., Kerst, S., & Karge, E. (2003). Evaluation of possible pro- or antioxidative properties and of the interaction capacity with the microsomal cytochrome P450 system of different NMDA-receptor ligands and of taurine in vitro. *Experimental and Toxicologic Pathology: Official Journal of the Gesellschaft Fur Toxikologische Pathologie*, *54*(5-6), 441-448. <https://doi.org/10.1078/0940-2993-00280>
- Lussier, M. P., Sanz-Clemente, A., & Roche, K. W. (2015). Dynamic Regulation of N-Methyl-d-aspartate (NMDA) and α -Amino-3-hydroxy-5-methyl-4-isoxazolepropionic Acid (AMPA) Receptors by Posttranslational Modifications. *The Journal of Biological Chemistry*, *290*(48), 28596-28603. <https://doi.org/10.1074/jbc.R115.652750>
- Lv, X., Li, Q., Mao, S., Qin, L., & Dong, P. (2020). The protective effects of memantine against inflammation and impairment of endothelial tube formation induced by oxygen-glucose deprivation/reperfusion. *Aging*, *12*(21), 21469-21480. <https://doi.org/10.18632/aging.103914>
- Lyman, M., Lloyd, D. G., Ji, X., Vizcaychipi, M. P., & Ma, D. (2014). Neuroinflammation: the role and consequences. *Neuroscience Research*, *79*, 1-12. <https://doi.org/10.1016/j.neures.2013.10.004>
- Ma, T., Cheng, Q., Chen, C., Luo, Z., & Feng, D. (2020). Excessive Activation of NMDA Receptors in the Pathogenesis of Multiple Peripheral Organs via Mitochondrial Dysfunction, Oxidative Stress, and Inflammation. *SN Comprehensive Clinical Medicine*, *2*(5), 551-569. <https://doi.org/10.1007/s42399-020-00298-w>
- MacMicking, J., Xie, Q. W., & Nathan, C. (1997). Nitric oxide and macrophage

- function. *Annual Review of Immunology*, 15, 323-350. <https://doi.org/10.1146/annurev.immunol.15.1.323>
- Mahaman, Y. A. R., Huang, F., Afewerky, H. K., Maibouge, T. M. S., Ghose, B., & Wang, X. (2019). Involvement of calpain in the neuropathogenesis of Alzheimer's disease. *Medicinal Research Reviews*, 39(2), 608-630. <https://doi.org/10.1002/MED.21534>
- Mahase, E. (2021). FDA approves controversial Alzheimer's drug despite uncertainty over effectiveness. *BMJ*, 373, n1462. <https://doi.org/10.1136/bmj.n1462>
- Mair, W., Muntel, J., Tepper, K., Tang, S., Biernat, J., Seeley, W. W., ... Steen, J. A. (2016). FLEXITau: quantifying post-translational modifications of tau protein in vitro and in human disease. *Analytical chemistry*, 88(7), 3704-3714.
- Marder, K. (2004). Memantine approved to treat moderate to severe Alzheimer's disease. *Current Neurology and Neuroscience Reports*, 4(5), 349-350. <https://doi.org/10.1007/s11910-004-0080-y>
- Martinez-Coria, H., Green, K. N., Billings, L. M., Kitazawa, M., Albrecht, M., Rammes, G., ... LaFerla, F. M. (2010). Memantine improves cognition and reduces Alzheimer's-like neuropathology in transgenic mice. *American Journal of Pathology*, 176(2), 870-880. <https://doi.org/10.2353/ajpath.2010.090452>
- Marvanová, M., Lakso, M., Pirhonen, J., Nawa, H., Wong, G., & Castrén, E. (2001). The neuroprotective agent memantine induces brain-derived neurotrophic factor and trkB receptor expression in rat brain. *Molecular and Cellular Neuroscience*, 18(3), 247-258.
- Masliah, E., Alford, M., DeTeresa, R., Mallory, M., & Hansen, L. (1996). Deficient glutamate transport is associated with neurodegeneration in Alzheimer's disease. *Annals of Neurology*, 40(5), 759-766. <https://doi.org/10.1002/ana.410400512>
- Masliah, E., Hansen, L., Albright, T., Mallory, M., & Terry, R. D. (1991). Immunoelectron microscopic study of synaptic pathology in Alzheimer's disease. *Acta Neuropathologica*, 81(4), 428-433. <https://doi.org/10.1007/BF00293464>
- Matthews, F. E., Arthur, A., Barnes, L. E., Bond, J., Jagger, C., Robinson, L., & Brayne, C. (2013). A two-decade comparison of prevalence of dementia in individuals aged 65 years and older from three geographical areas of England: results of the Cognitive Function and Ageing Study I and II. *Lancet (London, England)*, 382(9902), 1405-1412. [https://doi.org/10.1016/S0140-6736\(13\)61570-6](https://doi.org/10.1016/S0140-6736(13)61570-6)

- McQuate, A., & Barria, A. (2020). Rapid exchange of synaptic and extrasynaptic NMDA receptors in hippocampal CA1 neurons. *Journal of Neurophysiology*, *123*(3), 1004-1014. <https://doi.org/10.1152/jn.00458.2019>
- McShane, R., Westby, M. J., Roberts, E., Minakaran, N., Schneider, L., Farrimond, L. E., ... Debarros, J. (2019). Memantine for dementia. *Cochrane database of systematic reviews*, (3).
- Medeiros, R., Baglietto-Vargas, D., & LaFerla, F. M. (2011). The role of tau in Alzheimer's disease and related disorders. *CNS Neuroscience & Therapeutics*, *17*(5), 514-524. <https://doi.org/10.1111/j.1755-5949.2010.00177.x>
- Meeker, H. C., Chadman, K. K., Heaney, A. T., & Carp, R. I. (2013). Assessment of social interaction and anxiety-like behavior in senescence-accelerated-prone and -resistant mice. *Physiology and Behavior*, *118*, 97-102. <https://doi.org/10.1016/j.physbeh.2013.05.003>
- Meisner, F., Scheller, C., Kneitz, S., Sopper, S., Neuen-Jacob, E., Riederer, P., ... Koutsilieri, E. (2008). Memantine upregulates BDNF and prevents dopamine deficits in SIV-infected macaques: a novel pharmacological action of memantine. *Neuropsychopharmacology: Official Publication of the American College of Neuropsychopharmacology*, *33*(9), 2228-2236. <https://doi.org/10.1038/sj.npp.1301615>
- Meldrum, B. S. (2000). Glutamate as a neurotransmitter in the brain: review of physiology and pathology. *The Journal of nutrition*, *130*(4), 1007S-1015S.
- Mendez, M. F. (2017). Early-Onset Alzheimer Disease. *Neurologic Clinics*, *35*(2), 263-281. <https://doi.org/10.1016/j.ncl.2017.01.005>
- Micu, I., Jiang, Q., Coderre, E., Ridsdale, A., Zhang, L., Woulfe, J., ... Stys, P. K. (2006). NMDA receptors mediate calcium accumulation in myelin during chemical ischaemia. *Nature*, *439*(7079), 988-992. <https://doi.org/10.1038/nature04474>
- Mishizen-Eberz, A. J., Rissman, R. A., Carter, T. L., Ikonovic, M. D., Wolfe, B. B., & Armstrong, D. M. (2004). Biochemical and molecular studies of NMDA receptor subunits NR1/2A/2B in hippocampal subregions throughout progression of Alzheimer's disease pathology. *Neurobiology of Disease*, *15*(1), 80-92. <https://doi.org/10.1016/j.nbd.2003.09.016>
- Mishra, A., Kim, H. J., Shin, A. H., & Thayer, S. A. (2012). Synapse loss induced by interleukin-1 β requires pre- and post-synaptic mechanisms. *Journal of Neuroimmune Pharmacology: The Official Journal of the Society on NeuroImmune Pharmacology*, *7*(3), 571-578. <https://doi.org/10.1007/s11481-012-9342-7>

- Mishra, S. K., Hidau, M., & Rai, S. (2021). Memantine and Ibuprofen pretreatment exerts anti-inflammatory effect against streptozotocin-induced astroglial inflammation via modulation of NMDA receptor-associated downstream calcium ion signaling. *Inflammopharmacology*, *29*(1), 183-192. <https://doi.org/10.1007/s10787-020-00760-0>
- Miyamoto, M., Kiyota, Y., Nishiyama, M., & Nagaoka, A. (1992). Senescence-accelerated mouse (SAM): age-related reduced anxiety-like behavior in the SAM-P/8 strain. *Physiology & Behavior*, *51*(5), 979-985. [https://doi.org/10.1016/0031-9384\(92\)90081-c](https://doi.org/10.1016/0031-9384(92)90081-c)
- Monastero, R., Mangialasche, F., Camarda, C., Ercolani, S., & Camarda, R. (2009). A systematic review of neuropsychiatric symptoms in mild cognitive impairment. *Journal of Alzheimer's Disease: JAD*, *18*(1), 11-30. <https://doi.org/10.3233/JAD-2009-1120>
- Mondragón-Rodríguez, S., Perry, G., Luna-Muñoz, J., Acevedo-Aquino, M. C., & Williams, S. (2014). Phosphorylation of tau protein at sites Ser(396-404) is one of the earliest events in Alzheimer's disease and Down syndrome. *Neuropathology and Applied Neurobiology*, *40*(2), 121-135. <https://doi.org/10.1111/nan.12084>
- Mondragón-Rodríguez, Siddhartha, Basurto-Islas, G., Binder, L. I., & García-Sierra, F. (2009). Conformational changes and cleavage; are these responsible for the tau aggregation in Alzheimer's disease?
- Mondragón-Rodríguez, Siddhartha, Basurto-Islas, G., Santa-Maria, I., Mena, R., Binder, L. I., Avila, J., ... García-Sierra, F. (2008). Cleavage and conformational changes of tau protein follow phosphorylation during Alzheimer's disease. *International Journal of Experimental Pathology*, *89*(2), 81-90. <https://doi.org/10.1111/j.1365-2613.2007.00568.x>
- Morgan, A. H., Hammond, V. J., Sakoh-Nakatogawa, M., Ohsumi, Y., Thomas, C. P., Blanchet, F., ... O'Donnell, V. B. (2015). A novel role for 12/15-lipoxygenase in regulating autophagy. *Redox Biology*, *4*, 40-47. <https://doi.org/10.1016/j.redox.2014.11.005>
- Morley, J. E., Armbrecht, H. J., Farr, S. A., & Kumar, V. B. (2012). The senescence accelerated mouse (SAMP8) as a model for oxidative stress and Alzheimer's disease. *Biochimica et Biophysica Acta*, *1822*(5), 650-656. <https://doi.org/10.1016/j.bbadis.2011.11.015>
- Morley, J. E., Kumar, V. B., Bernardo, A. E., Farr, S. A., Uezu, K., Tumosa, N., & Flood, J. F. (2000). β -Amyloid precursor polypeptide in SAMP8 mice affects learning and memory. *Peptides*, *21*(12), 1761-1767.
- Morris, R. G., & Baddeley, A. D. (1988). Primary and working memory functioning in Alzheimer-type dementia. *Journal of clinical and*

- experimental neuropsychology*, 10(2), 279-296.
- Morrison, J. H., & Baxter, M. G. (2012). The ageing cortical synapse: hallmarks and implications for cognitive decline. *Nature Reviews. Neuroscience*, 13(4), 240-250. <https://doi.org/10.1038/nrn3200>
- Mothet, J.-P., Le Bail, M., & Billard, J.-M. (2015). Time and space profiling of NMDA receptor co-agonist functions. *Journal of Neurochemistry*, 135(2), 210-225. <https://doi.org/10.1111/jnc.13204>
- Mullard, A. (2021, juliol). Controversial Alzheimer's drug approval could affect other diseases. *Nature*. England. <https://doi.org/10.1038/d41586-021-01763-9>
- Müller, T. (2007). Rivastigmine in the treatment of patients with Alzheimer's disease. *Neuropsychiatric Disease and Treatment*, 3(2), 211-218. <https://doi.org/10.2147/ndt.2007.3.2.211>
- Munder, M. (2009). Arginase: an emerging key player in the mammalian immune system. *British Journal of Pharmacology*, 158(3), 638-651. <https://doi.org/10.1111/j.1476-5381.2009.00291.x>
- Murakawa-Hirachi, T., Mizoguchi, Y., Ohgidani, M., Haraguchi, Y., & Monji, A. (2021). Effect of memantine, an anti-Alzheimer's drug, on rodent microglial cells in vitro. *Scientific Reports*, 11(1), 6151. <https://doi.org/10.1038/s41598-021-85625-4>
- Murman, D. L. (2015). The Impact of Age on Cognition. *Seminars in Hearing*, 36(3), 111-121. <https://doi.org/10.1055/s-0035-1555115>
- Murphy, T. H., & Baraban, J. M. (1990). Glutamate toxicity in immature cortical neurons precedes development of glutamate receptor currents. *Brain Research. Developmental Brain Research*, 57(1), 146-150. [https://doi.org/10.1016/0165-3806\(90\)90195-5](https://doi.org/10.1016/0165-3806(90)90195-5)
- Nabavi, S., Fox, R., Proulx, C. D., Lin, J. Y., Tsien, R. Y., & Malinow, R. (2014). Engineering a memory with LTD and LTP. *Nature*, 511(7509), 348-352. <https://doi.org/10.1038/nature13294>
- Nagakura, A., Shitaka, Y., Yarimizu, J., & Matsuoka, N. (2013). Characterization of cognitive deficits in a transgenic mouse model of Alzheimer's disease and effects of donepezil and memantine. *European Journal of Pharmacology*, 703(1-3), 53-61. <https://doi.org/10.1016/J.EJPHAR.2012.12.023>
- Nagele, R. G., D'Andrea, M. R., Lee, H., Venkataraman, V., & Wang, H.-Y. (2003). Astrocytes accumulate A beta 42 and give rise to astrocytic amyloid plaques in Alzheimer disease brains. *Brain Research*, 971(2), 197-209. [https://doi.org/10.1016/s0006-8993\(03\)02361-8](https://doi.org/10.1016/s0006-8993(03)02361-8)
- Nelson, P. T., Alafuzoff, I., Bigio, E. H., Bouras, C., Braak, H., Cairns, N. J., ... Beach, T. G. (2012). Correlation of Alzheimer disease neuropathologic

- changes with cognitive status: a review of the literature. *Journal of Neuropathology and Experimental Neurology*, 71(5), 362-381. <https://doi.org/10.1097/NEN.0b013e31825018f7>
- Nikoletopoulou, V., & Tavernarakis, N. (2018). Regulation and Roles of Autophagy at Synapses. *Trends in Cell Biology*, 28(8), 646-661. <https://doi.org/10.1016/j.tcb.2018.03.006>
- Nilsson, P., Sekiguchi, M., Akagi, T., Izumi, S., Komori, T., Hui, K., ... Saido, T. C. (2015). Autophagy-related protein 7 deficiency in amyloid β (A β) precursor protein transgenic mice decreases A β in the multivesicular bodies and induces A β accumulation in the Golgi. *The American Journal of Pathology*, 185(2), 305-313. <https://doi.org/10.1016/j.ajpath.2014.10.011>
- Nimmerjahn, A., Kirchhoff, F., & Helmchen, F. (2005). Resting microglial cells are highly dynamic surveillants of brain parenchyma in vivo. *Science (New York, N.Y.)*, 308(5726), 1314-1318. <https://doi.org/10.1126/science.1110647>
- Nixon, R. A. (2007). Autophagy, amyloidogenesis and Alzheimer disease. *Journal of Cell Science*, 120(23), 4081-4091. <https://doi.org/10.1242/jcs.019265>
- Norden, D. M., & Godbout, J. P. (2013). Review: microglia of the aged brain: primed to be activated and resistant to regulation. *Neuropathology and Applied Neurobiology*, 39(1), 19-34. <https://doi.org/10.1111/j.1365-2990.2012.01306.x>
- Nowak, L., Bregestovski, P., Ascher, P., Herbet, A., & Prochiantz, A. (1984). Magnesium gates glutamate-activated channels in mouse central neurones. *Nature*, 307(5950), 462-465. <https://doi.org/10.1038/307462a0>
- Nygaard, H. B., van Dyck, C. H., & Strittmatter, S. M. (2014). Fyn kinase inhibition as a novel therapy for Alzheimer's disease. *Alzheimer's Research & Therapy*, 6(1), 8. <https://doi.org/10.1186/alzrt238>
- O'Brien, R. J., & Wong, P. C. (2011). Amyloid precursor protein processing and Alzheimer's disease. *Annual Review of Neuroscience*, 34, 185-204. <https://doi.org/10.1146/annurev-neuro-061010-113613>
- O'Keefe, L. M., Doran, S. J., Mwilambwe-Tshilobo, L., Conti, L. H., Venna, V. R., & McCullough, L. D. (2014). Social isolation after stroke leads to depressive-like behavior and decreased BDNF levels in mice. *Behavioural Brain Research*, 260, 162-170. <https://doi.org/10.1016/j.bbr.2013.10.047>
- O'Leary, T. P., Mantolino, H. M., Stover, K. R., & Brown, R. E. (2018). Age-related deterioration of motor function in male and female 5xFAD mice from 3 to 16 months of age. *Genes Brain Behav.*, 19(3), e12538. <https://doi.org/10.1111/gbb.12538>

- Oakley, H., Cole, S. L., Logan, S., Maus, E., Shao, P., Craft, J., ... Vassar, R. (2006). Intraneuronal β -amyloid aggregates, neurodegeneration, and neuron loss in transgenic mice with five familial Alzheimer's disease mutations: Potential factors in amyloid plaque formation. *Journal of Neuroscience*, 26(40), 10129-10140. <https://doi.org/10.1523/JNEUROSCI.1202-06.2006>
- Ogata, M., Hino, S., Saito, A., Morikawa, K., Kondo, S., Kanemoto, S., ... Imaizumi, K. (2006). Autophagy is activated for cell survival after endoplasmic reticulum stress. *Molecular and Cellular Biology*, 26(24), 9220-9231. <https://doi.org/10.1128/MCB.01453-06>
- Oh, J., Lee, Y. D., & Wagers, A. J. (2014). Stem cell aging: mechanisms, regulators and therapeutic opportunities. *Nature Medicine*, 20(8), 870-880. <https://doi.org/10.1038/nm.3651>
- Oka, M., Fujisaki, N., Maruko-Otake, A., Ohtake, Y., Shimizu, S., Saito, T., ... Ando, K. (2017). Ca²⁺/calmodulin-dependent protein kinase II promotes neurodegeneration caused by tau phosphorylated at Ser262/356 in a transgenic *Drosophila* model of tauopathy. *Journal of Biochemistry*, 162(5), 335-342. <https://doi.org/10.1093/jb/mvx038>
- Okouchi, R., Sakanoi, Y., & Tsuduki, T. (2019). The Effect of Carbohydrate-Restricted Diets on the Skin Aging of Mice. *Journal of Nutritional Science and Vitaminology*, 65(Supplement), S67-S71. <https://doi.org/10.3177/jnsv.65.S67>
- Osborn, L. M., Kamphuis, W., Wadman, W. J., & Hol, E. M. (2016). Astrogliosis: An integral player in the pathogenesis of Alzheimer's disease. *Progress in Neurobiology*, 144, 121-141. <https://doi.org/https://doi.org/10.1016/j.pneurobio.2016.01.001>
- Overk, C. R., & Masliah, E. (2014). Pathogenesis of synaptic degeneration in Alzheimer's disease and Lewy body disease. *Biochemical Pharmacology*, 88(4), 508-516. <https://doi.org/10.1016/j.bcp.2014.01.015>
- Pallas-Bazarra, N., Draffin, J., Cuadros, R., Antonio Esteban, J., & Avila, J. (2019). Tau is required for the function of extrasynaptic NMDA receptors. *Scientific Reports*, 9(1), 9116. <https://doi.org/10.1038/s41598-019-45547-8>
- Pankiv, S., Clausen, T. H., Lamark, T., Brech, A., Bruun, J.-A., Outzen, H., ... Johansen, T. (2007). p62/SQSTM1 binds directly to Atg8/LC3 to facilitate degradation of ubiquitinated protein aggregates by autophagy. *The Journal of Biological Chemistry*, 282(33), 24131-24145. <https://doi.org/10.1074/jbc.M702824200>
- Pannese, E. (2011). Morphological changes in nerve cells during normal aging. *Brain Structure & Function*, 216(2), 85-89. <https://doi.org/10.1007/s00429-011-0308-y>

- Panza, F., Lozupone, M., Logroscino, G., & Imbimbo, B. P. (2019). A critical appraisal of amyloid- β -targeting therapies for Alzheimer disease. *Nature Reviews. Neurology*, *15*(2), 73-88. <https://doi.org/10.1038/s41582-018-0116-6>
- Paoletti, P., Bellone, C., & Zhou, Q. (2013, gener 1). NMDA receptor subunit diversity: Impact on receptor properties, synaptic plasticity and disease. *Nature Reviews Neuroscience*. Nature Publishing Group. <https://doi.org/10.1038/nrn3504>
- Parameshwaran, K., Dhanasekaran, M., & Suppiramaniam, V. (2008, març). Amyloid beta peptides and glutamatergic synaptic dysregulation. *Experimental Neurology*. Exp Neurol. <https://doi.org/10.1016/j.expneurol.2007.10.008>
- Parsons, C. G., Danysz, W., & Quack, G. (1999). Memantine is a clinically well tolerated N-methyl-D-aspartate (NMDA) receptor antagonist - A review of preclinical data. *Neuropharmacology*, *38*(6), 735-767. [https://doi.org/10.1016/S0028-3908\(99\)00019-2](https://doi.org/10.1016/S0028-3908(99)00019-2)
- Parsons, Chris G, Danysz, W., Bartmann, A., Spielmanns, P., Frankiewicz, T., Hesselink, M., ... Quack, G. (1999). Amino-alkyl-cyclohexanes are novel uncompetitive NMDA receptor antagonists with strong voltage-dependency and fast blocking kinetics: in vitro and in vivo characterization. *Neuropharmacology*, *38*(1), 85-108.
- Patterson, C., Feightner, J. W., Garcia, A., Hsiung, G.-Y. R., MacKnight, C., & Sadvnick, A. D. (2008). Diagnosis and treatment of dementia: 1. Risk assessment and primary prevention of Alzheimer disease. *Cmaj*, *178*(5), 548-556.
- Pei, J. J., Tanaka, T., Tung, Y. C., Braak, E., Iqbal, K., & Grundke-Iqbal, I. (1997). Distribution, levels, and activity of glycogen synthase kinase-3 in the Alzheimer disease brain. *Journal of Neuropathology and Experimental Neurology*, *56*(1), 70-78. <https://doi.org/10.1097/00005072-199701000-00007>
- Pekny, M., Pekna, M., Messing, A., Steinhäuser, C., Lee, J.-M., Parpura, V., ... Verkhratsky, A. (2016). Astrocytes: a central element in neurological diseases. *Acta Neuropathologica*, *131*(3), 323-345. <https://doi.org/10.1007/s00401-015-1513-1>
- Pekny, M., Wilhelmsson, U., & Pekna, M. (2014). The dual role of astrocyte activation and reactive gliosis. *Neuroscience Letters*, *565*, 30-38. <https://doi.org/10.1016/j.neulet.2013.12.071>
- Peng, S., Wu, J., Mufson, E. J., & Fahnstock, M. (2005). Precursor form of brain-derived neurotrophic factor and mature brain-derived neurotrophic

- factor are decreased in the pre-clinical stages of Alzheimer's disease. *Journal of Neurochemistry*, 93(6), 1412-1421. <https://doi.org/10.1111/j.1471-4159.2005.03135.x>
- Pérez-Ortiz, J. M., Serrano-Pérez, M. C., Pastor, M. D., Martín, E. D., Calvo, S., Rincón, M., & Tranque, P. (2008). Mechanical lesion activates newly identified NFATc1 in primary astrocytes: implication of ATP and purinergic receptors. *The European Journal of Neuroscience*, 27(9), 2453-2465. <https://doi.org/10.1111/j.1460-9568.2008.06197.x>
- Perl, D. P. (2010). Neuropathology of Alzheimer's disease. *The Mount Sinai Journal of Medicine, New York*, 77(1), 32-42. <https://doi.org/10.1002/msj.20157>
- Perry, R. J., Watson, P., & Hodges, J. R. (2000). The nature and staging of attention dysfunction in early (minimal and mild) Alzheimer's disease: relationship to episodic and semantic memory impairment. *Neuropsychologia*, 38(3), 252-271.
- Petrovic, M., Hurt, C., Collins, D., Burns, A., Camus, V., Liperoti, R., ... Byrne, E. J. (2007). Clustering of behavioural and psychological symptoms in dementia (BPSD): A european alzheimer's disease consortium (EADC) study. *Acta Clinica Belgica*, 62(6), 426-432. <https://doi.org/10.1179/acb.2007.062>
- Phillips, H. S., Hains, J. M., Armanini, M., Laramée, G. R., Johnson, S. A., & Winslow, J. W. (1991). BDNF mRNA is decreased in the hippocampus of individuals with Alzheimer's disease. *Neuron*, 7(5), 695-702. [https://doi.org/10.1016/0896-6273\(91\)90273-3](https://doi.org/10.1016/0896-6273(91)90273-3)
- Pickford, F., Masliah, E., Britschgi, M., Lucin, K., Narasimhan, R., Jaeger, P. A., ... Wyss-Coray, T. (2008). The autophagy-related protein beclin 1 shows reduced expression in early Alzheimer disease and regulates amyloid beta accumulation in mice. *The Journal of Clinical Investigation*, 118(6), 2190-2199. <https://doi.org/10.1172/JCI33585>
- Pietá Dias, C., Martins de Lima, M. N., Presti-Torres, J., Dornelles, A., Garcia, V. A., Siciliani Scalco, F., ... Schröder, N. (2007). Memantine reduces oxidative damage and enhances long-term recognition memory in aged rats. *Neuroscience*, 146(4), 1719-1725. <https://doi.org/10.1016/j.neuroscience.2007.03.018>
- Popugaeva, E., & Bezprozvanny, I. (2013). Role of endoplasmic reticulum Ca²⁺ signaling in the pathogenesis of Alzheimer disease. *Frontiers in molecular neuroscience*, 6, 29.
- Prvulovic, D., Hampel, H., & Pantel, J. (2010). Galantamine for Alzheimer's disease. *Expert opinion on drug metabolism & toxicology*, 6(3), 345-354.

- Puzzo, D., Gulisano, W., Palmeri, A., & Arancio, O. (2015). Rodent models for Alzheimer's disease drug discovery. *Expert Opinion on Drug Discovery*, *10*(7), 703-711. <https://doi.org/10.1517/17460441.2015.1041913>
- Qiu, L.-L., Pan, W., Luo, D., Zhang, G.-F., Zhou, Z.-Q., Sun, X.-Y., ... Ji, M.-H. (2020). Dysregulation of BDNF/TrkB signaling mediated by NMDAR/Ca(2+)/calpain might contribute to postoperative cognitive dysfunction in aging mice. *Journal of Neuroinflammation*, *17*(1), 23. <https://doi.org/10.1186/s12974-019-1695-x>
- Reese, L. C., & Tagliatela, G. (2010). Neuroimmunomodulation by calcineurin in aging and Alzheimer's disease. *Aging and Disease*, *1*(3), 245-253.
- Rego, A. C., & Oliveira, C. R. (2003). Mitochondrial dysfunction and reactive oxygen species in excitotoxicity and apoptosis: implications for the pathogenesis of neurodegenerative diseases. *Neurochemical Research*, *28*(10), 1563-1574. <https://doi.org/10.1023/a:1025682611389>
- Reiner, A., & Levitz, J. (2018). Glutamatergic Signaling in the Central Nervous System: Ionotropic and Metabotropic Receptors in Concert. *Neuron*, *98*(6), 1080-1098. <https://doi.org/https://doi.org/10.1016/j.neuron.2018.05.018>
- Reisberg, B., Doody, R., Stöffler, A., Schmitt, F., Ferris, S., & Möbius, H. J. (2003). Memantine in moderate-to-severe Alzheimer's disease. *The New England Journal of Medicine*, *348*(14), 1333-1341. <https://doi.org/10.1056/NEJMoa013128>
- Reynolds, A., Laurie, C., Lee Mosley, R., & Gendelman, H. E. (2007). Oxidative Stress and the Pathogenesis of Neurodegenerative Disorders. En *Neuroinflammation in Neuronal Death and Repair* (Vol. 82, p. 297-325). Academic Press. [https://doi.org/https://doi.org/10.1016/S0074-7742\(07\)82016-2](https://doi.org/https://doi.org/10.1016/S0074-7742(07)82016-2)
- Rivers-Auty, J., Mather, A. E., Peters, R., Lawrence, C. B., Brough, D., & Initiative, A. D. N. (2020). Anti-inflammatories in Alzheimer's disease—potential therapy or spurious correlate? *Brain Communications*, *2*(2), fcaa109. <https://doi.org/10.1093/braincomms/fcaa109>
- Rogawski, M. A., & Wenk, G. L. (2003). The neuropharmacological basis for the use of memantine in the treatment of Alzheimer's disease. *CNS drug reviews*, *9*(3), 275-308.
- Rönicke, R., Mikhaylova, M., Rönicke, S., Meinhardt, J., Schröder, U. H., Fändrich, M., ... Reymann, K. G. (2011). Early neuronal dysfunction by amyloid β oligomers depends on activation of NR2B-containing NMDA receptors. *Neurobiology of Aging*, *32*(12), 2219-2228. <https://doi.org/10.1016/j.neurobiolaging.2010.01.011>
- Rose, M. R. (2009). Adaptation, aging, and genomic information. *Aging (Albany*

- NY), 1(5), 444.
- Rosi, S., Vazdarjanova, A., Ramirez-Amaya, V., Worley, P. F., Barnes, C. A., & Wenk, G. L. (2006). Memantine protects against LPS-induced neuroinflammation, restores behaviorally-induced gene expression and spatial learning in the rat. *Neuroscience*, 142(4), 1303-1315. <https://doi.org/10.1016/j.neuroscience.2006.08.017>
- Roth, K. A. (2001). Caspases, Apoptosis, and Alzheimer Disease: Causation, Correlation, and Confusion. *Journal of Neuropathology & Experimental Neurology*, 60(9), 829-838. <https://doi.org/10.1093/jnen/60.9.829>
- Rothstein, J. D., Martin, L., Levey, A. I., Dykes-Hoberg, M., Jin, L., Wu, D., ... Kuncl, R. W. (1994). Localization of neuronal and glial glutamate transporters. *Neuron*, 13(3), 713-725. [https://doi.org/10.1016/0896-6273\(94\)90038-8](https://doi.org/10.1016/0896-6273(94)90038-8)
- Russo, R., Berliocchi, L., Adornetto, A., Varano, G., Cavaliere, F., Nucci, C., ... Corasaniti, M. (2011). Calpain-mediated cleavage of Beclin-1 and autophagy deregulation following retinal ischemic injury in vivo. *Cell death & disease*, 2(4). <https://doi.org/10.1038/CDDIS.2011.29>
- Ryman, D. C., Acosta-Baena, N., Aisen, P. S., Bird, T., Danek, A., Fox, N. C., ... Bateman, R. J. (2014). Symptom onset in autosomal dominant Alzheimer disease: a systematic review and meta-analysis. *Neurology*, 83(3), 253-260. <https://doi.org/10.1212/WNL.0000000000000596>
- Saito, K., Elce, J. S., Hamos, J. E., & Nixon, R. A. (1993). Widespread activation of calcium-activated neutral proteinase (calpain) in the brain in Alzheimer disease: a potential molecular basis for neuronal degeneration. *Proceedings of the National Academy of Sciences of the United States of America*, 90(7), 2628-2632. <https://doi.org/10.1073/pnas.90.7.2628>
- Salmon, D. P., Heindel, W. C., & Lange, K. L. (1999). Differential decline in word generation from phonemic and semantic categories during the course of Alzheimer's disease: Implications for the integrity of semantic memory. *Journal of the International Neuropsychological Society*, 5(7), 692-703.
- Salter, M. G., & Fern, R. (2005). NMDA receptors are expressed in developing oligodendrocyte processes and mediate injury. *Nature*, 438(7071), 1167-1171. <https://doi.org/10.1038/nature04301>
- Salter, M. W., & Stevens, B. (2017). Microglia emerge as central players in brain disease. *Nature Medicine*, 23(9), 1018-1027. <https://doi.org/10.1038/nm.4397>
- Sattler, R., & Tymianski, M. (2001). Molecular mechanisms of glutamate receptor-mediated excitotoxic neuronal cell death. *Molecular Neurobiology*, 24(1-3), 107-129. <https://doi.org/10.1385/MN:24:1-3:107>

- Scarmeas, N., Luchsinger, J. A., Schupf, N., Brickman, A. M., Cosentino, S., Tang, M. X., & Stern, Y. (2009). Physical activity, diet, and risk of Alzheimer disease. *JAMA*, 302(6), 627-637. <https://doi.org/10.1001/jama.2009.1144>
- Schindowski, K., Belarbi, K., & Buée, L. (2008). Neurotrophic factors in Alzheimer's disease: role of axonal transport. *Genes, Brain, and Behavior*, 7 Suppl 1(1), 43-56. <https://doi.org/10.1111/j.1601-183X.2007.00378.x>
- Schneider, L. S., Mangialasche, F., Andreasen, N., Feldman, H., Giacobini, E., Jones, R., ... Kivipelto, M. (2014). Clinical trials and late-stage drug development for Alzheimer's disease: an appraisal from 1984 to 2014. *Journal of Internal Medicine*, 275(3), 251-283. <https://doi.org/10.1111/joim.12191>
- Scholtzova, H., Wadghiri, Y. Z., Douadi, M., Sigurdsson, E. M., Li, Y.-S., Quartermain, D., ... Wisniewski, T. (2008). Memantine Leads to Behavioral Improvement and Amyloid Reduction in Alzheimer's-Disease-Model Transgenic Mice Shown as by Micromagnetic Resonance Imaging. *Journal of neuroscience research*, 86(12), 2784. <https://doi.org/10.1002/jnr.21713>
- Schrijvers, E. M. C., Verhaaren, B. F. J., Koudstaal, P. J., Hofman, A., Ikram, M. A., & Breteler, M. M. B. (2012). Is dementia incidence declining?: Trends in dementia incidence since 1990 in the Rotterdam Study. *Neurology*, 78(19), 1456-1463. <https://doi.org/10.1212/WNL.0b013e3182553be6>
- Scott, D. B., Blanpied, T. A., Swanson, G. T., Zhang, C., & Ehlers, M. D. (2001). An NMDA receptor ER retention signal regulated by phosphorylation and alternative splicing. *The Journal of Neuroscience: The Official Journal of the Society for Neuroscience*, 21(9), 3063-3072. <https://doi.org/10.1523/JNEUROSCI.21-09-03063.2001>
- Segura-Aguilar, J. (2015). A new mechanism for protection of dopaminergic neurons mediated by astrocytes. *Neural Regeneration Research*, 10(8), 1225-1227. <https://doi.org/10.4103/1673-5374.162750>
- Sengupta, A., Kabat, J., Novak, M., Wu, Q., Grundke-Iqba, I., & Iqbal, K. (1998). Maximal inhibition of tau binding to microtubules requires the phosphorylation of tau at both Thr 231 and Ser 262. *Neurobiol Aging*, 19(4S), S124-S524.
- Sengupta, U., Nilson, A. N., & Kaye, R. (2016). The Role of Amyloid- β Oligomers in Toxicity, Propagation, and Immunotherapy. *EBioMedicine*, 6, 42-49. <https://doi.org/10.1016/j.ebiom.2016.03.035>
- Serrano-Pozo, A., Frosch, M. P., Masliah, E., & Hyman, B. T. (2011). Neuropathological alterations in Alzheimer disease. *Cold Spring Harbor Perspectives in Medicine*, 1(1), a006189.

- <https://doi.org/10.1101/cshperspect.a006189>
- Serrano-Pozo, A., Mielke, M. L., Gómez-Isla, T., Betensky, R. A., Growdon, J. H., Frosch, M. P., & Hyman, B. T. (2011). Reactive glia not only associates with plaques but also parallels tangles in Alzheimer's disease. *The American journal of pathology*, *179*(3), 1373-1384.
- Sevigny, J., Chiao, P., Bussière, T., Weinreb, P. H., Williams, L., Maier, M., ... Sandrock, A. (2016). The antibody aducanumab reduces A β plaques in Alzheimer's disease. *Nature*, *537*(7618), 50-56. <https://doi.org/10.1038/nature19323>
- Sharma, K. (2019). Cholinesterase inhibitors as Alzheimer's therapeutics (Review). *Molecular Medicine Reports*, *20*(2), 1479-1487. <https://doi.org/10.3892/mmr.2019.10374>
- Shaye, D. D., & Greenwald, I. (2011). OrthoList: a compendium of *C. elegans* genes with human orthologs. *PloS One*, *6*(5), e20085. <https://doi.org/10.1371/journal.pone.0020085>
- Shimokawa, I., & Trindade, L. S. (2010). Dietary restriction and aging in rodents: A current view on its molecular mechanisms. *Aging and Disease*. International Society on Aging and Disease.
- Silva, M. V. F., Loures, C. de M. G., Alves, L. C. V., de Souza, L. C., Borges, K. B. G., & Carvalho, M. das G. (2019). Alzheimer's disease: risk factors and potentially protective measures. *Journal of Biomedical Science*, *26*(1), 33. <https://doi.org/10.1186/s12929-019-0524-y>
- Sofroniew, M. V. (2009). Molecular dissection of reactive astrogliosis and glial scar formation. *Trends in neurosciences*, *32*(12), 638-647.
- Sofroniew, M. V., & Vinters, H. V. (2010). Astrocytes: biology and pathology. *Acta Neuropathologica*, *119*(1), 7-35. <https://doi.org/10.1007/s00401-009-0619-8>
- Solito, E., & Sastre, M. (2012). Microglia function in Alzheimer's disease. *Frontiers in Pharmacology*, *3*, 14. <https://doi.org/10.3389/fphar.2012.00014>
- Sompol, P., Furman, J. L., Pleiss, M. M., Kraner, S. D., Artiushin, I. A., Batten, S. R., ... Norris, C. M. (2017). Calcineurin/NFAT Signaling in Activated Astrocytes Drives Network Hyperexcitability in A β -Bearing Mice. *The Journal of Neuroscience*, *37*(25), 6132 LP - 6148. <https://doi.org/10.1523/JNEUROSCI.0877-17.2017>
- Song, G., Li, Y., Lin, L., & Cao, Y. (2015). Anti-autophagic and anti-apoptotic effects of memantine in a SH-SY5Y cell model of Alzheimer's disease via mammalian target of rapamycin-dependent and -independent pathways. *Mol Med Rep*, *12*(5), 7615-7622. <https://doi.org/10.3892/mmr.2015.4382>
- Song, Z., Bian, Z., Zhang, Z., Wang, X., Zhu, A., & Zhu, G. (2021). Astrocytic

- Kir4.1 regulates NMDAR/calpain signaling axis in lipopolysaccharide-induced depression-like behaviors in mice. *Toxicology and Applied Pharmacology*, 429, 115711. <https://doi.org/10.1016/j.taap.2021.115711>
- Sonkusare, S. K., Kaul, C. L., & Ramarao, P. (2005). Dementia of Alzheimer's disease and other neurodegenerative disorders—memantine, a new hope. *Pharmacological Research*, 51(1), 1-17. <https://doi.org/https://doi.org/10.1016/j.phrs.2004.05.005>
- Stroebel, D., & Paoletti, P. (2021). Architecture and function of NMDA receptors: an evolutionary perspective. *The Journal of Physiology*, 599(10), 2615-2638. <https://doi.org/10.1113/JP279028>
- Strong, R., Reddy, V., & Morley, J. E. (2003). Cholinergic deficits in the septal–hippocampal pathway of the SAM-P/8 senescence accelerated mouse. *Brain research*, 966(1), 150-156.
- Sturchio, A., Dwivedi, A. K., Young, C. B., Malm, T., Marsili, L., Sharma, J. S., ... Espay, A. J. (2021). High cerebrospinal amyloid- β ; 42 is associated with normal cognition in individuals with brain amyloidosis. *eClinicalMedicine*, 38. <https://doi.org/10.1016/j.eclinm.2021.100988>
- Stutzmann, G. E., & Mattson, M. P. (2011). Endoplasmic reticulum Ca(2+) handling in excitable cells in health and disease. *Pharmacological Reviews*, 63(3), 700-727. <https://doi.org/10.1124/pr.110.003814>
- Subramanian, J., Savage, J. C., & Tremblay, M.-È. (2020). Synaptic Loss in Alzheimer's Disease: Mechanistic Insights Provided by Two-Photon in vivo Imaging of Transgenic Mouse Models. *Frontiers in Cellular Neuroscience*, 14, 592607. <https://doi.org/10.3389/fncel.2020.592607>
- Sulston, J. E., & Horvitz, H. R. (1977). Post-embryonic cell lineages of the nematode, *Caenorhabditis elegans*. *Developmental Biology*, 56(1), 110-156. [https://doi.org/10.1016/0012-1606\(77\)90158-0](https://doi.org/10.1016/0012-1606(77)90158-0)
- Suzuki, K., & Terry, R. D. (1967). Fine structural localization of acid phosphatase in senile plaques in Alzheimer's presenile dementia. *Acta Neuropathologica*, 8(3), 276-284. <https://doi.org/10.1007/BF00688828>
- Swerdlow, R. H., Burns, J. M., & Khan, S. M. (2010). The Alzheimer's disease mitochondrial cascade hypothesis. *Journal of Alzheimer's Disease : JAD*, 20 Suppl 2(Suppl 2), S265-79. <https://doi.org/10.3233/JAD-2010-100339>
- Tackenberg, C., & Nitsch, R. M. (2019). The secreted APP ectodomain sAPP α , but not sAPP β , protects neurons against A β oligomer-induced dendritic spine loss and increased tau phosphorylation. *Molecular Brain*, 12(1), 27. <https://doi.org/10.1186/s13041-019-0447-2>
- Tagliavini, F., Tiraboschi, P., & Federico, A. (2021). Alzheimer's disease: the controversial approval of Aducanumab. *Neurological Sciences*, 42(8), 3069-

3070. <https://doi.org/10.1007/s10072-021-05497-4>
- Takahashi-Ito, K., Makino, M., Okado, K., & Tomita, T. (2017). Memantine inhibits β -amyloid aggregation and disassembles preformed β -amyloid aggregates. *Biochemical and Biophysical Research Communications*, 493(1), 158-163. <https://doi.org/https://doi.org/10.1016/j.bbrc.2017.09.058>
- Takeda, T. (1997). Senescence-accelerated mouse (SAM): A novel murine model of senescence. *Experimental Gerontology*, 32(1-2), 105-109. [https://doi.org/10.1016/S0531-5565\(96\)00036-8](https://doi.org/10.1016/S0531-5565(96)00036-8)
- Takeda, T., Hosokawa, M., Takeshita, S., Irino, M., Higuchi, K., Matsushita, T., ... Yamamuro, T. (1981). A new murine model of accelerated senescence. *Mechanisms of ageing and development*, 17(2), 183-194.
- Tan, C. C., Yu, J. T., Tan, M. S., Jiang, T., Zhu, X. C., & Tan, L. (2014). Autophagy in aging and neurodegenerative diseases: Implications for pathogenesis and therapy. *Neurobiology of Aging*, 35(5), 941-957. <https://doi.org/10.1016/j.neurobiolaging.2013.11.019>
- Tan, Y. J., Ng, A. S. L., Vipin, A., Lim, J. K. W., Chander, R. J., Ji, F., ... Zhou, J. (2017). Higher Peripheral TREM2 mRNA Levels Relate to Cognitive Deficits and Hippocampal Atrophy in Alzheimer's Disease and Amnesic Mild Cognitive Impairment. *Journal of Alzheimer's Disease*, 58, 413-423. <https://doi.org/10.3233/JAD-161277>
- Tang, S. J., Fesharaki-Zadeh, A., Takahashi, H., Nies, S. H., Smith, L. M., Luo, A., ... Strittmatter, S. M. (2020). Fyn kinase inhibition reduces protein aggregation, increases synapse density and improves memory in transgenic and traumatic Tauopathy. *Acta Neuropathologica Communications*, 8(1), 96. <https://doi.org/10.1186/s40478-020-00976-9>
- Tanzi, R. E., Gusella, J. F., Watkins, P. C., Bruns, G. A., St George-Hyslop, P., Van Keuren, M. L., ... Neve, R. L. (1987). Amyloid beta protein gene: cDNA, mRNA distribution, and genetic linkage near the Alzheimer locus. *Science (New York, N.Y.)*, 235(4791), 880-884. <https://doi.org/10.1126/science.2949367>
- Tapia-Rojas, C., Cabezas-Opazo, F., Deaton, C. A., Vergara, E. H., Johnson, G. V. W., & Quintanilla, R. A. (2019). It's all about tau. *Progress in Neurobiology*, 175, 54-76. <https://doi.org/10.1016/j.pneurobio.2018.12.005>
- Tariot, P. N., Farlow, M. R., Grossberg, G. T., Graham, S. M., McDonald, S., Gergel, I., ... Group, M. S. (2004). Memantine treatment in patients with moderate to severe Alzheimer disease already receiving donepezil: a randomized controlled trial. *Jama*, 291(3), 317-324.
- Teich, A. F., Nicholls, R. E., Puzzo, D., Fiorito, J., Purgatorio, R., Fa', M., & Arancio, O. (2015). Synaptic therapy in Alzheimer's disease: a CREB-

- centric approach. *Neurotherapeutics : The Journal of the American Society for Experimental NeuroTherapeutics*, 12(1), 29-41. <https://doi.org/10.1007/s13311-014-0327-5>
- Terry, R. D., Masliah, E., Salmon, D. P., Butters, N., DeTeresa, R., Hill, R., ... Katzman, R. (1991). Physical basis of cognitive alterations in alzheimer's disease: Synapse loss is the major correlate of cognitive impairment. *Annals of Neurology*, 30(4), 572-580. <https://doi.org/10.1002/ana.410300410>
- Thomas, C. G., Miller, A. J., & Westbrook, G. L. (2006). Synaptic and extrasynaptic NMDA receptor NR2 subunits in cultured hippocampal neurons. *Journal of Neurophysiology*, 95(3), 1727-1734. <https://doi.org/10.1152/jn.00771.2005>
- Tingley, W. G., Ehlers, M. D., Kameyama, K., Doherty, C., Ptak, J. B., Riley, C. T., & Huganir, R. L. (1997). Characterization of protein kinase A and protein kinase C phosphorylation of the N-methyl-D-aspartate receptor NR1 subunit using phosphorylation site-specific antibodies. *The Journal of Biological Chemistry*, 272(8), 5157-5166. <https://doi.org/10.1074/jbc.272.8.5157>
- Tong, B. C.-K., Wu, A. J., Li, M., & Cheung, K.-H. (2018). Calcium signaling in Alzheimer's disease & therapies. *Biochimica et Biophysica Acta (BBA) - Molecular Cell Research*, 1865(11, Part B), 1745-1760. <https://doi.org/https://doi.org/10.1016/j.bbamcr.2018.07.018>
- Traynelis, S. F., Wollmuth, L. P., McBain, C. J., Menniti, F. S., Vance, K. M., Ogden, K. K., ... Dingledine, R. (2010). Glutamate receptor ion channels: structure, regulation, and function. *Pharmacological Reviews*, 62(3), 405-496. <https://doi.org/10.1124/pr.109.002451>
- Trepanier, C. H., Jackson, M. F., & MacDonald, J. F. (2012). Regulation of NMDA receptors by the tyrosine kinase Fyn. *The FEBS Journal*, 279(1), 12-19. <https://doi.org/https://doi.org/10.1111/j.1742-4658.2011.08391.x>
- Trushina, E., & McMurray, C. T. (2007). Oxidative stress and mitochondrial dysfunction in neurodegenerative diseases. *Neuroscience*, 145(4), 1233-1248. <https://doi.org/10.1016/j.neuroscience.2006.10.056>
- Tseng, H. C., Zhou, Y., Shen, Y., & Tsai, L. H. (2002). A survey of Cdk5 activator p35 and p25 levels in Alzheimer's disease brains. *FEBS Letters*, 523(1-3), 58-62. [https://doi.org/10.1016/s0014-5793\(02\)02934-4](https://doi.org/10.1016/s0014-5793(02)02934-4)
- Tsujimoto, Y. (1998). Role of Bcl-2 family proteins in apoptosis: apoptosomes or mitochondria? *Genes to Cells: Devoted to Molecular & Cellular Mechanisms*, 3(11), 697-707. <https://doi.org/10.1046/j.1365-2443.1998.00223.x>
- Turcu, A. L., Companys-Aleman, J., Phillips, M. B., Patel, D. S., Griñán-Ferré,

- C., Loza, M. I., ... Vázquez, S. (2022). Design, synthesis, and in vitro and in vivo characterization of new memantine analogs for Alzheimer's Disease. *European Journal of Medicinal Chemistry*, 236, 114354. <https://doi.org/https://doi.org/10.1016/j.ejmech.2022.114354>.
- Tuszynski, M. H., Thal, L., Pay, M., Salmon, D. P., U, H. S., Bakay, R., ... Conner, J. (2005). A phase 1 clinical trial of nerve growth factor gene therapy for Alzheimer disease. *Nature Medicine*, 11(5), 551-555. <https://doi.org/10.1038/nm1239>
- Uttara, B., Singh, A. V., Zamboni, P., & Mahajan, R. T. (2009). Oxidative stress and neurodegenerative diseases: a review of upstream and downstream antioxidant therapeutic options. *Current Neuropharmacology*, 7(1), 65-74. <https://doi.org/10.2174/157015909787602823>
- Valverde, E., Sureda, F. X., & Vázquez, S. (2014). Novel benzopolycyclic amines with NMDA receptor antagonist activity. *Bioorganic and Medicinal Chemistry*, 22(9), 2678-2683. <https://doi.org/10.1016/j.bmc.2014.03.025>
- Van Dam, D., & De Deyn, P. P. (2006). Cognitive evaluation of disease-modifying efficacy of galantamine and memantine in the APP23 model. *European Neuropsychopharmacology: The Journal of the European College of Neuropsychopharmacology*, 16(1), 59-69. <https://doi.org/10.1016/j.euroneuro.2005.06.005>
- VanItallie, T. B. (2017). Alzheimer's disease: Innate immunity gone awry? *Metabolism: Clinical and Experimental*, 69S, S41-S49. <https://doi.org/10.1016/j.metabol.2017.01.014>
- Varin, A., & Gordon, S. (2009). Alternative activation of macrophages: immune function and cellular biology. *Immunobiology*, 214(7), 630-641. <https://doi.org/10.1016/j.imbio.2008.11.009>
- Vaz, M., & Silvestre, S. (2020, novembre 15). Alzheimer's disease: Recent treatment strategies. *European Journal of Pharmacology*. Elsevier B.V. <https://doi.org/10.1016/j.ejphar.2020.173554>
- Vissel, B., Krupp, J. J., Heinemann, S. F., & Westbrook, G. L. (2001). A use-dependent tyrosine dephosphorylation of NMDA receptors is independent of ion flux. *Nature Neuroscience*, 4(6), 587-596. <https://doi.org/10.1038/88404>
- Walsh, D. M., & Selkoe, D. J. (2007). A beta oligomers - a decade of discovery. *Journal of Neurochemistry*, 101(5), 1172-1184. <https://doi.org/10.1111/j.1471-4159.2006.04426.x>
- Wang, F., Zou, Z., Gong, Y., Yuan, D., Chen, X., & Sun, T. (2017). Regulation of Human Brain Microvascular Endothelial Cell Adhesion and Barrier Functions by Memantine. *Journal of Molecular Neuroscience*, 62(1), 123-

129. <https://doi.org/10.1007/s12031-017-0917-x>
- Wang, H. G., Pathan, N., Ethell, I. M., Krajewski, S., Yamaguchi, Y., Shibasaki, F., ... Reed, J. C. (1999). Ca²⁺-induced apoptosis through calcineurin dephosphorylation of BAD. *Science (New York, N.Y.)*, 284(5412), 339-343. <https://doi.org/10.1126/science.284.5412.339>
- Wang, J., Zhang, X., Cheng, X., Cheng, J., Liu, F., Xu, Y., ... Zhang, Y. (2017). LW-AFC, A New Formula Derived from Liuwei Dihuang Decoction, Ameliorates Cognitive Deterioration and Modulates Neuroendocrine-Immune System in SAMP8 Mouse. *Current Alzheimer Research*, 14(2), 221-238. <https://doi.org/10.2174/1567205013666160603001637>
- Wang, Q., Yao, H., Liu, W., Ya, B., Cheng, H., Xing, Z., & Wu, Y. (2021). Microglia Polarization in Alzheimer's Disease: Mechanisms and a Potential Therapeutic Target. *Frontiers in Aging Neuroscience*, 13, 772717. <https://doi.org/10.3389/fnagi.2021.772717>
- Wang, R., & Reddy, P. H. (2017). Role of Glutamate and NMDA Receptors in Alzheimer's Disease. *Journal of Alzheimer's Disease*, 57(4), 1041-1048. <https://doi.org/10.3233/JAD-160763>
- Wang, Y., Cella, M., Mallinson, K., Ulrich, J. D., Young, K. L., Robinette, M. L., ... Colonna, M. (2015). TREM2 lipid sensing sustains the microglial response in an Alzheimer's disease model. *Cell*, 160(6), 1061-1071. <https://doi.org/10.1016/j.cell.2015.01.049>
- Wang, Y. T., & Salter, M. W. (1994). Regulation of NMDA receptors by tyrosine kinases and phosphatases. *Nature*, 369(6477), 233-235. <https://doi.org/10.1038/369233a0>
- Wegiel, J., Wang, K.-C., Tarnawski, M., & Lach, B. (2000). Microglial cells are the driving force in fibrillar plaque formation, whereas astrocytes are a leading factor in plaque degradation. *Acta neuropathologica*, 100(4), 356-364.
- Weingarten, M. D., Lockwood, A. H., Hwo, S. Y., & Kirschner, M. W. (1975). A protein factor essential for microtubule assembly. *Proceedings of the National Academy of Sciences of the United States of America*, 72(5), 1858-1862. <https://doi.org/10.1073/pnas.72.5.1858>
- Welsh, K., Butters, N., Hughes, J., Mohs, R., & Heyman, A. (1991). Detection of abnormal memory decline in mild cases of Alzheimer's disease using CERAD neuropsychological measures. *Archives of neurology*, 48(3), 278-281.
- Wenk, G. L. (2006). Neuropathologic changes in Alzheimer's disease: potential targets for treatment. *The Journal of Clinical Psychiatry*, 67 Suppl 3, 3-7; quiz 23.

- Wilkinson, D., & Andersen, H. F. (2007). Analysis of the effect of memantine in reducing the worsening of clinical symptoms in patients with moderate to severe Alzheimer's disease. *Dementia and geriatric cognitive disorders*, *24*(2), 138-145.
- Wilson, R. S., Evans, D. A., Bienias, J. L., Mendes de Leon, C. F., Schneider, J. A., & Bennett, D. A. (2003). Proneness to psychological distress is associated with risk of Alzheimer's disease. *Neurology*, *61*(11), 1479-1485. <https://doi.org/10.1212/01.wnl.0000096167.56734.59>
- Winblad, B., & Poritis, N. (1999). Memantine in severe dementia: results of the 9M-best study (benefit and efficacy in severely demented patients during treatment with memantine). *International journal of geriatric psychiatry*, *14*(2), 135-146.
- World Alzheimer Report. (2016).
- World Health Organization. (2016). *WHO | Dementia: a public health priority*. World Health Organization.
- Wu, L., Zhou, X., Cao, Y., Mak, S. H., Zha, L., Li, N., ... Yang, X. (2021). Therapeutic efficacy of novel memantine nitrate MN-08 in animal models of Alzheimer's disease. *Aging Cell*, *20*(6), e13371. <https://doi.org/10.1111/acel.13371>
- Wu, S.-Z., Bodles, A. M., Porter, M. M., Griffin, W. S. T., Basile, A. S., & Barger, S. W. (2004). Induction of serine racemase expression and D-serine release from microglia by amyloid beta-peptide. *Journal of Neuroinflammation*, *1*(1), 2. <https://doi.org/10.1186/1742-2094-1-2>
- Wu, Y., Wu, Z., Butko, P., Christen, Y., Lambert, M. P., Klein, W. L., ... Luo, Y. (2006). Amyloid-beta-induced pathological behaviors are suppressed by Ginkgo biloba extract EGb 761 and ginkgolides in transgenic *Caenorhabditis elegans*. *The Journal of Neuroscience : The Official Journal of the Society for Neuroscience*, *26*(50), 13102-13113. <https://doi.org/10.1523/JNEUROSCI.3448-06.2006>
- Wyss-Coray, T., Loike, J. D., Brionne, T. C., Lu, E., Anankov, R., Yan, F., ... Husemann, J. (2003). Adult mouse astrocytes degrade amyloid-beta in vitro and in situ. *Nature Medicine*, *9*(4), 453-457. <https://doi.org/10.1038/nm838>
- Wyss-Coray, T., & Rogers, J. (2012). Inflammation in Alzheimer disease—a brief review of the basic science and clinical literature. *Cold Spring Harbor Perspectives in Medicine*, *2*(1), a006346. <https://doi.org/10.1101/cshperspect.a006346>
- Xia, P., Chen, H. V., Zhang, D., & Lipton, S. A. (2010). Memantine preferentially blocks extrasynaptic over synaptic NMDA receptor currents in hippocampal autapses. *The Journal of Neuroscience : The Official Journal of the Society*

- for *Neuroscience*, 30(33), 11246-11250.
<https://doi.org/10.1523/JNEUROSCI.2488-10.2010>
- XiangWei, W., Jiang, Y., & Yuan, H. (2018). De Novo Mutations and Rare Variants Occurring in NMDA Receptors. *Current Opinion in Physiology*, 2, 27-35. <https://doi.org/10.1016/j.cophys.2017.12.013>
- Xu, G., Ran, Y., Fromholt, S. E., Fu, C., Yachnis, A. T., Golde, T. E., & Borchelt, D. R. (2015). Murine A β over-production produces diffuse and compact Alzheimer-type amyloid deposits. *Acta Neuropathologica Communications*, 3, 72. <https://doi.org/10.1186/s40478-015-0252-9>
- Yamazaki, Y., Takahashi, T., Hiji, M., Kurashige, T., Izumi, Y., Yamawaki, T., & Matsumoto, M. (2010). Immunopositivity for ESCRT-III subunit CHMP2B in granulovacuolar degeneration of neurons in the Alzheimer's disease hippocampus. *Neuroscience Letters*, 477(2), 86-90. <https://doi.org/10.1016/j.neulet.2010.04.038>
- Yan, X., Liu, J., Ye, Z., Huang, J., He, F., Xiao, W., ... Luo, Z. (2016). CaMKII-Mediated CREB Phosphorylation Is Involved in Ca²⁺-Induced BDNF mRNA Transcription and Neurite Outgrowth Promoted by Electrical Stimulation. *PLoS One*, 11(9), e0162784. <https://doi.org/10.1371/journal.pone.0162784>
- Yang, M., & Leonard, J. P. (2001). Identification of mouse NMDA receptor subunit NR2A C-terminal tyrosine sites phosphorylated by coexpression with v-Src. *Journal of Neurochemistry*, 77(2), 580-588. <https://doi.org/10.1046/j.1471-4159.2001.00255.x>
- Yang, T., Shi, Y., Lin, C., Yan, C., Zhang, D., & Lin, J. (2019). Pharmacokinetics, bioavailability and tissue distribution study of JCC-02, a novel N-methyl-d-aspartate (NMDA) receptor inhibitor, in rats by LC-MS/MS. *European Journal of Pharmaceutical Sciences : Official Journal of the European Federation for Pharmaceutical Sciences*, 131, 146-152. <https://doi.org/10.1016/j.ejps.2019.02.018>
- Yang, Y., Ji, W.-G., Zhu, Z.-R., Wu, Y.-L., Zhang, Z.-Y., & Qu, S.-C. (2018). Rhynchophylline suppresses soluble A β (1-42)-induced impairment of spatial cognition function via inhibiting excessive activation of extrasynaptic NR2B-containing NMDA receptors. *Neuropharmacology*, 135, 100-112. <https://doi.org/10.1016/j.neuropharm.2018.03.007>
- Yasutake, C., Kuroda, K., Yanagawa, T., Okamura, T., & Yoneda, H. (2006). Serum BDNF, TNF-alpha and IL-1beta levels in dementia patients: comparison between Alzheimer's disease and vascular dementia. *European Archives of Psychiatry and Clinical Neuroscience*, 256(7), 402-406. <https://doi.org/10.1007/s00406-006-0652-8>

- Yu, X. M., Askalan, R., Keil, G. J. 2nd, & Salter, M. W. (1997). NMDA channel regulation by channel-associated protein tyrosine kinase Src. *Science (New York, N.Y.)*, 275(5300), 674-678. <https://doi.org/10.1126/science.275.5300.674>
- Yue, J., & López, J. M. (2020). Understanding MAPK Signaling Pathways in Apoptosis. *International Journal of Molecular Sciences*, 21(7). <https://doi.org/10.3390/ijms21072346>
- Zachari, M., & Ganley, I. G. (2017). The mammalian ULK1 complex and autophagy initiation. *Essays in Biochemistry*, 61(6), 585-596. <https://doi.org/10.1042/EBC20170021>
- Zamzow, D. R., Elias, V., Acosta, V. A., Escobedo, E., & Magnusson, K. R. (2016). Higher levels of phosphorylated Y1472 on GluN2B subunits in the frontal cortex of aged mice are associated with good spatial reference memory, but not cognitive flexibility. *Age (Dordrecht, Netherlands)*, 38(3), 50. <https://doi.org/10.1007/s11357-016-9913-2>
- Zhang, L., Zhang, J., & You, Z. (2018). Switching of the Microglial Activation Phenotype Is a Possible Treatment for Depression Disorder. *Frontiers in Cellular Neuroscience*, 12, 306. <https://doi.org/10.3389/fncel.2018.00306>
- Zhang, Yan, Li, P., Feng, J., & Wu, M. (2016). Dysfunction of NMDA receptors in Alzheimer's disease. *Neurological Sciences*, 37(7), 1039-1047. <https://doi.org/10.1007/s10072-016-2546-5>
- Zhang, Yun-wu, Thompson, R., Zhang, H., & Xu, H. (2011). APP processing in Alzheimer's disease. *Molecular Brain*, 4, 3. <https://doi.org/10.1186/1756-6606-4-3>
- Zhao, X., Yang, Z., Liang, G., Wu, Z., Peng, Y., Joseph, D. J., ... Wei, H. (2013). Dual effects of isoflurane on proliferation, differentiation, and survival in human neuroprogenitor cells. *Anesthesiology*, 118(3), 537-549. <https://doi.org/10.1097/ALN.0b013e3182833fae>
- Zheng, L., Kågedal, K., Dehvari, N., Benedikz, E., Cowburn, R., Marcusson, J., & Terman, A. (2009). Oxidative stress induces macroautophagy of amyloid beta-protein and ensuing apoptosis. *Free Radical Biology & Medicine*, 46(3), 422-429. <https://doi.org/10.1016/j.freeradbiomed.2008.10.043>
- Zhu, X. C., Yu, J. T., Jiang, T., & Tan, L. (2013). *Autophagy modulation for alzheimer's disease therapy*. *Molecular Neurobiology* (Vol. 48). Humana Press Inc. <https://doi.org/10.1007/s12035-013-8457-z>

Annex

Annex 1

Resultats preliminars sobre l'efecte de l'UB-ALT-EV sobre la neurogènesi en femelles SAMP8 de 10 mesos d'edat

1. Antecedents

La neurogènesi és el procés pel qual es generen noves neurones a partir de cèl·lules mare i cèl·lules progenitores, que es produeix durant el desenvolupament embrionari del cervell (Götz, Nakafuku, & Petrik, 2016). No obstant això, durant la vida adulta, els mamífers segueixen presentant neurogènesi en dues àrees cerebrals, la zona subventricular i la zona subgranular del gir dentat a l'hipocamp, gràcies a la presència de les cèl·lules mare neurals (Ihrle & Álvarez-Buylla, 2011; Zhao, Deng, & Gage, 2008). Aquest procés s'entén com una forma de plasticitat neuronal (Lledo, Alonso, & Grubb, 2006). Durant l'envelliment s'han identificat alteracions en el procés neurogènic (Lee, Clemenson, & Gage, 2012; Trinchero et al., 2017), que es veuen agreujades per la presència de malalties neurodegeneratives com la MA (Lazarov & Marr, 2010; Mu & Gage, 2011). De fet, diversos estudis en ratolins vells indiquen que les noves cèl·lules generades es desenvolupen a un ritme més lent (Trinchero et al., 2017), tenen una supervivència reduïda (Kempermann, Kuhn, & Gage, 1998), i es diferencien menys en neurones i més en astròcits (Encinas et al., 2011), però encara se'n desconeix en gran mesura el perquè es produeix aquesta alteració neurogènica (Díaz-Moreno et al., 2018).

Els receptors NMDA, a part de tenir un paper important en la supervivència neuronal són també essencials pel procés de neurogènesi (Åmellem et al., 2021). S'ha demostrat com la supervivència de les neurones nascudes al cervell adult estaria regulada per l'activitat neuronal en el gir dentat mitjançant l'LTP dependent dels receptors NMDA (Åmellem et al., 2021; Bruel-Jungerman, Davis, Rampon, & Laroche, 2006). La memantina, ha demostrat un efecte potenciador de la proliferació cel·lular d'un 26% al gir dentat de ratolins adults i d'un 27% a la zona subventricular, de la mateixa manera que altres antagonistes del receptor NMDA com l'MK-801 o l' àcid D(-)-2-amino-5-fosfonopentanoic (D-APV) (Hirasawa, Wada, Kohsaka, & Uchino, 2003; Nacher, Alonso-Llosa, Rosell, & McEwen, 2003; Nacher, Rosell, Alonso-Llosa, & McEwen, 2001; Okuyama, Takagi, Kawai, Miyake-Takagi, & Takeo, 2004), així com també ha demostrat

incluir la producció de neurones madures (Maekawa et al., 2009). Per aquest motiu, i donat el potencial terapèutic de compostos inductors del procés neurogènic en processos neurodegeneratius, es va decidir avaluar l'efecte del compost **UB-ALT-EV** sobre la neurogènesi a la zona del gir dentat de l'hipocamp en ratolins SAMP8 de 10 mesos d'edat.

2. Materials i mètodes

2.1. Tractament animals

Ratolins femella SAMR1 i SAMP8 de 9 mesos d'edat es van dividir aleatòriament en tres grups (n=37): SAMR1 (n=10), SAMP8 (n=11) i SAMP8 tractats amb UB-ALT-EV (n=10). Els animals van tenir accés lliure al menjar i a l'aigua, es van mantenir en condicions de temperatura estàndards (22 ± 2 °C) i es van mantenir en cicles de llum i foscor de 12h:12h (300lux/ 0lux). El consum d'aigua i el pes dels animals es va controlar cada setmana i la concentració de fàrmac es va ajustar quan va ser necessari. El compost UB-ALT-EV es va dissoldre en 2-hidroxipropil-b-ciclodextrina al 1,8% i es va administrar als ratolins a una dosi de 5mg/Kg/dia a través de l'aigua de beguda durant 28 dies fins l'eutanàsia. Els animals de 9 mesos d'edat el mateix dia d'inici tractament se'ls va injectar una solució de Bromodeoxiuridina (BrdU) i NaCl de 50 mg/Kg de pes dels animals en intervals de 2 hores, tres cops. Els animals es van sacrificar 28 dies després de la injecció de BrdU. Els estudis van ser aprovats pel Comitè Ètic d'Experimentació Animal (CEEA) de la Universitat de Barcelona.

2.2. Test de reconeixement de l'objecte nou:

La prova NORT és una prova cognitiva utilitzada per avaluar la memòria de reconeixement a curt i llarg termini. L'aparell utilitzat consisteix en un laberint negre de clorur de polivinil amb dos braços de 25 x 20 x 5 cm amb una orientació de 90°. Els objectes a discriminar eren de plàstic i sense cap part que pogués ser mossegada. La prova es va realitzar durant 5 dies. En els primers tres dies, els animals van ser habituats individualment a l'aparell durant 10 min cada dia. El quart dia, els animals van ser exposats individualment durant els 10 min de l'aparell i se'ls va permetre explorar lliurement la zona dins de l'aparell (fase de familiarització) on havíem col·locat dos objectes idèntics (A+A o B+B) al final de cada braç. Després de 10 min, els animals van ser retirats i retornats a la seva gàbia, i 2 h més tard es va realitzar la primera prova (memòria de curt termini). En aquesta segona fase del test, els objectes A i B van ser intercanviats (A+B o B+A) i els ratolins van poder explorar el laberint durant 10 minuts. 24 hores

després del primer assaig, els animals van ser exposats de nou a l'aparell, i en aquest cas, els objectes A i B van ser substituïts per dos nous objectes amb diferents formes i colors (A+C o B+C), i es va permetre als animals explorar-los durant 10 minuts. Es va mesurar el temps d'exploració de l'objecte nou (TN) i de l'objecte conegut (TC). L'exploració d'un objecte es va definir com el temps que passa el rosegador apuntant el nas cap a l'objecte a una distància de 2 cm i/o tocant-lo amb el nas. Girar o seure al voltant de l'objecte no es va considerar exploració. Per evitar els prejudicis de preferència de l'objecte, els objectes A i B es van contraequilibrar de manera que la meitat dels animals de

cada grup experimental es van exposar primer a l'objecte A i després a l'objecte B, mentre que l'altra meitat primer va veure l'objecte B i després l'objecte A. Finalment, per quantificar la funció cognitiva, es va calcular l'índex de discriminació (ID), que es defineix com $(TN-TC)/(TN+TC)$.

2.3. Tinció immunofluorescent:

Els ratolins van ser anestesiats (cetemamina 100 mg/Kg i xilazina 10 mg/Kg, per via intraperitoneal) i després es van perfondre intracardiacament amb una solució de PBS seguida d'una solució de paraformaldehid (PFA) al 4% diluït en una solució de tampó de fosfat 0,1 M. Els cervells van ser retirats i fixats en PFA al 4% durant la nit a 4°C. Posteriorment, els cervells es van canviar a una solució de PFA 4% i sucrosa 15%. Finalment, es van congelar en gel sec i es van emmagatzemar a -80°C. Es van tallar seccions de cervell coronals de 30 µm mitjançant un criostat (Leica Microsystems CM 3050S criostat, Wetzlar, Alemanya) i es van emmagatzemar en solució crioprotectora a -20°C.

Per a la tinció, es van permeabilitzar les seccions en un tampó Tris-Tween al 0,3% durant 20 min, seguit d'un bloqueig d'una hora amb albúmina de sèrum boví (BSA) al 0,5% en TBST. La incubació de l'anticòs primari es va realitzar a 4°C durant la nit. A continuació, es van realitzar tres rondes de rentats de 10 min de duració amb TBST a temperatura ambient, seguides d'una hora d'incubació a temperatura ambient de l'anticòs secundari. Les mostres es van rentar posteriorment en tres rondes de 10 min per finalment dur a terme una incubació de 5 min amb Hoescht a una dilució 1:500 per a tenyir els nuclis. Finalment es van rentar les seccions i es van muntar amb Fluoromount (Thermo Scientific). Els anticòssos utilitzats van ser: BrdU (Abcam/Ab6326; a una dilució 1:800), DCX (Santa Cruz Biotechnology/SC271390; a una dilució 1:50), GFAP (Dako/GA524; a una dilució 1:200), Alexa Fluor® 568 anti-goat (Invitrogen/A21206; a una dilució 1:500), Alexa Fluor® 488 anti-rabbit (Invitrogen/A11057; a una dilució 1:800). Les imatges es van obtenir amb un microscopi confocal espectral d'alta

velocitat Zeiss LSM880. Les imatges es van analitzar amb el programari ImageJ. Es van analitzar com a mínim 5 imatges de 5 individus per grup. I es van contar el nombre de cèl·lules positives per cadascuna de les tincions a la zona del gir dentat.

2.4. Anàlisi estadístic:

L'adquisició de dades i l'anàlisi estadística de les dades es va dur a terme utilitzant el programari GraphPad Prism. Les dades s'expressen com a mitjana \pm error estàndard de la mitjana (SEM) d'almenys 3 mostres per grup. L'anàlisi estadística es va realitzar a través de la prova *t-student* de dues cues o l'anàlisi de la variància d'una via (ANOVA) seguida per l'anàlisi *post-hoc* de Tukey. La importància estadística es va definir com a valor $p < 0,05$. Els valors atípics es van determinar amb la prova de Grubbs i, es van retirar de l'anàlisi quan va ser necessari. L'anàlisi dels paràmetres cognitius es va realitzar a cegues.

3. Resultats

En primer lloc, es va avaluar l'estat cognitiu dels animals SAMR1 i SAMP8 de 10 mesos d'edat, i l'efecte del tractament durant quatre setmanes amb el compost UB-ALT-EV sobre animals SAMP8. La prova de memòria NORT es va utilitzar per avaluar la memòria de reconeixement de curt i llarg termini. Els resultats van mostrar una disminució significativa de l'índex de discriminació del grup SAMP8 en comparació amb el grup de ratolins SAMR1 de 10 mesos d'edat (**Figura A1**). Per altra banda, el compost UB-ALT-EV va demostrar el seu efecte beneficiós sobre la memòria de reconeixement tant a curt com a llarg termini en els animals SAMP8 de 10 mesos d'edat.

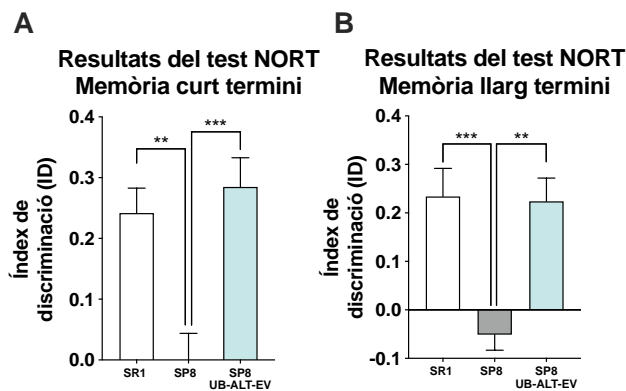


Figura A1. Resultats obtinguts mitjançant el test NORT en ratolins SAMR1, SAMP8 i SAMP8 tractats amb UB-ALT-EV de 10 mesos d'edat. Índex de discriminació del test de memòria de curt termini (**A**), índex de discriminació del test de memòria de llarg termini (**B**). Valors representants com la mitjana \pm error estàndard de la mitjana; (n=37): SAMR1 (n=10), SAMP8 (n=11) i SAMP8 tractats amb UB-ALT-EV (n=10). **p<0.01, ***p<0.001.

Seguidament, per avaluar la supervivència de les cèl·lules en el gir dentat de l'hipocamp, es van contar les cèl·lules positives pel marcatge amb BrdU a l'hipocamp dels ratolins SAMR1, SAMP8 i SAMP8 tractats amb el compost UB-ALT-EV. El BrdU és un anàleg de la timidina que s'incorpora a l'ADN de les cèl·lules en divisió durant la fase S del cicle cel·lular pel que s'utilitza per al seguiment de la proliferació cel·lular (Taupin, 2007). Els ratolins SAMP8 van mostrar una reducció del 50% de les cèl·lules BrdU positives en comparació amb el grup de ratolins SAMR1 de 10 mesos d'edat. Per altra banda, el tractament amb UB-ALT-EV va ser capaç d'augmentar significativament la supervivència cel·lular en els animals SAMP8 tractats (**Figura A2**). Cal destacar però que el nombre de cèl·lules BrdU positives a aquesta edat dels rosegadors va ser extremadament baixa, pel que l'efecte positiu sobre la supervivència per part del nou compost, és d'especial rellevància.

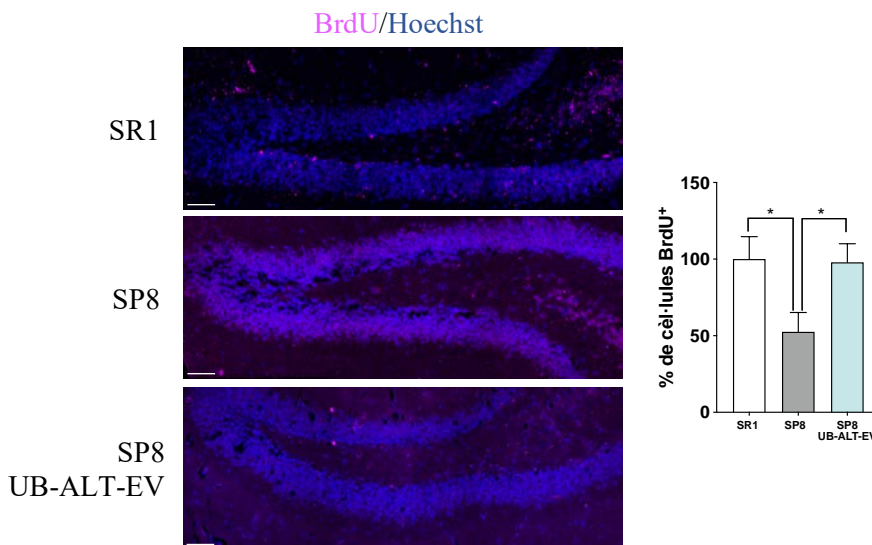


Figura A2. Nombre de cèl·lules BrdU positives al gir dentat de l'hipocamp dels animals SAMR1 i SAMP8 de 10 mesos d'edat. La gràfica representa el % de cèl·lules BrdU positives respecte els animals SAMR1. *p<0.05. L'escala representa 40µm.

Posteriorment, es va avaluar el marcador Doblecortina (DCX), una proteïna de migració neuronal que s'expressa a les neurones immadures (Francis et al., 1999). Així doncs, volíem avaluar el nombre de neurones en procés de maduració en els grups estudiats. En la mateixa línia que l'estudi del marcador BrdU, els animals SAMP8 de 10 mesos d'edat van mostrar una disminució del 50% en l'expressió d'aquest marcador de proliferació. En canvi, els animals SAMP8 tractats amb el compost UB-ALT-EV van augmentar en un 30% el marcatge DCX positiu en comparació amb el grup SAMP8, indicant un efecte inductor de la proliferació neuronal per part del nou compost (**Figura A3**). A més, l'avaluació del marcador d'activació astrocítica GFAP va mostrar una reducció d'aquest marcador en els animals SAMP8 en comparació amb els animals SAMR1, que no va ser revertida pel tractament amb UB-ALT-EV (**Figura A4**).

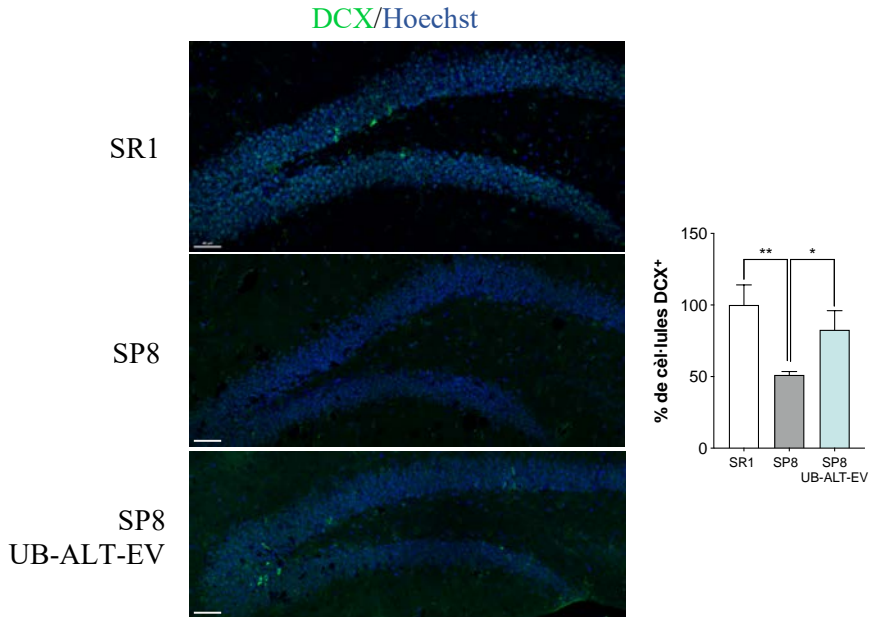


Figura A3. Nombre de cèl·lules DCX positives al gir dentat de l'hipocamp dels animals SAMR1 i SAMP8 de 10 mesos d'edat. La gràfica representa el % de cèl·lules DCX positives respecte els animals SAMR1. * $p < 0.05$, ** $p < 0.01$. L'escala representa $40\mu\text{m}$.

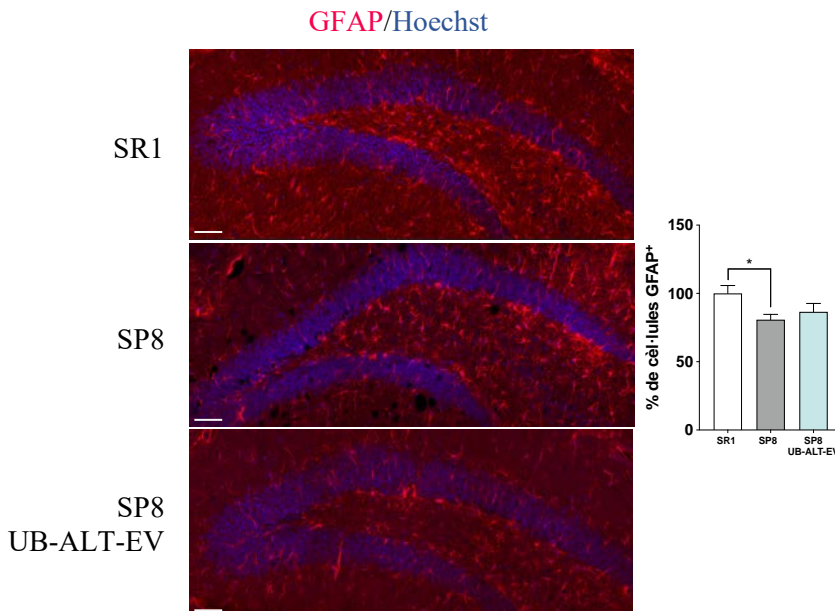


Figura A4. Nombre de cèl·lules GFAP positives al gir dentat de l'hipocamp dels animals SAMR1 i SAMP8 de 10 mesos d'edat. La gràfica representa el % de cèl·lules GFAP positives respecte els animals SAMR1. * $p < 0.05$. L'escala representa 40 μ m.

4. Discussió

Efectes del tractament amb UB-ALT-EV sobre el procés neurogènic en ratolins SAMP8 de 10 mesos d'edat

La neurogènesi durant l'edat adulta té un paper important en la millora i el manteniment de funcions com l'aprenentatge i la memòria (Yau, Li, & So, 2015). Per aquest motiu, s'ha postulat que teràpies dirigides a la potenciació de la neurogènesi podrien representar una estratègia per a reduir la progressió de la MA (Blennow, de Leon, & Zetterberg, 2006). De fet, s'ha demostrat com en el model de ratolí SAMP8, mitjançant l'ús d'agents inductors de la neurogènesi, es pot regular el microambient del nínxol neurogènic, rescatant el nombre de cèl·lules mare i així revertint el fenotip neurogènic patològic (Díaz-Moreno et al., 2018).

Particularment, el model SAMP8 en edats joves mostra un augment considerable de la neurogènesi en comparació amb els animals SAMR1 (Gang et al., 2011). S'ha suggerit que aquest increment en la neurogènesi en edats joves és un mecanisme per fer front a alteracions patològiques del cervell com l'estrès oxidatiu, la inflamació i l'activació de vies de mort neuronal, que afecten

principalment l'escorça cerebral i l'hipocamp (Cristòfol et al., 2012; Morley, Farr, Kumar, & Armbrecht, 2012; Surenda et al., 2006). Cal destacar però, que els ratolins SAMP8 presenten una disminució dràstica de la neurogènesi amb la progressió de la senescència (Gang et al., 2011). Per aquest motiu, és interessant l'estudi de l'efecte d'agents inductors de la neurogènesi en edats avançades d'aquest model donada la disminució de l'activitat neurogènica.

En primera instància, la millora de la memòria de reconeixement induïda pel tractament amb **UB-ALT-EV**, demostra una vegada més el potencial terapèutic del nou compost sobre la cognició, aquest cop, en ratolins SAMP8 de 10 mesos d'edat. A més, tenint en compte l'evidència demostrada per diferents antagonistes del receptor NMDA, actuant tots ells com a inductors de la neurogènesi (Hirasawa et al., 2003; Nacher et al., 2003, 2001; Okuyama et al., 2004), els nostres resultats preliminars sobre aquest procés (**Annex 1**), encara que són discrets, segueixen la mateixa línia d'evidència. En primer lloc, l'augment del percentatge de supervivència i de proliferació cel·lular observat en els animals SAMP8 envellits després del tractament amb **UB-ALT-EV** sembla indicar una vegada més, l'activitat inductora de la neurogènesi per part d'antagonistes del receptor NMDA. En segon lloc, tal i com s'ha descrit prèviament, vam trobar una disminució dels nivells del marcador GFAP al gir dentat dels ratolins SAMP8 de 10 mesos d'edat en comparació amb els animals SAMR1 (Gang et al., 2011), que no va ser revertida pel tractament amb **UB-ALT-EV**. En aquest sentit, s'ha suggerit que aquesta disminució en l'activació astrocítica dels animals SAMP8 podria ser responsable del deteriorament del nínxol neurogènic durant la senescència (Gang et al., 2011). En el nostre cas, l'avançada edat dels animals podria ser la causa de l'absència d'efecte del compost **UB-ALT-EV**.

En conjunt, els resultats preliminars obtinguts després del tractament d'animals SAMP8 de 10 mesos d'edat amb el compost **UB-ALT-EV** són molt esperançadors i, suggereixen un efecte inductor de la neurogènesi per part del nou compost, tot i l'avançat procés senescent que presenten els ratolins SAMP8.

5. Referències

- Åmellem, I., Yovianto, G., Chong, H. T., Nair, R. R., Cnops, V., Thanawalla, A., & Tashiro 田代 歩, A. (2021). Role of NMDA Receptors in Adult Neurogenesis and Normal Development of the Dentate Gyrus. *ENeuro*, 8(4). <https://doi.org/10.1523/ENEURO.0566-20.2021>
- Blennow, K., de Leon, M. J., & Zetterberg, H. (2006). Alzheimer's disease. *The Lancet*, 368(9533), 387-403. <https://doi.org/10.1016/S0140->

6736(06)69113-7

- Bruel-Jungerman, E., Davis, S., Rampon, C., & Laroche, S. (2006). Long-term potentiation enhances neurogenesis in the adult dentate gyrus. *The Journal of Neuroscience: The Official Journal of the Society for Neuroscience*, 26(22), 5888-5893. <https://doi.org/10.1523/JNEUROSCI.0782-06.2006>
- Cristòfol, R., Porquet, D., Corpas, R., Coto-Montes, A., Serret, J., Camins, A., ... Sanfeliu, C. (2012). Neurons from senescence-accelerated SAMP8 mice are protected against frailty by the sirtuin 1 promoting agents melatonin and resveratrol. *Journal of Pineal Research*, 52(3), 271-281. <https://doi.org/10.1111/j.1600-079X.2011.00939.x>
- Díaz-Moreno, M., Armenteros, T., Gradari, S., Hortigüela, R., García-Corzo, L., Fontán-Lozano, Á., ... Mira, H. (2018). Noggin rescues age-related stem cell loss in the brain of senescent mice with neurodegenerative pathology. *Proceedings of the National Academy of Sciences of the United States of America*, 115(45), 11625-11630. <https://doi.org/10.1073/pnas.1813205115>
- Encinas, J. M., Michurina, T. V., Peunova, N., Park, J.-H., Tordo, J., Peterson, D. A., ... Enikolopov, G. (2011). Division-coupled astrocytic differentiation and age-related depletion of neural stem cells in the adult hippocampus. *Cell Stem Cell*, 8(5), 566-579. <https://doi.org/10.1016/j.stem.2011.03.010>
- Francis, F., Koulakoff, A., Boucher, D., Chafey, P., Schaar, B., Vinet, M. C., ... Chelly, J. (1999). Doublecortin is a developmentally regulated, microtubule-associated protein expressed in migrating and differentiating neurons. *Neuron*, 23(2), 247-256. [https://doi.org/10.1016/s0896-6273\(00\)80777-1](https://doi.org/10.1016/s0896-6273(00)80777-1)
- Gang, B., Yue, C., Han, N., Xue, H., Li, B., Sun, L., ... Zhao, Q. (2011). Limited hippocampal neurogenesis in SAMP8 mouse model of Alzheimer's disease. *Brain Research*, 1389, 183-193. <https://doi.org/10.1016/j.brainres.2011.03.039>
- Götz, M., Nakafuku, M., & Petrik, D. (2016). Neurogenesis in the Developing and Adult Brain-Similarities and Key Differences. *Cold Spring Harbor Perspectives in Biology*, 8(7). <https://doi.org/10.1101/cshperspect.a018853>
- Hirasawa, T., Wada, H., Kohsaka, S., & Uchino, S. (2003). Inhibition of NMDA receptors induces delayed neuronal maturation and sustained proliferation of progenitor cells during neocortical development. *Journal of neuroscience research*, 74(5), 676-687.
- Ihrle, R. A., & Álvarez-Buylla, A. (2011). Lake-front property: a unique germinal niche by the lateral ventricles of the adult brain. *Neuron*, 70(4), 674-686.
- Kempermann, G., Kuhn, H. G., & Gage, F. H. (1998). Experience-induced neurogenesis in the senescent dentate gyrus. *The Journal of Neuroscience: The Official Journal of the Society for Neuroscience*, 18(9), 3206-3212.

- <https://doi.org/10.1523/JNEUROSCI.18-09-03206.1998>
- Lazarov, O., & Marr, R. A. (2010). Neurogenesis and Alzheimer's disease: at the crossroads. *Experimental Neurology*, 223(2), 267-281. <https://doi.org/10.1016/j.expneurol.2009.08.009>
- Lee, S. W., Clemenson, G. D., & Gage, F. H. (2012). New neurons in an aged brain. *Behavioural Brain Research*, 227(2), 497-507. <https://doi.org/10.1016/j.bbr.2011.10.009>
- Lledo, P.-M., Alonso, M., & Grubb, M. S. (2006). Adult neurogenesis and functional plasticity in neuronal circuits. *Nature Reviews. Neuroscience*, 7(3), 179-193. <https://doi.org/10.1038/nrn1867>
- Maekawa, M., Namba, T., Suzuki, E., Yuasa, S., Kohsaka, S., & Uchino, S. (2009). NMDA receptor antagonist memantine promotes cell proliferation and production of mature granule neurons in the adult hippocampus. *Neuroscience Research*, 63(4), 259-266. <https://doi.org/10.1016/j.neures.2008.12.006>
- Morley, J. E., Farr, S. A., Kumar, V. B., & Armbrecht, H. J. (2012). The SAMP8 mouse: a model to develop therapeutic interventions for Alzheimer's disease. *Current pharmaceutical design*, 18(8), 1123-1130.
- Mu, Y., & Gage, F. H. (2011, desembre 22). Adult hippocampal neurogenesis and its role in Alzheimer's disease. *Molecular Neurodegeneration*. <https://doi.org/10.1186/1750-1326-6-85>
- Nacher, J., Alonso-Llosa, G., Rosell, D. R., & McEwen, B. S. (2003). NMDA receptor antagonist treatment increases the production of new neurons in the aged rat hippocampus. *Neurobiology of aging*, 24(2), 273-284.
- Nacher, J., Rosell, D. R., Alonso-Llosa, G., & McEwen, B. S. (2001). NMDA receptor antagonist treatment induces a long-lasting increase in the number of proliferating cells, PSA-NCAM-immunoreactive granule neurons and radial glia in the adult rat dentate gyrus. *European Journal of Neuroscience*, 13(3), 512-520.
- Okuyama, N., Takagi, N., Kawai, T., Miyake-Takagi, K., & Takeo, S. (2004). Phosphorylation of extracellular-regulating kinase in NMDA receptor antagonist-induced newly generated neurons in the adult rat dentate gyrus. *Journal of neurochemistry*, 88(3), 717-725.
- Sureda, F. X., Gutierrez-Cuesta, J., Romeu, M., Mulero, M., Canudas, A. M., Camins, A., ... Pallàs, M. (2006). Changes in oxidative stress parameters and neurodegeneration markers in the brain of the senescence-accelerated mice SAMP-8. *Experimental Gerontology*, 41(4), 360-367. <https://doi.org/10.1016/j.exger.2006.01.015>
- Taupin, P. (2007). BrdU immunohistochemistry for studying adult neurogenesis:

- paradigms, pitfalls, limitations, and validation. *Brain Research Reviews*, 53(1), 198-214. <https://doi.org/10.1016/j.brainresrev.2006.08.002>
- Trincherro, M. F., Buttner, K. A., Sulkes Cuevas, J. N., Temprana, S. G., Fontanet, P. A., Monzón-Salinas, M. C., ... Schinder, A. F. (2017). High Plasticity of New Granule Cells in the Aging Hippocampus. *Cell Reports*, 21(5), 1129-1139. <https://doi.org/10.1016/j.celrep.2017.09.064>
- Yau, S., Li, A., & So, K.-F. (2015). Involvement of Adult Hippocampal Neurogenesis in Learning and Forgetting. *Neural Plasticity*, 2015, 717958. <https://doi.org/10.1155/2015/717958>
- Zhao, C., Deng, W., & Gage, F. H. (2008). Mechanisms and functional implications of adult neurogenesis. *Cell*, 132(4), 645-660.

